

Title	Synthesis of nitrogen-containing heterocycles
Authors	Shanahan, Rachel
Publication date	2019-07
Original Citation	Shanahan, R. M. 2019. Synthesis of nitrogen-containing heterocycles. PhD Thesis, University College Cork.
Type of publication	Doctoral thesis
Rights	© 2019, Rachel M. Shanahan. - https://creativecommons.org/licenses/by-nc-nd/4.0/
Download date	2023-05-05 00:20:19
Item downloaded from	http://hdl.handle.net/10468/10087

Synthesis of Nitrogen-Containing Heterocycles



Rachel M. Shanahan BSc

*A thesis presented for the degree of
Doctor of Philosophy*

to

NATIONAL UNIVERSITY OF IRELAND, CORK

School of Chemistry
University College Cork

Supervisor: Dr. Gerard P. McGlacken
Head of School: Dr. Humphrey A. Moynihan

July 2019

Table of Contents

Declaration.....	i
Acknowledgements.....	ii
Abstract.....	iv
Abbreviations and Acronyms	v
Chapter 1 Synthesis of Biologically Active HHQ Analogues	
Introduction.....	1
1.1. Antibiotic Resistance	2
1.2. Quorum Sensing.....	2
1.3. <i>Pseudomonas aeruginosa</i>	4
1.3.1. Quorum Sensing in <i>Pseudomonas aeruginosa</i>	4
1.4. Previous Structure-Activity Relationship Studies of HHQ	6
1.5. Aims of this Chapter	9
Results & Discussion.....	10
1.6. Objectives	11
1.7. β -Ketoester Synthesis	12
1.8. Synthesis of HHQ	13
1.8.1. Synthesis of Aryl-Substituted HHQ Analogues	14
1.8.2. Synthesis of C-2 Nonyl Chain Analogues	15
1.8.3. Methylation of HHQ Analogues.....	17
1.9. Quinazolinone Synthesis.....	19
1.10. Synthesis of HHQ Analogue with a C-2 Terminal Alkene.....	20
1.11. Synthesis of Potential PqsR Antagonists	21
1.11.1. Synthesis of Substituted Analogues of Hartmann's Antagonist.....	22
1.12. Conclusions.....	23

1.13. Biological Results	24
Experimental	37
1.14. General Considerations.....	38
1.15. Synthesis of β -Ketoesters.....	39
1.16. General Procedure for the Synthesis of HHQ and HHQ Analogues	41
1.17. General Procedure for the Methylation of HHQ Analogues	47
1.18. Synthesis of Quinazolinone Compound 28.....	49
1.19. Synthesis of 6-Nitro HHQ 3	50
1.20. Synthesis of Carboxylic Acid Precursor 32	51
1.21. General Procedure for the Synthesis of Hartmann's Amide and Methylated Analogues	52
1.22. Chapter 1 References.....	55
Chapter 2 Towards the Synthesis of PHT	
Introduction.....	59
2.1. Crop Protection	60
2.2. Syngenta.....	60
2.3. Nicotinic Acetylcholine Receptor (nAChR) Agonists as Insecticides	60
2.4. Pyridohomotropane (PHT) - Design.....	62
2.4.1. PHT - Previous Synthetic Routes	63
2.5. Aims of this Chapter	65
Results & Discussion.....	66
2.6. Retrosynthetic Analysis of PHT – Strategy 1	67
2.7. Route 1 – Beginning from Aldehyde Starting Material.....	67
2.8. Retrosynthetic Analysis of PHT – Strategy 2	69
2.9. Route 2 – Utilising the Nitrile Group as a 'Masked' Aldehyde	69
2.10. Accessing Key Intermediate 47	70
2.11. Building the Bicyclic PHT Framework	72

2.12. Krapcho Decarboxylation – Removing the First Ester Group.....	73
2.13. Barton Decarboxylation – Removing the Remaining Ester Group	74
2.13.1. Barton Decarboxylation of Model Substrates	75
2.13.2. Attempts to Perform Barton Decarboxylation on PHT Substrate	79
2.14. Proof-of-Principle Debenzylation.....	83
2.15. Conclusions.....	85
2.16. Publication of Completed Total Synthesis of PHT in 2018.....	86
Experimental	88
2.17. General Considerations.....	89
2.18. Aldehyde Route	90
2.18.1. Synthesis of Compound 37.....	90
2.18.2. Synthesis of Compound 38.....	90
2.18.3. Synthesis of Diazo Compound 40	91
2.18.4. Synthesis of Compound 41	92
2.19. Nitrile Route.....	93
2.19.1. Synthesis of Nitrile Compound 43	93
2.19.2. Synthesis of Compound 44.....	93
2.19.3. Synthesis of Compound 45.....	94
2.19.4. Synthesis of Compound 47	95
2.19.5. Synthesis of Cyclised Diester Compound 49	96
2.19.6. Synthesis of Monoester Compound 50.....	97
2.19.7. Synthesis of Carboxylic Acid Compound 62	97
2.19.8. Synthesis of Debenzylated Monoester Compound 67.....	98

2.20. Barton Model System	99
2.21. Chapter 2 References.....	100
Chapter 3 Direct Arylation of Phenoxyquinolines	
Introduction.....	103
3.1. Direct Arylation	104
3.2. Quinolines	108
3.3. One-Pot Reactions	110
3.3.1. Literature Examples of One-Pot Suzuki-Miyaura/Direct Arylation....	111
3.4. Dihalogenated Substrates – Chemoselectivity and Regioselectivity	112
3.5. Reversible Oxidative Addition	114
3.6. Aims of this Chapter	115
Results & Discussion.....	116
3.7. Objectives	117
3.8. Attempts at Double C-H Activation	118
3.9. Single C-H Coupling.....	120
3.9.1. Substrate Scope.....	122
3.9.2. Substrates that Failed to Cyclise.....	130
3.10. One-Pot Tandem Suzuki-Miyaura/Direct Arylation Reactions	131
3.10.1. Substrate Scope.....	135
3.10.2. One-Pot Tandem Mizoroki-Heck/Direct Arylation Reactions	140
3.10.3. Tandem Reaction on Pyridine Substrates	141
3.11. Reversible Oxidative Addition	148
3.12. Conclusions.....	154
Experimental	155
3.13. General Considerations	156

3.14. Synthesis of 4-Chloroquinolines.....	157
3.15. General Procedure for Synthesis of 4-Phenoxy Quinoline Substrates – NaOH Method.....	158
3.16. General Procedure for Synthesis of 4-Phenoxy Quinoline Substrates – DMAP Method.....	167
3.17. General Procedure for Pd-Catalysed Intramolecular Direct Arylation.....	171
3.18. Synthesis of Compound 106.....	180
3.19. Synthesis of Compound 107.....	180
3.20. Synthesis of Compound 110.....	181
3.21. Synthesis of Compound 108.....	182
3.22. General Procedure for Synthesis of 4-Phenoxy Quinoline Substrates.....	183
3.23. General Procedure for Pd-Catalysed One-Pot Tandem Suzuki-Miyaura/Direct Arylation Reactions	186
3.24. General Procedure for Pd-Catalysed One-Pot Mizoroki-Heck and Intramolecular Direct Arylation Reactions.....	196
3.25. General Procedure for Synthesis of 4-Phenoxy Pyridine Substrates.....	198
3.26. Synthesis of Compound 148.....	200
3.27. Synthesis of Compound 150.....	201
3.28. Synthesis of Compound 157.....	201
3.29. General Procedure for Synthesis of Iodinated 4-Chloroquinolines	202
3.30. Synthesis of Compound 164.....	205
3.31. Chapter 3 References.....	206
General Conclusions	211
Appendix I	213
Appendix II.....	248

Declaration

This is to certify that the work I am submitting is my own and has not been submitted for another degree, either at University College Cork or elsewhere. All external references and sources are clearly acknowledged and identified within the contents. I have read and understood the regulations of University College Cork concerning plagiarism.

Rachel M. Shanahan

22nd July 2019

Acknowledgements

To those who inspired it and will not read it.

Firstly, I want to thank my supervisor, Dr Gerard McGlacken, for answering my eager request for a summer placement in his research group as an undergraduate back in 2012. Little did I know then that, one-quarter of my lifetime later, I would be saddened to move on from what has become my GMG family. I am very grateful for all of your advice when I didn't know what to do next, your encouragement when I didn't know how, and your understanding when I simply couldn't.

I wish to thank the Irish Research Council for funding this research, and to Syngenta Crop Protection for hosting me in 2015. I am grateful to Dr Florence McCarthy for acting as my advisor. I also thank Dr McCarthy and Prof Frances Heaney for examining this thesis.

I express my appreciation for the staff of the School of Chemistry who provide the many services that supported this work. Firstly, to Claire Tobin, Mary O'Neill, Claire O'Sullivan and Niamh Daly, as well as all previous staff of the Chemistry Office, for keeping the place running day-to-day. Thanks to Dr Dan McCarthy, Dr Lorraine Bateman and Dr Denis Lynch for the NMR service, to Dr Florence McCarthy and Mick O'Shea for the mass spectrometry service, to the technical staff, Dr Tom O'Mahony, Dr Trevor Carey, Dr Ian O'Connor, Dr Aoife O'Sullivan, Dr Francis Harrington, Dr Donncha O'Connell, Tina Kent, Denis Duggan, Johnny Ryan, Tony Hogan, Noel Browne and Derry Kearney for all that you do. Special thanks to Trevor, Ian and Fran for helping me keep a roof over my head, food in my belly, and a smile on my face.

I have had the privilege to work with many talented people, all of whom have contributed to my becoming the chemist and the person I am today. Firstly, to my favourite Postdocs, Dr Rafael Cano and Dr Leticia Pardo, for passing on their knowledge and experience, both inside and outside the lab. Rafa, we will always be Team Quinolone! Leti, you will always be my lab mom/big sister and proof-reader extraordinaire. To all of the past members of the GMG group – Tina, Marie-Therese, Sarah, Eoin, and Vera. Thank you all for everything you taught me and for welcoming

me into the lab. To Aisling, my lab buddy...it was the best of times, it was the worst of times, but I'm glad we went through it together and supported each other as best we could! And to those who came after us, Pamela, Katrina, Emma and Aobha, thanks for all the fun and emotional support, I hope you all continue to look out for each other and keep the lab tidy! Aobha, you were my best FYP student and quickly became a dear friend. Thank you for all the hard work you have put into our projects, I couldn't have done it without you. I'm very proud of the chemists you have all grown into, keep up the great work! And to everyone else who has crossed my path on the 4th floor of the Kane and 2nd floor of the CPB, thank you all for your friendship. Special mention to Patrick, I toast our success and our friendship with an ice-cream cookie sandwich.

I am especially grateful to my Mum, Dad and sister Alison, who have provided moral, emotional and, lest I forget, financial support in my life. I am also grateful to my extended family members and friends who have supported me along the way, including through their regular requests for updates on the estimated time of completion for this PhD. I can now tell you all that it's (pretty much) finished. Special thanks to Cas for always being there.

To Mark, thanks for keeping me sane and looking after me when I was too worn out to look after myself. And thanks for ensuring I had plenty of procrastinating to do around the house during the last six years of this four year PhD program. I needed those breaks!

Y xxx

Abstract

The sharp rise in antimicrobial resistance has been matched by a decline in the identification and clinical introduction of new classes of drugs to treat microbial infections. Thus new approaches are being sought to target pathogenic microorganisms. In that context, the use of non-biocidal small molecules, that target quorum sensing signalling networks in pathogens, has emerged as a solution with real clinical potential. Previous work has shown that two alkyl quinolone signal molecules (HHQ and PQS) from the nosocomial pathogen *Pseudomonas aeruginosa* have modulatory activity towards other microorganisms. Chapter 1 of this thesis outlines the synthesis of analogues of HHQ with the aim of learning more about the structure-activity relationship of alkyl quinolone quorum sensing molecules.

Chapter 2 of this thesis describes work carried out during a six-month work placement at Syngenta Crop Protection in Stein, Switzerland. The project involved efforts towards a new total synthesis of pyridohomotropane (PHT), a synthetic alkaloid which has shown agonistic activity towards nicotinic acetylcholine receptors (nAChRs). Since they are found in the central nervous system of insects, nAChRs are a key target of insecticidal crop protection products. This chapter outlines the retrosynthetic analysis and synthesis of key intermediates towards the total synthesis of PHT.

The formation of aryl-aryl bonds is an important transformation in organic synthesis due to the abundance of aryl-aryl moieties in natural products and pharmaceuticals. Direct arylation strategies aim to avoid the installation of one or both of the activating groups typically required for traditional cross-coupling methods. The application of direct arylation protocols towards the synthesis of polycyclic benzofuroquinoline compounds is described in Chapter 3. Expansion of the methodology to facilitate a one-pot tandem reaction combining Suzuki-Miyaura and direct arylation transformations is also discussed. Finally, the retention of specific carbon-bromide bonds of the quinoline substrates is achieved via a reversible oxidative addition protocol.

Abbreviations and Acronyms

Å	ångström
ABSA	acetamidobenzene sulfonyl azide
Ac	acetyl
AcOH	acetic acid
Add.	additive
aq.	aqueous
Ar	aryl
BINAP	2,2'-bis(diphenylphosphino)-1,1'-binaphthyl
Bn	benzyl
Boc	<i>tert</i> -butyloxycarbonyl
Bu	butyl
c	centi (10^{-2})
°C	Celsius
^{13}C -NMR	carbon nuclear magnetic resonance
ca.	circa
calcd	calculated
cataCXiumA	di(1-adamantyl)- <i>n</i> -butylphosphine
CDI	<i>N,N'</i> -carbonyldiimidazole
conc.	concentrated
COSY	correlation spectroscopy
Cy	cyclohexyl
δ	NMR chemical shift
D, d	deuterium
DABCO	1,4-diazabicyclo[2.2.2]octane
DavePhos	2-dicyclohexylphosphino-2'-(<i>N,N</i> -dimethylamino)biphenyl
dba	dibenzylideneacetone
DCC	<i>N,N'</i> -dicyclohexylcarbodiimide
DCE	dichloroethane
DCM	dichloromethane
DEPT	distortionless enhancement by polarisation transfer
DIBAL	diisobutyl aluminium hydride
DIPEA	<i>N,N</i> -diisopropyl ethyl amine
DMA	dimethylacetamide
DMAP	4-dimethylaminopyridine
DME	dimethoxyethane
DMF	dimethylformamide
DMSO	dimethylsulfoxide
DPEphos	bis[(2-diphenylphosphino)phenyl] ether
dppf	1,1'-bis(diphenylphosphino)ferrocene
e.g.	for example
EDC	1-ethyl-3-(3-dimethylaminopropyl)carbodiimide
equiv.	equivalent(s)
ESI	electrospray ionisation
esp	$\alpha,\alpha,\alpha',\alpha'$ -tetramethyl-1,3-benzenedipropionic acid
Et	ethyl
<i>et al.</i>	and others
^{19}F -NMR	fluorine nuclear magnetic resonance
FDA	Food and Drug Administration

FT-IR	Fourier-transform infrared spectroscopy
g	gram(s)
h	hour(s)
¹ H-NMR	proton nuclear magnetic resonance
HMBC	heteronuclear multiple-bond correlation spectroscopy
HMDS	hexamethyldisilazane
HRMS	high-resolution mass spectrometry
HSQC	heteronuclear single-quantum correlation spectroscopy
Hz	Hertz
<i>i</i>	iso
i.e.	that is
IR	infrared
<i>J</i>	coupling constant
John Phos	(2-biphenyl)di- <i>tert</i> -butylphosphine
L	ligand
	litre
LCMS	liquid chromatography mass spectrometry
LDA	lithium diisopropylamide
LED	light-emitting diode
lit.	literature
μ	micro (10 ⁻⁶)
m	metre
	milli (10 ⁻³)
<i>m</i>	meta
M	metal
	molar
m/z	mass-to-charge ratio
max	maximum
Me	methyl
MIC	methylisocyanide
mg	milligram
MHz	megahertz
min	minute(s)
	minimum
mL	millilitre
mmol	millimole
mol	mole
	molecular
mol%	mole percent
m.p.	melting point
MS	mass spectrometry
	molecular sieves
ν	frequency of absorption
n	nano (10 ⁻⁹)
<i>n</i>	normal
<i>n</i> -BuLi	<i>n</i> -butyllithium
NMP	<i>N</i> -methyl-2-pyrrolidone
NMR	nuclear magnetic resonance
<i>o</i>	ortho
OAc	acetate

OTBS	<i>tert</i> -butyldimethylsilyl ether
OTf	triflate
	trifluoromethanesulfonate
<i>p</i>	para
Ph	phenyl
PivOH	pivalic acid
PMP	1,2,2,6,6-pentamethylpiperidine
ppm	parts per million
Pr	propyl
<i>p</i> -TsOH	<i>p</i> -toluenesulfonic acid
q	quaternary
QPhos	1,2,3,4,5-pentaphenyl-1'-(di- <i>tert</i> -butylphosphino)ferrocene
R.T.	room temperature
RuPhos	2-dicyclohexylphosphino-2',6'-diisopropoxybiphenyl
s	second(s)
sat.	saturated
SPhos	2-dicyclohexylphosphino-2',6'-dimethoxybiphenyl
t	time
<i>t</i> , <i>tert</i>	tertiary
T	temperature
TEA	triethylamine
TFA	trifluoroacetic acid
	trifluoroacetate
TFE	2,2,2-trifluoroethanol
THF	tetrahydrofuran
TLC	thin-layer chromatography
TMS	tetramethylsilane
	trimethylsilyl
TOF LC-MS	time-of-flight liquid chromatography-mass spectrometry
Tol	tolyl
Ts	4-toluenesulfonyl, tosyl
USD	United States Dollars
UV	ultraviolet
W	Watt
Xantphos	4,5-bis(diphenylphosphino)-9,9-dimethylxanthene
XPhos	2-dicyclohexylphosphino-2',4',6'-triisopropylbiphenyl

Nothing in life is to be feared, it is only to be understood. Now is the time to understand more, so that we may fear less.

Marie Skłodowska Curie

Chapter 1

Synthesis of Biologically Active HHQ Analogues

Introduction

1.1. Antibiotic Resistance

The discovery, isolation and development of antibiotics revolutionised medicine in the 20th century.^[1] Antibiotics have successfully prevented or treated previously fatal infections, greatly contributing to longevity and quality of life. In developing countries, antibiotics decrease morbidity and mortality caused by poverty-related infections.^[2] Unsurprisingly, antibiotics can be considered one of the most successful forms of chemotherapy in the history of medicine.

Nowadays however, there is evidence to suggest that the widespread use of broad-spectrum antibiotics has contributed to the emergence of resistance among both targeted and non-targeted microbes, since current antibiotic therapies tend to be non-pathogen specific.^[3] Consequently, there is an urgent need to create innovative new medicines for the prevention of microbial infections, while avoiding the development of resistance.^[3-4] In contrast to classical antibiotic drug targets, which are involved in vital processes of the bacterial cell, ‘antivirulence’ strategies aim to abolish pathogenic behaviours without affecting cell viability, circumventing the problem of acquired resistance.^[5-6]

1.2. Quorum Sensing

One way in which microorganisms coordinate their behaviour is by utilising a system of chemical regulation of gene expression in response to population density, known as quorum sensing (QS).^[7] QS involves the production, release and detection of small molecules, known as autoinducers (AIs), which accumulate in the extracellular environment as the population increases. Once the concentration of AIs rises to a minimal threshold, population-wide alterations of gene expression are triggered, leading to a coordinated response.^[7] In this manner, QS regulates the expression of genes that underpin various biological processes.^[8]

Importantly, among the behaviours controlled by QS in pathogenic microorganisms are those that promote infection or circumvent the host immune system.^[9] Using QS, pathogenic bacteria can coordinate critical pathogenicity traits, like the production of virulence factors or biofilm formation. A biofilm can be defined as a structure consisting of surface-attached microbial cells that is enclosed in an extracellular

polysaccharide matrix (**Figure 1**).^[10] They can grow on living or inert surfaces, such as lung tissue or medical implants. Bacterial biofilms can cause chronic infections because they display increased tolerance to antibiotics and resist phagocytosis by the host immune system.

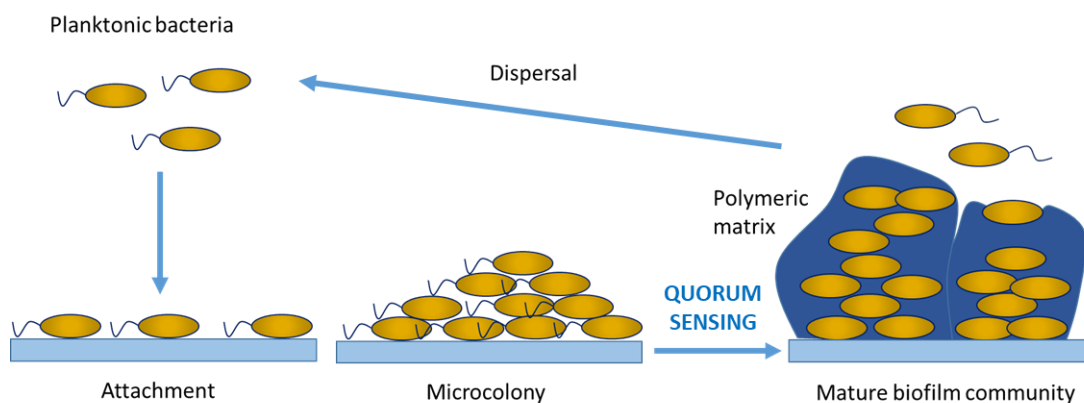


Figure 1 Biofilm formation in pathogenic bacteria.

Targeting the QS networks that are responsible for virulence factors and biofilm formation in pathogens constitutes an attractive alternative to antibiotics for the control of microbial diseases. The term ‘antivirulence therapy’ has emerged to describe this strategy.^[11] This intervention does not directly lead to bacterial death or growth inhibition, but instead it suppresses pathogenic behaviour.^[12] As the viability of the target population is not directly affected, it is proposed that development of resistance to drug candidates would be stunted.^[6] Thus, interference with the QS network responsible for virulence behaviour in pathogens represents an excellent therapeutic strategy. ‘Quorum quenching’ as an antivirulence target is a rapidly-growing area of research.^[13-14] Synthetic molecules capable of interfering with bacterial QS networks are known as quorum sensing inhibitors (QSIs).^[15] In order to design effective QSIs, it is important to understand the native AIs that operate in the QS networks of the target pathogen.

1.3. *Pseudomonas aeruginosa*

Pseudomonas aeruginosa is a Gram-negative pathogenic bacteria often associated with hospital acquired infections, particularly in immunocompromised patients. For example, it is a common cause of morbidity and death in people with cystic fibrosis (CF).^[16] *P. aeruginosa* is one of the so-called ESKAPE pathogens (*Enterococcus faecium*, *Staphylococcus aureus*, *Klebsiella pneumoniae*, *Acinetobacter baumannii*, *P. aeruginosa*, and *Enterobacter* species) which are responsible for the majority of nosocomial infections.^[17-18] In 2017, the World Health Organization (WHO) published a priority list of pathogens with an urgent need for new treatment options.^[19] *P. aeruginosa* ranked in the highest ‘critical’ category.

The persistence of chronic *P. aeruginosa* lung infections in CF patients, for example, can be largely attributed to the establishment of a biofilm mode of growth. Prevention of chronic biofilm lung infections is only possible by early, aggressive antibiotic intervention. However, once chronic biofilm infections are established, permanent eradication is almost impossible to achieve.^[20]

1.3.1. Quorum Sensing in *Pseudomonas aeruginosa*

A complex QS network controls virulent behaviour and the development of biofilms in *P. aeruginosa* (**Figure 2**).^[21] Typically, the QS system of Gram-negative bacteria consists of a transcription regulator, the AI molecules and one or several enzymes involved in the synthesis of the latter. The transcription regulator controls the transcription of the biosynthetic enzymes and also functions as a receptor for the signal molecules themselves. In *P. aeruginosa*, there are three different chemotypes of AIs: alkyl homoserine lactones (AHLs) used by both the *las* and *rhl* QS systems,^[5, 18] alkyl quinolones (AHQs) used by the *pqs* system,^[22] and the integrating quorum sensing signal (IQS) 2-(2-hydroxyphenyl)thiazole-4-carbaldehyde used by the *iqs* system.^[23] The focus of this thesis chapter is the *pqs* network and the AHQ signalling molecules.

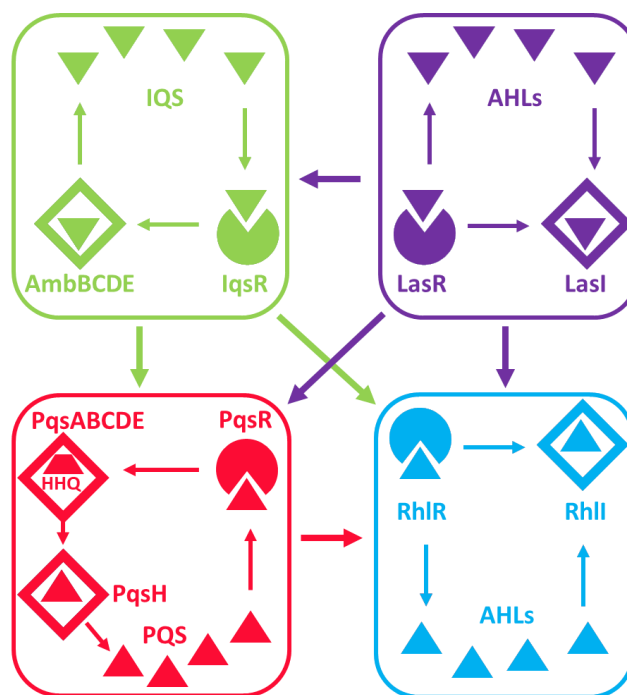


Figure 2 The four QS networks of *P. aeruginosa*.

The primary AIs of the *P. aeruginosa* AHQ QS pathway are 2-heptyl-4-quinolone (HHQ, **1**) and 2-heptyl-3-hydroxy-4-quinolone, known as the Pseudomonas quinolone signal (PQS, **2**).^[24] HHQ is converted to PQS in *P. aeruginosa* by the monooxygenase PqsH (**Figure 3**). Both PQS and HHQ are agonists of the transcription regulator called ‘multiple virulence factor regulator’ (MvfR), more commonly referred to as PqsR. Through interaction with this receptor, HHQ and PQS induce the transcription of a variety of genes, including their own biosynthetic enzyme cascade (PqsABCDE), as well as genes responsible for the production of virulence factors and biofilm formation.^[14]

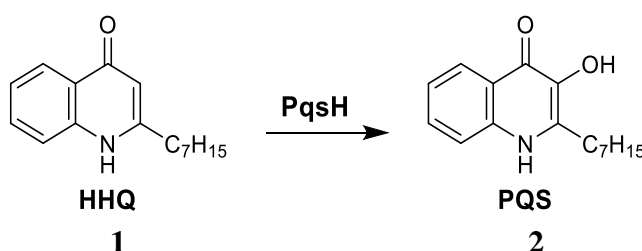


Figure 3 *P. aeruginosa* QS molecules HHQ **1** and PQS **2**.

Thus, AHQ-derived QSIs capable of interrupting the QS network responsible for virulence behaviour in *P. aeruginosa* potentially represent a new generation of antimicrobial agents.^[14, 25-26] Encouragingly, it has been shown that PqsR-targeting

QSIs are able to increase the susceptibility of *P. aeruginosa* biofilms against antibiotics.^[27] Therefore, integrated treatment approaches where a conventional antibiotic therapy is potentiated by quorum quenching agents could also be an effective treatment option.

The *P. aeruginosa* signalling molecules HHQ and PQS have also been shown to possess interspecies and even interkingdom activity, influencing the phenotypic and transcriptional behaviour of other pathogenic microorganisms, such as fungi and yeasts.^[28-30] This may be a consequence of the proximity in which these organisms co-exist in clinical and environmental niches, including the lungs of immunocompromised patients and plant ecosystems. Interactions between co-existing organisms have been widely reported, and many signalling molecules display activity ranging from interspecies to interkingdom.^[31-32] Exploiting interspecies and interkingdom communication networks, and the mode of action of the chemical signals employed therein, offers a powerful platform from which to combat a range of microbial diseases.^[33]

1.4. Previous Structure-Activity Relationship Studies of HHQ

In light of the important roles played by PQS and HHQ in virulence, both molecular structures have been the subject of a number of structure–activity relationship (SAR) studies in recent years (**Figure 4**). The Welch group was among the first to undertake a SAR approach to the PQS framework.^[34] Around the same time, Spring and co-workers developed an excellent high throughput method for the preparation of PQS analogues using flow techniques.^[35] Overall, these studies indicated that almost every part of the PQS molecule appears to contribute in some way towards its function as a signalling molecule. Most of the alterations to the quinolone backbone and the alkyl chain resulted in reduced agonistic activity towards PqsR. For example, shortening or lengthening the C-2 alkyl chain resulted in diminished activation of the receptor. In addition, substitution of the quinolone ring with electron-withdrawing groups appeared to increase agonistic activity, while a decrease was observed with electron-donating substituents.

The McGlacken group is engaged in a long-standing collaboration with Dr Jerry Reen and Prof Fergal O’Gara from the BIOMERIT Research Centre at UCC. Their research

focuses on contributing to further understanding of the SAR of *P. aeruginosa* QS molecules and the development of quorum quenching antivirulence treatments.

In 2011, they demonstrated that PQS and HHQ modulate interspecies and interkingdom behaviour in a variety bacterial and yeast strains.^[28] McGlacken and co-workers also published the synthesis of C-3 halogenated and other analogues of HHQ, and reported the first crystal structure of PQS.^[36] An investigation carried out in 2012 focused on the implications of substitution at the C-3 position of AHQs on biofilm formation in bacterial and yeast species that coexist with *P. aeruginosa*.^[37] HHQ was shown to inhibit biofilm formation in species that inhabit the same environment as *P. aeruginosa*, whereas PQS and 3-halo analogues did not (**Figure 4**).

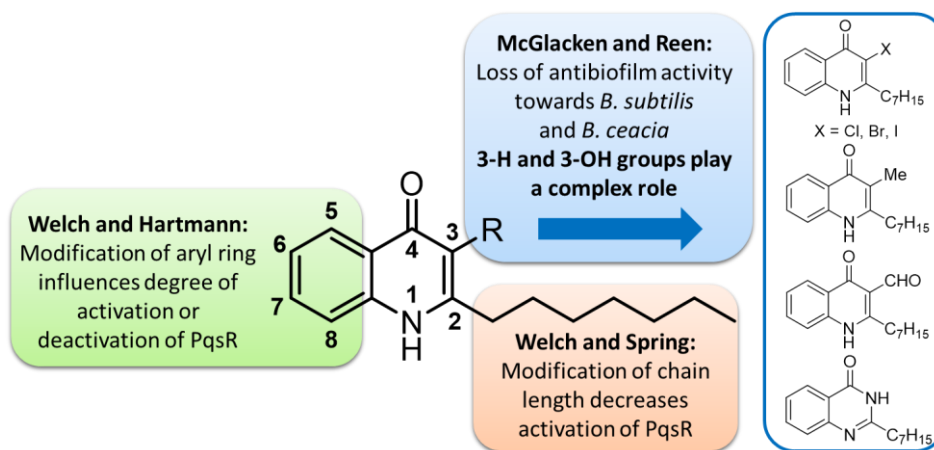
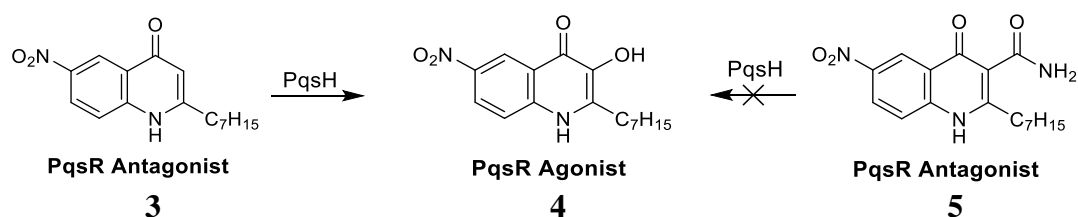


Figure 4 Structure-activity relationship analysis of the HHQ/PQS framework.

The influence of PQS and HHQ on the pathogenic capabilities of *P. aeruginosa* is complex,^[38] but is known to be dependent on the PqsABCDE biosynthetic operon which is positively regulated by the transcriptional regulator PqsR.^[39-40] As already mentioned, PQS and HHQ are PqsR agonists, and thus enhance the expression of this operon and the production of virulence factors. Therefore PqsR is a key target in the search for a *P. aeruginosa* QS inhibitor. Hartmann and co-workers showed that analogues of HHQ which possess strong electron-withdrawing groups at the C-6 position were antagonistic towards PqsR in *E. coli* reporter gene assays.^[41-42] With reference to structural data related to the binding pocket of PqsR,^[43] it was suggested that interaction of the strong electron-withdrawing group at the C-6 position with an isoleucine residue (Ile-149) decreases activation of the receptor. However, when tested *in vivo* on *P. aeruginosa*, the lead compound 6-NO₂ HHQ (**3**) seemed to display agonistic behaviour, reminiscent of PQS (**Scheme 1**).



Scheme 1 Hartmann's antagonists **3** and **5** and their interaction with PqsH.

Further investigation led to the discovery that the supposed antagonist was being hydroxylated by PqsH in *P. aeruginosa* into the corresponding PQS-like analogue (**4**), which was a strong PqsR agonist. In order to suppress this functional inversion, the authors 'blocked' the C-3 position, thus preventing hydroxylation by PqsH. Of the derivatives tested, the C-3 carboxamide (**5**) proved to be a highly active antagonist, and was even shown to reduce mortality caused by *P. aeruginosa* in an animal model.^[41]

1.5. Aims of this Chapter

Given the continuing development of antibiotic resistance, there is an urgent need for innovative strategies to tackle infection. This is particularly prevalent in species such as *P. aeruginosa*, and co-habiting pathogens such as *Bacillus* species, *Candida albicans* and *Aspergillus fumigatus*. The established roles of HHQ and PQS as key virulence factor determinants provides the opportunity to interrupt the *P. aeruginosa* QS network by designing structurally modified analogues. In addition, by taking advantage of the cross-species and cross-kingdom influences of HHQ and PQS, treatments for tackling infections caused by mixed-microbial communities can be investigated. This non-biocidal approach should dramatically reduce the evolutionary pressure on microbes to develop resistance.

This thesis chapter outlines the synthesis of functionalised analogues of HHQ, with alterations to the aryl ring, the alkyl chain, and the C-3 position. The compounds described herein were synthesised as part of a larger substrate scope of AHQ derivatives. McGlacken group member Dr Rafael Cano also worked on this project and synthesised a selection of substrates. Any compounds made by Dr Cano are labelled **RC**, and are only included to provide context when summarising the results of the SAR analysis. All of the AHQ analogues prepared during this project were sent to Dr Reen at the BIOMERIT Research Centre at UCC for inclusion in various biological studies, the results of which are summarised at the end of the Results & Discussion section. The aim of these SAR studies was to further delineate the interspecies and interkingdom influence of these molecules, and to further define the role of the C-3 position in the development of PqsR antagonists.

Chapter 1

Synthesis of Biologically Active HHQ Analogues

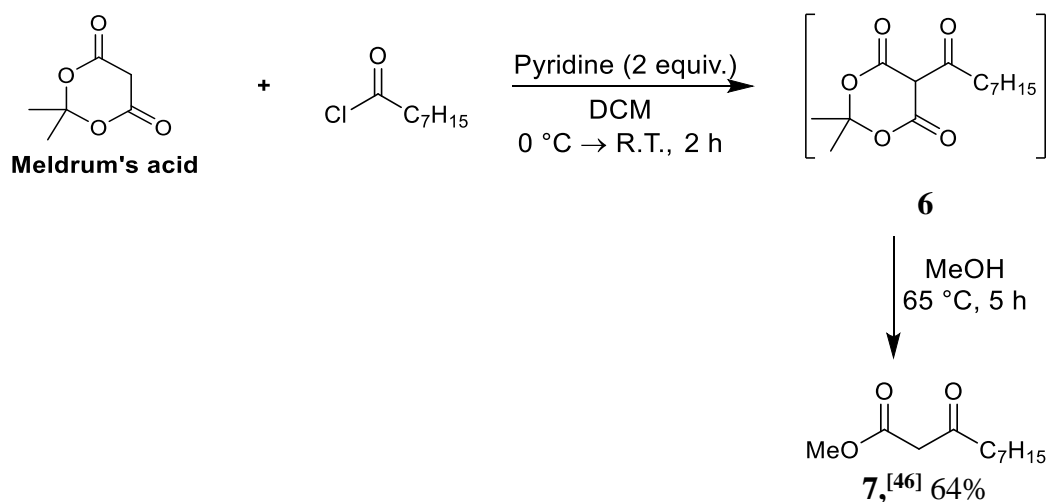
Results & Discussion

1.6. Objectives

The aim of this project was to synthesise a variety of analogues of HHQ, substituted at the C-5, C-6, C-7 and C-8 positions of the quinolone ring. In addition, C-3 substituted derivatives of HHQ were also prepared to see if these would display activity similar to either PQS or HHQ in species that coexist with *P. aeruginosa*. Functionalising the C-3 position of the quinolone also prevents hydroxylation of this position by PqsH to PQS-type compounds in *P. aeruginosa*. All of the compounds were sent to Dr Reen to be included in biological studies to learn more about the SAR of AHQs within the QS system of *P. aeruginosa*, and to determine their influence on pathogenic species of bacteria, fungi and yeast. As stated in the introduction, several compounds were synthesised by Dr Cano, and these are labelled **RC**. Experimental data for those compounds are not included in this thesis.

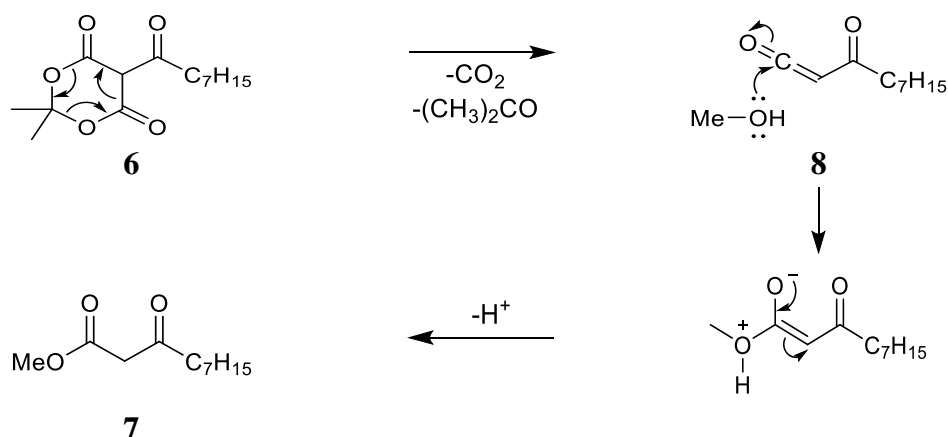
1.7. β -Ketoester Synthesis

The synthesis of quinolones like HHQ began with the preparation of β -ketoesters which determine the length of the alkyl chain at the C-2 position of the quinolone product. For example, a β -ketoester bearing a heptyl chain (**7**) is required for the synthesis of HHQ. The β -ketoesters used in this project were synthesised using methodology developed by Oikawa *et al.*^[44] Deprotonation of the highly acidic proton ($pK_a = 4.97$)^[45] of Meldrum's acid by pyridine and subsequent reaction with octanoyl chloride led to formation of acylated Meldrum's acid **6** (**Scheme 2**). Thermal decomposition of this intermediate, releasing carbon dioxide and acetone, resulted in the formation of β -ketoester **7**.



Scheme 2 Synthesis of β -ketoester **7** from Meldrum's acid.

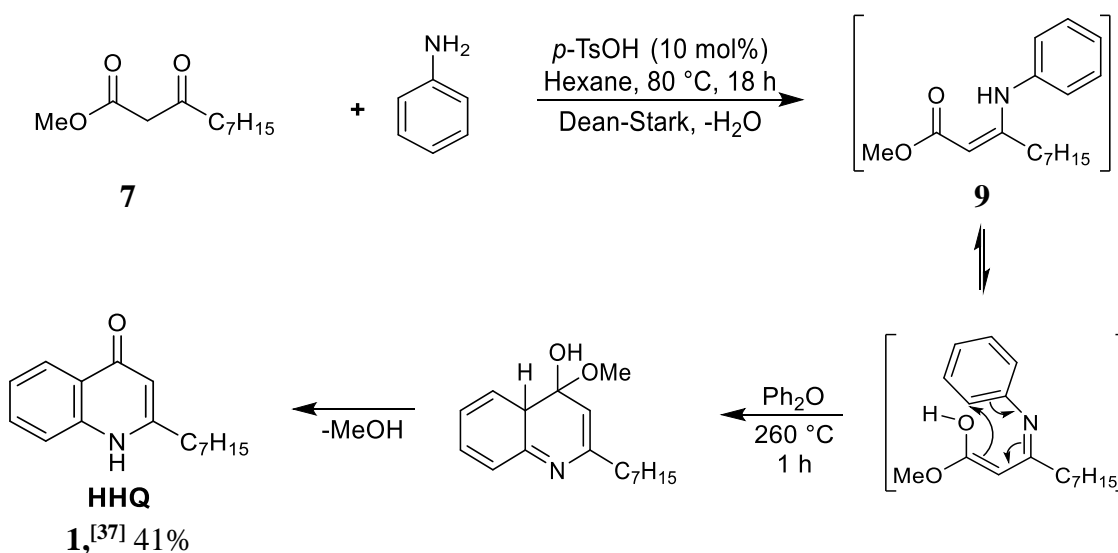
The amenability of acyl Meldrum's acid adducts such as **6** to react with various nucleophiles allows quick access to a variety of functionalised compounds.^[47] The mechanism for the fragmentation process was studied in detail by Xu *et al.* in 2004.^[48] Based on rate law calculations and reaction monitoring by IR spectroscopy, the authors concluded that heat initiates the decomposition of acyl Meldrum's acid adducts like **6** into an α -oxoketene species **8**, which then undergoes methanolysis to yield the β -ketoester product **7** (**Scheme 3**).



Scheme 3 Mechanism for decomposition of acyl Meldrum's acid **6** to form β -ketoester product **7**.

1.8. Synthesis of HHQ

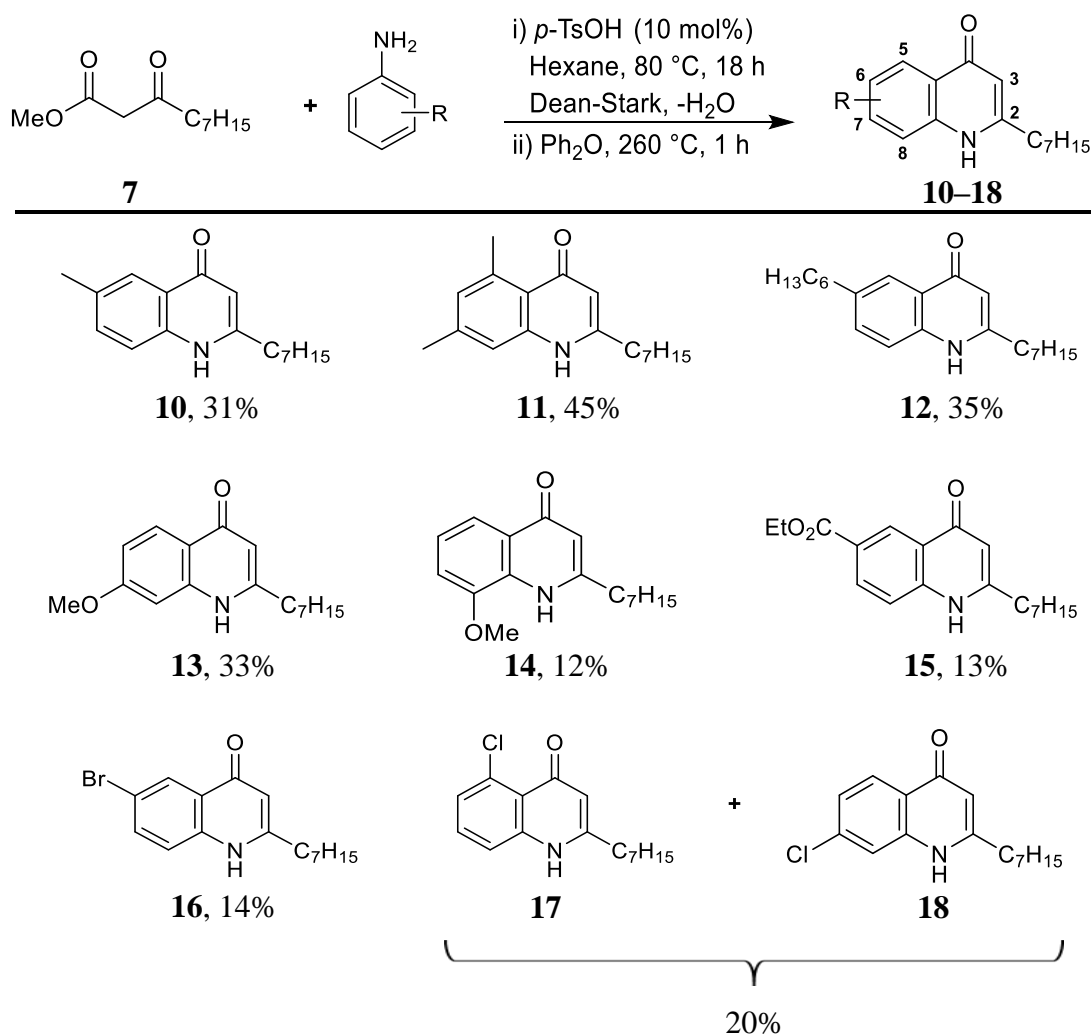
The next step in the synthesis of HHQ involved reaction of the β -ketoester **7** with aniline in the presence of a catalytic amount of an organic acid, forming the enamine intermediate **9** in near quantitative yield (**Scheme 4**). The enamine then underwent a Conrad-Limpach cyclisation in refluxing diphenyl ether to give the HHQ product **1**.^[36] A very high temperature ($>250^\circ\text{C}$) was required for the Conrad-Limpach cyclisation step. Once cyclisation occurred, methanol was expelled and aromaticity restored to form the quinolone framework. Due to the harsh conditions required, yields for this step were low to moderate.



Scheme 4 Synthesis of HHQ **1**.

1.8.1. Synthesis of Aryl-Substituted HHQ Analogues

In order to carry out further SAR studies on the quinolone framework, a range of novel aryl-substituted analogues was prepared. Aryl-substituted HHQ derivatives were prepared by reacting β -ketoester **7** with a variety of substituted anilines under the same conditions as for the synthesis of HHQ **1** (Scheme 5).



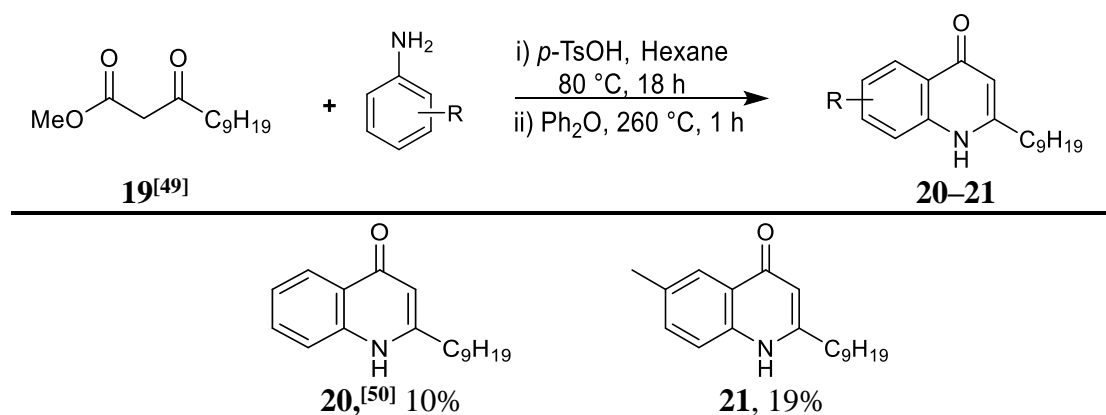
Scheme 5 Synthesis of aryl-substituted HHQ analogues.

As previously mentioned, owing to the harsh reaction conditions, the products were obtained in low to moderate yields. Overall, anilines bearing electron-donating substituents gave rise to higher yields of the quinolone products (**10–13**) compared to those with electron-withdrawing groups (**15–18**). Quinolone product **14** was an exception to this trend, having a very low yield of 12%. This may be due to steric interference of the *ortho*-methoxy group of the enamine intermediate during the cyclisation step. In the case of *meta*-substituted anilines, two different isomers of the

quinolone product are possible due to free rotation about the Ar-N bond in the enamine intermediate (like **9** in **Scheme 4**), resulting in a mixture of C-5 and C-7 substituted products. Interestingly, in the case of *meta*-anisidine, only the C-7 isomer **13** of the product was isolated, possibly due to unfavourable steric interactions between the methoxy and carbonyl groups of the C-5 isomer. In the case of *meta*-chloroaniline, a mixture of both products was obtained, in a ratio of 1:0.7 in favour of the C-7 substituted product **18**. Attempts to separate these two isomers by column chromatography or crystallisation methods were unsuccessful.

1.8.2. Synthesis of C-2 Nonyl Chain Analogues

In addition to these aryl-substituted HHQ analogues, two compounds were synthesised with a nonyl chain at the C-2 position in order to expand the scope of the SAR investigation. Once again, these compounds were prepared from the appropriate β -ketoester and substituted aniline. The β -ketoester bearing a nonyl chain was prepared as described in **Scheme 2** from decanoyl chloride.



Scheme 6 Synthesis of aryl-substituted quinolones bearing a nonyl chain at the C-2 position.

Compounds **10–21** (**Scheme 5** and **Scheme 6**) were synthesised as part of a larger substrate scope contributing to the McGlacken group and BIOMERIT collaborative projects. Also working on the synthesis of AHQs was Dr Rafael Cano. The structures of Dr Cano's compounds are shown in **Figure 5**, and were prepared using the same methods outlined above. All of the HHQ analogues prepared during this project were sent to Dr Reen in the BIOMERIT Research Centre at UCC for inclusion in various biological studies, the results of which are summarised at the end of this **Results & Discussion** section.

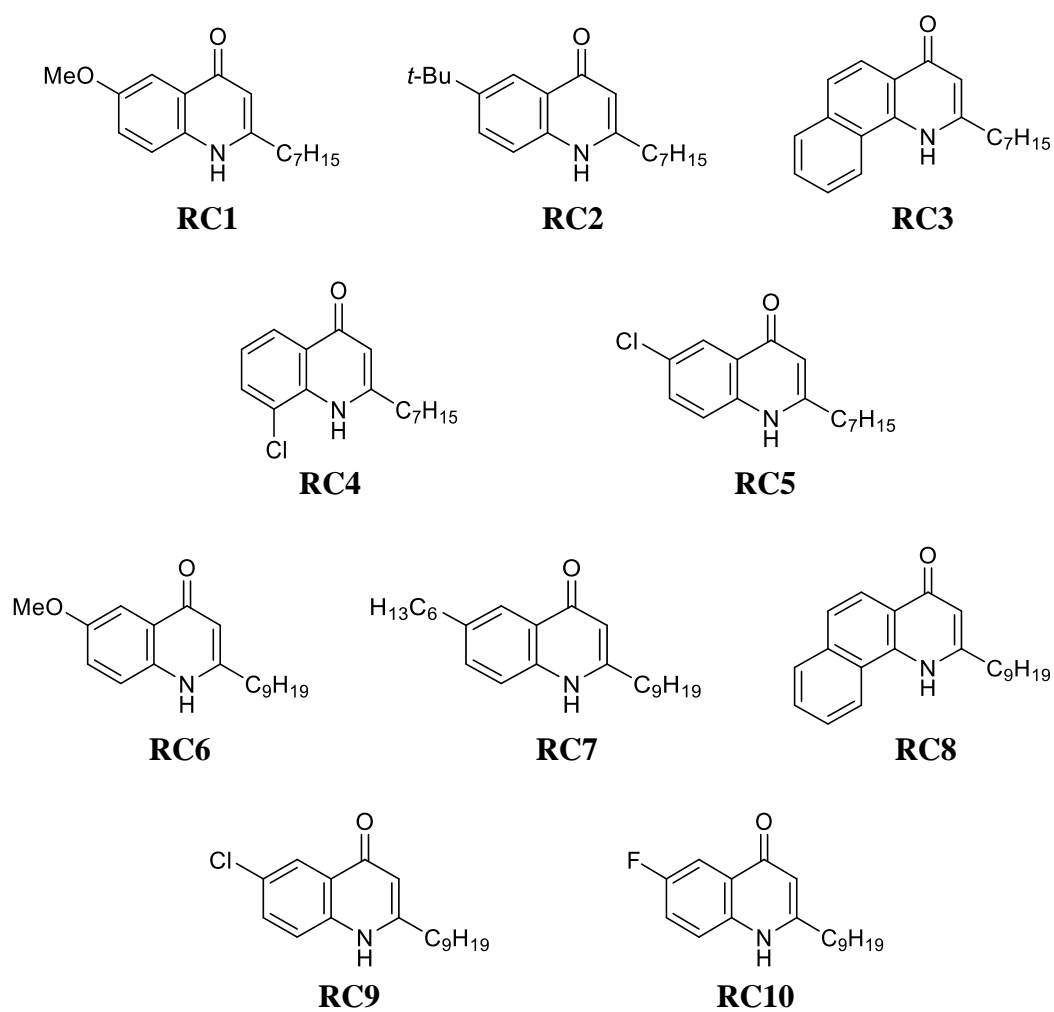
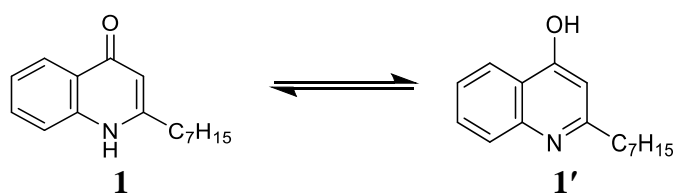


Figure 5 Compounds synthesised by Dr Rafael Cano (McGlacken group) as part of this project.

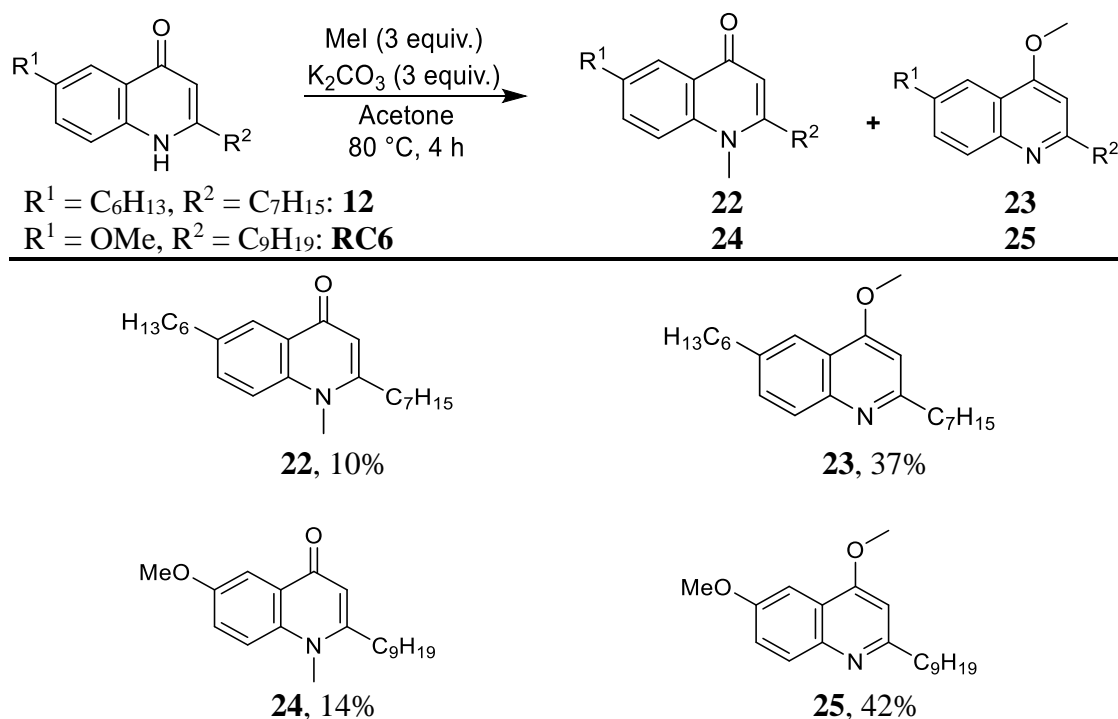
1.8.3. Methylation of HHQ Analogues

4-Quinolones like HHQ exist as two tautomeric forms – a 4-quinolone (**1**) and a 4-hydroxyquinoline (**1'**) (**Scheme 7**). Equilibrium tends towards the quinolone form under physiological conditions.^[51] Since proton transfer from the nitrogen atom to the oxygen atom drives tautomerisation, substitution of this proton forces the molecule to stay ‘locked’ in one of the isomeric forms. Hence, further insight can be gained into the biological activity of the quinolone or the quinoline framework specifically.



Scheme 7 Quinolone/quinoline tautomerisation.

Two of the aryl-substituted quinolones were chosen to undergo methylation based on results obtained from a study on the influence of the HHQ analogues on swarming motility in *Bacillus atrophaeus*, which will be discussed later. To prepare the *N*- and *O*-methylated isomers, compound **12** was reacted with methyl iodide in acetone and K_2CO_3 . The resulting isomeric mixture was purified by column chromatography to afford the desired products **22** (quinolone) and **23** (quinoline) in 10% and 37% yield, respectively (**Scheme 8**). A C-2 nonyl analogue previously synthesised by Dr Cano (**RC6**) was subjected to the same methylation conditions to yield compounds **24** and **25**, in 14% and 42% yield, respectively.

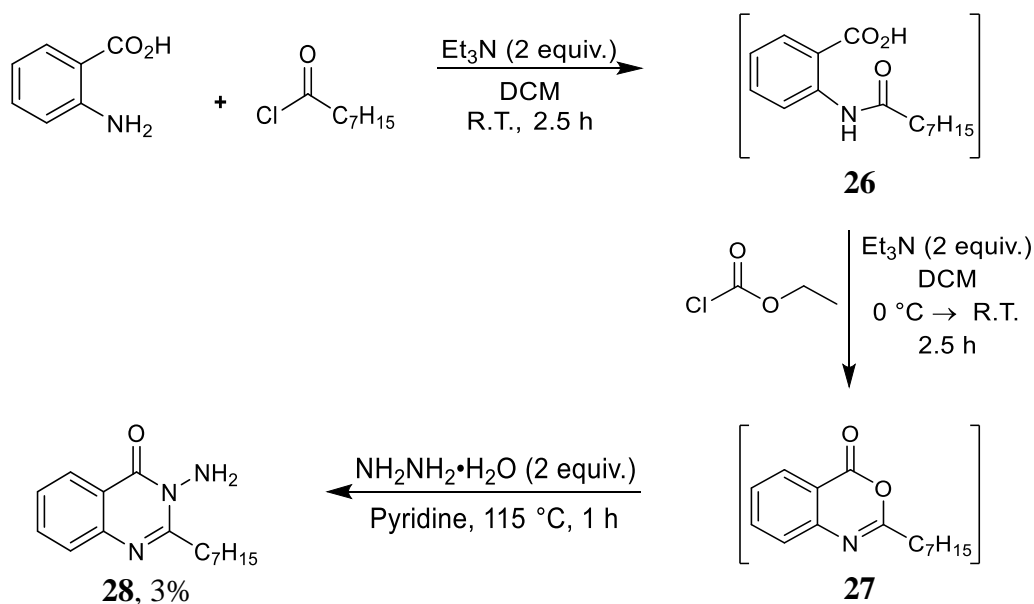


Scheme 8 Methylation of quinolones.

When the methylated compounds **22–25** were subjected to the same biological tests as N-H quinolones **12** and **RC6**, there was a detectable difference in activity. This will be discussed further in the **Biological Results Section 1.13**.

1.9. Quinazolinone Synthesis

As discussed in the introduction, HHQ and PQS differ by the presence of a hydrogen atom (HHQ) or hydroxyl group (PQS) at the C-3 position. Modification of this site is known to play an important role in dictating the biological activity of the molecule.^[37] The 3-aminoquinazolinone compound **28** was synthesised for inclusion in biological studies to determine whether it displayed activity similar to PQS (**Scheme 9**).

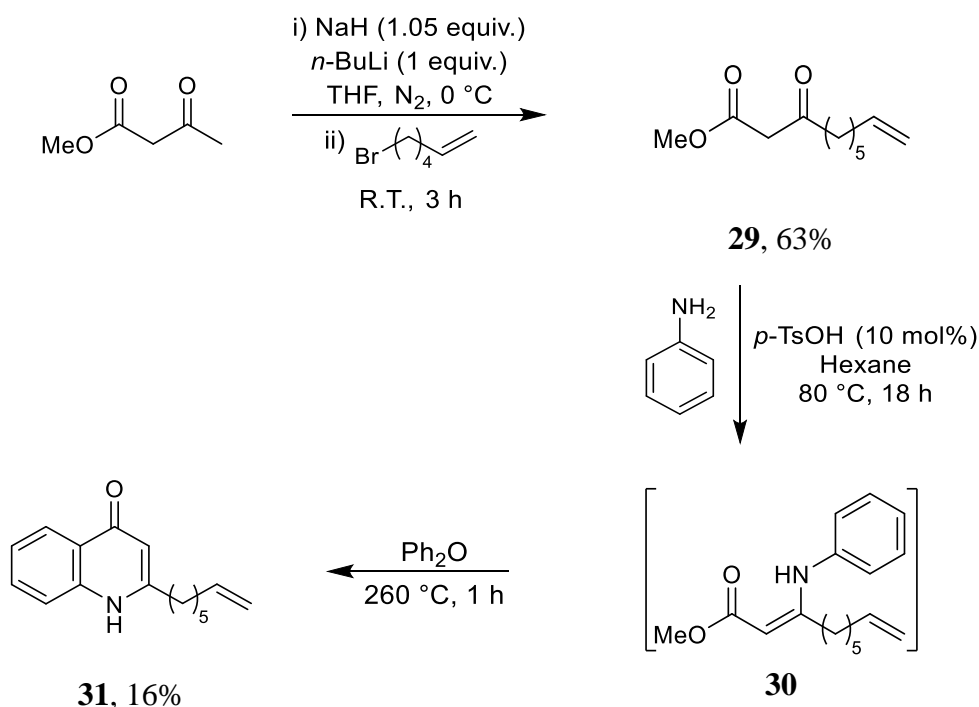


Scheme 9 Synthesis of quinazolinone compound **28**.

The synthesis of the quinazolinone compound began with acylation of commercially available anthranillic acid with octanoyl chloride to give the amide intermediate **26**. Cyclisation of this compound to form intermediate compound **27** and subsequent reaction with hydrazine hydrate led to formation of the desired product **28**. Problems with the purification process resulted in a very low isolated yield of 3% pure product over three steps, although there was still enough material to obtain full characterisation and submit for biological analysis.

1.10. Synthesis of HHQ Analogue with a C-2 Terminal Alkene

As discussed in the introduction, the alkyl chain at the C-2 position of HHQ and PQS seems to play an important role in the biological activity of the molecule. Having already extended the chain length by two carbon atoms (compounds **20** and **21**), the effect of a terminal alkene was also of interest, and thus HHQ analogue **31** was synthesised (**Scheme 10**).



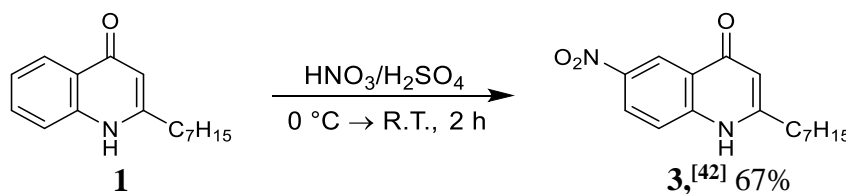
Scheme 10 Synthesis of HHQ analogue **31** with a terminal alkene.

In order to incorporate the terminal alkene into the alkyl chain, a novel β -ketoester was prepared. This was achieved by deprotonation of methyl acetoacetate at the less-acidic C-4 position and subsequent reaction with 6-bromohex-1-ene to yield β -ketoester **29** in 63% isolated yield. This β -ketoester was then subjected to the same reaction conditions used for the synthesis of HHQ to form the desired product **31** in 16% isolated yield. This novel HHQ analogue was also sent to Dr Reen for biological analysis, and a publication describing those results is in preparation.

1.11. Synthesis of Potential PqsR Antagonists

Hartmann and co-workers developed potent HHQ-derived antagonists of the PqsR regulator of *P. aeruginosa*.^[41-42, 52] As outlined in the introduction, antagonistic activity is dependent on two key features of the molecule. Firstly, the presence of the NO₂ group at C-6 greatly improves the antagonistic effects towards PqsR. Secondly, insertion of a C-3 blocking group prevents hydroxylation by PqsH in *P. aeruginosa*, and thus the *in vivo* formation of agonistic molecules (**Scheme 1**). Thus, understanding the mode of action of the blocking group is of interest. For example, does the installed C-3 group merely block the hydroxylation site? Or does it infer additional biological activity? The addition of the amide group in compound **5** (**Scheme 1**) likely contributes additional properties to the molecule, such as H-donor/acceptor capabilities. Therefore, it is unlikely that the C-3 group only acts to prevent hydroxylation.

To gain further understanding of the role of the C-3 group in Hartmann's PqsR antagonist, the McGlacken group prepared a number of analogues of 6-NO₂ HHQ (**3**) with different groups at C-3. This project began by developing a new route to **3**. Hartmann found that when using the same conditions as for the synthesis of HHQ (**Scheme 4**) to access **3**, the Conrad-Limpach cyclisation step was very low yielding (1%).^[42] This result is probably due to the lower nucleophilicity of the nitroaniline group in the Conrad-Limpach cyclisation step. Instead, HHQ **1** itself was selectively nitrated in one step via electrophilic aromatic substitution in 67% yield (**Scheme 11**).

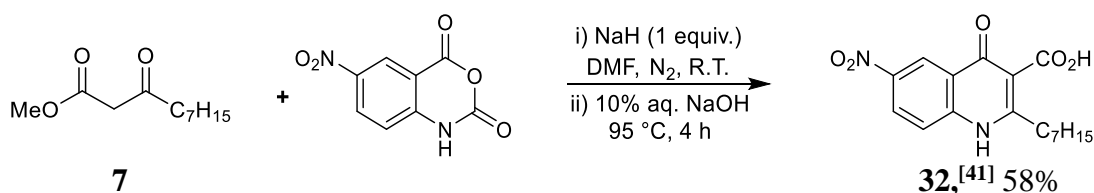


Scheme 11 Nitration of HHQ.

Importantly, this improvement allowed access to greater quantities of **3**. Next, a number of blocking groups were then installed at the C-3 position, namely -F, -Cl, -Br, -I, -D and -Me. These compounds were prepared by McGlacken group member Dr Rafael Cano.^[53]

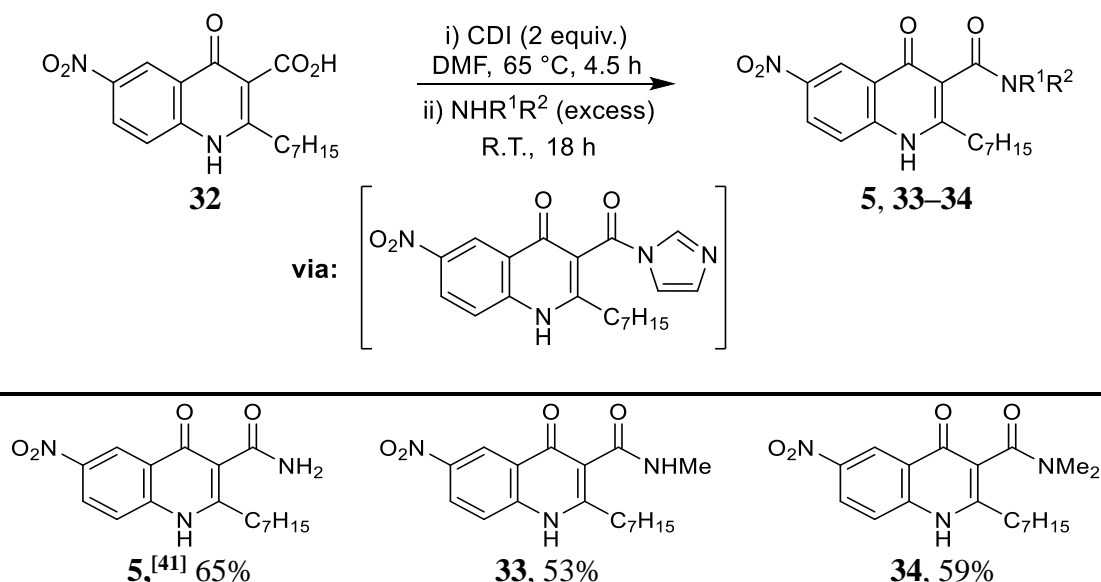
1.11.1. Synthesis of Substituted Analogues of Hartmann's Antagonist

In addition to testing analogues with non-amide functional groups at the C-3 position, understanding the H-donor/acceptor properties of the amide group in Hartmann's antagonist **5** was also of interest. Therefore, it was necessary to prepare compound **5** to act as a comparator in the biological tests. In addition, the corresponding secondary and tertiary amides were also synthesised. All three amide compounds were prepared by initially following Hartmann's synthesis of the carboxylic acid precursor (**Scheme 12**).^[41]



Scheme 12 Synthesis of carboxylic acid compound **32**.

Compound **32** was then reacted with the coupling reagent 1,1'-carbonyldiimidazole (CDI), and treatment of the resulting imidazolyl intermediate with an excess of the appropriately substituted amine afforded the corresponding primary (**5**), secondary (**33**) or tertiary (**34**) amide.



Scheme 13 Synthesis of Hartmann's amide (**5**) and secondary (**33**) and tertiary (**34**) derivatives.

1.12. Conclusions

Analogues of HHQ were synthesised with substitutions at the C-5 to C-8 positions (**10–21**). Two of the quinolone compounds were methylated to give the *N*-Me quinolone and *O*-Me quinoline isomeric products (**Scheme 8**). A C-3 substituted quinazolinone analogue (**28**) was prepared, and a HHQ analogue with a terminal alkene on the heptyl chain at C-2 was also synthesised (**31**). An improved route to access 6-NO₂ HHQ **3** via regioselective nitration of HHQ **1** was developed, and the secondary (**33**) and tertiary (**34**) methylated analogues of Hartmann's antagonist **5** were prepared.

All of the HHQ analogues prepared were sent to Dr Reen at the BIOMERIT Research Centre at UCC to be tested in various biological studies. The experimental details of these tests are outside the scope of this thesis. However, due to the fact that the results of the biological analysis often guide the design of structural analogues of lead compounds, the results of the studies are summarised in the next section. Full details of the biological experiments can be found in the various publications, and are included in **Appendix I**.

1.13. Biological Results

A Structure Activity-Relationship Study of Bacterial Signal Molecule HHQ Reveals Swarming Motility Inhibition in *Bacillus atrophaeus* (*Organic & Biomolecular Chemistry*, **2015**, *13*, 5537–5541)

Bacillus atrophaeus is a Gram-positive species of bacteria that co-inhabits with *P. aeruginosa* in soil. *P. aeruginosa* QS molecules have been shown to influence behaviour in *B. atrophaeus*.^[28, 54] *B. atrophaeus* also exhibits strong swarming and biofilm phenotypes that are characteristic of the multicellular behaviour underpinning virulence in many pathogens.^[9] Swarming motility is considered a key virulence phenotype in many organisms controlled by QS.^[55]

The aim of the SAR in this study was to learn more about the influence of AHQs on Gram-positive bacteria and provide a platform for therapeutic developments. To achieve this, a diverse range of novel aryl-substituted HHQ analogues were tested on *B. atrophaeus*. A previous report from Reen *et al.* showed that swarming motility of *B. atrophaeus* was abolished in the presence of PQS, while use of HHQ showed little reduction.^[28] Interestingly, some of the aryl-substituted HHQ analogues showed significant alteration in activity relative to the parent HHQ, with some compounds exhibiting inhibition comparable to PQS. In particular, **RC5** and **RC6** completely inhibited swarming, despite differing in the alkyl chain length at C-2. It appears that for compounds with a C-2 heptyl chain, an electron-withdrawing substituent at C-6 is required for anti-swarming activity, while for compounds with a C-2 nonyl chain, an electron-donating substituent at C-6 is required.

As mentioned, 4-quinolones such as HHQ exist as two interconverting tautomeric forms: 4-quinolone and 4-hydroxyquinoline. It would be interesting to determine if either structure maintained anti-swarming activity if ‘locked’ in these tautomeric forms by methylation at the oxygen or nitrogen atom. Indeed, when anti-swarming molecule **RC6** was methylated, both the quinolone form **24** and the quinoline form **25** lost this activity (**Figure 6**). Compound **12** was also methylated and both isomers tested for their impact on swarming motility in *B. atrophaeus*. Again, both methylated derivatives **22** and **23** exhibited reduced activity relative to the parent molecule. In fact, the quinoline analogue **23** appeared to promote swarming.

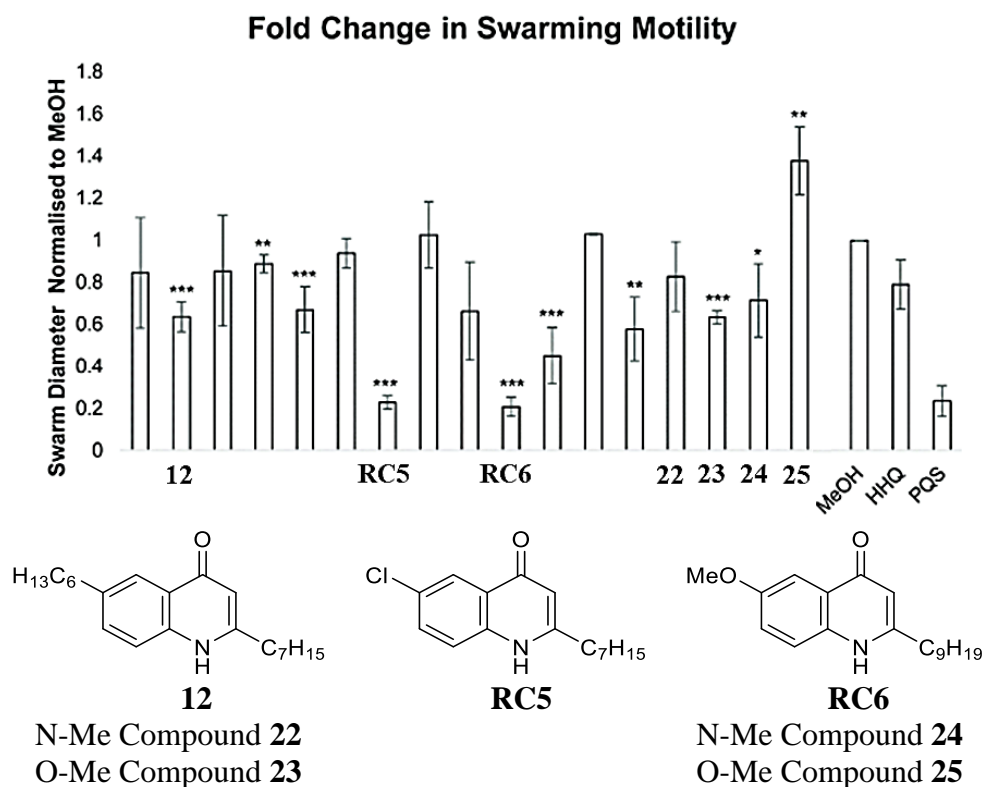


Figure 6 Impact of HHQ analogues on swarming motility of *B. atrophaeus*. The smaller the swarming diameter, the greater the anti-swarming activity of the compound.^[56]

Modification of the quinolone at C-6 resulted in compounds possessing anti-swarming activity similar to that of PQS. These results suggest that the C-3 hydroxyl group of PQS is not essential for anti-swarming activity of AHQs towards *B. atrophaeus*.

Exploiting Interkingdom Interactions for Development of Small Molecule Inhibitors of *Candida albicans* Biofilm Formation (*Antimicrobial Agents and Chemotherapy*, **2016**, 60, 5894–5905)

Candida albicans causes a variety of complications ranging from mucosal disease to deep-seated mycoses, particularly in immunocompromised individuals.^[57-58] Along with other bacterial, fungal and yeast pathogens, *C. albicans* is known to form biofilms on medical devices, leading to recurring infections and in some cases death.^[59-60] Once established in the biofilm phase, *C. albicans* presents a significant clinical problem, as biofilms themselves are considered a breeding ground for the emergence of antibiotic-resistant strains.^[61]

C. albicans is known to coexist with *P. aeruginosa* in the cystic fibrosis lung, and interkingdom communication between the two organisms has previously been reported.^[62-63] Previously, Reen *et al.* have shown that HHQ, but not PQS, suppresses biofilm formation in *C. albicans* (**Figure 7**).^[28] In order to visualize the biofilm structures, attached cells were treated with specific intracellular stains to assess impact on key cellular components. These included cellulose and chitin with **Calcofluor**; lectin (carbohydrate) structures with **Concanavalin A**; and live cellular vacuolar stain **FUN-1** which functions as a live/dead stain. As both PQS and HHQ promote virulence and pathogenicity in *P. aeruginosa*,^[24, 64] these compounds fall short of being a viable antifungal treatment. However, chemical modification of these molecules provides an opportunity to develop compounds with greater specificity of function.

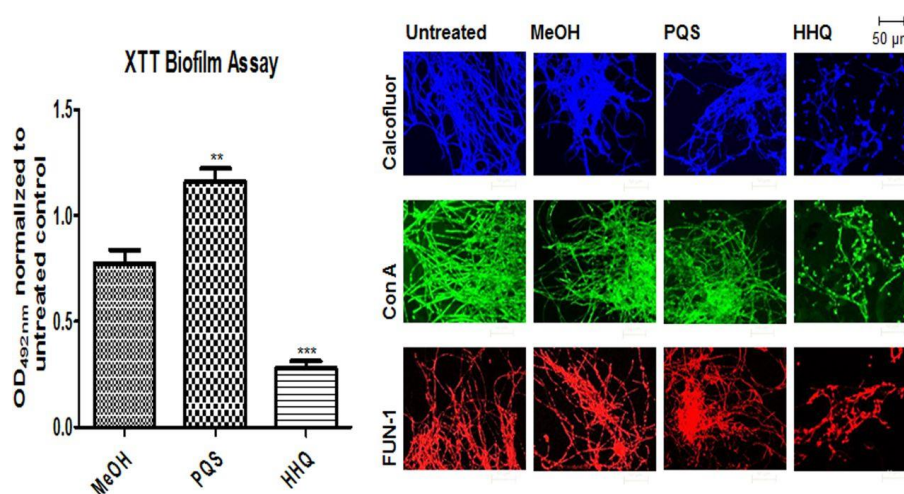


Figure 7 *C. albicans* biofilms grown in the presence of PQS and HHQ.^[65]

Analysis of the suite of analogues based on the core HHQ quinolone framework led to the identification of compounds that retain anti-biofilm activity toward *C. albicans*. Several analogues displayed anti-biofilm activity similar to HHQ, including the C-3 substituted quinazolinone analogue **28**. Overall, electron-withdrawing substituents (e.g. compounds **RC4**, **RC5**) promoted anti-biofilm activity in a similar manner to the HHQ parent, while electron-donating substituents (e.g. compounds **12**, **13**, **RC3**) resulted in some loss of activity. Extension of C-2 chain (**20**) did not seem to alter activity. Microscopic staining revealed that, like HHQ, the active compounds caused structural changes in the biofilm, causing atypical morphologies.

Importantly, the new compounds exhibited significantly reduced cytotoxicity toward IB3-1 airway epithelial cells compared with the parent HHQ molecule. Evaluating the cytotoxicity of synthetic compounds is crucial in the context of developing targeted therapeutics that are benign to human cellular physiology and ideal for use in a clinical environment. Furthermore, unlike HHQ, the lead compounds were inactive toward the *P. aeruginosa* PqsR receptor system, a critical requirement for their potential future development as anti-biofilm therapeutics.

Harnessing Bacterial Signals for Suppression of Biofilm Formation in the Nosocomial Fungal Pathogen *Aspergillus fumigatus* (*Frontiers in Microbiology*, 2016, 7, 2074)

Aspergillus fumigatus is a pathogenic fungus associated with hospital-acquired infections. *A. fumigatus* infections contribute to morbidity and mortality in people with respiratory diseases such as cystic fibrosis, as well as infecting open skin wounds in burn patients and areas surrounding medical implants.^[66-67] However, as with its bacterial counterparts, the defensive biofilm of *A. fumigatus* has led to conventional antifungal therapies rapidly becoming redundant.^[68] Additionally, the co-existence and mutual interaction of bacteria and fungi at the site of infection contributes to the pathogenesis of disease. In the case of CF, *A. fumigatus* has been isolated in up to 60% of patients with *P. aeruginosa* infection, suggesting a close relationship between colonisation by *P. aeruginosa* and chronic infection by *A. fumigatus*.^[69-70]

In this study, the anti-biofilm activity of *P. aeruginosa* AHQs against *A. fumigatus* was investigated. Biofilm biomass and structure was significantly altered in the presence of both HHQ and PQS. Confocal microscopic analysis revealed that cells treated with either HHQ or PQS appeared locked in a spore form, with minimal evidence for formation of hyphal structures, characteristic of *A. fumigatus* biofilms. Next, the suite of analogues was tested and lead compounds were identified that retained activity against *A. fumigatus* (**11**, **12**, **13**, **20**, **28**). Of these, compound **12** (*n*-hexyl group at C-6) and compound **13** (methoxy group at C-7) gave the greatest reduction in biofilm formation. Compound **20**, in which the alkyl chain length was extended relative to the parent molecule HHQ, retained its anti-biofilm activity. Quinazolinone compound **28** also displayed good anti-biofilm activity.

Importantly, anti-biofilm activity was retained against clinical isolates from paediatric samples. It has been shown that the genomes of clinical isolates can vary markedly from typed environmental strains, with niche-specific selective pressures manifesting with considerable specificity, even within species.^[71] Both HHQ and PQS were capable of suppressing biofilm formation in each of the clinical isolates. Lead compounds **11** and **28** were also found to be effective against biofilm formation in clinical strains, underpinning their suitability for further therapeutic development (**Figure 8**). As expected, anti-biofilm compounds disrupted the formation of hyphal

structures, and appeared to lock the fungal cells in the spore state. Notably, however, the suppression of biofilm formation was not to the same extent as that seen against the lab strain Af293, suggesting some degree of tolerance or adaptation in the clinical isolates.

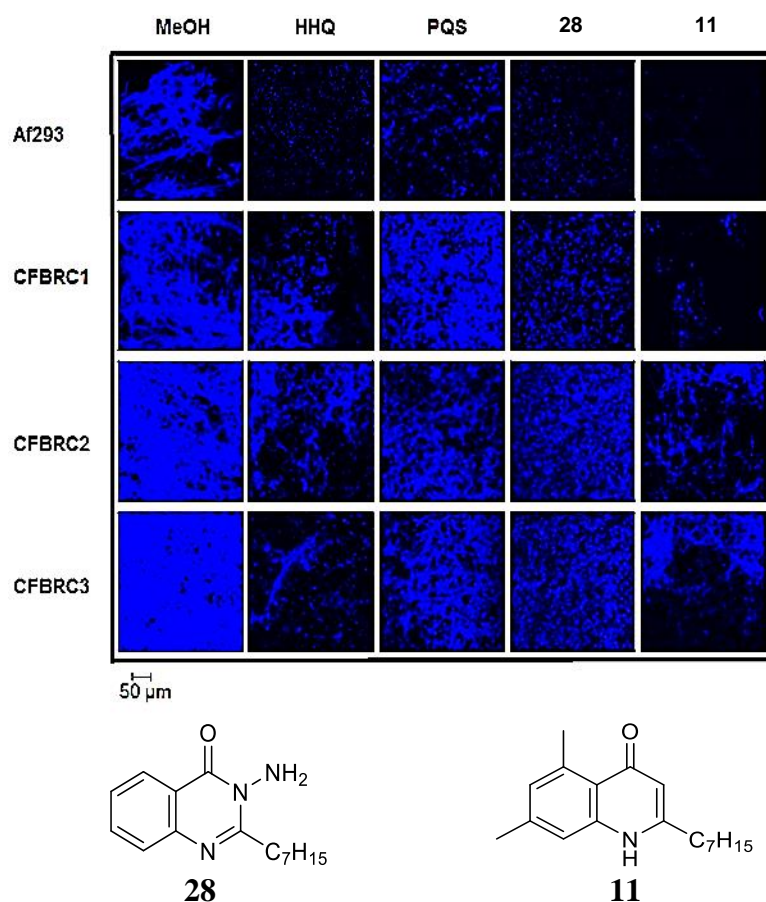


Figure 8 Confocal laser scanning microscopy analysis of biofilm formation in model strain (Af293) and clinical isolates (CFBRC1, CFBRC2, CFBRC3) in the presence of HHQ, PQS and lead compounds **28** and **11**.^[72]

This study identified compounds with anti-biofilm activity comparable to the parent HHQ molecule, providing important insights into the SAR underpinning the suppression of fungal biofilms.

The Requirements at the C-3 Position of Alkylquinolones for Signalling in *Pseudomonas aeruginosa* (*Organic & Biomolecular Chemistry*, **2017**, *15*, 306–310)

As described in the introduction, Hartmann and co-workers reported a potent PqsR antagonist could be accessed by placing a nitro group at the C-6 position of HHQ (**Scheme 1**).^[41–42, 52] In order to suppress functional inversion by in vivo hydroxylation of the C-3 position, the C-3 position was ‘blocked’ with a primary amide, leading to the development of a highly active antagonist **5**. Previous work from the McGlacken group and collaborators showed that altering the C-3 position of HHQ prevented restoration of phenazine production in *P. aeruginosa* mutants, and also resulted in loss of anti-biofilm activity displayed by HHQ towards *B. subtilis*.^[37] However, since then, the observations made by Hartmann compel further investigation of the role played by the C-3 position of AHQs.

As previously stated, the *P. aeruginosa* QS system is known to be dependent on the PqsABCDE biosynthetic operon, which is positively regulated by PqsR. As PqsR controls the expression of PqsA, the monitoring of PqsA promoter activity can be used to determine PqsR agonism and antagonism. Thus all of the C-3 substituted 6-NO₂ HHQ analogues were tested using promotor fusion analysis of the PqsR-regulated PqsABCDE operon. Two genotypes of *P. aeruginosa* were chosen to be tested with the prepared molecules: a wild-type *P. aeruginosa* (PAO1) which would appropriately reflect the natural biochemistry of the species, and an isogenic PqsA mutant (PAO1pqs[–]) in which the ability to produce HHQ and PQS has been abolished (**Figure 9**). Overall, while all of the compounds showed some decrease in PqsR activity, none proved to be as potent as Hartmann’s amide **5**, particularly when tested on the wild-type strain PAO1.

Substituted amide compounds **33** and **34** showed minimal inhibition and were less potent than compound **5** (**Figure 9**). Inhibitory effects decreased with increasing substitution of the amide, indicating that the amide group is not acting solely as a blocking group. Furthermore, this result suggests that the H-bond donor capability of the amide N-H is important. This is in agreement with an extensive study on AHQ receptor interactions by Williams and co-workers,^[43] which highlighted the requirement for an -NH₂ group at the C-3 position of HHQ derivatives for competitive antagonism of PqsR. They suggested that strengthened electrostatic interactions

between the -NH₂ group and carbonyl groups in the Leu207 backbone within the receptor pocket results in stronger binding than with native ligands such as PQS.

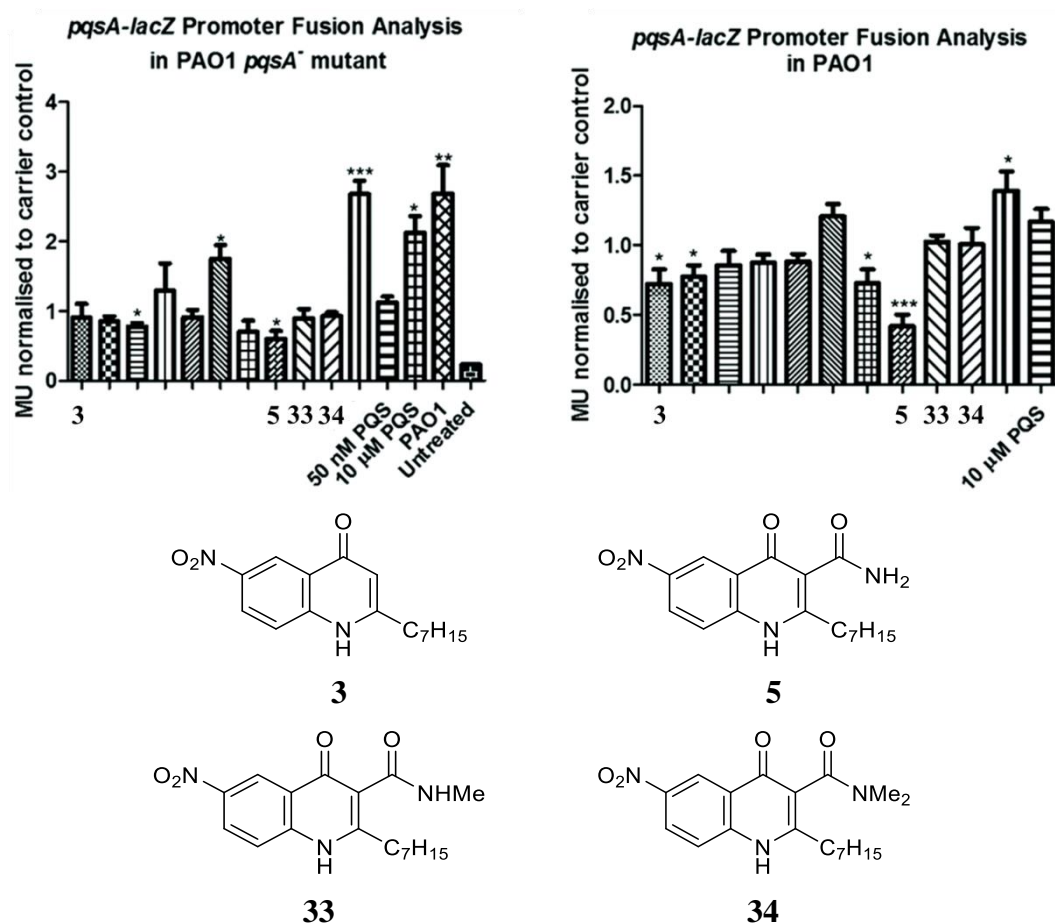


Figure 9 PqsR activation in the presence of 6-NO₂ HHQ analogues.^[53]

From this study, it is clear that the substituent at C-3 has a more complex role beyond acting as a blocking group to prevent hydroxylation by PqsH. Overall, it appears that antagonistic behaviour seems to be strongly dependent on the ability of the molecule to engage in hydrogen-bonding interactions at the C-3 position.

Chapter 1

Synthesis of Biologically Active HHQ Analogues

Experimental

1.14. General Considerations

Solvents and reagents were used as obtained from commercial sources, without purification. Unless otherwise indicated, starting materials were also obtained from commercial sources. Column chromatography was carried out using 60 Å (35-70 µm) silica. TLC was carried out on pre-coated silica gel plates (Merck 60 PF254). The developed plates were visualised under UV light.

Melting points were measured in a Thomas Hoover Capillary Melting Point apparatus. Infrared spectra were measured on a Perkin-Elmer FT-IR spectrometer. High resolution precise mass spectra (HRMS) were recorded on a Waters LCT Premier TOF LC-MS instrument in electrospray ionisation (ESI) mode using 50% acetonitrile-water containing 0.1% formic acid as eluent; samples were made up in acetonitrile at a concentration of *ca.* 1 mg/mL. Reported results are all within the range of \pm 5ppm of the calculated mass. For brominated compounds, Br⁸⁰ was used for the calculated and reported molecular ion mass.

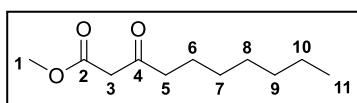
Nuclear Magnetic Resonance (NMR) samples were run in deuterated chloroform (CDCl₃) or deuterated dimethylsulfoxide (DMSO-d₆), as specified. ¹H-NMR (600 MHz), ¹H-NMR (500 MHz), ¹H-NMR (400 MHz), and ¹H-NMR (300 MHz) spectra were recorded on Bruker Avance 600, Bruker Avance 500, Bruker Avance 400 and Bruker Avance 300 NMR spectrometers, respectively, in proton coupled mode using tetramethylsilane (TMS) as the internal standard. ¹³C-NMR (150 MHz), ¹³C-NMR (125 MHz), ¹³C-NMR (100 MHz) and ¹³C-NMR (75 MHz) spectra were recorded on Bruker Avance 600, Bruker Avance 500, Bruker Avance 400 and Bruker Avance 300 NMR spectrometers, respectively, in proton decoupled mode at 20 °C using tetramethylsilane (TMS) as the internal standard. All spectra were run at University College Cork. Chemical shifts (δ) are expressed as parts per million (ppm), positive shift being downfield from TMS; coupling constants (*J*) are expressed in hertz (Hz). Splitting patterns in ¹H-NMR spectra are designated as: s (singlet), br s (broad singlet), d (doublet), dd (doublet of doublets), ddd (doublet of doublets of doublets), t (triplet), td (triplet of doublets), q (quartet), quin (quintet) and m (multiplet). Please note that the numbering system displayed on the structures is to assign the NMR data, and differs from the IUPAC system used for naming.

1.15. Synthesis of β -Ketoesters

Methyl 3-oxodecanoate^[46] (**7**)

2,2-Dimethyl-1,3-dioxane-4,6-dione (Meldrum's acid) (1 equiv.) was dissolved in dry DCM (1.5 mL/mmol). The solution was cooled to 0 °C under a nitrogen atmosphere. To the cooled solution were added pyridine (2 equiv.) and octanoyl chloride (1.1 equiv.), dropwise. The solution was stirred at 0 °C for 1 h and then at room temperature for 1 h. The mixture was washed with 5% HCl (3 \times 0.5 mL/mmol) and water (0.5 mL/mmol). The organic layer was dried with MgSO₄, filtered and concentrated *in vacuo* to yield acyl Meldrum's acid **6** as a brown oil, which was used in the next step without purification.

Acyl Meldrum's acid **6** was dissolved in MeOH (1.4 mL/mmol) and heated at reflux for 5 h with constant stirring. After cooling to room temperature, the reaction mixture was concentrated *in vacuo* to yield the crude product as an orange oil. Purification by fractional distillation afforded the β -keto ester **7** as a colourless oil (16.7 g, 64 % yield).

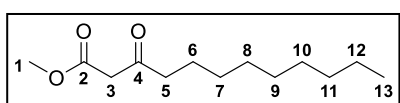


Colourless oil; yield: 16.7 g (64%); ¹H-NMR (300 MHz, CDCl₃, only signals of the predominant keto tautomer are given) δ : 0.88 (t, J = 6.7 Hz, 3H, CH₃-**11**), 1.19–1.40 (m, 8H, CH₂-**7**, CH₂-**8**, CH₂-**9**, CH₂-**10**), 1.52–1.68 (m, 2H, CH₂-**6**), 2.53 (t, J = 7.4 Hz, 2H, CH₂-**5**), 3.45 (s, 2H, CH₂-**3**), 3.73 (s, 3H, CH₃-**1**); ¹³C-NMR (75 MHz, CDCl₃, only signals of the predominant keto tautomer are given) δ : 13.8 (CH₃-**11**), 22.4 (CH₂-**10**), 23.3 (CH₂-**6**), 28.8 (CH₂-**8**), 28.9 (CH₂-**7**), 31.5 (CH₂-**9**), 42.8 (CH₂-**5**), 48.8 (CH₂-**3**), 52.0 (CH₃-**1**), 167.6 (qC-**2**), 202.7 (qC-**4**); HRMS (ESI-TOF) m/z : [M+H]⁺ calcd. for C₁₁H₂₁O₃: 201.1491; found: 201.1482.

Spectral data were consistent with those reported in the literature.

Methyl 3-oxododecanoate^[49] (**19**)

Synthesised according to the same procedure as for **7** using decanoyl chloride.



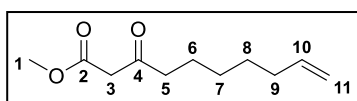
Colourless oil; yield: 8.08 g (59%); ¹H-NMR (300 MHz, CDCl₃, only signals of the predominant keto tautomer are given) δ : 0.88 (t, J = 6.7 Hz, 3H, CH₃-**13**), 1.15–1.41 (m, 12H, CH₂-**7**, CH₂-**8**, CH₂-**9**, CH₂-**10**, CH₂-**11**, CH₂-**12**), 1.49–1.71 (m, 2H, CH₂-**6**), 2.53 (t, J = 7.4

Hz, 2H, CH₂-5), 3.45 (s, 2H, CH₂-3), 3.73 (s, 3H, CH₃-1); ¹³C-NMR (100 MHz, CDCl₃, only signals of the predominant keto tautomer are given) δ: 14.1 (CH₃-13), 22.7 (CH₂-12), 23.5 (CH₂-6), 29.0 (CH₂-7), 29.3 (CH₂-10), 29.35 (CH₂-8), 29.39 (CH₂-9), 31.9 (CH₂-11), 43.1 (CH₂-5), 49.0 (CH₂-3), 52.4 (CH₃-1), 167.8 (qC-2), 203.0 (qC-4); HRMS (ESI-TOF) *m/z*: [M-H]⁻ calcd. for C₁₃H₂₃O₃: 227.16527; found: 227.16487.

Spectral data were consistent with those reported in the literature.

Methyl 3-oxodec-9-enoate (29)

A mixture of NaH (1.05 equiv.) in dry THF (2.5 mL/mmol) was cooled to 0 °C under a nitrogen atmosphere. Methyl acetoacetate (1 equiv.) was added dropwise, and the resulting white suspension was stirred at this 0 °C for 15 mins. Next, *n*-BuLi (1 equiv.) was added dropwise and the resulting bright yellow mixture was stirred at 0 °C for a further 20 mins. To this dianion mixture was added 6-bromohex-1-ene (1 equiv.) dropwise, and the resulting orange mixture was allowed to warm to room temperature and stirred until complete consumption of the starting materials was observed by TLC analysis (hexane/EtOAc 8:2), 3 h in total. The reaction was quenched with saturated aq. NH₄Cl (3 mL/mmol) and extracted with EtOAc (3 × 1.5 mL/mmol). The combined organic layers were washed with brine (2 mL/mmol), dried over MgSO₄, filtered and concentrated *in vacuo* to yield the crude product as an orange oil. Purification by column chromatography (hexane/EtOAc 9:1) yielded the product as yellow oil (1.25 g, 63%).



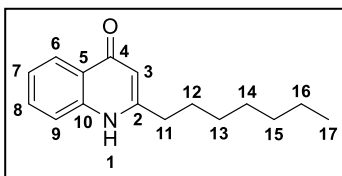
Pale yellow oil; yield: 1.25 g (63%); IR (NaCl): ν 3081 (C-H stretch), 2932 (C-H stretch), 1740 (ester C=O stretch), 1701 (ketone C=O stretch), 1506 (alkene C=C stretch), 1477 (alkyl C-H bend), 1264 (C-O stretch) cm⁻¹; ¹H-NMR (300 MHz, CDCl₃, signals of the predominant keto tautomer are given) δ: 1.21–1.47 (m, 4H, CH₂-7, CH₂-8), 1.52–1.69 (m, 2H, CH₂-6), 1.99–2.12 (m, 2H, CH₂-9), 2.53 (t, *J* = 7.3 Hz, 2H, CH₂-5), 3.44 (s, 2H, CH₂-3), 3.74 (s, 3H, CH₃-1), 4.86–5.09 (m, 2H, CH₂-11), 5.68–5.92 (m, 1H, CH-10); ¹³C-NMR (75 MHz, CDCl₃, signals of the predominant keto tautomer are given) δ: 23.3 (CH₂-6), 28.4 (CH₂-8), 28.6 (CH₂-7), 33.5 (CH₂-9), 43.0 (CH₂-5), 49.0

(CH₂-3), 52.3 (CH₃-1), 114.5 (CH₂-11), 138.7 (CH-10), 167.7 (qC-2), 202.7 (qC-4); HRMS (ESI-TOF) m/z : [M+2H]⁺ calcd. for C₁₁H₂₀O₃: 199.1339; found: 199.1338.

1.16. General Procedure for the Synthesis of HHQ and HHQ Analogues

To a solution of methyl 3-oxodecanoate **7** (or, for C-2 nonyl analogues, methyl 3-oxododecanoate **19**) (1 equiv.) in hexane (1.5 mL/mmol) were added the appropriate substituted aniline (1 equiv.) and *p*-TsOH (2 mol%). The reaction mixture was heated at reflux overnight under a Dean-Stark system. The reaction mixture was concentrated *in vacuo* to afford the crude β -enamino ester as an orange oil. This enamine intermediate was added dropwise (max. 10 mins for addition) via syringe to refluxing (>260 °C) diphenyl ether (0.5 mL/mmol) and left to cyclise at this temperature for 1.5 h. After cooling to room temperature, diethyl ether (approx. 400 mL) was added to the reaction residue and left overnight at 5 °C, allowing the quinolone product to precipitate. The product was collected by vacuum filtration and washed with diethyl ether. If necessary, the quinolone was recrystallised from methanol.

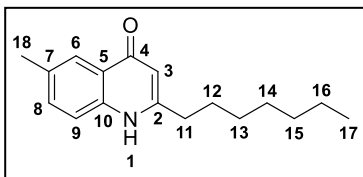
2-Heptylquinolin-4(1H)-one (HHQ)^[37] (**1**)



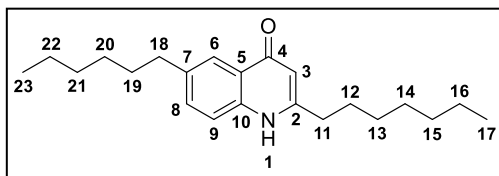
Pale yellow solid; yield: 10.01 g (41%); m.p. = 143–146 °C (lit. 146–147 °C); IR (KBr): ν 3253 (N-H stretch), 2956 (C-H stretch), 1636 (C=O stretch), 1596 (aromatic C-C stretch), 1465 (alkyl C-H bend), 1196 (C-N stretch)

cm⁻¹; ¹H-NMR (300 MHz, CDCl₃) δ : 0.81 (t, J = 6.8 Hz, 3H, CH₃-17), 1.09–1.37 (m, 8H, CH₂-13, CH₂-14, CH₂-15, CH₂-16), 1.64–1.79 (m, 2H, CH₂-12), 2.39 (t, J = 7.7 Hz, 2H, CH₂-11), 6.24 (s, 1H, CH-3), 7.28–7.37 (m, 1H, CH-7), 7.53–7.63 (m, 1H, CH-8), 7.75 (d, J = 8.3 Hz, 1H, CH-9), 8.36 (dd, J = 8.2, 1.1 Hz, 1H, CH-6), 12.04 (br s, 1H, NH-1); ¹³C-NMR (75 MHz, CDCl₃) δ : 14.0 (CH₃-17), 22.6 (CH₂-16), 28.96 (CH₂-14), 29.05 (CH₂-12), 29.2 (CH₂-13), 31.6 (CH₂-15), 34.4 (CH₂-11), 108.2 (CH-3), 118.5 (CH-9), 123.5 (CH-7), 125.0 (qC-5), 125.3 (CH-6), 131.8 (CH-8), 140.6 (qC-10), 155.1 (qC-2), 178.9 (qC-4); HRMS (ESI-TOF) m/z : [M+H]⁺ calcd. for C₁₆H₂₂NO: 244.1701; found: 244.1692.

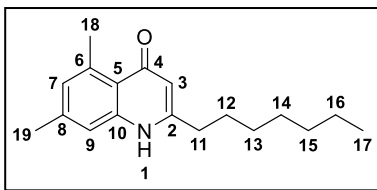
Spectral data were consistent with those reported in the literature.

2-Heptyl-6-methylquinolin-4(1H)-one (10)

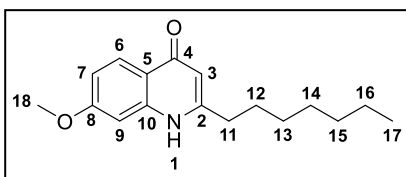
Pale yellow solid; yield: 398 mg (31%); m.p. = 177–179 °C; IR (KBr): ν 3259 (N-H stretch), 2956 (C-H stretch), 1644 (C=O stretch), 1593 (aromatic C-C stretch), 1490 (alkyl C-H bend), 1203 (C-N stretch) cm^{-1} ; $^1\text{H-NMR}$ (300 MHz, DMSO-d_6) δ : 0.85 (t, J = 6.8 Hz, 3H, CH_3 -17), 1.17–1.40 (m, 8H, CH_2 -13, CH_2 -14, CH_2 -15, CH_2 -16), 1.59–1.74 (m, 2H, CH_2 -12), 2.38 (s, 3H, CH_3 -18), 2.56 (t, J = 7.7 Hz, 2H, CH_2 -11), 5.87 (s, 1H, CH -3), 7.40–7.46 (m, 2H, CH -8, CH -9), 7.82 (s, 1H, CH -6), 11.37 (br s, 1H, NH -1); $^{13}\text{C-NMR}$ (75 MHz, DMSO-d_6) δ : 13.9 (CH_3 -17), 20.7 (CH_3 -18), 22.0 (CH_2 -16), 28.4 (CH_2 -12, CH_2 -14), 28.5 (CH_2 -13), 31.1 (CH_2 -15), 33.2 (CH_2 -11), 107.3 (CH -3), 117.8 (CH -9), 124.0 (CH -6), 124.6 (qC-5), 131.8 (qC-7), 132.7 (CH -8), 138.2 (qC-10), 153.1 (qC-2), 176.6 (qC-4); HRMS (ESI-TOF) m/z : $[\text{M}+\text{H}]^+$ calcd. for $\text{C}_{17}\text{H}_{24}\text{NO}$: 258.1858; found: 258.1848.

2-Heptyl-6-hexylquinolin-4(1H)-one (12)

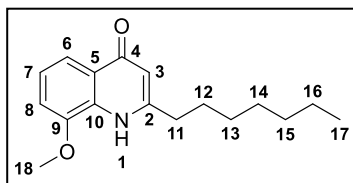
Pale pink solid; yield: 580 mg (35%); m.p. = 112–113 °C; IR (KBr): ν 3245 (N-H stretch), 3051 (C-H stretch), 2926 (C-H stretch), 2741 (C-H stretch), 1643 (C=O stretch), 1590 (aromatic C-C stretch), 1486 (alkyl C-H bend), 1362 (alkyl C-H bend), 1112 (C-N stretch) cm^{-1} ; $^1\text{H-NMR}$ (300 MHz, DMSO-d_6) δ : 0.80–0.95 (m, 6H, CH_3 -17, CH_3 -23), 1.19–1.40 (m, 14H, CH_2 -13, CH_2 -14, CH_2 -15, CH_2 -16, CH_2 -20, CH_2 -21, CH_2 -22), 1.52–1.75 (m, 4H, CH_2 -12, CH_2 -19), 2.53–2.71 (m, 4H, CH_2 -11, CH_2 -18), 5.88 (s, 1H, CH -3), 7.45 (s, 2H, CH -8, CH -9), 7.82 (s, 1H, CH -6), 11.37 (br s, 1H, NH -1); $^{13}\text{C-NMR}$ (150 MHz, DMSO-d_6) δ : 13.9 (CH_3 -17, CH_3 -23), 22.0 (CH_2 -16, CH_2 -22), 28.2 (CH_2 -20), 28.35 (CH_2 -12), 28.37 (CH_2 -14), 28.4 (CH_2 -13), 30.9 (CH_2 -19), 31.1 (CH_2 -15, CH_2 -21), 33.2 (CH_2 -11), 34.7 (CH_2 -18), 107.3 (CH -3), 117.8 (CH -9), 123.3 (CH -6), 124.5 (qC-5), 132.2 (CH -8), 136.9 (qC-7), 138.4 (qC-10), 153.2 (qC-2), 176.8 (qC-4); HRMS (ESI-TOF) m/z : $[\text{M}+\text{H}]^+$ calcd. for $\text{C}_{22}\text{H}_{34}\text{NO}$: 328.2640; found: 328.2628.

2-Heptyl-5,7-dimethylquinolin-4(1H)-one (11)

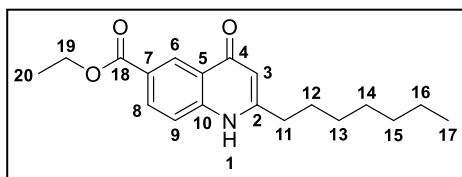
Pale yellow solid; yield: 612 mg (45%); m.p. = 158–160 °C; IR (KBr): ν 3329 (N-H stretch), 3091 (C-H stretch), 2959 (C-H stretch), 1641 (C=O stretch), 1551 (aromatic C-C stretch), 1462 (alkyl C-H bend), 1227 (C-N stretch) cm^{-1} ; $^1\text{H-NMR}$ (300 MHz, DMSO-d_6) δ : 0.88 (t, J = 7.0 Hz, 3H, CH_3 -17), 1.20–1.36 (m, 8H, CH_2 -13, CH_2 -14, CH_2 -15, CH_2 -16), 1.56–1.70 (m, 2H, CH_2 -12), 2.32 (s, 3H, CH_3 -19), 2.44–2.56 (m, 2H, CH_2 -11), 2.74 (s, 3H, CH_3 -18), 5.76 (s, 1H, CH -3), 6.77 (s, 1H, CH -7), 7.10 (s, 1H, CH -9), 11.05 (br s, 1H, NH -1); $^{13}\text{C-NMR}$ (75 MHz, DMSO-d_6) δ : 14.4 (CH_3 -17), 21.5 (CH_3 -19), 22.5 (CH_2 -16), 23.5 (CH_3 -18), 28.6 (CH_2 -14), 28.88 (CH_2 -13), 28.90 (CH_2 -12), 31.7 (CH_2 -15), 33.1 (CH_2 -11), 109.7 (CH -3), 115.9 (CH -9), 121.4 (qC-5), 127.2 (CH -7), 139.3 (qC-6), 140.7 (qC-8), 142.5 (qC-10), 152.0 (qC-2), 179.9 (qC-4); HRMS (ESI-TOF) m/z : $[\text{M}+\text{H}]^+$ calcd. for $\text{C}_{18}\text{H}_{26}\text{NO}$: 272.2014; found: 272.2009.

2-Heptyl-7-methoxyquinolin-4(1H)-one (13)

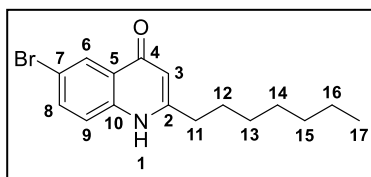
Recrystallised from hot methanol. Pale yellow solid; yield: 450 mg (33%); m.p. = 135–138 °C; IR (KBr): ν 3199 (N-H stretch), 2929 (C-H stretch), 1638 (C=O stretch), 1508 (aromatic C-C stretch), 1466 (alkyl C-H bend), 1257 (C-O stretch), 1168 (C-N stretch) cm^{-1} ; $^1\text{H-NMR}$ (300 MHz, DMSO-d_6) δ : 0.85 (t, J = 6.9 Hz, 3H, CH_3 -17), 1.16–1.39 (m, 8H, CH_2 -13, CH_2 -14, CH_2 -15, CH_2 -16), 1.55–1.73 (m, 2H, CH_2 -12), 2.54 (t, J = 5.9 Hz, 2H, CH_2 -11), 3.83 (s, 3H, CH_3 -18), 5.82 (s, 1H, CH -3), 6.74–6.99 (m, 2H, CH -7, CH -9), 7.92 (d, J = 8.9 Hz, 1H, CH -6), 11.32 (br s, 1H, NH -1); $^{13}\text{C-NMR}$ (75 MHz, DMSO-d_6) δ : 14.4 (CH_3 -17), 22.5 (CH_2 -16), 28.7 (CH_2 -12), 28.8 (CH_2 -14), 28.9 (CH_2 -13), 31.6 (CH_2 -15), 33.7 (CH_2 -11), 55.8 (CH_3 -18), 99.4 (CH -9), 107.9 (CH -3), 113.1 (CH -7), 119.4 (qC-5), 127.0 (CH -6), 142.4 (qC-10), 153.5 (qC-2), 162.1 (qC-8), 176.9 (qC-4); HRMS (ESI-TOF) m/z : $[\text{M}+\text{H}]^+$ calcd. for $\text{C}_{17}\text{H}_{24}\text{NO}_2$: 274.1807; found: 274.1805.

2-Heptyl-8-methoxyquinolin-4(1H)-one (14)

Recrystallised from hot methanol. Pale yellow solid; yield: 167 mg (12%); m.p. = 111–113 °C; IR (KBr): ν 3372 (N-H stretch), 2923 (C-H stretch), 1634 (C=O stretch), 1592 (aromatic C-C stretch), 1435 (alkyl C-H bend), 1263 (C-O stretch) 1198 (C-N stretch) cm^{-1} ; $^1\text{H-NMR}$ (300 MHz, DMSO- d_6) δ : 0.86 (t, J = 6.8 Hz, 3H, CH_3 -17), 1.15–1.42 (m, 8H, CH_2 -13, CH_2 -14, CH_2 -15, CH_2 -16), 1.52–1.73 (m, 2H, CH_2 -12), 2.67 (t, J = 7.6 Hz, 2H, CH_2 -11), 3.99 (s, 3H, CH_3 -18), 5.92 (s, 1H, CH -3), 7.17–7.23 (m, 2H, CH -7, CH -8), 7.56–7.65 (m, 1H, CH -6), 10.88 (br s, 1H, NH -1); $^{13}\text{C-NMR}$ (75 MHz, DMSO- d_6) δ : 14.4 (CH_3 -17), 22.6 (CH_2 -16), 28.9 (CH_2 -14), 29.0 (CH_2 -13), 29.5 (CH_2 -12), 31.7 (CH_2 -15), 33.2 (CH_2 -11), 56.6 (CH_3 -18), 108.7 (CH -3), 111.4 (CH -8), 116.5 (CH -6), 123.0 (CH -7), 126.1 (qC-5), 131.3 (qC-10), 148.8 (qC-9), 154.2 (qC-2), 177.0 (qC-4); HRMS (ESI-TOF) m/z : $[\text{M}+\text{H}]^+$ calcd. for $\text{C}_{17}\text{H}_{24}\text{NO}_2$: 274.1807; found: 274.1801.

Ethyl 2-heptyl-4-oxo-1,4-dihydroquinoline-6-carboxylate (15)

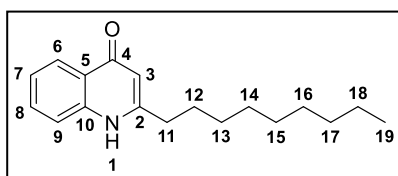
Pale yellow solid; yield: 202 mg (13%); m.p. = 197–198 °C; IR (KBr): ν 3258 (N-H stretch), 3057 (C-H stretch), 2926 (C-H stretch), 1719 (ester C=O stretch), 1645 (C=O stretch), 1593 (aromatic C-C stretch), 1495 (alkyl C-H bend), 1278 (C-O stretch), 1172 (C-N stretch) cm^{-1} ; $^1\text{H-NMR}$ (300 MHz, DMSO- d_6) δ : 0.86 (t, J = 6.8 Hz, 3H, CH_3 -17), 1.21–1.41 (m, 11H, CH_2 -13, CH_2 -14, CH_2 -15, CH_2 -16, CH_3 -20), 1.60–1.75 (m, 2H, CH_2 -12), 2.60 (t, J = 7.6 Hz, 2H, CH_2 -11), 4.34 (q, J = 7.1 Hz, 2H, CH_2 -19), 6.01 (s, 1H, CH -3), 7.61 (d, J = 8.7 Hz, 1H, CH -9), 8.12 (dd, J = 8.7, 2.1 Hz, 1H, CH -8), 8.66 (d, J = 1.9 Hz, 1H, CH -6), 11.75 (br s, 1H, NH -1); $^{13}\text{C-NMR}$ (150 MHz, DMSO- d_6) δ : 13.9 (CH_3 -20), 14.2 (CH_3 -17), 22.0 (CH_2 -16), 28.2 (CH_2 -12), 28.3 (CH_2 -14), 28.5 (CH_2 -13), 31.1 (CH_2 -15), 33.2 (CH_2 -11), 60.8 (CH_2 -19), 108.7 (CH -3), 118.5 (CH -9), 123.8 (qC-7), 123.9 (qC-5), 127.1 (CH -6), 131.3 (CH -8), 143.0 (qC-10), 154.5 (qC-2), 165.3 (qC-18), 176.7 (qC-4); HRMS (ESI-TOF) m/z : $[\text{M}+\text{H}]^+$ calcd. for $\text{C}_{19}\text{H}_{26}\text{NO}_3$: 316.1913; found: 316.1913.

6-Bromo-2-heptylquinolin-4(1H)-one (16)

Recrystallised from hot methanol. Light brown solid; yield: 355 mg (14%); m.p. = 186–188 °C; IR (KBr): ν 3319 (N-H stretch), 2926 (C-H stretch), 1632 (C=O stretch), 1595 (aromatic C-C stretch), 1467 (alkyl C-H bend), 1129 (C-N stretch), 842 (C-Br stretch) cm^{-1} ; $^1\text{H-NMR}$ (300 MHz, DMSO-d_6) δ : 0.86 (t, J = 6.8 Hz, 3H, CH_3 -17), 1.15–1.42 (m, 8H, CH_2 -13, CH_2 -14, CH_2 -15, CH_2 -16), 1.57–1.76 (m, 2H, CH_2 -12), 2.61 (t, J = 6.9 Hz, 2H, CH_2 -11), 6.04 (s, 1H, CH -3), 7.53 (d, J = 8.7 Hz, 1H, CH -9), 7.79 (dd, J = 8.8, 2.4 Hz, 1H, CH -8), 8.13 (d, J = 2.3 Hz, 1H, CH -6), 11.81 (br s, 1H, NH -1); $^{13}\text{C-NMR}$ (75 MHz, DMSO-d_6) δ : 14.4 (CH_3 -17), 22.5 (CH_2 -16), 28.8 (CH_2 -12, CH_2 -14), 28.9 (CH_2 -13), 31.6 (CH_2 -15), 33.8 (CH_2 -11), 108.1 (CH -3), 116.6 (qC-7), 121.3 (CH -9), 125.6 (qC-5), 127.2 (CH -6), 135.1 (CH -8), 139.3 (qC-10), 155.8 (qC-2), 174.8 (qC-4); HRMS (ESI-TOF) m/z : $[\text{M}+\text{H}]^+$ calcd. for $\text{C}_{16}\text{H}_{21}\text{BrNO}$: 322.0807; found: 322.0798.

2-Nonylquinolin-4(1H)-one^[50] (20)

Synthesised according to the same procedure as for HHQ using β -ketoester **19**.

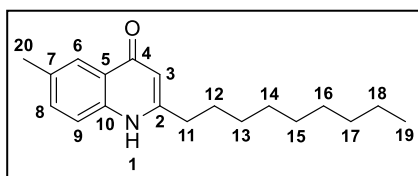


Off-white solid; yield: 312 mg (23%); m.p. = 133–134 °C (lit. 138–139 °C); IR (KBr): ν 3256 (N-H stretch), 2923 (C-H stretch), 1641 (C=O stretch), 1503 (aromatic C-C stretch), 1472 (alkyl C-H bend), 1137 (C-N stretch) cm^{-1} ; $^1\text{H-NMR}$ (300 MHz, CDCl_3) δ : 0.84 (t, J = 6.8 Hz, 3H, CH_3 -19), 1.05–1.43 (m, 12H, CH_2 -13, CH_2 -14, CH_2 -15, CH_2 -16, CH_2 -17, CH_2 -18), 1.62–1.82 (m, 2H, CH_2 -12), 2.69 (t, J = 7.6 Hz, 2H, CH_2 -11), 6.24 (s, 1H, CH -3), 7.27–7.38 (m, 1H, CH -7), 7.50–7.66 (m, 1H, CH -8), 7.77 (d, J = 8.3 Hz, 1H, CH -9), 8.36 (dd, J = 8.1, 1.2 Hz, 1H, CH -6), 12.16 (br s, 1H, NH -1); $^{13}\text{C-NMR}$ (75 MHz, CDCl_3) δ : 14.1 (CH_3 -19), 22.6 (CH_2 -18), 29.1 (CH_2 -12), 29.25 (CH_2 -15, CH_2 -16), 29.32 (CH_2 -14), 29.4 (CH_2 -13), 31.8 (CH_2 -17), 34.4 (CH_2 -11), 108.2 (CH -3), 118.5 (CH -9), 123.5 (CH -7), 125.0 (qC-5), 125.3 (CH -6), 131.7 (CH -8), 140.7 (qC-10), 155.2 (qC-2), 178.9 (qC-4); HRMS (ESI-TOF) m/z : $[\text{M}+\text{H}]^+$ calcd. for $\text{C}_{18}\text{H}_{26}\text{NO}$: 272.2014; found: 272.2012.

Spectral data were consistent with those reported in the literature.

6-Methyl-2-nonylquinolin-4(1H)-one (21)

Synthesised according to the same procedure as for HHQ using β -ketoester **19**.

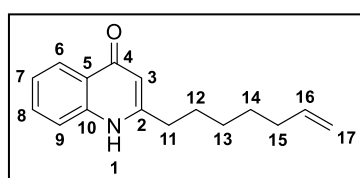


Pale yellow solid; yield: 109 mg (19%); m.p. = 172–174 °C; IR (KBr): ν 3261 (N-H stretch), 2954 (C-H stretch), 1647 (C=O stretch), 1589 (aromatic C-C stretch), 1495 (alkyl C-H bend), 1198 (C-N

stretch) cm^{-1} ; $^1\text{H-NMR}$ (300 MHz, DMSO-d_6) δ : 0.85 (t, $J = 6.7$ Hz, 3H, CH_3 -**19**), 1.17–1.40 (m, 12H, CH_2 -**13**, CH_2 -**14**, CH_2 -**15**, CH_2 -**16**, CH_2 -**17**, CH_2 -**18**), 1.57–1.75 (m, 2H, CH_2 -**12**), 2.39 (s, 3H, CH_3 -**20**), 2.53–2.60 (m, 2H, CH_2 -**11**), 5.88 (s, 1H, CH -**3**), 7.41–7.46 (m, 2H, CH -**8**, CH -**9**), 7.83 (d, $J = 0.9$ Hz, 1H, CH -**6**), 11.35 (br s, 1H, NH -**1**); $^{13}\text{C-NMR}$ (75 MHz, DMSO-d_6) δ : 14.4 (CH_3 -**19**), 21.2 (CH_3 -**20**), 22.5 (CH_2 -**18**), 28.8 (CH_2 -**12**), 29.0 (CH_2 -**16**), 29.1 (CH_2 -**15**), 29.2 (CH_2 -**14**), 29.3 (CH_2 -**13**), 31.7 (CH_2 -**17**), 33.7 (CH_2 -**11**), 107.8 (CH -**3**), 118.3 (CH -**9**), 124.5 (CH -**6**), 125.0 (qC-**5**), 132.3 (qC-**7**), 133.2 (CH -**8**), 138.7 (qC-**10**), 153.6 (qC-**2**), 177.1 (qC-**4**); HRMS (ESI-TOF) m/z : $[\text{M}+\text{H}]^+$ calcd. for $\text{C}_{19}\text{H}_{28}\text{NO}$: 286.2171; found: 286.2167.

2-(Hept-6-en-1-yl)quinolin-4(1H)-one (31)

Synthesised according to the same procedure as for HHQ using β -ketoester **29**.



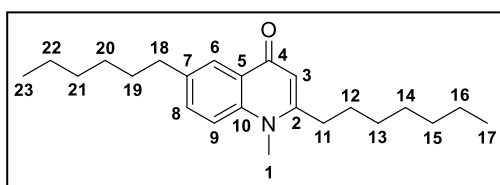
Pale yellow solid; yield: 109 mg (16%); m.p. = 122–124 °C; IR (NaCl): ν 3426 (N-H stretch), 2929 (C-H stretch), 1638 (C=O stretch), 1595 (aromatic C-C stretch), 1505 (alkene C=C stretch), 1472 (alkyl C-H bend), 1137 (C-N

stretch) cm^{-1} ; $^1\text{H-NMR}$ (300 MHz, CDCl_3) δ : 1.26–1.44 (m, 4H, CH_2 -**13**, CH_2 -**14**), 1.67–1.82 (m, 2H, CH_2 -**12**), 1.93–2.08 (m, 2H, CH_2 -**15**), 2.66 (t, $J = 7.7$ Hz, 2H, CH_2 -**11**), 4.86–5.01 (m, 2H, CH_2 -**17**), 5.73 (ddt, $J = 16.9, 10.2, 6.7$ Hz, 1H, CH -**16**), 6.20 (s, 1H, CH -**3**), 7.32 (ddd, $J = 8.1, 5.9, 2.2$ Hz, 1H, CH -**7**), 7.51–7.64 (m, 2H, CH -**8**, CH -**9**), 8.35 (d, $J = 7.9$ Hz, 1H, CH -**6**), 10.43 (br s, 1H, NH -**1**); $^{13}\text{C-NMR}$ (75 MHz, CDCl_3) δ : 28.4 (CH_2 -**12**, CH_2 -**14**), 28.6 (CH_2 -**13**), 33.5 (CH_2 -**15**), 33.6 (CH_2 -**11**), 108.1 (CH -**3**), 115.2 (CH_2 -**17**), 118.3 (CH -**9**), 123.2 (CH -**7**), 125.1 (qC-**5**), 125.2 (CH -**6**), 131.9 (CH -**8**), 139.1 (CH -**16**), 140.6 (qC-**10**), 153.9 (qC-**2**), 177.3 (qC-**4**); HRMS (ESI-TOF) m/z : $[\text{M}+\text{H}]^+$ calcd. for $\text{C}_{16}\text{H}_{20}\text{NO}$: 242.1545; found: 242.1535.

1.17. General Procedure for the Methylation of HHQ Analogues

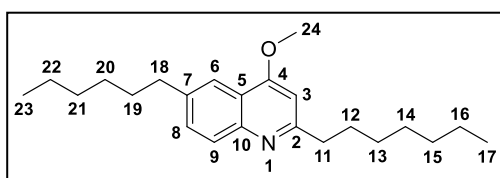
To a solution of the quinolone substrate **12** or **RC6** (compound synthesised by Dr Rafael Cano, refer to **Figure 5** for structure) (1 equiv.) in acetone (6 mL/mmol) were added K_2CO_3 (3 equiv.) and MeI (3 equiv.). The resulting mixture was stirred at 79 °C for 4 h. The cooled reaction mixture was poured into deionised water (25 mL/mmol) and extracted with EtOAc (3×10 mL/mmol). The combined organic extracts were dried over $MgSO_4$, filtered and concentrated *in vacuo* to yield the crude isomeric mixture of the *N*- and *O*-methylated products. Separation of the mixture by column chromatography (hexane/EtOAc 8:2) afforded the pure products.

2-Heptyl-6-hexyl-1-methylquinolin-4(1H)-one (**22**)



Yellow oil; yield: 13 mg (10%); [not enough material was obtained for IR analysis]; 1H -NMR (300 MHz, $CDCl_3$) δ : 0.75–1.00 (m, 6H, CH_3 -**17**, CH_3 -**23**), 1.13–1.53 (m, 14H, CH_2 -**13**, CH_2 -**14**, CH_2 -**15**, CH_2 -**16**, CH_2 -**20**, CH_2 -**21**, CH_2 -**22**), 1.57–1.79 (m, 4H, CH_2 -**12**, CH_2 -**19**), 2.62–2.81 (m, 4H, CH_2 -**11**, CH_2 -**18**), 3.72 (s, 3H, CH_3 -**1**), 6.22 (s, 1H, CH -**3**), 7.38–7.53 (m, 2H, CH -**8**, CH -**9**), 8.25 (d, $J = 1.7$ Hz, 1H, CH -**6**); ^{13}C -NMR (75 MHz, $CDCl_3$) δ : 14.1 (CH_3 -**17**, CH_3 -**23**), 22.6 (CH_2 -**16**, CH_2 -**22**), 28.6 (CH_2 -**20**), 28.9 (CH_2 -**12**), 29.0 (CH_2 -**14**), 29.2 (CH_2 -**13**), 31.4 (CH_2 -**19**), 31.7 (CH_2 -**15**, CH_2 -**21**), 34.1 (CH_2 -**11**), 34.7 (CH_2 -**18**), 35.2 (CH_3 -**1**), 110.9 (CH -**3**), 115.3 (CH -**9**), 125.5 (CH -**6**), 126.5 (qC-**5**), 132.7 (CH -**8**), 138.3 (qC-**7**), 140.2 (qC-**10**), 154.3 (qC-**2**), 177.8 (qC-**4**); HRMS (ESI-TOF) m/z : $[M+H]^+$ calcd. for $C_{23}H_{36}NO$: 342.2797; found: 342.2788.

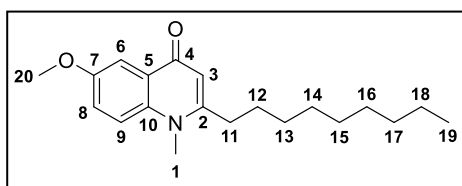
2-Heptyl-6-hexyl-4-methoxyquinoline (**23**)



Orange oil; yield: 46 mg (37%); IR (NaCl): ν 3583 (C-H stretch), 2926 (C-H stretch), 2854 (C-H stretch), 1596 (aromatic C-C stretch), 1462 (alkyl C-H bend), 1362 (C-N stretch), 1112 (C-O stretch) cm^{-1} ; 1H -NMR (300 MHz, $CDCl_3$) δ : 0.81–0.96 (m, 6H, CH_3 -**17**, CH_3 -**23**), 1.18–1.50 (m, 14H, CH_2 -**13**, CH_2 -**14**, CH_2 -**15**, CH_2 -**16**, CH_2 -**20**, CH_2 -**21**, CH_2 -**22**), 1.60–1.87 (m, 4H, CH_2 -**12**, CH_2 -**19**), 2.70–2.97 (m, 4H, CH_2 -**11**,

CH_2 -18), 4.02 (s, 3H, CH_3 -24), 6.60 (s, 1H, CH -3), 7.49 (dd, J = 8.6, 2.0 Hz, 1H, CH -8), 7.83–7.94 (m, 2H, CH -6, CH -9); ^{13}C -NMR (75 MHz, $CDCl_3$) δ : 14.1 (CH_3 -17, CH_3 -23), 22.0 (CH_2 -16, CH_2 -22), 29.0 (CH_2 -20), 29.2 (CH_2 -14), 29.6 (CH_2 -13), 30.3 (CH_2 -12), 31.5 (CH_2 -19), 31.7 (CH_2 -15), 31.8 (CH_2 -21), 36.1 (CH_2 -18), 40.0 (CH_2 -11), 55.4 (CH_3 -24), 99.7 (CH -3), 119.8 (qC-5, CH -9), 128.1 (CH -6), 131.1 (CH -8), 139.6 (qC-7), 147.5 (qC-10), 162.0 (qC-4), 163.3 (qC-2); HRMS (ESI-TOF) m/z : $[M+H]^+$ calcd. for $C_{23}H_{36}NO$: 342.2797; found: 342.2784.

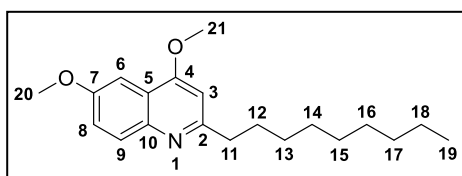
6-Methoxy-1-methyl-2-nonylquinolin-4(1H)-one (24)



Pale yellow oil; yield: 22 mg (14%); IR (KBr): ν 3369 (C-H stretch), 2929 (C-H stretch), 1599 (C=O stretch), 1566 (aromatic C-C stretch), 1493 (alkyl C-H bend), 1318 (C-N stretch),

1069 (C-O stretch) cm^{-1} ; 1H -NMR (500 MHz, $CDCl_3$) δ : 0.88 (t, J = 6.6 Hz, 3H, CH_3 -19), 1.20–1.50 (m, 12H, CH_2 -13, CH_2 -14, CH_2 -15, CH_2 -16, CH_2 -17, CH_2 -18), 1.65–1.75 (m, 2H, CH_2 -12), 2.72 (t, J = 7.5 Hz, 2H, CH_2 -11), 3.75 (s, 3H, CH_3 -1), 3.93 (s, 3H, CH_3 -20), 6.23 (s, 1H, CH -3), 7.25–7.30 (m, 1H, CH -8), 7.46 (d, J = 9.3 Hz, 1H, CH -9), 7.86 (s, 1H, CH -6); ^{13}C -NMR (125 MHz, $CDCl_3$) δ : 14.1 (CH_3 -19), 22.7 (CH_2 -18), 28.7 (CH_2 -12), 29.25 (CH_2 -16), 29.29 (CH_2 -15), 29.32 (CH_2 -14), 29.4 (CH_2 -13), 31.8 (CH_2 -17), 34.3 (CH_3 -1), 34.7 (CH_2 -11), 55.8 (CH_3 -20), 105.7 (CH -6), 110.4 (CH -3), 117.0 (CH -9), 122.6 (CH -8), 127.8 (qC-5), 136.7 (qC-10), 153.8 (qC-2), 156.0 (qC-7), 177.2 (qC-4); HRMS (ESI-TOF) m/z : $[M+H]^+$ calcd. for $C_{20}H_{30}NO_2$: 316.2277; found: 316.2282.

4,6-Dimethoxy-2-nonylquinoline (25)



Orange oil; yield: 66 mg (42%); IR (NaCl): ν 3583 (C-H stretch), 2925 (C-H stretch), 1599 (aromatic C-C stretch), 1489 (alkyl C-H bend), 1223 (C-N stretch), 1089 (C-O stretch) cm^{-1} ;

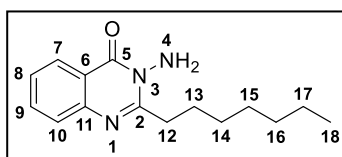
1H -NMR (300 MHz, $CDCl_3$) δ : 0.87 (t, J = 6.6 Hz, 3H, CH_3 -19), 1.20–1.50 (m, 12H, CH_2 -13, CH_2 -14, CH_2 -15, CH_2 -16, CH_2 -17, CH_2 -18), 1.75–1.85 (m, 2H, CH_2 -12), 2.88 (t, J = 7.6 Hz, 2H, CH_2 -11), 3.92 (s, 3H, CH_3 -20), 4.03 (s, 3H, CH_3 -21), 6.61 (s, 1H, CH -3), 7.30 (dd, J = 9.1, 2.9 Hz, 1H, CH -8), 7.40 (d, J = 2.8 Hz, 1H, CH -6), 7.87 (d, J = 9.2 Hz, 1H, CH -9); ^{13}C -NMR (75 MHz, $CDCl_3$) δ : 14.1 (CH_3 -19), 22.7

(CH₂-**18**), 29.3 (CH₂-**12**), 29.54 (CH₂-**16**), 29.56 (CH₂-**15**), 29.6 (CH₂-**14**), 30.3 (CH₂-**13**), 31.9 (CH₂-**17**), 39.7 (CH₂-**11**), 55.5 (CH₃-**20**, CH₃-**21**), 99.7 (CH-**3**), 100.0 (CH-**9**), 120.5 (qC-**5**), 121.8 (CH-**6**), 129.8 (CH-**8**), 144.7 (qC-**10**), 156.8 (qC-**7**), 161.4 (qC-**4**), 161.7 (qC-**2**); HRMS (ESI-TOF) *m/z*: [M+H]⁺ calcd. for C₂₀H₃₀NO₂: 316.2277; found: 316.2270.

1.18. Synthesis of Quinazolinone Compound **28**

3-Amino-2-heptylquinazolin-4(3*H*)-one (**28**)

Triethylamine (2 equiv.) was added to a suspension of anthranilic acid (1 equiv.) in DCM (3.5 mL/mmol). The mixture was cooled to 0 °C and octanoyl chloride (1 equiv.) was added dropwise, and the reaction mixture was stirred at room temperature for 2.5 h. After this time the reaction mixture was again cooled to 0 °C, and more triethylamine (1.1 equiv.) and ethyl chloroformate (1.1 equiv.) were added dropwise to the mixture, successively. The reaction mixture was then stirred at 0 °C for 1 h and at room temperature for 1.5 h, and then concentrated *in vacuo* to yield intermediate **27** as a pale yellow solid, which was carried through to the next step without further purification. Compound **27** was dissolved in pyridine (2.5 mL/mmol). Hydrazine hydrate (2 equiv.) was added and the reaction mixture was stirred at 115 °C for 1 h. After cooling to room temperature, conc. HCl (2 mL/mmol) and ice (2 g/mmol) were added to the mixture which was left to stand at room temperature overnight. A small amount of solid precipitated and was collected by vacuum filtration and washed with water. The solid was then recrystallised from ethanol to yield the pure product **28** as an off-white solid (52 mg, 3%).



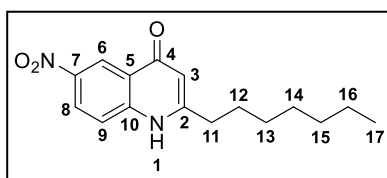
Off-white solid; yield: 52 mg (3%); m.p. = 73–75 °C; IR (KBr): ν 3300 (N-H stretch), 3202 (C-H stretch), 2927 (C-H stretch), 1665 (C=O stretch), 1591 (aromatic C-C stretch), 1474 (alkyl C-H bend), 1230 (C-N stretch), 1108 (N-N stretch) cm⁻¹; ¹H-NMR (300 MHz, CDCl₃) δ : 0.89 (t, *J* = 6.8 Hz, 3H, CH₃-**18**), 1.23–1.54 (m, 8H, CH₂-**14**, CH₂-**15**, CH₂-**16**, CH₂-**17**), 1.76–1.90 (m, 2H, CH₂-**13**), 2.94–3.10 (m, 2H, CH₂-**12**), 4.86 (s, 2H, NH₂-**4**), 7.44 (ddd, *J* = 8.1, 6.8, 1.5 Hz, 1H, CH-**8**), 7.63–7.78 (m, 2H, CH-**9**, CH-**10**), 8.24 (dd, *J* = 8.0, 0.9 Hz, 1H, CH-**7**); ¹³C-NMR (75 MHz, CDCl₃) δ : 14.1 (CH₃-**18**), 22.6 (CH₂-**17**), 27.2 (CH₂-**13**), 29.1 (CH₂-**15**), 29.4 (CH₂-**14**), 31.7 (CH₂-**16**), 34.6 (CH₂-**12**), 120.0 (qC-**6**), 126.2 (CH-**7**), 126.5 (CH-**10**),

127.2 (CH-8), 134.2 (CH-9), 147.1 (qC-11), 158.4 (qC-2), 161.9 (qC-5); HRMS (ESI-TOF) m/z : $[M+H]^+$ calcd. for $C_{15}H_{22}N_3O$: 260.1763; found: 260.1752.

1.19. Synthesis of 6-Nitro HHQ 3

2-Heptyl-6-nitroquinolin-4(1H)-one^[42] (3)

HHQ **1** (1 equiv.) was dissolved in conc. H_2SO_4 (1.2 mL/mmol) and the solution was cooled to 0 °C on an ice bath. In a separate vessel, conc. H_2SO_4 (0.12 mL/mmol) and conc. HNO_3 (0.12 mL/mmol) were combined and also cooled to 0 °C on ice. The HNO_3/H_2SO_4 solution was added dropwise over approx. 5 min to the HHQ solution whilst maintaining the temperature between 0–5 °C (this proved to be important for selective nitration at the C-6 position and minimising the formation of other nitrated isomers). The resulting yellow solution was allowed to warm to room temperature with stirring for a further 2 h. Ice-water (2.5 mL/mmol) was added to the solution and a bright yellow solid precipitated, which was collected by vacuum filtration and recrystallised from hot methanol and diethyl ether. The yellow solid obtained was collected by vacuum filtration, washed with diethyl ether, yielding the pure product **3** (388 mg, 67 %).

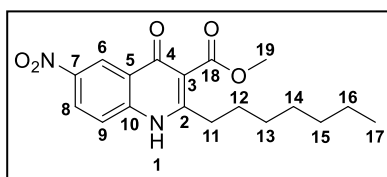


Yellow solid; yield: 388 mg (67%); m.p. = 183–185 °C (lit. 185–186 °C); IR (KBr): ν 3102 (C-H stretch), 2921 (C-H stretch), 1658 (C=O stretch), 1616 (N-O stretch), 1494 (aromatic C-C stretch), 1468 (alkyl C-H bend), 1355 (N-O stretch), 1193 (C-N stretch) cm^{-1} ; 1H -NMR (300 MHz, DMSO- d_6) δ : 0.86 (t, J = 6.8 Hz, 3H, CH_3 -17), 1.16–1.44 (m, 8H, CH_2 -13, CH_2 -14, CH_2 -15, CH_2 -16), 1.59–1.81 (m, 2H, CH_2 -12), 2.68 (t, J = 7.7 Hz, 2H, CH_2 -11), 6.22 (s, 1H, CH-3), 7.78 (d, J = 9.2 Hz, 1H, CH-9), 8.44 (dd, J = 9.2, 2.7 Hz, 1H, CH-8), 8.82 (d, J = 2.6 Hz, 1H, CH-6), 12.37 (br s, 1H, NH-1); ^{13}C -NMR (75 MHz, DMSO- d_6) δ : 14.4 (CH_3 -17), 22.5 (CH_2 -16), 28.6 (CH_2 -12), 28.8 (CH_2 -14), 28.9 (CH_2 -13), 31.6 (CH_2 -15), 33.8 (CH_2 -11), 109.2 (CH-3), 120.5 (CH-9), 121.8 (CH-6), 123.5 (qC-5), 126.5 (CH-8), 143.2 (qC-7), 144.1 (qC-10), 156.8 (qC-2), 176.0 (qC-4); HRMS (ESI-TOF) m/z : $[M+H]^+$ calcd. for $C_{16}H_{21}N_2O_3$: 289.1552; found: 289.1538.

Spectral data were consistent with those reported in the literature.

1.20. Synthesis of Carboxylic Acid Precursor 32**Methyl 2-heptyl-6-nitro-4-oxo-1,4-dihydroquinoline-3-carboxylate**

To a suspension of NaH (1.1 equiv.) in dry DMF (3 mL/mmol) was added a solution of methyl 3-oxodecanoate **7** (1.1 equiv.) in dry DMF (2 mL/mmol) via a dropping funnel under a nitrogen atmosphere, and the reaction mixture stirred at room temperature. Once the evolution of H₂ had ceased, a solution of 5-nitroisotoic anhydride (1 equiv.) in dry DMF (2 mL/mmol) was added dropwise via a dropping funnel. The resulting orange reaction mixture was then stirred at room temperature overnight. The reaction mixture was concentrated *in vacuo* (Kugelrohr) to approximately 25% the original volume. HCl (1 M aq.) was then added to precipitate the crude product as a yellow solid, which was collected by vacuum filtration and dried *in vacuo*. The crude product was recrystallised from hot methanol, collected by vacuum filtration and dried *in vacuo* to yield the pure product as a pale yellow solid (0.859 g, 31%).

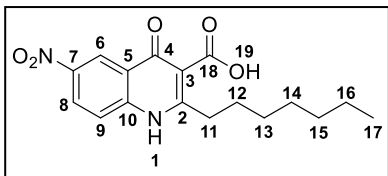


Pale yellow solid; yield: 859 mg (31%); m.p. = 235–239 °C; IR (KBr): ν 3101 (C-H stretch), 2927 (C-H stretch), 1727 (ester C=O stretch), 1661 (C=O stretch), 1615 (N-O stretch), 1504 (aromatic C-C stretch), 1469 (alkyl C-H bend), 1343 (N-O stretch), 1200 (C-N stretch), 1065 (C-O stretch) cm⁻¹; ¹H-NMR (300 MHz, DMSO-d₆) δ : 0.86 (t, *J* = 6.8 Hz, 3H, CH₃-**17**), 1.18–1.45 (m, 8H, CH₂-**13**, CH₂-**14**, CH₂-**15**, CH₂-**16**), 1.61–1.74 (m, 2H, CH₂-**12**), 2.65 (t, *J* = 7.8 Hz, 2H, CH₂-**11**), 3.80 (s, 3H, CH₃-**19**), 7.77 (d, *J* = 9.1 Hz, 1H, CH-**9**), 8.45 (dd, *J* = 9.1, 2.6 Hz, 1H, CH-**8**), 8.81 (d, *J* = 2.6 Hz, 1H, CH-**6**), 12.30 (br s, 1H, NH-**1**); ¹³C-NMR (75 MHz, DMSO-d₆) δ : 14.4 (CH₃-**17**), 22.5 (CH₂-**16**), 28.7 (CH₂-**12**), 29.1 (CH₂-**14**), 29.2 (CH₂-**13**), 31.5 (CH₂-**15**), 32.5 (CH₂-**11**), 52.5 (CH₃-**19**), 116.2 (qC-**3**), 120.6 (CH-**9**), 122.0 (CH-**6**), 124.1 (qC-**5**), 127.0 (CH-**8**), 143.5 (qC-**7**), 143.6 (qC-**10**), 154.7 (qC-**2**), 167.1 (qC-**18**), 173.6 (qC-**4**); HRMS (ESI-TOF) *m/z*: [M+H]⁺ calcd. for C₁₈H₂₃N₂O₅: 347.1607; found: 347.1594.

2-Heptyl-6-nitro-4-oxo-1,4-dihydroquinoline-3-carboxylic acid^[41] (32)

A suspension of methyl 2-heptyl-6-nitro-4-oxo-1,4-dihydroquinoline-3-carboxylate (1 equiv.) in 10% aq. NaOH (70 mL/mmol) was heated at 97 °C with stirring for 4 h.

The reaction mixture was then cooled to room temperature and extracted with EtOAc (3×5 mL/mmol). The aqueous layer was then acidified to pH 4.5 with conc. HCl on ice, causing a white solid to precipitate. The crude product was collected by vacuum filtration, and recrystallised from hot methanol to yield the pure product **32** as a white solid (0.209 g, 58%).



White solid; yield: 209 mg (58%); m.p. = 194–197 °C (lit. 192–194 °C); IR (KBr): ν 3439 (N-H stretch), 3099 (C-H stretch), 2932 (C-H stretch), 2852 (O-H stretch), 1737 (acid C=O stretch), 1681 (C=O

stretch), 1619 (N-O stretch), 1515 (aromatic C-C stretch), 1418 (alkyl C-H bend), 1344 (N-O stretch), 1251 (C-O stretch), 1225 (C-N stretch) cm^{-1} ; ^1H -NMR (300 MHz, DMSO- d_6) δ : 0.87 (t, J = 6.7 Hz, 3H, CH_3 -**17**), 1.20–1.52 (m, 8H, CH_2 -**13**, CH_2 -**14**, CH_2 -**15**, CH_2 -**16**), 1.61–1.79 (m, 2H, CH_2 -**12**), 3.18–3.45 (m, 2H, CH_2 -**11**), 7.93 (d, J = 9.2 Hz, 1H, CH -**9**), 8.59 (dd, J = 9.1, 2.6 Hz, 1H, CH -**8**), 8.94 (d, J = 2.6 Hz, 1H, CH -**6**), 13.23 (br s, 1H, NH -**1**), 15.67 (br s, 1H, OH -**19**); ^{13}C -NMR (75 MHz, DMSO- d_6) δ : 14.4 (CH_3 -**17**), 22.5 (CH_2 -**16**), 28.8 (CH_2 -**12**), 29.6 (CH_2 -**13**, CH_2 -**14**), 31.6 (CH_2 -**15**), 33.9 (CH_2 -**11**), 108.2 (qC-**3**), 121.4 (CH -**9**), 122.0 (CH -**6**), 123.2 (qC-**5**), 128.1 (CH -**8**), 142.3 (qC-**7**), 144.7 (qC-**10**), 164.5 (qC-**2**), 166.0 (qC-**18**), 179.0 (qC-**4**); HRMS (ESI-TOF) m/z : $[\text{M}+\text{H}]^+$ calcd. for $\text{C}_{17}\text{H}_{21}\text{N}_2\text{O}_5$: 333.1450; found: 333.1451.

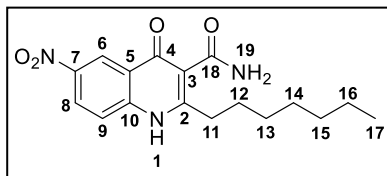
Spectral data were consistent with those reported in the literature.

1.21. General Procedure for the Synthesis of Hartmann's Amide and Methylated Analogues

N,N'-Carbonyldiimidazole (CDI) (2 equiv.) was added to a solution of **32** (1 equiv.) in dry DMF (5 mL/mmol), and the resulting yellow mixture was stirred for 4 h at 65 °C. The cooled reaction mixture was then added to a solution of the appropriate amine, 30 wt% NH_4OH for **5**, 40 wt% NH_2Me in H_2O for **33**, or 30 wt% NHMe_2 in Et_2O for **34** (25 mL/mmol) on an ice bath and the resulting mixture was stirred at room temperature overnight. The reaction mixture was then concentrated by approx. 50% *in vacuo* (Kugelrohr) and iced water (15 mL/mmol) was added, causing the product to

precipitate as a pale yellow solid which was collected by vacuum filtration and dried *in vacuo*.

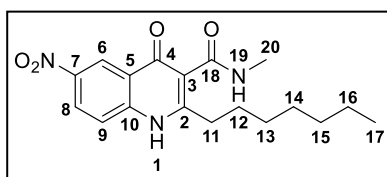
2-Heptyl-6-nitro-4-oxo-1,4-dihydroquinoline-3-carboxamide^[41] (5)



Pale yellow solid; yield: 129 mg (65%); m.p. = 238–241 °C (lit. 237–239 °C); IR (KBr): ν 3392 (N-H stretch), 3222 (N-H stretch), 3091 (C-H stretch), 2927 (C-H stretch), 1684 (C=O stretch), 1651 (amide C=O stretch), 1595 (N-O stretch), 1501 (aromatic C-C stretch), 1409 (alkyl C-H bend), 1342 (N-O stretch), 1223 (C-N stretch) cm^{-1} ; $^1\text{H-NMR}$ (300 MHz, DMSO-d_6) δ : 0.87 (t, $J = 6.7$ Hz, 3H, CH_3 -17), 1.19–1.47 (m, 8H, CH_2 -13, CH_2 -14, CH_2 -15, CH_2 -16), 1.62–1.79 (m, 2H, CH_2 -12), 3.02 (t, $J = 7.8$ Hz, 2H, CH_2 -11), 7.36 (br s, 1H, one of NH_2 -19), 7.77 (d, $J = 9.1$ Hz, 1H, CH -9), 8.46 (dd, $J = 9.1, 2.7$ Hz, 1H, CH -8), 8.55 (br s, 1H, one of NH_2 -19), 8.88 (d, $J = 2.6$ Hz, 1H, CH -6), 12.30 (br s, 1H, NH -1); $^{13}\text{C-NMR}$ (75 MHz, DMSO-d_6) δ : 14.4 (CH_3 -17), 22.5 (CH_2 -16), 28.8 (CH_2 -12), 29.5 (CH_2 -14), 29.7 (CH_2 -13), 31.6 (CH_2 -15), 33.2 (CH_2 -11), 115.8 (qC-3), 120.4 (CH -9), 122.4 (CH -6), 124.4 (qC-5), 126.8 (CH -8), 142.9 (qC-7), 143.6 (qC-10), 158.2 (qC-2), 167.2 (qC-18), 175.5 (qC-4); HRMS (ESI-TOF) m/z : $[\text{M}+\text{H}]^+$ calcd. for $\text{C}_{17}\text{H}_{22}\text{N}_3\text{O}_4$: 332.1610; found: 332.1597.

Spectral data were consistent with those reported in the literature.

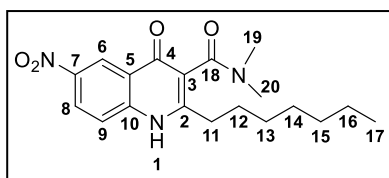
2-Heptyl-*N*-methyl-6-nitro-4-oxo-1,4-dihydroquinoline-3-carboxamide (33)



Pale yellow solid; yield: 11 mg (53%); m.p. = 243–245 °C; IR (KBr): ν 3302 (N-H stretch), 3100 (C-H stretch), 2928 (C-H stretch), 1677 (C=O stretch), 1634 (amide C=O stretch), 1568 (N-O stretch), 1501 (aromatic C-C stretch), 1410 (alkyl C-H bend), 1337 (N-O stretch), 1216 (C-N stretch) cm^{-1} ; $^1\text{H-NMR}$ (300 MHz, DMSO-d_6) δ : 0.79–0.96 (m, 3H, CH_3 -17), 1.17–1.48 (m, 8H, CH_2 -13, CH_2 -14, CH_2 -15, CH_2 -16), 1.58–1.79 (m, 2H, CH_2 -12), 2.77 (d, $J = 4.5$ Hz, 3H, CH_3 -20), 2.94 (t, $J = 7.6$ Hz, 2H, CH_2 -11), 7.76 (d, $J = 9.1$ Hz, 1H, CH -9), 8.45 (dd, $J = 9.1, 2.2$ Hz, 1H, CH -8), 8.86 (d, $J = 2.2$ Hz, 1H, CH -6), 9.01 (m, 1H, NH -19), 12.28 (br s, 1H, NH -1); $^{13}\text{C-NMR}$ (75 MHz, DMSO-d_6) δ : 14.4 (CH_3 -17), 22.5 (CH_2 -16), 26.2 (CH_3 -20), 28.8 (CH_2 -12), 29.5 (CH_2 -14), 29.7 (CH_2 -13), 31.6

(CH₂-15), 33.1 (CH₂-11), 116.0 (qC-3), 120.6 (CH-9), 122.3 (CH-6), 124.3 (qC-5), 126.7 (CH-8), 143.1 (qC-7), 143.4 (qC-10), 157.8 (qC-2), 165.9 (qC-18), 175.3 (qC-4); HRMS (ESI-TOF) *m/z*: [M+H]⁺ calcd. for C₁₈H₂₄N₃O₄: 346.1767; found: 346.1773.

2-Heptyl-*N,N*-dimethyl-6-nitro-4-oxo-1,4-dihydroquinoline-3-carboxamide (34)



Pale yellow solid; yield: 59 mg (59%); m.p. = 236–238 °C; IR (KBr): ν 3229 (N-H stretch), 3096 (C-H stretch), 2922 (C-H stretch), 1667 (C=O stretch), 1621 (amide C=O stretch), 1556 (N-O stretch), 1504

(aromatic C-C stretch), 1394 (alkyl C-H bend), 1334 (N-O stretch), 1062 (C-N stretch) cm⁻¹; ¹H-NMR (300 MHz, DMSO-d₆) δ : 0.86 (t, *J* = 6.5 Hz, 3H, CH₃-17), 1.17–1.42 (m, 8H, CH₂-13, CH₂-14, CH₂-15, CH₂-16), 1.53–1.79 (m, 2H, CH₂-12), 2.84 (s, 3H, CH₃-19/20), 2.99 (s, 3H, CH₃-20/19), 2.40–2.57 (m, 2H, CH₂-11), 7.76 (d, *J* = 9.1 Hz, 1H, CH-9), 8.44 (dd, *J* = 9.1, 2.6 Hz, 1H, CH-8), 8.82 (d, *J* = 2.6 Hz, 1H, CH-6), 12.25 (br s, 1H, NH-1); ¹³C-NMR (75 MHz, DMSO-d₆) δ : 14.4 (CH₃-17), 22.5 (CH₂-16), 28.7 (CH₂-12, CH₂-14), 29.2 (CH₂-13), 31.5 (CH₂-15), 32.1 (CH₂-11), 34.6 (CH₃-19/20), 37.7 (CH₃-19/20), 119.5 (qC-3), 120.4 (CH-9), 122.1 (CH-6), 123.6 (qC-5), 126.6 (CH-8), 143.2 (qC-7), 143.7 (qC-10), 153.0 (qC-2), 166.6 (qC-18), 173.3 (qC-4); HRMS (ESI-TOF) *m/z*: [M+H]⁺ calcd. for C₁₉H₂₆N₃O₄: 360.1923; found: 360.1919.

1.22. Chapter 1 References

1. R. I. Aminov, *Front. Microbiol.* **2010**, *1*, 134.
2. C. L. Ventola, *Pharm. Ther.* **2015**, *40*, 277-283.
3. A. Casadevall, *Expert Opin. Pharmacother.* **2009**, *10*, 1699-1703.
4. B. Spellberg, J. H. Rex, *Nat. Rev. Drug Discov.* **2013**, *12*, 963-964.
5. S. Wagner, R. Sommer, S. Hinsberger, C. Lu, R. W. Hartmann, M. Empting, A. Titz, *J. Med. Chem.* **2016**, *59*, 5929-5969.
6. S. W. Dickey, G. Y. Cheung, M. Otto, *Nat. Rev. Drug Discov.* **2017**, *16*, 457-471.
7. M. B. Miller, B. L. Bassler, *Ann. Rev. Microbiol.* **2001**, *55*, 165-199.
8. K. Papenfort, B. L. Bassler, *Nat. Rev. Microbiol.* **2016**, *14*, 576-588.
9. S. T. Rutherford, B. L. Bassler, *Cold Spring Harbor Perspect. Med.* **2012**, *2*, a012427.
10. R. M. Donlan, *Emerging Infect. Dis.* **2002**, *8*, 881-890.
11. T. Defoirdt, *Trends Microbiol.* **2018**, *26*, 313-328.
12. D. A. Rasko, V. Sperandio, *Nat. Rev. Drug Discov.* **2010**, *9*, 117-128.
13. Y.-H. Dong, L.-H. Wang, J.-L. Xu, H.-B. Zhang, X.-F. Zhang, L.-H. Zhang, *Nature* **2001**, *411*, 813-817.
14. E. Ó. Muimhneacháin, F. J. Reen, F. O'Gara, G. P. McGlacken, *Org. Biomol. Chem.* **2018**, *16*, 169-179.
15. V. C. Kalia, *Biotechnol. Adv.* **2013**, *31*, 224-245.
16. A. Y. Peleg, D. C. Hooper, *New Engl. J. Med.* **2010**, *362*, 1804-1813.
17. J. N. Pendleton, S. P. Gorman, B. F. Gilmore, *Expert Rev. Anti-Infect. Ther.* **2013**, *11*, 297-308.
18. F. Soukarieh, P. Williams, M. J. Stocks, M. Cámara, *J. Med. Chem.* **2018**, *61*, 10385-10402.
19. WHO Global Priority List of Antibiotic-Resistant Bacteria to Guide Research, Discovery, and Development of New Antibiotics, **2017**, <https://www.who.int/medicines/publications/global-priority-list-antibiotic-resistant-bacteria/en/>, accessed 26 March 2019.
20. N. Høiby, O. Ciofu, T. Bjarnsholt, *Future Microbiol.* **2010**, *5*, 1663-1674.

21. C. T. O'Loughlin, L. C. Miller, A. Siryaporn, K. Drescher, M. F. Semmelhack, B. L. Bassler, *Proc. Natl. Acad. Sci.* **2013**, *110*, 17981-17986.
22. S. P. Diggle, P. Cornelis, P. Williams, M. Camara, *Int. J. Med. Microbiol.* **2006**, *296*, 83-91.
23. S. Li, S. Chen, J. Fan, Z. Cao, W. Ouyang, N. Tong, X. Hu, J. Hu, P. Li, Z. Feng, *Eur. J. Med. Chem.* **2018**, *145*, 64-73.
24. S. P. Diggle, S. Matthijs, V. J. Wright, M. P. Fletcher, S. R. Chhabra, I. L. Lamont, X. Kong, R. C. Hider, P. Cornelis, M. Camara, P. Williams, *Chem. Biol.* **2007**, *14*, 87-96.
25. S. Heeb, M. P. Fletcher, S. R. Chhabra, S. P. Diggle, P. Williams, M. Cámara, *FEMS Microbiol. Rev.* **2011**, *35*, 247-274.
26. C. Schütz, M. Empting, *Beilstein J. Org. Chem.* **2018**, *14*, 2627-2645.
27. D. Maura, L. G. Rahme, *Antimicrob. Agents Chemother.* **2017**, *61*, e0136217.
28. F. J. Reen, M. J. Mooij, L. J. Holcombe, C. M. McSweeney, G. P. McGlacken, J. P. Morrissey, F. O'Gara, *FEMS Microbiol. Ecol.* **2011**, *77*, 413-428.
29. Y. Tashiro, Y. Yawata, M. Toyofuku, H. Uchiyama, N. Nomura, *Microbes Environ.* **2013**, *28*, 13-24.
30. A. Trejo-Hernández, A. Andrade-Domínguez, M. Hernández, S. Encarnacion, *ISME J.* **2014**, *8*, 1974-1988.
31. A. I. Chen, E. F. Dolben, C. Okegbe, C. E. Harty, Y. Golub, S. Thao, D. G. Ha, S. D. Willger, G. A. O'Toole, C. S. Harwood, *PLoS Path.* **2014**, *10*, e1004480.
32. M. M. Kendall, V. Sperandio, *MBio* **2016**, *7*, e0174815.
33. F. J. Reen, G. P. McGlacken, F. O'Gara, *FEMS Microbiol. Lett.* **2018**, *365*, fny076.
34. J. T. Hodgkinson, S. D. Bowden, W. R. Galloway, D. R. Spring, M. Welch, *J. Bacteriol.* **2010**, *192*, 3833-3837.
35. J. T. Hodgkinson, W. R. J. D. Galloway, S. Saraf, I. R. Baxendale, S. V. Ley, M. Ladlow, M. Welch, D. R. Spring, *Org. Biomol. Chem.* **2011**, *9*, 57-61.
36. G. P. McGlacken, C. M. McSweeney, T. O'Brien, S. E. Lawrence, C. J. Elcoate, F. J. Reen, F. O'Gara, *Tetrahedron Lett.* **2010**, *51*, 5919-5921.
37. F. J. Reen, S. L. Clarke, C. Legendre, C. M. McSweeney, K. S. Eccles, S. E. Lawrence, F. O'Gara, G. P. McGlacken, *Org. Biomol. Chem.* **2012**, *10*, 8903-8910.

38. P. N. Jimenez, G. Koch, J. A. Thompson, K. B. Xavier, R. H. Cool, W. J. Quax, *Microbiol. Mol. Biol. Rev.* **2012**, 76, 46-65.
39. H. Cao, G. Krishnan, B. Goumnerov, J. Tsongalis, R. Tompkins, L. G. Rahme, *Proc. Natl. Acad. Sci. USA* **2001**, 98, 14613-14618.
40. L. A. Gallagher, S. L. McKnight, M. S. Kuznetsova, E. C. Pesci, C. Manoil, *J. Bacteriol.* **2002**, 184, 6472-6480.
41. C. Lu, C. K. Maurer, B. Kirsch, A. Steinbach, R. W. Hartmann, *Angew. Chem. Int. Ed.* **2014**, 53, 1109-1112.
42. C. Lu, B. Kirsch, C. Zimmer, J. C. De Jong, C. Henn, C. K. Maurer, M. Musken, S. Haussler, A. Steinbach, R. W. Hartmann, *Chem. Biol.* **2012**, 19, 381-390.
43. A. Ilangovan, M. Fletcher, G. Rampioni, C. Pustelny, K. Rumbaugh, S. Heeb, M. Cámara, A. Truman, S. R. Chhabra, J. Emsley, *PLoS Path.* **2013**, 9, e1003508.
44. Y. Oikawa, K. Sugano, O. Yonemitsu, *J. Org. Chem.* **1978**, 43, 2087-2088.
45. K. Pihlaja, M. Seilo, U. Svanholm, A. Duffield, A. Balaban, J. Craig, *Acta Chem. Scand.* **1969**, 23, 3003-3010.
46. J. T. Hodgkinson, W. R. J. D. Galloway, M. Casoli, H. Keane, X. Su, G. P. C. Salmond, M. Welch, D. R. Spring, *Tetrahedron Lett.* **2011**, 52, 3291-3294.
47. A. S. Ivanov, *Chem. Soc. Rev.* **2008**, 37, 789-811.
48. F. Xu, J. D. Armstrong, G. X. Zhou, B. Simmons, D. Hughes, Z. Ge, E. J. Grabowski, *J. Am. Chem. Soc.* **2004**, 126, 13002-13009.
49. G. L. Thomas, C. M. Böhner, H. E. Williams, C. M. Walsh, M. Ladlow, M. Welch, C. E. Bryant, D. R. Spring, *Mol. Biosyst.* **2006**, 2, 132-137.
50. H. Z. Jin, J. H. Lee, D. Lee, H. S. Lee, Y. S. Hong, Y. H. Kim, J. J. Lee, *Biol. Pharm. Bull.* **2004**, 27, 926-928.
51. P. K. Singh, A. L. Schaefer, M. R. Parsek, T. O. Moninger, M. J. Welsh, E. Greenberg, *Nature* **2000**, 407, 762-764.
52. C. Lu, B. Kirsch, C. K. Maurer, J. C. de Jong, A. Braunshausen, A. Steinbach, R. W. Hartmann, *Eur. J. Med. Chem.* **2014**, 79, 173-183.
53. R. Shanahan, F. J. Reen, R. Cano, F. O'Gara, G. P. McGlacken, *Org. Biomol. Chem.* **2017**, 15, 306-310.
54. Y. Tashiro, S. Ichikawa, T. Nakajima-Kambe, H. Uchiyama, N. Nomura, *Microbes Environ.* **2010**, 25, 120-125.
55. D. B. Kearns, *Nat. Rev. Microbiol.* **2010**, 8, 634-644.

56. F. J. Reen, R. Shanahan, R. Cano, F. O'Gara, G. P. McGlacken, *Org. Biomol. Chem.* **2015**, *13*, 5537-5541.
57. J. Perlroth, B. Choi, B. Spellberg, *Med. Mycol.* **2007**, *45*, 321-346.
58. V. Moudgal, J. Sobel, *Expert Opin. Pharmacother.* **2010**, *11*, 2037-2048.
59. J. Chandra, P. K. Mukherjee, M. A. Ghannoum, *Mycoses* **2012**, *55*, 46-57.
60. A. S. Lynch, G. T. Robertson, *Annu. Rev. Med.* **2008**, *59*, 415-428.
61. A. Bink, K. Pellens, B. PA Cammue, K. Thevissen, *Open Mycol.* **2011**, *5*, 29-38.
62. L. J. Holcombe, G. McAlester, C. A. Munro, B. Enjalbert, A. J. Brown, N. A. Gow, C. Ding, G. Butler, F. O'Gara, J. P. Morrissey, *Microbiology* **2010**, *156*, 1476-1486.
63. C. Cugini, D. K. Morales, D. A. Hogan, *Microbiology* **2010**, *156*, 3096-3107.
64. E. Deziel, F. Lepine, S. Milot, J. He, M. N. Mindrinos, R. G. Tompkins, L. G. Rahme, *Proc. Natl. Acad. Sci.* **2004**, *101*, 1339-1344.
65. F. J. Reen, J. P. Phelan, L. Gallagher, D. F. Woods, R. M. Shanahan, R. Cano, E. Ó. Muimhneacháin, G. P. McGlacken, F. O'Gara, *Antimicrob. Agents Chemother.* **2016**, *60*, 5894-5905.
66. A. Y. Peleg, D. A. Hogan, E. Mylonakis, *Nat. Rev. Microbiol.* **2010**, *8*, 340-349.
67. J. J. Speirs, C. K. van der Ent, J. M. Beekman, *Curr. Opin. Pulm. Med.* **2012**, *18*, 632-638.
68. G. Ramage, C. Williams, *Adv. Appl. Microbiol.* **2013**, *84*, 27-83.
69. B. Briard, P. Bomme, B. E. Lechner, G. L. Mislin, V. Lair, M.-C. Prévost, J.-P. Latgé, H. Haas, A. Beauvais, *Sci. Rep.* **2015**, *5*, 8220.
70. A. Paugam, M.-T. Baixench, N. Demazes-Dufeu, P.-R. Burgel, E. Sauter, R. Kanaan, D. Dusser, J. Dupouy-Camet, D. Hubert, *Med. Mycol.* **2010**, *48*, S32-S36.
71. C. Fux, M. Shirtliff, P. Stoodley, J. W. Costerton, *Trends Microbiol.* **2005**, *13*, 58-63.
72. F. J. Reen, J. P. Phelan, D. F. Woods, R. Shanahan, R. Cano, S. Clarke, G. P. McGlacken, F. O'Gara, *Front. Microbiol.* **2016**, *7*(2074).

Chapter 2

Towards the Synthesis of PHT

Introduction

2.1. Crop Protection

The science of crop protection involves managing plant diseases, weeds and other pests (both vertebrate and invertebrate) that damage or inhibit the growth of agricultural crops.^[1] As the world's population continues to grow, the agricultural industry is under increasing pressure to provide not only food, but also crops for conversion into renewable fuels and other raw materials. The demand for higher crop yields per unit area requires chemicals used in crop protection to become ever more sophisticated. In order to contribute to programmes of sustainable crop management, new treatment and prevention products need to display high target specificity, demonstrate benign environmental and toxicological profiles, and be biodegradable.^[2-3] Improved manufacturing processes are also required, because waste generated by the production process mitigates the overall benefit.

2.2. Syngenta

Syngenta is a global agribusiness company that produces agrochemicals and seeds. Headquartered in Basel, Switzerland, Syngenta was formed in 2000 by the merger of the Swiss company Novartis Agribusiness and the British company Zeneca Agrochemicals. In 2017, the company was acquired by ChemChina, a Chinese state-owned chemical enterprise. As a leading agriculture company Syngenta is committed to helping improve global food security by enabling farmers to meet the challenge of feeding a fast-growing population in a sustainable manner.^[4]

2.3. Nicotinic Acetylcholine Receptor (nAChR) Agonists as Insecticides

Nicotinic acetylcholine receptors (nAChRs) are found in the central and peripheral nervous system and muscle tissue of many organisms, including humans.^[5] At the neuromuscular junction, nAChRs are the primary receptor controlling the nerve-muscle communication that controls muscle contraction. Pharmacophores of nAChRs (such as nicotine analogues) continue to be of interest in pharmacological studies on central nervous system (CNS) diseases in humans. In particular, synthetic nAChR ligands have emerged as potential treatments for Parkinson's disease, Alzheimer's disease, Tourette's syndrome, epilepsy, schizophrenia, attention-deficit hyperactivity disorder (ADHD), and depression.^[5-6] In insects, nAChRs are limited to the CNS, and have been a molecular target site in crop protection research for many years.^[7]

The global market for insecticides in 2015 was valued at \$2.6 billion USD, and is estimated to reach almost \$3.5 billion USD by 2021.^[8] The most widely-used class of insecticides are neonicotinoids, which accounted for more than 25% of the global insecticide market in 2014, and are beginning to replace many conventional insecticide classes, such as chlorinated hydrocarbons and organophosphates.^[9] The insecticidal activity of neonicotinoids, which are designed to be chemically similar to nicotine, is attributed to their agonistic action on the nAChRs found in the CNS of insects. Since they selectively target insects, neonicotinoids have been considered to be of low toxicity risk to mammals and humans in comparison to more conventional insecticides.^[10] The first neonicotinoid released to market was imidacloprid in 1991 by Bayer Crop Science AG.^[11-12] Today, imidacloprid and thiamethoxam (Syngenta AG 1998) occupy the leading market share of commercial neonicotinoid insecticides (**Figure 10**).^[13]

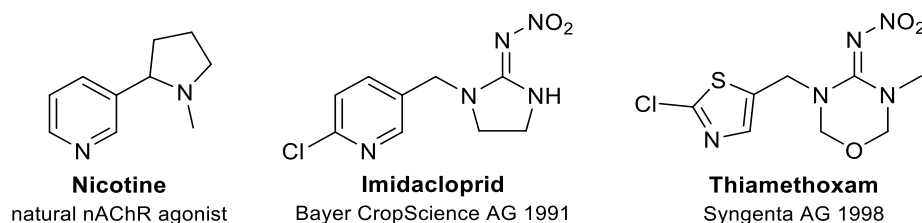


Figure 10 Nicotine and structurally related commercial neonicotinoid insecticides.

As part of the vast research that has gone into developing novel nAChR agonists, the design of nicotine analogues that are more rigid in their structure has been helpful in evaluating the SAR of the receptors.^[14-15] The first highly potent bridged nicotinoid, exhibiting bioactivity surpassing that of the conformationally free parent, was designed and synthesised by Kanne in 1986.^[16] The new derivative, pyrido[3,4-*b*]homotropane (PHT), exhibited three times the toxicological activity and 16 times the receptor binding affinity of nornicotine.^[16]

2.4. Pyridohomotropane (PHT) - Design

PHT is a synthetic bridged hybrid of anatoxin-a and nornicotine (**Figure 11**). Anatoxin-a is a semi-rigid alkaloid toxin which has an affinity for nAChRs that is about 20 times that of acetylcholine.^[17] This highly potent agonist binds irreversibly to the receptor, preventing neuromuscular transmissions and resulting in convulsions, respiratory failure, and eventually death. Due to its superior binding affinity, anatoxin-a has been used in medical studies to evaluate newly-developed agonists or antagonists of nAChRs.^[18-19] Nornicotine is also a potent nAChR agonist in its own right, although its toxicity is significantly less than that of anatoxin-a.^[20] The design of PHT was based on the observation that one of the conformers of nornicotine would position the pyrrolidine *N*-hydrogen (a hydrogen-bond donor) and the pyridine nitrogen lone pair (a hydrogen-bond acceptor) in the same spatial orientation as those found in the *s-cis* conformation of anatoxin-a (**Figure 11**). Insertion of a two-carbon bridge in nornicotine between the C-4 of the pyridine and C-5' of the pyrrolidine would 'freeze' the structure in this conformation.^[16]

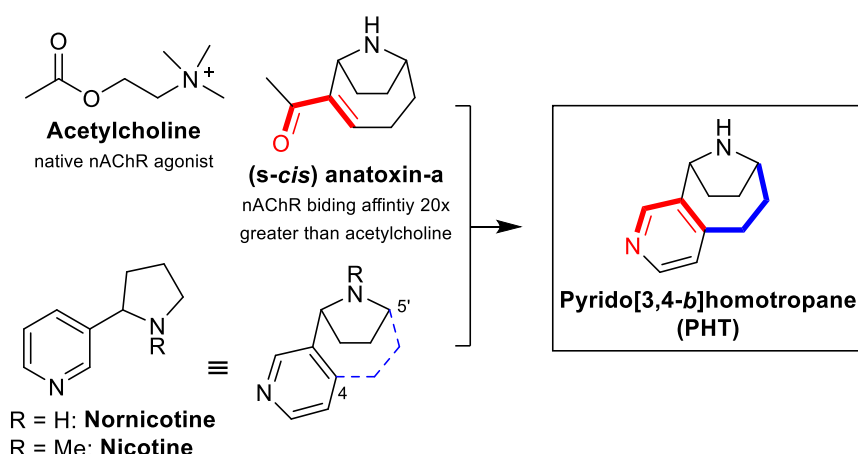
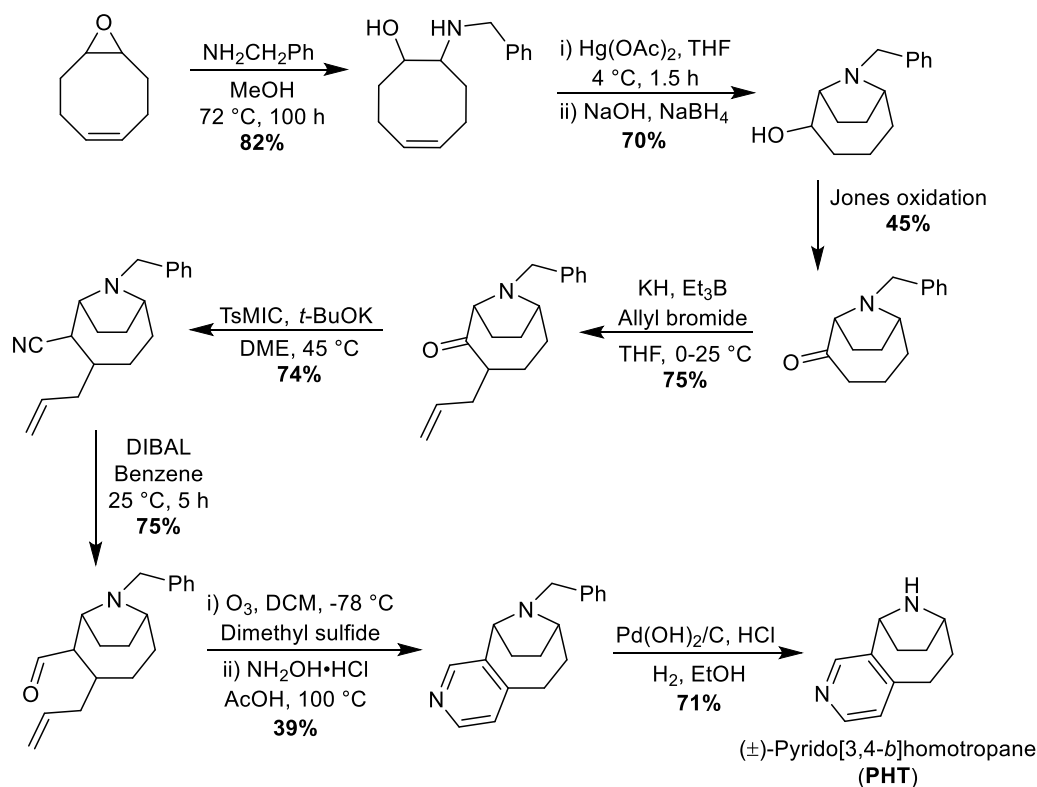


Figure 11 Design of PHT - a hybrid of anatoxin-a and nornicotine.

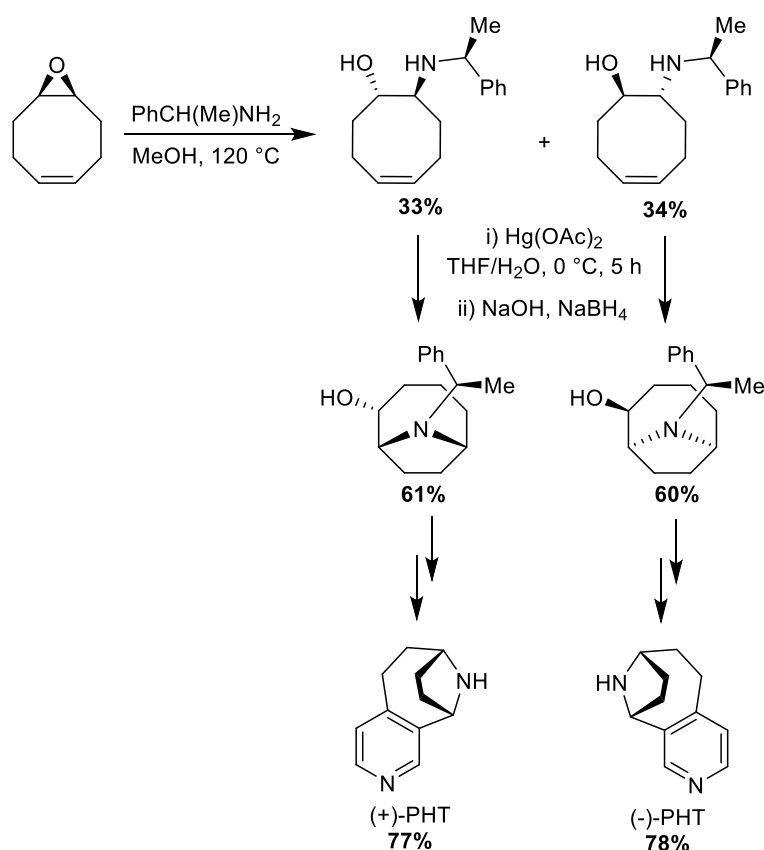
2.4.1. PHT - Previous Synthetic Routes

Kanne and co-workers first described the synthesis of PHT in 1986^[16] and again in 1988^[20] along with some new PHT analogues. This method used 1,2-oxido-5-cyclooctene as the starting material, with eight steps required to reach PHT (**Scheme 14**).



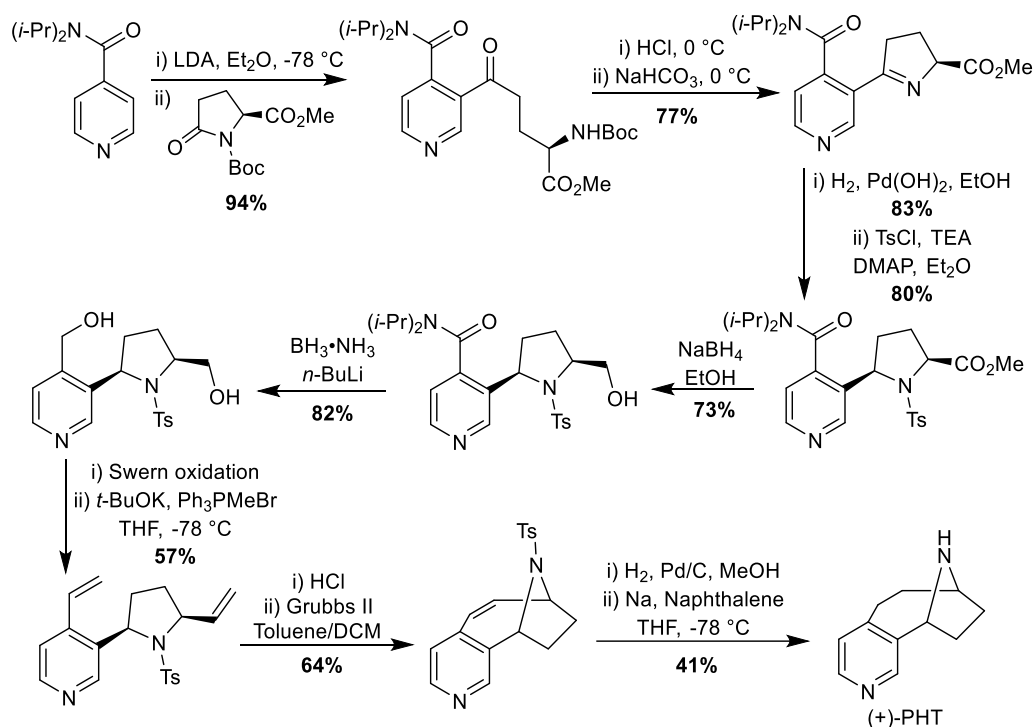
Scheme 14 First synthesis of PHT by Kanne and co-workers (1986).

The first asymmetric synthesis of PHT was described by Carroll and co-workers in 2006, and was carried out using a procedure similar to that reported by Kanne (**Scheme 15**).^[21] (*R*)-(+)-Methylbenzylamine was used instead of benzylamine in the first step to produce diastereomers that could be separated and then converted to (+)-PHT and (-)-PHT using Kanne's method.



Scheme 15 First asymmetric synthesis of PHT by Carroll and co-workers (2006).

This was an important development in the synthesis of PHT as now, for the first time, further insight into the receptor pharmacophore could be established. Indeed, the (+) and (-) enantiomers of PHT exhibit different binding selectivities for different nAChR subtypes, meaning both are highly useful pharmacological probes for studying nAChRs.^[21-22] For example, (+)-PHT exhibits 260 times higher binding affinity than (-)-PHT for the $\alpha 4\beta 2$ nAChR, a major subtype present in the human brain.^[21-22] In 2008, Zhai and co-workers reported a new asymmetric total synthesis of (+)-PHT over 12 steps (**Scheme 16**).^[23]



Scheme 16 Asymmetric synthesis of (+)-PHT by Zhai and co-workers (2008).

2.5. Aims of this Chapter

Despite the interesting bioactivities displayed by PHT in pharmacological studies, there is virtually no data on the insecticidal activity of the compound. The project undertaken at Syngenta Crop Protection in Stein, Switzerland during this PhD was aimed at developing a new total synthesis of PHT that would allow for derivatisation and scale-up to provide material for in-house biological studies. This chapter describes the retrosynthetic analysis and synthetic steps carried out towards a new total synthesis of PHT.

Chapter 2

Towards the Synthesis of PHT

Results & Discussion

2.6. Retrosynthetic Analysis of PHT – Strategy 1

The retrosynthetic strategy for the synthesis of PHT designed during this project is outlined (**Figure 12**). The key step would involve an intramolecular [3+2] cycloaddition of a cyclopropane 1,1-diester with a protected imine. The imine would be derived from an aldehyde on the pyridine ring, therefore compound **47** was a key target in the retrosynthetic plan. Cyclopropanation of a terminal alkene such as **46** with a diazodiester would give access to the cyclopropane diester of **47**. Compound **46** could be formed by alkylation of commercially available 4-methylnicotinaldehyde **36**.

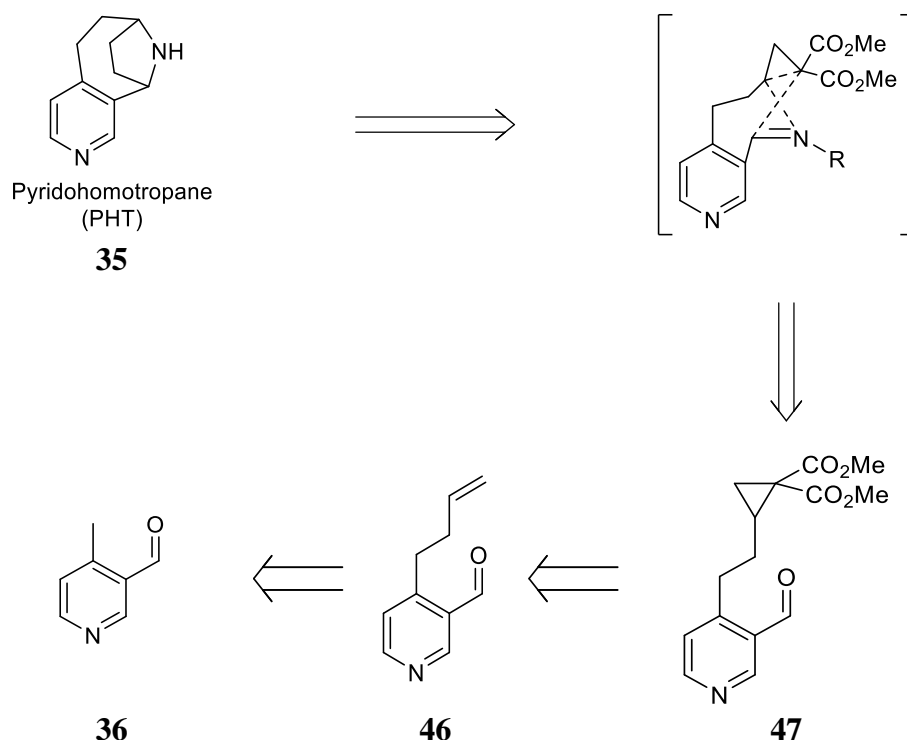
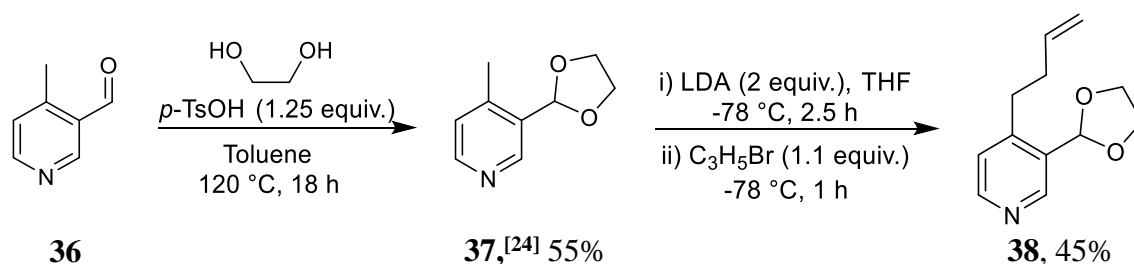


Figure 12 Initial retrosynthetic analysis of PHT **35**.

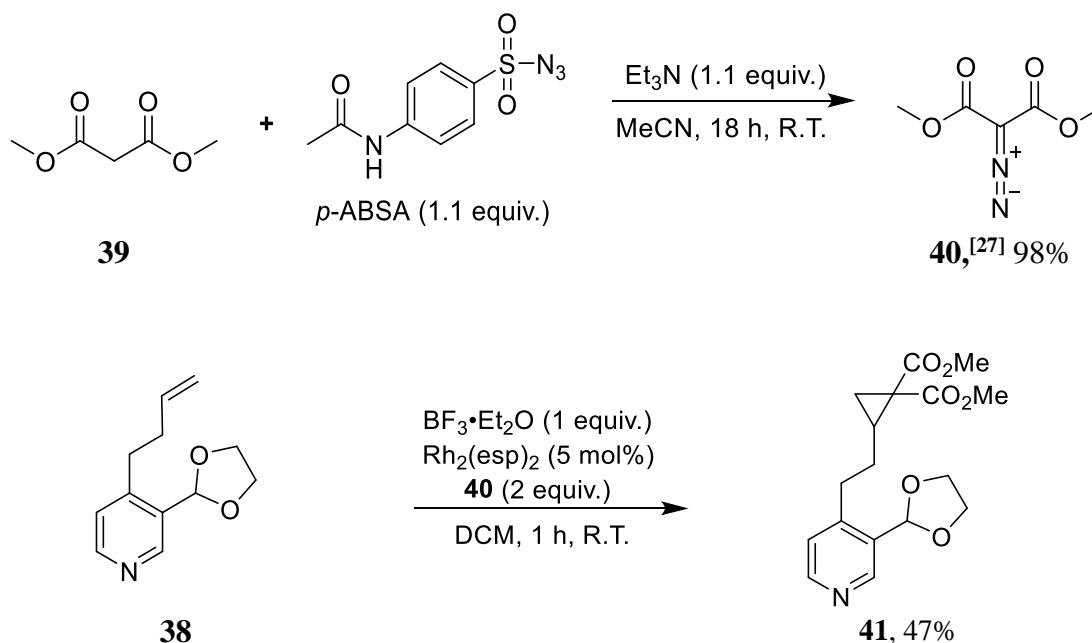
2.7. Route 1 – Beginning from Aldehyde Starting Material

The first challenge was accessing the key cyclopropanated intermediate **47** with the aldehyde at the C-3 position. Commercially available 4-methylnicotinaldehyde **36** was chosen as the starting material for the synthesis of **47**. The idea was to protect the aldehyde as its corresponding acetal **37** while carrying out the alkylation and cyclopropanation steps (**Scheme 17**). Acetal protection was achieved in a moderate 55% isolated yield despite optimisation efforts, while alkylation of **37** gave product **38** in a maximum isolated yield of 45% (formation of di-alkylated side-products proved difficult to completely eliminate).



Scheme 17 Acetal protection and alkylation of the aldehyde precursor.

The next step was to cyclopropanate the terminal alkene of **38** using diazo intermediate **40**. This was synthesised from dimethyl malonate **39** and 4-acetamidobenzene sulfonyl azide (*p*-ABSA) in 98% isolated yield (**Scheme 18**).^[25] This diazo compound **40** was reacted with **38** via rhodium catalysis resulting in cyclopropanation of the terminal alkene to give **41** in 47% isolated yield.^[26] Boron trifluoride diethyl etherate (1 equiv.) was required as an additive to coordinate to the pyridine nitrogen in order to prevent unproductive coordination of the rhodium catalyst. Whilst addition of the diazo compound was carried out dropwise via syringe, it was important to add the diazo reagent over a period of no more than five minutes.



Scheme 18 Synthesis of diazo reagent and subsequent cyclopropanation of **38**.

2.8. Retrosynthetic Analysis of PHT – Strategy 2

Concurrently with the synthetic strategy outlined above, an alternative route to access the key intermediate **47** was investigated. This route was based on the idea of using a nitrile group on intermediate **44** as a ‘masked aldehyde’ rather than acetal protection (**Figure 13**).

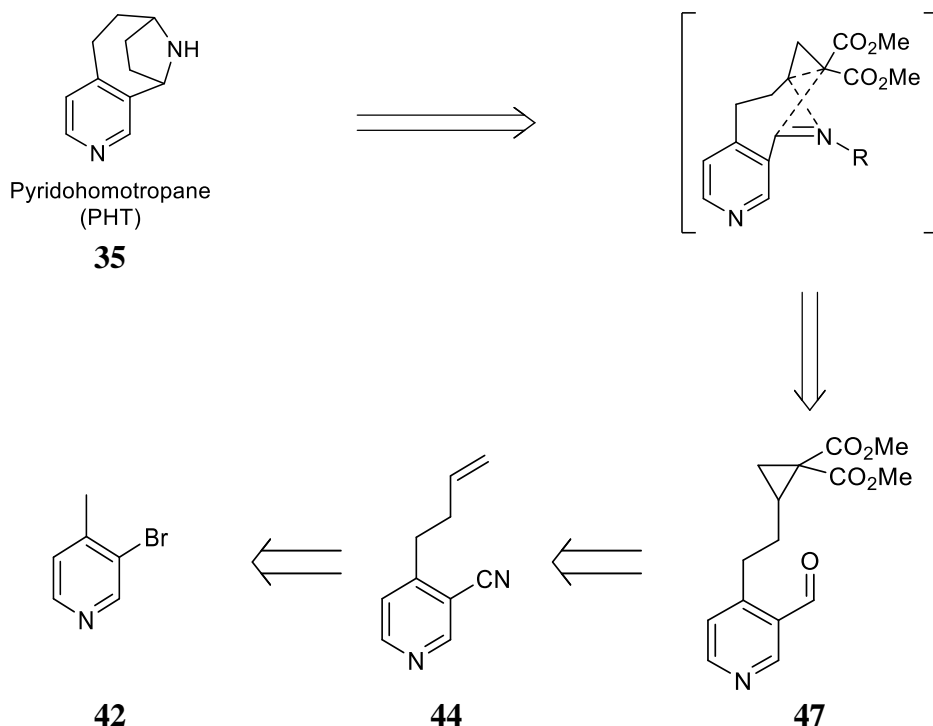
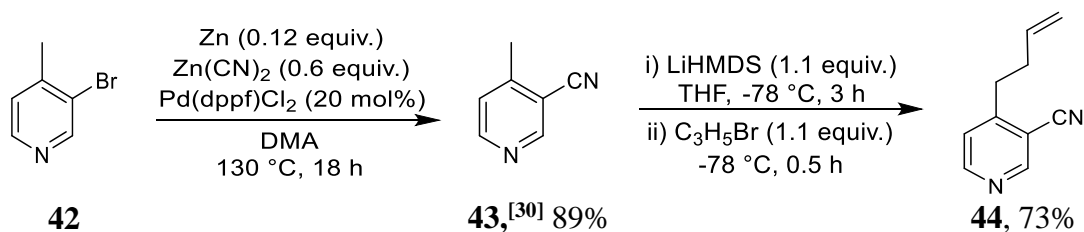


Figure 13 Alternative retrosynthetic plan for PHT synthesis.

2.9. Route 2 – Utilising the Nitrile Group as a ‘Masked’ Aldehyde

This route began with commercially available 3-bromo picoline **42**, which underwent cyanation at the C-3 position (**Scheme 19**).^[28] This gave access to the ‘masked aldehyde’ precursor **43** in 89% isolated yield, which then underwent alkylation at the methyl group to give compound **44** in 73% isolated yield (**Scheme 19**).^[29]

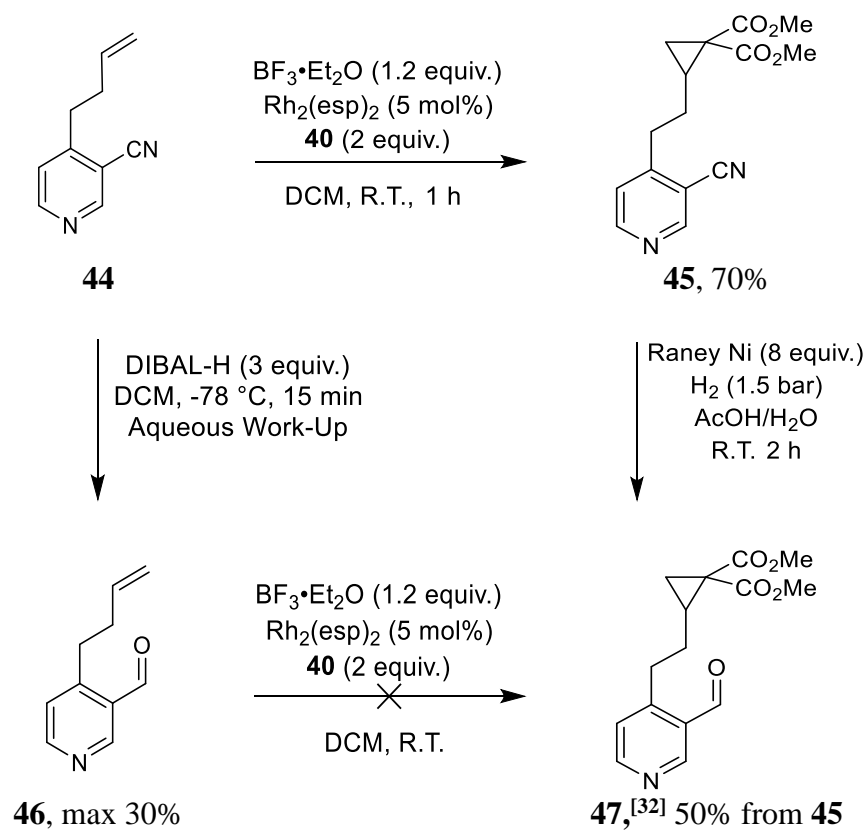


Scheme 19 Nitrile synthesis and subsequent alkylation.

Gratifyingly, these yields were a significant improvement on the first two steps compared to the original aldehyde route which gave maximum isolated yields of 55% (**37**) and 45% (**38**), respectively (**Scheme 17**). This was an important factor to consider when choosing which synthetic route to progress with later, as it would be necessary to access large quantities of intermediate products. Clearly, using the nitrile-masked aldehyde rather than the acetal-protected aldehyde was a better choice as it provided access to intermediate **44** with better yields in each step.

2.10. Accessing Key Intermediate **47**

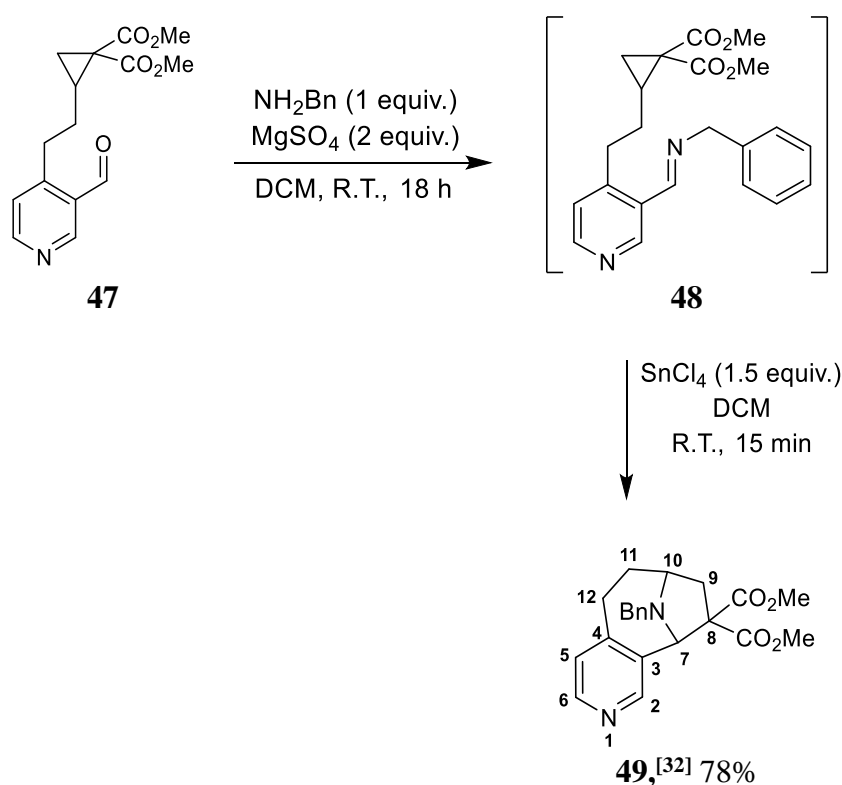
At this point the next goal was to reach the key aldehyde intermediate **47**, which could be obtained via either of two approaches: 1) first reduce the nitrile to the aldehyde, followed by cyclopropanation of the terminal alkene, or 2) carry out cyclopropanation first and then reduce the nitrile (**Scheme 20**). The determining step turned out to be the cyclopropanation – while this proceeded well in the presence of the nitrile, furnishing the cyclopropanated product **45** in 70% isolated yield, attempts to carry out the same reaction in the presence of the aldehyde **46** failed to yield any product. Notwithstanding this, reducing the nitrile group on compound **45** proved challenging due to the tendency of the aldehyde product to further reduce to the corresponding primary alcohol. Under optimum conditions,^[31] the desired aldehyde **47** could be obtained in 50% isolated yield, with the remainder of the mixture comprising of starting material and the alcohol side-product.



Scheme 20 Options for synthesis of aldehyde intermediate **47** from **44**.

2.11. Building the Bicyclic PHT Framework

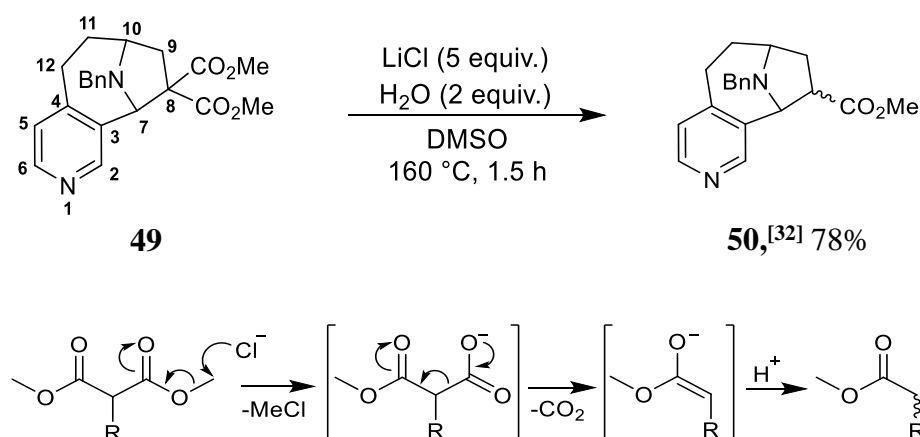
Next was the key step in this strategy, an intramolecular [3+2] cycloaddition of the cyclopropane 1,1-diester with a protected imine, forming the structural framework of the PHT molecule. First, the aldehyde was stirred with benzylamine in the presence of a drying agent (magnesium sulphate proved best) to give the imine intermediate **48** in quantitative yield (**Scheme 21**). Tin (IV) chloride was employed as a Lewis acid to promote the cycloaddition reaction; pleasingly, this reaction led to isolation of compound **49** in 78% isolated yield.^[33]



Scheme 21 Imine formation and intramolecular [3+2] cycloaddition.

2.12. Krapcho Decarboxylation – Removing the First Ester Group

With the PHT framework now constructed, the following steps were to involve removing the extraneous functional groups (i.e. the diester at C-8 and the benzyl group on the amine) from the molecule. Krapcho decarboxylation conditions^[34] were used to remove the first ester group, which gave the monoester **50** as a 1:1 mixture of diastereomers in 78% isolated yield (**Scheme 22**). Separation of the diastereomers was not attempted as this was not deemed necessary at the time (**Figure 14**).



Scheme 22 Krapcho decarboxylation of the diester **49** and associated mechanism.

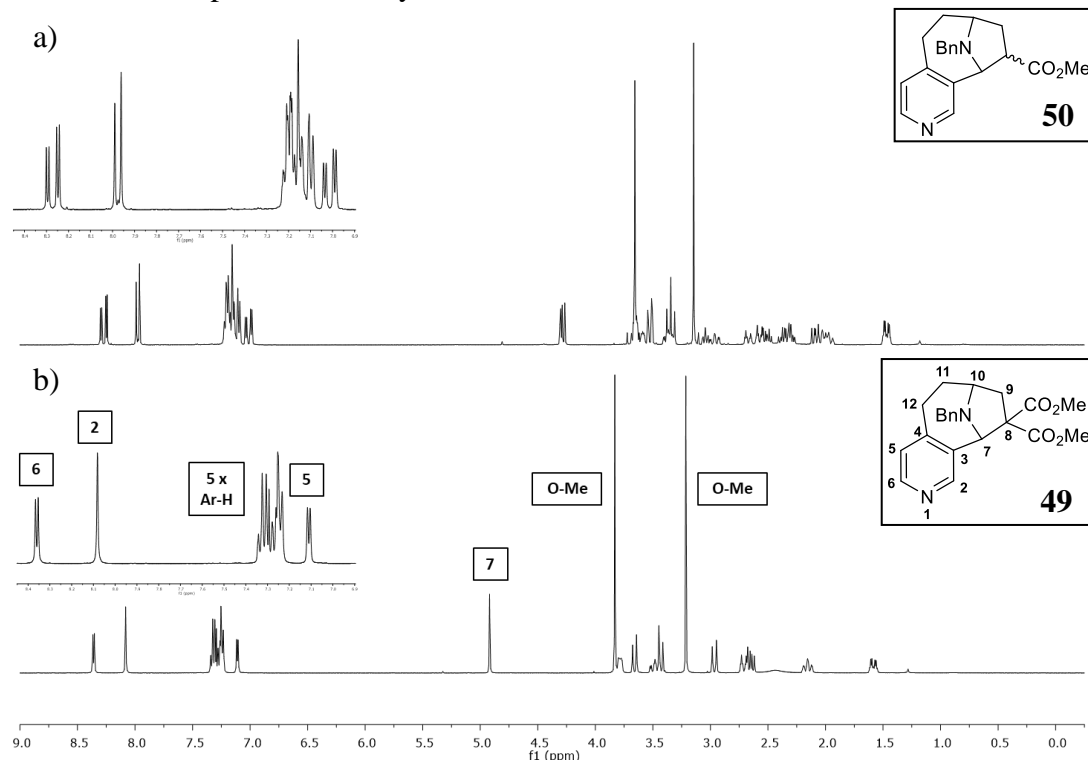


Figure 14 a) ¹H-NMR (CDCl₃) spectrum of diastereomeric mixture of **50**. b) ¹H-NMR (CDCl₃) spectrum of diester **49**.

2.13. Barton Decarboxylation – Removing the Remaining Ester Group

To remove the remaining ester group, a Barton decarboxylation was investigated. This involves a radical-mediated reaction in which a carboxylic acid or acid chloride is first converted to a thiohydroxamate ester (commonly referred to as a Barton ester) by coupling with pyrrhione.^[35-36] This intermediate is then heated in the presence of a radical initiator and a suitable hydrogen donor to complete the reductive decarboxylation of the carbonyl compound (**Figure 15**). For carboxylic acids, the reaction with pyrrhione requires the addition of a stoichiometric coupling reagent, such as DCC or EDC, as well as a non-nucleophilic base such as DMAP, to generate the thiohydroxamate ester.^[37] In reactions where the carboxylic acid is first converted to the corresponding acid chloride, the sodium salt of pyrrhione along with a catalytic amount of DMAP is used to form the Barton ester.^[37]

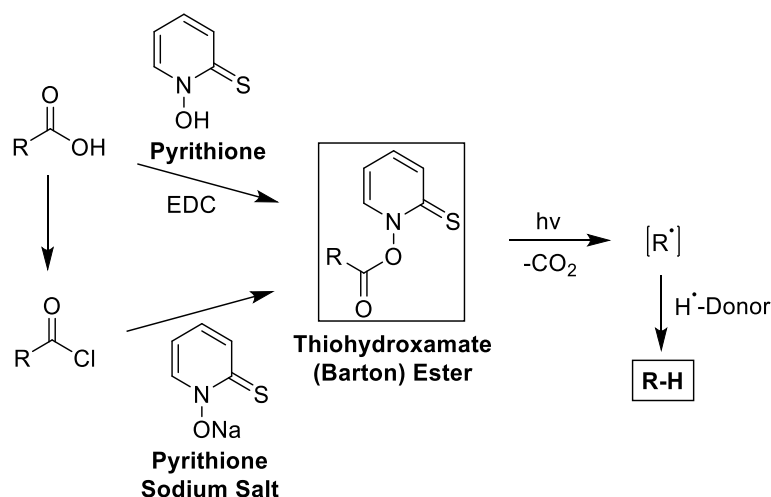
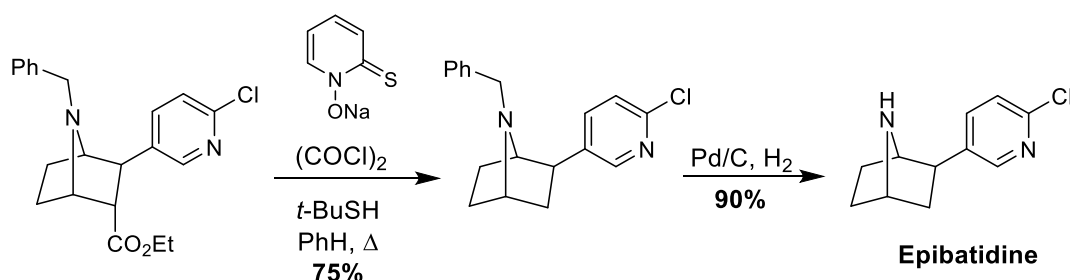


Figure 15 Barton decarboxylation of carboxylic acids and acid chlorides.^[37]

This method was chosen based on a literature precedent for the synthesis of epibatidine by Pandey and co-workers,^[38] which also provided a precedent for the final debenzylation step. For the decarboxylation, Pandey and co-workers converted their ethyl ester to the acid chloride and then treated this with the sodium salt of pyrrhione to produce the Barton ester. This highly reactive intermediate then underwent radical decarboxylation as per Barton's conditions to give the desired product in 75% isolated yield. The subsequent debenzylation step furnished epibatidine in 90% isolated yield (**Scheme 23**).



Scheme 23 Barton decarboxylation and debenzylation steps in the synthesis of epibatidine.

Under Barton's original decarboxylation conditions, the hydrogen-donor reagents typically used are tributyltin hydride or *tert*-butyl thiol, which are not only highly toxic (organotin compounds) and pungent (thiols), but their by-products are often difficult to separate from the target compound. Whilst reviewing the literature in an effort to find conditions which avoid these complications, a report from Williams and co-workers in 2011 proved insightful.^[37] Therein, the use of chloroform as both a suitable solvent and convenient H-donor for the Barton decarboxylation was demonstrated on a range of substrates, producing yields that were comparable to (and in some cases better than) those obtained from traditional H-donors such as organotin and thiol reagents. Given these apparent advantages, the Williams version of the Barton conditions was chosen as a starting point for carrying out the desired transformation.

2.13.1. Barton Decarboxylation of Model Substrates

To garner some experience on this type of chemistry, the Williams method was tried on a selection of model substrates (**Figure 16**). The models were chosen based on their structural similarity to PHT (compounds **51** and **52**). A substrate similar to one used in the Williams paper (compound **53**) was also included.

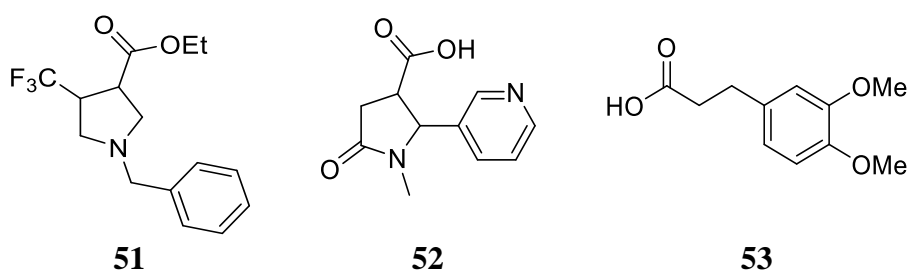
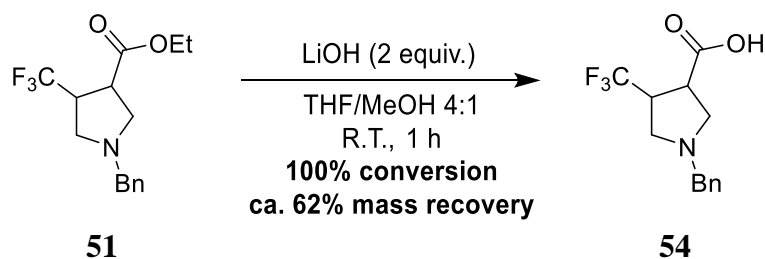


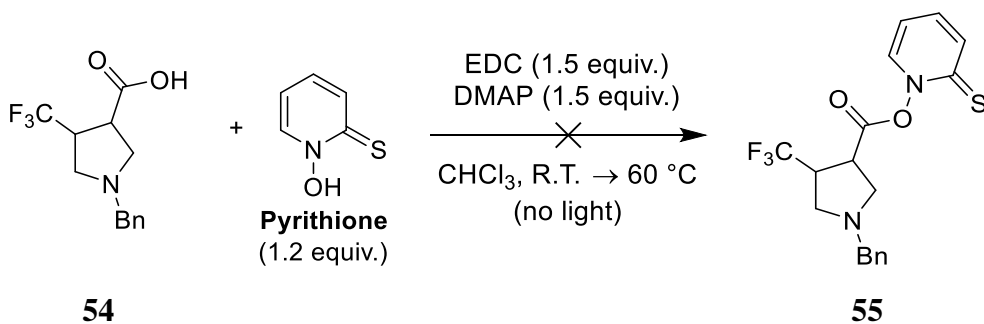
Figure 16 Model substrates for Barton decarboxylation.

Model compound **51** was first hydrolysed to the corresponding acid **54** using lithium hydroxide in a mixture of methanol and THF (**Scheme 24**).



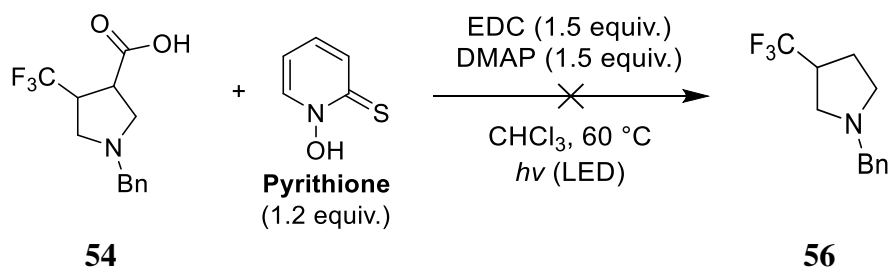
Scheme 24 Hydrolysis of ester **51**.

The carboxylic acid was then subjected to Williams' decarboxylation conditions in the absence of light and heat, in an effort to form the Barton ester **55** (**Scheme 25**). After 2 h only starting material and no product could be observed by LCMS analysis. The reaction was heated at reflux for a further 2 h but no improvement was observed.



Scheme 25 Attempted formation of the Barton ester of **54**.

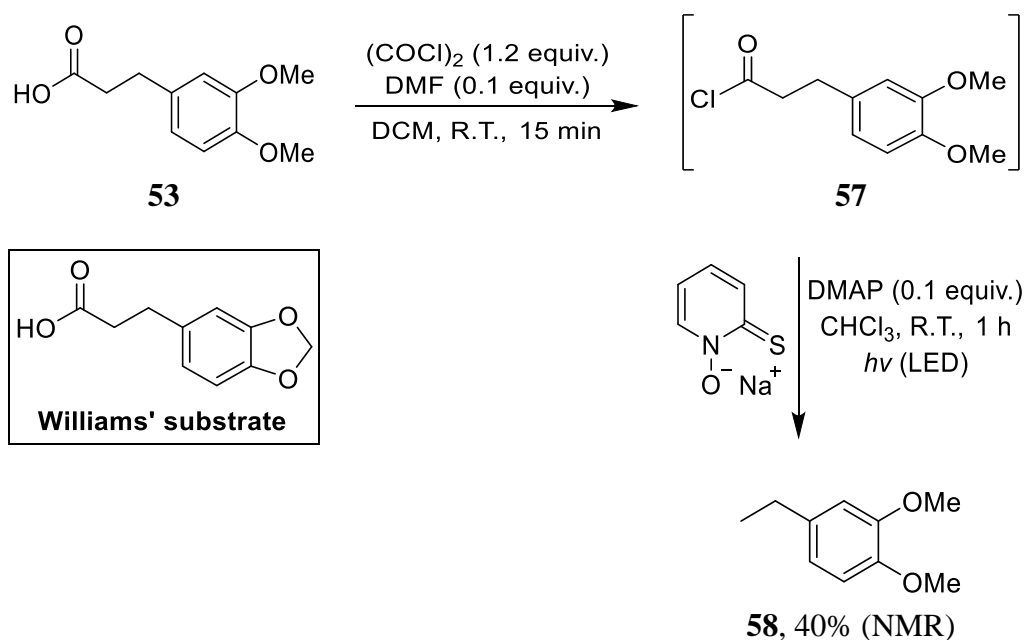
At this point, after reviewing the literature, it became evident that the Barton ester itself would be very difficult to isolate. Instead, the formation of the Barton ester and the decarboxylation was tried in one pot. This time, the pyridine-2-thione was added to a pre-mixed suspension of **54**, EDC and DMAP, and the reaction mixture was immediately irradiated with visible light from an LED lamp and heated at reflux (**Scheme 26**). The decision to use an LED lamp rather than a tungsten light bulb was made with the intention to eliminate an additional heat source from the reaction set-up, and allow for controlled monitoring and manipulation of the reaction temperature through use of an oil bath. As both light sources emit visible light, failure of the decarboxylation reaction merely due to the choice of lamp was not considered likely.



Scheme 26 Attempted Barton decarboxylation of **54**.

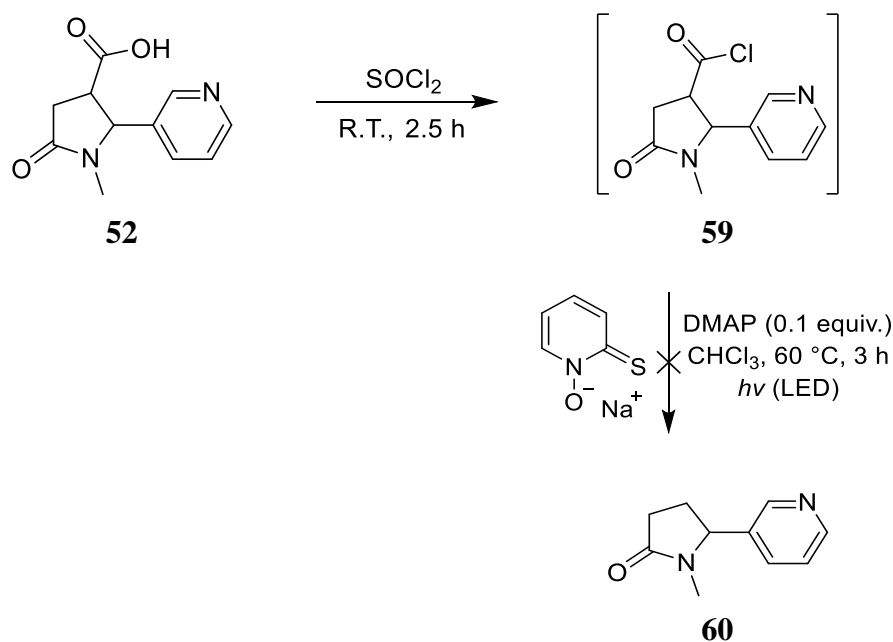
Unfortunately, only starting material could be observed by LCMS analysis, even after 6 h. At this point, having consumed all of model compound **51**, attention was turned to the remaining model compounds **52** and **53**.

Model compound **53** was chosen from an in-house library of compounds as it was very similar to one of Williams' substrates which was decarboxylated in 77% isolated yield.^[37] Following Williams' method, compound **53** was first converted to the corresponding acid chloride **57** and used immediately in the Barton step without further purification (**Scheme 27**).^[37] This time, the decarboxylated product **58** could be obtained in 40% yield by quantitative ¹H-NMR analysis of the crude reaction mixture. This was a poorer yield than expected, however the fact that the reaction yielded some product was a positive outcome.



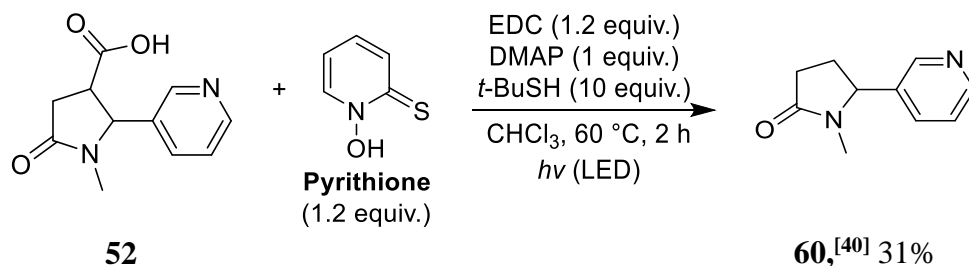
Scheme 27 Chlorination and decarboxylation of **53**.

A more substantial proof-of-principle for these conditions would be their successful application to a heterocyclic compound like the target PHT. Therefore, the acid chloride decarboxylation that proved successful for **53** was performed on nicotine analogue **52**. In this case, thionyl chloride proved to be a better chlorinating agent than oxalyl chloride and gave the acid chloride **59** in quantitative yield (**Scheme 28**). However, after **59** was added to the reaction mixture for the subsequent decarboxylation, no decarboxylated product **60** could be detected by analytical methods, even after stirring for 3 h at 60 °C.



Scheme 28 Chlorination and attempted decarboxylation of model compound **52**.

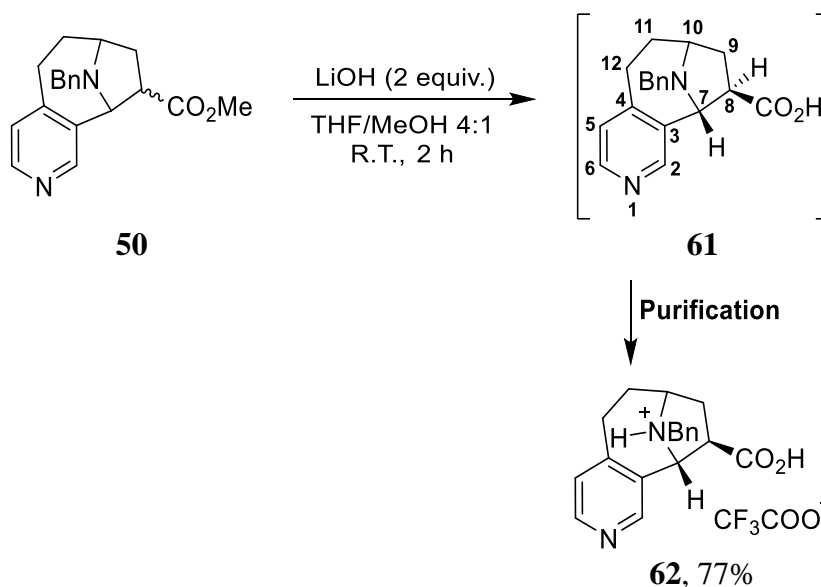
At this point it was clear that the acid chloride **59** was unsuitable for this reaction and so focus returned to decarboxylation conditions for carboxylic acid **52**. An observation, made by Martin and co-workers,^[39] regarding the inefficacy of chloroform as a H-atom donor in these types of reactions led to the decision to include *t*-butyl thiol in the reaction conditions. Pleasingly, using the original conditions for the decarboxylation of carboxylic acids reported by Williams and co-workers and by including *t*-butyl thiol as a more reactive H-atom donor, the decarboxylated nicotine analogue **60** was obtained in 31% isolated yield (**Scheme 29**).



Scheme 29 Decarboxylation of model compound **52**.

2.13.2. Attempts to Perform Barton Decarboxylation on PHT Substrate

Having achieved a better understanding of the intricacies of this transformation, the decarboxylation of the PHT framework could now be pursued. Hydrolysis of the monoester **50** proceeded well under the same conditions used for model substrate **51**. Unfortunately, several attempts to isolate **61** from the reaction mixture with aqueous work-ups led to loss of product to the aqueous layer each time. However, the product could be isolated in an analytically pure form (as its TFA salt) by reverse phase chromatography, to give **62** in 77% isolated yield (**Scheme 30**). Isolation of **62** in this manner was performed by a dedicated purifications laboratory at Syngenta.



Scheme 30 Hydrolysis of monoester **50**.

Interestingly, despite starting with a mixture of diastereomers of **50**, only the *anti*-isomer of the carboxylic acid was observed, probably due to epimerisation to the more stable configuration during the hydrolysis reaction. The *anti*-isomer was identified based on the coupling constant of the C-7 proton in the ¹H-NMR spectrum ($J = 2.3\text{ Hz}$). Computational work carried out by a

previous member of the group predicted the 3J coupling constants of both the *syn*- and *anti*-isomers of compound **50** (Figure 17).^[41] On that occasion, the diastereomers of **50** had been separated by chiral chromatography, and their individual coupling constants were also measured experimentally. As mentioned earlier, the diastereomers of **50** were not separated during this PhD project.

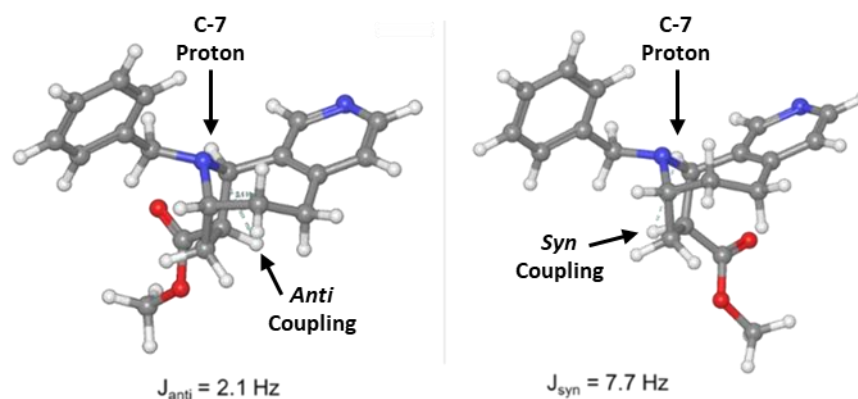
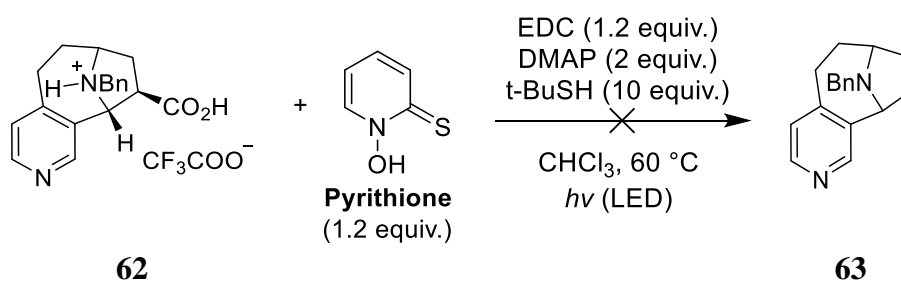


Figure 17 Computed 3J coupling constants for compound **50**, calculated with Maestro software by Schrödinger on the optimized structures. Experimental ^1H -NMR coupling constants are: $J_{\text{anti}} = 2.2 \text{ Hz}$ and $J_{\text{syn}} = 9.2 \text{ Hz}$. This work was carried out prior to the project discussed in this PhD thesis.^[41]

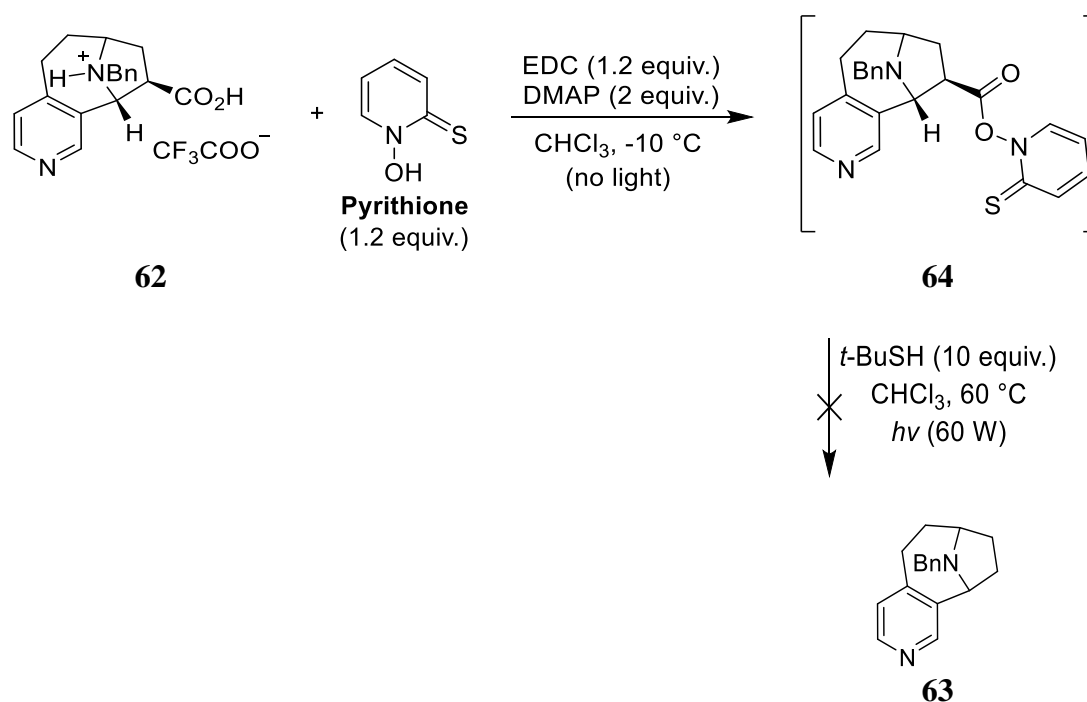
The carboxylic acid salt **62** was subjected to the same decarboxylation conditions that proved effective on the model substrate **52**. However, this did not yield any of the decarboxylated product **63** (Scheme 31).



Scheme 31 Attempted decarboxylation of **62**.

Next, a more careful, step-wise approach was tried whereby a chloroform solution of **62**, EDC and DMAP was first cooled to $-10\text{ }^{\circ}\text{C}$ and shielded from any light by wrapping the reaction vessel in aluminium foil (Scheme 32). Next, pyridine was added and the resulting mixture stirred in darkness at $-10\text{ }^{\circ}\text{C}$ for 1 h and then at room temperature for 1 h. This was done in an effort to allow the formation of the Barton ester **64** which is the key intermediate in the decarboxylation. Unsurprisingly however, efforts to observe this intermediate by LCMS, TLC

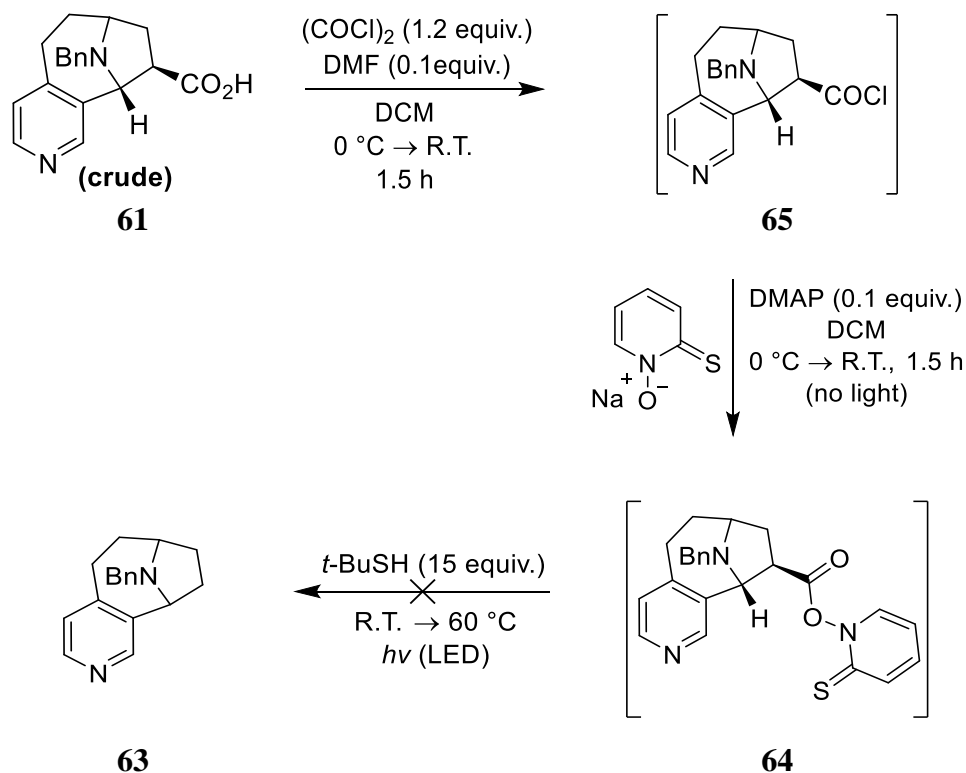
or $^1\text{H-NMR}$ proved unsuccessful. Nevertheless, *t*-butyl thiol was added and the reaction mixture was immediately irradiated with visible light, this time from a tungsten lamp, and heated at reflux. Unfortunately, reaction monitoring by LCMS showed no trace of the decarboxylated product **63** after 3 h, and so the reaction was cooled and concentrated *in vacuo*. $^1\text{H-NMR}$ analysis of the crude reaction mixture revealed a complex mixture comprising mainly of an unknown compound retaining the carbonyl group at C-8. No signals consistent with the desired product could be detected.



Scheme 32 Step-wise approach to decarboxylation of **62**.

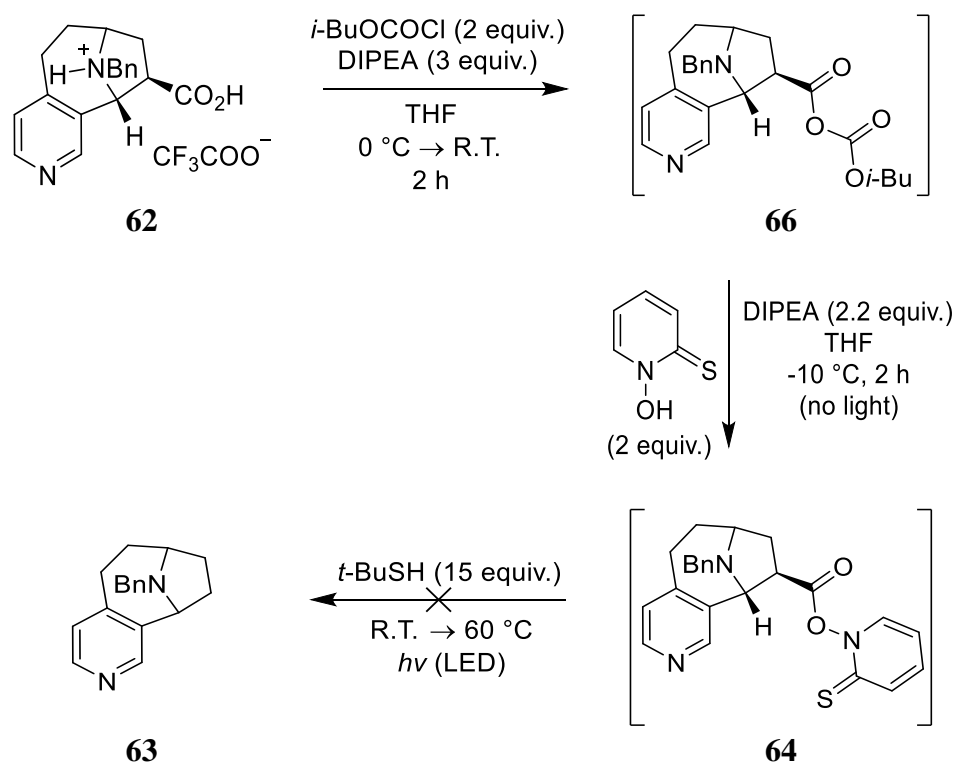
Given that decarboxylation of the acid chloride variant of model compound **53** proved to be effective (**Scheme 27**), the next approach was to apply these conditions to the PHT analogue. Hsung and Gerasyuto used a similar approach in their synthesis of the quinolizidine alkaloid 2-deoxylasubine II.^[42] On this occasion, the crude carboxylic acid product **61** was used, as there was not enough time left in the project to wait for purification (as mentioned previously, the isolation of the TFA salt **62** was carried out by a different lab and could take up to 2 weeks to complete). The crude acid was then chlorinated using oxalyl chloride as per Hsung's procedure (**Scheme 33**). The crude acid chloride **65** was then added to a chilled solution of the pyridithione sodium salt and DMAP in DCM and stirred in darkness for 1.5 h in an attempt to form the Barton ester **64**. However, in line with previous attempts, **64** could not be observed by analytical methods. Next, *t*-butyl thiol was added to the reaction mixture, which was

immediately irradiated with visible light from an LED lamp. After stirring at room temperature for 1 h and then heating at reflux for 3 h, no decarboxylated product **63** could be observed by LCMS analysis.



Scheme 33 Chlorination and attempted decarboxylation of **61**.

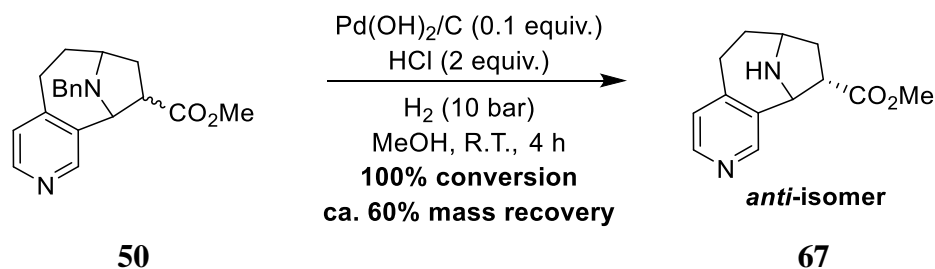
At this point, with only a small amount of the TFA salt **62** left, one final attempt at the decarboxylation was made. This was once again based on Hsung's work, and methodology used for the total synthesis of myrrhine.^[43] Rather than an acid chloride, this method uses a mixed anhydride intermediate to activate the carbonyl group. Although complete consumption of the starting material **62** and formation of the mixed anhydride intermediate **66** was observed by LCMS analysis, once again the decarboxylated product **63** could not be detected (**Scheme 34**).



Scheme 34 Attempted decarboxylation of **62** via a mixed anhydride intermediate.

2.14. Proof-of-Principle Debenzylation

At this point it became clear that the second decarboxylation of compound **50** was not going to be achieved during the timeframe of this work placement. In an effort to support that the final product PHT could be reached once the decarboxylation step was accomplished, debenzylation of monoester **50** was carried out. Indeed, hydrogenolysis of **50** using Pearlman's catalyst led to formation of the free amine **67** (**Scheme 35**).^[20]



Scheme 35 Debenzylation of **50**.

Evidence for the disappearance of the benzyl group can be seen in the ^1H -NMR spectra below (**Figure 18**). For clarity, the ^1H -NMR spectrum of the diester **49** is shown, as the monoester **50** was isolated as a 1:1 mixture of diastereomers. The two 1H doublets corresponding to the diastereotopic benzylic protons at 3.40 and 3.65 ppm, as well as the 5H multiplet of the phenyl

group at 7.21-7.36 ppm, are no longer present in the ^1H -NMR spectrum of **67**. This is a good indication that, providing that the Barton decarboxylation be optimised, this total synthesis of PHT could be completed.

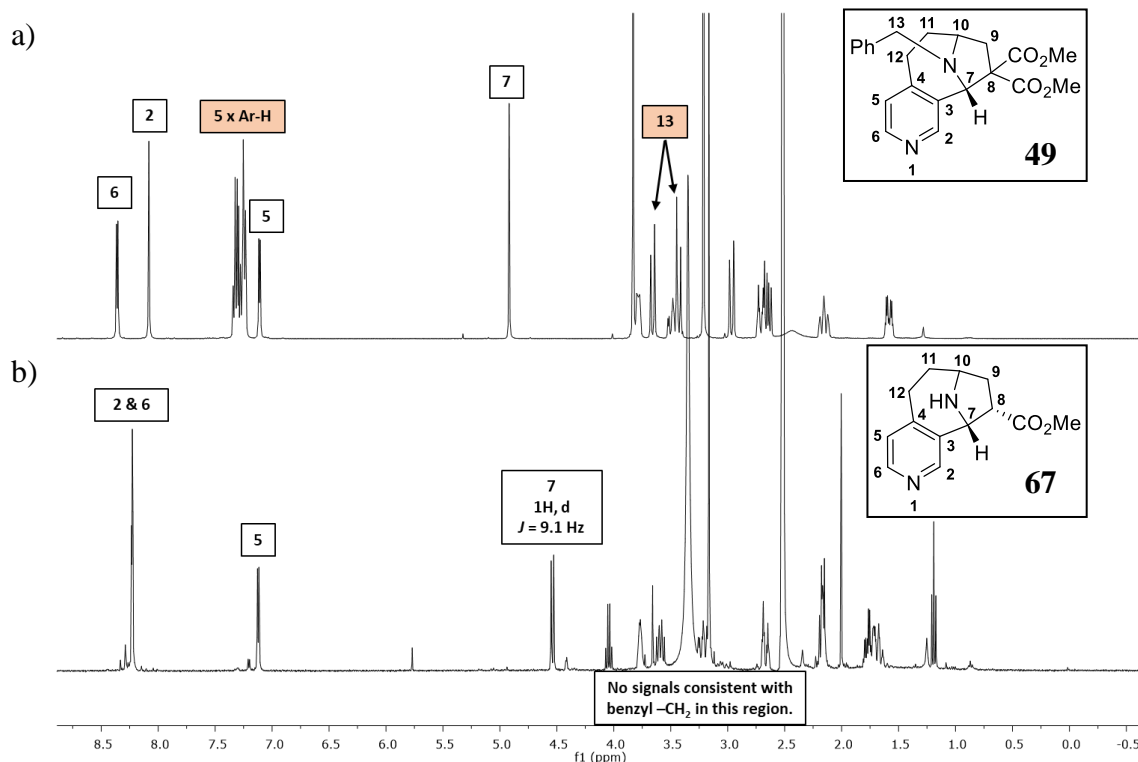


Figure 18 a) ^1H -NMR (CDCl_3) spectrum of diester compound **49**. b) ^1H -NMR ($\text{DMSO}-d_6$) spectrum of crude product **67** from debenzilation of monoester **50**.

Interestingly, the free amine product **67** was observed as a single, *syn*-isomer, as indicated by the large coupling constant ($J = 9.1$ Hz) of the CH -7 doublet at 4.55 ppm. The *anti*-isomer may have become trapped in the aqueous layer during work-up due to coordination with water molecules (**Figure 19**). Indeed, LCMS analysis of the aqueous layer indicated that some product was still present after several extractions with EtOAc.

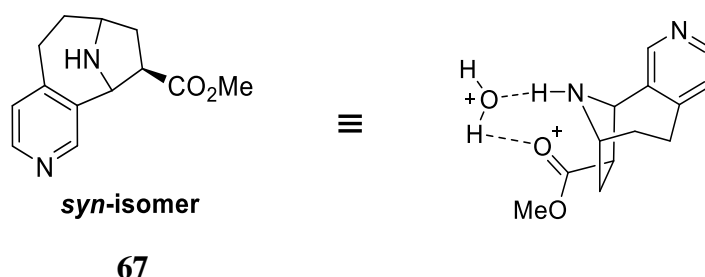


Figure 19 Possible trapping of *syn*-isomer of **67** in aqueous layer due to H-bonding.

Unfortunately, the contract under which the above work was carried out came to an end before any further attempts at completing the total synthesis could be made. In compliance with a

confidentiality agreement between the student and Syngenta, no further investigations could be carried out upon returning to University College Cork.

2.15. Conclusions

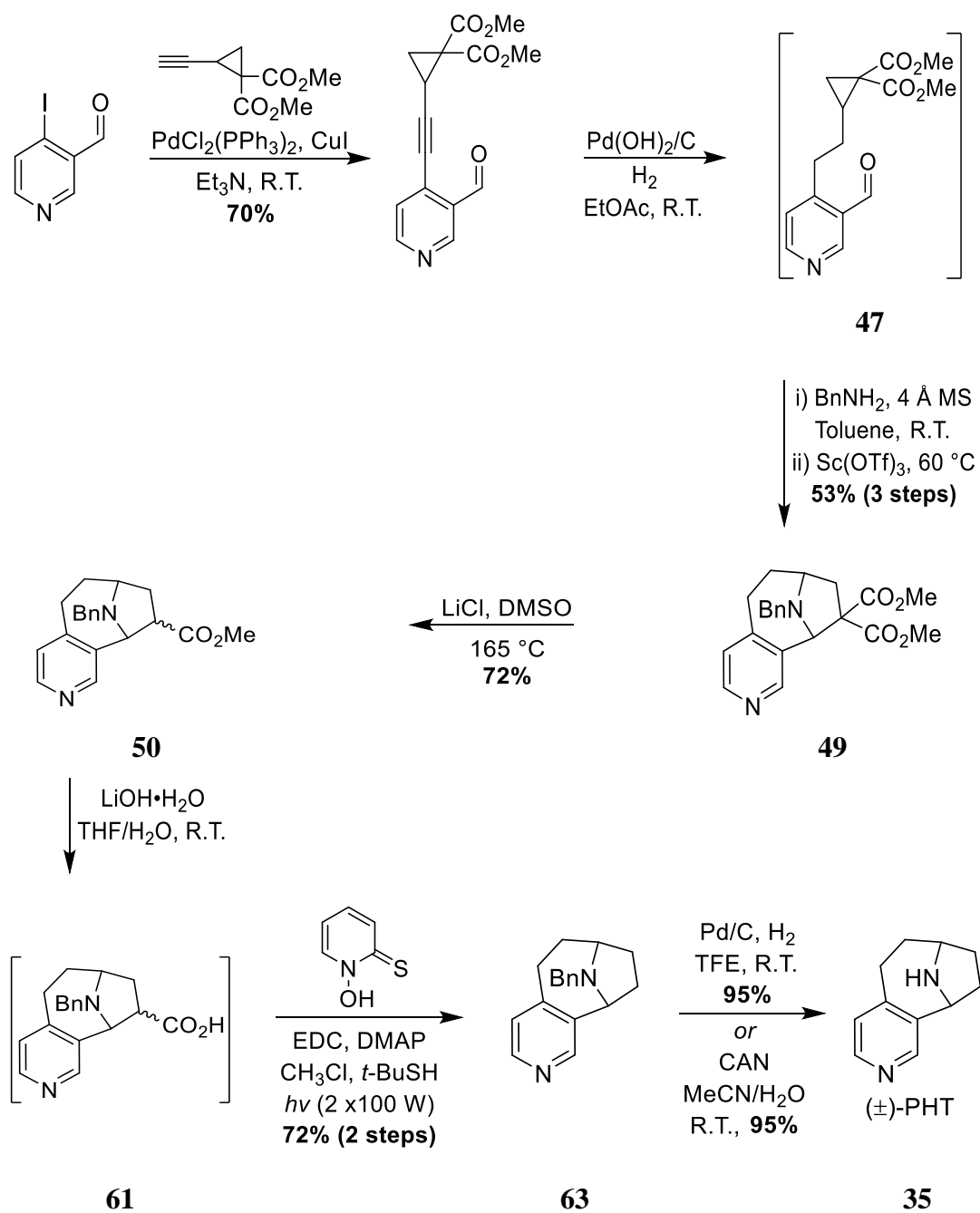
A new route towards the total synthesis of PHT was developed, which was envisaged to be completed in eight steps. After investigating two different retrosynthetic plans, the first six steps were optimised to produce good to excellent yields of compounds **43**, **44**, **45**, **47**, **49** and **50**. Pleasingly, the key [3+2] cycloaddition step, which was required to access the bridged bicyclic framework of PHT, worked efficiently (**Scheme 21**). The methodology of the photochemical Barton decarboxylation proved very difficult to apply consistently to model substrates, although some proof-of-principle results were achieved, such as the decarboxylation of models **52** (**Scheme 29**) and **53** (**Scheme 27**). However, ultimately, decarboxylation of the PHT substrate **61** could not be achieved despite several attempts using various different approaches. A proof-of-concept debenzoylation of intermediate compound **50** indicated that if the challenges of the decarboxylation step could be overcome, the target compound **35** would indeed be accessible using this novel synthetic route (**Scheme 35**).

2.16. Publication of Completed Total Synthesis of PHT in 2018

Interestingly, in 2018 Wang and co-workers published their total synthesis of PHT (**Scheme 36**) using the same intramolecular [3+2] cycloaddition strategy we had planned (**Scheme 21**).^[32] Most importantly, they were able to perform the Barton decarboxylation of compound **61**, under conditions similar to those in **Scheme 31**, in 72% yield. Their success appears to be owed to the use of two 100 W tungsten lamps as the light source, as opposed to our use of an LED lamp or a single 60 W tungsten lamp. Additionally, Wang and co-workers managed to extract the neutral carboxylic acid compound **61** from the hydrolysis reaction mixture by using a sat. NH₄Cl aqueous work-up. Our initial attempt at an aqueous work-up of this reaction mixture (**Scheme 30**) led to significant loss of material to the water layer. Not wanting to waste anymore of the monoester **50**, on the next attempt, reverse-phase chromatography of the reaction mixture was used to isolate the carboxylic acid as its TFA salt (**62**), without pursuing any other work-up methods. Our use of the salt **62** and insufficient light power appear to be the reasons why our decarboxylation reactions failed.

After obtaining the decarboxylated product **63**, Wang and co-workers next carried out the debenzylation of this compound, which led to isolation of the target, PHT (**Scheme 36**). This report also included an asymmetric synthesis of (-)-PHT, using the same approach as shown in **Scheme 36**.

This publication proves that the synthetic strategy outlined in the above work was viable and that, perhaps with more time, completion of this total synthesis of PHT would have been achieved.



Scheme 36 Total synthesis of PHT by Wang and co-workers (2018).^[32]

Chapter 2

Towards the Synthesis of PHT

Experimental

2.17. General Considerations

Solvents and reagents were used as obtained from commercial sources, without purification. Unless otherwise indicated, starting materials were also obtained from commercial sources. Flash chromatography was carried out on a Teledyne Isco Combiflash® Rf 200i automated chromatography machine. TLC was carried out on pre-coated silica gel glass plates (Merck 60G F254). The developed plates were visualised under UV light.

Melting points were obtained using SRS (Stanford Research Systems) Optimelt V.1.107. IR spectra were recorded on a Perkin Elmer UATR Two spectrometer. All samples were examined as neat oil or solid samples. LCMS analysis was obtained on a Waters SQD/SQDII single quadrupole mass spectrometer equipped with an electrospray source and a Waters Acquity UPLC; column: Waters UPLC HSS T3, 1.8 μm , 30 x 2.1 mm, Temp: 60 °C, DAD Wavelength range (nm): 210 to 500; solvent gradient: A = water + 5% MeOH + 0.05 % HCOOH, B= Acetonitrile + 0.05 % HCOOH, gradient: 10-100% B in 1.2 min; flow (ml/min) 0.85. HRMS were recorded on a Thermo Q Exactive in ESI+ mode. Reported results are all within the range of ± 5 ppm of the calculated mass. For brominated compounds, Br⁸⁰ was used for the calculated and reported molecular ion mass.

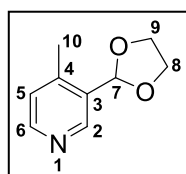
NMR spectra were run in CDCl₃ using TMS as the internal standard at 25 °C unless otherwise stated. ¹H-NMR (400 MHz) spectra were recorded on a Bruker Avance 400 NMR spectrometer. ¹³C-NMR (100 MHz) spectra were recorded on a Bruker Avance 400 NMR spectrometer in proton decoupled mode. Chemical shifts (δ) are expressed as parts per million (ppm), positive shift being downfield from TMS; coupling constants (J) are expressed in hertz (Hz). Splitting patterns in ¹H-NMR spectra are designated as s (singlet), br s (broad singlet), d (doublet), dd (doublet of doublets), dt (doublet of triplets), ddt (double of doublet of triplets), t (triplet), m (multiplet). For ¹³C-NMR spectra, the number of attached protons for each signal was determined using the DEPT pulse sequence run in the DEPT-90 and DEPT-135 modes. COSY, HSQC and HMBC experiments were routinely performed to aid the NMR assignment of novel chemical structures. Please note that the numbering system displayed on the structures is to assign the NMR data, and differs from the IUPAC system used for naming.

2.18. Aldehyde Route

2.18.1. Synthesis of Compound 37

3-(1,3-Dioxolan-2-yl)-4-methylpyridine^[24] (37)

The following procedure was carried out using Dean-Stark apparatus. 4-Methylpyridine-3-carboxaldehyde **36** (1 equiv.) and *p*-TsOH monohydrate (1.25 equiv.) were dissolved in toluene (4 mL/mmol) and the resulting mixture was stirred at 90 °C under an argon atmosphere for 15 min. Ethylene glycol (5 equiv.) was added and the reaction was stirred at 120 °C overnight. The cooled reaction mixture was quenched with sat. NaHCO₃ (equal volume to reaction solvent). The aqueous layer was extracted with DCM (3 × 2.5 mL/mmol) and the combined organic layers were washed with brine (2 mL/mmol), dried over NaSO₄, filtered and concentrated *in vacuo* to yield the crude product as a yellow oil. Purification by column chromatography (cyclohexane/EtOAc 6:4) afforded the pure product **37** as a pale yellow oil (0.865 g, 55% yield).



Yellow oil; yield: 865 mg (55%); IR (neat): ν 3100 (C-H stretch), 2888 (C-H stretch), 1598 (aromatic C-C stretch), 1393 (pyridine C-N stretch), 1058 (ether C-O stretch) cm⁻¹; ¹H-NMR (400 MHz, CDCl₃): δ 2.42 (s, 3H, CH₃-**10**), 4.01–4.10 (m, 4H, CH₂-**8**, CH₂-**9**), 5.98 (s, 1H, CH-**7**), 7.09 (d, *J* = 4.9 Hz, 1H, CH-**5**), 8.46 (d, *J* = 5.0 Hz, 1H, CH-**6**), 8.66 (s, 1H, CH-**2**); ¹³C-NMR (100 MHz, CDCl₃): δ 18.5 (CH₃-**10**), 65.3 (CH₂-**8**, CH₂-**9**), 101.3 (CH-**7**), 125.6 (CH-**5**), 131.4 (qC-**3**), 146.5 (qC-**4**), 147.5 (CH-**2**), 149.9 (CH-**6**); HRMS (ESI-TOF) *m/z*: [M+H]⁺ calcd. for C₉H₁₂NO₂: 166.0868 found: 166.0860.

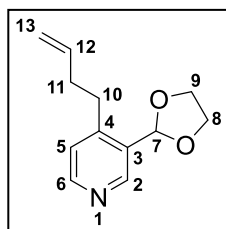
Spectral data were consistent with those reported in the literature.

2.18.2. Synthesis of Compound 38

4-(But-3-en-1-yl)-3-(1,3-dioxolan-2-yl)pyridine (38)

3-(1,3-Dioxolan-2-yl)-4-methylpyridine **37** (1 equiv.) was dissolved in THF (4 mL/mmol) and the solution (yellow/brown) cooled to -78°C. LDA (2 equiv.) was added slowly, temperature maintained below -75 °C. The resulting orange solution was stirred at -78 °C for 2.5 h to complete deprotonation. Allyl bromide (1.1 equiv.) was added dropwise, maintaining temperature below -75 °C, and the reaction mixture stirred at this temperature for 1 h until alkylation was complete as determined by LCMS. The reaction mixture was quenched with

sat. NH_4Cl solution (3.5 mL/mmol) at $-78\text{ }^\circ\text{C}$ and then allowed to warm to room temperature. The aqueous layer was extracted with EtOAc (3×2.5 mL/mmol) and the combined organic layers were washed with brine (2 mL/mmol), dried over NaSO_4 , filtered and concentrated *in vacuo* to yield the crude product as an orange oil. Purification by column chromatography (cyclohexane/EtOAc 1:1) afforded the pure product **38** as a pale yellow oil (0.114 g, 46% yield).

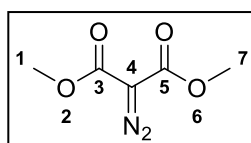


Yellow oil; yield: 114 mg (46%); IR (neat): ν 3150 (C-H stretch), 2889 (C-H stretch), 1640 (alkene C-C stretch), 1597 (aromatic C-C stretch), 1415 (pyridine C-N stretch), 1054 (ether C-O stretch) cm^{-1} ; $^1\text{H-NMR}$ (400 MHz, CDCl_3): δ 2.40 (dt, $J = 7.7, 6.6$ Hz, 2H, $\text{CH}_2\text{-11}$), 2.84 (dd, $J = 9.0, 6.9$ Hz, 2H, $\text{CH}_2\text{-10}$), 4.00–4.21 (m, 4H, $\text{CH}_2\text{-8}$, $\text{CH}_2\text{-9}$), 4.98–5.11 (m, 2H, $\text{CH}_2\text{-13}$), 5.86 (ddt, $J = 16.9, 10.2, 6.6$ Hz, 1H, CH-12), 6.01 (s, 1H, CH-7), 7.12 (d, $J = 5.1$ Hz, 1H, CH-5), 8.50 (d, $J = 5.1$ Hz, 1H, CH-6), 8.71 (s, 1H, CH-2); $^{13}\text{C-NMR}$ (100 MHz, CDCl_3): δ 30.9 ($\text{CH}_2\text{-11}$), 34.2 ($\text{CH}_2\text{-10}$), 65.3 ($\text{CH}_2\text{-8}$, $\text{CH}_2\text{-9}$), 101.0 (CH-7), 115.6 ($\text{CH}_2\text{-13}$), 124.2 (CH-5), 130.9 (qC-3), 137.2 (CH-12), 148.1 (CH-2), 149.8 (qC-4), 150.1 (CH-6); HRMS (ESI-TOF) m/z : $[\text{M}+\text{H}]^+$ calcd. for $\text{C}_{12}\text{H}_{16}\text{NO}_2$: 206.1181 found: 206.1180.

2.18.3. Synthesis of Diazo Compound 40

Dimethyldiazomalonate^[27] (**40**)

To a solution of 4-acetamidobenzenesulfonyl azide (1.1 equiv.) in acetonitrile (4 mL/mmol) under argon were added dimethyl malonate **39** (1 equiv.) and triethyl amine (1.1 equiv.). The resulting pale yellow solution was stirred at room temperature. After 1 h a beige precipitate formed, and more solvent was added if necessary to improve stirring. The resulting beige suspension was stirred overnight at room temperature. The insoluble material (sulfonamide by-product) was removed by filtration and the filtrate concentrated *in vacuo* (**water bath at $20\text{ }^\circ\text{C}$ – diazo thermally unstable at $40\text{ }^\circ\text{C}$**). Chloroform was added to the residue and the mixture filtered to remove any remaining sulfonamide. The filtrate was concentrated *in vacuo* to yield the crude product as a yellow oil. Purification by column chromatography (cyclohexane/EtOAc 3:7) afforded the pure product **40** as a yellow oil (2.97 g, 99% yield).



Yellow oil; yield: 2.97 g (99%); IR (neat): ν 2958 (C-H stretch), 2132 (diazo C=N stretch), 1734 (ester C=O stretch), 1083 (ester C-O stretch) cm^{-1} ; $^1\text{H-NMR}$ (400 MHz, CDCl_3): δ 3.81 (s, 6H, $\text{CH}_3\text{-1}$, $\text{CH}_3\text{-7}$);

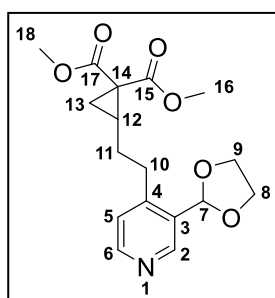
^{13}C -NMR* (100 MHz, CDCl_3): δ 52.5 (CH_3 -**1**, CH_3 -**7**), 161.4 (qC-**3**, qC-**5**) *Diazo carbon cannot be detected^[27]; HRMS (ESI-TOF) m/z : $[\text{M}+\text{H}]^+$ calcd. for $\text{C}_5\text{H}_7\text{N}_2\text{O}_4$: 159.0406 found: 159.0410.

Spectral data were consistent with those reported in the literature.

2.18.4. Synthesis of Compound 41

Dimethyl 2-(2-(3-(1,3-dioxolan-2-yl)pyridin-4-yl)ethyl)cyclopropane-1,1-dicarboxylate (**41**)

A solution of 4-but-3-enyl-3-(1,3-dioxolan-2-yl)pyridine **38** (1 equiv.) in DCM (2 mL/mmol) was cooled to 0 °C under argon. $\text{BF}_3 \cdot \text{Et}_2\text{O}$ (1 equiv.) was added and the reaction mixture stirred at 0 °C for 30 min. $\text{Rh}_2(\text{esp})_2$ (5 mol%) was added followed by a solution of dimethyldiazomalonate **40** (2 equiv.) in DCM (1 mL/mmol diazo) which was added dropwise over no more than 5 min. The reaction mixture was stirred at room temperature for 1 h. Once the reaction was completed, as determined by ^1H -NMR, the reaction mixture was quenched with NaHCO_3 (equal volume to reaction solvent) and extracted with DCM (3×50 mL/mmol). The combined organic layers were washed with brine (50 mL/mmol), dried over NaSO_4 , filtered and concentrated *in vacuo* to yield the crude product as a red oil. Purification by column chromatography (cyclohexane/EtOAc 6:4) afforded the pure product **41** as pale yellow oil (0.038 g, 47% yield).



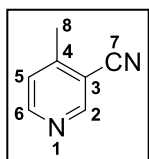
Yellow oil; yield: 38 mg (47%); IR (neat): ν 2954 (C-H stretch), 2892 (C-H stretch), 1724 (ester C=O stretch), 1598 (aromatic C-C stretch), 1437 (pyridine C-N stretch), 1213 (ester C-O stretch), 1065 (ether C-O stretch) cm^{-1} ; ^1H -NMR (400 MHz, CDCl_3): δ 1.36–1.48, (m, 2H, CH_2 -**11**), 1.57–1.82 (m, 2H, CH_2 -**13**), 1.90–2.01 (m, 1H, CH -**12**), 2.89 (t, $J = 7.9$ Hz, 2H, CH_2 -**10**), 3.74 (s, 3H, CH_3 -**16** or **18**), 3.76 (s, 3H, CH_3 -**16** or **18**), 4.03–4.22 (m, 4H, CH_2 -**8**, CH_2 -**9**), 6.00 (s, 1H, CH -**7**), 7.16 (d, $J = 5.1$ Hz, 1H, CH -**5**), 8.53 (d, $J = 5.1$ Hz, 1H, CH -**6**), 8.73 (s, 1H, CH -**2**); ^{13}C -NMR (100 MHz, CDCl_3): δ 21.0 (CH_2 -**11**), 28.0 (CH -**12**), 29.5 (CH_2 -**13**), 31.1 (CH_2 -**10**), 34.0 (qC-**14**), 52.6 (CH_3 -**16** or **18**), 52.7 (CH_3 -**16** or **18**), 65.4 (CH_2 -**8**, CH_2 -**9**), 100.5 (CH -**7**), 124.8 (CH -**5**), 131.9 (qC-**3**), 146.8 (CH -**2**), 148.7 (CH -**6**), 151.2 (qC-**4**), 168.5 (qC-**15** or **17**), 170.6 (qC-**15** or **17**); HRMS (ESI-TOF) m/z : $[\text{M}+\text{H}]^+$ calcd. for $\text{C}_{17}\text{H}_{22}\text{NO}_6$: 336.1447 found: 336.1440.

2.19. Nitrile Route

2.19.1. Synthesis of Nitrile Compound 43

4-Methylpyridine-3-carbonitrile^[30] (43)

3-Bromo-4-methylpyridine **42** (1 equiv.) was dissolved in DMA (3.7 mL/mmol) under an argon atmosphere. Zinc dust (0.12 equiv.) and zinc cyanide (0.6 equiv.) were added (grey suspension) and argon was bubbled through the reaction mixture for 20 min with stirring. Pd(dppf)Cl₂ (20 mol%) was added (red/orange mixture) and the reaction mixture was stirred at reflux (130 °C) overnight under argon. After cooling, the reaction mixture was filtered through Celite and the filtrate poured onto 2 M NH₄OH solution (4 mL/mmol) while cooling on an ice bath. The aqueous layer was extracted with EtOAc (3 × 2.5 mL/mmol) and the combined organic layers were washed with water (2 mL/mmol), brine (2 mL/mmol), dried over NaSO₄, filtered through Celite and concentrated *in vacuo* to yield the crude product as a dark red/brown oil. Purification by column chromatography (cyclohexane/EtOAc 6:4) afforded the pure product **43** as a light brown crystalline solid (1.8 g, 89% yield).



Beige crystalline solid; yield: 1.8 g (89%); m.p. = 45–47 °C (lit. 44–46 °C); IR (neat): ν 2942 (C-H stretch), 2227 (nitrile C \equiv N stretch), 1593 (aromatic C-C stretch), 1487 (pyridine C-N stretch) cm⁻¹; ¹H-NMR (400 MHz, CDCl₃): δ 2.58 (s, 3H, CH₃-8), 7.30 (d, J = 5.1 Hz, 1H, CH-5), 8.65 (d, J = 5.1 Hz, 1H, CH-6), 8.79 (s, 1H, CH-2); ¹³C-NMR (100 MHz, CDCl₃): δ 20.1 (CH₃-8), 110.9 (qC-4), 115.9 (qC-3), 124.8 (CH-5), 150.8 (qC-7), 152.5 (CH-6), 152.7 (CH-2); HRMS (ESI-TOF) m/z : [M+H]⁺ calcd. for C₇H₇N₂: 119.0609 found: 119.0610.

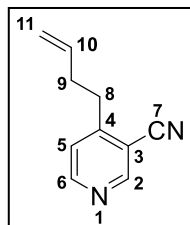
Spectral data were consistent with those reported in the literature.

2.19.2. Synthesis of Compound 44

4-But-3'-enylpyridine-3-carbonitrile (44)

A solution of 4-methylpyridine-3-carbonitrile **43** (1 equiv.) was dissolved in THF (4 mL/mmol) and the solution (yellow/brown) cooled to -78 °C. LiHMDS (1.1 equiv.) was added slowly, temperature maintained below -75 °C. The resulting orange solution was stirred at -78 °C for 3 h to complete deprotonation. Allyl bromide (1.1 equiv.) was added dropwise, maintaining temperature below -75 °C, and the reaction mixture stirred at this temperature for 15 min until alkylation was complete as determined by LCMS. The reaction mixture was quenched with

sat. NH_4Cl solution (3.5 mL/mmol) at $-78\text{ }^\circ\text{C}$ and then allowed to warm to room temperature. The aqueous layer was extracted with EtOAc (3×2.5 mL/mmol) and the combined organic layers were washed with brine (2 mL/mmol), dried over NaSO_4 , filtered and concentrated *in vacuo* to yield the crude product as an orange oil. Purification by column chromatography (cyclohexane/EtOAc 6:4) afforded the pure product **44** as a yellow oil (1.65 g, 73% yield).

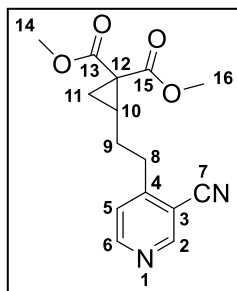


Yellow oil; yield: 1.65 g (73%); IR (neat): ν 2934 (C-H stretch), 2228 (nitrile $\text{C}\equiv\text{N}$ stretch), 1641 (alkene $\text{C}=\text{C}$ stretch), 1589 (aromatic C-C stretch), 1405 (pyridine C-N stretch) cm^{-1} ; ^1H -NMR (400 MHz, CDCl_3): δ 2.47 (m, 2H, CH_2 -9), 2.95 (t, $J = 7.5$ Hz, 2H, CH_2 -8), 5.03–5.08 (m, 2H, CH_2 -11), 5.75–5.88 (m, 1H, CH -10), 7.28 (d, $J = 5.1$ Hz, 1H, CH -5), 8.68 (d, $J = 5.1$ Hz, 1H, CH -6), 8.81 (s, 1H, CH -2); ^{13}C -NMR (100 MHz, CDCl_3): δ 33.4 (CH_2 -9), 33.5 (CH_2 -8), 110.6 (qC-4), 115.8 (qC-3), 116.8 (CH_2 -11), 124.0 (CH -5), 135.7 (CH -10), 152.5 (CH -6), 152.9 (CH -2), 154.3 (qC-7); HRMS (ESI-TOF) m/z : $[\text{M}+\text{H}]^+$ calcd. for $\text{C}_{10}\text{H}_{11}\text{N}_2$: 159.0922 found: 159.0920.

2.19.3. Synthesis of Compound 45

Dimethyl 2-[2-(3-cyano-4-pyridyl)ethyl]cyclopropane-1,1-dicarboxylate (**45**)

A solution of 4-but-3'-enylpyridine-3-carbonitrile **44** (1 equiv.) in DCM (2 mL/mmol) was cooled to $0\text{ }^\circ\text{C}$ under argon. $\text{BF}_3\cdot\text{Et}_2\text{O}$ (1 equiv.) was added and the reaction mixture stirred at $0\text{ }^\circ\text{C}$ for 30 min. $\text{Rh}_2(\text{esp})_2$ (2 mol%) was added followed by a solution of dimethyldiazomalonate **40** (2 equiv.) in DCM (1 mL/mmol diazo). The reaction mixture was stirred at room temperature for 1 h. Once the reaction was completed, as determined by ^1H -NMR, the reaction mixture was quenched with NaHCO_3 (equal volume to reaction solvent) and extracted with DCM (3×50 mL/mmol). Combined organic layers were washed with brine (50 mL/mmol), dried over NaSO_4 , filtered and concentrated *in vacuo* to yield the crude product as a red oil. Purification by column chromatography (cyclohexane/EtOAc 4:6) afforded the pure product **45** as a red oil (0.67 g, 70% yield).

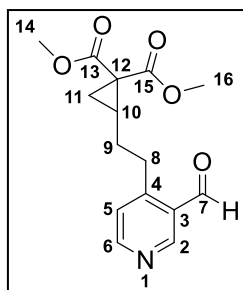


Red oil; yield: 0.67 g (70%); IR (neat): ν 2954 (C-H stretch), 2229 (nitrile C \equiv N stretch), 1722 (ester C=O stretch), 1589 (aromatic C-C stretch), 1436 (pyridine C-N stretch), 1213 (ester C-O stretch) cm^{-1} ; ^1H -NMR (400 MHz, CDCl_3): δ 1.35–1.51 (m, 2H, CH_2 -9), 1.67–1.98, (m, 3H, CH -10, CH_2 -11), 2.93–3.00 (m, 2H, CH_2 -8), 3.74 (s, 3H, CH_3 -14/16), 3.77 (s, 3H, CH_3 -14/16), 7.28 (d, J = 4.8 Hz, 1H, CH -5), 8.69 (d, J = 5.2 Hz, 1H, CH -6), 8.82 (s, 1H, CH -2); ^{13}C -NMR (100 MHz, CDCl_3): δ 20.8 (CH_2 -9), 27.3 (CH -10), 28.8 (CH_2 -11), 33.3 (CH_2 -8), 33.9 (qC-12), 52.7 (CH_3 -14, CH_3 -16), 110.5 (qC-4), 115.7 (qC-3), 124.0 (CH -5), 152.7 (CH -6), 153.1 (CH -2), 153.7 (qC-7), 168.8 (qC-13/15), 170.3 (qC-13/15); HRMS (ESI-TOF) m/z : $[\text{M}+\text{H}]^+$ calcd. for $\text{C}_{15}\text{H}_{17}\text{N}_2\text{O}_4$: 289.1188 found: 289.1180.

2.19.4. Synthesis of Compound 47

Dimethyl 2-[2-(3-formyl-4-pyridyl)ethyl]cyclopropane-1,1-dicarboxylate^[32] (47)

A solution of dimethyl 2-[2-(3-cyano-4-pyridyl)ethyl]cyclopropane-1,1-dicarboxylate **45** (1 equiv.) in 1:1 acetic acid and water (1.5 mL/mmol) was added to a hydrogenation reaction vessel containing Raney nickel (7.6 equiv.) under an argon atmosphere. The reaction mixture was stirred at room temperature in the presence of hydrogen gas (1.5 bar) for 2 h. The nickel catalyst was removed by filtration through Celite and washed several times with water and EtOAc. The aqueous layer was adjusted to pH 9 and extracted with EtOAc (3×2.5 mL/mmol). Combined organic layers were washed with sat. NaHCO_3 (2 mL/mmol), brine (2 mL/mmol), dried over NaSO_4 , filtered through Celite and concentrated *in vacuo* to yield the crude product as a red oil. Purification by column chromatography (DCM/MeOH 95:5) afforded the pure product **47** as a yellow oil (0.48 g, 50% yield).



Yellow oil; yield: 0.48 g (50%); IR (neat): ν 2954 (C-H stretch), 2725 (aldehyde C-H stretch), 1721 (ester C=O stretch), 1698 (aldehyde C=O stretch), 1590 (aromatic C-C stretch), 1436 (pyridine C-N stretch), 1210 (ester C-O stretch) cm^{-1} ; ^1H -NMR (400 MHz, CDCl_3): δ 1.41–1.48, (m, 2H, CH_2 -9), 1.57–1.66 (m, 1H, one of CH_2 -11), 1.75–1.84 (m, 1H, one of CH_2 -11), 1.93–2.01 (m, 1H, CH -10), 3.19 (t, J = 7.1 Hz, 2H, CH_2 -8), 3.75 (s, 3H, CH_3 -14/16), 3.78 (s, 3H, CH_3 -14/16), 7.25 (d, J = 5.1 Hz, 1H, CH -5), 8.69 (d, J = 5.1 Hz, 1H, CH -6), 8.97 (s, 1H, CH -2), 10.26 (s, 1H, CH -7); ^{13}C -NMR (100 MHz, CDCl_3): δ 21.0 (CH_2 -9), 27.8 (CH -10), 29.5 (CH_2 -11), 31.6 (CH_2 -8), 33.9 (qC-12), 52.6 (CH_3 -14 or 16), 52.7 (CH_3 -14 or 16), 125.8 (CH -5), 129.4 (qC-3), 152.3 (qC-4), 153.6 (CH -6), 154.8 (CH -2),

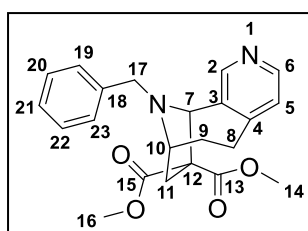
168.5 (qC-**13** or **15**), 170.5 (qC-**13** or **15**), 191.5 (qC-**7**); HRMS (ESI-TOF) m/z : $[M+H]^+$ calcd. for $C_{15}H_{18}NO_5$: 292.1185 found: 292.1170.

Spectral data were consistent with those reported in the literature.

2.19.5. Synthesis of Cyclised Diester Compound **49**

Dimethyl-11-benzyl-5,7,8,10-tetrahydro-7,10-epiminocycloocta[*c*]pyridine-9,9(6*H*)-dicarboxylate^[32] (**49**)

A solution of dimethyl 2-[2-(3-formyl-4-pyridyl)ethyl]cyclopropane-1,1-dicarboxylate **47** (1 equiv.) in DCM (14 mL/mmol) under an argon atmosphere containing $MgSO_4$ (2 equiv.) was treated with benzylamine (1 equiv.). The resulting pale yellow mixture was stirred overnight at room temperature. The reaction mixture was filtered and the filtrate concentrated *in vacuo* to yield the crude imine **48** intermediate as a yellow oil which was used directly without purification. The imine intermediate was dissolved in DCM (14 mL/mmol) under argon and $SnCl_4$ solution (1 M in DCM, 1.5 equiv.) was added dropwise at room temperature. The resulting bright yellow suspension was stirred for 15 min. The reaction mixture was quenched with sat. $NaHCO_3$ solution (equivalent volume to solvent) and the resulting mixture stirred for 30 min at room temperature. The aqueous layer was extracted with EtOAc (3 \times 2.5 mL/mmol) and the combined organic layers were washed with sat. $NaHCO_3$ (2 mL/mmol), brine (2 mL/mmol), dried over $NaSO_4$, filtered and concentrated *in vacuo* to yield the crude product as a brown solid. Purification by column chromatography (cyclohexane/EtOAc 1:1) afforded the pure product **49** as a white solid (0.37 g, 78% yield).



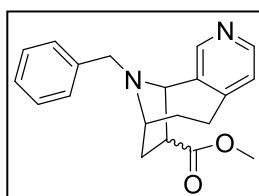
White solid; yield: 0.37 g (78%); m.p. = 115–117 °C (lit. 117–118 °C); IR (neat): ν 2951 (C-H stretch), 1735 (ester C=O stretch), 1591 (aromatic C-C stretch), 1434 (pyridine C-N stretch), 1266 (amine C-N stretch), 1227 (ester C-O stretch) cm^{-1} ; 1H -NMR (400 MHz, $CDCl_3$): δ 1.52–1.62, (m, 1H, one of CH_2 -**9**), 2.08–2.20 (m, 1H, one of CH_2 -**9**), 2.60–2.77 (m, 2H, one of CH_2 -**8**, one of CH_2 -**11**), 2.97 (d, J = 14.5 Hz, 1H, one of CH_2 -**11**), 3.21 (s, 3H, CH_3 -**14/16**), 3.38–3.55 (m, 2H, one of CH_2 -**8**, one of CH_2 -**17**), 3.66 (d, J = 13.6 Hz, 1H, one of CH_2 -**17**), 3.74–3.83 (m, 1H, CH -**10**), 3.83 (s, 3H, CH_3 -**14/16**), 4.92 (s, 1H, CH -**7**), 7.11 (d, J = 4.9 Hz, 1H, CH -**5**), 7.21–7.36 (m, 5H, CH -**19**, CH -**20**, CH -**21**, CH -**22**, CH -**23**), 8.08 (s, 1H, CH -**2**), 8.36 (d, J = 5.0 Hz, 1H, CH -**6**); ^{13}C -NMR (100 MHz, $CDCl_3$): δ 24.2 (CH_2 -**9**), 31.9 (CH_2 -**8**), 35.7 (CH_2 -**11**), 51.4 (CH_2 -**17**), 52.4 (CH_3 -**14** or **16**), 53.1 (CH_3 -**14**

or **16**), 60.1 (CH-**10**), 65.4 (qC-**12**), 68.6 (CH-**7**), 124.9 (CH-**5**), 127.1 (CH-**21**), 128.2 (CH-**20**, CH-**22**), 128.4 (CH-**19**, CH-**23**), 134.1 (qC-**3**), 138.0 (qC-**18**), 148.6 (CH-**6**), 150.5 (qC-**4**), 151.8 (CH-**2**), 169.3 (qC-**13** or **15**), 171.9 (qC-**13** or **15**); HRMS (ESI-TOF) m/z : $[M+H]^+$ calcd. for $C_{22}H_{25}N_2O_4$: 381.1814 found: 381.1810.

Spectral data were consistent with those reported in the literature.

2.19.6. Synthesis of Monoester Compound **50**

Methyl-11-benzyl-5,6,7,8,9,10-hexahydro-7,10-epiminocycloocta[*c*]pyridine-9-carboxylate^[32] (**50**)

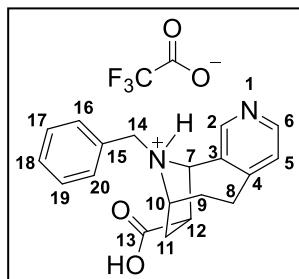


A solution of **49** (1 equiv.) in DMSO (14 mL/mmol) under an argon atmosphere containing LiCl (5 equiv.) and water (2 equiv.) was placed under a slight vacuum and heated at 160 °C for 1.5 h. The cooled reaction mixture was diluted with water and extracted with EtOAc (3 × 5 mL/mmol). The combined organic layers were washed with water (3 × 5 mL/mmol), brine (5 mL/mmol), dried over $NaSO_4$, filtered and concentrated *in vacuo* to yield the crude product as a brown oil. Purification by column chromatography (cyclohexane/EtOAc 4:6) afforded the product **50** as a 1:1 mixture of diastereomers (yellow oil, 1.67 g, 78% yield). This mixture of diastereomers was used directly in the next step without further separation.

2.19.7. Synthesis of Carboxylic Acid Compound **62**

11-Benzyl-5,6,7,8,9,10-hexahydro-7,10-epiminocycloocta[*c*]pyridine-9-carboxylic acid TFA salt (**62**)

A solution of **50** (1 equiv.) in THF (7 mL/mmol) and methanol (1.6 mL/mmol) was cooled on an ice bath. LiOH (2 equiv.) was added followed by 0.5 mL water. The resulting pale yellow solution was stirred at room temperature overnight, then concentrated *in vacuo* to yield the crude product **61** as an orange oil. The TFA salt of the product (**62**) was isolated as a single (*anti*) isomer by reverse-phase chromatography (water/acetonitrile/1% aq. formic acid 3:6:1) in 77% yield (0.22 g). This purification step was carried out by analysts at a dedicated purifications laboratory at Syngenta.

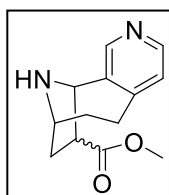


White solid; yield: 0.22 g (77%); IR (neat): ν 2925 (C-H stretch), 2493 (acid O-H stretch), 1667 (acid C=O stretch), 1601 (aromatic C-C stretch), 1455 (pyridine C-N stretch), 1195 (amine C-N stretch) cm^{-1} ; ^1H -NMR (400 MHz, CDCl_3): δ 1.66–1.80 (m, 1H, one of CH_2 -9), 2.14–2.37 (m, 2H, one of CH_2 -9, one of CH_2 -11), 2.74–2.94 (m, 2H, one of CH_2 -8, one of CH_2 -11), 3.07–3.29 (m, 2H, one of CH_2 -8, CH -12), 3.90 (apparent s, 3H, CH -10, CH_2 -14), 4.95 (d, $J = 2.3$ Hz, 1H, CH -7), 7.21–7.37 (m, 6H, CH -5, CH -16, CH -17, CH -18, CH -19, CH -20), 8.34 (s, 1H, CH -2), 8.47 (d, $J = 5.1$ Hz, 1H, CH -6), 10.03 (br s, 2H, qC-13OH, CH_2 -14N ^+H); ^{13}C -NMR (100 MHz, CDCl_3): δ 26.0 (CH_2 -9), 31.3 (CH_2 -8), 32.1 (CH_2 -11), 49.8 (CH -12), 53.4 (CH_2 -14), 61.9 (CH -10), 68.2 (CH -7), 116.5 (q, $^1J_{\text{C-F}} = 290$ Hz, TFA- CF_3), 125.9 (CH -5), 128.4 (CH -18), 128.8 (CH -16, CH -20), 129.4 (CH -17, CH -19), 134.2 (qC-15), 136.1 (qC-3), 147.5 (CH -6), 147.8 (CH -2), 151.6 (qC-4), 162.1 (q, $^2J_{\text{C-F}} = 35$ Hz, TFA-q CO_2), 176.4 (qC-13); HRMS (ESI-TOF) m/z : $[\text{M}+\text{H}]^+$ calcd. for the free amine $\text{C}_{19}\text{H}_{21}\text{N}_2\text{O}_2$: 309.1603 found: 309.1600.

Melting point and ^{19}F -NMR for this compound were not obtained.

2.19.8. Synthesis of Debenzylated Monoester Compound 67

Methyl(7R,10R)-5,6,7,8,9,10-hexahydro-7,10-epiminocycloocta[c]pyridine-9-carboxylate^[20] (67)

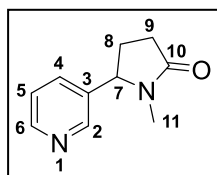


A solution of **50** (1 equiv.) in MeOH (8 mL/mmol) was degassed using argon in a hydrogenation reactor. Pearlmann's catalyst ($\text{Pd}(\text{OH})_2/\text{C}$, 0.1 equiv.) was added to the reactor, followed by a 2.0 M solution of HCl in MeOH (2 equiv.). The reaction mixture was stirred at room temperature in the presence of hydrogen gas (10 bar) for 2 h. The catalyst was removed by filtration of the reaction mixture through Celite and washed several times with water and MeOH. The filtrate was concentrated *in vacuo* and the aqueous solution was adjusted to pH 10 and extracted with EtOAc (5×20 mL/mmol). Combined organic layers were washed with sat. NaHCO_3 (10 mL/mmol), brine (10 mL/mmol), dried over NaSO_4 , filtered through Celite and concentrated *in vacuo* to yield the crude product as an orange oil (ca. 60% mass recovery). NMR and LCMS analysis of the crude product indicated that debenzylation of **50** to give the free amine **67** had occurred. Further purification of this mixture was not carried out.

2.20. Barton Model System

1-Methyl-5-(pyridin-3-yl)pyrrolidin-2-one^[40] (**60**)

1-Methyl-5-oxo-2-(pyridin-3-yl)pyrrolidine-3-carboxylic acid **52** (1 equiv.), DMAP (1 equiv.), EDC hydrochloride (1.2 equiv.) and pyridine (1.2 equiv.) were dissolved in chloroform (9 mL/mmol) resulting in a bright yellow solution. 2-Methyl-2-propanethiol (10 equiv.) was added and the mixture was immediately irradiated with an LED lamp, with CO₂ evolution monitored via use of an oil bubbler. The reaction mixture was stirred at room temperature for 2.5 h, and then at 60 °C for 2 h (monitored by LCMS). The cooled reaction was then concentrated *in vacuo* to yield the crude product as a brown oil. Purification by column chromatography (DCM/MeOH 9:1) afforded the pure product **60** as a pale yellow oil (0.013 g, 31%).



Pale yellow oil; yield: 0.013 g (31%); IR (neat): ν 2923 (C-H stretch), 1674 (amide C=O stretch), 1421 (aromatic C-C stretch), 1393 (pyridine C-N stretch), 1115 (amine C-N stretch) cm⁻¹; ¹H-NMR (400 MHz, CDCl₃): δ 1.84–2.00 (m, 1H, one of CH₂-**8**), 2.48–2.68 (m, 3H, one of CH₂-**8**, CH₂-**9**), 2.72 (s, 3H, CH₃-**11**), 4.62 (dd, J = 7.7, 6.0 Hz, 1H, CH-**7**), 7.45 (dd, J = 7.9, 4.9 Hz, 1H, CH-**5**), 7.64 (dt, J = 7.9, 1.8 Hz, 1H, CH-**4**), 8.51 (d, J = 1.7 Hz, 1H, CH-**2**), 8.65 (dd, J = 4.8, 1.3 Hz, 1H, CH-**6**); ¹³C-NMR (100 MHz, CDCl₃): δ 28.28 (CH₂-**8**), 28.30 (CH₃-**11**), 30.0 (CH₂-**9**), 62.2 (CH-**7**), 124.1 (CH-**5**), 134.0 (CH-**4**), 136.7 (qC-**3**), 148.3 (CH-**2**), 149.6 (CH-**6**), 175.4 (qC-**10**); HRMS (ESI-TOF) m/z : [M+H]⁺ calcd. for C₁₀H₁₃N₂O: 177.1028 found: 177.1020.

Spectral data were consistent with those reported in the literature.

2.21. Chapter 2 References

1. R. Heitefuss, J. Welch *Crop and plant protection: the practical foundations*, Ellis Horwood Limited, **1989**.
2. Pesticides-Explained,
<http://ec.europa.eu/assets/sante/food/plants/pesticides/lop/index.html>, accessed 1 May 2019.
3. European Crop Protection - Regulatory and Policy Topics,
<https://www.ecpa.eu/regulatory-policy-topics>, accessed 1 May 2019.
4. Syngenta At A Glance, <https://www.syngenta.com/who-we-are/about-our-business/syngenta-at-a-glance>, accessed 1 May 2019.
5. A. Taly, P.-J. Corringer, D. Guedin, P. Lestage, J.-P. Changeux, *Nat. Rev. Drug Discov.* **2009**, 8, 733-750.
6. S. P. Arneric, M. Holladay, M. Williams, *Biochem. Pharmacol.* **2007**, 74, 1092-1101.
7. P. Jeschke, R. Nauen, M. E. Beck, *Angew. Chem. Int. Ed.* **2013**, 52, 9464-9485.
8. <https://www.zionmarketresearch.com/market-analysis/insecticides-market>, accessed 27 September 2018.
9. C. Bass, I. Denholm, M. S. Williamson, R. Nauen, *Pestic. Biochem. Physiol.* **2015**, 121, 78-87.
10. M. Tomizawa, J. E. Casida, *Annu. Rev. Pharmacol. Toxicol.* **2005**, 45, 247-268.
11. A. Elbert, B. Becker, J. Hartwig, C. Erdelen, *Pflanzenschutz-Nachrichten Bayer (Germany, FR)* **1991**.
12. A. Elbert, H. Overbeck, K. Iwaya, S. Tsuboi, *Brighton Crop Protection Conference, Pests and Diseases-1990. Vol. 1.*, (British Crop Protection Council), **1990**, 21-28.
13. A. J. Crossthwaite, A. Bigot, P. Camblin, J. Goodchild, R. J. Lind, R. Slater, P. Maienfisch, *J. Pestic. Sci.* **2017**, 42, 67-83.
14. T. E. Catka, E. Leete, *J. Org. Chem.* **1978**, 43, 2125-2127.
15. C. G. Chavdarian, J. I. Seeman, J. B. Wooten, *J. Org. Chem.* **1983**, 48, 492-494.
16. D. B. Kanne, D. J. Ashworth, M. T. Cheng, L. C. Mutter, L. G. Abood, *J. Am. Chem. Soc.* **1986**, 108, 7864-7865.
17. A. M. Koskinen, H. Rapoport, *J. Med. Chem.* **1985**, 28, 1301-1309.
18. C. Spivak, J. Waters, B. Witkop, E. Albuquerque, *Mol. Pharmacol.* **1983**, 23, 337-343.
19. R. S. Aronstam, B. Witkop, *Proc. Natl. Acad. Sci.* **1981**, 78, 4639-4643.

20. D. B. Kanne, L. G. Abood, *J. Med. Chem.* **1988**, *31*, 506-509.
21. F. I. Carroll, X. Hu, H. A. Navarro, J. Deschamps, G. R. Abdrakhmanova, M. I. Damaj, B. R. Martin, *J. Med. Chem.* **2006**, *49*, 3244-3250.
22. F. I. Carroll, H. A. Navarro, S. W. Mascarella, A. H. Castro, C. W. Luetje, C. R. Wageman, M. J. Marks, A. Jackson, M. I. Damaj, *ACS Chem. Neurosci.* **2015**, *6*, 920-926.
23. Y. Sang, J. Zhao, X. Jia, H. Zhai, *J. Org. Chem.* **2008**, *73*, 3589-3592.
24. A. Shariff, S. McLean, *Can. J. Chem.* **1983**, *61*, 2813-2820.
25. F. De Nanteuil, J. Loup, J. Waser, *Org. Lett.* **2013**, *15*, 3738-3741.
26. F. González-Bobes, M. D. B. Fenster, S. Kiau, L. Kolla, S. Kolotuchin, M. Soumeillant, *Adv. Synth. Catal.* **2008**, *350*, 813-816.
27. F. de Nanteuil, J. Waser, *Angew. Chem.* **2011**, *123*, 12281-12285.
28. F. A. Davis, J. Y. Melamed, S. S. Sharik, *J. Org. Chem.* **2006**, *71*, 8761-8766.
29. W. H. Miller, S. P. Romeril, X. Tian, S. K. Verma (GlaxoSmithKline), US20170015666A1, **2017**.
30. B. Di Rienzo, P. Mellini, S. Tortorella, D. De Vita, L. Scipione, *Synthesis* **2010**, *22*, 3835-3838.
31. L. P. Zhang, Y. Bao, Y. Y. Kuang, F. E. Chen, *Helv. Chim. Acta* **2008**, *91*, 2057-2061.
32. B. Sun, J. Ren, S. Xing, Z. Wang, *Adv. Synth. Catal.* **2018**, *360*, 1529-1537.
33. S. Xing, W. Pan, C. Liu, J. Ren, Z. Wang, *Angew. Chem. Int. Ed.* **2010**, *49*, 3215-3218.
34. A. P. Krapcho, J. Weimaster, J. Eldridge, E. Jahngen Jr, A. Lovey, W. Stephens, *J. Org. Chem.* **1978**, *43*, 138-147.
35. D. H. Barton, D. Crich, W. B. Motherwell, *J. Chem. Soc., Chem. Commun.* **1983**, 939-941.
36. D. H. Barton, Y. Hervé, P. Potier, J. Thierry, *Tetrahedron* **1988**, *44*, 5479-5486.
37. E. J. Ko, G. P. Savage, C. M. Williams, J. Tsanaktsidis, *Org. Lett.* **2011**, *13*, 1944-1947.
38. G. Pandey, T. D. Bagul, G. Lakshmaiah, *Tetrahedron Lett.* **1994**, *35*, 7439-7442.
39. C. S. Shanahan, C. Fang, D. H. Paull, S. F. Martin, *Tetrahedron* **2013**, *69*, 7592-7607.
40. T. Sato, N. Chono, H. Ishibashi, M. Ikeda, *J. Chem. Soc., Perkin Trans. I* **1995**, 1115-1120.
41. This computational work, as well as separation and NMR analysis of the two diastereomers, was carried out by a previous member of Dr Benfatti's group prior to

this placement project. This information and the accompanying figure has been included with permission from Dr Benfatti.

42. Y. Zhang, A. I. Gerasyuto, Q. A. Long, R. P. Hsung, *Synlett* **2008**, 2009, 237-240.
43. A. I. Gerasyuto, R. P. Hsung, *J. Org. Chem.* **2007**, 72, 2476-2484.

Chapter 3

Direct Arylation of Phenoxyquinolines

Introduction

3.1. Direct Arylation

One of the most important transformations in organic synthesis is the linking of two (hetero)aryl groups via a new carbon-carbon bond.^[1] The biaryl motif is an important substructure of many medically relevant compounds and is thus a critical synthetic target.^[2] Traditionally, the most reliable class of aryl-aryl bond forming reactions involved the palladium-catalysed coupling of an ‘activated’ aryl halide with another ‘activated’ organometallic reagent.^[3-6] Examples include the Suzuki-Miyaura coupling,^[7] Stille coupling,^[8] and Negishi coupling^[9] (**Figure 20**).



Figure 20 Traditional aryl-aryl bond forming methods.

While reliable and robust, the above named reactions have their drawbacks. Most notably, pre-activation of the coupling partners requires the use of stoichiometric amounts of expensive organometallic compounds, such as boron, tin or zinc reagents. The installation of the activating groups themselves is not trivial, often requiring several synthetic steps and suffering from regioselectivity problems, as well as the secondary issues of generating more waste from reagents, solvents and purification methods. Furthermore, subsequent disposal of the organometallic by-products of the coupling reaction renders these methods inherently wasteful. In addition, the organometallic waste is often toxic and therefore costly to dispose of.

In recent years, there have been significant advances toward more cost effective and environmentally friendly cross-coupling methods. The aim is to eliminate the necessity for pre-activation, thus increasing atom economy and reducing waste output. This approach is termed direct arylation (DA), and utilises protocols which are less reliant on the installation of a reactive functionality to activate the coupling partners, prior to cross-coupling (**Figure 21**).^[10-12] Modern methods to synthesise these compounds via direct arylation are among the ‘Wanted List’ of top pharmaceutical companies.^[13]

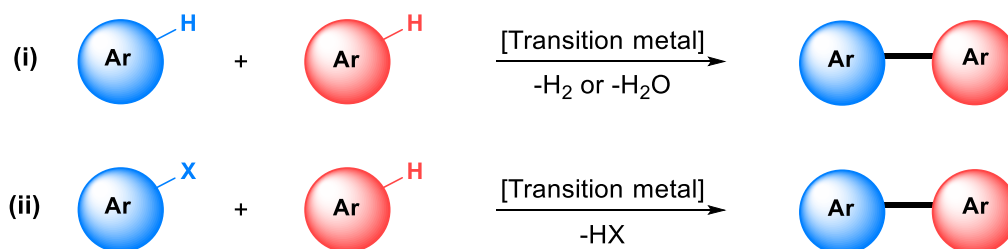
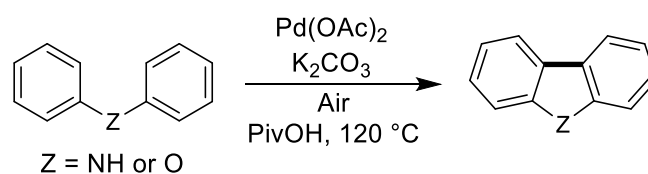


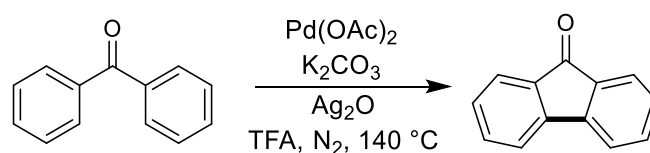
Figure 21 Methods of aryl-aryl bond formation via direct arylation.

Ideally, neither partner requires pre-activation. This methodology is termed double C-H activation or dehydrogenative coupling. Often, the only by-products are H_2 or H_2O (**Figure 21 (i)**).^[14] This type of reaction is usually performed in an intramolecular fashion to minimise chemoselectivity and regioselectivity issues. In 2008, Fagnou and co-workers published the synthesis of dibenzofurans and carbazoles via double C-H activation of diarylethers and diarylamines (**Scheme 37 (i)**).^[15] In 2012, Shi and co-workers reported the synthesis of fluorenone derivatives via Pd-catalysed double C-H activation of benzophenones (**Scheme 37 (ii)**).^[16] The McGracken group developed a route to polycyclic pyrones and coumarins by intramolecular double C-H coupling of phenoxy-substituted substrates (**Scheme 37 (iii)**).

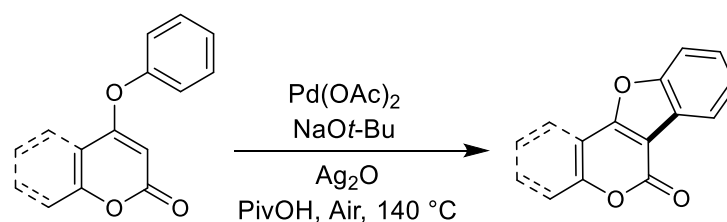
(i) Fagnou, *J. Org. Chem.*, 2008, 73, 5022-5028



(ii) Shi, *Org. Lett.*, 2012, 14, 4850-4853



(iii) McGracken, *Org. Lett.*, 2016, 18, 2540-2543

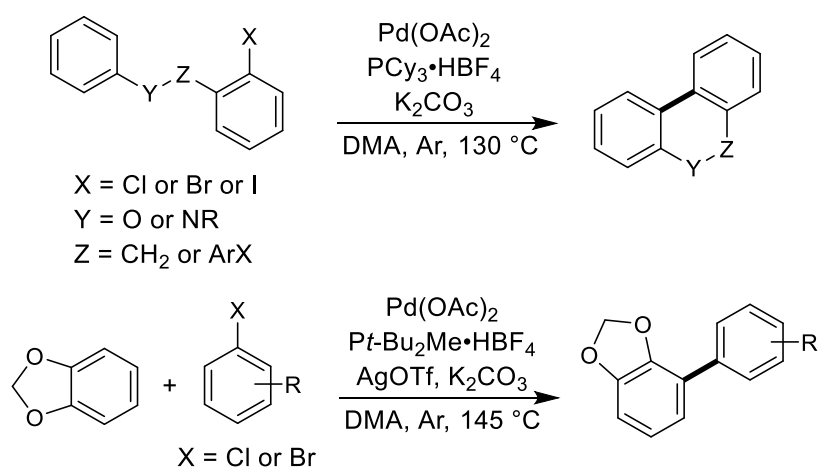


Scheme 37 Literature examples of direct arylation via double C-H activation.

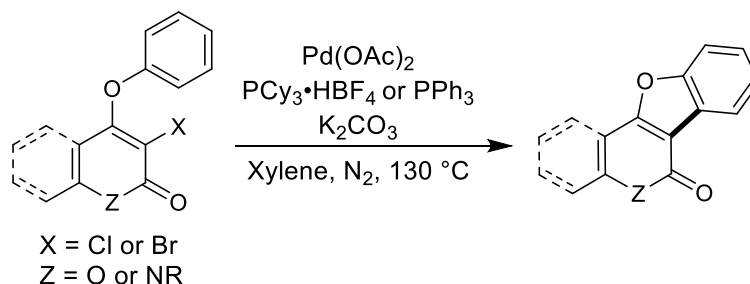
However, dehydrogenative coupling can be very difficult to achieve selectively, given that a number of C-H sites are usually available. Additionally, the reaction is thermodynamically disfavoured due to the strength of the aromatic C-H bond.^[17]

Alternatively, a chemical compromise can be reached whereby one of the coupling partners is pre-activated. This methodology is known as single C-H activation (**Figure 21 (ii)**).^[11] Once again, a transition metal catalyst is used to couple a pre-activated species (often a carbon-halogen bond) with a specific C-H site on another aryl ring. This can be performed in an intermolecular or intramolecular system, and regioselectivity can be controlled by use of a directing group, manipulation of steric effects or the latent electronics of the aryl ring.^[18] In 2006, Fagnou and co-workers reported both intermolecular and intramolecular single C-H activation reactions of simple arenes (**Scheme 38 (i)**).^[19] An intramolecular single C-H activation of privileged biological scaffolds was reported by the McGlacken group in 2015 (**Scheme 38 (ii)**).^[20]

(i) Fagnou, *J. Am. Chem. Soc.*, 2006, 128, 581-590



(ii) McGlacken, *J. Org. Chem.*, 2015, 80, 10904-10913



Scheme 38 Literature examples of direct arylation via single C-H activation.

Direct arylation of simple arenes has been used routinely in organic synthesis to access complex polycyclic ring systems.^[20-24] By comparison, similar reactions involving heterocycles tend to require specialised catalyst/ligand systems and are therefore less prevalent in the literature.^[25] One of the earliest examples of an intramolecular direct arylation of a heteroarene was reported in 1984 by Ames and Opalko.^[26] More recently, Ha *et al.* reported a palladium-catalysed synthesis of benzofuopyridines in moderate to excellent yields.^[27] As illustrated in Scheme 37 and Scheme 38, the McGlacken group have reported direct arylation methodologies involving pyrone, coumarin, pyridone and quinolone heterocycles.^[20, 22-23, 28-29]

Whether carrying out aryl-aryl bond formation by traditional or modern direct arylation methodologies, the mechanism of palladium-catalysed coupling reactions are expected to follow the same general steps (Figure 22). The catalytic cycle typically begins with **oxidative addition** of Pd(0) to the carbon-halide (or carbon-hydrogen) bond of the first coupling partner. Subsequently, the second partner undergoes **transmetallation**, which places both coupling partners on the metal centre. The final step is **reductive elimination** of the product to regenerate the catalyst.

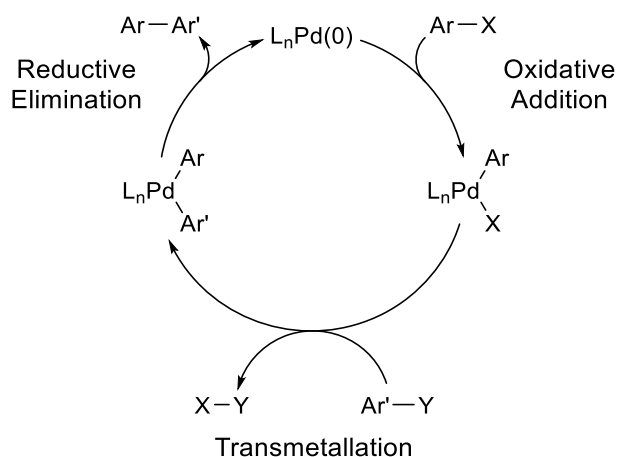


Figure 22 General catalytic cycle for palladium-catalysed cross-coupling reactions.

3.2. Quinolines

The quinoline nucleus occurs in many natural and synthetic pharmacologically active compounds,^[30] and is ranked 22nd in the top 100 most frequent ring systems present in FDA approved drugs (**Figure 23**).^[31] Thus, the quinoline motif is considered a privileged biological scaffold, utilised by synthetic chemists to build molecular complexity, and ultimately improve biological activity. As a versatile heterocycle, it displays reactivity similar to that of other aromatic (pyridine/benzene) analogues, and thus can undergo a wide range of synthetic transformations.^[32-33]

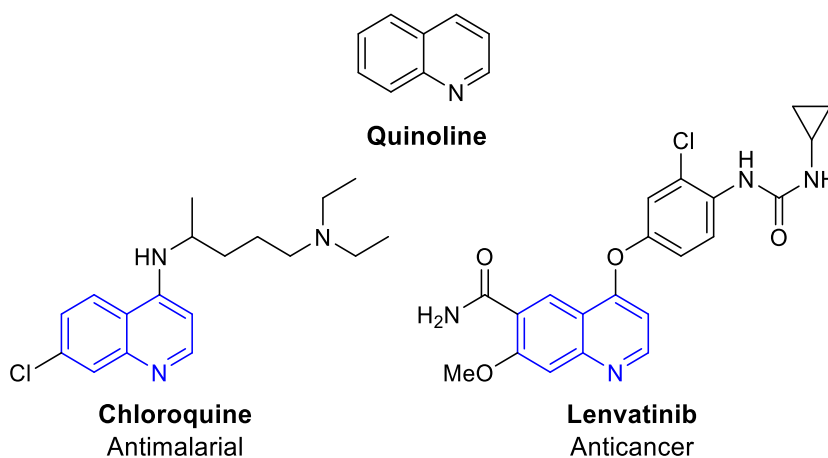


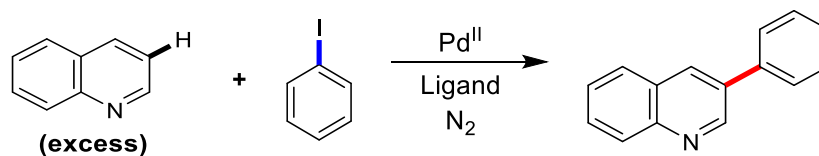
Figure 23 Quinoline and the quinoline-containing drugs Chloroquine and Lenvatinib.

This thesis chapter describes the development of a palladium-catalysed direct arylation of 4-phenoxyquinolines as a route to benzofuro[3,2-*c*]quinolines. Access to these products will aid exploration of their untapped biological potential, given that similar quinoline-based compounds exhibit anticancer,^[34] antimalarial^[35] and antibacterial^[36] effects.

Previous syntheses of some of similar benzofuroquinolines via direct arylation have relied upon positioning the activated carbon-halide bond on the C-3 position of the quinoline coupling partner,^[37-38] which limits the accessibility and versatility of the products formed. The first example of a (non-directed) C-H activation selectively at the C-3 position of unprotected pyridines and quinolines was reported by Yu and co-workers (**Figure 24 (i)**), using phosphine ligands and inert reaction conditions.^[39] Yu's method relies upon the use of a large excess of the quinoline or pyridine substrate, which is only applicable to an intermolecular system. The work in this chapter outlines

the development of an air-stable C-H activation of the C-3 position of the quinoline ring via intramolecular direct arylation with no added ligand required (**Figure 24 (ii)**).

(i) Yu, *J. Am. Chem. Soc.*, 2011, 133, 19090-19093



(ii) This work

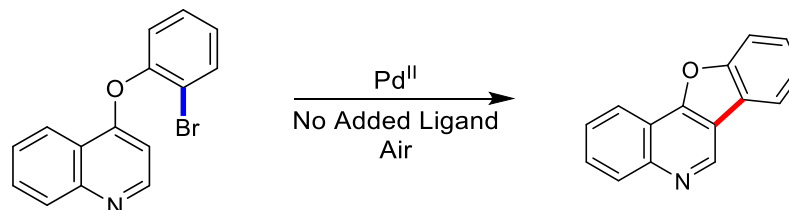
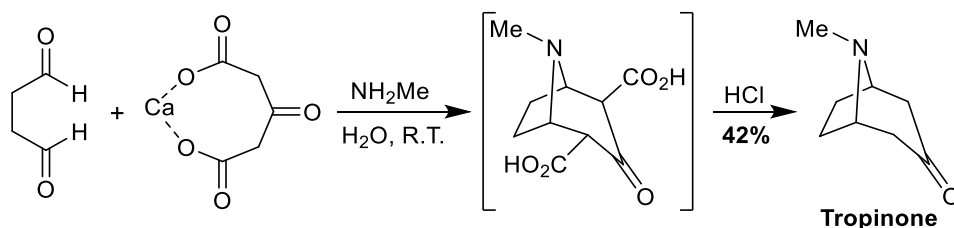


Figure 24 Palladium-catalysed C-H activation at the C-3 position of quinolines.

3.3. One-Pot Reactions

Efficient and environmentally-friendly approaches to the construction of new chemical entities are highly desirable to synthetic chemists both in academic and industrial settings. Such methods aim to avoid or reduce the number of work-ups and purification steps and, when feasible, involve carrying out the entire synthesis in a single reaction vessel. Step-economic, telescoped procedures allow for a dramatic reduction of costs, mostly associated with operator time and chemical waste.^[40-41] However, carrying out two or more reactions in a single step within a single pot places significant demands on the methodologies involved, specifically in terms of solvent, reagent and substrate compatibility. In addition, avoiding secondary manipulation of the system during the reaction (by the addition of a new reactant, reagent, or catalyst, for example) is preferable.

Despite the associated challenges, one-pot synthetic strategies have been successfully employed to access valuable target molecules for over 100 years. In 1917, Sir Robert Robinson published his ground-breaking one-pot total synthesis of tropinone (**Scheme 39**).^[42] By comparison, the first total synthesis of tropinone, published in 1901 by Willstätter,^[43] involved 21 steps with an overall yield of <1%. The step-economic and biomimetic approach displayed in Robinson's tropinone synthesis serve as inspiration for the development of new, efficient strategies for complex molecule synthesis.



Scheme 39 Robinson's one-pot synthesis of tropinone in 1917.

One-pot strategies are frequently employed to streamline the synthesis of complex natural products and pharmaceutically active compounds.^[44] In a more recent example, Hayashi and colleagues have developed a powerful one-pot reaction for the rapid construction of the polyfunctionalized cyclohexene core of Tamiflu.^[45-46]

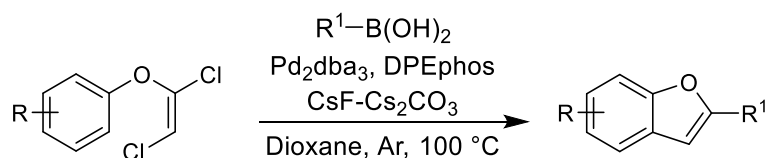
Considering the variety of transformations that can be performed in a one-pot system, a complete summary of the topic is not possible within the scope of this thesis. Instead,

the focus of this introduction will be on reactions combining a Pd-catalysed Suzuki-Miyaura and direct arylation transformation in one pot. While there are several different terminologies used to describe multiple transformations taking place in one pot,^[40] the term ‘tandem reaction’, whereby transformations occur one after the other, is the most applicable here.

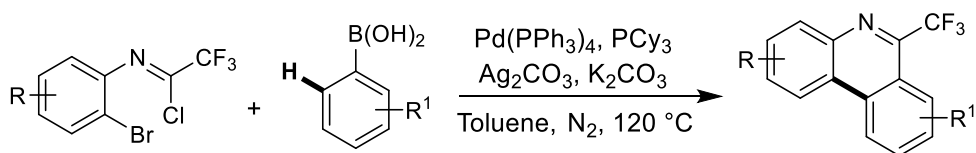
3.3.1. Literature Examples of One-Pot Suzuki-Miyaura/Direct Arylation

Several tandem reactions combining a direct arylation step with a Suzuki-Miyaura reaction have been reported.^[47-51] However, we are aware of a very limited number of protocols that do not require perturbation of the reaction set-up by the addition of secondary reactants, reagents or catalysts (**Scheme 40**).^[52-55]

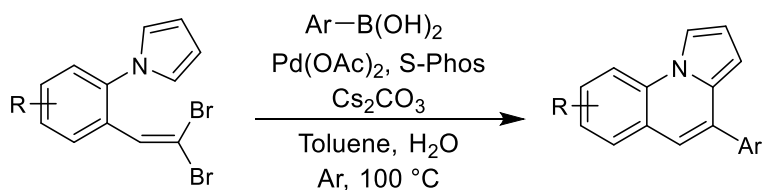
Hultin, *Org. Lett.* 2009, 11, 5478-5481



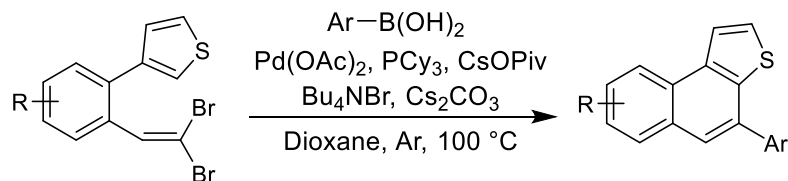
Zhang, *J. Org. Chem.* 2013, 78, 6025-6030



Lautens, *J. Org. Chem.* 2009, 74, 3054-3061

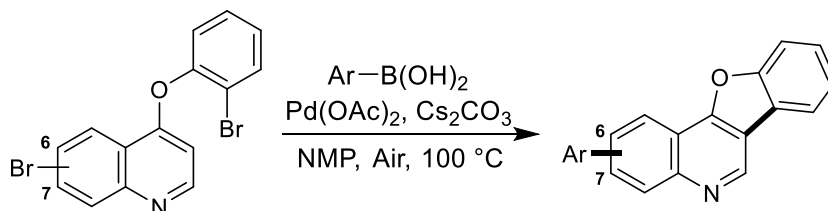


Lautens, *Org. Lett.* 2011, 13, 4236-4239



Scheme 40 One-pot tandem Suzuki-Miyaura/direct arylation reactions in the literature.

As outlined above, tandem cross-coupling reactions can increase the efficiency and modularity of synthetic transformations. All of the examples shown in **Scheme 40** fall under this category, as does the one-pot tandem Suzuki-Miyaura/direct arylation reaction shown in **Scheme 41**, which was discovered and optimised during this PhD project (see **Section 3.10**).



Scheme 41 One-pot tandem Suzuki-Miyaura/direct arylation of dibrominated 4-phenoxyquinolines.

What separates this work from the examples in **Scheme 40**, however, is that neither phosphine ligands nor an inert atmosphere are required for this tandem reaction. This reduces the associated cost and simplifies the set-up of the one-pot reaction. The novel benzofuroquinoline products make for excellent molecular frameworks for further modification and structure-activity studies.

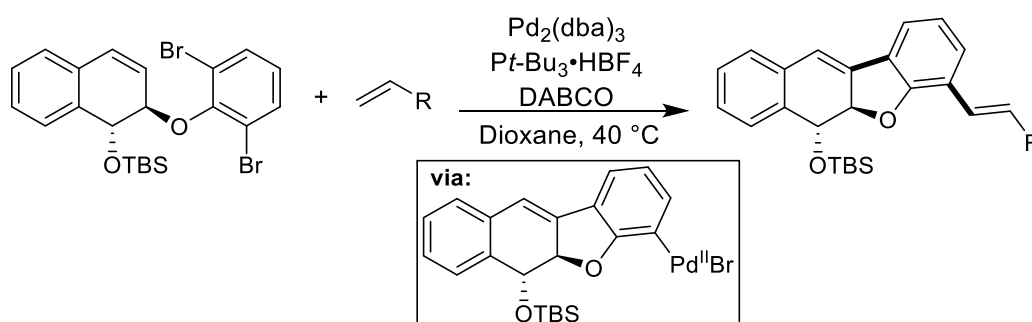
3.4. Dihalogenated Substrates – Chemoselectivity and Regioselectivity

In direct arylation reactions, chemoselectivity and regioselectivity are somewhat predictable in monohalogenated systems. Even when working with polyhalogenated starting materials, chemoselectivity can often be controlled by using two different halogens, since there is a marked difference in reactivity between the various carbon-halogen bonds of aromatic compounds.^[56] The order of reactivity ($\text{Ar-I} > \text{Ar-Br} > \text{Ar-Cl} \gg \text{Ar-F}$) is consistent with the strength of the C-X bond. The experimentally measured bond dissociation energies (BDEs) for phenyl C-X bonds are 126, 96, 81, and 65 kcal/mol at 298 K for X = F, Cl, Br, and I, respectively.^[57]

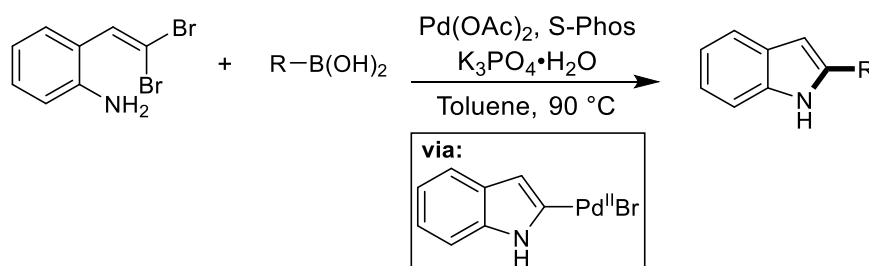
However, the outcome of cross-coupling reactions involving substrates bearing multiple identical halogens can be considerably more difficult to control, as rate-differences in the oxidative addition step (I vs. Br or Br vs. Cl) can be difficult to harness. One potential problem that can arise when using dihalogenated substrates is irreversible oxidative addition of the catalyst to one of the C-X bonds, leading to a shutdown of the catalytic cycle. This type of catalyst deactivation can be avoided by

adding an intermolecular coupling partner, such as an alkene or boronic acid, to the reaction mixture. This strategy facilitates the conversion of the otherwise unproductive ArPd(II)X species through an intermolecular cross-coupling reaction, regenerating the active catalyst. Lautens^[58-59] and Cramer^[60] have reported employing tandem processes in this manner when working with dibrominated substrates (**Scheme 42**). In all three examples, the authors reported that the dibrominated substrates failed to undergo complete conversion to the ring-closed product in the absence of an intermolecular coupling partner.

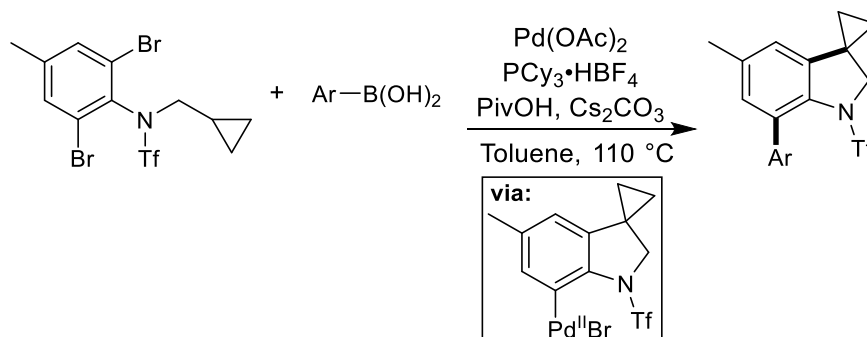
(i) Lautens, *Org. Lett.*, 2003, 5, 3679-3682



(ii) Lautens, *J. Org. Chem.*, 2008, 73, 538-549



(ii) Cramer, *Org. Lett.*, 2013, 15, 1354-1357

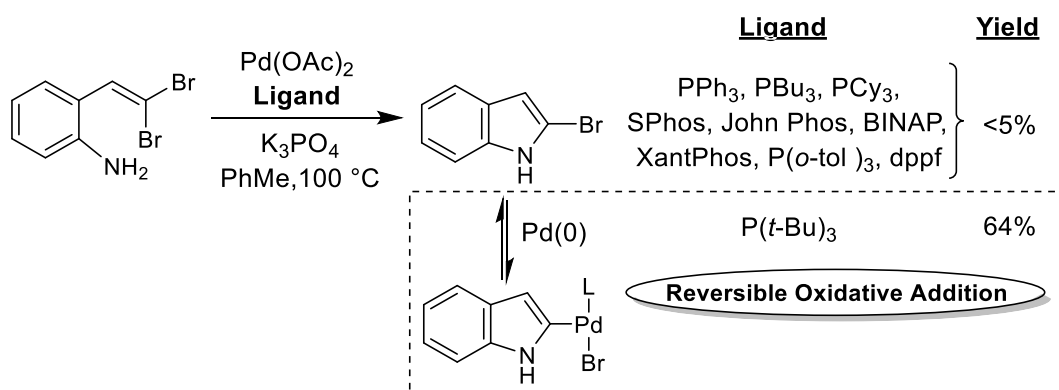


Scheme 42 Tandem reactions of dihalogenated substrates.

However, this tandem reaction strategy is not applicable when there is a desire to retain a particular halogen in the product. In the examples shown in **Scheme 42**, the authors noted in each case that the monobrominated product of their ring-closing reaction could not be obtained in high yield. Rather, the second bromide always had to undergo coupling for the overall catalytic cycle to remain productive. Lautens has speculated that the termination of the catalytic due to unproductive C-X oxidative addition is responsible for the notable absence of polyhalogenated substrates in the majority of scope evaluations.^[61]

3.5. Reversible Oxidative Addition

While oxidative addition of Pd(0) to aryl halides is generally considered irreversible (**Figure 22**), Hartwig and Roy discovered that by using a large excess of a bulky phosphine ligand, it was possible to induce reductive elimination of ArPd(II)Br complexes to liberate Pd(0).^[62-64] They found that the steric crowding and strongly electron-donating nature of ligands such as P(*t*-Bu)₃ accelerated the rate of reductive elimination to such an extent that elimination became thermodynamically favoured. This work suggests that oxidative addition of specific Pd(0) complexes to carbon-halogen bonds can occur in a reversible manner. Inspired by these findings, Lautens hypothesised that a catalyst capable of both oxidative addition to and reductive elimination from C-X bonds could facilitate site-selective cross-coupling reactions of substrates bearing identical halides. In 2010, Lautens and Newman reported a modification of their tandem synthesis of 2-substituted indoles from *gem*-dibromoalkenes (**Scheme 42 (ii)**) that allowed for isolation of 2-bromoindole products (**Scheme 43**).^[61] These brominated indoles had proved to be inaccessible under the previously reported conditions.^[59]



Scheme 43 Importance of ligand choice in Lautens' synthesis of 2-bromoindoles. Reversible oxidative addition occurs only when L = P(*t*-Bu)₃.

The key to their success was the choice of phosphine ligand, with bulky P(*t*-Bu)₃ proving capable of promoting the desired reaction. The reaction failed in the presence of all of the other phosphine ligands screened due to the irreversible oxidative addition of the palladium catalyst to the 2-bromoindole product after one turnover of the catalytic cycle.

Since this seminal report, Lautens and co-workers have developed other Pd(0)-catalysed transformations whereby reversible oxidative addition is the key to catalysis.^[65-70] As well as P(*t*-Bu)₃, the ferrocene-derived QPhos ligand has also proved effective at promoting reversible oxidative addition in site-selective reactions.^[67-69]

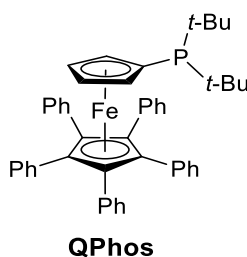


Figure 25 QPhos = 1,2,3,4,5-pentaphenyl-1'-(di-*tert*-butylphosphino) ferrocene.

3.6. Aims of this Chapter

The three key concepts discussed in this introduction (**Direct Arylation**, **One-Pot Synthesis** and **Reversible Oxidative Addition**) will be applied to the synthesis of a range of quinoline-derived compounds containing the benzofuroquinoline scaffold.

Chapter 3

Direct Arylation of Phenoxyquinolines

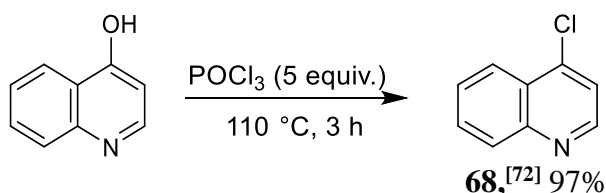
Results & Discussion

3.7. Objectives

As discussed in the introduction, direct arylation protocols aim to eliminate the requirement for pre-activation of the coupling partners prior to cross-coupling. Ideally, neither coupling partner requires the installation of a reactive functionality, and the direct arylation reaction proceeds by double C-H activation. Previous success in this area within the McGlacken group^[22, 29] (**Scheme 37 (iii)**) inspired the following work on exploring conditions for the intramolecular double C-H activation of 4-phenoxyquinolines as a route to benzofuroquinolines.

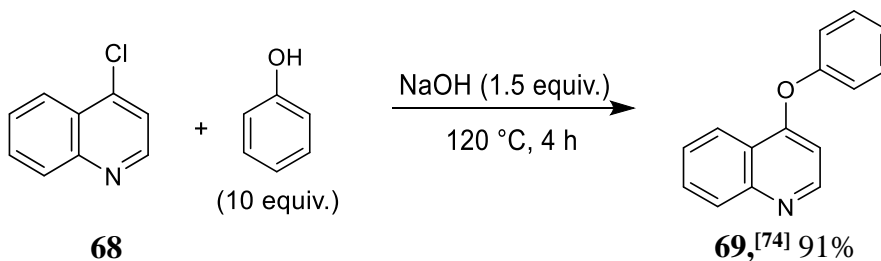
3.8. Attempts at Double C-H Activation

To begin, 4-chloroquinoline **68** was synthesised by chlorination of commercially available 4-quinolinol using phosphorus oxychloride in near quantitative yield.^[71] Multiple grams of **68** could be synthesised at a time to serve as a useful starting material for many of the substrates discussed in this chapter.



Scheme 44 Chlorination of 4-quinolinol to form 4-chloroquinoline **68**.

Next, 4-chloroquinoline **68** underwent substitution of the chlorine atom with a phenoxide group, formed in situ by deprotonation with sodium hydroxide.^[73] A large excess of phenol was used to act as the solvent for the reaction. A lower excess can be used in the case of more expensive substituted phenols, and this will be discussed further later. This method allowed access to the 4-phenoxyquinoline substrate **69** in high yield.

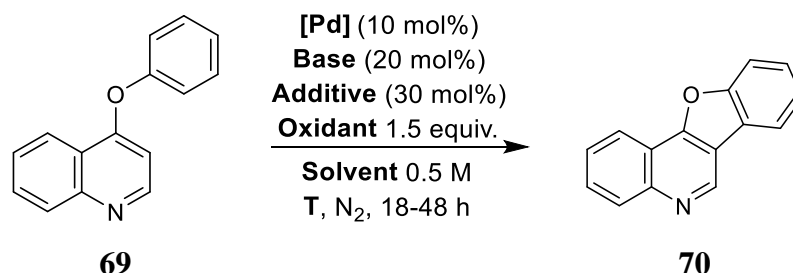


Scheme 45 Synthesis of 4-phenoxyquinoline **69**.

Although there are examples of dehydrogenative coupling reactions involving heterocycles in the literature,^[24] the transformation of **69** to **70** has yet to be reported. The investigation began with state-of-the-art conditions from reports by Shi^[16] (**Table 1, entry 1**) and Fagnou^[15] (**Table 1, entry 2**). Unfortunately, neither of these reactions resulted in good conversion to product. Instead, a complex mixture of degradation products was observed. The literature example most similar to our substrate was found in a report by Miura and co-workers.^[75] The substrate in Miura's report was a 2-phenoxyquinoline rather than a 4-phenoxyquinoline. Nevertheless, the new C-C bond formed was between the 3-position of the quinoline and the 2'-position of the

phenoxy ring, as would be the case in our target product. However, Miura's conditions (**Table 1, entry 3**) failed to promote the intramolecular cyclisation of **69**.

Table 1 Screen of conditions for double C-H activation of substrate **69**.



Entry	[Pd]	Base	Oxidant	Solvent	Add.	T (°C)	%Yield (NMR) ^[a]
1 ^[b]	Pd(OAc) ₂	K ₂ CO ₃	Ag ₂ O	TFA	-	140	<10
2 ^[c]	Pd(OAc) ₂	K ₂ CO ₃	-	PivOH	-	120	13
3 ^[d]	Pd(TFA) ₂	AgOAc	Air	PivOH	-	150	6
4	Pd(OAc) ₂	NaOt-Bu	Ag ₂ O	PivOH	-	140	22
5	Pd(OAc) ₂	NaOt-Bu	Ag ₂ O	PivOH	-	155	16
6	Pd(OAc) ₂	NaOt-Bu	Ag ₂ O	PivOH	-	120	20
7	Pd(OAc) ₂	NaOt-Bu	Ag ₂ O	DMF	PivOH	140	<1
8	Pd(OAc) ₂	NaOt-Bu	Ag ₂ O	NMP	PivOH	140	<1
9	Pd(OAc) ₂	NaOt-Bu	Ag ₂ O	DMSO	PivOH	140	<1
10	Pd(OAc) ₂	NaOt-Bu	Ag ₂ O	PivOH	-	140	13
11	Pd(OAc) ₂	NaOt-Bu	Air	PivOH	-	140	14

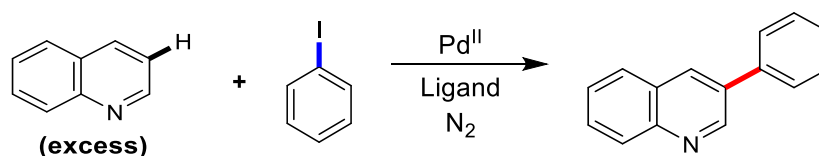
^[a]Yields were determined by ¹H-NMR analysis of the C-2 proton of the product in the crude reaction mixture using 1,3,5-trimethoxybenzene as the internal standard. ^[b]Shi's conditions (5 mol% Pd(OAc)₂ and 2.5 equiv. K₂CO₃). ^[c]Fagnou's conditions (5 mol% Pd(OAc)₂ and 10 mol% K₂CO₃). ^[d]Miura's conditions (3 mol% Pd(OAc)₂ and 2 equiv. AgOAc).

Subsequent investigations were based on conditions previously optimised within the McGlacken group for the cyclisation of 4-phenoxy-2-coumarins and 4-phenoxy-2-yrone via double C-H Activation (**Table 1, entry 4**).^[22] Whilst these conditions gave the highest yield of **70**, significant degradation of starting material was also observed. Increasing (**Table 1, entry 5**) or decreasing (**Table 1, entry 6**) the reaction temperature did not improve the outcome. Using a substoichiometric amount of pivalic acid in high boiling-point solvents (**Table 1, entry 7–9**) resulted in degradation of starting material, and no evidence of product formation was observed. Using a carbonate base instead of NaOt-Bu (**Table 1, entry 10**), or using air rather than Ag₂O as the oxidant (**Table 1, entry 11**) did not result in greater product formation. Given the difficulties associated with trying to cleave two C-H bonds on the quinoline substrate, the decision was made to try a single C-H activation approach.

3.9. Single C-H Coupling

As mentioned in the introduction, methods for accessing the framework of **70** via C-H bond activation of the C-3 position of the quinoline were lacking in the literature. The first example of a non-directed C-H activation of the C-3 position of pyridines and quinolines was reported by Yu and co-workers (**Figure 26 (i)**), using phosphine ligands.^[39] The following section describes a ligand-free C-H activation of the C-3 position of the quinoline via intramolecular direct arylation, in air (**Figure 26 (ii)**).

(i) Yu, *J. Am. Chem. Soc.*, 2011, **133**, 19090-19093



(ii) This work

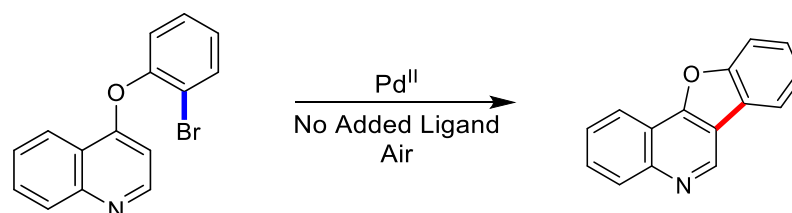
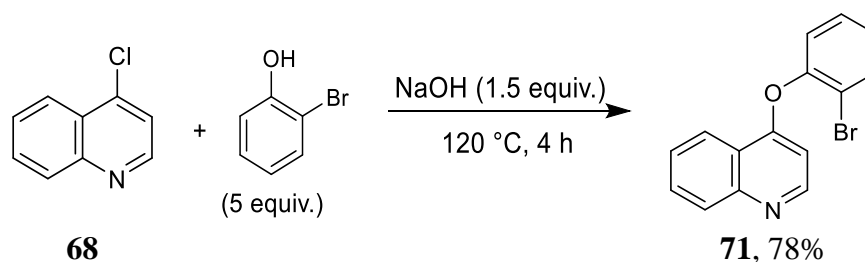


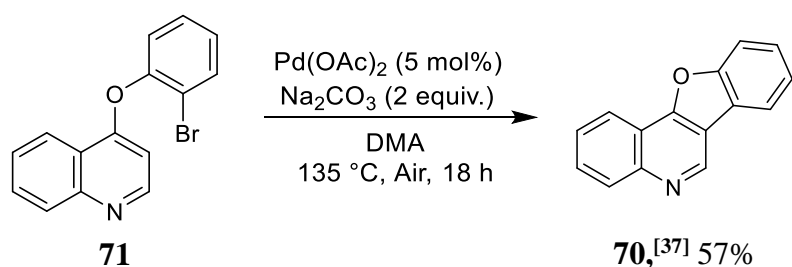
Figure 26 Palladium-catalysed C-H activation at the C-3 position of quinolines.

To begin, 4-(2-bromophenoxy)quinoline **71** was chosen as the substrate, synthesised by reaction of 4-chloroquinoline **68** with 2-bromophenol. This transformation proceeds via nucleophilic attack of the phenoxide anion (generated in situ) at the 4-position of the quinoline (**Scheme 46**).



Scheme 46 Synthesis of 4-(2-bromophenoxy)quinoline substrate **71**.

To achieve the intramolecular cyclisation of **71**, a relatively simple system of a palladium catalyst, inorganic base, and high-boiling polar solvent was first applied. Pleasingly, our initial coupling conditions allowed formation of the fused product **70** in 57% isolated yield, in air (**Scheme 47**).



Scheme 47 Initial conditions for single C-H functionalisation of **71**.

Next, a variety of reaction parameters was assessed (**Table 2**). A solvent screen indicated that high-boiling point amide solvents were necessary for good conversion (**Table 2**, entry 1–3). Other solvents gave little or no conversion to product (**Table 2**, entry 4–8). Changing the base from Na_2CO_3 to K_2CO_3 or Cs_2CO_3 resulted in an increase in the isolated yield of the product (**Table 2**, entry 9–10), while use of a stronger butoxide base resulted in decomposition of the starting material (**Table 2**, entry 11). A further reduction in catalyst loading to 2 mol% was also achieved (**Table 2**, entry 12), allowing the desired product **70** to be isolated in 95% yield.

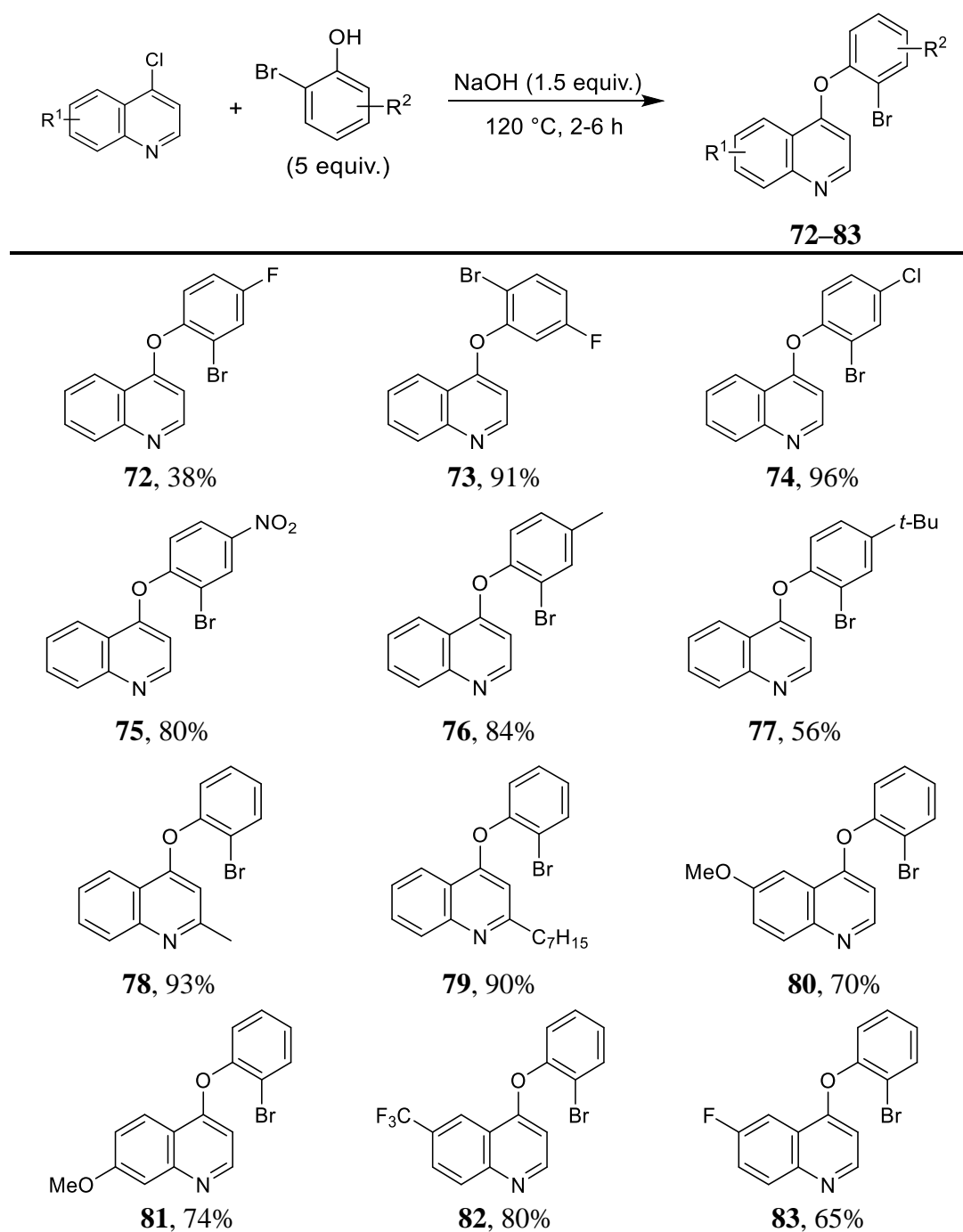
Table 2 Optimisation of direct arylation conditions for 4-(2-bromophenoxy)phenol.

Entry	Pd(OAc)_2	Base	Solvent	T (°C)	%Yield NMR ^[a] (Isolated Yield)
1	5 mol%	Na_2CO_3	DMA	135	(57)
2	5 mol%	Na_2CO_3	DMF	135	67
3	5 mol%	Na_2CO_3	NMP	135	70 (72)
4	5 mol%	Na_2CO_3	DMSO	135	0
5 ^[b]	5 mol%	Na_2CO_3	1,4-Dioxane	100	0
6 ^[b]	5 mol%	Na_2CO_3	EtOH	78	0
7 ^[b]	5 mol%	Na_2CO_3	1,2-DCE	55	0
8 ^[b]	5 mol%	Na_2CO_3	MeCN	82	0
9	5 mol%	K_2CO_3	NMP	135	72
10	5 mol%	Cs_2CO_3	NMP	135	83
11	5 mol%	NaOt-Bu	NMP	135	39 ^[c]
12	2 mol%	Cs_2CO_3	NMP	135	99 (95)
13	1 mol%	Cs_2CO_3	NMP	135	33

^[a]Yields determined by $^1\text{H-NMR}$ analysis of the C-2 proton of the product in the crude reaction mixture using 1,3,5-trimethoxybenzene as internal standard. ^[b]Reaction carried out at the boiling point of the solvent. ^[c]Decomposition of starting material observed.

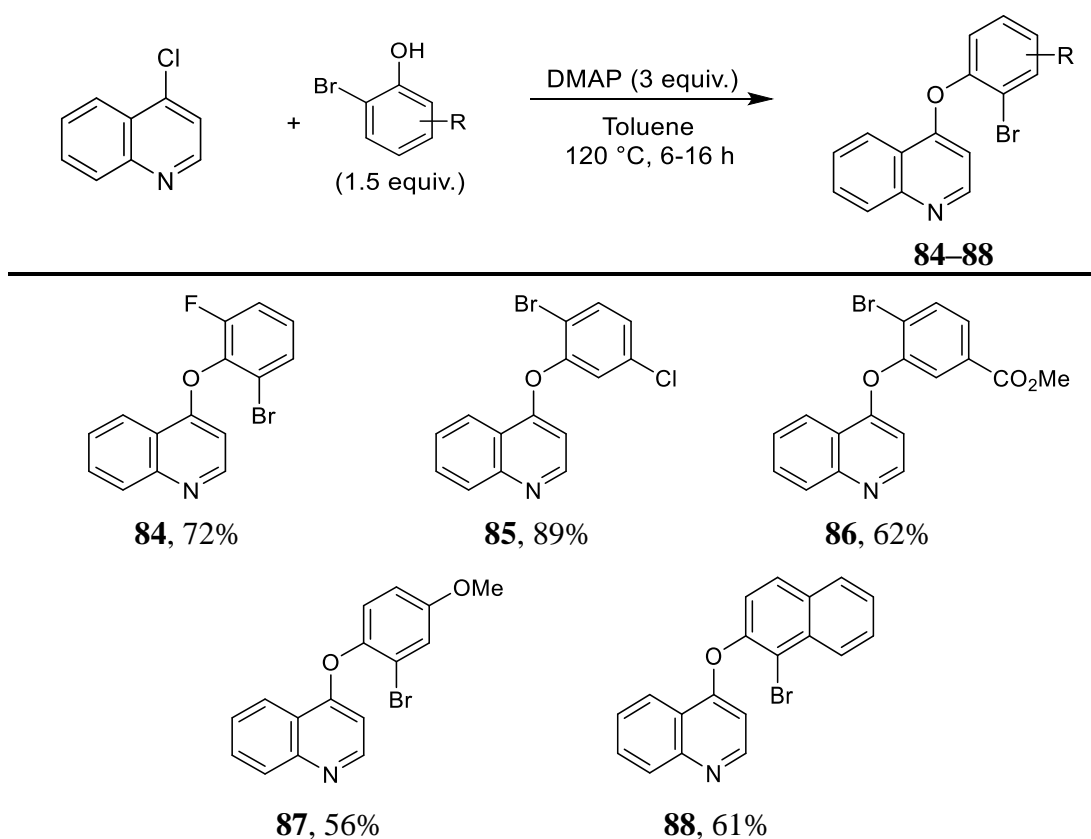
3.9.1. Substrate Scope

With optimised conditions in hand, an examination of the functional group tolerance under the optimised conditions was planned. For this investigation, a range of novel substituted analogues of **71** was synthesised. Compounds **72–83** were prepared using the same method as described for **71**.



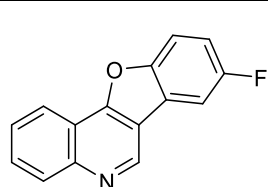
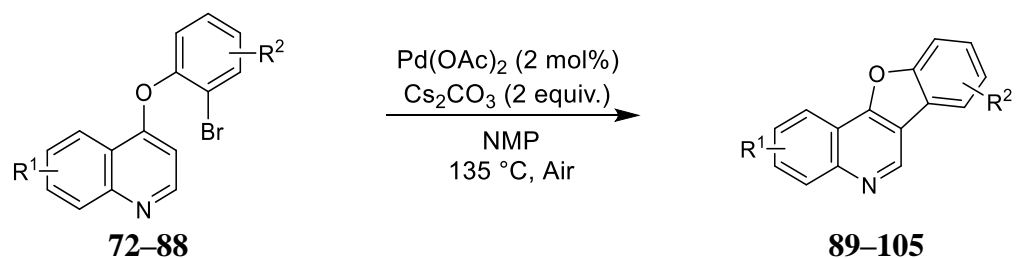
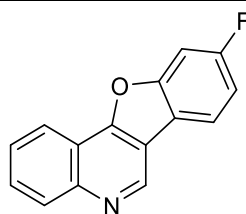
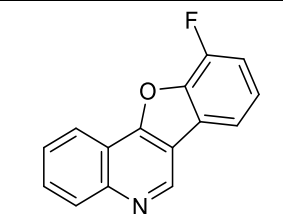
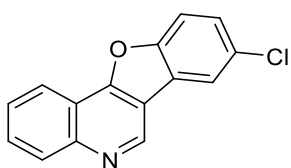
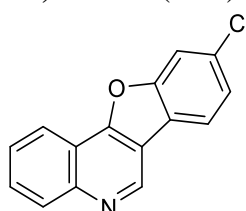
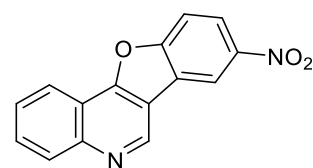
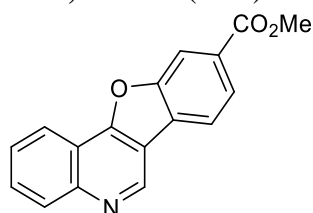
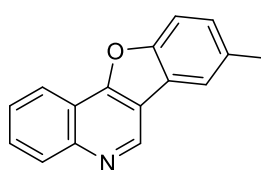
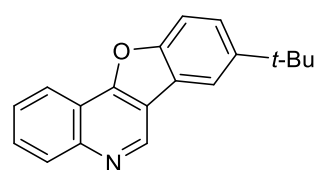
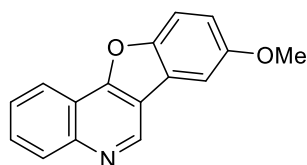
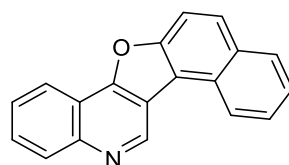
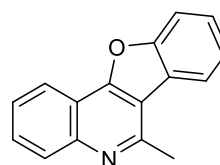
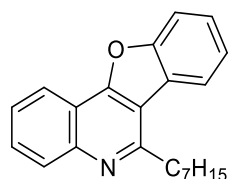
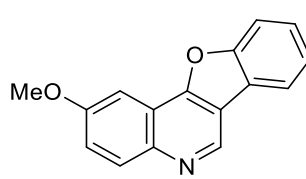
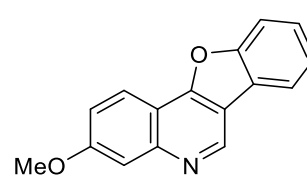
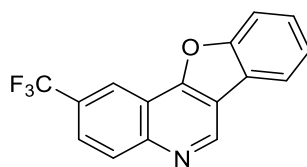
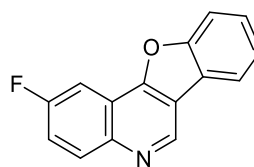
Scheme 48 Synthesis of 4-phenoxyquinoline substrates.

However, in the case of a few of the substituted 2-bromophenols, this method proved unsuitable. The reactions did not proceed as desired in the presence of sodium hydroxide, resulting in unreacted starting materials or complex mixtures. It was suspected that the nucleophilic nature of the hydroxide base was incompatible with these 2-bromophenols. As it was of interest to expand the variety of substrates bearing both electron-rich and electron-poor substituents, an alternative method was employed using the non-nucleophilic base DMAP. Gratifyingly, under these conditions the desired novel substrates could be obtained and included in the substrate scope. This method was also favourable as it required a lesser excess of the phenol, thus avoiding wasting large amounts of the more expensive phenol starting materials.



Scheme 49 Synthesis of 4-phenoxyquinoline substrates using DMAP as base.

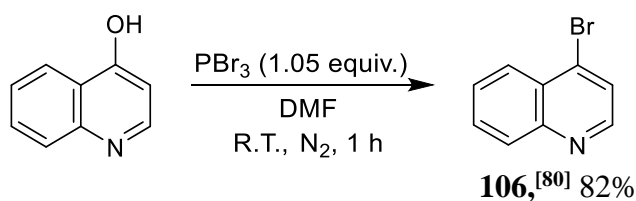
Next, each of these substrates were subjected to the optimised direct arylation conditions (**Scheme 50**). Overall, it was observed that the reaction allows for a variety of functional groups on both the phenoxy and quinoline coupling partners. Substrates with weakly electron-withdrawing substituents (**72**, **73**, **74**, **84**, **85**) on the phenoxy ring were well tolerated. Additionally, the chlorides in **74** and **85** were retained as a synthetic handle for further cross-coupling. Moderate yields of cyclised product were observed in the case of the nitro (**75**) and ester (**86**) containing analogues. Longer reaction times were required in the case of electron-rich phenoxy substrates (**76**, **77**). In the case of the naphthyl analogue **88**, the desired product could only be obtained in 17% isolated yield, with the majority of the remaining product attributed to unreacted starting material. This may be due to the steric bulk of the naphthyl group hindering access to the coupling site. The scope of the reaction with respect to the quinoline was also examined. A methyl group at the C-2 position was well tolerated (**78**), as was the heptyl chain of the HHQ-derived substrate (**79**). As discussed in Chapter 1, quinolones/quinolines bearing a heptyl chain at the C-2 position display signalling activity in the QS network of *P. aeruginosa* and other microorganisms. On the aryl backbone, both electron donating -OMe substituents (**80**, **81**) and electron withdrawing -CF₃ (**82**) and -F (**83**) substituents also led to very good yields of product.

**89**,^[37] 91% (18 h)**90**,^[76] 87% (18 h)**91**,^[37] 93% (18 h)**92**,^[37] 93% (18 h)**93**, 79% (18 h)**94**, 46% (18 h)**95**, 56% (18 h)**96**,^[37] 71% (48 h)**97**,^[37] 50% (48 h)**98**,^[38] 42% (48 h)**99**, 17% (48 h)**100**,^[37] 78% (30 h)**101**, 70% (30 h)**102**,^[37] 84% (18 h)^[a]**103**, 81% (18 h)^[a]**104**, 63% (24 h)**105**,^[76] 67% (24 h)

Scheme 50 Investigation of substrate scope. All yields are isolated yields. ^[a]5 mol% Pd(OAc)₂ required.

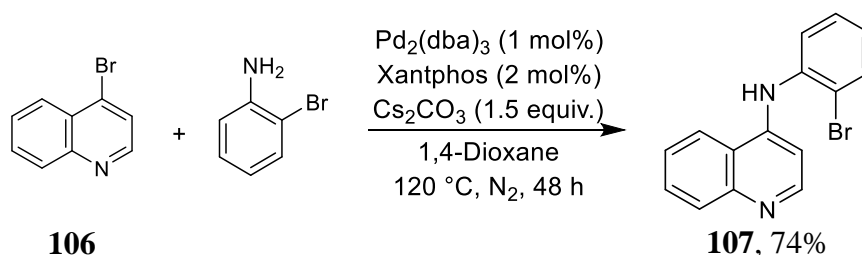
In an effort to expand the substrate scope beyond 4-phenoxyquinolines, the ether linker was replaced with an amine, which would allow access to fused indoloquinolines. Compounds containing fused indoloquinoline rings are known to possess antimalarial^[77] and anticancer activity.^[78]

It was envisaged that the amine-linked substrate could be accessed by performing a Hartwig-Buchwald coupling reaction between the 4-bromoquinoline starting material and an aniline. First, 4-bromoquinoline **106** was synthesised from 4-quinolinol (Scheme 51).^[79]



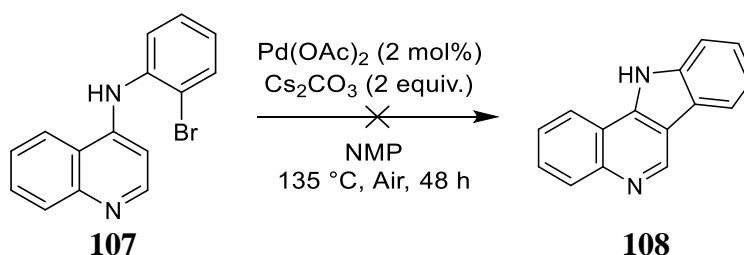
Scheme 51 Bromination of 4-quinolinol.

Next, the amine-linked substrate **107** was synthesised via Hartwig-Buchwald coupling of 4-bromoquinoline with 2-bromoaniline (Scheme 52).^[77]



Scheme 52 Synthesis of amine-linked substrate **107**.

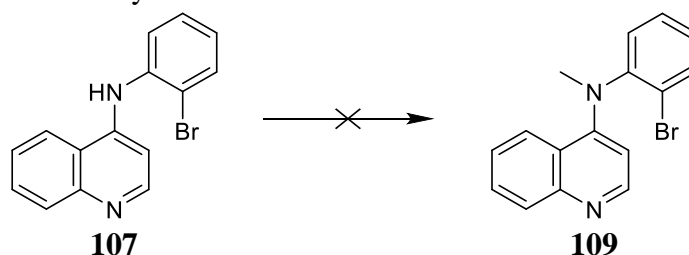
When **107** was subjected to the previously-optimised direct arylation conditions that worked for the 4-phenoxyquinolines, no cyclised product **108** was observed, even after prolonged reaction time (Scheme 53).



Scheme 53 Attempted cyclisation of **107** using previously optimised direct arylation conditions.

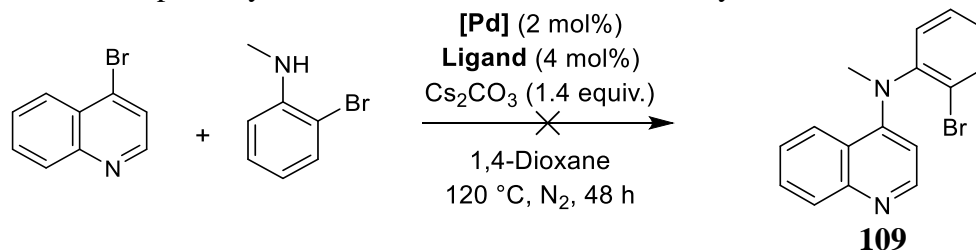
Given the possibility that the secondary amine was coordinating to the palladium and hindering catalysis of the desired reaction,^[81] methylation of the amine was envisaged to hinder ligation of the linker to the catalyst by creating steric bulk around the nitrogen atom. However, this seemingly straightforward transformation proved difficult to achieve, and after several attempts using various approaches (outlined in **Table 3**), this strategy was abandoned.

Table 3 Attempts at methylation of **107**.



Entry	Conditions	Result
1 ^[82]	NaH, MeI, DMF, N ₂ , 0 °C	Complex mixture
2 ^[83]	<i>n</i> -BuLi, MeI, THF, N ₂ , -40 °C	Debromination
3	KOH, MeI, Acetone, 65 °C	Complex mixture
4	KOH, MeI, DMF, 25 °C	Complex mixture
5 ^[84]	Paraformaldehyde, NaBH ₄ , TFE	Unreacted starting material
6 ^[85]	Aq. formaldehyde, AcOH, Zn, 1,4-Dioxane, 35 °C	Unreacted starting material

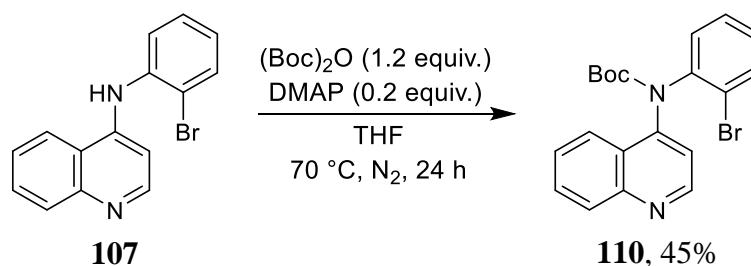
An alternative strategy for the synthesis of *N*-Me amine **109**, whereby the methyl group was installed by using 2-bromo-*N*-methylaniline as the starting material in the Hartwig-Buchwald reaction, was also tried.^[77] Unfortunately, multiple attempts using this approach also proved unsuccessful (**Table 4**).

Table 4 Attempts to synthesise **109** from 2-bromo-*N*-methylaniline.

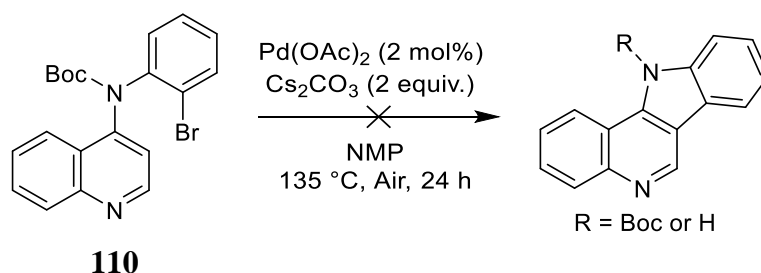
Entry	[Pd]	Ligand	Result
1	Pd ₂ (dba) ₃	Xantphos	Unreacted starting material
2	Pd ₂ (dba) ₃	dppf	Unreacted starting material
3	Pd ₂ (dba) ₃	RuPhos	Unreacted starting material
4 ^[a]	Pd(OAc) ₂	RuPhos	Unreacted starting material
5 ^[b]	Pd ₂ (dba) ₃	Xantphos	Unreacted starting material

^[a] 1 mol% Pd(OAc)₂ and 2 mol% RuPhos, NaO*t*-Bu (1.2 equiv.) used as base.^[86] ^[b] 4-Iodoquinoline used as starting material.

Given the difficulties associated with installing the methyl group on the amine linker, and since the methyl group itself would be difficult to remove or functionalise later, a removable protecting group strategy was pursued next. Gratifyingly, addition of a Boc group proved to be much more straightforward (**Scheme 54**).

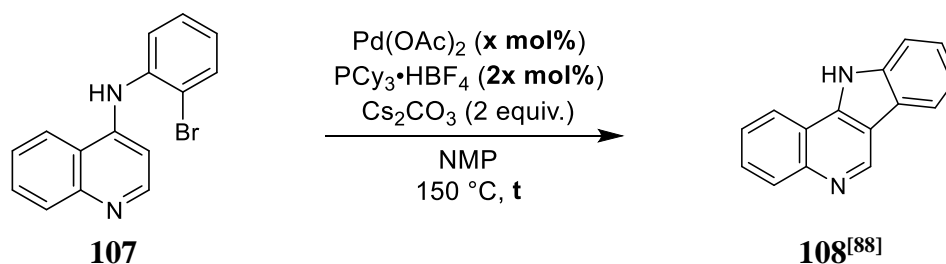
**Scheme 54** Boc protection of **107**.

Unfortunately, when **110** was subjected to the previously optimised direct arylation conditions, no cyclisation was observed and only deprotected starting material **107** was present in the crude reaction mixture.

**Scheme 55** Attempted direct arylation of **110**.

At this point, it seemed that inhibitive *N*-ligation to palladium could only be avoided by the addition of competitive phosphine ligands.^[87] Indeed, when a new catalytic system of 2 mol% Pd(OAc)₂ and 4 mol% PCy₃·HBF₄ was employed, approximately 20% conversion to the fused product was observed (**Table 5, entry 1**). Increasing the amount of catalyst and ligand led to 100% conversion, and now the product could be isolated in 83% yield after column chromatography (**Table 5, entry 2**). In contrast to the optimised conditions for the 4-phenoxyquinoline substrates, an inert atmosphere was required for efficient cyclisation of **107**. Under aerobic conditions the reaction proceeded sluggishly, with concomitant decomposition of starting material (**Table 5, entry 3**).

Table 5 Screen of modified conditions for direct arylation of **107**.



Entry	Mol% Pd	Mol% PCy ₃ ·HBF ₄	Atmosphere	t (h)	Conversion (Isolated Yield)
1	2	4	N ₂	24	20%
2	5	10	N ₂	3	100% (83%)
3	5	10	Air	3	~50% ^[a]

^[a]Prolonging reaction time to 24 h did not improve conversion, instead resulting in a complex mixture of by-products.

3.9.2. Substrates that Failed to Cyclise

As is to be expected when carrying out a substrate investigation, some functional groups were incompatible with the optimised direct arylation conditions. Four of the compounds that were synthesised for inclusion in the substrate scope failed to cyclise under the optimised direct arylation conditions (**Figure 27**). Reasons may be attributed to the electronics (**111**), steric effects (**112**), catalyst poisoning (**113**) or incompatible functionality (**114**). Compounds **111**, **112** and **113** were prepared using the same conditions depicted in **Scheme 48** (substrate **113** was synthesised under an inert atmosphere to prevent dimerisation of the thiol). Compound **114** was prepared using the same conditions as depicted in **Scheme 49**.

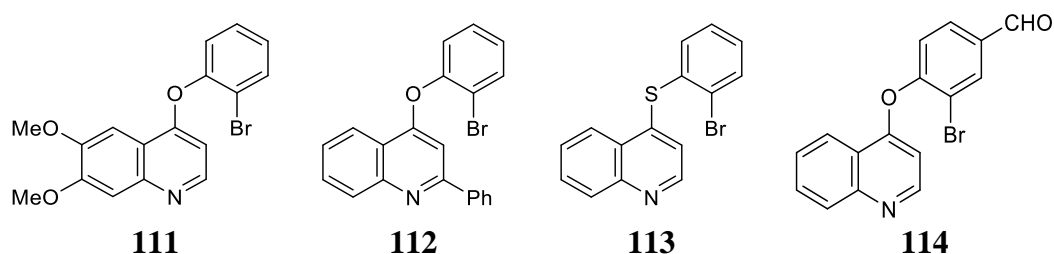
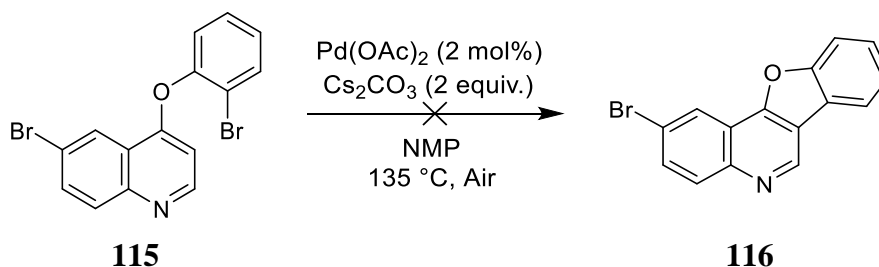


Figure 27 Substrates that failed to cyclise under the optimised conditions.

This work on the direct arylation of 4-phenoxyquinolines was published in a Special Issue of the European Journal of Organic Chemistry in 2018, and is included in **Appendix II**.

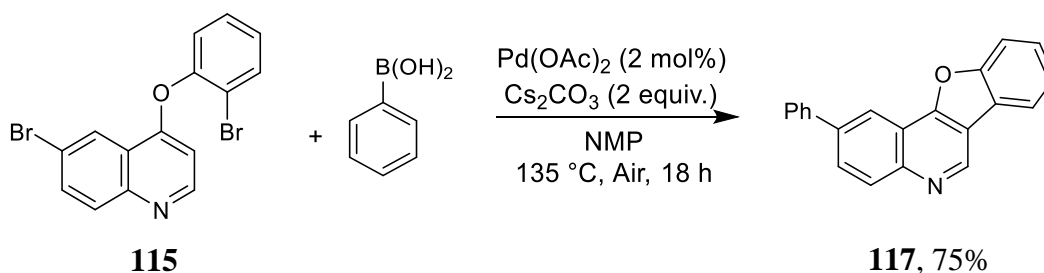
3.10. One-Pot Tandem Suzuki-Miyaura/Direct Arylation Reactions

One other substrate (**115**) initially failed to cyclise under the optimised direct arylation conditions (**Scheme 56**). This result was reminiscent of observations made by Lautens^[58-59] and Cramer^[60] when working with polyhalogenated substrates.



Scheme 56 Substrate **115** failed to undergo cyclisation under the optimised reaction conditions.

Due to the presence of a second site where oxidative addition of the palladium catalyst could occur, the catalyst was irreversibly inserting into the carbon-bromine bond at the C-6 position. In the absence of an obvious coupling partner, the catalytic cycle reached a dead-end. To test this hypothesis, the reaction was repeated under the same conditions with the addition of phenylboronic acid, which could potentially undergo a Suzuki-Miyaura coupling at the C-6 position of the substrate. Indeed, on this occasion a single novel product (**117**) was isolated (**Scheme 57**).

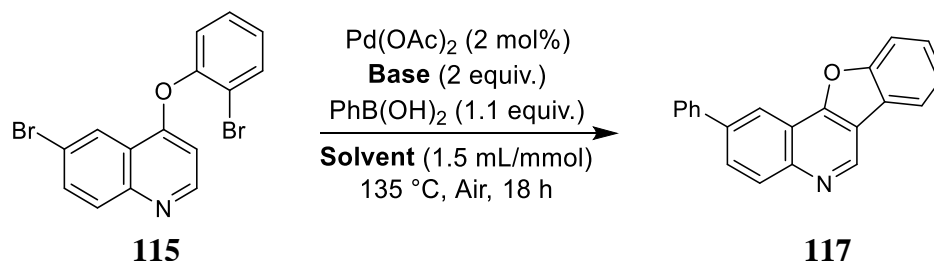


Scheme 57 Tandem Suzuki-Miyaura and direct arylation of **115**.

A range of different solvents was screened (**Table 6, entry 1–7**) in an effort to optimise the reaction, but ultimately, NMP proved to be superior in terms of conversion and isolated yield (**Table 6, entry 1**). It is worth noting, however, that 1,4-dioxane was almost as effective as NMP at promoting the reaction (**Table 6, entry 2**). Because dioxane is much easier to remove from the reaction mixture, this solvent was sometimes used in place of NMP for some investigative reactions. For substrate

scope reactions, where the final isolated yield was important, NMP was used. Replacing Cs_2CO_3 with K_2CO_3 (Table 6, entry 8–12) increased the isolated yield to 83% (Table 6, entry 9).

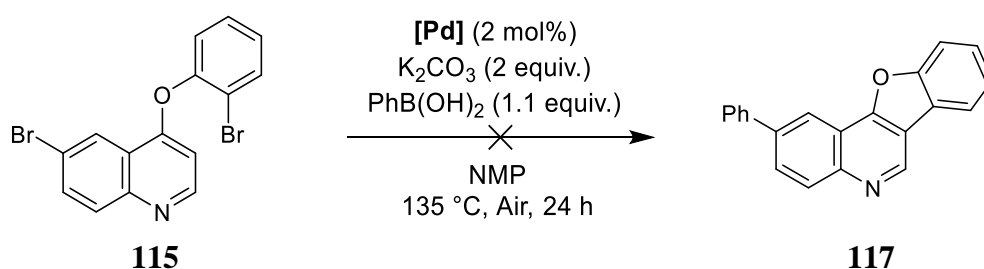
Table 6 Solvent and base screen for tandem Suzuki-Miyaura/direct arylation of **115**.



Entry	Base	Solvent	%Conversion ^[a]	%Yield NMR ^[b] (Isolated Yield)
1	Cs_2CO_3	NMP	100	73 (75)
2 ^[c]	Cs_2CO_3	1,4-Dioxane	90	68
3 ^[d]	Cs_2CO_3	Toluene	25	-
4 ^[d]	Cs_2CO_3	Xylene	16	-
5 ^[d]	Cs_2CO_3	Cyclohexanone	85	61
6 ^[d]	Cs_2CO_3	<i>i</i> -PrOAc	25	-
7 ^[d]	Cs_2CO_3	<i>n</i> -BuOAc	20	-
8	Na_2CO_3	NMP	100	80
9	K_2CO_3	NMP	100	86 (83)
10	KOH	NMP	30	20
11	NaOH	NMP	65	44
12	NaOt-Bu	NMP	decomposition	-

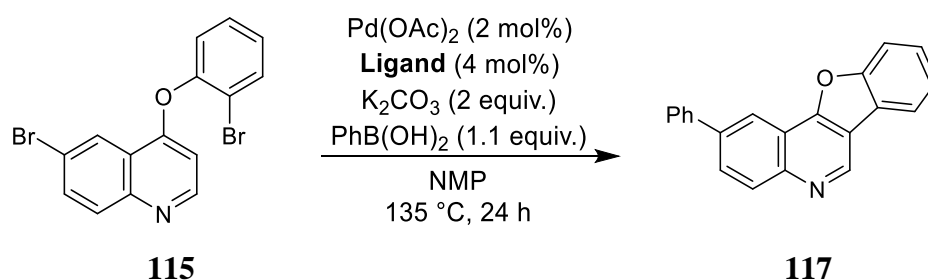
^[a]%Conversion determined as consumption of starting material by ^1H -NMR analysis of the crude reaction mixture. ^[b]Yields determined by ^1H -NMR analysis of the crude reaction mixture using 1,3,5-trimethoxybenzene as internal standard. ^[c]Reaction carried out at 125 °C. ^[d]Reaction carried out at 110 °C.

The use of heterogeneous palladium catalysts (i.e. Pd on charcoal, alumina or carbon) instead of $\text{Pd}(\text{OAc})_2$ resulted in degradation of the starting material, and no evidence for the formation of product was observed (Table 7, entry 1–3).

Table 7 Screen of heterogeneous palladium catalysts.

Entry	Pd Source	Result
1	10% Pd on charcoal	Decomposition
2	10% Pd on alumina	Decomposition
3	10% Pd on carbon	Decomposition

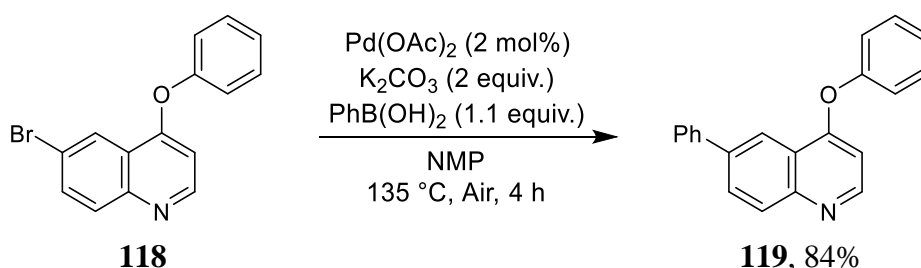
The effect of adding phosphine ligands to the reaction was also evaluated (**Table 8**). Under aerobic conditions, the ligands inhibited the reaction (**Table 8, entry 1–2**), in comparison to the optimum ligand-free conditions (**Table 6, entry 9**). Under inert conditions, the reaction did proceed in the presence of PPh_3 (**Table 8, entry 3**), although periodic $^1\text{H-NMR}$ analysis of the reaction mixture indicated that the rate of reaction was slower than in the absence of added ligand (**Table 6, entry 9**). The bulky ligand $\text{P}(t\text{-Bu})_3\cdot\text{HBF}_4$ failed to promote the reaction under inert conditions (**Table 8, entry 4**). Like PPh_3 , QPhos also allowed the reaction to proceed under inert conditions, but once again, not to full conversion, even after prolonged reaction time (**Table 8, entry 5**).

Table 8 Investigation of effect of adding phosphine ligands to the tandem reaction.

Entry	Ligand	Atmosphere	% Yield (NMR) ^[a]
1	PPh_3	Air	0
2	$\text{P}(t\text{-Bu})_3\cdot\text{HBF}_4$	Air	0
3	PPh_3	N_2	57
4 ^[b]	$\text{P}(t\text{-Bu})_3\cdot\text{HBF}_4$	N_2	0
5 ^[b]	QPhos	N_2	64

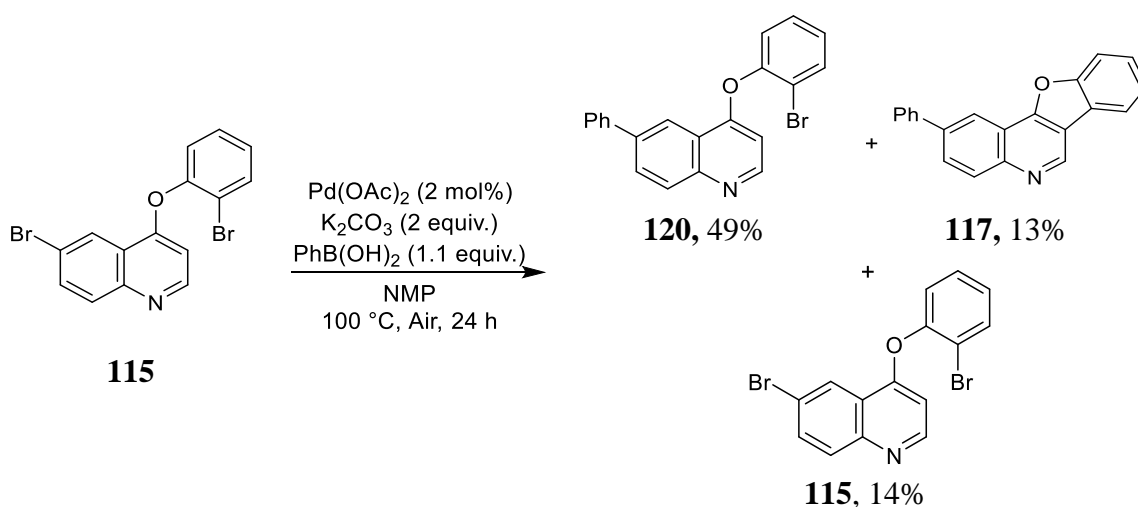
^[a]Yields determined by $^1\text{H-NMR}$ analysis of the crude reaction mixture using 1,3,5-trimethoxybenzene as internal standard. ^[b]Reaction stirred for 48 h at 135 °C.

To further probe the hypothesis that the Suzuki-Miyaura reaction was occurring at the C-6 position before direct arylation at the C-3 position, substrate **118** was synthesised using the same methodology described in **Scheme 48**. This substrate could only undergo the Suzuki-Miyaura reaction, and therefore if this reaction did not work efficiently under the optimised conditions, a more complicated catalytic cycle may be at play in the tandem reaction. The reaction proceeded as anticipated and in a much shorter reaction time of just four hours (**Scheme 58**), compared to overnight (18 h) for the tandem Suzuki-Miyaura/direct arylation reaction.



Scheme 58 Suzuki-Miyaura coupling of substrate **118**.

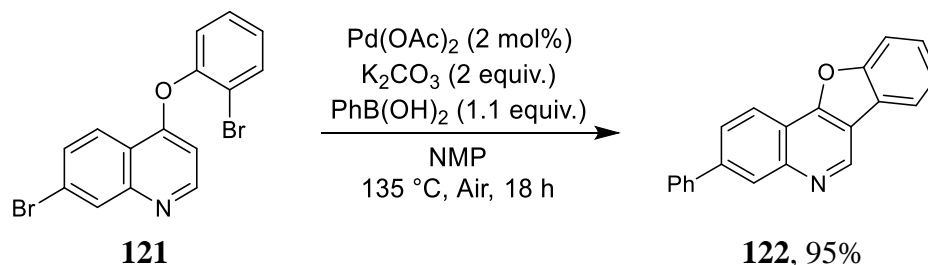
Next, the tandem reaction was carried out at a lower temperature of $100\text{ }^\circ\text{C}$ to see if only the Suzuki-Miyaura product could be isolated (**Scheme 59**). This would add further evidence that oxidative addition was occurring at the C-6 position initially. Indeed, at this temperature the major product was the uncyclised Suzuki-Miyaura product **120**, although some of the tandem product **117** and starting material **115** were also isolated.



Scheme 59 Tandem reaction carried out at $100\text{ }^\circ\text{C}$. Yields are isolated yields.

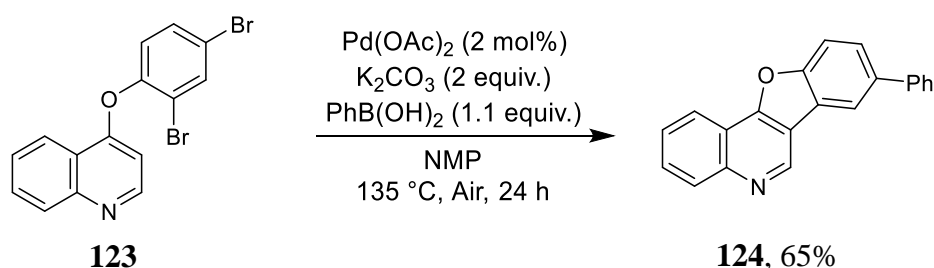
3.10.1. Substrate Scope

Moving the second C-Br bond to the C-7 position of the quinoline (**121**) also facilitated the tandem reaction, with respect to the isolated yield of the product **122** (Scheme 60).



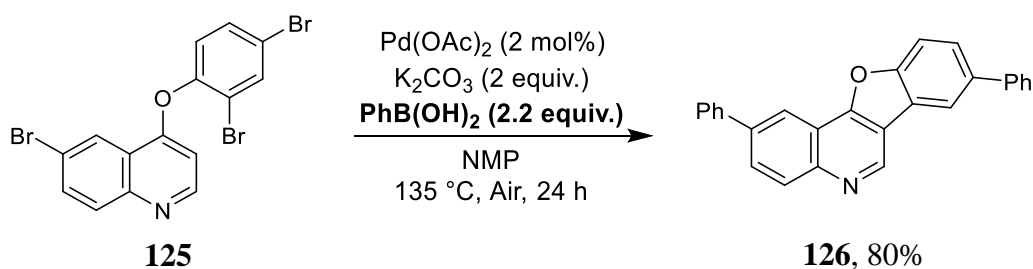
Scheme 60 One-pot reaction of the C-7 substrate **121**.

Both transformations of the tandem reaction could also be carried out on the phenoxy ring of substrate **123**. However, the isolated yield of product **124** was lower than that of the quinoline-substituted compounds (Scheme 61).



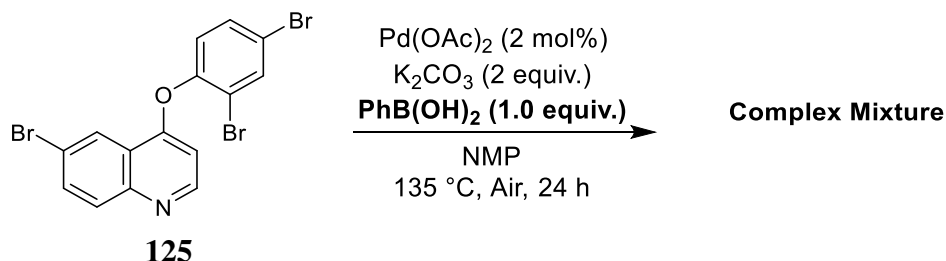
Scheme 61 Tandem reaction involving a Suzuki-Miyaura reaction on the phenoxy ring of **123**.

Next, tri-brominated substrate **125** was synthesised to see if three transformations could be carried out in the one pot. Indeed, when two equivalents of phenylboronic acid were included in the reaction mixture using the optimised reaction conditions, compound **126** could be isolated in high yield (Scheme 62).



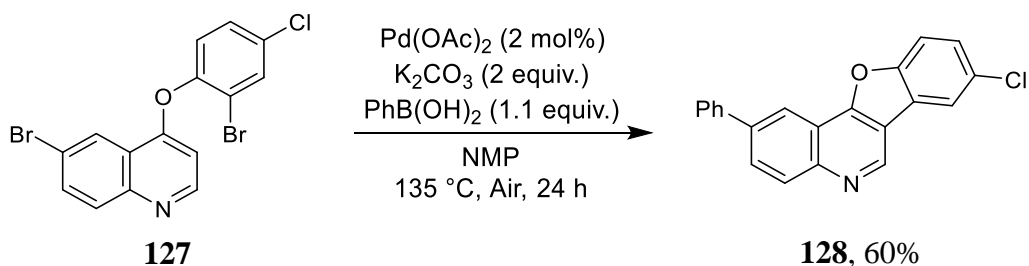
Scheme 62 Tandem reaction of **125** involving two Suzuki-Miyaura couplings and one direct arylation reaction on a single substrate.

However, when only one equivalent of phenylboronic acid was included, the reaction did not seem to show any overriding regioselectivity in the Suzuki-Miyaura reaction. The resulting complex mixture of products could not be separated (**Scheme 63**).



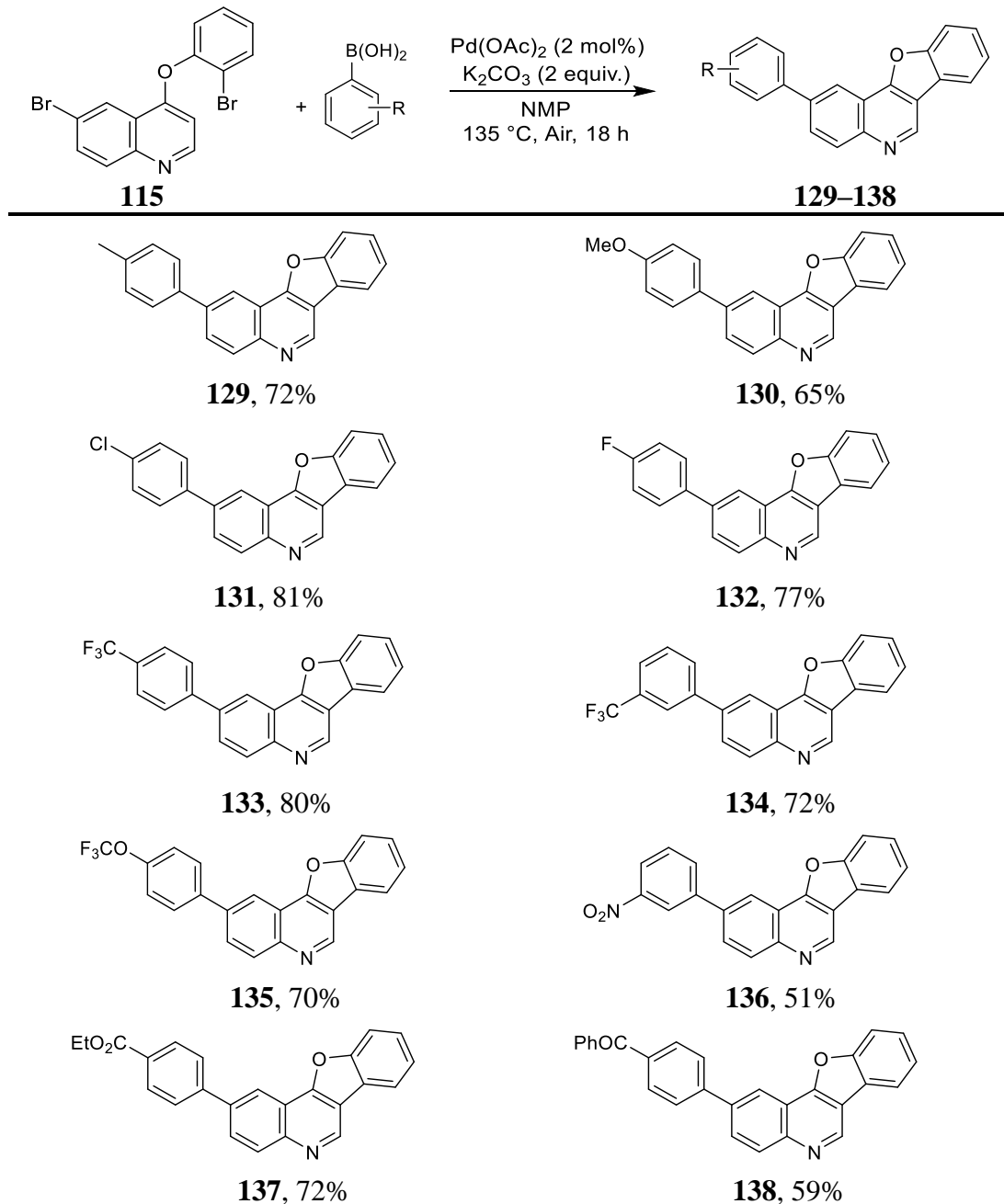
Scheme 63 Tandem reaction of **125** with only one equivalent of phenylboronic acid.

To allow for differentiation between the two Suzuki-Miyaura coupling sites, one of the bromine atoms was replaced with a chlorine (**127**). The product **128** was isolated, with the C-Cl bond retained (**Scheme 64**).



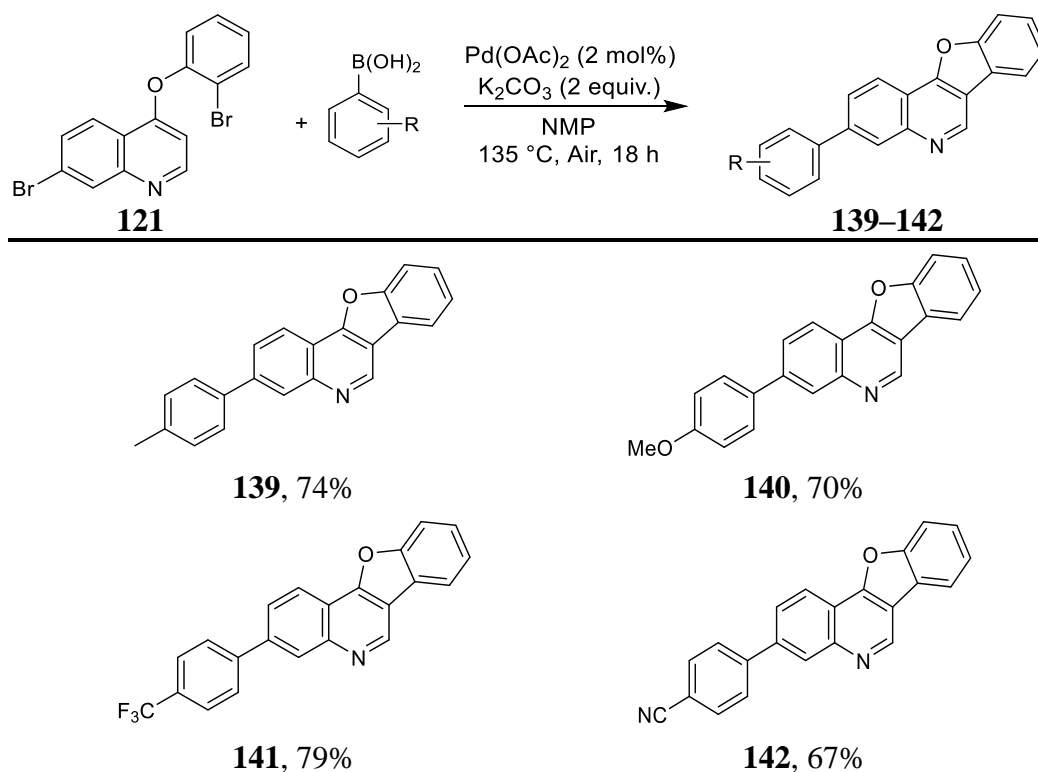
Scheme 64 Tandem reaction of **127** with retention of the C-Cl bond.

Next, several substituted phenylboronic acids were screened to assess the performance of various functional groups under the optimised reaction conditions (**Scheme 65**). The products of successful reactions were isolated in moderate to good yields.



Scheme 65 Substrate scope of tandem reaction with various substituted phenyl boronic acids using the 6-bromo substrate **115**.

A selection of four tandem products that were substituted at the C-7 position was synthesised from substrate **121**.



Scheme 66 Substrate scope of the tandem reaction with various substituted phenyl boronic acids using substrate **121**.

Unfortunately, several of the substituted phenylboronic acids that were subjected to the optimised tandem reaction conditions failed to yield the desired products (**Figure 28**). Additionally, the reaction conditions proved to be incompatible with both alkyl and heteroaryl boronic acids. Radically different, specialised conditions will be required to allow heteroaryl boronic acids to be included.

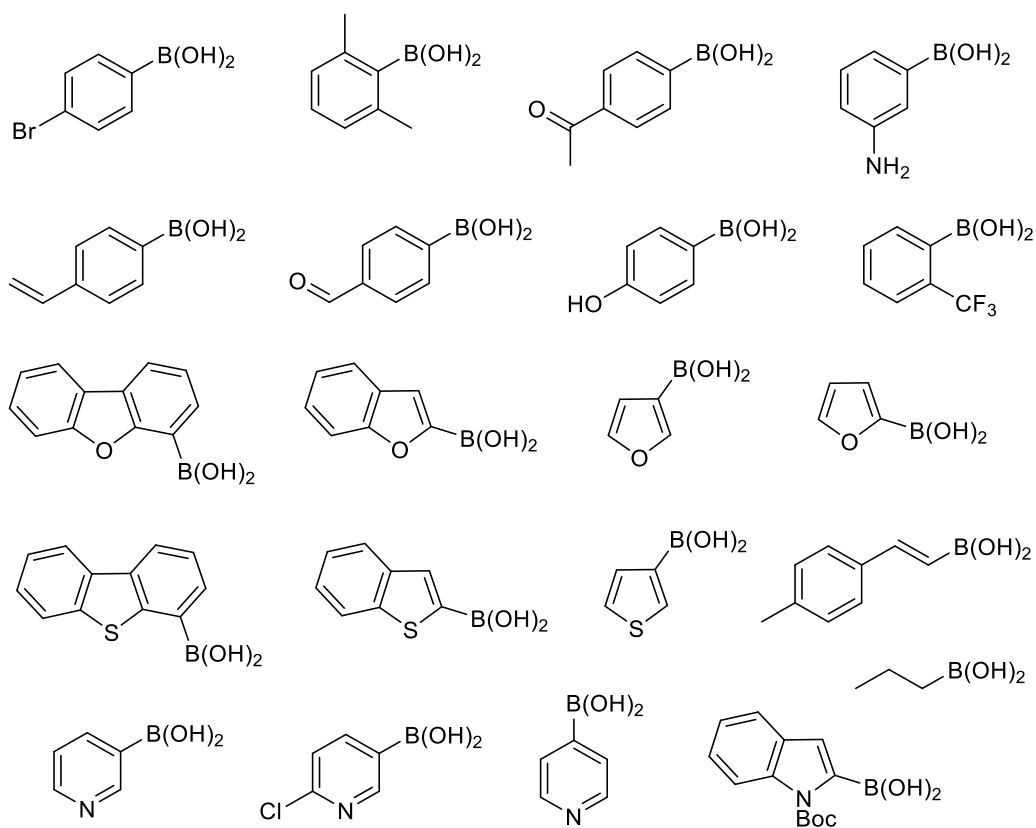
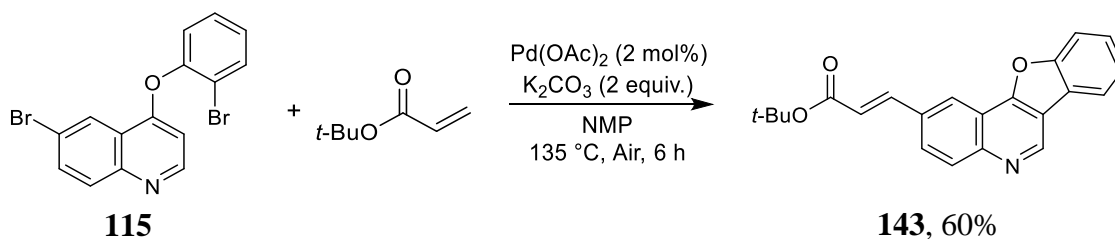


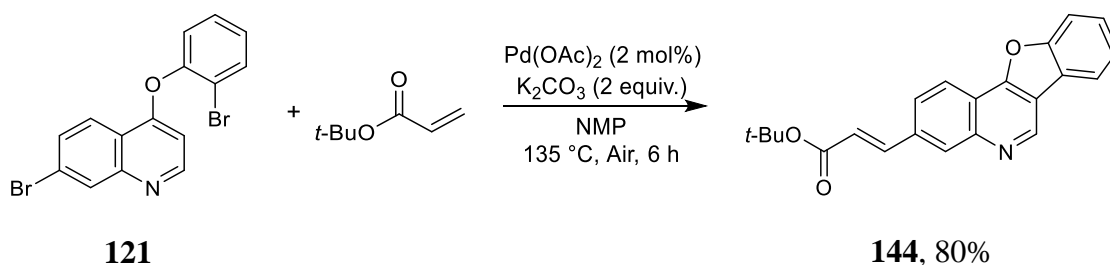
Figure 28 Boronic acids that were not compatible with the tandem reaction.

3.10.2. One-Pot Tandem Mizoroki-Heck/Direct Arylation Reactions

Interestingly, the reaction conditions described here could also facilitate tandem Mizoroki-Heck/direct arylation transformations (**Scheme 67** and **Scheme 68**) to yield products **143** and **144**.



Scheme 67 One-pot Mizoroki-Heck/direct arylation of **115**.



Scheme 68 One-pot Mizoroki-Heck/direct arylation of **121**.

This work, in combination with a larger substrate scope of the tandem Mizoroki-Heck/direct arylation products which subsequently undertaken within the McGlacken group, was published post examination of this thesis in The Journal of Organic Chemistry in January 2020.^[89]

3.10.3. Tandem Reaction on Pyridine Substrates

Like quinoline, the pyridine nucleus is also present in many biologically active compounds, including vitamins such as niacin (a form of vitamin B3), coenzymes such as nicotinamide adenine dinucleotide (NAD), and alkaloids such as nicotine.^[90] Pyridine is the 2nd most frequently occurring ring system in FDA approved drugs, after benzene (**Figure 29**).^[31] Therefore, carrying out similar tandem reactions on a pyridine scaffold would allow access to novel polycyclic pyridines.

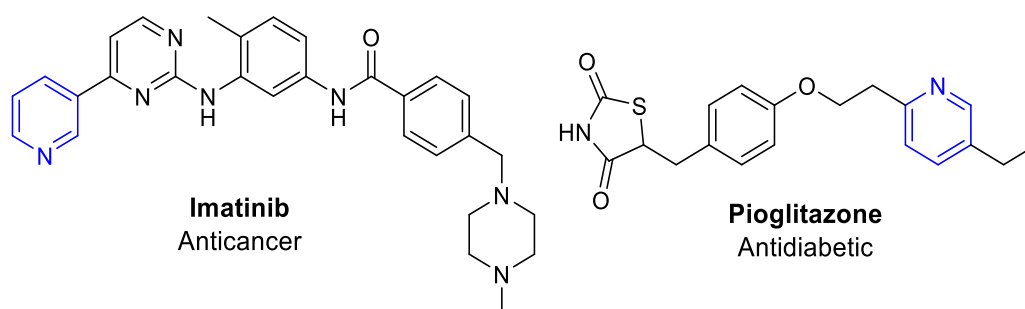
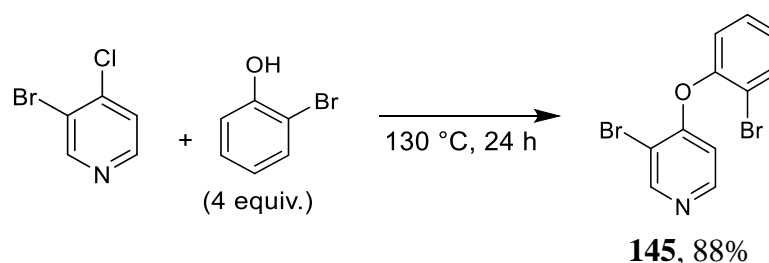


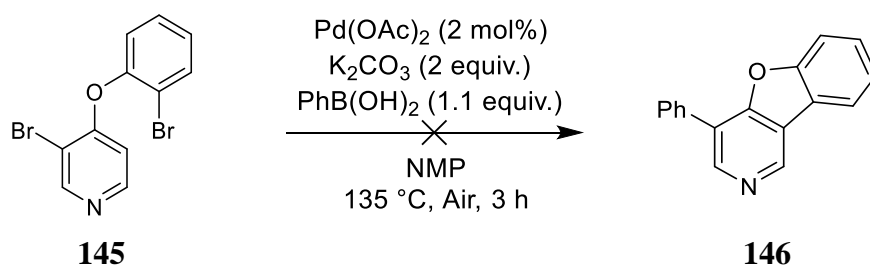
Figure 29 Pyridine-containing drugs Imatinib and Pioglitazone.

Firstly, the dibrominated 4-phenoxy pyridine substrate **145** was synthesised from 3-bromo-4-chloropyridine and 2-bromophenol (**Scheme 69**).



Scheme 69 Synthesis of substrate **145**.

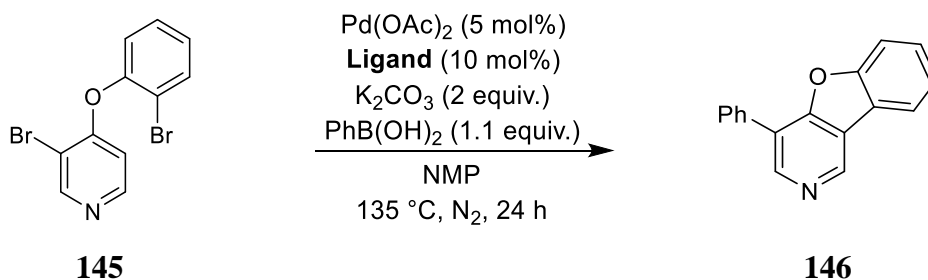
Next, the tandem reaction conditions optimised for the quinoline substrates were applied. However, clean conversion to the desired product was not achieved (**Scheme 70**). Although complete consumption of **145** was observed after 3 h, a complex mixture of products was observed by ¹H-NMR analysis of the crude reaction mixture.



Scheme 70 Substrate **145** failed to undergo tandem Suzuki-Miyaura/direct arylation in a clean manner, under the previously optimised conditions.

Nitrogen-containing heterocycles, such as pyridines and quinolines, are known to coordinate to transition metal catalysts such as palladium.^[91] As such, they can be used as ligands to facilitate certain transformations.^[92] On the other hand, the nitrogen atom may coordinate to the catalyst in an unproductive manner, occupying coordination sites needed for oxidative addition or transmetalation. Whilst this was not the case in the reactions carried out on the quinoline substrates, the pyridine substrate **145** may be susceptible to unproductive coordination to the catalyst. In an effort to improve the outcome of the reaction depicted in **Scheme 70**, phosphine ligands were included in the reaction mixture. (**Table 9**). Unfortunately, the addition of these ligands did not improve the one-pot reaction and no product formation could be detected.

Table 9 Screen of ligands for one-pot reaction with **145**.

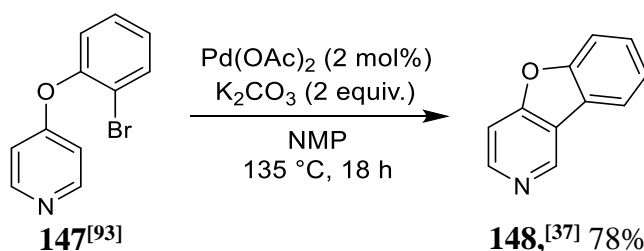


Entry	Ligand	%Conversion ^[a]
1	PPh_3	0
2	$\text{Pt-Bu}_3\cdot\text{HBF}_4$	0
3	QPhos	0

^[a]Some degradation of starting material was observed as indicated by the $^1\text{H-NMR}$ spectra of the reaction mixtures.

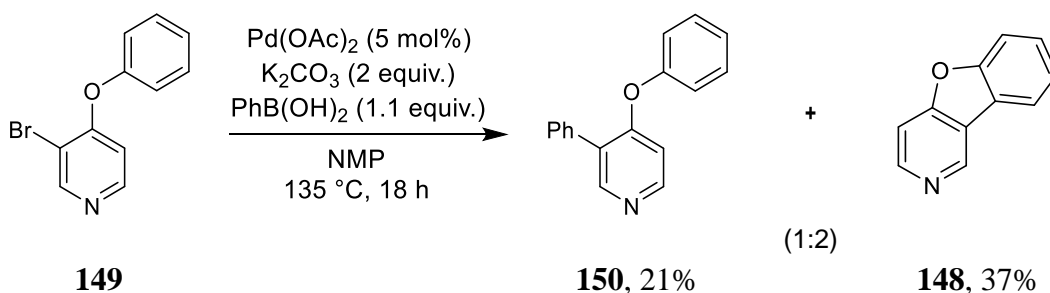
In order to gain better insight into the problem point of this transformation, a step-wise approach was taken whereby both the Suzuki-Miyaura and direct arylation reactions were performed individually before proceeding to the tandem transformation. First, the ring-closing direct arylation reaction was performed. This is a known

transformation carried out by Ha and co-workers,^[27] using Pd(OAc)₂, an imidazolyl carbene ligand (IPr·HCl) and K₂CO₃ in DME. However, it was important to confirm that the reaction would proceed under our optimised conditions.



Scheme 71 Direct arylation reaction of **147**.

Next, substrate **149** was subjected to the reaction conditions along with phenylboronic acid, to see if the Suzuki-Miyaura reaction would occur efficiently at the C-3 position (**Scheme 72**).

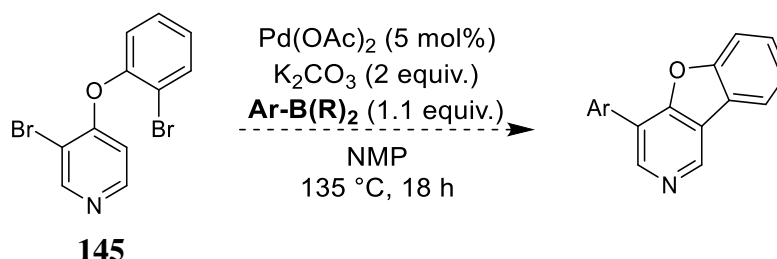


Scheme 72 Substrate **149** was subjected to the one-pot reaction conditions to see if the Suzuki-Miyaura reaction would occur efficiently at the C-3 position.

However, rather than obtaining the Suzuki-Miyaura product **150** exclusively, a mixture of the Suzuki-Miyaura product **150** and the ring-closed product **148** was observed. There was no evidence of unreacted starting material post-reaction. Complete separation of these two products by column chromatography proved difficult. Nevertheless, there was sufficient pure material isolated for the structure of both products to be confirmed. Presumably, when the oxidative addition product of **149** is formed, there is competition between intramolecular direct arylation of the phenoxy ring and the intermolecular Suzuki-Miyaura reaction, with the former being favoured. This, together with the result from **Scheme 71** explains the complex mixture of products observed when the dibrominated substrate **145** was subjected to the tandem reaction conditions (**Scheme 70**).

To investigate if the Suzuki-Miyaura reaction could be forced to occur selectively over the competing direct arylation reaction, a variety of boron-based coupling partners that can undergo Suzuki-Miyaura coupling was screened.

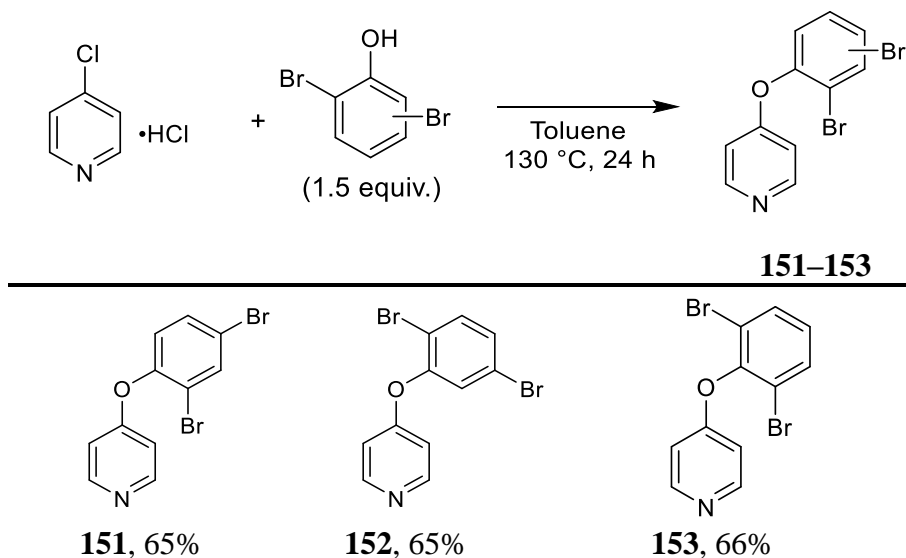
Table 10 Screen of coupling partners for the tandem Suzuki-Miyaura/direct arylation reaction of **145**.



Entry	Boron Coupling Partner	Result
1		Complex mixture
2		Complex mixture
3		Complex mixture
4		Complex mixture
5		Unreacted starting material
6	No added coupling partner	Unreacted starting material

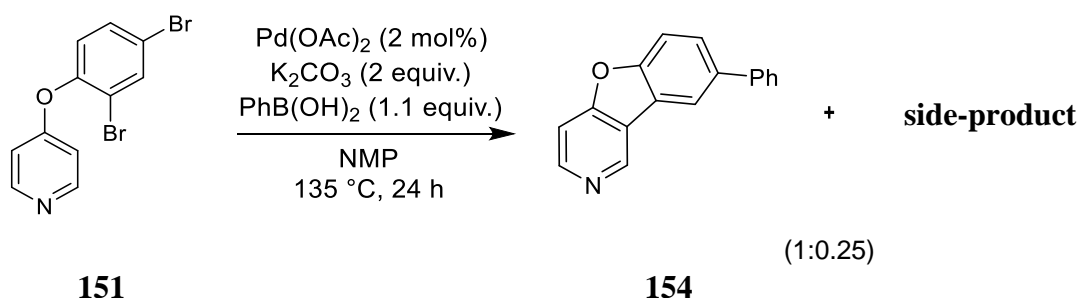
Unfortunately, none of the boron reagents screened promoted any improvement in the outcome of the reaction. In addition, the control experiment, which had no added coupling partner, only yielded unreacted starting material. This may be due to oxidative addition occurring preferentially at the C-3 position of the pyridine, resulting in shutdown of the catalytic cycle. At this point it was clear that an alternative strategy would need to be considered.

Looking at the various quinoline substrates that were tolerated under the optimised reaction conditions, substrate **123**, with both bromides on the phenoxy ring, underwent both transformations of the tandem reaction (**Scheme 61**). Therefore, the same result might be achievable with the pyridine framework. Thus, substrates **151–153** bearing both C-Br sites on the phenoxy ring were synthesised (**Scheme 73**).



Scheme 73 Synthesis of dibromophenoxy pyridine substrates.

To begin, substrate **151** was subjected to the optimised tandem reaction conditions (**Scheme 74**).

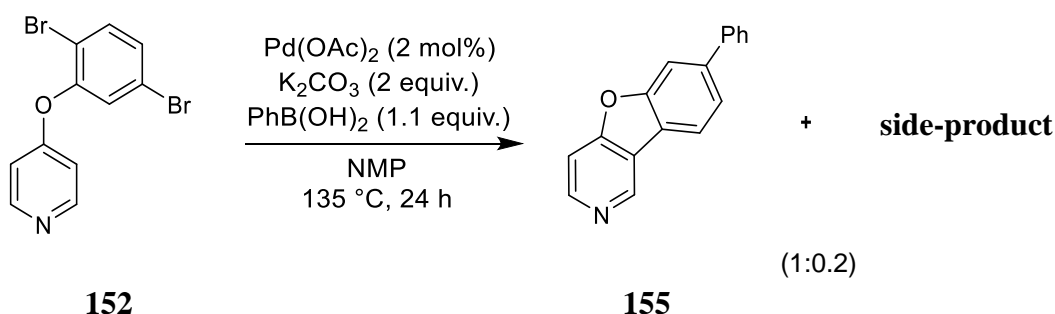


Scheme 74 Tandem reaction of substrate **151**. The ratio of the products is based on the ratio of the signals for the C-2 proton(s) of each product.

Whilst $^1\text{H-NMR}$ analysis of the crude reaction mixture indicated that all of the starting material had been consumed, peaks corresponding to an uncyclised side-product were also present in a ratio of approximately 1:0.25 (**154:side-product**). Attempts to cleanly separate the two products by column chromatography proved unsuccessful. To determine if the side-product was a brominated compound, the purified mixture of the two products was added to a new system containing Pd(OAc)_2 (2 mol%), K_2CO_3 (2 equiv.) and PhB(OH)_2 (1.1 equiv.) in NMP, and heated at 135 °C overnight. $^1\text{H-NMR}$ and $^{13}\text{C-NMR}$ analysis of this crude reaction mixture showed little change in the spectra, implying that the mixture of compounds obtained from the reaction depicted

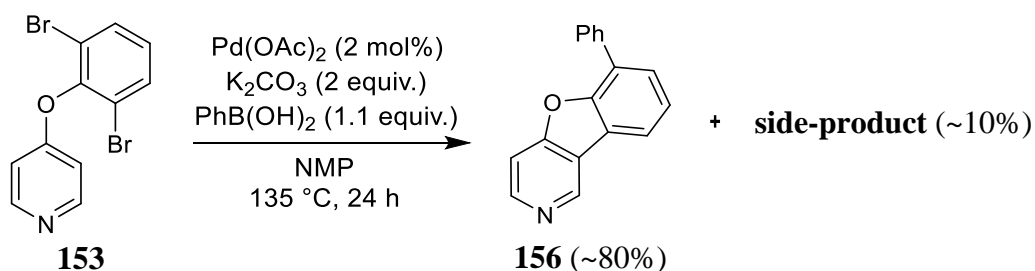
in **Scheme 74** most likely did not contain any reactive C-Br bonds. Elucidation of the correct structure of the side-product will be discussed later.

Next, substrates **152** and **153** were subjected to the tandem conditions to see if varying the substitution pattern of the phenoxy ring would improve the outcome of the reaction in favour of the desired one-pot Suzuki-Miyaura/direct arylation product. Using regioisomer **152** with the bromide *meta* to the oxygen atom only slightly improved conversion to the tandem reaction product (**Scheme 75**). Once again, clean separation of the products by column chromatography proved unsuccessful.



Scheme 75 Tandem reaction of substrate **152**. The ratio of the products is based on the ratio of the signals for the C-2 proton(s) of each product.

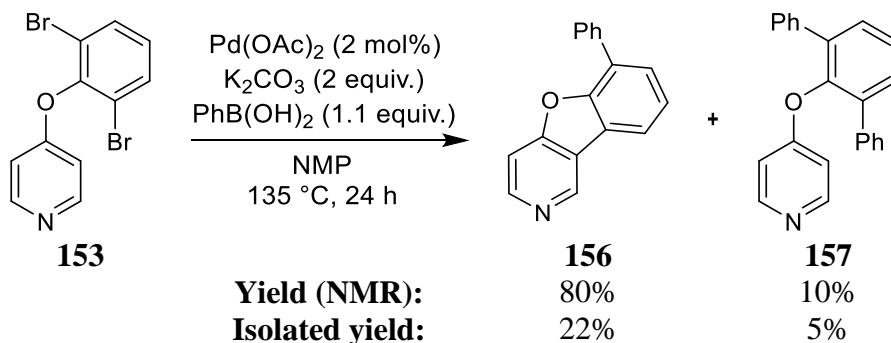
In the case of substrate **153**, which is symmetrically substituted on the phenoxy ring, less of the uncyclised side-product was formed, resulting in very good conversion to the desired product (**Scheme 76**). Quantitative ^1H -NMR analysis of the crude mixture indicated yields of approximately 80% (**156**) and 10% (**side-product**).



Scheme 76 Tandem reaction of substrate **153**.

Column chromatography of the crude mixture was carried out to see if it would be possible to isolate some clean fractions of the desired product. Gratifyingly, on this occasion it was possible to obtain a pure sample of **156** in 22% isolated yield. In addition, a sample of the side-product in 5% isolated yield was obtained. From careful consideration of the NMR spectra of the side-product, possible reaction pathways and

the stoichiometry of the reaction, the structure of the side-product was determined to be **157** as shown in **Scheme 77**. The side-product was also identified by HRMS analysis.

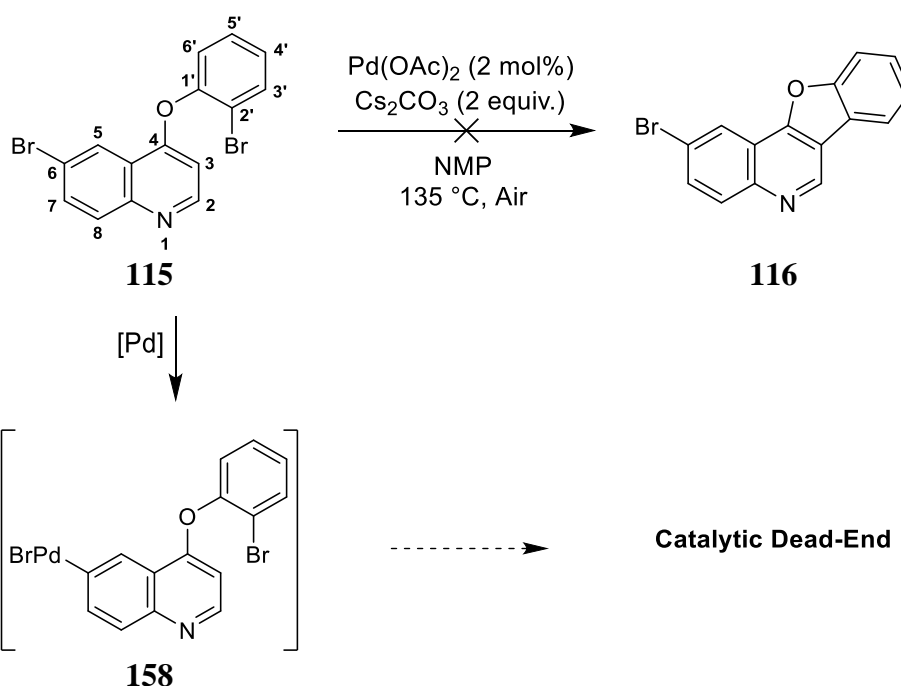


Scheme 77 Overall outcome of the tandem reaction of **153** yielding the major desired product **156** and diarylated side-product **157**.

Having determined the side-product formed during the tandem reaction of **153**, it is likely that side-products depicted in **Scheme 74** and **Scheme 75** were also formed as the result of a double Suzuki-Miyaura reaction on substrates **151** and **152**, respectively. Indeed, subsequent HRMS analysis of the mixtures identified the presence of a double Suzuki-Miyaura side-product in both cases.

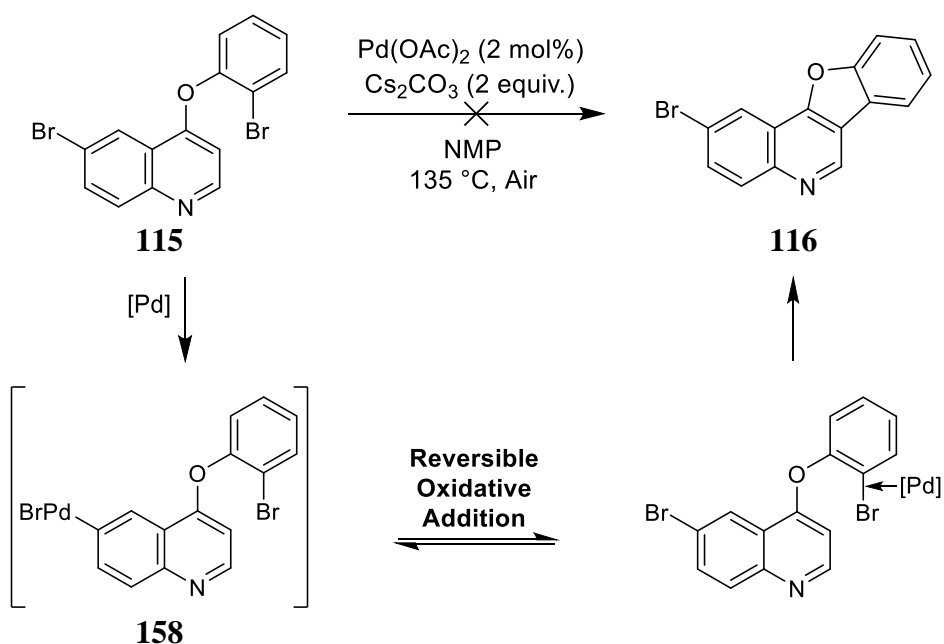
3.11. Reversible Oxidative Addition

Returning to the ‘failed’ reaction (**Scheme 56**) that initiated the one-pot reactions project, it is most likely that oxidative addition of the palladium catalyst to the carbon-bromine bond at the C-6 position of the quinoline is more favourable than at the C-2’ position of the phenoxy ring. As a result, in the absence of an intermolecular coupling partner that will release the catalyst from the C-6 position, the intramolecular cyclisation reaction at the C-2’ position of this particular substrate cannot proceed (**Scheme 78**).



Scheme 78 Irreversible oxidative addition of the catalyst into the C-6 C-Br bond of **115** causes the catalytic cycle to reach a dead-end in the absence of an intermolecular coupling partner.

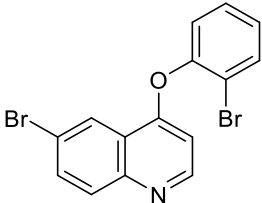
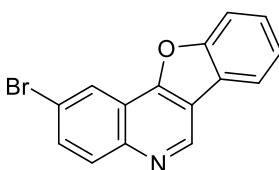
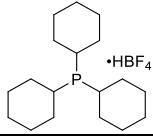
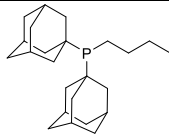
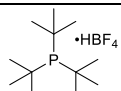
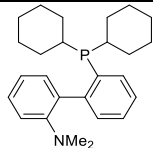
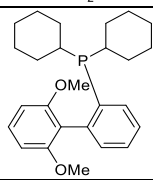
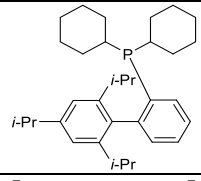
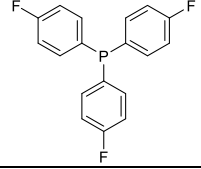
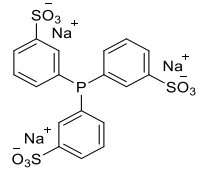
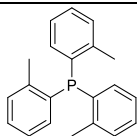
However, if the oxidative addition of the catalyst to the C-6 position was reversible, this might allow the intramolecular reaction to proceed and allow formation of compound **116** (**Scheme 79**). As discussed in the introduction, the use of conditions which allow reversible oxidative addition to occur can provide access to products that retain certain carbon-halogen bonds, as reported by Lautens.^[61]

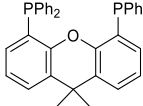
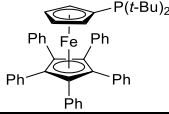
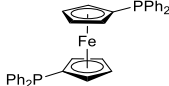


Scheme 79 Promoting reversible oxidative addition of the palladium catalyst could allow formation of the cyclised product **116** with retention of the quinoline C-Br bond.

Initially, several phosphine ligands were screened in an effort to observe any evidence for the formation of **116** (**Table 11**). The optimised conditions for the intramolecular cyclisation of compound **71** were chosen, as the desired reaction in this case was the cyclisation. However, 1,4-dioxane was used instead of NMP as the reaction solvent for ease of work-up.

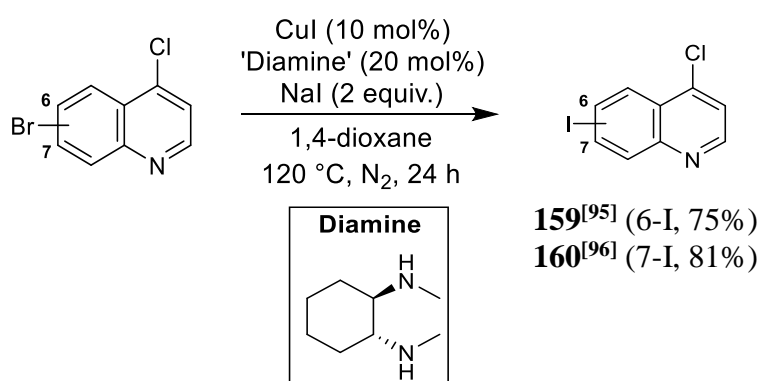
Table 11 Screen of phosphine ligands to determine conditions for promoting reversible oxidative addition.

<div style="display: flex; align-items: center; justify-content: space-around;"> <div style="text-align: center;">  <p>115</p> </div> <div style="text-align: center;"> <p>Pd(OAc)₂ (5 mol%) Ligand (10 mol%) Cs₂CO₃ (2 equiv.) 1,4-dioxane 125 °C, N₂, 24 h</p> </div> <div style="text-align: center;">  <p>116</p> </div> </div>			
Entry	Ligand	Structure	%Conversion
1	PCy ₃ ·HBF ₄		0
2	cataCXium A		0
3	P(<i>t</i> -Bu) ₃ ·HBF ₄		0
4	DavePhos		0
5	SPhos		0
6	XPhos		0
7	Tris(4-fluorophenyl) phosphine		0
8	Triphenylphosphine-3,3',3''-trisulfonic acid trisodium		0
9	Tri- <i>o</i> -tolylphosphine		0

10	Xantphos		0
11	QPhos		0
12	dppf		0

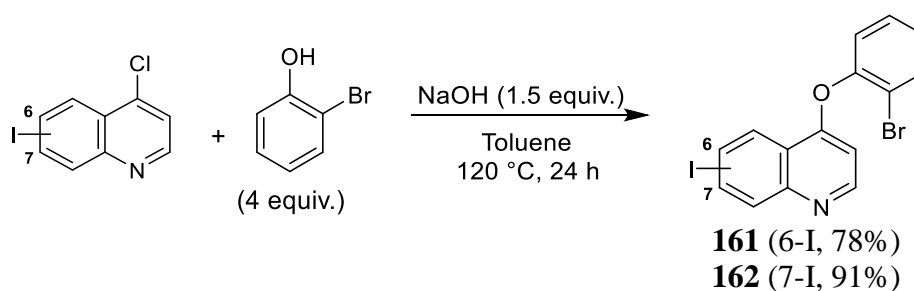
Unfortunately, none of the ligands screened promoted the cyclisation reaction. Even the ligands that worked well in Lautens' reactions, $P(t\text{-Bu})_3 \cdot \text{HBF}_4$ (**Table 11, entry 3**) and QPhos (**Table 11, entry 11**), failed to induce reversible oxidative addition.

To further probe how to promote the cyclisation reaction in the presence of a second C-X bond, iodinated analogues of the substrates were synthesised. To achieve this, first an aromatic Finklestein reaction was performed on the commercially available brominated starting materials to give iodinated compounds **159** and **160**.^[94]



Scheme 80 Aromatic Finklestein reaction of 6- and 7-bromo-4-chloroquinoline to form the 6-iodo (**159**) and 7-iodo (**160**) analogues.

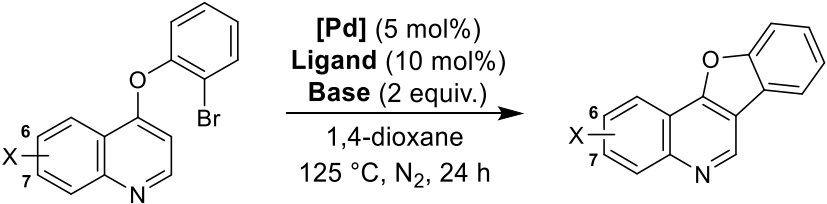
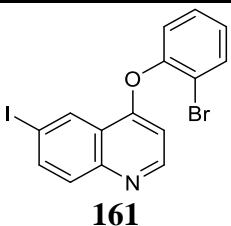
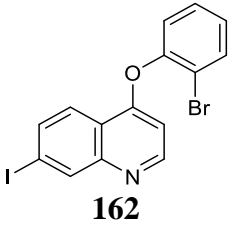
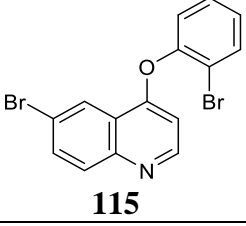
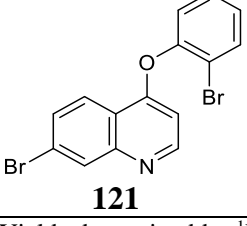
Next, both **159** and **160** were reacted with 2-bromophenol to give the iodinated quinolines **161** and **162** (**Scheme 81**).



Scheme 81 Synthesis of 6-iodo and 7-iodo 4-phenoxyquinolines.

At this point, another screen of conditions was devised for the four dihalogenated compounds – the C-6 bromo (**115**), C-6 iodo (**161**), C-7 bromo (**121**) and C-7 iodo (**162**) substrates. It was thought that sticking with the ligands that worked for Lautens and varying other parameters would be the best place to start. Thus, three different sets of conditions were chosen varying the catalyst, ligand and base: 1) Pd(OAc)₂, P(*t*-Bu)₃·HBF₄ and Cs₂CO₃ (already tried with the brominated substrates **115** and **121** but not with **161** and **162**); 2) Pd(OAc)₂, QPhos and PMP (our catalyst, Lautens' ligand and base) and 3) Pd(QPhos)₂, QPhos and PMP (Lautens' exact conditions).^[68] The results of this investigation are outlined in **Table 12**.

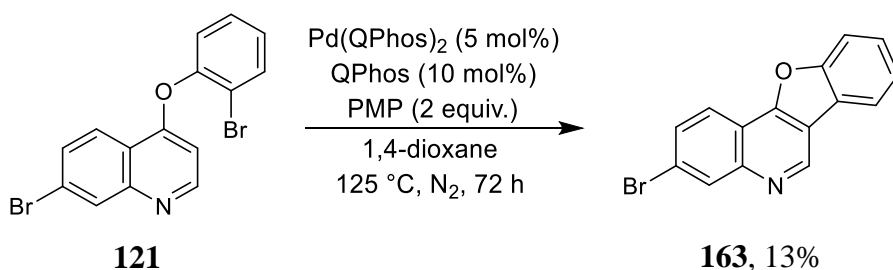
Table 12 Screen of conditions for reversible oxidative addition.

					
Substrate	Entry	[Pd]	Ligand	Base	%Yield (NMR) ^[a]
 161	1	Pd(OAc) ₂	P(<i>t</i> -Bu) ₃ ·HBF ₄	Cs ₂ CO ₃	0
	2	Pd(OAc) ₂	QPhos	PMP	0
	3	Pd(QPhos) ₂	QPhos	PMP	0
 162	4	Pd(OAc) ₂	P(<i>t</i> -Bu) ₃ ·HBF ₄	Cs ₂ CO ₃	0
	5	Pd(OAc) ₂	QPhos	PMP	0
	6	Pd(QPhos) ₂	QPhos	PMP	0
 115	7	Pd(OAc) ₂	QPhos	PMP	0
	8	Pd(QPhos) ₂	QPhos	PMP	24%
 121	9	Pd(OAc) ₂	QPhos	PMP	0
	10	Pd(QPhos) ₂	QPhos	PMP	20%

^[a]Yields determined by ¹H-NMR analysis of the crude reaction mixture using 1,3,5-trimethoxybenzene as internal standard.

To our delight, on this occasion two of the reactions showed some formation of a cyclised product (**Table 12, entry 8** and **entry 10**). Indeed, in addition to using QPhos as an added ligand, it was also necessary to include Pd(QPhos)₂ as the pre-catalyst, as noted by Lautens.^[68]

In order to confirm the structure of the products that were observed, the reaction of dibromide **121** under Lautens' conditions (**Table 12, entry 10**) was repeated on a larger scale in an effort to obtain enough product for isolation and characterisation (**Scheme 82**). The reaction was sampled periodically and analysed by ¹H-NMR spectrometry to monitor the progress of product formation. Careful monitoring of the reaction progress revealed that catalytic turnover decreased dramatically after approximately 48 h. Thus, throughout the experiment, new batches of catalyst and ligand were added whenever the reaction halted. This was continued until the majority of the starting material had been consumed and the product constituted the majority of the reaction mixture. Under these forcing conditions, some material may have been lost to degradation pathways. Nevertheless, after careful column chromatography of the crude reaction mixture, a pure sample of the product **163** was isolated, albeit in 13% yield.



Scheme 82 Scale up of reaction depicted in **Table 12, entry 10**.

The structure of novel cyclised product **163** was confirmed by NMR and HRMS analysis. The ¹H-NMR spectrum of **163** is shown in **Figure 30** below. The singlet peak at 9.49 ppm is indicative of an intramolecular direct arylation having occurred at the C-3 position. The shift and splitting pattern of the peaks for protons at C-5, C-6 and C-8 are also consistent with other 7-substituted products synthesised in this project. Retention of the C-Br bond was indicated by the minimal shift of the quaternary C-7 peak in the ¹³C-NMR spectra of the substrate **121** ($\delta = 124.6$ ppm) and the product **163** ($\delta = 123.4$ ppm). By comparison, the quaternary C-14 peak for the phenoxy C-Br of substrate **121** occurs at 116.3 ppm. Upon cyclisation, this quaternary C-14 peak shifts

to 122.4 ppm. The HRMS data also confirmed the presence of **163** (ESI-TOF m/z : $[M+H]^+$ calcd. for $C_{15}H_9BrNO$: 297.9862; found: 297.9865).

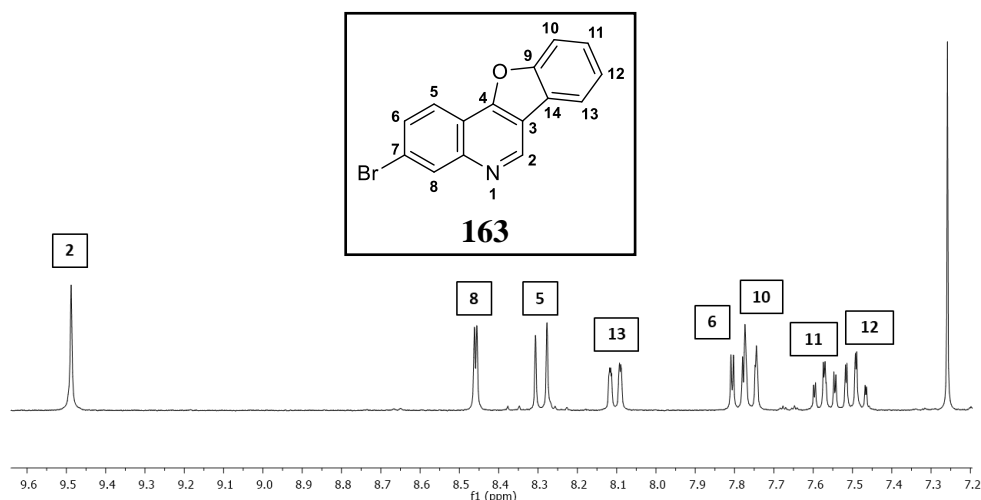


Figure 30 1H -NMR ($CDCl_3$) spectrum of product **163**.

This work proves that cyclised products such as **116** (C-6 Br) and **163** (C-7 Br), which retain the quinoline C-Br bonds, can be accessed under conditions that allow reversible oxidative addition of the palladium catalyst at the more favoured site. Optimisation of the reaction conditions for reversible oxidative addition and substrate scope investigations are currently ongoing within the McGlacken group.

3.12. Conclusions

The application of direct arylation methodology towards the synthesis of fused benzofuroquinoline products was demonstrated. Placement of the halide on the phenoxy component of the coupling precursor allowed for easy access to cyclised products. No added phosphine was required and the reactions were carried out in air. Modification of the methodology allowed for the inclusion of a 4-anilinoquinoline substrate, without the requirement for *N*-protection. Under virtually the same conditions, using dibrominated substrates, a new one-pot tandem reaction was discovered whereby a Suzuki-Miyaura coupling and direct arylation reaction occur on the same substrate, without requiring additional reagents or catalyst. Again, this tandem reaction occurs in the absence of added ligand and in air. Finally, reversible oxidative conditions allowed for the isolation of the C-7 brominated product of the direct arylation reaction.

Chapter 3

Direct Arylation of Phenoxyquinolines

Experimental

3.13. General Considerations

Solvents, reagents and starting materials were used as obtained from commercial sources, without purification. Column chromatography was carried out using 60 Å (35-70 µm) silica. TLC was carried out on pre-coated silica gel plates (Merck 60 PF254). The developed plates were visualised under UV light.

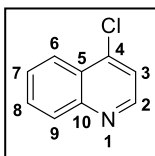
Melting points were measured in a Thomas Hoover Capillary Melting Point apparatus. Infrared spectra were measured on a Perkin-Elmer FT-IR spectrometer. High resolution mass spectra (HRMS) were recorded on a Waters LCT Premier TOF LC-MS instrument in electrospray ionisation (ESI) mode using 50% acetonitrile-water containing 0.1% formic acid as eluent; samples were prepared in acetonitrile at a concentration of *ca.* 1 mg/mL. Reported results are within the range of ± 5 ppm of the calculated mass. For brominated compounds, Br⁸⁰ was used for the calculated and reported molecular ion mass.

Nuclear Magnetic Resonance (NMR) samples were run in deuterated chloroform (CDCl₃) or deuterated dimethylsulfoxide (DMSO-d₆), as specified. ¹H-NMR (600 MHz), ¹H-NMR (500 MHz), ¹H-NMR (400 MHz), and ¹H-NMR (300 MHz) spectra were recorded on Bruker Avance 600, Bruker Avance 500, Bruker Avance 400 and Bruker Avance 300 NMR spectrometers, respectively, in proton coupled mode using tetramethylsilane (TMS) as the internal standard. ¹³C-NMR (150 MHz), ¹³C-NMR (125 MHz), ¹³C-NMR (100 MHz) and ¹³C-NMR (75 MHz) spectra were recorded on Bruker Avance 600, Bruker Avance 500, Bruker Avance 400 and Bruker Avance 300 NMR spectrometers, respectively, in proton decoupled mode at 20 °C using tetramethylsilane (TMS) as the internal standard. ¹⁹F-NMR (282 MHz) spectra were recorded on a Bruker Avance 300 NMR spectrometer in proton decoupled mode at 20 °C. All spectra were run at University College Cork. Chemical shifts (δ) are expressed as parts per million (ppm), positive shift being downfield from TMS; coupling constants (*J*) are expressed in hertz (Hz). Splitting patterns in ¹H-NMR spectra are designated as: s (singlet), br s (broad singlet), d (doublet), dd (doublet of doublets), ddd (doublet of doublets of doublets), t (triplet), td (triplet of doublets), q (quartet), quin (quintet) and m (multiplet). Please note that the numbering system used on the structures is to assign the NMR data, and differs from the IUPAC system used for naming.

3.14. Synthesis of 4-Chloroquinolines

4-Chloroquinoline^[72] (**68**)

A mixture of 4-quinolinol (1 equiv.) and POCl₃ (5 equiv.) was stirred at 110 °C for 3 h, until full consumption of the starting material was observed by TLC analysis of the reaction mixture (eluent DCM/MeOH 9:1). The cooled reaction mixture was slowly poured onto ice water (~4 mL/mmol) with stirring. Solid NaHCO₃ was added portion-wise until the mixture reached pH 7–8. This aqueous mixture was transferred to a separating funnel and extracted with DCM (3 × 1.5 mL/mmol). The combined organic layers were washed with water (1.5 mL/mmol), brine (1.5 mL/mmol), dried over MgSO₄, filtered and concentrated *in vacuo* to yield the crude product as a yellow oil. Purification by column chromatography (DCM/MeOH 95:5) afforded the pure product **68** as a yellow solid (2.17 g, 96% yield).

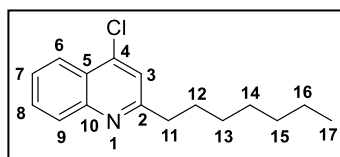


Yellow solid; yield: 2.17 g (96%); m.p. = 29–30 °C (lit. 28–31 °C); IR (NaCl): ν 2462 (C-H stretch), 1617 (aromatic C-C stretch), 1381 (C-N stretch), 759 (C-Cl stretch) cm⁻¹; ¹H-NMR (300 MHz, CDCl₃) δ : 7.50 (d, J = 4.7 Hz, 1H, CH-3), 7.66 (ddd, J = 8.2, 6.9, 1.2 Hz, 1H, CH-7), 7.79 (ddd, J = 8.4, 6.9, 1.5 Hz, 1H, CH-8), 8.14 (d, J = 8.4 Hz, 1H, CH-9), 8.25 (dd, J = 8.4, 1.0 Hz, 1H, CH-6), 8.79 (d, J = 4.7 Hz, 1H, CH-2); ¹³C-NMR (75 MHz, CDCl₃) δ : 121.2 (CH-3), 124.1 (CH-6), 126.5 (qC-5), 127.6 (CH-7), 129.8 (CH-9), 130.3 (CH-8), 142.6 (qC-4), 149.1 (qC-10), 149.8 (CH-2); HRMS (ESI-TOF) m/z : [M+H]⁺ calcd. for C₉H₇ClN: 164.0267; found: 164.0265.

Spectral data were consistent with those reported in the literature.

4-Chloro-2-heptylquinoline (precursor to compound **79**)

Prepared using the same procedure as for 4-chloroquinoline (**68**) using HHQ **1** as starting material.



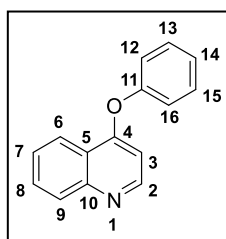
Orange sticky oil; yield: 0.461 mg, (86%); IR (NaCl): ν 3410 (C-H stretch), 2926 (C-H stretch), 1585 (aromatic C-C stretch), 1493 (aromatic C-C stretch), 1378 (C-N stretch), 761 (C-Cl stretch) cm⁻¹; ¹H-NMR (300 MHz, CDCl₃) δ : 0.88 (t, J = 6.8 Hz, 3H, CH₃-17), 1.19–1.49 (m, 8H, CH₂-13, CH₂-14, CH₂-15, CH₂-16), 1.73–1.87 (m,

2H, CH₂-12), 2.93 (t, J = 7.9 Hz, 2H, CH₂-11), 7.40 (s, 1H, CH-3), 7.57 (ddd, J = 8.2, 6.9, 1.1 Hz, 1H, CH-7), 7.73 (ddd, J = 8.4, 6.9, 1.4 Hz, 1H, CH-8), 8.05 (d, J = 8.4 Hz, 1H, CH-9), 8.17 (dd, J = 8.4, 1.0 Hz, 1H, CH-6); ¹³C-NMR (75 MHz, CDCl₃) δ : 14.1 (CH₃-17), 22.7 (CH₂-16), 29.2 (CH₂-14), 29.5 (CH₂-13), 29.9 (CH₂-12), 31.8 (CH₂-15), 39.2 (CH₂-11), 121.4 (CH-3), 123.9 (CH-6), 124.9 (qC-5), 126.6 (CH-7), 129.2 (CH-9), 130.3 (CH-8), 142.5 (qC-4), 148.7 (qC-10), 163.1 (qC-2); HRMS (ESI-TOF) m/z : [M+H]⁺ calcd. for C₁₆H₂₁ClN: 262.1363; found: 262.1352.

3.15. General Procedure for Synthesis of 4-Phenoxy Quinoline Substrates – NaOH Method

A mixture of the 4-chloroquinoline substrate (1 equiv.), the substituted 2-bromophenol (5 equiv.) and NaOH (crushed pellets) (1.5 equiv.) was stirred at 120 °C until reaction was completed (2–6 h) as evident by TLC (hexane/EtOAc 8:2). The cooled reaction mixture was diluted with 10% aq. NaOH (0.5 mL/mmol) and stirred at room temperature for 1 h. The aqueous phase was extracted with DCM (3 \times 1.5 mL/mmol). The combined organic layers were washed with 6M NaOH (3 \times 1 mL/mmol), water (1 mL/mmol) and brine (1 mL/mmol), dried over MgSO₄, filtered and concentrated *in vacuo*. The crude mixture was purified by column chromatography over silica gel using hexane/EtOAc (8:2) as eluent.

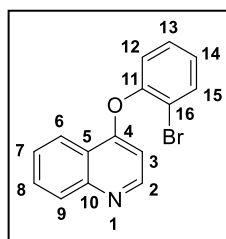
4-Phenoxyquinoline^[74] (69)



Yellow oil; yield: 2.45 g (91%); IR (NaCl): ν 3392 (C-H stretch), 3063 (C-H stretch), 1595 (aromatic C-C stretch), 1487 (aromatic C-C stretch), 1393 (C-N stretch), 1207 (C-O stretch) cm⁻¹; ¹H-NMR (300 MHz, CDCl₃) δ : 6.55 (d, J = 5.2 Hz, 1H, CH-3), 7.17–7.22 (m, 2H, CH-12, CH-16), 7.26–7.33 (m, 1H, CH-14), 7.42–7.52 (m, 2H, CH-13, CH-15), 7.58 (ddd, J = 8.1, 6.9, 1.1 Hz, 1H, CH-7), 7.76 (ddd, J = 8.5, 6.9, 1.5 Hz, 1H, CH-8), 8.10 (d, J = 8.5 Hz, 1H, CH-9), 8.37 (dd, J = 8.4, 0.9 Hz, 1H, CH-6), 8.67 (d, J = 5.2 Hz, 1H, CH-2); ¹³C-NMR (75 MHz, CDCl₃) δ : 104.4 (CH-3), 121.1 (CH-12, CH-16), 121.5 (qC-5), 121.8 (CH-6), 125.6 (CH-14), 126.1 (CH-7), 129.1 (CH-9), 130.1 (CH-8), 130.3 (CH-13, CH-15), 149.8 (qC-10), 151.1 (CH-2), 154.4 (qC-11), 161.9 (qC-4); HRMS (ESI-TOF) m/z : [M+H]⁺ calcd. for C₁₅H₁₂NO: 222.0919; found: 222.0915.

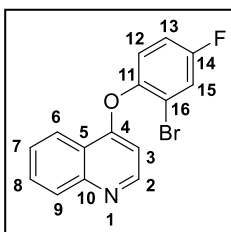
Spectral data were consistent with those reported in the literature.

4-(2-Bromophenoxy)quinoline (71)

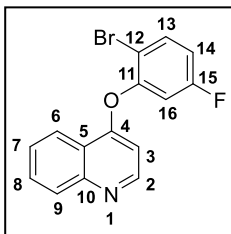


White solid; yield: 2.89 g (78%); m.p. = 62–64 °C; IR (NaCl): ν 3434 (C-H stretch), 1596 (aromatic C-C stretch), 1305 (C-N stretch), 1223 (C-O stretch), 659 (C-Br stretch) cm^{-1} ; $^1\text{H-NMR}$ (300 MHz, CDCl_3) δ : 6.41 (d, $J = 5.1$ Hz, 1H, CH-3), 7.18–7.27 (m, 2H, CH-12, CH-14), 7.43 (ddd, $J = 8.1, 7.3, 1.6$ Hz, 1H, CH-13), 7.61 (ddd, $J = 8.2, 6.9, 1.1$ Hz, 1H, CH-7), 7.70–7.82 (m, 2H, CH-8, CH-15), 8.12 (d, $J = 8.2$ Hz, 1H, CH-9), 8.42 (dd, $J = 8.3, 0.9$ Hz, 1H, CH-6), 8.68 (d, $J = 5.1$ Hz, 1H, CH-2); $^{13}\text{C-NMR}$ (75 MHz, CDCl_3) δ : 103.7 (CH-3), 116.4 (qC-16), 121.1 (qC-5), 121.9 (CH-6), 123.2 (CH-12), 126.3 (CH-7), 127.3 (CH-14), 129.1 (CH-9), 129.2 (CH-13), 130.2 (CH-8), 134.3 (CH-15), 149.8 (qC-10), 151.0 (CH-2), 151.2 (qC-11), 160.7 (qC-4); HRMS (ESI-TOF) m/z : $[\text{M}+\text{H}]^+$ calcd. for $\text{C}_{15}\text{H}_{11}\text{BrNO}$: 300.0024; found: 300.0016.

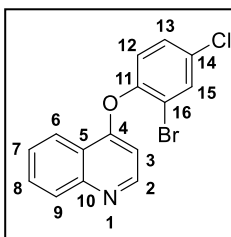
4-(2-Bromo-4-fluorophenoxy)quinoline (72)



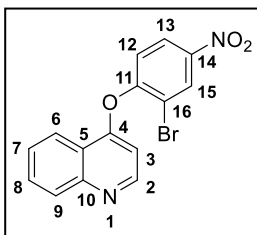
Pale yellow solid; yield: 188 mg (38%); m.p. = 100–103 °C; IR (NaCl): ν 3065 (C-H stretch), 1480 (aromatic C-C stretch), 1305 (C-N stretch), 1248 (C-O stretch), 1183 (C-F stretch), 765 (C-Br stretch) cm^{-1} ; $^1\text{H-NMR}$ (300 MHz, CDCl_3) δ : 6.39 (d, $J = 5.1$ Hz, 1H, CH-3), 7.10–7.29 (m, 2H, CH-12, CH-13), 7.48 (dd, $^3J_{\text{H,F}} = 7.7$, $^4J_{\text{H,H}} = 2.8$ Hz, 1H, CH-15), 7.62 (ddd, $J = 8.2, 5.5, 1.2$ Hz, 1H, CH-7), 7.79 (ddd, $J = 8.5, 6.9, 1.5$ Hz, 1H, CH-8), 8.12 (d, $J = 8.5$ Hz, 1H, CH-9), 8.40 (dd, $J = 8.3, 0.9$ Hz, 1H, CH-6), 8.69 (d, $J = 5.1$ Hz, 1H, CH-2); $^{13}\text{C-NMR}$ (75 MHz, CDCl_3) δ : 103.4 (CH-3), 116.1 (d, $^2J_{\text{C,F}} = 23$ Hz, CH-13), 116.9 (d, $^3J_{\text{C,F}} = 10$ Hz, qC-16), 120.9 (qC-5), 121.3 (d, $^2J_{\text{C,F}} = 26$ Hz, CH-15), 121.8 (CH-6), 124.3 (d, $^3J_{\text{C,F}} = 9$ Hz, CH-12), 126.4 (CH-7), 129.2 (CH-9), 130.3 (CH-8), 147.4 (qC-11), 149.8 (qC-10), 151.0 (CH-2), 159.9 (d, $^1J_{\text{C,F}} = 250$ Hz, qC-14), 160.7 (qC-4); $^{19}\text{F-NMR}$ (282 MHz, CDCl_3) δ : -114 (CF-14); HRMS (ESI-TOF) m/z : $[\text{M}+\text{H}]^+$ calcd. for $\text{C}_{15}\text{H}_{10}\text{BrFNO}$: 317.9930; found: 317.9935.

4-(2-Bromo-5-fluorophenoxy)quinoline (73)

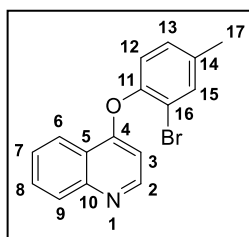
Pale yellow solid; yield: 891 mg (91%); m.p. = 77–78 °C; IR (NaCl): ν 3066 (C-H stretch), 1476 (aromatic C-C stretch), 1305 (C-N stretch), 1252 (C-O stretch), 1159 (C-F stretch), 601 (C-Br stretch) cm^{-1} ; $^1\text{H-NMR}$ (300 MHz, CDCl_3) δ : 6.49 (d, $J = 5.1$ Hz, 1H, CH-3), 6.94–7.01 (m, 1H, CH-14), 6.99 (d, $^3J_{\text{H,F}} = 8.1$ Hz, 1H, CH-16), 7.57–7.74 (m, 2H, CH-7, CH-13), 7.80 (ddd, $J = 8.4, 6.9, 1.4$ Hz, 1H, CH-8), 8.13 (d, $J = 8.5$ Hz, 1H, CH-9), 8.37 (dd, $J = 8.4, 1.0$ Hz, 1H, CH-6), 8.73 (d, $J = 5.1$ Hz, 1H, CH-2); $^{13}\text{C-NMR}$ (75 MHz, CDCl_3) δ : 104.1 (CH-3), 110.7 (qC-12), 110.9 (d, $^2J_{\text{C,F}} = 25$ Hz, CH-16), 114.5 (d, $^2J_{\text{C,F}} = 22$ Hz, CH-14), 120.9 (qC-5), 121.7 (CH-6), 126.5 (CH-7), 129.2 (CH-9), 130.4 (CH-8), 134.7 (d, $^3J_{\text{C,F}} = 9$ Hz, CH-13), 149.9 (qC-10), 151.0 (CH-2), 152.0 (d, $^3J_{\text{C,F}} = 11$ Hz, qC-11), 160.1 (qC-4), 162.4 (d, $^1J_{\text{C,F}} = 250$ Hz, qC-15); $^{19}\text{F-NMR}$ (282 MHz, CDCl_3) δ : -111 (CF-15); HRMS (ESI-TOF) m/z : $[\text{M}+\text{H}]^+$ calcd. for $\text{C}_{15}\text{H}_{10}\text{BrFNO}$: 317.9930; found: 317.9936.

4-(2-Bromo-4-chlorophenoxy)quinoline (74)

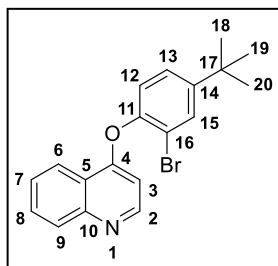
Off-white solid; yield: 1.97 g (96%); m.p. = 112–115 °C; IR (NaCl): ν 3403 (C-H stretch), 1596 (aromatic C-C stretch), 1465 (aromatic C-C stretch), 1392 (C-N stretch), 1257 (C-O stretch), 824 (C-Cl stretch), 765 (C-Br stretch) cm^{-1} ; $^1\text{H-NMR}$ (300 MHz, CDCl_3) δ : 6.42 (d, $J = 5.1$ Hz, 1H, CH-3), 7.17 (d, $J = 8.6$ Hz, 1H, CH-12), 7.40 (dd, $J = 8.7, 2.5$ Hz, 1H, CH-13), 7.61 (ddd, $J = 8.2, 6.9, 1.2$ Hz, 1H, CH-7), 7.70–7.84 (m, 2H, CH-8, CH-15), 8.12 (d, $J = 8.5$ Hz, 1H, CH-9), 8.38 (dd, $J = 8.4, 0.9$ Hz, 1H, CH-6), 8.70 (d, $J = 5.1$ Hz, 1H, CH-2); $^{13}\text{C-NMR}$ (75 MHz, CDCl_3) δ : 103.7 (CH-3), 117.0 (qC-16), 120.9 (qC-5), 121.7 (CH-6), 123.8 (CH-12), 126.4 (CH-7), 129.2 (CH-9), 129.3 (CH-13), 130.3 (CH-8), 132.0 (qC-14), 133.9 (CH-15), 149.9 (qC-10), 150.0 (qC-11), 151.0 (CH-2), 160.4 (qC-4); HRMS (ESI-TOF) m/z : $[\text{M}+\text{H}]^+$ calcd. for $\text{C}_{15}\text{H}_{10}\text{BrClNO}$: 333.9634; found: 333.9629.

4-(2-Bromo-4-nitrophenoxy)quinoline (75)

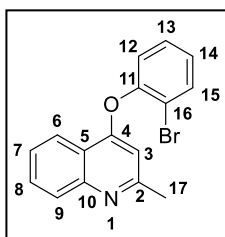
Pale yellow solid; yield: 192 mg (80%); m.p. = 151–152 °C; IR (NaCl): ν 3376 (C-H stretch), 1523 (aromatic C-C stretch), 1346 (N-O stretch), 1305 (C-N stretch), 1257 (C-O stretch), 665 (C-Br stretch) cm^{-1} ; $^1\text{H-NMR}$ (300 MHz, CDCl_3) δ : 6.65 (d, J = 5.0 Hz, 1H, CH-3), 7.23 (d, J = 8.9 Hz, 1H, CH-15), 7.64 (ddd, J = 8.1, 7.1, 0.7 Hz, 1H, CH-7), 7.83 (ddd, J = 8.4, 7.0, 1.3 Hz, 1H, CH-8), 8.17 (d, J = 8.5 Hz, 1H, CH-9), 8.25 (d, J = 8.8 Hz, 1H, CH-6), 8.27 (dd, J = 8.9, 2.7 Hz, 1H, CH-13), 8.65 (d, J = 2.6 Hz, 1H, CH-12), 8.80 (d, J = 5.0 Hz, 1H, CH-2); $^{13}\text{C-NMR}$ (75 MHz, CDCl_3) δ : 106.0 (CH-3), 115.9 (qC-16), 121.1 (qC-5), 121.2 (CH-12), 121.5 (CH-6), 124.6 (CH-13), 127.1 (CH-7), 129.5 (CH-9), 129.9 (CH-15), 130.7 (CH-8), 144.9 (qC-14), 150.2 (qC-10), 151.0 (CH-2), 157.2 (qC-11), 159.1 (qC-4); HRMS (ESI-TOF) m/z : $[\text{M}+\text{H}]^+$ calcd. for $\text{C}_{15}\text{H}_{10}\text{BrN}_2\text{O}_3$: 344.9875; found: 344.9865.

4-(2-Bromo-4-methylphenoxy)quinoline (76)

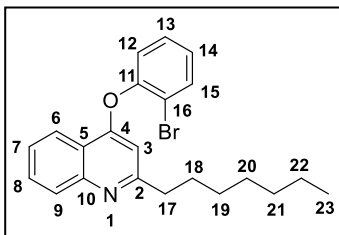
Orange solid; yield: 242 mg (84%); m.p. = 122–125 °C; IR (NaCl): ν 3064 (C-H stretch), 1568 (aromatic C-C stretch), 1485 (aromatic C-C stretch), 1392 (C-N stretch), 1255 (C-O stretch), 765 (C-Br stretch) cm^{-1} ; $^1\text{H-NMR}$ (300 MHz, CDCl_3) δ : 2.41 (s, 3H, CH₃-17), 6.40 (d, J = 5.2 Hz, 1H, CH-3), 7.13 (d, J = 8.2 Hz, 1H, CH-12), 7.22 (dd, J = 8.2, 1.5 Hz, 1H, CH-13), 7.54 (d, J = 1.4 Hz, 1H, CH-15), 7.61 (ddd, J = 8.1, 6.9, 1.1 Hz, 1H, CH-7), 7.78 (ddd, J = 8.4, 6.9, 1.4 Hz, 1H, CH-8), 8.11 (d, J = 8.5 Hz, 1H, CH-9), 8.43 (dd, J = 8.3, 1.0 Hz, 1H, CH-6), 8.67 (d, J = 5.1 Hz, 1H, CH-2); $^{13}\text{C-NMR}$ (75 MHz, CDCl_3) δ : 20.7 (CH₃-17), 103.5 (CH-3), 115.9 (qC-16), 121.1 (qC-5), 121.9 (CH-6), 122.9 (CH-12), 126.2 (CH-7), 129.1 (CH-9), 129.8 (CH-13), 130.1 (CH-8), 134.5 (CH-15), 137.5 (qC-14), 148.8 (qC-11), 149.8 (qC-10), 151.0 (CH-2), 161.0 (qC-4); HRMS (ESI-TOF) m/z : $[\text{M}+\text{H}]^+$ calcd. for $\text{C}_{16}\text{H}_{13}\text{BrNO}$: 314.0181; found: 314.0169.

4-(2-Bromo-4-(*tert*-butyl)phenoxy)quinoline (77)

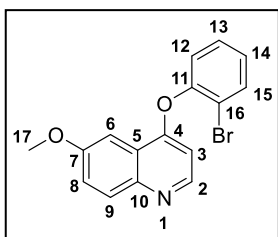
Pale yellow solid; yield: 73 mg (56%); m.p. = 68–70 °C; IR (NaCl): ν 2963 (C-H stretch), 1568 (aromatic C-C stretch), 1488 (aromatic C-C stretch), 1391 (C-H bend), 1306 (C-N stretch) 1263 (C-O stretch), 766 (C-Br stretch) cm^{-1} ; $^1\text{H-NMR}$ (300 MHz, CDCl_3) δ : 1.36 (s, 9H, CH_3 -**18**, CH_3 -**19**, CH_3 -**20**), 6.43 (d, $J = 5.1$ Hz, 1H, CH -**3**), 7.16 (d, $J = 8.5$ Hz, 1H, CH -**12**), 7.41 (dd, $J = 8.5$, 2.2 Hz, 1H, CH -**13**), 7.60 (t, $J = 7.6$ Hz, 1H, CH -**7**), 7.65–7.83 (m, 2H, CH -**8**, CH -**15**), 8.11 (d, $J = 8.5$ Hz, 1H, CH -**9**), 8.42 (d, $J = 8.3$ Hz, 1H, CH -**6**), 8.67 (d, $J = 5.0$ Hz, 1H, CH -**2**); $^{13}\text{C-NMR}$ (75 MHz, CDCl_3) δ : 31.3 (CH_3 -**18**, CH_3 -**19**, CH_3 -**20**), 34.7 (qC-**17**), 103.6 (CH -**3**), 115.8 (qC-**16**), 121.1 (qC-**5**), 121.9 (CH -**6**), 122.6 (CH -**12**), 126.2 (CH -**7**), 126.3 (CH -**13**), 129.0 (CH -**9**), 130.2 (CH -**8**), 131.2 (CH -**15**), 148.5 (qC-**11**), 149.7 (qC-**10**), 150.9 (qC-**14**), 151.1 (CH -**2**), 160.9 (qC-**4**); HRMS (ESI-TOF) m/z : $[\text{M}+\text{H}]^+$ calcd. for $\text{C}_{19}\text{H}_{19}\text{BrNO}$: 356.0650; found: 356.0642.

4-(2-Bromophenoxy)-2-methylquinoline (78)

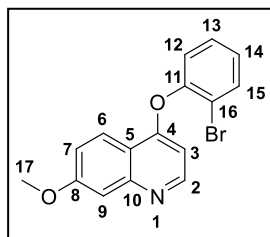
Pale pink solid; yield: 331 mg (93%); m.p. = 98–101 °C; IR (NaCl): ν 2923 (C-H stretch), 1599 (aromatic C-C stretch), 1470 (aromatic C-C stretch), 1342 (C-N stretch), 1235 (C-O stretch), 754 (C-Br stretch) cm^{-1} ; $^1\text{H-NMR}$ (300 MHz, CDCl_3) δ : 2.60 (s, 3H, CH_3 -**17**), 6.29 (s, 1H, CH -**3**), 7.15–7.29 (m, 2H, CH -**12**, CH -**14**), 7.42 (ddd, $J = 8.6$, 7.3, 1.6 Hz, 1H, CH -**13**), 7.54 (ddd, $J = 8.2$, 6.9, 1.2 Hz, 1H, CH -**7**), 7.68–7.79 (m, 2H, CH -**8**, CH -**15**), 8.02 (d, $J = 8.4$ Hz, 1H, CH -**9**), 8.35 (dd, $J = 8.4$, 1.0 Hz, 1H, CH -**6**); $^{13}\text{C-NMR}$ (75 MHz, CDCl_3) δ : 25.8 (CH_3 -**17**), 104.2 (CH -**3**), 116.3 (qC-**16**), 119.5 (qC-**5**), 121.7 (CH -**6**), 123.2 (CH -**12**), 125.4 (CH -**7**), 127.1 (CH -**14**), 128.3 (CH -**9**), 129.1 (CH -**13**), 130.2 (CH -**8**), 134.3 (CH -**15**), 149.4 (qC-**10**), 151.3 (qC-**11**), 159.9 (qC-**2**), 160.8 (qC-**4**); HRMS (ESI-TOF) m/z : $[\text{M}+\text{H}]^+$ calcd. for $\text{C}_{16}\text{H}_{13}\text{BrNO}$: 314.0181; found: 314.0179.

4-(2-Bromophenoxy)-2-heptylquinoline (79)

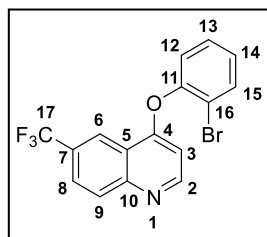
Off-white solid; yield: 205 mg (90%); m.p. = 75–77 °C; IR (NaCl): ν 2926 (C-H stretch), 2855 (C-H stretch), 1600 (aromatic C-C stretch), 1470 (aromatic C-C stretch), 1359 (C-N stretch), 1234 (C-O stretch), 763 (C-Br stretch) cm^{-1} ; $^1\text{H-NMR}$ (300 MHz, CDCl_3) δ : 0.85 (t, J = 6.7 Hz, 3H, CH_3 -23), 1.14–1.42 (m, 8H, CH_2 -19, CH_2 -20, CH_2 -21, CH_2 -22), 1.60–1.73 (m, 2H, CH_2 -18), 2.80 (t, J = 8.1 Hz, 2H, CH_2 -17), 6.30 (s, 1H, CH -3), 7.17–7.25 (m, 2H, CH -12, CH -14), 7.42 (ddd, J = 8.5, 7.2, 1.5 Hz, 1H, CH -13), 7.53 (ddd, J = 8.1, 7.0, 1.1 Hz, 1H, CH -7), 7.63–7.81 (m, 2H, CH -8, CH -15), 8.05 (d, J = 8.4 Hz, 1H, CH -9), 8.34 (dd, J = 8.3, 0.9 Hz, 1H, CH -6); $^{13}\text{C-NMR}$ (75 MHz, CDCl_3) δ : 14.1 (CH_3 -23), 22.6 (CH_2 -22), 29.2 (CH_2 -18), 29.4 (CH_2 -20), 30.0 (CH_2 -19), 31.8 (CH_2 -21), 39.7 (CH_2 -17), 103.8 (CH -3), 116.3 (qC-16), 119.7 (qC-5), 121.7 (CH -6), 123.1 (CH -12), 125.4 (CH -7), 127.1 (CH -14), 128.5 (CH -9), 129.2 (CH -13), 130.1 (CH -8), 134.3 (CH -15), 149.5 (qC-10), 151.4 (qC-11), 160.7 (qC-4), 164.2 (qC-2); HRMS (ESI-TOF) m/z : $[\text{M}+\text{H}]^+$ calcd. for $\text{C}_{22}\text{H}_{25}\text{BrNO}$: 398.1120; found: 398.1135.

4-(2-Bromophenoxy)-6-methoxyquinoline (80)

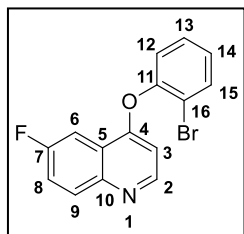
Yellow sticky oil; yield: 599 mg (70%); IR (NaCl): ν 3392 (C-H stretch), 1596 (aromatic C-C stretch), 1467 (aromatic C-C stretch), 1365 (C-N stretch), 1262 (C-O stretch), 1223 (C-O stretch), 778 (C-Br stretch) cm^{-1} ; $^1\text{H-NMR}$ (300 MHz, CDCl_3) δ : 3.98 (s, 3H, CH_3 -17), 6.40 (d, J = 5.1 Hz, 1H, CH -3), 7.16–7.29 (m, 2H, CH -12, CH -14), 7.37–7.47 (m, 2H, CH -8, CH -13), 7.64 (d, J = 2.8 Hz, 1H, CH -6), 7.73 (dd, J = 8.0, 1.5 Hz, 1H, CH -15), 8.01 (d, J = 9.2 Hz, 1H, CH -9), 8.54 (d, J = 5.1 Hz, 1H, CH -2); $^{13}\text{C-NMR}$ (75 MHz, CDCl_3) δ : 55.7 (CH_3 -17), 99.4 (CH -6), 104.2 (CH -3), 116.4 (qC-16), 121.8 (qC-5), 122.9 (CH -8), 123.2 (CH -12), 127.2 (CH -14), 129.2 (CH -13), 130.7 (CH -9), 134.3 (CH -15), 145.9 (qC-10), 148.4 (CH -2), 151.3 (qC-11), 157.8 (qC-7), 159.7 (qC-4); HRMS (ESI-TOF) m/z : $[\text{M}+\text{H}]^+$ calcd. for $\text{C}_{16}\text{H}_{13}\text{BrNO}_2$: 330.0130; found: 330.0127.

4-(2-Bromophenoxy)-7-methoxyquinoline (81)

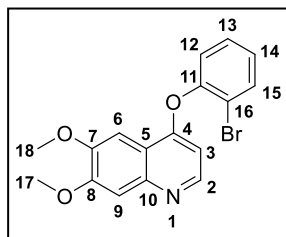
Pale yellow solid; yield: 380 mg (74%); m.p. = 99–100 °C; IR (NaCl): ν 3388 (C-H stretch), 1622 (aromatic C-C stretch), 1428 (aromatic C-C stretch), 1315 (C-N stretch), 1227 (C-O stretch), 665 (C-Br stretch) cm^{-1} ; $^1\text{H-NMR}$ (300 MHz, CDCl_3) δ : 3.98 (s, 3H, CH_3 -17), 6.30 (d, J = 5.2 Hz, 1H, CH -3), 7.15–7.29 (m, 3H, CH -7, CH -12, CH -14), 7.36–7.47 (m, 2H, CH -9, CH -13), 7.72 (dd, J = 7.9, 1.5 Hz, 1H, CH -15), 8.29 (d, J = 9.2 Hz, 1H, CH -6), 8.59 (d, J = 5.2 Hz, 1H, CH -2); $^{13}\text{C-NMR}$ 75 MHz, CDCl_3) δ : 55.5 (CH_3 -17), 102.4 (CH -3), 107.3 (CH -9), 115.8 (qC-5), 116.3 (qC-16), 119.2 (CH -7), 123.1 (CH -6), 123.2 (CH -12), 127.1 (CH -14), 129.1 (CH -13), 134.2 (CH -15), 151.2 (qC-11), 151.5 (CH -2), 151.8 (qC-10), 160.7 (qC-4), 161.3 (qC-8); HRMS (ESI-TOF) m/z : $[\text{M}+\text{H}]^+$ calcd. for $\text{C}_{16}\text{H}_{13}\text{BrNO}_2$: 330.0130; found: 330.0128.

4-(2-Bromophenoxy)-6-(trifluoromethyl)quinoline (82)

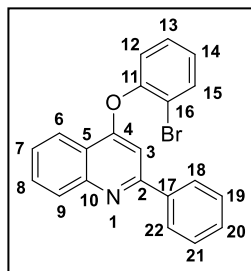
Off-white solid; yield: 254 mg (80%); m.p. = 67–69 °C; IR (NaCl): ν 3069 (C-H stretch), 1570 (aromatic C-C stretch), 1467 (aromatic C-C stretch), 1316 (C-N stretch), 1224 (C-O stretch), 1126 (C-F stretch), 739 (C-Br stretch) cm^{-1} ; $^1\text{H-NMR}$ (300 MHz, CDCl_3) δ : 6.47 (d, J = 5.2 Hz, 1H, CH -3), 7.21–7.32 (m, 2H, CH -12, CH -14), 7.46 (ddd, J = 8.1, 7.3, 1.6 Hz, 1H, CH -13), 7.75 (dd, J = 7.9, 1.3 Hz, 1H, CH -15), 7.95 (dd, J = 8.9, 2.1 Hz, 1H, CH -8), 8.22 (d, J = 8.9 Hz, 1H, CH -9), 8.76 (s, 1H, CH -6), 8.77 (d, J = 5.2 Hz, 1H, CH -2); $^{13}\text{C-NMR}$ (125 MHz, CDCl_3) δ : 104.4 (CH -3), 116.4 (qC-16), 120.2 (qC-5), 120.3 (q, $^3J_{\text{C,F}}$ = 5 Hz, CH -6), 123.4 (CH -12), 124.1 (q, $^1J_{\text{C,F}}$ = 272 Hz, qC-17), 126.0 (q, $^3J_{\text{C,F}}$ = 3 Hz, CH -8), 127.8 (CH -14), 128.2 (q, $^2J_{\text{C,F}}$ = 33 Hz, qC-7), 129.4 (CH -13), 130.3 (CH -9), 134.5 (CH -15), 150.6 (qC-11), 150.7 (qC-10), 153.2 (CH -2), 161.3 (qC-4); $^{19}\text{F-NMR}$ (282 MHz, CDCl_3) δ : -62 (CF_3 -17); HRMS (ESI-TOF) m/z : $[\text{M}+\text{H}]^+$ calcd. for $\text{C}_{16}\text{H}_{10}\text{BrF}_3\text{NO}$: 367.9898; found: 367.9894.

4-(2-Bromophenoxy)-6-fluoroquinoline (83)

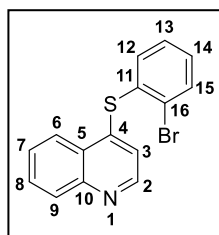
Pale yellow solid; yield: 344 mg (65%); m.p. = 75–79 °C; IR (NaCl): ν 3422 (C-H stretch), 1630 (aromatic C-C stretch), 1262 (C-N stretch), 1222 (C-O stretch), 1177 (C-F stretch), 657 (C-Br stretch) cm^{-1} ; $^1\text{H-NMR}$ (300 MHz, CDCl_3) δ : 6.43 (d, $J = 5.1$ Hz, 1H, CH-3), 7.19–7.24 (m, 1H, CH-14), 7.25 (d, $J = 8.7$ Hz, 1H, CH-12), 7.44 (t, $J = 7.4$ Hz, 1H, CH-13), 7.54 (td, $J = 8.7, 2.8$ Hz, 1H, CH-8), 7.73 (d, $J = 9.9$ Hz, 1H, CH-15), 8.02 (dd, $^3J_{\text{H,F}} = 9.3$, $^4J_{\text{H,H}} = 2.8$ Hz, 1H, CH-6), 8.12 (dd, $^3J_{\text{H,H}} = 9.2$, $^4J_{\text{H,F}} = 5.2$ Hz, 1H, CH-9), 8.64 (d, $J = 5.1$ Hz, 1H, CH-2); $^{13}\text{C-NMR}$ (75 MHz, CDCl_3) δ : 104.0 (CH-3), 105.7 (d, $^2J_{\text{C,F}} = 24$ Hz, CH-6), 116.3 (qC-16), 120.4 (d, $^2J_{\text{C,F}} = 26$ Hz, CH-8), 121.7 (d, $^3J_{\text{C,F}} = 10$ Hz, qC-5), 123.3 (CH-12), 127.5 (CH-14), 129.3 (CH-13), 131.7 (d, $^3J_{\text{C,F}} = 10$ Hz, CH-9), 134.4 (CH-15), 146.9 (qC-10), 150.3 (d, $^6J_{\text{C,F}} = 3$ Hz, CH-2), 150.8 (qC-11), 160.3 (d, $^4J_{\text{C,F}} = 5$ Hz, qC-4), 160.4 (d, $^1J_{\text{C,F}} = 248$ Hz, qC-7); $^{19}\text{F-NMR}$ (282 MHz, CDCl_3) δ : -113 (CF-7); HRMS (ESI-TOF) m/z : $[\text{M}+\text{H}]^+$ calcd. for $\text{C}_{15}\text{H}_{10}\text{BrFNO}$: 317.9930; found: 317.9917.

4-(2-Bromophenoxy)-6,7-dimethoxyquinoline (111)

Yellow solid; yield: 294 mg (91%); m.p. = 89–91 °C; IR (NaCl): ν 3373 (C-H stretch), 2932 (C-H stretch), 1572 (aromatic C-C stretch), 1467 (aromatic C-C stretch), 1349 (C-N stretch), 1250 (C-O stretch), 1225 (C-O stretch), 667 (C-Br stretch) cm^{-1} ; $^1\text{H-NMR}$ (300 MHz, CDCl_3) δ : 4.07 (s, 6H, CH₃-17, CH₃-18), 6.33 (d, $J = 5.2$ Hz, 1H, CH-3), 7.16–7.29 (m, 2H, CH-12, CH-14), 7.38–7.48 (m, 2H, CH-9, CH-13), 7.61 (s, 1H, CH-6), 7.73 (dd, $J = 8.0, 1.5$ Hz, 1H, CH-15), 8.50 (d, $J = 5.2$ Hz, 1H, CH-2); $^{13}\text{C-NMR}$ 75 MHz, CDCl_3) δ : 56.2 (CH₃-17, CH₃-18), 99.6 (CH-6), 103.0 (CH-3), 108.0 (CH-9), 115.8 (qC-5), 116.3 (qC-16), 123.2 (CH-12), 127.1 (CH-14), 129.1 (CH-13), 134.3 (CH-15), 147.1 (qC-10), 148.8 (CH-2), 149.7 (qC-7), 151.4 (qC-11), 152.9 (qC-8), 159.5 (qC-4); HRMS (ESI-TOF) m/z : $[\text{M}+\text{H}]^+$ calcd. for $\text{C}_{17}\text{H}_{15}\text{BrNO}_3$: 360.0235; found: 360.0225.

4-(2-Bromophenoxy)-2-phenylquinoline (112)

Pale yellow solid; yield: 185 mg (79%); m.p. = 112–113 °C; IR (NaCl): ν 3583 (C-H stretch), 3291 (C-H stretch), 1596 (aromatic C-C stretch), 1470 (aromatic C-C stretch), 1353 (C-N stretch), 1225 (C-O stretch), 667 (C-Br stretch) cm^{-1} ; $^1\text{H-NMR}$ (300 MHz, CDCl_3) δ : 6.87 (s, 1H, CH-3), 7.15–7.31 (m, 2H, CH-12, CH-14), 7.35–7.51 (m, 4H, CH-13, CH-19, CH-20, CH-21), 7.58 (t, $J = 7.5$ Hz, 1H, CH-7), 7.68–7.86 (m, 2H, CH-8, CH-15), 7.87–8.02 (m, 2H, CH-18, CH-22), 8.18 (d, $J = 8.4$ Hz, 1H, CH-9), 8.39 (d, $J = 8.1$ Hz, 1H, CH-6); $^{13}\text{C-NMR}$ (75 MHz, CDCl_3) δ : 101.9 (CH-3), 116.3 (qC-16), 120.1 (qC-5), 121.8 (CH-6), 123.0 (CH-12), 126.0 (CH-7), 127.2 (CH-14), 127.5 (CH-18, CH-22), 128.7 (CH-19, CH-21), 129.2 (CH-13), 129.35 (CH-20), 129.41 (CH-9), 130.4 (CH-8), 134.4 (CH-15), 139.8 (qC-17), 149.9 (qC-10), 151.4 (qC-11), 158.6 (qC-2), 161.3 (qC-4); HRMS (ESI-TOF) m/z : $[\text{M}+\text{H}]^+$ calcd. for $\text{C}_{21}\text{H}_{15}\text{BrNO}$: 376.0337; found: 376.0323.

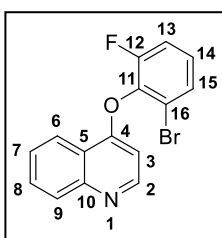
4-((2-Bromophenyl)thio)quinoline (113)

Off-white solid; yield: 226 mg (78%); m.p. = 72–73 °C; IR (NaCl): ν 3059 (C-H stretch), 1560, 1496 (aromatic C-C stretch), 831 (C-S stretch), 755 (C-Br stretch) cm^{-1} ; $^1\text{H-NMR}$ (300 MHz, CDCl_3) δ : 6.83 (d, $J = 4.7$ Hz, 1H, CH-3), 7.27–7.32 (m, 1H, CH-14), 7.32–7.38 (m, 1H, CH-13), 7.49 (dd, $J = 7.2, 2.2$ Hz, 1H, CH-12), 7.60 (ddd, $J = 8.3, 6.9, 1.3$ Hz, 1H, CH-7), 7.72–7.80 (m, 2H, CH-8, CH-15), 8.12 (dd, $J = 8.5, 0.7$ Hz, 1H, CH-9), 8.23 (dd, $J = 8.4, 0.9$ Hz, 1H, CH-6), 8.65 (d, $J = 4.7$ Hz, 1H, CH-2); $^{13}\text{C-NMR}$ (75 MHz, CDCl_3) δ : 119.4 (CH-3), 123.9 (CH-6), 126.4 (qC-5), 126.8 (CH-7), 128.6 (CH-13), 129.0 (qC-16), 130.0 (CH-8), 130.1 (CH-9), 130.7 (CH-14), 132.1 (qC-11), 134.1 (CH-15), 136.0 (CH-12), 145.6 (qC-4), 148.0 (qC-10), 149.6 (CH-2); HRMS (ESI-TOF) m/z : $[\text{M}+\text{H}]^+$ calcd. for $\text{C}_{15}\text{H}_{11}\text{BrNS}$: 315.9796; found: 315.9795.

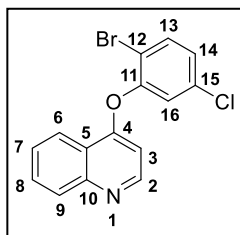
3.16. General Procedure for Synthesis of 4-Phenoxy Quinoline Substrates – DMAP Method

A mixture of 4-chloroquinoline (1 equiv.), the substituted 2-bromophenol (1.5 equiv.) in toluene (1.5 mL/mmol) was stirred at 130 °C until the reaction was completed as evident by TLC (hexane/EtOAc 8:2). The cooled reaction mixture was diluted with 10% aq. NaOH (0.5 mL/mmol) and stirred at room temperature for 1 h. The aqueous phase was extracted with DCM (3 × 1.5 mL/mmol). The combined organic layers were washed with 3M NaOH (3 × 1 mL/mmol), 1M HCl (2 × 1 mL/mmol), water (1 mL/mmol) and brine (1 mL/mmol), dried over MgSO₄, filtered and concentrated *in vacuo*. The crude mixture was purified by column chromatography over silica gel using hexane/EtOAc (8:2) as eluent.

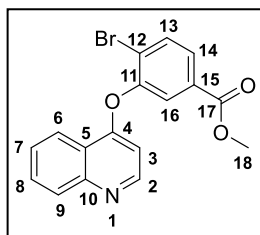
4-(2-Bromo-6-fluorophenoxy)quinoline (84)



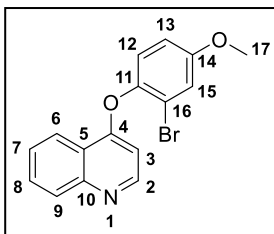
Pale yellow solid; yield: 318 mg (72%); m.p. = 118–119 °C; IR (NaCl): ν 3064 (C-H stretch), 1502 (aromatic C-C stretch), 1471 (aromatic C-C stretch), 1305 (C-N stretch), 1271 (C-O stretch), 1042 (C-F stretch), 665 (C-Br stretch) cm⁻¹; ¹H-NMR (300 MHz, CDCl₃) δ : 6.39 (d, J = 5.1 Hz, 1H, CH-3), 7.15–7.30 (m, 2H, CH-13, CH-14), 7.47–7.54 (m, 1H, CH-15), 7.63 (ddd, J = 8.1, 7.0, 1.1 Hz, 1H, CH-7), 7.79 (ddd, J = 8.4, 6.9, 1.5 Hz, 1H, CH-8), 8.13 (d, J = 8.5 Hz, 1H, CH-9), 8.46 (dd, J = 8.3, 1.1 Hz, 1H, CH-6), 8.69 (d, J = 5.0 Hz, 1H, CH-2); ¹³C-NMR (75 MHz, CDCl₃) δ : 102.5 (CH-3), 116.5 (d, ² $J_{\text{C,F}}$ = 19 Hz, CH-13), 118.3 (qC-16), 120.6 (qC-5), 121.9 (CH-6), 126.4 (CH-7), 127.7 (d, ³ $J_{\text{C,F}}$ = 8 Hz, CH-14), 129.1 (CH-9), 129.2 (CH-15), 130.2 (CH-8), 139.3 (d, ² $J_{\text{C,F}}$ = 14 Hz, qC-11), 149.8 (qC-10), 150.9 (CH-2), 155.6 (d, ¹ $J_{\text{C,F}}$ = 255 Hz, qC-12), 159.8 (qC-4); ¹⁹F-NMR (282 MHz, CDCl₃) δ : -124 (CF-12); HRMS (ESI-TOF) m/z : [M+H]⁺ calcd. for C₁₅H₁₀BrFNO: 317.9930; found: 317.9921.

4-(2-Bromo-5-chlorophenoxy)quinoline (85)

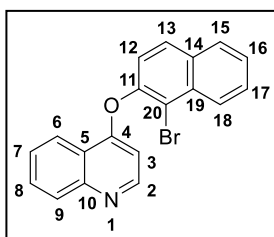
White solid; yield: 290 mg (89%); m.p. = 79–81 °C; IR (NaCl): ν 3370 (C-H stretch), 1562 (aromatic C-C stretch), 1464 (aromatic C-C stretch), 1305 (C-N stretch), 1252 (C-O stretch), 765 (C-Cl stretch), 665 (C-Br stretch) cm^{-1} ; $^1\text{H-NMR}$ (300 MHz, CDCl_3) δ : 6.48 (d, $J = 5.1$ Hz, 1H, CH-3), 7.16–7.29 (m, 2H, CH-14, CH-16), 7.57–7.69 (m, 2H, CH-7, CH-13), 7.79 (ddd, $J = 8.5, 6.9, 1.5$ Hz, 1H, CH-8), 8.13 (d, $J = 8.6$ Hz, 1H, CH-9), 8.36 (dd, $J = 8.4, 0.9$ Hz, 1H, CH-6), 8.72 (d, $J = 5.1$ Hz, 1H, CH-2); $^{13}\text{C-NMR}$ (75 MHz, CDCl_3) δ : 104.1 (CH-3), 114.4 (qC-12), 120.9 (qC-5), 121.7 (CH-6), 123.3 (CH-16), 126.5 (CH-7), 127.4 (CH-14), 129.2 (CH-9), 130.4 (CH-8), 134.5 (qC-15), 134.8 (CH-13), 149.9 (qC-10), 151.0 (CH-2), 151.9 (qC-11), 160.1 (qC-4); HRMS (ESI-TOF) m/z : $[\text{M}+\text{H}]^+$ calcd. for $\text{C}_{15}\text{H}_{10}\text{BrClNO}$: 333.9634; found: 333.9622.

Methyl 4-bromo-3-(quinolin-4-yloxy)benzoate (86)

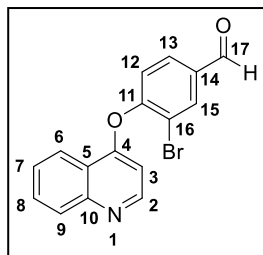
Off white solid; yield: 258 mg (62%); m.p. = 87–89 °C; IR (NaCl): ν 3586 (C-H stretch), 2950 (C-H stretch), 1724 (ester C=O stretch), 1565 (aromatic C-C stretch), 1502 (aromatic C-C stretch), 1392 (C-N stretch), 1294 (C-O stretch), 1241 (C-O stretch), 765 (C-Br stretch) cm^{-1} ; $^1\text{H-NMR}$ (300 MHz, CDCl_3) δ : 3.92 (s, 3H, CH₃-18), 6.43 (d, $J = 5.1$ Hz, 1H, CH-3), 7.63 (ddd, $J = 8.2, 6.9, 1.1$ Hz, 1H, CH-7), 7.76–7.90 (m, 4H, CH-8, CH-13, CH-14, CH-16), 8.13 (d, $J = 8.5$ Hz, 1H, CH-9), 8.40 (dd, $J = 8.3, 0.9$ Hz, 1H, CH-6), 8.70 (d, $J = 5.1$ Hz, 1H, CH-2); $^{13}\text{C-NMR}$ (75 MHz, CDCl_3) δ : 52.6 (CH₃-18), 103.9 (CH-3), 121.0 (qC-5), 121.7 (CH-6), 122.0 (qC-12), 123.9 (CH-16), 126.5 (CH-7), 128.0 (CH-14), 129.2 (CH-9), 130.4 (CH-8), 131.6 (qC-15), 134.5 (CH-13), 149.9 (qC-10), 151.0 (CH-2), 151.4 (qC-11), 160.3 (qC-4), 165.4 (qC-17); HRMS (ESI-TOF) m/z : $[\text{M}+\text{H}]^+$ calcd. for $\text{C}_{17}\text{H}_{13}\text{BrNO}_3$: 358.0079; found: 358.0089.

4-(2-Bromo-4-methoxyphenoxy)quinoline (87)

Beige solid; yield: 304 mg (56%); m.p. = 184–185 °C; IR (NaCl): ν 3062 (C-H stretch), 2835 (C-H stretch), 1595 (aromatic C-C stretch), 1487 (aromatic C-C stretch), 1392 (C-N stretch), 1212 (C-O stretch), 765 (C-Br stretch) cm^{-1} ; $^1\text{H-NMR}$ (300 MHz, CDCl_3) δ : 3.86 (s, 3H, CH_3 -17), 6.38 (d, $J = 5.2$ Hz, 1H, CH -3), 6.96 (dd, $J = 8.9, 2.9$ Hz, 1H, CH -13), 7.17 (d, $J = 8.9$ Hz, 1H, CH -12), 7.24 (d, $J = 2.9$ Hz, 1H, CH -15), 7.60 (ddd, $J = 8.1, 6.9, 1.1$ Hz, 1H, CH -7), 7.77 (ddd, $J = 8.5, 6.9, 1.5$ Hz, 1H, CH -8), 8.11 (d, $J = 8.5$ Hz, 1H, CH -9), 8.43 (dd, $J = 8.3, 0.9$ Hz, 1H, CH -6), 8.67 (d, $J = 5.0$ Hz, 1H, CH -2); $^{13}\text{C-NMR}$ (75 MHz, CDCl_3) δ : 55.9 (CH_3 -17), 103.3 (CH -3), 114.9 (CH -13), 116.7 (qC-16), 118.9 (CH -15), 121.0 (qC-5), 121.9 (CH -6), 123.7 (CH -12), 126.2 (CH -7), 129.0 (CH -9), 130.1 (CH -8), 144.5 (qC-11), 149.7 (qC-10), 151.0 (CH -2), 157.9 (qC-14), 161.3 (qC-4); HRMS (ESI-TOF) m/z : $[\text{M}+\text{H}]^+$ calcd. for $\text{C}_{16}\text{H}_{13}\text{BrNO}_2$: 330.0130; found: 330.0125.

4-((1-Bromonaphthalen-2-yl)oxy)quinoline (88)

Off-white solid; yield: 318 mg (61%); m.p. = 197–200 °C; IR (NaCl): ν 3062 (C-H stretch), 1594 (aromatic C-C stretch), 1568 (aromatic C-C stretch), 1499 (aromatic C-C stretch), 1392 (C-N stretch), 1253 (C-O stretch), 764 (C-Br stretch) cm^{-1} ; $^1\text{H-NMR}$ (300 MHz, CDCl_3) δ : 6.42 (d, $J = 5.1$ Hz, 1H, CH -3), 7.36 (d, $J = 8.8$ Hz, 1H, CH -12), 7.55–7.72 (m, 3H, CH -7, CH -16, CH -17), 7.80 (ddd, $J = 8.5, 6.9, 1.5$ Hz, 1H, CH -8), 7.92 (d, $J = 8.1$ Hz, 1H, CH -15), 7.93 (d, $J = 8.8$ Hz, 1H, CH -13), 8.14 (d, $J = 8.5$ Hz, 1H, CH -9), 8.33 (d, $J = 8.5$ Hz, 1H, CH -18), 8.51 (dd, $J = 8.3, 1.0$ Hz, 1H, CH -6), 8.56 (d, $J = 5.1$ Hz, 1H, CH -2); $^{13}\text{C-NMR}$ (75 MHz, CDCl_3) δ : 103.9 (CH -3), 115.2 (qC-20), 121.1 (qC-5), 121.3 (CH -12), 122.0 (CH -6), 126.3 (CH -7), 126.6 (CH -16), 127.1 (CH -18), 128.2 (CH -17), 128.4 (CH -15), 129.1 (CH -9), 129.8 (CH -13), 130.3 (CH -8), 132.4 (qC-14), 133.2 (qC-19), 149.0 (qC-11), 149.8 (qC-10), 151.1 (CH -2), 160.8 (qC-4); HRMS (ESI-TOF) m/z : $[\text{M}+\text{H}]^+$ calcd. for $\text{C}_{19}\text{H}_{13}\text{BrNO}$: 350.0181; found: 350.0178.

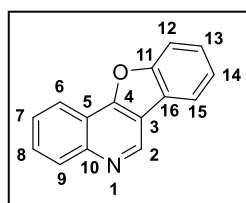
3-Bromo-4-(quinolin-4-yloxy)benzaldehyde (114)

Pale yellow solid; yield: 215 mg (79%); m.p. = 139–141 °C; IR (NaCl): ν 3063, 2849 (C-H stretch), 1703 (aldehyde C=O stretch), 1566, 1503 (aromatic C-C stretch), 1392 (C-N stretch), 1257 (C-O stretch), 765 (C-Br stretch) cm^{-1} ; $^1\text{H-NMR}$ (300 MHz, CDCl_3) δ : 6.59 (d, $J = 5.0$ Hz, 1H, CH-3), 7.29 (d, $J = 8.3$ Hz, 1H, CH-12), 7.58–7.68 (m, 1H, CH-7), 7.81 (ddd, $J = 8.1, 7.0, 1.2$ Hz, 1H, CH-8), 7.90 (dd, $J = 8.3, 1.9$ Hz, 1H, CH-13), 8.16 (d, $J = 8.5$ Hz, 1H, CH-9), 8.22–8.37 (m, 2H, CH-6, CH-15), 8.76 (d, $J = 4.9$ Hz, 1H, CH-2), 9.99 (s, 1H, CH-17); $^{13}\text{C-NMR}$ (75 MHz, CDCl_3) δ : 105.4 (CH-3), 116.7 (qC-16), 121.1 (qC-5), 121.7 (CH-6), 122.2 (CH-12), 126.8 (CH-7), 129.3 (CH-9), 130.53 (CH-13), 130.56 (CH-8), 134.7 (qC-14), 135.6 (CH-15), 150.1 (qC-10), 151.0 (CH-2), 156.5 (qC-11), 159.5 (qC-4), 189.4 (CH-17); HRMS (ESI-TOF) m/z : $[\text{M}+\text{H}]^+$ calcd. for $\text{C}_{16}\text{H}_{11}\text{BrNO}_2$: 327.9973; found: 327.9970.

3.17. General Procedure for Pd-Catalysed Intramolecular Direct Arylation

A mixture of the 4-(2-bromophenoxy)quinoline substrate (1 equiv.), Pd(OAc)₂ (2-5 mol%), and anhydrous Cs₂CO₃ (2 equiv.) in anhydrous NMP (1.5 mL/mmol) was stirred at 135 °C in a sealed reaction tube. The reaction progress was monitored by periodically sampling the reaction mixture for ¹H-NMR analysis in CDCl₃. Once complete, the cooled reaction mixture was diluted with DCM, filtered through a short plug of Celite and concentrated *in vacuo*. The crude mixture was purified by column chromatography over silica gel using DCM/EtOAc (99:1–95:5) as eluent.

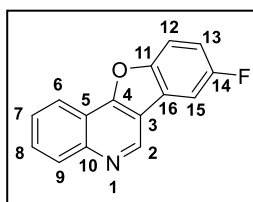
Benzofuro[3,2-*c*]quinoline (70)^[37]



2 mol% Pd(OAc)₂ used. White solid; yield: 68 mg (95%); m.p. = 132–135 °C (lit. 135–138 °C); IR (NaCl): ν 3369 (C-H stretch), 1566 (aromatic C-C stretch), 1510 (aromatic C-C stretch), 1399 (C-N stretch), 1190 (C-O stretch) cm⁻¹; ¹H-NMR (300 MHz, CDCl₃) δ : 7.44–7.58 (m, 2H, CH-13, CH-14), 7.65–7.83 (m, 3H, CH-7, CH-8, CH-12), 8.12 (dd, J = 7.2, 0.9 Hz, 1H, CH-15), 8.28 (d, J = 8.4 Hz, 1H, CH-9), 8.44 (dd, J = 8.1, 1.0 Hz, 1H, CH-6), 9.51 (s, 1H, CH-2); ¹³C-NMR (75 MHz, CDCl₃) δ : 112.1 (CH-12), 116.3 (qC-3), 117.2 (qC-5), 120.6 (CH-15), 120.8 (CH-6), 122.7 (qC-16), 124.1 (CH-14), 127.0 (CH-7), 127.2 (CH-13), 129.3 (CH-8), 129.9 (CH-9), 144.4 (CH-2), 147.4 (qC-10), 156.0 (qC-11), 157.5 (qC-4); HRMS (ESI-TOF) m/z : [M+H]⁺ calcd. for C₁₅H₁₀NO: 220.0762; found: 220.0755.

Spectral data were consistent with those reported in the literature.

8-Fluorobenzofuro[3,2-*c*]quinoline (89)^[37]

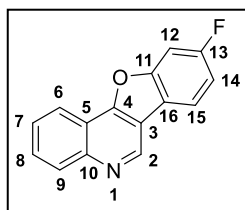


2 mol% Pd(OAc)₂ used. White solid; yield: 87 mg (91%); m.p. = 163–164 °C (lit. 162–163 °C); IR (NaCl): ν 3368 (C-H stretch), 1565 (aromatic C-C stretch), 1479 (aromatic C-C stretch), 1319 (C-N stretch), 1247 (C-O stretch), 1146 (C-F stretch) cm⁻¹; ¹H-NMR (300 MHz, CDCl₃) δ : 7.21–7.33 (m, 1H, CH-13), 7.65–7.87 (m, 4H, CH-7, CH-8, CH-12, CH-15), 8.28 (d, J = 8.4 Hz, 1H, CH-9), 8.41 (dd, J = 8.1, 1.0 Hz, 1H, CH-6), 9.45 (s, 1H, CH-2); ¹³C-NMR (75 MHz, CDCl₃) δ : 106.7 (d, ² $J_{\text{C,F}}$ = 26 Hz, CH-15), 112.9 (d, ³ $J_{\text{C,F}}$ = 9 Hz, CH-12), 114.7 (d, ² $J_{\text{C,F}}$ = 26 Hz,

CH-13), 116.1 (d, $^4J_{(C,F)} = 4$ Hz, qC-3), 117.0 (qC-5), 120.8 (CH-6), 123.6 (d, $^3J_{(C,F)} = 11$ Hz, qC-16), 127.2 (CH-7), 129.6 (CH-8), 129.9 (CH-9), 144.2 (CH-2), 147.5 (qC-10), 151.9 (qC-11), 158.6 (qC-4), 159.7 (d, $^1J_{(C,F)} = 241$ Hz, qC-14); ^{19}F -NMR (282 MHz, CDCl_3) δ : -118 (CF-14); HRMS (ESI-TOF) m/z : $[\text{M}+\text{H}]^+$ calcd. for $\text{C}_{15}\text{H}_9\text{FNO}$: 238.0668; found: 238.0659.

Spectral data were consistent with those reported in the literature.

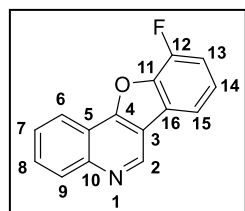
9-Fluorobenzofuro[3,2-*c*]quinoline (90)^[76]



2 mol% $\text{Pd}(\text{OAc})_2$ used. White solid; yield: 64 mg (88%); m.p. = 149–150 °C (lit. 148–150 °C); IR (NaCl): ν 3052 (C-H stretch), 1564 (aromatic C-C stretch), 1512 (aromatic C-C stretch), 1396 (C-N stretch), 1254 (C-O stretch), 1134 (C-F stretch) cm^{-1} ; ^1H -NMR (300 MHz, CDCl_3) δ : 7.22 (ddd, $^3J_{(H,F)} = 8.9$, $^3J_{(H,H)} = 6.9$, $^4J_{(H,H)} = 2.2$ Hz, 1H, CH-14), 7.45 (dd, $^3J_{(H,F)} = 8.6$, $^4J_{(H,H)} = 2.2$ Hz, 1H, CH-12), 7.63–7.85 (m, 2H, CH-7, CH-8), 8.00 (dd, $^3J_{(H,H)} = 8.6$, $^4J_{(H,F)} = 5.3$ Hz, 1H, CH-15), 8.25 (d, $J = 8.3$ Hz, 1H, CH-9), 8.36 (dd, $J = 8.1$, 1.1 Hz, 1H, CH-6), 9.43 (s, 1H, CH-2); ^{13}C -NMR (75 MHz, CDCl_3) δ : 100.3 (d, $^2J_{(C,F)} = 27$ Hz, CH-12), 112.3 (d, $^2J_{(C,F)} = 24$ Hz, CH-14), 115.8 (qC-3), 117.0 (qC-5), 118.9 (d, $^4J_{(C,F)} = 2$ Hz, qC-16), 120.6 (CH-6), 121.2 (d, $^3J_{(C,F)} = 10$ Hz, CH-15), 127.2 (CH-7), 129.4 (CH-8), 129.8 (CH-9), 143.9 (CH-2), 147.1 (qC-10), 156.1 (d, $^3J_{(C,F)} = 14$ Hz, qC-11), 158.1 (d, $^5J_{(C,F)} = 3$ Hz, qC-4), 162.2 (d, $^1J_{(C,F)} = 247$ Hz, qC-13); ^{19}F -NMR (282 MHz, CDCl_3) δ : -112 (CF-13); HRMS (ESI-TOF) m/z : $[\text{M}+\text{H}]^+$ calcd. for $\text{C}_{15}\text{H}_9\text{FNO}$: 238.0668; found: 238.0668.

Spectral data were consistent with those reported in the literature.

10-Fluorobenzofuro[3,2-*c*]quinoline (91)^[37]

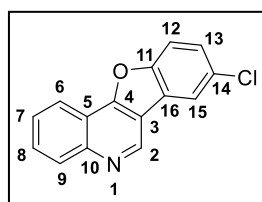


2 mol% $\text{Pd}(\text{OAc})_2$ used. White solid; yield: 104 mg (93%); m.p. = 156–157 °C (lit. 157–158 °C); IR (NaCl): ν 3368 (C-H stretch), 1564 (aromatic C-C stretch), 1496 (aromatic C-C stretch), 1347 (C-N stretch), 1200 (C-O stretch), 1189 (C-F stretch) cm^{-1} ; ^1H -NMR (300 MHz, CDCl_3) δ : 7.27–7.35 (m, 1H, CH-13), 7.42 (td, $^3J_{(H,H)} = 8.0$, $^4J_{(H,F)} = 4.4$ Hz, 1H, CH-14), 7.73 (ddd, $J = 8.1$, 7.0, 1.2 Hz, 1H, CH-7), 7.79–7.92 (m, 2H, CH-8, CH-15), 8.29 (d, $J = 8.2$ Hz, 1H, CH-9), 8.49 (dd, $J = 8.1$, 0.9 Hz, 1H, CH-6),

9.50 (s, 1H, CH-2); ^{13}C -NMR (75 MHz, CDCl_3) δ : 113.7 (d, $^2J_{\text{C,F}} = 16$ Hz, CH-13), 116.0 (qC-3), 116.1 (d, $^4J_{\text{C,F}} = 4$ Hz, CH-15), 117.0 (qC-5), 120.8 (CH-6), 124.8 (d, $^3J_{\text{C,F}} = 6$ Hz, CH-14), 126.2 (d, $^3J_{\text{C,F}} = 3$ Hz, qC-16), 127.3 (CH-7), 129.7 (CH-8), 129.8 (CH-9), 142.7 (d, $^2J_{\text{C,F}} = 11$ Hz, qC-11), 144.3 (CH-2), 147.7 (qC-10), 148.3 (d, $^1J_{\text{C,F}} = 251$ Hz, qC-12), 157.8 (qC-4); ^{19}F -NMR (282 MHz, CDCl_3) δ : -135 (CF-12); HRMS (ESI-TOF) m/z : $[\text{M}+\text{H}]^+$ calcd. for $\text{C}_{15}\text{H}_9\text{FNO}$: 238.0668; found: 238.0662.

Spectral data were consistent with those reported in the literature.

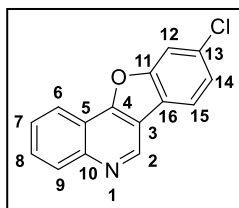
8-Chlorobenzofuro[3,2-*c*]quinoline (92)^[37]



2 mol% $\text{Pd}(\text{OAc})_2$ used. White solid; yield: 71 mg (93%); m.p. = 187–189 °C (lit. 189–190 °C); IR (NaCl): ν 2917 (C-H stretch), 1564 (C aromatic C-C stretch), 1511 (aromatic C-C stretch), 1395 (C-N stretch), 1194 (C-O stretch), 871 (C-Cl stretch) cm^{-1} ; ^1H -NMR (300 MHz, CDCl_3) δ : 7.51 (dd, $J = 8.8, 2.2$ Hz, 1H, CH-13), 7.69 (dd, $J = 8.8, 0.4$ Hz, 1H, CH-12), 7.72 (ddd, $J = 8.1, 7.0, 1.2$ Hz, 1H, CH-7), 7.82 (ddd, $J = 8.5, 7.0, 1.5$ Hz, 1H, CH-8), 8.08 (dd, $J = 2.2, 0.4$ Hz, 1H, CH-15), 8.28 (d, $J = 8.2$ Hz, 1H, CH-9), 8.41 (dd, $J = 8.2, 0.9$ Hz, 1H, CH-6), 9.46 (s, 1H, CH-2); ^{13}C -NMR (100 MHz, CDCl_3) δ : 113.1 (CH-12), 115.5 (qC-3), 117.0 (qC-5), 120.5 (CH-15), 120.8 (CH-6), 124.1 (qC-16), 127.28 (CH-7), 127.34 (CH-13), 129.75 (qC-14), 129.78 (CH-8), 130.0 (CH-9), 144.2 (CH-2), 147.6 (qC-10), 154.2 (qC-11), 158.2 (qC-4); HRMS (ESI-TOF) m/z : $[\text{M}+\text{H}]^+$ calcd. for $\text{C}_{15}\text{H}_9\text{ClNO}$: 254.0373; found: 254.0370.

Spectral data were consistent with those reported in the literature.

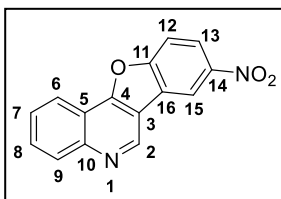
9-Chlorobenzofuro[3,2-*c*]quinoline (93)



2 mol% $\text{Pd}(\text{OAc})_2$ used. White solid; yield: 86 mg (79%); m.p. = 198–199 °C; IR (NaCl): ν 3047 (C-H stretch), 1562 (aromatic C-C stretch), 1508 (aromatic C-C stretch), 1338 (C-N stretch), 1049 (C-O stretch), 755 (C-Cl stretch) cm^{-1} ; ^1H -NMR (300 MHz, CDCl_3) δ : 7.47 (dd, $J = 8.3, 1.8$ Hz, 1H, CH-14), 7.66–7.87 (m, 3H, CH-7, CH-8, CH-12), 8.00 (d, $J = 8.3$ Hz, 1H, CH-15), 8.27 (d, $J = 8.4$ Hz, 1H, CH-9), 8.40 (d, J

= 8.0 Hz, 1H, *CH-6*), 9.46 (s, 1H, *CH-2*); ^{13}C -NMR (75 MHz, CDCl_3) δ : 112.8 (*CH-12*), 115.7 (q*C-3*), 117.0 (q*C-5*), 120.7 (*CH-6*), 121.1 (*CH-15*), 121.4 (q*C-16*), 124.8 (*CH-14*), 127.2 (*CH-7*), 129.6 (*CH-8*), 129.9 (*CH-9*), 132.9 (q*C-13*), 144.1 (*CH-2*), 147.5 (q*C-10*), 156.0 (q*C-11*), 157.8 (q*C-4*); HRMS (ESI-TOF) m/z : $[\text{M}+\text{H}]^+$ calcd. for $\text{C}_{15}\text{H}_9\text{ClNO}$: 254.0373; found: 254.0363.

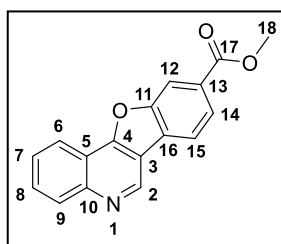
8-Nitrobenzofuro[3,2-*c*]quinoline (94)



2 mol% $\text{Pd}(\text{OAc})_2$ used. Orange solid; yield: 28 mg (46%); m.p. $>250\text{ }^\circ\text{C}$; IR (NaCl): ν 3030 (C-H stretch), 1528 (aromatic C-C stretch), 1397 (C-N stretch), 1344 (N-O stretch), 1200 (C-O stretch) cm^{-1} ; ^1H -NMR (300 MHz, CDCl_3)

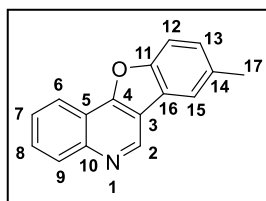
δ : 7.77 (ddd, $J = 8.1, 7.2, 1.0$ Hz, 1H, *CH-7*), 7.84–7.91 (m, 2H, *CH-8*, *CH-12*), 8.32 (d, $J = 8.5$ Hz, 1H, *CH-9*), 8.41–8.52 (m, 2H, *CH-6*, *CH-13*), 9.02 (d, $J = 2.3$ Hz, 1H, *CH-15*), 9.56 (s, 1H, *CH-2*); ^{13}C -NMR (100 MHz, CDCl_3) δ : 112.6 (*CH-12*), 115.4 (q*C-3*), 116.8 (q*C-5*), 117.1 (*CH-15*), 120.8 (*CH-6*), 123.0 (*CH-13*), 123.6 (q*C-16*), 127.8 (*CH-7*), 130.1 (*CH-9*), 130.5 (*CH-8*), 144.1 (*CH-2*), 144.9 (q*C-14*), 148.1 (q*C-10*), 158.6 (q*C-11*), 159.3 (q*C-4*); HRMS (ESI-TOF) m/z : $[\text{M}+\text{H}]^+$ calcd. for $\text{C}_{15}\text{H}_9\text{N}_2\text{O}_3$: 265.0613; found: 265.0611.

Methyl benzofuro[3,2-*c*]quinoline-9-carboxylate (95)



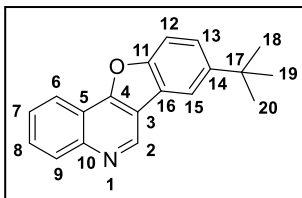
2 mol% $\text{Pd}(\text{OAc})_2$ used. Beige solid; yield: 43 mg (56%); m.p. = 192–193 $^\circ\text{C}$; IR (NaCl): ν 3402 (C-H stretch), 1717 (C=O stretch), 1565 (aromatic C-C stretch), 1434 (aromatic C-C stretch), 1397 (C-N stretch), 1281 (C-O stretch), 1234 (C-O stretch) cm^{-1} ; ^1H -NMR (300 MHz, CDCl_3) δ : 4.00 (s, 3H,

*CH*₃-18), 7.66–7.74 (m, 1H, *CH-7*), 7.81 (ddd, $J = 8.5, 7.0, 1.5$ Hz, 1H, *CH-8*), 8.09 (d, $J = 7.8$ Hz, 1H, *CH-15*), 8.16 (dd, $J = 8.2, 1.3$ Hz, 1H, *CH-14*), 8.26 (d, $J = 8.4$ Hz, 1H, *CH-9*), 8.36–8.43 (m, 2H, *CH-6*, *CH-12*), 9.46 (s, 1H, *CH-2*); ^{13}C -NMR (75 MHz, CDCl_3) δ : 52.5 (*CH*₃-18), 113.6 (*CH-12*), 115.5 (q*C-3*), 116.9 (q*C-5*), 120.2 (*CH-15*), 121.0 (*CH-6*), 125.5 (*CH-14*), 126.8 (q*C-16*), 127.3 (*CH-7*), 129.0 (q*C-13*), 129.9 (*CH-9*), 130.0 (*CH-8*), 144.5 (*CH-2*), 147.8 (q*C-10*), 155.4 (q*C-11*), 159.0 (q*C-4*), 166.6 (q*C-17*); HRMS (ESI-TOF) m/z : $[\text{M}+\text{H}]^+$ calcd. for $\text{C}_{17}\text{H}_{12}\text{NO}_3$: 278.0817; found: 278.0811.

8-Methylbenzofuro[3,2-*c*]quinoline (96)^[37]

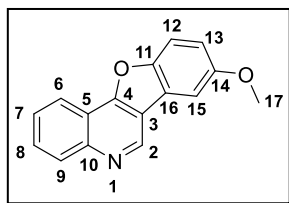
2 mol% Pd(OAc)₂ used. White solid; yield: 62 mg (71%); m.p. = 145–148 °C (lit. 149–150 °C); IR (NaCl): ν 2917 (C-H stretch), 1564 (C aromatic C-C stretch), 1510 (C aromatic C-C stretch), 1321 (C-N stretch), 1192 (C-O stretch) cm⁻¹; ¹H-NMR (300 MHz, CDCl₃) δ : 2.57 (s, 3H, CH₃-17), 7.32–7.39 (ddd, J = 8.5, 1.8, 0.5 Hz, 1H, CH-13), 7.61–7.73 (m, 2H, CH-7, CH-12), 7.78 (ddd, J = 8.5, 6.9, 1.6 Hz, 1H, CH-8), 7.89–7.92 (m, 1H, CH-15), 8.26 (d, J = 8.5 Hz, 1H, CH-9), 8.41 (dd, J = 8.1, 0.9 Hz, 1H, CH-6), 9.47 (s, 1H, CH-2); ¹³C-NMR (75 MHz, CDCl₃) δ : 21.4 (CH₃-17), 111.5 (CH-12), 116.2 (qC-3), 117.2 (qC-5), 120.5 (CH-15), 120.8 (CH-6), 122.6 (qC-16), 126.8 (CH-7), 128.3 (CH-13), 129.1 (CH-8), 129.8 (CH-9), 133.7 (qC-14), 144.3 (CH-2), 147.3 (qC-10), 154.3 (qC-11), 157.6 (qC-4); HRMS (ESI-TOF) m/z : [M+H]⁺ calcd. for C₁₆H₁₂NO: 234.0919; found: 234.0921.

Spectral data were consistent with those reported in the literature.

8-(*tert*-Butyl)benzofuro[3,2-*c*]quinoline (97)^[37]

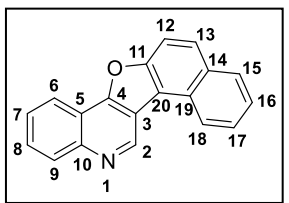
2 mol% Pd(OAc)₂ used. Pale yellow solid; yield: 25 mg (50%); m.p. = 97–100 °C (lit. 99–100 °C); IR (NaCl): ν 2962 (C-H stretch), 1567 (aromatic C-C stretch), 1488 (aromatic C-C stretch), 1392 (C-N stretch), 1201 (C-O stretch) cm⁻¹; ¹H-NMR (600 MHz, CDCl₃) δ : 1.47 (s, 9H, CH₃-18, CH₃-19, CH₃-20), 7.61 (dd, J = 8.7, 2.0 Hz, 1H, CH-13), 7.67–7.72 (m, 2H, CH-7, CH-12), 7.79 (ddd, J = 8.4, 6.9, 1.5 Hz, 1H, CH-8), 8.10 (d, J = 1.7 Hz, 1H, CH-15), 8.27 (d, J = 8.4 Hz, 1H, CH-9), 8.42 (dd, J = 8.2, 1.0 Hz, 1H, CH-6), 9.52 (s, 1H, CH-2); ¹³C-NMR (150 MHz, CDCl₃) δ : 31.9 (CH₃-18, CH₃-19, CH₃-20), 35.0 (qC-17), 111.4 (CH-12), 116.7 (qC-3), 116.9 (CH-15), 117.3 (qC-5), 120.8 (CH-6), 122.3 (qC-16), 125.1 (CH-13), 126.9 (CH-7), 129.2 (CH-8), 129.8 (CH-9), 144.4 (CH-2), 147.3 (qC-10), 147.4 (qC-14), 154.2 (qC-11), 157.8 (qC-4); HRMS (ESI-TOF) m/z : [M+H]⁺ calcd. for C₁₉H₁₈NO: 276.1388; found: 276.1377.

Spectral data were consistent with those reported in the literature.

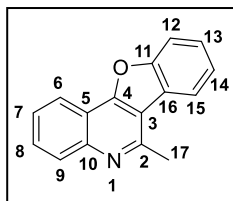
8-Methoxybenzofuro[3,2-*c*]quinoline (98)^[38]

2 mol% Pd(OAc)₂ used. Off-white solid; yield: 32 mg (42%); m.p. = 165–167 °C (lit. 160–162 °C); IR (NaCl): ν 3350 (C-H stretch), 1570 (aromatic C-C stretch), 1486 (aromatic C-C stretch), 1330 (C-N stretch), 1186 (C-O stretch), 1164 (C-O stretch) cm⁻¹; ¹H-NMR (300 MHz, CDCl₃) δ : 3.96 (s, 3H, CH₃-17), 7.13 (dd, J = 9.0, 2.6 Hz, 1H, CH-13), 7.54 (d, J = 2.6 Hz, 1H, CH-15), 7.59–7.85 (m, 3H, CH-7, CH-8, CH-12), 8.26 (d, J = 8.4 Hz, 1H, CH-9), 8.40 (dd, J = 8.1, 1.0 Hz, 1H, CH-6), 9.46 (s, 1H, CH-2); ¹³C-NMR (75 MHz, CDCl₃) δ : 56.1 (CH₃-17), 103.3 (CH-15), 112.6 (CH-12), 115.5 (CH-13), 116.6 (qC-3), 117.3 (qC-5), 120.8 (CH-6), 123.3 (qC-16), 127.0 (CH-7), 129.3 (CH-8), 129.8 (CH-9), 144.4 (CH-2), 147.3 (qC-10), 150.7 (qC-11), 156.9 (qC-14), 158.1 (qC-4); HRMS (ESI-TOF) m/z : [M+H]⁺ calcd. for C₁₆H₁₂NO₂: 250.0868; found: 250.0858.

Spectral data were consistent with those reported in the literature.

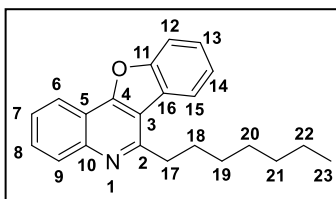
Naphtho[1',2':4,5]furo[3,2-*c*]quinoline (99)

2 mol% Pd(OAc)₂ used. Off-white solid; yield: 14 mg (17%); m.p. = 203–205 °C; IR (NaCl): ν 2919 (C-H stretch), 1562 (aromatic C-C stretch), 1507 (aromatic C-C stretch), 1310 (C-N stretch), 1223 (C-O stretch) cm⁻¹; ¹H-NMR (600 MHz, CDCl₃) δ : 7.64 (ddd, J = 8.0, 6.9, 1.1 Hz, 1H, CH-16), 7.75 (ddd, J = 8.0, 6.9, 1.1 Hz, 1H, CH-7), 7.79–7.85 (m, 2H, CH-8, CH-17), 7.94 (d, J = 8.9 Hz, 1H, CH-12), 8.02 (d, J = 8.9 Hz, 1H, CH-13), 8.09 (d, J = 8.2 Hz, 1H, CH-15), 8.33 (d, J = 8.4 Hz, 1H, CH-9), 8.51 (dd, J = 8.4, 1.1 Hz, 1H, CH-6), 8.69 (d, J = 8.2 Hz, 1H, CH-18), 9.97 (s, 1H, CH-2); ¹³C-NMR (150 MHz, CDCl₃) δ : 112.7 (CH-12), 117.0 (qC-20), 117.3 (qC-5), 117.7 (qC-3), 120.7 (CH-6), 124.2 (CH-18), 125.3 (CH-16), 127.2 (CH-7), 127.7 (CH-17), 128.5 (qC-19), 128.8 (CH-13), 129.2 (CH-8), 129.4 (CH-15), 129.8 (CH-9), 131.0 (qC-14), 145.1 (CH-2), 146.4 (qC-10), 154.1 (qC-11), 157.0 (qC-4); HRMS (ESI-TOF) m/z : [M+H]⁺ calcd. for C₁₉H₁₂NO: 270.0919; found: 270.0916.

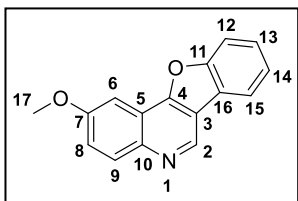
6-Methylbenzofuro[3,2-*c*]quinoline (100)^[37]

2 mol% Pd(OAc)₂ used. Pale yellow solid; yield: 29 mg (78%); m.p. = 132–134 °C (lit. 132–133 °C); IR (NaCl): ν 3380 (C-H stretch), 1563 (aromatic C-C stretch), 1509 (aromatic C-C stretch), 1364 (C-N stretch), 1084 (C-O stretch) cm⁻¹; ¹H-NMR (300 MHz, CDCl₃) δ : 3.16 (s, 3H, CH₃-17), 7.41–7.69 (m, 3H, CH-7, CH-13, CH-14), 7.72–7.79 (m, 2H, CH-8, CH-12), 8.10 (dd, J = 7.6, 2.1 Hz, 1H, CH-15), 8.18 (d, J = 8.4 Hz, 1H, CH-9), 8.38 (dd, J = 8.1, 2.1 Hz, 1H, CH-6); ¹³C-NMR (75 MHz, CDCl₃) δ : 24.3 (CH₃-17), 112.1 (CH-12), 115.5 (qC-3), 116.2 (qC-5), 120.7 (CH-6), 121.8 (CH-15), 123.5 (qC-16), 124.0 (CH-14), 126.1 (CH-7), 126.7 (CH-13), 128.9 (CH-9), 129.4 (CH-8), 146.9 (qC-10), 154.8 (qC-2), 155.9 (qC-11), 157.5 (qC-4); HRMS (ESI-TOF) m/z : [M+H]⁺ calcd. for C₁₆H₁₂NO: 234.0919; found: 234.0915.

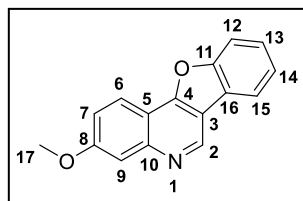
Spectral data were consistent with those reported in the literature.

6-Heptylbenzofuro[3,2-*c*]quinoline (101)

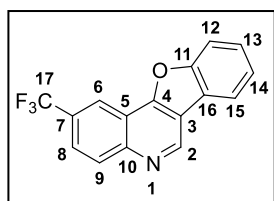
2 mol% Pd(OAc)₂ used. White solid; yield: 56 mg (70%); m.p. = 90–92 °C; IR (NaCl): ν 2917 (C-H stretch), 1559 (aromatic C-C stretch), 1445 (aromatic C-C stretch), 1363 (C-N stretch), 1202 (C-O stretch) cm⁻¹; ¹H-NMR (300 MHz, CDCl₃) δ : 0.88 (t, J = 6.7 Hz, 3H, CH₃-23), 1.22–1.64 (m, 8H, CH₂-19, CH₂-20, CH₂-21, CH₂-22), 1.95 (dt, J = 15.7, 7.7 Hz, 2H, CH₂-18), 3.40 (t, J = 8.0 Hz, 2H, CH₂-17), 7.40–7.67 (m, 3H, CH-7, CH-13, CH-14), 7.69–7.79 (m, 2H, CH-8, CH-12), 8.00 (d, J = 7.3 Hz, 1H, CH-15), 8.19 (d, J = 8.4 Hz, 1H, CH-9), 8.35 (d, J = 8.1 Hz, 1H, CH-6); ¹³C-NMR (75 MHz, CDCl₃) δ : 14.1 (CH₃-23), 22.7 (CH₂-22), 28.6 (CH₂-18), 29.2 (CH₂-20), 29.9 (CH₂-19), 31.8 (CH₂-21), 38.0 (CH₂-17), 112.1 (CH-12), 114.8 (qC-3), 116.2 (qC-5), 120.7 (CH-6), 121.8 (CH-15), 123.1 (qC-16), 124.0 (CH-14), 126.0 (CH-7), 126.6 (CH-13), 129.1 (CH-9), 129.3 (CH-8), 146.9 (qC-10), 155.9 (qC-11), 157.7 (qC-4), 159.0 (qC-2); HRMS (ESI-TOF) m/z : [M+H]⁺ calcd. for C₂₂H₂₄NO: 318.1858; found: 318.1845.

2-Methoxybenzofuro[3,2-*c*]quinoline (102)^[37]

5 mol% Pd(OAc)₂ used. Off-white solid; yield: 95 mg (84%); m.p. = 150–152 °C (lit. 150–153 °C); IR (NaCl): ν 2954 (C-H stretch), 1350 (C-H bend), 1514 (aromatic C-C stretch), 1468 (aromatic C-C stretch), 1228 (C-N stretch), 1191 (C-O stretch), 1031 (C-O stretch) cm⁻¹; ¹H-NMR (300 MHz, CDCl₃) δ : 3.96 (s, 3H, CH₃-17), 7.28–7.53 (m, 4H, CH-6, CH-8, CH-13, CH-14), 7.64 (d, *J* = 8.1 Hz, 1H, CH-12), 7.97 (dd, *J* = 7.4, 0.8 Hz, 1H, CH-15), 8.08 (d, *J* = 9.2 Hz, 1H, CH-9), 9.23 (s, 1H, CH-2); ¹³C-NMR (75 MHz, CDCl₃) δ : 55.6 (CH₃-17), 98.5 (CH-6), 111.9 (CH-12), 116.4 (qC-3), 117.7 (qC-5), 120.6 (CH-15), 121.7 (CH-8), 122.8 (qC-16), 123.9 (CH-14), 127.1 (CH-13), 131.3 (CH-9), 141.5 (CH-2), 143.3 (qC-10), 155.8 (qC-11), 156.7 (qC-4), 158.2 (qC-7); HRMS (ESI-TOF) *m/z*: [M+H]⁺ calcd. for C₁₆H₁₂NO₂: 250.0868; found: 250.0858.

3-Methoxybenzofuro[3,2-*c*]quinoline (103)

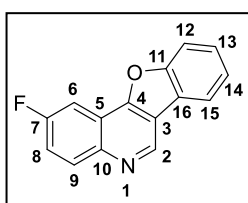
5 mol% Pd(OAc)₂ used. Off-white solid; yield: 91 mg (81%); m.p. = 146–147 °C; IR (NaCl): ν 3022 (C-H stretch), 1345 (C-H bend), 1639 (aromatic C-C stretch), 1452 (aromatic C-C stretch), 1324 (C-N stretch), 1242 (C-O stretch), 1168 (C-O stretch) cm⁻¹; ¹H-NMR (300 MHz, CDCl₃) δ : 3.97 (s, 3H, CH₃-17), 7.31 (dd, *J* = 9.0, 2.3 Hz, 1H, CH-7), 7.36–7.54 (m, 2H, CH-13, CH-14), 7.58 (d, *J* = 2.3 Hz, 1H, CH-9), 7.68 (d, *J* = 8.0 Hz, 1H, CH-12), 7.99 (d, *J* = 7.1 Hz, 1H, CH-15), 8.25 (d, *J* = 9.0 Hz, 1H, CH-6), 9.37 (s, 1H, CH-2); ¹³C-NMR (75 MHz, CDCl₃) δ : 55.5 (CH₃-17), 108.4 (CH-9), 111.7 (qC-5), 112.0 (CH-12), 115.0 (qC-3), 119.7 (CH-7), 120.3 (CH-15), 121.9 (CH-6), 122.8 (qC-16), 123.9 (CH-14), 126.7 (CH-13), 144.6 (CH-2), 149.3 (qC-10), 155.8 (qC-11), 157.8 (qC-4), 160.7 (qC-8); HRMS (ESI-TOF) *m/z*: [M+H]⁺ calcd. for C₁₆H₁₂NO₂: 250.0868; found: 250.0865.

2-(Trifluoromethyl)benzofuro[3,2-*c*]quinoline (104)

2 mol% Pd(OAc)₂ used. Yellow solid; yield: 49 mg (63%); m.p. = 141–143 °C; IR (NaCl): ν 2917 (C-H stretch), 1567 (aromatic C-C stretch), 1443 (aromatic C-C stretch), 1348 (C-N stretch), 1167 (C-O stretch), 1111 (C-F stretch) cm⁻¹;

^1H -NMR (300 MHz, CDCl_3) δ : 7.43–7.67 (m, 2H, *CH*-13, *CH*-14), 7.80 (d, J = 8.2 Hz, 1H, *CH*-12), 7.96 (dd, J = 9.0, 2.0 Hz, 1H, *CH*-8), 8.13 (d, J = 8.4 Hz, 1H, *CH*-15), 8.38 (d, J = 8.9 Hz, 1H, *CH*-9), 8.75 (s, 1H, *CH*-6), 9.60 (s, 1H, *CH*-2); ^{13}C -NMR (100 MHz, CDCl_3) δ : 112.3 (*CH*-12), 116.3 (qC-5), 117.3 (qC-3), 119.1 (q, $^3J_{\text{C,F}}$ = 5 Hz, *CH*-6), 120.8 (*CH*-15), 122.1 (qC-16), 124.3 (q, $^1J_{\text{C,F}}$ = 270 Hz, qC-17), 124.5 (*CH*-14), 124.9 (q, $^3J_{\text{C,F}}$ = 3 Hz, *CH*-8), 127.9 (*CH*-13), 128.8 (q, $^2J_{\text{C,F}}$ = 33 Hz, qC-7), 131.0 (*CH*-9), 146.4 (*CH*-2), 148.0 (qC-10), 156.1 (qC-11), 157.5 (qC-4); ^{19}F -NMR (282 MHz, CDCl_3) δ : -62 (CF_3 -17); HRMS (ESI-TOF) m/z : $[\text{M}+\text{H}]^+$ calcd. for $\text{C}_{16}\text{H}_9\text{F}_3\text{NO}$: 288.0636; found: 288.0634.

2-Fluorobenzofuro[3,2-*c*]quinoline (105)^[76]



2 mol% $\text{Pd}(\text{OAc})_2$ used. White solid; yield: 25 mg (67%); m.p. = 146–148 °C (lit. 148–149 °C); IR (NaCl): ν 3399 (C-H stretch), 1515 (aromatic C-C stretch), 1462 (aromatic C-C stretch), 1364 (C-N stretch), 1195 (C-O stretch), 1175 (C-F stretch) cm^{-1} ;

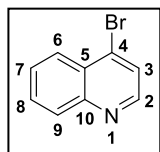
^1H -NMR (300 MHz, CDCl_3) δ : 7.45–7.61 (m, 3H, *CH*-8, *CH*-13, *CH*-14), 7.76 (d, J = 8.1 Hz, 1H, *CH*-12), 8.00 (dd, $^3J_{\text{H,H}} = 8.6$, $^4J_{\text{H,H}} = 2.8$ Hz, 1H, *CH*-6), 8.10 (dd, J = 7.6, 0.8 Hz, 1H, *CH*-15), 8.26 (dd, $^3J_{\text{H,H}} = 9.3$, $^4J_{\text{H,F}} = 5.2$ Hz, 1H, *CH*-9), 9.45 (s, 1H, *CH*-2); ^{13}C -NMR (75 MHz, CDCl_3) δ : 104.7 (d, $^2J_{\text{C,F}}$ = 24 Hz, *CH*-6), 112.2 (*CH*-12), 116.8 (qC-3), 117.8 (d, $^3J_{\text{C,F}}$ = 11 Hz, qC-5), 119.3 (d, $^2J_{\text{C,F}}$ = 26 Hz, *CH*-8), 120.8 (*CH*-15), 122.5 (qC-16), 124.2 (*CH*-14), 127.6 (*CH*-13), 132.5 (d, $^3J_{\text{C,F}}$ = 9 Hz, *CH*-9), 143.6 (d, $^6J_{\text{C,F}}$ = 3 Hz, *CH*-2), 144.4 (qC-10), 156.1 (qC-11), 157.1 (d, $^4J_{\text{C,F}}$ = 5 Hz, qC-4), 160.8 (d, $^1J_{\text{C,F}}$ = 249 Hz, qC-7); ^{19}F -NMR (282 MHz, CDCl_3) δ : -111 (CF -7); HRMS (ESI-TOF) m/z : $[\text{M}+\text{H}]^+$ calcd. for $\text{C}_{15}\text{H}_9\text{FNO}$: 238.0668; found: 238.0659.

Spectral data were consistent with those reported in the literature.

3.18. Synthesis of Compound 106

4-Bromoquinoline^[80] (106)

A mixture of 4-quinolinol (1 equiv.) and PBr_3 (1.05 equiv.) in dry DMF (1.7 mL/mmol) was stirred at room temperature for 45 min under N_2 , until full consumption of the starting material was observed by TLC analysis of the reaction mixture (eluent DCM/MeOH 9:1). The cooled reaction mixture was slowly poured onto ice water (~8 mL/mmol) with stirring. Solid NaHCO_3 was added portion-wise until the mixture reached pH 9–10. This aqueous mixture was transferred to a separating funnel and extracted with EtOAc (3×5 mL/mmol). The combined organic layers were washed with water (5 mL/mmol), brine (5 mL/mmol), dried over MgSO_4 , filtered and concentrated *in vacuo* to yield the crude product as an orange oil. Purification by column chromatography (DCM/MeOH 95:5) afforded the pure product 106 as a yellow solid (0.597 g, 83% yield).



Yellow solid; yield: 597 mg (83%); m.p. = 28–30 °C (lit. 29–30 °C); IR (NaCl): ν 2549 (C-H stretch), 1492 (aromatic C-C stretch), 1377 (C-N stretch), 651 (C-Cl stretch) cm^{-1} ; $^1\text{H-NMR}$ (300 MHz, CDCl_3) δ : 7.62–7.82 (m, 3H, CH-3, CH-7, CH-8), 8.11 (d, J = 8.4 Hz, 1H, CH-9), 8.20 (dd, J = 8.4, 0.9 Hz, 1H, CH-6), 8.68 (d, J = 4.7 Hz, 1H, CH-2); $^{13}\text{C-NMR}$ (75 MHz, CDCl_3) δ : 125.1 (CH-3), 126.8 (CH-6), 127.88 (CH-7), 127.93 (qC-5), 129.9 (CH-9), 130.4 (CH-8), 134.2 (qC-4), 149.0 (qC-10), 149.9 (CH-2); HRMS (ESI-TOF) m/z : $[\text{M}+\text{H}]^+$ calcd. for $\text{C}_9\text{H}_7\text{BrN}$: 207.9762; found: 207.9760.

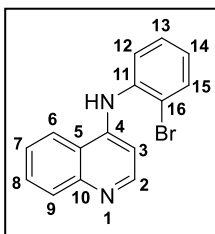
Spectral data were consistent with those reported in the literature.

3.19. Synthesis of Compound 107

N-(2-bromophenyl)quinolin-4-amine (107)

To a degassed solution of $\text{Pd}_2(\text{dba})_3$ (2 mol%) and XantPhos (4 mol%) in anhydrous 1,4-dioxane (4 mL/mmol) were added Cs_2CO_3 (1.4 equiv.), 4-bromoquinoline (1 equiv.) and 2-bromoaniline (1.1 equiv.) under a nitrogen atmosphere. The reaction mixture was stirred at 120 °C under N_2 for 24 h. The cooled reaction mixture was diluted with DCM, filtered through Celite and concentrated *in vacuo*. The crude

mixture was purified by column chromatography over silica gel using DCM/EtOAc (3:1) as eluent to yield the product **107** as a yellow solid (0.322 g, 74%).

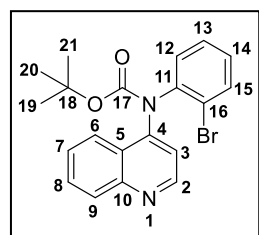


Yellow/orange solid; yield: 322 mg (74%); m.p. = 238–241 °C; IR (NaCl): ν 3360 (N-H stretch), 3061 (C-H stretch), 1572 (aromatic C-C stretch), 1526 (aromatic C-C stretch), 1335 (C-N stretch), 747 (C-Br stretch) cm^{-1} ; $^1\text{H-NMR}$ (300 MHz, CDCl_3) δ : 6.88 (br s, 1H, NH), 7.02 (td, $J = 8.0, 1.5$ Hz, 1H, CH-14), 7.08 (d, $J = 5.2$ Hz, 1H, CH-3), 7.31–7.38 (m, 1H, CH-13), 7.51–7.61 (m, 2H, CH-7, CH-12), 7.65–7.78 (m, 2H, CH-8, CH-15), 8.01 (d, $J = 8.3$ Hz, 1H, CH-6), 8.09 (d, $J = 8.0$ Hz, 1H, CH-9), 8.66 (d, $J = 5.2$ Hz, 1H, CH-2); $^{13}\text{C-NMR}$ (75 MHz, CDCl_3) δ : 103.4 (CH-3), 116.9 (qC-16), 120.0 (CH-6), 120.3 (qC-5), 122.2 (CH-12), 125.0 (CH-14), 125.8 (CH-7), 128.4 (CH-13), 129.6 (CH-8), 130.1 (CH-9), 133.5 (CH-15), 138.3 (qC-11), 146.2 (qC-4), 149.2 (qC-10), 150.8 (CH-2); HRMS (ESI-TOF) m/z : $[\text{M}+\text{H}]^+$ calcd. for $\text{C}_{15}\text{H}_{12}\text{BrN}_2$: 299.0184; found: 299.0187.

3.20. Synthesis of Compound 110

tert-Butyl (2-bromophenyl)(quinolin-4-yl)carbamate (**110**)

N-(2-Bromophenyl)quinolin-4-amine **107** (1 equiv.) and DMAP (0.2 equiv.) were added to a solution of $(\text{Boc})_2\text{O}$ (1.2 equiv.) in dry THF (1 mL/mmol) and the mixture was stirred at 70 °C for 24 h. After cooling to room temperature, the reaction mixture was concentrated *in vacuo*. Purification by column chromatography (hexane/EtOAc 8:2) afforded the product **110** as a yellow solid (0.09 g, 45 %).



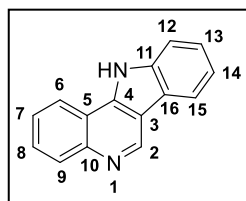
Yellow solid; yield: 90 mg (45%); m.p. = 165–167 °C; IR (NaCl): ν 3583 (C-H stretch), 2924 (C-H stretch), 1745 (ester C=O stretch), 1641 (aromatic C-C stretch), 1578 (aromatic C-C stretch), 1349 (C-N stretch), 12899 (C-O stretch), 734 (C-Br stretch) cm^{-1} ; $^1\text{H-NMR}$ (300 MHz, CDCl_3) δ : 1.62 (s, 9H, CH₃-19, CH₃-20, CH₃-21), 5.80 (d, $J = 8.6$ Hz, 1H, CH-3), 6.83–6.97 (m, 2H, CH-12, CH-14), 7.21–7.31 (m, 1H, CH-13), 7.39 (ddd, $J = 8.1, 7.2, 1.1$ Hz, 1H, CH-7), 7.50–7.64 (m, 2H, CH-8, CH-15), 7.78 (d, $J = 8.7$ Hz, 1H, CH-2), 8.51 (dd, $J = 8.8, 0.6$ Hz, 1H, CH-9), 8.61 (dd, $J = 8.0, 1.7$ Hz, 1H, CH-6); $^{13}\text{C-NMR}$ (75 MHz, CDCl_3) δ : 28.0 (CH₃-19, CH₃-20, CH₃-21), 85.3 (qC-18), 103.8 (CH-3), 115.9 (qC-16), 120.1 (CH-9),

121.9 (CH-12), 124.0 (CH-14), 125.2 (qC-5), 125.4 (CH-7), 125.9 (CH-6), 128.1 (CH-13), 131.0 (CH-8), 133.1 (CH-15), 134.1 (CH-2), 137.1 (qC-10), 150.26 (qC-11), 150.30 (qC-17), 154.3 (qC-4); HRMS (ESI-TOF) m/z : [M+H]⁺ calcd. for C₁₆H₁₁BrN₂O₂: 343.0077; found: 343.0074.

3.21. Synthesis of Compound 108

11*H*-Indolo[3,2-*c*]quinoline^[88] (**108**)

N-(2-bromophenyl)quinolin-4-amine **107** (1 equiv.), Pd(OAc)₂ (5 mol%), PCy₃·HBF₄ (10 mol%) and Cs₂CO₃ (2 equiv.) were added to degassed NMP (1.5 mL/mmol) in an inert Schlenk tube under a nitrogen atmosphere. The reaction mixture was stirred at 150 °C (sand bath) for 3 h. The cooled reaction mixture was diluted with DCM and filtered through Celite. The mixture was washed with water (3 × 60 mL/mmol) and brine (90 mL/mmol), dried over MgSO₄, filtered and concentrated *in vacuo*. The crude mixture was purified by column chromatography over silica gel using DCM/EtOAc (7:3) as eluent to yield the product **108** as an off-white solid (0.030 g, 83%).



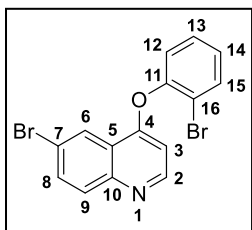
Off-white solid; yield: 30 mg (83%); m.p. >250 °C (lit. 340–341 °C); IR (NaCl): ν 3355 (N-H stretch), 2916 (C-H stretch), 2849 (C-H stretch), 1567 (aromatic C-C stretch), 1512 (aromatic C-C stretch), 1459 (C-N stretch), 1236 (C-N stretch) cm⁻¹; ¹H-NMR (300 MHz, DMSO-d₆) δ : 7.35 (t, J = 7.5 Hz, 1H, CH-14), 7.51 (t, J = 7.6 Hz, 1H, CH-13), 7.63–7.81 (m, 3H, CH-7, CH-8, CH-12), 8.15 (dd, J = 8.2, 1.3 Hz, 1H, CH-9), 8.33 (d, J = 7.8 Hz, 1H, CH-15), 8.53 dd, J = 8.0, 1.4 Hz, 1H, CH-6), 9.60 (s, 1H, CH-2), 12.72 (br s, 1H, N-H); ¹³C-NMR (75 MHz, DMSO-d₆) δ : 112.3 (CH-12), 114.8 (qC-3), 117.6 (qC-5), 120.6 (CH-15), 121.1 (CH-14), 122.4 (qC-16), 122.6 (CH-6), 126.0 (CH-13), 126.1 (CH-7), 128.5 (CH-8), 130.0 (CH-9), 139.3 (qC-11), 140.2 (qC-4), 145.3 (CH-2), 145.9 (qC-10); HRMS (ESI-TOF) m/z : [M+H]⁺ calcd. for C₁₅H₁₁N₂: 219.0922; found: 219.0911.

Spectral data were consistent with those reported in the literature.

3.22. General Procedure for Synthesis of 4-Phenoxy Quinoline Substrates

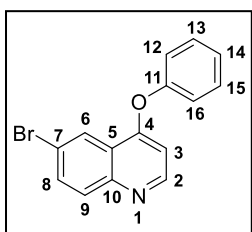
A mixture of the 6-bromo or 7-bromo-4-chloroquinoline substrate (1 equiv.), the 2-bromophenol (5 equiv.) and NaOH (crushed pellets) (1.5 equiv.) was stirred at 120 °C until reaction was completed (2–6 h) as evident by TLC (hexane/EtOAc 8:2). The cooled reaction mixture was diluted with 10% aq. NaOH (0.5 mL) and stirred at room temperature for 1 h. The aqueous phase was extracted with DCM (3 × 1.5 mL/mmol). The combined organic layers were washed with 6M NaOH (3 × 1 mL/mmol), water (1 mL/mmol) and brine (1 mL/mmol), dried over MgSO₄, filtered and concentrated *in vacuo*. The crude mixture was purified by column chromatography over silica gel using hexane/EtOAc (8:2) as eluent.

6-Bromo-4-(2-bromophenoxy)quinoline (115)



Pale yellow solid; yield: 1.53 g (83%); m.p. = 97–98 °C; IR (NaCl): ν 3399 (C-H stretch), 1590 (aromatic C-C stretch), 1491 (aromatic C-C stretch), 1350 (C-N stretch), 1221 (C-O stretch), 665 (C-Br stretch) cm⁻¹; ¹H-NMR (300 MHz, CDCl₃) δ : 6.41 (d, J = 5.2 Hz, 1H, CH-3), 7.19–7.28 (m, 2H, CH-12, CH-14), 7.39–7.47 (m, 1H, CH-13), 7.73 (dd, J = 8.3, 1.5 Hz, 1H, CH-15), 7.84 (dd, J = 9.0, 2.2 Hz, 1H CH-8), 7.98 (d, J = 9.0 Hz, 1H, CH-9), 8.58 (d, J = 2.2 Hz, 1H, CH-6), 8.67 (d, J = 5.2 Hz, 1H, CH-2); ¹³C-NMR (75 MHz, CDCl₃) δ : 104.2 (CH-3), 116.4 (qC-16), 120.3 (qC-7), 122.2 (qC-5), 123.3 (CH-12), 124.3 (CH-6), 127.6 (CH-14), 129.3 (CH-13), 130.9 (CH-9), 133.7 (CH-8), 134.4 (CH-15), 148.4 (qC-10), 150.8 (qC-11), 151.4 (CH-2), 159.8 (qC-4); HRMS (ESI-TOF) m/z : [M+H]⁺ calcd. for C₁₅H₁₀Br₂NO: 377.9129; found: 377.9132.

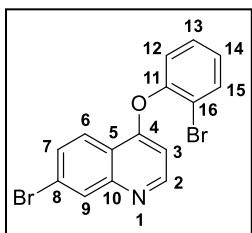
6-Bromo-4-phenoxyquinoline (118)



Pale yellow solid; yield: 517 mg (83%); m.p. = 84–86 °C; IR (NaCl): ν 3401 (C-H stretch), 1561 (aromatic C-C stretch), 1487 (aromatic C-C stretch), 1351 (C-N stretch), 1213 (C-O stretch), 667 (C-Br stretch) cm⁻¹; ¹H-NMR (300 MHz, CDCl₃) δ : 6.54 (d, J = 5.2 Hz, 1H, CH-3), 7.13–7.22 (m, 2H, CH-12, CH-16), 7.25–7.36 (m, 1H, CH-14), 7.41–7.53 (m, 2H, CH-13, CH-15), 7.80 (dd, J = 9.0, 2.2 Hz, 1H, CH-8), 7.95 (d, J = 9.0 Hz, 1H CH-9), 8.53 (d, J = 2.2 Hz, 1H CH-6), 8.65 (d, J =

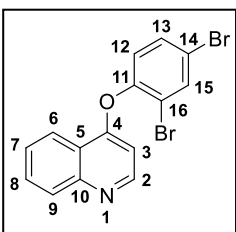
5.2 Hz, 1H, CH-2); ^{13}C -NMR (75 MHz, CDCl_3) δ : 104.7 (CH-3), 120.2 (qC-7), 121.1 (CH-12, CH-16), 122.6 (qC-5), 124.3 (CH-6), 125.9 (CH-14), 130.4 (CH-13, CH-15), 130.9 (CH-9), 133.6 (CH-8), 148.3 (qC-10), 151.5 (CH-2), 154.0 (qC-11), 161.0 (qC-4); HRMS (ESI-TOF) m/z : $[\text{M}+\text{H}]^+$ calcd. for $\text{C}_{15}\text{H}_{11}\text{BrNO}$: 300.0024; found: 300.0013.

7-Bromo-4-(2-bromophenoxy)quinoline (121)

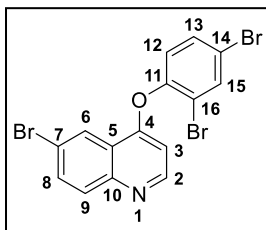


Pale yellow solid; yield: 409 mg (87%); m.p. = 73–74 °C; IR (NaCl): ν 3064 (C-H stretch), 1561 (aromatic C-C stretch), 1468 (aromatic C-C stretch), 1301 (C-N stretch), 1220 (C-O stretch), 657 (C-Br stretch) cm^{-1} ; ^1H -NMR (300 MHz, CDCl_3) δ : 6.41 (d, $J = 5.2$ Hz, 1H, CH-3), 7.19–7.30 (m, 2H, CH-12, CH-14), 7.39–7.48 (m, 1H, CH-13), 7.66–7.76 (m, 2H, CH-7, CH-15), 8.25–8.33 (m, 2H, CH-6, CH-9), 8.66 (d, $J = 5.2$ Hz, 1H, CH-2); ^{13}C -NMR (75 MHz, CDCl_3) δ : 103.9 (CH-3), 116.3 (qC-16), 119.7 (qC-5), 123.3 (CH-12), 123.5 (CH-6), 124.6 (qC-8), 127.6 (CH-14), 129.3 (CH-13), 129.8 (CH-7), 131.4 (CH-9), 134.4 (CH-15), 150.5 (qC-10), 150.8 (qC-11), 152.1 (CH-2), 160.8 (qC-4); HRMS (ESI-TOF) m/z : $[\text{M}+\text{H}]^+$ calcd. for $\text{C}_{15}\text{H}_{10}\text{Br}_2\text{NO}$: 377.9129; found: 377.9119.

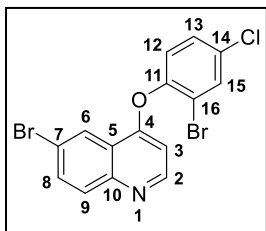
4-(2,4-Dibromophenoxy)quinoline (123)



Pale yellow solid; yield: 517 mg (85%); m.p. = 125–126 °C; IR (NaCl): ν 3394 (C-H stretch), 1596 (aromatic C-C stretch), 1464 (aromatic C-C stretch), 1305 (C-N stretch), 1224 (C-O stretch), 667 (C-Br stretch) cm^{-1} ; ^1H -NMR (300 MHz, CDCl_3) δ : 6.43 (d, $J = 5.1$ Hz, 1H, CH-3), 7.13 (d, $J = 8.6$ Hz, 1H, CH-12), 7.50–7.68 (m, 2H, CH-7, CH-13), 7.79 (ddd, $J = 8.5, 6.9, 1.4$ Hz, 1H, CH-8), 7.88 (d, $J = 2.3$ Hz, 1H, CH-15), 8.12 (d, $J = 8.4$ Hz, 1H, CH-9), 8.38 (dd, $J = 8.4, 0.9$ Hz, 1H, CH-6), 8.70 (d, $J = 5.1$ Hz, 1H, CH-2); ^{13}C -NMR (75 MHz, CDCl_3) δ : 103.8 (CH-3), 117.4 (qC-16), 119.3 (qC-14), 120.9 (qC-5), 121.8 (CH-6), 124.3 (CH-12), 126.5 (CH-7), 129.2 (CH-9), 130.4 (CH-8), 132.3 (CH-13), 136.6 (CH-15), 149.8 (qC-10), 150.5 (qC-11), 151.0 (CH-2), 160.3 (qC-4); HRMS (ESI-TOF) m/z : $[\text{M}+\text{H}]^+$ calcd. for $\text{C}_{15}\text{H}_{10}\text{Br}_2\text{NO}$: 377.9129; found: 377.9114.

6-Bromo-4-(2,4-dibromophenoxy)quinoline (125)

Pale yellow solid; yield: 268 mg (57%); m.p. = 162–163 °C; IR (NaCl): ν 3370 (C-H stretch), 1590 (aromatic C-C stretch), 1449 (aromatic C-C stretch), 1349 (C-N stretch), 1255 (C-O stretch), 665 (C-Br stretch) cm^{-1} ; $^1\text{H-NMR}$ (300 MHz, CDCl_3) δ : 6.42 (d, J = 5.1 Hz, 1H, CH-3), 7.12 (d, J = 8.6 Hz, 1H, CH-12), 7.56 (dd, J = 8.6, 2.3 Hz, 1H, CH-13), 7.80–7.91 (m, 2H, CH-8, CH-15), 7.98 (d, J = 9.0 Hz, 1H, CH-9), 8.54 (d, J = 2.2 Hz, 1H CH-6), 8.68 (d, J = 5.1 Hz, 1H, CH-2); $^{13}\text{C-NMR}$ (75 MHz, CDCl_3) δ : 104.2 (CH-3), 117.4 (qC-16), 119.7 (qC-14), 120.5 (qC-7), 122.0 (qC-5), 124.2 (CH-6), 124.4 (CH-12), 131.0 (CH-9), 132.4 (CH-13), 133.9 (CH-8), 136.7 (CH-15), 148.4 (qC-10), 150.1 (qC-11), 151.3 (CH-2), 159.4 (qC-4); HRMS (ESI-TOF) m/z : $[\text{M}+\text{H}]^+$ calcd. for $\text{C}_{15}\text{H}_9\text{Br}_3\text{NO}$: 455.8234; found: 455.8233.

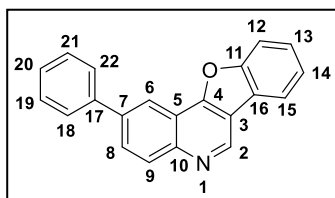
6-Bromo-4-(2-bromo-4-chlorophenoxy)quinoline (127)

Pale pink solid; yield: 531 mg (77%); m.p. = 157–159 °C; IR (NaCl): ν 3392 (C-H stretch), 1590 (aromatic C-C stretch), 1467 (aromatic C-C stretch), 1349 (C-N stretch), 1256 (C-O stretch), 729 (C-Cl stretch), 667 (C-Br stretch) cm^{-1} ; $^1\text{H-NMR}$ (300 MHz, CDCl_3) δ : 6.41 (d, J = 5.1 Hz, 1H, CH-3), 7.18 (d, J = 8.6 Hz, 1H, CH-12), 7.42 (dd, J = 8.6, 2.5 Hz, 1H, CH-13), 7.74 (d, J = 2.4 Hz, 1H, CH-15), 7.84 (dd, J = 9.0, 2.2 Hz, 1H, CH-8), 7.98 (d, J = 9.0 Hz, 1H, CH-9), 8.55 (d, J = 2.2 Hz, 1H CH-6), 8.68 (d, J = 5.1 Hz, 1H, CH-2); $^{13}\text{C-NMR}$ (75 MHz, CDCl_3) δ : 104.1 (CH-3), 117.0 (qC-16), 120.5 (qC-7), 122.0 (qC-5), 124.0 (CH-12), 124.2 (CH-6), 129.4 (CH-13), 131.0 (CH-9), 132.4 (qC-14), 133.9 (CH-8), 134.0 (CH-15), 148.4 (qC-10), 149.6 (qC-11), 151.3 (CH-2), 159.5 (qC-4); HRMS (ESI-TOF) m/z : $[\text{M}+\text{H}]^+$ calcd. for $\text{C}_{15}\text{H}_9\text{Br}_2\text{ClNO}$: 411.8739; found: 411.8730.

3.23. General Procedure for Pd-Catalysed One-Pot Tandem Suzuki-Miyaura/Direct Arylation Reactions

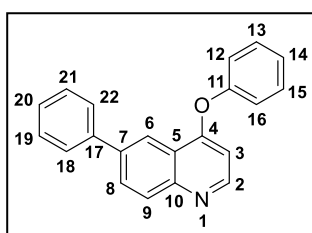
A mixture of the 4-(2-bromophenoxy)quinoline substrate (1 equiv.), PhB(OH)_2 (1.1 equiv.), Pd(OAc)_2 (2 mol%), and anhydrous K_2CO_3 (2 equiv.) in anhydrous NMP (1.5 mL/mmol) was stirred at 135 °C in a sealed reaction tube. The reaction progress was monitored by periodically sampling the reaction mixture for $^1\text{H-NMR}$ analysis in CDCl_3 . Once complete, the cooled reaction mixture was diluted with DCM, filtered through a short plug of Celite and concentrated *in vacuo*. The crude mixture was purified by column chromatography over silica gel using DCM/EtOAc (99:1–95:5) as eluent.

2-Phenylbenzofuro[3,2-*c*]quinoline (117)



Pale yellow solid; yield: 63 mg (83%); m.p. = 169–171 °C; IR (NaCl): ν 3450 (C-H stretch), 1559 (aromatic C-C stretch), 1460 (aromatic C-C stretch), 1359 (C-N stretch), 1193 (C-O stretch) cm^{-1} ; $^1\text{H-NMR}$ (300 MHz, CDCl_3) δ : 7.39–7.61 (m, 5H, CH-13, CH-14, CH-19, CH-20, CH-21), 7.74–7.87 (m, 3H, CH-12, CH-18, CH-22), 8.02–8.15 (m, 2H, CH-8, CH-15), 8.33 (d, J = 8.8 Hz, 1H, CH-9), 8.62 (d, J = 1.7 Hz, 1H, CH-6), 9.49 (s, 1H, CH-2); $^{13}\text{C-NMR}$ (75 MHz, CDCl_3) δ : 112.1 (CH-12), 116.6 (qC-3), 117.3 (qC-5), 118.4 (CH-6), 120.6 (CH-15), 122.7 (qC-16), 124.1 (CH-14), 127.3 (CH-13), 127.5 (CH-18, CH-22), 127.9 (CH-20), 128.8 (CH-8), 129.0 (CH-19, CH-21), 130.2 (CH-9), 139.7 (qC-7), 140.1 (qC-17), 144.2 (CH-2), 146.7 (qC-10), 156.0 (qC-11), 157.6 (qC-4); HRMS (ESI-TOF) m/z : $[\text{M}+\text{H}]^+$ calcd. for $\text{C}_{21}\text{H}_{14}\text{NO}$: 296.1075; found: 296.1062.

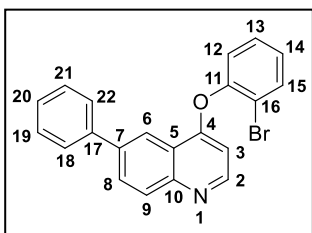
4-Phenoxy-6-phenylquinoline (119)



Pale yellow solid; yield: 168 mg (84%); m.p. = 78–80 °C; IR (NaCl): ν 3058 (C-H stretch), 1562 (aromatic C-C stretch), 1487 (aromatic C-C stretch), 1460 (aromatic C-C stretch), 1360 (C-N stretch), 1203 (C-O stretch) cm^{-1} ; $^1\text{H-NMR}$ (300 MHz, CDCl_3) δ : 6.58 (d, J = 5.1 Hz, 1H, CH-3), 7.16–7.57 (m, 8H, CH-19, CH-20, CH-21, CH-12, CH-13, CH-14, CH-15, CH-16), 7.72–7.74 (m, 2H, CH-18, CH-22), 8.03 (dd, J = 8.8, 2.1 Hz, 1H, CH-8), 8.17

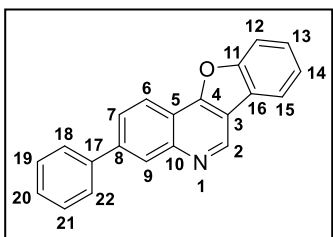
(d, $J = 8.8$ Hz, 1H, CH-9), 8.58 (d, $J = 2.0$ Hz, 1H, CH-6), 8.67 (d, $J = 4.9$ Hz, 1H, CH-2); ^{13}C -NMR (75 MHz, CDCl_3) δ : 104.6 (CH-3), 119.6 (CH-6), 121.2 (CH-12, CH-16), 121.7 (qC-5), 125.7 (CH-14), 127.5 (CH-18, CH-22), 127.7 (CH-20), 129.0 (CH-19, CH-21), 129.6 (CH-9), 129.8 (CH-8), 130.3 (CH-13, CH-15), 139.0 (qC-7), 140.5 (qC-17), 149.1 (qC-10), 151.1 (CH-2), 154.4 (qC-11), 162.1 (qC-4); HRMS (ESI-TOF) m/z : $[\text{M}+\text{H}]^+$ calcd. for $\text{C}_{21}\text{H}_{16}\text{NO}$: 298.1226; found: 298.1228.

4-(2-Bromophenoxy)-6-phenylquinoline (120)



Pale yellow solid; yield: 73 mg (49%); m.p. = 85–87 °C; IR (NaCl): ν 3059 (C-H stretch), 1564 (aromatic C-C stretch), 1460 (aromatic C-C stretch), 1361 (C-N stretch), 1222 (C-O stretch), 667 (C-Br stretch) cm^{-1} ; ^1H -NMR (300 MHz, CDCl_3) δ : 6.43 (d, $J = 5.2$ Hz, 1H, CH-3), 7.16–7.32 (m, 2H, CH-12, CH-14), 7.34–7.57 (m, 4H, CH-13, CH-19, CH-20, CH-21), 7.70–7.84 (m, 3H, CH-15, CH-18, CH-22), 8.05 (dd, $J = 8.8, 2.1$ Hz, 1H, CH-8), 8.20 (d, $J = 8.7$ Hz, 1H, CH-9), 8.62 (d, $J = 2.0$ Hz, 1H, CH-6), 8.69 (d, $J = 5.3$ Hz, 1H, CH-2); ^{13}C -NMR (75 MHz, CDCl_3) δ : 103.9 (CH-3), 116.4 (qC-16), 119.6 (CH-6), 121.3 (qC-5), 123.3 (CH-12), 127.6 (CH-14, CH-18, CH-22), 127.9 (CH-20), 129.0 (CH-9, CH-19, CH-21), 129.3 (CH-13), 130.2 (CH-8), 134.4 (CH-15), 139.4 (qC-7), 140.3 (qC-17), 148.2 (qC-10), 150.5 (CH-2), 151.0 (qC-11), 161.5 (qC-4); HRMS (ESI-TOF) m/z : $[\text{M}+\text{H}]^+$ calcd. for $\text{C}_{21}\text{H}_{15}\text{BrNO}$: 376.0332; found: 376.0331.

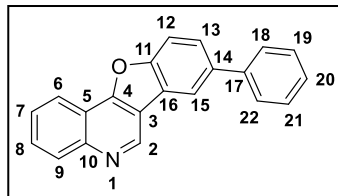
3-Phenylbenzofuro[3,2-c]quinoline (122)



Pale yellow solid; yield: 146 mg (95%); m.p. = 172–173 °C; IR (NaCl): ν 3275 (C-H stretch), 1559 (aromatic C-C stretch), 1452 (aromatic C-C stretch), 1379 (C-N stretch), 1188 (C-O stretch) cm^{-1} ; ^1H -NMR (300 MHz, CDCl_3) δ : 7.37–7.64 (m, 5H, CH-13, CH-14, CH-19, CH-20, CH-21), 7.72–7.88 (m, 3H, CH-12, CH-18, CH-22), 7.98 (dd, $J = 8.5, 1.7$ Hz, 1H, CH-7), 8.12 (dd, $J = 7.5, 1.0$ Hz, 1H, CH-15), 8.42–8.59 (m, 2H, CH-6, CH-9), 9.54 (s, 1H, CH-2); ^{13}C -NMR (75 MHz, CDCl_3) δ : 112.2 (CH-12), 116.1 (qC-5), 116.4 (qC-3), 120.6 (CH-15), 121.3 (CH-6), 122.8 (qC-16), 124.1 (CH-14), 126.6 (CH-7), 127.3 (CH-13), 127.5 (CH-18, CH-22), 127.6 (CH-9), 128.0 (CH-20), 129.1 (CH-19, CH-21), 140.2 (qC-17), 142.2 (qC-8), 144.9 (CH-2), 147.8 (qC-10), 156.1 (qC-11),

157.5 (qC-4); HRMS (ESI-TOF) m/z : $[M+H]^+$ calcd. for $C_{21}H_{14}NO$: 296.1070; found: 296.1072.

8-Phenylbenzofuro[3,2-*c*]quinoline (124)

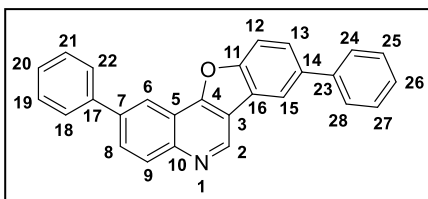


Yellow solid; yield: 103 mg (65%); m.p. = 153–155 °C;

IR (NaCl): ν 2922 (C-H stretch), 1567 (aromatic C-C stretch), 1460 (aromatic C-C stretch), 1325 (C-N stretch), 1202 (C-O stretch) cm^{-1} ; 1H -NMR (300 MHz, $CDCl_3$) δ :

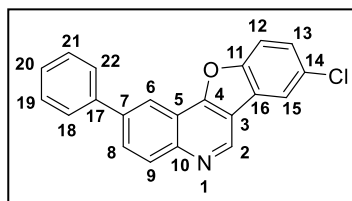
7.36–7.45 (m, 1H, CH-20), 7.46–7.56 (m, 2H, CH-19, CH-21), 7.67–7.86 (m, 6H, CH-7, CH-8, CH-12, CH-13, CH-18, CH-22), 8.24–8.35 (m, 2H, CH-9, CH-15), 8.45 (dd, J = 8.1, 1.6 Hz, 1H, CH-6), 9.55 (s, 1H, CH-2); ^{13}C -NMR (75 MHz, $CDCl_3$) δ : 112.2 (CH-12), 116.4 (qC-3), 117.2 (qC-5), 119.1 (CH-15), 120.8 (CH-6), 123.3 (qC-16), 126.7 (CH-13), 127.1 (CH-7), 127.4 (CH-20), 127.5 (CH-18, CH-22), 128.9 (CH-19, CH-21), 129.4 (CH-8), 129.9 (CH-9), 137.9 (qC-14), 140.9 (qC-17), 144.4 (CH-2), 147.5 (qC-10), 155.5 (qC-11), 158.0 (qC-4); HRMS (ESI-TOF) m/z : $[M+H]^+$ calcd. for $C_{21}H_{14}NO$: 296.1070; found: 296.1072.

2,8-Diphenylbenzofuro[3,2-*c*]quinoline (126)

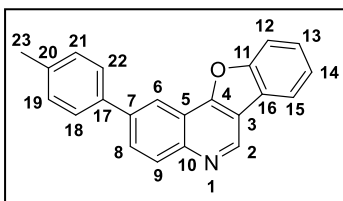


Pale yellow solid; yield: 129 mg (80%); m.p. = 206–207 °C; IR (NaCl): ν 3054 (C-H stretch), 2920 (C-H stretch), 1682 (aromatic C-C stretch), 1560 (aromatic C-C stretch), 1460 (aromatic C-C

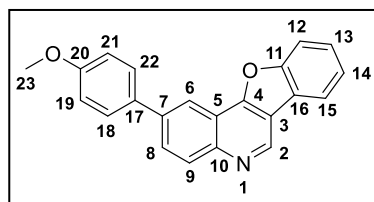
stretch), 1358 (C-N stretch), 1200 (C-O stretch) cm^{-1} ; 1H -NMR (300 MHz, $CDCl_3$) δ : 7.37–7.60 (m, 6H, CH-19, CH-20, CH-21, CH-25, CH-26, CH-27), 7.68–7.88 (m, 6H, CH-12, CH-13, CH-18, CH-22, CH-24, CH-28), 8.07 (dd, J = 8.8, 2.1 Hz, 1H, CH-8), 8.28–8.40 (m, 2H, CH-9, CH-15), 8.64 (d, J = 1.7 Hz, 1H, CH-6), 9.54 (s, 1H, CH-2); ^{13}C -NMR (75 MHz, $CDCl_3$) δ : 112.2 (CH-12), 116.6 (qC-3), 117.4 (qC-5), 118.4 (CH-6), 119.1 (CH-15), 123.3 (qC-16), 126.8 (CH-13), 127.4 (CH-26), 127.50 (CH-24, CH-28), 127.54 (CH-18, CH-22), 128.0 (CH-20), 128.9 (CH-8, CH-25, CH-27), 129.0 (CH-19, CH-21), 130.3 (CH-9), 137.9 (qC-14), 139.8 (qC-7), 140.1 (qC-17), 140.9 (qC-23), 144.2 (CH-2), 146.8 (qC-10), 155.5 (qC-11), 158.1 (qC-4); HRMS (ESI-TOF) m/z : $[M+H]^+$ calcd. for $C_{27}H_{18}NO$: 372.1388; found: 372.1384.

8-Chloro-2-phenylbenzofuro[3,2-*c*]quinoline (128)

Pale yellow solid; yield: 118 mg (60%); m.p. = 213–214 °C; IR (NaCl): ν 3583 (C-H stretch), 1461 (aromatic C-C stretch), 1359 (C-N stretch), 1192 (C-O stretch), 665 (C-Cl stretch) cm^{-1} ; $^1\text{H-NMR}$ (300 MHz, CDCl_3) δ : 7.38–7.60 (m, 4H, CH-13, CH-19, CH-20, CH-21), 7.66 (d, J = 8.8 Hz, 1H, CH-12), 7.75–7.87 (m, 2H, CH-18, CH-22), 7.99–8.12 (m, 2H, CH-8, CH-15), 8.31 (d, J = 8.8 Hz, 1H CH-9), 8.55 (d, J = 1.8 Hz, 1H, CH-6), 9.41 (s, 1H, CH-2); $^{13}\text{C-NMR}$ (75 MHz, CDCl_3) δ : 113.1 (CH-12), 115.8 (qC-3), 117.2 (qC-5), 118.4 (CH-6), 120.5 (CH-15), 124.2 (qC-16), 127.4 (CH-13), 127.5 (CH-18, CH-22), 128.1 (CH-20), 129.1 (CH-19, CH-21), 129.3 (CH-8), 129.9 (qC-14), 130.4 (CH-9), 140.0 (qC-17), 140.1 (qC-7), 144.0 (CH-2), 147.0 (qC-10), 154.3 (qC-11), 158.4 (qC-4); HRMS (ESI-TOF) m/z : $[\text{M}+\text{H}]^+$ calcd. for $\text{C}_{21}\text{H}_{13}\text{ClNO}$: 330.0681; found: 330.0684.

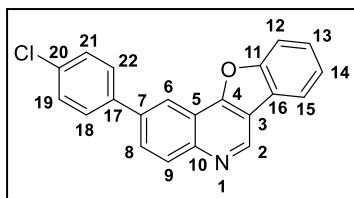
2-(*p*-Tolyl)benzofuro[3,2-*c*]quinoline (129)

White solid; yield: 89 mg (72%); m.p. = 183–185 °C; IR (NaCl): ν 3583 (C-H stretch), 3401 (C-H stretch), 1505 (aromatic C-C stretch), 1460 (aromatic C-C stretch), 1358 (C-N stretch), 1190 (C-O stretch) cm^{-1} ; $^1\text{H-NMR}$ (300 MHz, CDCl_3) δ : 2.45 (s, 3H, CH₃-23), 7.35 (d, J = 7.9 Hz, 2H, CH-19, CH-21), 7.44–7.62 (m, 2H, CH-13, CH-14), 7.69–7.82 (m, 3H, CH-12, CH-18, CH-22), 8.02–8.16 (m, 2H, CH-8, CH-15), 8.33 (d, J = 8.8 Hz, 1H, CH-9), 8.61 (d, J = 1.9 Hz, 1H, CH-6), 9.49 (s, 1H, CH-2); $^{13}\text{C-NMR}$ (75 MHz, CDCl_3) δ : 21.2 (CH₃-23), 112.1 (CH-12), 116.5 (qC-3), 117.4 (qC-5), 118.0 (CH-6), 120.7 (CH-15), 122.7 (qC-16), 124.1 (CH-14), 127.27 (CH-13), 127.34 (CH-18, CH-22), 128.8 (CH-8), 129.8 (CH-19, CH-21), 130.2 (CH-9), 137.2 (qC-17), 137.9 (qC-20), 139.6 (qC-7), 144.0 (CH-2), 146.6 (qC-10), 156.0 (qC-11), 157.6 (qC-4); HRMS (ESI-TOF) m/z : $[\text{M}+\text{H}]^+$ calcd. for $\text{C}_{22}\text{H}_{16}\text{NO}$: 310.1232; found: 310.1222.

2-(4-Methoxyphenyl)benzofuro[3,2-*c*]quinoline (130)

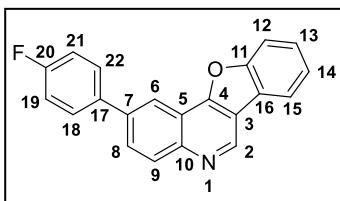
White solid; yield: 84 mg (65%); m.p. = 189–191 °C; IR (NaCl): ν 3320 (C-H stretch), 1505 (aromatic C-C stretch), 1460 (aromatic C-C stretch), 1359 (C-N stretch), 1246 (C-O stretch), 1190 (C-O stretch) cm^{-1} ;

^1H -NMR (300 MHz, CDCl_3) δ : 3.90 (s, 3H, CH_3 -23), 7.01–7.12 (m, 2H, CH -19, CH -21), 7.43–7.60 (m, 2H, CH -13, CH -14), 7.71–7.81 (m, 3H, CH -12, CH -18, CH -22), 8.01 (dd, J = 8.8, 2.1 Hz, 1H, CH -8), 8.10 (dd, J = 7.6, 0.9 Hz, 1H, CH -15), 8.30 (d, J = 8.8 Hz, 1H, CH -9), 8.55 (d, J = 1.9 Hz, 1H, CH -6), 9.46 (s, 1H, CH -2); ^{13}C -NMR (75 MHz, CDCl_3) δ : 55.4 (CH_3 -23), 112.1 (CH -12), 114.5 (CH -19, CH -21), 116.5 (qC-3), 117.4 (qC-5), 117.5 (CH -6), 120.6 (CH -15), 122.7 (qC-16), 124.1 (CH -14), 127.2 (CH -13), 128.56 (CH -18, CH -22), 128.61 (CH -8), 130.2 (CH -9), 132.6 (qC-17), 139.3 (qC-7), 143.9 (CH -2), 146.4 (qC-10), 156.0 (qC-11), 157.5 (qC-4), 159.7 (qC-20); HRMS (ESI-TOF) m/z : $[\text{M}+\text{H}]^+$ calcd. for $\text{C}_{22}\text{H}_{16}\text{NO}_2$: 326.1181; found: 326.1185.

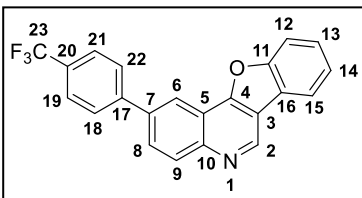
2-(4-Chlorophenyl)benzofuro[3,2-*c*]quinoline (131)

Pale yellow solid; yield: 106 mg (81%); m.p. = 191–192 °C; IR (NaCl): ν 3389 (C-H stretch), 1556 (aromatic C-C stretch), 1458 (aromatic C-C stretch), 1356 (C-N stretch), 1191 (C-O stretch), 821 (C-Cl stretch) cm^{-1} ;

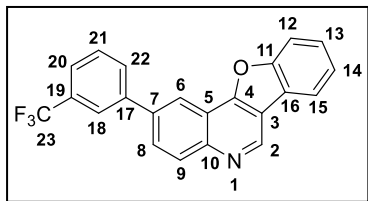
^1H -NMR (300 MHz, CDCl_3) δ : 7.38–7.57 (m, 4H, CH -13, CH -14, CH -19, CH -21), 7.61–7.75 (m, 3H, CH -12, CH -18, CH -22), 7.89 (dd, J = 8.8, 2.1 Hz, 1H, CH -8), 8.02 (dd, J = 7.6, 0.8 Hz, 1H, CH -15), 8.24 (d, J = 8.8 Hz, 1H, CH -9), 8.43 (d, J = 2.0 Hz, 1H, CH -6), 9.39 (s, 1H, CH -2); ^{13}C -NMR (75 MHz, CDCl_3) δ : 112.1 (CH -12), 116.7 (qC-3), 117.3 (qC-5), 118.2 (CH -6), 120.7 (CH -15), 122.6 (qC-16), 124.1 (CH -14), 127.3 (CH -13), 128.3 (CH -8), 128.6 (CH -18, CH -22), 129.1 (CH -19, CH -21), 130.4 (CH -9), 134.1 (qC-20), 138.3 (qC-7), 138.5 (qC-17), 144.4 (CH -2), 146.7 (qC-10), 155.9 (qC-11), 157.4 (qC-4); HRMS (ESI-TOF) m/z : $[\text{M}+\text{H}]^+$ calcd. for $\text{C}_{21}\text{H}_{13}\text{ClNO}$: 330.0680; found: 330.0676.

2-(4-Fluorophenyl)benzofuro[3,2-*c*]quinoline (132)

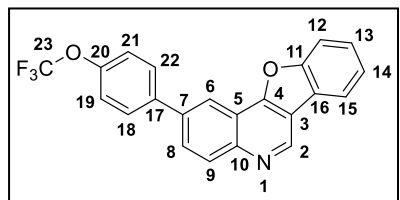
Pale yellow solid; yield: 95 mg (77%); m.p. = 185–186 °C; IR (NaCl): ν 3391 (C-H stretch), 1561 (aromatic C-C stretch), 1460 (aromatic C-C stretch), 1334 (C-N stretch), 1192 (C-O stretch), 1123 (C-F stretch) cm^{-1} ; $^1\text{H-NMR}$ (300 MHz, CDCl_3) δ : 7.16–7.29 (m, 2H, CH-19, CH-21), 7.46–7.62 (m, 2H, CH-13, CH-14), 7.72–7.83 (m, 3H, CH-12, CH-18, CH-22), 8.00 (dd, J = 8.8, 2.1 Hz, 1H, CH-8), 8.13 (dd, J = 7.2, 1.3 Hz, 1H, CH-15), 8.33 (d, J = 8.8 Hz, 1H, CH-9), 8.57 (d, J = 2.0 Hz, 1H, CH-6), 9.50 (s, 1H, CH-2); $^{13}\text{C-NMR}$ (75 MHz, CDCl_3) δ : 112.1 (CH-12), 115.9 (d, $^2J_{\text{C,F}}$ = 22 Hz, CH-19, CH-21), 116.7 (qC-3), 117.4 (qC-5), 118.2 (CH-6), 120.7 (CH-15), 122.7 (qC-16), 124.1 (CH-14), 127.3 (CH-13), 128.6 (CH-8), 129.1 (d, $^3J_{\text{C,F}}$ = 8 Hz, CH-18, CH-22), 130.4 (CH-9), 136.2 (qC-17), 138.7 (qC-7), 144.3 (CH-2), 146.6 (qC-10), 156.0 (qC-11), 157.5 (qC-4), 162.9 (d, $^1J_{\text{C,F}}$ = 247 Hz, qC-20); $^{19}\text{F-NMR}$ (282 MHz, CDCl_3) δ : -115; HRMS (ESI-TOF) m/z : $[\text{M}+\text{H}]^+$ calcd. for $\text{C}_{21}\text{H}_{13}\text{FNO}$: 314.0981; found: 314.0971.

2-(4-(Trifluoromethyl)phenyl)benzofuro[3,2-*c*]quinoline (133)

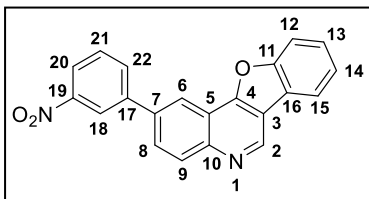
Pale yellow solid; yield: 114 mg (80%); m.p. = 194–195 °C; IR (NaCl): ν 3384 (C-H stretch), 1614 (aromatic C-C stretch), 1460 (aromatic C-C stretch), 1331 (C-N stretch), 1189 (C-O stretch), 1116 (C-F stretch) cm^{-1} ; $^1\text{H-NMR}$ (300 MHz, CDCl_3) δ : 7.46–7.63 (m, 2H, CH-13, CH-14), 7.74–7.85 (m, 3H, CH-12, CH-19, CH-21), 7.93 (d, J = 8.2 Hz, 2H, CH-18, CH-22), 8.04 (dd, J = 8.8, 2.1 Hz, 1H, CH-8), 8.13 (d, J = 7.4 Hz, 1H, CH-15), 8.37 (d, J = 8.8 Hz, 1H, CH-9), 8.65 (d, J = 1.9 Hz, 1H, CH-6), 9.53 (s, 1H, CH-2); $^{13}\text{C-NMR}$ (75 MHz, CDCl_3) δ : 112.1 (CH-12), 116.8 (qC-3), 117.3 (qC-5), 119.0 (CH-6), 120.7 (CH-15), 122.6 (qC-16), 124.22 (CH-14), 124.23 (q, $^1J_{\text{C,F}}$ = 270 Hz, qC-23), 125.9 (q, $^3J_{\text{C,F}}$ = 4 Hz, CH-19, CH-21), 127.5 (CH-13), 127.7 (CH-18, CH-22), 128.4 (CH-8), 130.0 (q, $^2J_{\text{C,F}}$ = 33 Hz, qC-20), 130.6 (CH-9), 138.1 (qC-7), 143.6 (qC-17), 144.8 (CH-2), 146.9 (qC-10), 156.0 (qC-11), 157.5 (qC-4); $^{19}\text{F-NMR}$ (282 MHz, CDCl_3) δ : -62; HRMS (ESI-TOF) m/z : $[\text{M}+\text{H}]^+$ calcd. for $\text{C}_{22}\text{H}_{13}\text{F}_3\text{NO}$: 364.0949; found: 364.0938.

2-(3-(Trifluoromethyl)phenyl)benzofuro[3,2-*c*]quinoline (134)

Pale yellow solid; yield: 104 mg (72%); m.p. = 171–173 °C; IR (NaCl): ν 3391 (C-H stretch), 1561 (aromatic C-C stretch), 1446 (aromatic C-C stretch), 1334 (C-N stretch), 1166 (C-O stretch), 1123 (C-F stretch) cm^{-1} ; ^1H -NMR (300 MHz, CDCl_3) δ : 7.45–7.73 (m, 4H, CH-13, CH-14, CH-20, CH-21), 7.79 (d, J = 7.9 Hz, 1H, CH-12), 7.95–8.09 (m, 3H, CH-8, CH-18, CH-22), 8.13 (dd, J = 7.6, 0.8 Hz, 1H, CH-15), 8.37 (d, J = 8.8 Hz, 1H, CH-9), 8.63 (d, J = 2.0 Hz, 1H, CH-6), 9.52 (s, 1H, CH-2); ^{13}C -NMR (75 MHz, CDCl_3) δ : 112.1 (CH-12), 116.8 (qC-3), 117.3 (qC-5), 118.7 (CH-6), 120.7 (CH-15), 122.6 (qC-16), 124.19 (CH-14), 124.20 (q, $^1J_{\text{C,F}}$ = 273 Hz, qC-23), 124.3 (q, $^3J_{\text{C,F}}$ = 4 Hz, CH-18), 124.6 (q, $^3J_{\text{C,F}}$ = 4 Hz, CH-20), 127.5 (CH-13), 128.4 (CH-8), 129.5 (CH-21), 130.6 (CH-9), 130.7 (CH-22), 131.5 (q, $^2J_{\text{C,F}}$ = 32 Hz, qC-19), 138.1 (qC-7), 140.9 (qC-17), 144.7 (CH-2), 146.8 (qC-10), 156.0 (qC-11), 157.5 (qC-4); ^{19}F -NMR (282 MHz, CDCl_3) δ : -62; HRMS (ESI-TOF) m/z : $[\text{M}+\text{H}]^+$ calcd. for $\text{C}_{22}\text{H}_{13}\text{F}_3\text{NO}$: 364.0944; found: 364.0947.

2-(4-(Trifluoromethoxy)phenyl)benzofuro[3,2-*c*]quinoline (135)

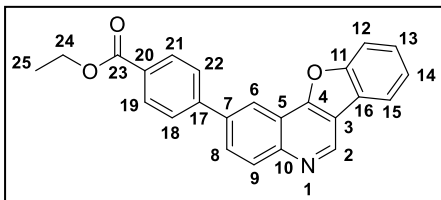
Yellow solid; yield: 105 mg (70%); m.p. = 148–150 °C; IR (NaCl): ν 3583 (C-H stretch), 1504 (aromatic C-C stretch), 1459 (aromatic C-C stretch), 1283 (C-N stretch), 1210 (C-O stretch), 1191 (C-O stretch), 1165 (C-F stretch) cm^{-1} ; ^1H -NMR (300 MHz, CDCl_3) δ : 7.37 (dd, J = 8.8, 0.9 Hz, 2H, CH-19, CH-21), 7.43–7.62 (m, 2H, CH-13, CH-14), 7.72–7.86 (m, 3H, CH-12, CH-18, CH-22), 7.97 (dd, J = 8.8, 2.1 Hz, 1H, CH-8), 8.09 (dd, J = 7.6, 0.8 Hz, 1H, CH-15), 8.31 (d, J = 8.8 Hz, 1H, CH-9), 8.54 (d, J = 2.0 Hz, 1H, CH-6), 9.47 (s, 1H, CH-2); ^{13}C -NMR (75 MHz, CDCl_3) δ : 112.1 (CH-12), 116.8 (qC-3), 117.4 (qC-5), 118.6 (CH-6), 120.5 (q, $^1J_{\text{C,F}}$ = 257 Hz, qC-23), 120.7 (CH-15), 121.4 (CH-19, CH-21), 122.6 (qC-16), 124.2 (CH-14), 127.4 (CH-13), 128.5 (CH-8), 128.9 (CH-18, CH-22), 130.5 (CH-9), 138.3 (qC-7), 138.9 (qC-17), 144.5 (CH-2), 146.7 (qC-10), 149.2 (q, $^3J_{\text{C,F}}$ = 2 Hz, qC-20), 156.0 (qC-11), 157.5 (qC-4); ^{19}F -NMR (282 MHz, CDCl_3) δ : -58; HRMS (ESI-TOF) m/z : $[\text{M}+\text{H}]^+$ calcd. for $\text{C}_{22}\text{H}_{13}\text{F}_3\text{NO}_2$: 380.0898; found: 380.0889.

2-(3-Nitrophenyl)benzofuro[3,2-*c*]quinoline (136)

Yellow solid; yield: 69 mg (51%); m.p. = 227–228 °C;

IR (NaCl): ν 3392 (C-H stretch), 1529 (aromatic C-C stretch), 1460 (aromatic C-C stretch), 1348 (N-O stretch), 1321 (C-N stretch), 1191 (C-O stretch) cm^{-1} ;

^1H -NMR (300 MHz, CDCl_3) δ : 7.47–7.64 (m, 2H, CH-13, CH-14), 7.72 (t, J = 8.0 Hz, 1H, CH-21), 7.80 (d, J = 8.0 Hz, 1H, CH-12), 8.06 (dd, J = 8.8, 2.2 Hz, 1H, CH-8), 8.10–8.19 (m, 2H, CH-15, CH-22), 8.30 (ddd, J = 8.2, 2.2, 1.0 Hz, 1H, CH-20), 8.40 (d, J = 8.8 Hz, 1H, CH-9), 8.65–8.73 (m, 2H, CH-6, CH-18), 9.55 (s, 1H, CH-2); ^{13}C -NMR (75 MHz, CDCl_3) δ : 112.2 (CH-12), 117.0 (qC-3), 117.4 (qC-5), 119.1 (CH-6), 120.8 (CH-15), 122.3 (CH-18), 122.5 (qC-16), 122.6 (CH-20), 124.3 (CH-14), 127.6 (CH-13), 128.2 (CH-8), 130.0 (CH-21), 131.0 (CH-9), 133.3 (CH-22), 137.1 (qC-7), 141.9 (qC-17), 145.1 (CH-2), 147.0 (qC-10), 148.9 (qC-19), 156.1 (qC-11), 157.5 (qC-4); HRMS (ESI-TOF) m/z : $[\text{M}+\text{H}]^+$ calcd. for $\text{C}_{21}\text{H}_{13}\text{N}_2\text{O}_3$: 341.0921; found: 341.0919.

Ethyl 4-(benzofuro[3,2-*c*]quinolin-2-yl)benzoate (137)

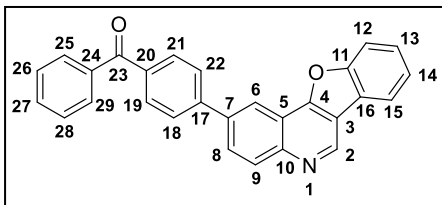
Beige solid; yield: 105 mg (72%); m.p. = 160–

161 °C; IR (NaCl): ν 2922 (C-H stretch), 1715

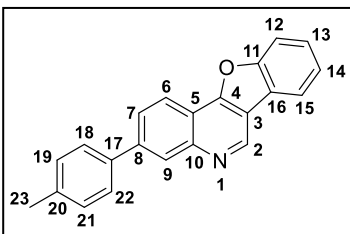
(ester C=O stretch), 1607 (aromatic C-C stretch),

1460 (aromatic C-C stretch), 1357 (C-N stretch),

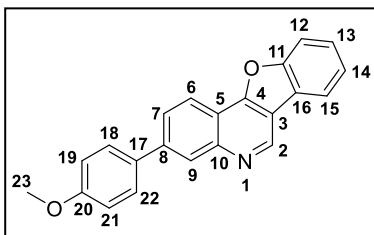
1278 (C-O stretch), 1190 (C-O stretch) cm^{-1} ; ^1H -NMR (300 MHz, CDCl_3) δ : 1.45 (t, J = 7.1 Hz, 3H, CH₃-25), 4.44 (q, J = 7.1 Hz, 2H, CH₂-24), 7.43–7.63 (m, 2H, CH-13, CH-14), 7.79 (d, J = 7.9 Hz, 1H, CH-12), 7.84–7.95 (m, 2H, CH-18, CH-22), 8.02–8.28 (m, 4H, CH-8, CH-15, CH-19, CH-21), 8.36 (d, J = 8.8 Hz, 1H, CH-9), 8.67 (d, J = 1.7 Hz, 1H, CH-6), 9.52 (s, 1H, CH-2); ^{13}C -NMR (75 MHz, CDCl_3) δ : 14.4 (CH₃-25), 61.1 (CH₂-24), 112.1 (CH-12), 116.7 (qC-3), 117.2 (qC-5), 118.8 (CH-6), 120.7 (CH-15), 122.5 (qC-16), 124.1 (CH-14), 127.3 (CH-18, CH-22), 127.4 (CH-13), 128.8 (CH-8), 129.8 (qC-20), 130.2 (CH-19, CH-21), 130.5 (CH-9), 138.3 (qC-7), 144.2 (qC-17), 144.6 (CH-2), 146.9 (qC-10), 155.9 (qC-11), 157.4 (qC-4), 166.4 (qC-23); HRMS (ESI-TOF) m/z : $[\text{M}+\text{H}]^+$ calcd. for $\text{C}_{24}\text{H}_{18}\text{NO}_3$: 368.1281; found: 368.1282.

(4-(Benzofuro[3,2-*c*]quinolin-2-yl)phenyl)(phenyl)methanone (138)

Pale yellow solid; yield: 94 mg (59%); m.p. = 184–187 °C; IR (NaCl): ν 3401 (C-H stretch), 1652 (C=O stretch), 1602 (aromatic C-C stretch), 1460 (aromatic C-C stretch), 1357 (C-N stretch), 1190 (C-O stretch) cm^{-1} ; ^1H -NMR (300 MHz, CDCl_3) δ : 7.46–7.70 (m, 5H, CH-13, CH-14, CH-26, CH-27, CH-28), 7.79 (d, J = 8.3 Hz, 1H, CH-12), 7.84–8.04 (m, 6H, CH-18, CH-19, CH-21, CH-22, CH-25, CH-29), 8.05–8.20 (m, 2H, CH-8, CH-15), 8.38 (d, J = 8.8 Hz, 1H, CH-9), 8.71 (d, J = 1.9 Hz, 1H, CH-6), 9.53 (s, 1H, CH-2); ^{13}C -NMR (75 MHz, CDCl_3) δ : 112.1 (CH-12), 116.8 (qC-3), 117.4 (qC-5), 119.0 (CH-6), 120.7 (CH-15), 122.6 (qC-16), 124.2 (CH-14), 127.3 (CH-18, CH-22), 127.5 (CH-13), 128.4 (CH-26, CH-28), 128.5 (CH-8), 130.0 (CH-25, CH-29), 130.6 (CH-9), 130.9 (CH-19, CH-21), 132.5 (CH-27), 136.8 (qC-20), 137.6 (qC-24), 138.4 (qC-7), 144.0 (qC-17), 144.7 (CH-2), 146.9 (qC-10), 156.0 (qC-11), 157.5 (qC-4), 196.2 (qC-23); HRMS (ESI-TOF) m/z : $[\text{M}+\text{H}]^+$ calcd. for $\text{C}_{28}\text{H}_{18}\text{NO}_2$: 400.1332; found: 400.1331.

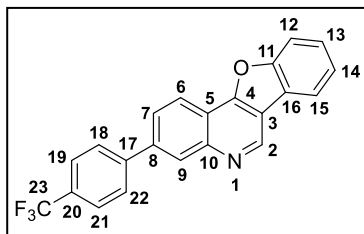
3-(*p*-Tolyl)benzofuro[3,2-*c*]quinoline (139)

White solid; yield: 90 mg (74%); m.p. = 200–202 °C; IR (NaCl): ν 3150 (C-H stretch), 1554 (aromatic C-C stretch), 1450 (aromatic C-C stretch), 1379 (C-N stretch), 1190 (C-O stretch) cm^{-1} ; ^1H -NMR (300 MHz, CDCl_3) δ : 2.45 (s, 3H, CH₃-23), 7.34 (d, J = 7.9 Hz, 2H, CH-19, CH-21), 7.44–7.60 (m, 2H, CH-13, CH-14), 7.66–7.81 (m, 3H, CH-12, CH-18, CH-22), 7.97 (dd, J = 8.5, 1.5 Hz, 1H, CH-7), 8.11 (dd, J = 7.6, 0.9 Hz, 1H, CH-15), 8.42–8.52 (m, 2H, CH-6, CH-9), 9.51 (s, 1H, CH-2); ^{13}C -NMR (75 MHz, CDCl_3) δ : 21.2 (CH₃-23), 112.1 (CH-12), 115.9 (qC-5), 116.2 (qC-3), 120.5 (CH-15), 121.1 (CH-6), 122.7 (qC-16), 124.0 (CH-14), 126.4 (CH-7), 127.1 (CH-13), 127.2 (CH-9), 127.3 (CH-18, CH-22), 129.8 (CH-19, CH-21), 137.3 (qC-20), 137.9 (qC-17), 142.0 (qC-8), 144.7 (CH-2), 147.9 (qC-10), 156.0 (qC-11), 157.4 (qC-4); HRMS (ESI-TOF) m/z : $[\text{M}+\text{H}]^+$ calcd. for $\text{C}_{22}\text{H}_{16}\text{NO}$: 310.1232; found: 310.1244.

3-(4-Methoxyphenyl)benzofuro[3,2-*c*]quinoline (140)

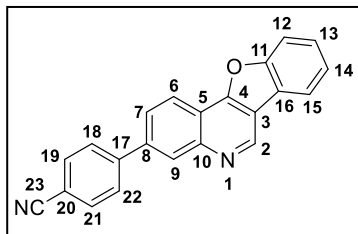
White solid; yield: 88 mg (70%); m.p. = 157–158 °C; IR (NaCl): ν 3369 (C-H stretch), 2998 (C-H stretch), 1607 (aromatic C-C stretch), 1450 (aromatic C-C stretch), 1303 (C-N stretch), 1245 (C-O stretch), 1188 (C-O stretch) cm^{-1} ; $^1\text{H-NMR}$ (300 MHz, CDCl_3) δ :

3.88 (s, 3H, CH_3 -**23**), 6.99–7.10 (m, 2H, CH -**19**, CH -**21**), 7.41–7.57 (m, 2H, CH -**13**, CH -**14**), 7.68–7.77 (m, 3H, CH -**12**, CH -**18**, CH -**22**), 7.91 (dd, $J = 8.6, 1.7$ Hz, 1H, CH -**7**), 8.07 (dd, $J = 7.5, 1.5$ Hz, 1H, CH -**15**), 8.37–8.45 (m, 2H, CH -**6**, CH -**9**), 9.47 (s, 1H, CH -**2**); $^{13}\text{C-NMR}$ (75 MHz, CDCl_3) δ : 55.4 (CH_3 -**23**), 112.1 (CH -**12**), 114.5 (CH -**19**, CH -**21**), 115.7 (qC-**5**), 116.1 (qC-**3**), 120.5 (CH -**15**), 121.2 (CH -**6**), 122.8 (qC-**16**), 124.1 (CH -**14**), 126.3 (CH -**7**), 126.8 (CH -**9**), 127.1 (CH -**13**), 128.5 (CH -**18**, CH -**22**), 132.7 (qC-**17**), 141.7 (qC-**8**), 144.8 (CH -**2**), 148.0 (qC-**10**), 156.0 (qC-**11**), 157.5 (qC-**4**), 159.8 (qC-**20**); HRMS (ESI-TOF) m/z : $[\text{M}+\text{H}]^+$ calcd. for $\text{C}_{22}\text{H}_{16}\text{NO}_2$: 326.1176; found: 326.1173.

3-(4-(Trifluoromethyl)phenyl)benzofuro[3,2-*c*]quinoline (141)

Yellow solid; yield: 114 mg (79%); m.p. = 205–208 °C; IR (NaCl): ν 3251 (C-H stretch), 1559 (aromatic C-C stretch), 1450 (aromatic C-C stretch), 1329 (C-N stretch), 1188 (C-O stretch), 1110 (C-F stretch) cm^{-1} ; $^1\text{H-NMR}$ (300 MHz, CDCl_3) δ :

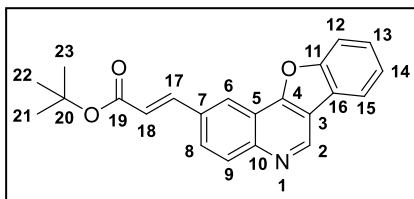
7.46–7.63 (m, 2H, CH -**13**, CH -**14**), 7.76–7.82 (m, 3H, CH -**12**, CH -**19**, CH -**21**), 7.86–8.02 (m, 3H, CH -**7**, CH -**18**, CH -**22**), 8.13 (dd, $J = 7.6, 0.9$ Hz, 1H, CH -**15**), 8.49–8.57 (m, 2H, CH -**6**, CH -**9**), 9.55 (s, 1H, CH -**2**); $^{13}\text{C-NMR}$ (75 MHz, CDCl_3) δ : 112.2 (CH -**12**), 116.7 (qC-**5**, qC-**3**), 120.7 (CH -**15**), 121.6 (CH -**6**), 122.6 (qC-**16**), 124.21 (CH -**14**), 124.22 (q, $^1J_{\text{C,F}} = 270$ Hz, qC-**23**), 126.0 (q, $^3J_{\text{C,F}} = 4$ Hz, CH -**19**, CH -**21**), 126.2 (CH -**7**), 127.5 (CH -**13**), 127.7 (CH -**18**, CH -**22**), 128.2 (CH -**9**), 129.9 (q, $^2J_{\text{C,F}} = 32$ Hz, qC-**20**), 140.4 (qC-**8**), 143.7 (qC-**17**), 145.1 (CH -**2**), 147.6 (qC-**10**), 156.1 (qC-**11**), 157.3 (qC-**4**); $^{19}\text{F-NMR}$ (282 MHz, CDCl_3) δ : -62; HRMS (ESI-TOF) m/z : $[\text{M}+\text{H}]^+$ calcd. for $\text{C}_{22}\text{H}_{13}\text{F}_3\text{NO}$: 364.0949; found: 364.0951.

4-(Benzofuro[3,2-*c*]quinolin-3-yl)benzonitrile (142)

White solid; yield: 85 mg (67%); m.p. >250 °C; IR (NaCl): ν 3348 (C-H stretch), 2223 (C \equiv N stretch), 1553 (aromatic C-C stretch), 1447 (aromatic C-C stretch), 1344 (C-N stretch), 1184 (C-O stretch) cm^{-1} ; $^1\text{H-NMR}$ (300 MHz, CDCl_3) δ : 7.45–7.64 (m, 2H, CH-13, CH-14), 7.73–7.80 (m, 6H, CH-7, CH-12, CH-18, CH-19, CH-21, CH-22), 8.13 (dd, J = 7.6, 0.8 Hz, 1H, CH-15), 8.45–8.60 (m, 2H, CH-6, CH-9), 9.55 (s, 1H, CH-2); $^{13}\text{C-NMR}$ (75 MHz, CDCl_3) δ : 111.7 (qC-20), 112.3 (CH-12), 116.9 (qC-5), 117.0 (qC-3), 118.8 (qC-23), 120.8 (CH-15), 121.9 (CH-6), 122.6 (qC-16), 124.3 (CH-14), 126.0 (CH-7), 127.6 (CH-13), 128.1 (CH-18, CH-22), 128.4 (CH-9), 132.9 (CH-19, CH-21), 139.9 (qC-8), 144.7 (qC-17), 145.3 (CH-2), 147.5 (qC-10), 156.2 (qC-11), 157.2 (qC-4); HRMS (ESI-TOF) m/z : $[\text{M}+\text{H}]^+$ calcd. for $\text{C}_{22}\text{H}_{13}\text{N}_2\text{O}$: 321.1028; found: 321.1033.

3.24. General Procedure for Pd-Catalysed One-Pot Mizoroki-Heck and Intramolecular Direct Arylation Reactions

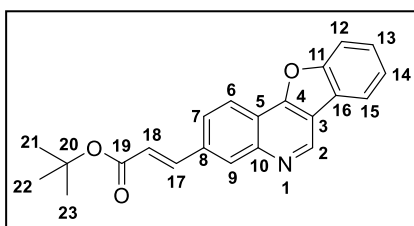
A mixture of the 4-(2-bromophenoxy)quinoline substrate (1 equiv.), *t*-BuOAc (1.1 equiv.), $\text{Pd}(\text{OAc})_2$ (2 mol%), and anhydrous K_2CO_3 (2 equiv.) in anhydrous NMP (1.5 mL/mmol) was stirred at 135 °C in a sealed reaction tube. The reaction progress was monitored by periodically sampling the reaction mixture for $^1\text{H-NMR}$ analysis in CDCl_3 . Once complete, the cooled reaction mixture was diluted with DCM, filtered through a short plug of Celite and concentrated *in vacuo*. The crude mixture was purified by column chromatography over silica gel using DCM/EtOAc (99:1–95:5) as eluent.

***tert*-Butyl (*E*)-3-(benzofuro[3,2-*c*]quinolin-2-yl)acrylate (143)**

White solid; yield: 27 mg (60%); m.p. = 169–170 °C; IR (NaCl): ν 3393 (C-H stretch), 2976 (C-H stretch), 1701 (ester C=O), 1560 (aromatic C-C stretch), 1460 (aromatic C-C stretch), 1366 (C-N stretch), 1238 (C-O stretch), 1151 (C-O stretch) cm^{-1} ; $^1\text{H-NMR}$ (300 MHz, CDCl_3) δ : 1.58 (s, 9H, CH₃-21, CH₃-22, CH₃-23), 6.60 (d, J = 16.0 Hz, 1H, CH-18), 7.44–7.65

(m, 2H, *CH*-13, *CH*-14), 7.73–7.89 (m, 2H, *CH*-12, *CH*-17), 7.94 (dd, $J = 8.9, 2.0$ Hz, 1H, *CH*-8), 8.11 (dd, $J = 7.6, 0.8$ Hz, 1H, *CH*-15), 8.24 (d, $J = 8.8$ Hz, 1H, *CH*-9), 8.51 (d, $J = 1.9$ Hz, 1H, *CH*-6), 9.49 (s, 1H, *CH*-2); ^{13}C -NMR (100 MHz, CDCl_3) δ : 28.2 (CH_3 -21, CH_3 -22, CH_3 -23), 80.9 (qC-20), 112.3 (*CH*-12), 117.0 (qC-3), 117.3 (qC-5), 120.8 (*CH*-15), 121.6 (*CH*-6), 122.0 (*CH*-18), 122.5 (qC-16), 124.3 (*CH*-14), 127.4 (*CH*-8), 127.6 (*CH*-13), 130.5 (*CH*-9), 133.4 (qC-7), 142.5 (*CH*-17), 145.1 (*CH*-2), 147.9 (qC-10), 156.1 (qC-11), 157.5 (qC-4), 166.1 (qC-19); HRMS (ESI-TOF) m/z : $[\text{M}+\text{H}]^+$ calcd. for $\text{C}_{22}\text{H}_{20}\text{NO}_3$: 346.1438; found: 346.1434.

***tert*-Butyl (*E*)-3-(benzofuro[3,2-*c*]quinolin-3-yl)acrylate (144)**



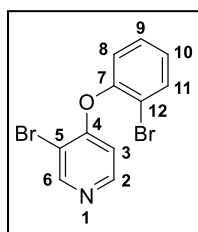
Pale yellow solid; yield: 36 mg (80%); m.p. = 160–162 °C; IR (NaCl): ν 3393 (C-H stretch), 2976 (C-H stretch), 1703 (ester C=O), 1560 (aromatic C-C stretch), 1452 (aromatic C-C stretch), 1366 (C-N stretch), 1285 (C-O stretch), 1149 (C-O stretch)

cm^{-1} ; ^1H -NMR (300 MHz, CDCl_3) δ : 1.58 (s, 9H, CH_3 -21, CH_3 -22, CH_3 -23), 6.59 (d, $J = 16.0$ Hz, 1H, *CH*-18), 7.44–7.63 (m, 2H, *CH*-13, *CH*-14), 7.71–7.92 (m, 3H, *CH*-6, *CH*-7, *CH*-12), 8.11 (dd, $J = 7.6, 0.8$ Hz, 1H, *CH*-15), 8.30–8.46 (m, 2H, *CH*-9, *CH*-17), 9.51 (s, 1H, *CH*-2); ^{13}C -NMR (75 MHz, CDCl_3) δ : 28.2 (CH_3 -21, CH_3 -22, CH_3 -23), 80.8 (qC-20), 112.2 (*CH*-12), 117.1 (qC-3), 117.7 (qC-5), 120.8 (*CH*-15), 121.4 (*CH*-6), 122.0 (*CH*-18), 122.5 (qC-16), 124.3 (*CH*-14), 125.1 (*CH*-7), 127.6 (*CH*-13), 130.7 (*CH*-9), 135.6 (qC-8), 142.8 (*CH*-17), 145.2 (*CH*-2), 147.4 (qC-10), 156.2 (qC-11), 157.1 (qC-4), 166.0 (qC-19); HRMS (ESI-TOF) m/z : $[\text{M}+\text{H}]^+$ calcd. for $\text{C}_{22}\text{H}_{20}\text{NO}_3$: 346.1438; found: 346.1432.

3.25. General Procedure for Synthesis of 4-Phenoxy Pyridine Substrates

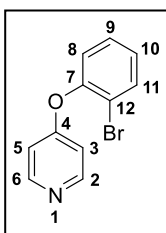
A mixture of the 4-chloropyridine (1 equiv.) and the 2-bromophenol (5 equiv.) was stirred at 130 °C until reaction was completed (18–24 h) as evident by ^1H -NMR analysis. The cooled reaction mixture was diluted with 10% aq. NaOH (0.5 mL/mmol) and stirred at room temperature for 1 h. The aqueous phase was extracted with DCM (3×1.5 mL/mmol). The combined organic layers were washed with 6M NaOH (3×1 mL/mmol), water (1 mL/mmol) and brine (1 mL/mmol), dried over MgSO_4 , filtered and concentrated *in vacuo*, yielding product which, if necessary, was recrystallised from cyclohexane.

3-Bromo-4-(2-bromophenoxy)pyridine (145)



Yellow solid; yield: 455 mg (88%); m.p. = 48–49 °C; IR (NaCl): ν 3369 (C-H stretch), 1566 (aromatic C-C stretch), 1467 (aromatic C-C stretch), 1267 (C-N stretch), 1029 (C-O stretch), 657 (C-Br stretch) cm^{-1} ; ^1H -NMR (300 MHz, CDCl_3) δ : 6.45 (d, $J = 5.6$ Hz, 1H, CH-3), 7.13–7.24 (m, 2H, CH-8, CH-10), 7.40 (td, $J = 7.8, 1.5$ Hz, 1H, CH-9), 7.70 (dd, $J = 7.9, 1.4$ Hz, 1H, CH-11), 8.31 (d, $J = 5.5$ Hz, 1H, CH-2), 8.72 (s, 1H, CH-6); ^{13}C -NMR (75 MHz, CDCl_3) δ : 110.4 (qC-5), 110.9 (CH-3), 116.1 (qC-12), 122.9 (CH-8), 127.6 (CH-10), 129.2 (CH-9), 134.4 (CH-11), 149.8 (CH-2), 150.6 (qC-7), 153.4 (CH-6), 160.4 (qC-4); HRMS (ESI-TOF) m/z : $[\text{M}+\text{H}]^+$ calcd. for $\text{C}_{11}\text{H}_8\text{Br}_2\text{NO}$: 327.8973; found: 327.8963.

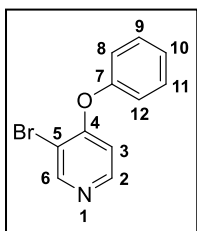
4-(2-Bromophenoxy)pyridine^[93] (147)



Yellow solid; yield: 301 mg (68%); m.p. = 64–65 °C (lit. 64–66 °C); IR (NaCl): ν 3038 (C-H stretch), 1575, 1467 (aromatic C-C stretch), 1269 (C-N stretch), 1047 (C-O stretch), 654 (C-Br stretch) cm^{-1} ; ^1H -NMR (300 MHz, CDCl_3) δ : 6.69 (d, $J = 6.0$ Hz, 2H, CH-3, CH-5), 7.11–7.24 (m, 2H, CH-8, CH-10), 7.38 (td, $J = 7.8, 1.5$ Hz, 1H, CH-9), 7.38 (dd, $J = 7.8, 1.2$ Hz, 1H, CH-11), 8.48 (s, 2H, CH-2, CH-6); ^{13}C -NMR (75 MHz, CDCl_3) δ : 111.6 (CH-3, CH-5), 116.3 (qC-12), 123.1 (CH-8), 127.2 (CH-10), 129.2 (CH-9), 134.2 (CH-11), 150.7 (qC-7), 151.5 (CH-2, CH-6), 163.9 (qC-4); HRMS (ESI-TOF) m/z : $[\text{M}+\text{H}]^+$ calcd. for $\text{C}_{11}\text{H}_9\text{BrNO}$: 249.9862; found: 249.9862.

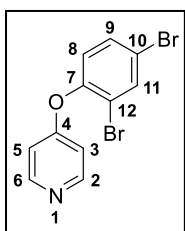
Spectral data were consistent with those reported in the literature.

3-Bromo-4-phenoxy pyridine (149)



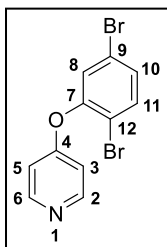
Yellow oil; yield: 345 mg (88%); IR (NaCl): ν 3046 (C-H stretch), 1568 (aromatic C-C stretch), 1480 (aromatic C-C stretch), 1273 (C-N stretch), 1099 (C-O stretch), 689 (C-Br stretch) cm^{-1} ; $^1\text{H-NMR}$ (300 MHz, CDCl_3) δ : 6.62 (d, $J = 5.6$ Hz, 1H, CH-3), 7.06–7.15 (m, 2H, CH-8, CH-12), 7.24–7.33 (m, 1H, CH-10), 7.40–7.50 (m, 2H, CH-9, CH-11), 8.30 (d, $J = 5.6$ Hz, 1H, CH-2), 8.70 (s, 1H, CH-6); $^{13}\text{C-NMR}$ (75 MHz, CDCl_3) δ : 110.9 (qC-5), 111.6 (CH-3), 120.7 (CH-8, CH-12), 125.8 (CH-10), 130.3 (CH-9, CH-11), 149.8 (CH-2), 153.4 (CH-6), 153.8 (qC-7), 161.4 (qC-4); HRMS (ESI-TOF) m/z : $[\text{M}+\text{H}]^+$ calcd. for $\text{C}_{11}\text{H}_9\text{BrNO}$: 249.9868; found: 249.9862.

4-(2,4-Dibromophenoxy)pyridine (151)



Yellow solid; yield: 381 mg (65%); m.p. = 43–45 °C; IR (NaCl): ν 3393 (C-H stretch), 1593 (aromatic C-C stretch), 1465 (aromatic C-C stretch), 1263 (C-N stretch), 1046 (C-O stretch), 665 (C-Br stretch) cm^{-1} ; $^1\text{H-NMR}$ (300 MHz, CDCl_3) δ : 6.78 (dd, $J = 4.8, 1.4$ Hz, 2H, CH-3, CH-5), 7.03 (d, $J = 8.6$ Hz, 1H, CH-8), 7.50 (dd, $J = 8.6, 2.3$ Hz, 1H, CH-9), 7.83 (d, $J = 2.3$ Hz, 1H, CH-11), 8.50 (d, $J = 5.2$ Hz, 2H, CH-2, CH-6); $^{13}\text{C-NMR}$ (75 MHz, CDCl_3) δ : 111.6 (CH-3, CH-5), 117.3 (qC-12), 119.2 (qC-10), 124.1 (CH-8), 132.2 (CH-9), 136.5 (CH-11), 150.1 (qC-7), 151.6 (CH-2, CH-6), 163.5 (qC-4); HRMS (ESI-TOF) m/z : $[\text{M}+\text{H}]^+$ calcd. for $\text{C}_{11}\text{H}_8\text{Br}_2\text{NO}$: 327.8973; found: 327.8971.

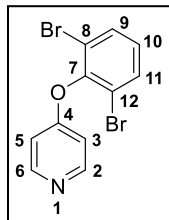
4-(2,5-Dibromophenoxy)pyridine (152)



Recrystallised from hot cyclohexane. Off-white solid; yield: 341 mg (65%); m.p. = 67–69 °C; IR (NaCl): ν 3035 (C-H stretch), 1565 (aromatic C-C stretch), 1463 (aromatic C-C stretch), 1257 (C-N stretch), 1037 (C-O stretch), 665 (C-Br stretch) cm^{-1} ; $^1\text{H-NMR}$ (300 MHz, CDCl_3) δ : 6.80 (dd, $J = 4.7, 1.6$ Hz, 2H, CH-3, CH-5), 7.27–7.35 (m, 2H, CH-8, CH-10), 7.50–7.60 (m, 1H, CH-11), 8.52 (dd, $J = 4.8, 1.5$ Hz, 2H, CH-2, CH-6); $^{13}\text{C-NMR}$ (75 MHz, CDCl_3) δ : 111.7 (CH-3, CH-5), 115.1 (qC-12), 121.8 (qC-9), 126.0 (CH-8), 130.2 (CH-10), 135.1 (CH-11), 151.6 (qC-7), 151.7

(CH-2, CH-6), 163.3 (qC-4); HRMS (ESI-TOF) m/z : $[M+H]^+$ calcd. for $C_{11}H_8Br_2NO$: 327.8973; found: 327.8971.

4-(2,6-Dibromophenoxy)pyridine (153)

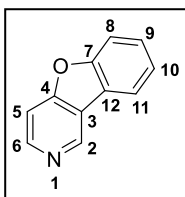


Recrystallised from hot cyclohexane. Off-white solid; yield: 365 mg (66%); m.p. = 91–93 °C; IR (NaCl): ν 3393 (C-H stretch), 1590 (aromatic C-C stretch), 1434 (aromatic C-C stretch), 1261 (C-N stretch), 1200 (C-O stretch), 665 (C-Br stretch) cm^{-1} ; 1H -NMR (300 MHz, $CDCl_3$) δ : 6.75 (d, J = 5.0 Hz, 2H, CH-3, CH-5), 7.07 (t, J = 8.1 Hz, 1H, CH-10), 7.63 (dd, J = 8.1, 1.9 Hz, 2H, CH-9, CH-11), 8.49 (d, J = 5.2 Hz, 2H, CH-2, CH-6); ^{13}C -NMR (75 MHz, $CDCl_3$) δ : 110.8 (CH-3, CH-5), 118.3 (qC-8, qC-12), 128.3 (CH-10), 133.1 (CH-9, CH-11), 147.7 (qC-7), 151.5 (CH-2, CH-6), 162.5 (qC-4); HRMS (ESI-TOF) m/z : $[M+H]^+$ calcd. for $C_{11}H_8Br_2NO$: 327.8973; found: 327.8961.

3.26. Synthesis of Compound 148

Benzofuro[3,2-*c*]pyridine^[37] (148)

A mixture of **147** (1 equiv.), $Pd(OAc)_2$ (2 mol%), and anhydrous Cs_2CO_3 (2 equiv.) in anhydrous NMP (1.5 mL/mmol) was stirred at 135 °C in a sealed reaction tube until the reaction was completed as evident by 1H -NMR analysis (20 h). The cooled reaction mixture was diluted with DCM, filtered through a short plug of Celite and concentrated *in vacuo*. The crude mixture was purified by column chromatography (DCM/EtOAc 95:5) to yield the product **148** as a yellow solid (0.026 g, 78%).

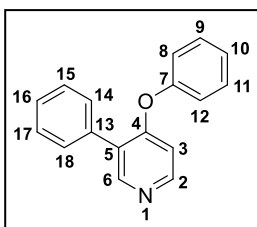


Yellow solid; yield: 26 mg (78%); m.p. = 73–74 °C (lit. 74–76 °C); IR (NaCl): ν 3393 (C-H stretch), 2918 (C-H stretch), 1575 (aromatic C-C stretch), 1447 (aromatic C-C stretch), 1266 (C-N stretch), 1107 (C-O stretch) cm^{-1} ; 1H -NMR (300 MHz, $CDCl_3$) δ : 7.38–7.46 (m, 1H, CH-10), 7.49–7.59 (m, 2H, CH-5, CH-9), 7.63 (d, J = 8.1 Hz, 1H, CH-8), 8.04 (d, J = 7.7 Hz, 1H, CH-11), 8.70 (d, J = 5.6 Hz, 1H, CH-6), 9.30 (s, 1H, CH-2); ^{13}C -NMR (75 MHz, $CDCl_3$) δ : 107.5 (CH-5), 112.0 (CH-8), 121.1 (CH-11), 121.7 (qC-3, qC-12), 123.9 (CH-10), 128.3 (CH-9), 143.5 (CH-2), 147.4 (CH-6), 155.9 (qC-7), 161.0 (qC-4); HRMS (ESI-TOF) m/z : $[M+H]^+$ calcd. for $C_{11}H_8NO$: 170.0600; found: 170.0598. Spectral data were consistent with those reported in the literature.

3.27. Synthesis of Compound 150

4-Phenoxy-3-phenylpyridine (150)

A mixture of **149** (1 equiv.), PhB(OH)₂ (1.1 equiv.), Pd(OAc)₂ (5 mol%), and anhydrous K₂CO₃ (2 equiv.) in anhydrous NMP (1.5 mL/mmol) was stirred at 135 °C in a sealed reaction tube until the reaction was completed as evident by ¹H-NMR analysis (18 h). The cooled reaction mixture was diluted with DCM, filtered through a short plug of Celite and concentrated *in vacuo*. The crude mixture was purified by column chromatography using DCM/EtOAc (99:1–95:5) as eluent to yield the product **150** as a pale yellow solid (0.010g, 21%). Compound **148** was also obtained as a side-product in 37% yield.

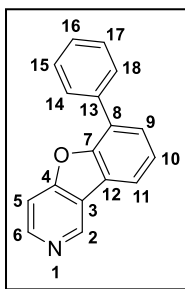


Yellow oil; yield: 10 mg (21%); IR (NaCl): ν 3374 (C-H stretch), 2923 (C-H stretch), 1575 (aromatic C-C stretch), 1447 (aromatic C-C stretch), 1333 (C-N stretch), 1107 (C-O stretch), cm^{-1} ; ¹H-NMR (300 MHz, CDCl₃) δ : 6.73 (d, J = 3.5 Hz, 1H, CH-3), 7.05-7.10 (m, 2H, CH-8, CH-12), 7.18-7.25 (m, 1H, CH-10), 7.35-7.49 (m, 5H, CH-9, CH-11, CH-15, CH-16, CH-17), 7.60-7.66 (m, 2H, CH-14, CH-18), 8.42 (d, J = 3.2 Hz, 1H, CH-2), 8.63 (s, 1H, CH-6); ¹³C-NMR (75 MHz, CDCl₃) δ : 111.3 (CH-3), 120.6 (CH-8, CH-12), 125.1 (CH-10), 127.5 (qC-5), 128.0 (CH-16), 128.5 (CH-15, CH-17), 129.4 (CH-14, CH-18), 130.2 (CH-9, CH-11), 134.3 (qC-13), 150.0 (CH-2), 151.8 (CH-6), 154.6 (qC-7), 161.6 (qC-4); HRMS (ESI-TOF) m/z : [M+H]⁺ calcd. for C₁₇H₁₄NO: 248.1070; found: 248.107.

3.28. Synthesis of Compound 156

6-Phenylbenzofuro[3,2-*c*]pyridine (156)

A mixture of **153** (1 equiv.), PhB(OH)₂ (1.1 equiv.), Pd(OAc)₂ (2 mol%), and anhydrous K₂CO₃ (2 equiv.) in anhydrous NMP (1.5 mL/mmol) was stirred at 135 °C in a sealed reaction tube until the reaction was completed as evident by ¹H-NMR analysis (18 h). The cooled reaction mixture was diluted with DCM, filtered through a short plug of Celite and concentrated *in vacuo*. The crude mixture was purified by column chromatography, first using DCM/EtOAc 99:1–95:5 as eluent, and then again using hexane/EtOAc (8:2–7:3), to yield the product **155** as a pale yellow solid (0.025g, 22%).

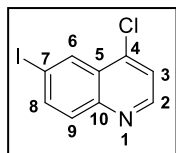


Pale yellow solid; yield: 25 mg (22%); m.p. = 66–68 °C; IR (NaCl): ν 3402 (C-H stretch), 3032 (C-H stretch), 1577 (aromatic C-C stretch), 1450 (aromatic C-C stretch), 1332 (C-N stretch), 1168 (C-O stretch) cm^{-1} ; $^1\text{H-NMR}$ (300 MHz, CDCl_3) δ : 7.35–7.63 (m, 5H, CH-5, CH-10, CH-15, CH-16, CH-17), 7.67 (dd, J = 7.6, 1.3 Hz, 1H, CH-9), 7.83–7.92 (m, 2H, CH-14, CH-18), 8.01 (dd, J = 7.7, 1.3 Hz, 1H, CH-11), 8.67 (d, J = 5.7 Hz, 1H, CH-6), 9.30 (s, 1H, CH-2); $^{13}\text{C-NMR}$ (75 MHz, CDCl_3) δ : 107.6 (CH-5), 120.1 (CH-11), 121.6 (qC-3), 122.4 (qC-12), 124.4 (CH-10), 126.4 (qC-8), 128.07 (CH-9), 128.13 (CH-16), 128.77 (CH-15, CH-17), 128.80 (CH-14, CH-18), 135.8 (qC-13), 143.7 (CH-2), 147.5 (CH-6), 153.1 (qC-7), 160.9 (qC-4); HRMS (ESI-TOF) m/z : $[\text{M}+\text{H}]^+$ calcd. for $\text{C}_{17}\text{H}_{12}\text{NO}$: 246.0913; found: 246.0914.

3.29. General Procedure for Synthesis of Iodinated 4-Chloroquinolines

6-Bromo or 7-bromo-4-chloroquinoline (1 equiv.) was added to an inert Schlenk tube under a nitrogen atmosphere, along with anhydrous NaI (2 equiv.), CuI (5 mol%) and *trans-N,N'*-dimethylcyclohexane-1,2-diamine (10 mol%). Anhydrous 1,4-dioxane (1 mL/mmol) was added and the reaction mixture was degassed with nitrogen for 10 min. The resulting green/blue mixture was stirred at 110 °C for 24 h under a nitrogen atmosphere, until the reaction was determined to be complete by $^1\text{H-NMR}$ analysis. The reaction mixture was cooled to room temperature and poured into ice water (15 mL/mmol) and extracted with DCM (3×25 mL/mmol). The combined organic extracts were washed with brine (25 mL/mmol), dried over MgSO_4 , filtered and concentrated *in vacuo* to yield the crude product as a grey solid, which was purified by column chromatography (DCM/EtOAc 95:5).

4-Chloro-6-iodoquinoline^[95] (159)

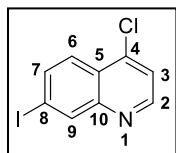


Pale yellow solid; yield: 180 mg (75%); m.p. = 138–139 °C (lit. 138–139 °C); IR (NaCl): ν 3382 (C-H stretch), 1549 (aromatic C-C stretch), 1468 (aromatic C-C stretch), 1340 (C-N stretch), 825 (C-Cl stretch), 570 (C-I stretch) cm^{-1} ; $^1\text{H-NMR}$ (300 MHz, CDCl_3) δ : 7.50 (d, J = 4.7 Hz, 1H, CH-3), 7.84 (d, J = 8.9 Hz, 1H, CH-9), 8.02 (dd, J = 8.9, 1.9 Hz, 1H, CH-8), 8.63 (d, J = 1.9 Hz, 1H, CH-6), 8.79 (d, J = 4.7 Hz, 1H, CH-2); $^{13}\text{C-NMR}$ (75 MHz, CDCl_3) δ : 93.6

(qC-7), 121.8 (CH-3), 128.0 (qC-5), 131.4 (CH-9), 133.1 (CH-6), 139.3 (CH-8), 141.3 (qC-4), 148.1 (qC-10), 150.4 (CH-2); HRMS (ESI-TOF) m/z : $[M+H]^+$ calcd. for C_9H_6ClIN : 289.9234; found: 289.9232.

Spectral data were consistent with those reported in the literature.

4-Chloro-7-iodoquinoline^[96] (160)

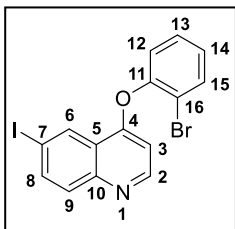


Pale yellow solid; yield: 195 mg (81%); m.p. = 99–101 °C (lit. 101–102 °C); IR (NaCl): ν 3399 (C-H stretch), 1576 (aromatic C-C stretch), 1547 (aromatic C-C stretch), 1365 (C-N stretch), 824 (C-Cl stretch), 576 (C-I stretch) cm^{-1} ; 1H -NMR (300 MHz, $CDCl_3$) δ : 7.51 (d, J = 4.7 Hz, 1H, CH-3), 7.88–7.99 (m, 2H, CH-6, CH-7), 8.56 (d, J = 1.1 Hz, 1H, CH-9), 8.77 (d, J = 4.7 Hz, 1H, CH-2); ^{13}C -NMR (75 MHz, $CDCl_3$) δ : 96.8 (qC-8), 121.7 (CH-3), 125.3 (CH-6), 125.6 (qC-5), 136.3 (CH-7), 138.8 (CH-9), 142.8 (qC-4), 1497 (qC-10), 150.6 (CH-2); HRMS (ESI-TOF) m/z : $[M+H]^+$ calcd. for C_9H_6ClIN : 289.9234; found: 289.9230.

Spectral data were consistent with those reported in the literature.

4-(2-Bromophenoxy)-6-iodoquinoline (161)

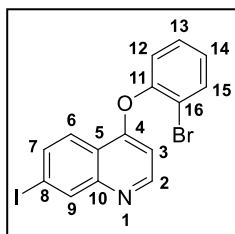
Synthesised according to the same procedure as for the other 4-phenoxyquinoline substrates (page 187) using 6-iodo-4-chloroquinoline 159.



Pale yellow solid; yield: 119 mg (78%); m.p. = 85–87 °C; IR (NaCl): ν 3392 (C-H stretch), 1585 (aromatic C-C stretch), 1468 (aromatic C-C stretch), 1348 (C-N stretch), 1094 (C-O stretch), 665 (C-Br stretch), 555 (C-I stretch) cm^{-1} ; 1H -NMR (300 MHz, $CDCl_3$) δ : 6.39 (d, J = 5.2 Hz, 1H, CH-3), 7.18–7.28 (m, 2H, CH-12, CH-14), 7.39–7.49 (m, 1H, CH-13), 7.73 (dd, J = 8.3, 1.6 Hz, 1H, CH-15), 7.83 (d, J = 8.9 Hz, 1H, CH-9), 8.01 (dd, J = 8.9, 2.0 Hz, 1H, CH-8), 8.66 (d, J = 4.9 Hz, 1H, CH-2), 8.81 (d, J = 1.9 Hz, 1H, CH-6); ^{13}C -NMR (75 MHz, $CDCl_3$) δ : 91.8 (qC-7), 104.1 (CH-3), 116.4 (qC-16), 122.6 (qC-5), 123.3 (CH-12), 127.6 (CH-14), 129.3 (CH-13), 130.8 (CH-9), 130.9 (CH-6), 134.4 (CH-15), 139.0 (CH-8), 148.7 (qC-10), 150.8 (qC-11), 151.5 (CH-2), 159.5 (qC-4); HRMS (ESI-TOF) m/z : $[M+H]^+$ calcd. for $C_{15}H_{10}BrINO$: 425.8991; found: 425.9001.

4-(2-Bromophenoxy)-7-iodoquinoline (162)

Synthesised according to the same procedure as for the other 4-phenoxyquinoline substrates (page 187) using 7-iodo-4-chloroquinoline **160**.

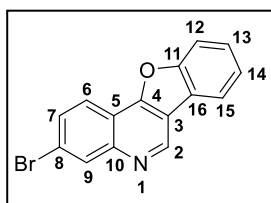


Pale yellow solid; yield: 134 mg (91%); m.p. = 113–115 °C; IR (NaCl): ν 3387 (C-H stretch), 1557 (aromatic C-C stretch), 1468 (aromatic C-C stretch), 1299 (C-N stretch), 1219 (C-O stretch), 665 (C-Br stretch), 575 (C-I stretch) cm^{-1} ; $^1\text{H-NMR}$ (300 MHz, CDCl_3) δ : 6.41 (d, $J = 5.2$ Hz, 1H, CH-3), 7.16–7.29 (m, 2H, CH-12, CH-14), 7.39–7.48 (m, 1H, CH-13), 7.73 (dd, $J = 7.8, 1.4$ Hz, 1H, CH-15), 7.87 (dd, $J = 8.8, 1.7$ Hz, 1H, CH-7), 8.13 (d, $J = 8.8$ Hz, 1H, CH-6), 8.54 (d, $J = 1.6$ Hz, 1H, CH-9), 8.64 (d, $J = 5.2$ Hz, 1H, CH-2); $^{13}\text{C-NMR}$ (75 MHz, CDCl_3) δ : 96.7 (qC-8), 104.1 (CH-3), 116.3 (qC-16), 120.2 (qC-5), 123.2 (CH-6), 123.3 (CH-12), 127.5 (CH-14), 129.3 (CH-13), 134.4 (CH-15), 135.0 (CH-7), 138.1 (CH-9), 150.5 (qC-10), 150.8 (qC-11), 151.8 (CH-2), 160.9 (qC-4); HRMS (ESI-TOF) m/z : $[\text{M}+\text{H}]^+$ calcd. for $\text{C}_{15}\text{H}_{10}\text{BrINO}$: 425.8991; found: 425.8982.

3.30. Synthesis of Compound 163

3-Bromobenzofuro[3,2-*c*]quinoline (163)

A mixture of **121** (1 equiv.), Pd(QPhos)₂ (5 mol%), QPhos (10 mol%) and PMP (2 equiv.) in anhydrous 1,4-dioxane (5 mL/mmol) was stirred at 125 °C in a sealed reaction tube under a nitrogen atmosphere. The reaction was periodically monitored by ¹H-NMR analysis, and additional Pd(QPhos)₂ and QPhos were added whenever the reaction seemed to stop progressing. Once the majority of the starting material was consumed and the cyclised product constituted the majority of the reaction mixture (72 h), the reaction was ceased. The cooled reaction mixture was diluted with DCM, filtered through a short plug of Celite and concentrated *in vacuo*. The crude mixture was purified by column chromatography (DCM/EtOAc 99:1–95:5) to yield the product **163** as a white solid (0.021 mg, 13%).



White solid; yield: 21 mg (13%); m.p. = 166–167 °C; IR (NaCl): ν 2921 (C-H stretch), 1558 (aromatic C-C stretch), 1449 (aromatic C-C stretch), 1369 (C-N stretch), 1186 (C-O stretch), 738 (C-Br stretch) cm⁻¹; ¹H-NMR (300 MHz, CDCl₃) δ : 7.44–7.62 (m, 2H, CH-13, CH-14), 7.71–7.83 (m, 2H, CH-7, CH-12), 8.10 (dd, *J* = 7.6, 0.8 Hz, 1H, CH-15), 8.29 (d, *J* = 8.8 Hz, 1H, CH-6), 8.46 (d, *J* = 1.8 Hz, 1H, CH-9), 9.49 (s, 1H, CH-2); ¹³C-NMR (75 MHz, CDCl₃) δ : 112.2 (CH-12), 115.8 (qC-5), 116.7 (qC-3), 120.7 (CH-15), 122.1 (CH-6), 122.4 (qC-16), 123.4 (qC-8), 124.3 (CH-14), 127.6 (CH-13), 130.5 (CH-7), 132.3 (CH-9), 145.4 (CH-2), 148.0 (qC-10), 156.0 (qC-11), 157.3 (qC-4); HRMS (ESI-TOF) *m/z*: [M+H]⁺ calcd. for C₁₅H₉BrNO: 297.9862; found: 297.9865.

3.31. Chapter 3 References

1. Y. Nishihara *Applied cross-coupling reactions*, Vol. 80, Springer Science & Business Media, **2012**.
2. D. A. Horton, G. T. Bourne, M. L. Smythe, *Chem. Rev.* **2003**, *103*, 893-930.
3. J. Stille, *Angew. Chem.* **1986**, *98*, 504-519.
4. S. L. Buchwald, K. Fugami, T. Hiyama, M. Kosugi, M. Miura, N. Miyauro, A. Muci, M. Nomura, E. Shirakawa, K. Tamao *Cross-coupling reactions: a practical guide*, Vol. 219, Springer, **2003**.
5. T.-Y. Luh, M.-k. Leung, K.-T. Wong, *Chem. Rev.* **2000**, *100*, 3187-3204.
6. J. Hassan, M. Sévignon, C. Gozzi, E. Schulz, M. Lemaire, *Chem. Rev.* **2002**, *102*, 1359-1470.
7. N. Miyauro, A. Suzuki, *Chem. Rev.* **1995**, *95*, 2457-2483.
8. D. Milstein, J. Stille, *J. Am. Chem. Soc.* **1978**, *100*, 3636-3638.
9. E.-I. Negishi, *Acc. Chem. Res.* **1982**, *15*, 340-348.
10. D. Alberico, M. E. Scott, M. Lautens, *Chem. Rev.* **2007**, *107*, 174-238.
11. G. P. McGlacken, L. M. Bateman, *Chem. Soc. Rev.* **2009**, *38*, 2447-2464.
12. L. Ackermann, R. Vicente, A. R. Kapdi, *Angew. Chem. Int. Ed.* **2009**, *48*, 9792-9826.
13. D. J. C. Constable, P. J. Dunn, J. D. Hayler, G. R. Humphrey, J. J. L. Leazer, R. J. Linderman, K. Lorenz, J. Manley, B. A. Pearlman, A. Wells, A. Zaks, T. Y. Zhang, *Green Chem.* **2007**, *9*, 411-420.
14. C. S. Yeung, V. M. Dong, *Chem. Rev.* **2011**, *111*, 1215-1292.
15. B. Liégault, D. Lee, M. P. Huestis, D. R. Stuart, K. Fagnou, *J. Org. Chem.* **2008**, *73*, 5022-5028.
16. H. Li, R.-Y. Zhu, W.-J. Shi, K.-H. He, Z.-J. Shi, *Org. Lett.* **2012**, *14*, 4850-4853.
17. X.-S. Xue, P. Ji, B. Zhou, J.-P. Cheng, *Chem. Rev.* **2017**, *117*, 8622-8648.
18. M. Kondrashov, D. Provost, O. F. Wendt, *Dalton Trans.* **2016**, *45*, 525-531.
19. L.-C. Campeau, M. Parisien, A. Jean, K. Fagnou, *J. Am. Chem. Soc.* **2006**, *128*, 581-590.
20. M.-T. Nolan, L. M. Pardo, A. M. Prendergast, G. P. McGlacken, *J. Org. Chem.* **2015**, *80*, 10904-10913.

21. L.-C. Campeau, M. Parisien, M. Leblanc, K. Fagnou, *J. Am. Chem. Soc.* **2004**, *126*, 9186-9187.
22. K. Mackey, L. M. Pardo, A. M. Prendergast, M.-T. Nolan, L. M. Bateman, G. P. McGlacken, *Org. Lett.* **2016**, *18*, 2540-2543.
23. M.-T. Nolan, J. T. W. Bray, K. Eccles, M. S. Cheung, Z. Lin, S. E. Lawrence, A. C. Whitwood, I. J. S. Fairlamb, G. P. McGlacken, *Tetrahedron* **2014**, *70*, 7120-7127.
24. Y. Yang, J. Lan, J. You, *Chem. Rev.* **2017**, *117*, 8787-8863.
25. R. Rossi, F. Bellina, M. Lessi, C. Manzini, *Adv. Synth. Catal.* **2014**, *356*, 17-117.
26. D. Ames, A. Opalko, *Tetrahedron* **1984**, *40*, 1919-1925.
27. W. S. Yoon, S. J. Lee, S. K. Kang, D.-C. Ha, J. Du Ha, *Tetrahedron Lett.* **2009**, *50*, 4492-4494.
28. A. M. Prendergast, G. P. McGlacken, *Eur. J. Org. Chem.* **2018**, *2018*, 6068-6082.
29. A. M. Prendergast, Z. Zhang, Z. Lin, G. P. McGlacken, *Dalton Trans.* **2018**, *47*, 6049-6053.
30. J. P. Michael, *Nat. Prod. Rep.* **2008**, *25*, 166-187.
31. R. D. Taylor, M. MacCoss, A. D. G. Lawson, *J. Med. Chem.* **2014**, *57*, 5845-5859.
32. G. Jones *The Chemistry of Heterocyclic Compounds - Quinolines*, Vol. 104, Wiley, **2009**.
33. T. Iwai, M. Sawamura, *ACS Catal.* **2015**, *5*, 5031-5040.
34. Y.-L. Chen, C.-H. Chung, I. L. Chen, P.-H. Chen, H.-Y. Jeng, *Bioorg. Med. Chem.* **2002**, *10*, 2705-2712.
35. Z. Xiao, N. C. Waters, C. L. Woodard, Z. Li, P.-K. Li, *Bioorg. Med. Chem. Lett.* **2001**, *11*, 2875-2878.
36. M. Zhao, T. Kamada, A. Takeuchi, H. Nishioka, T. Kuroda, Y. Takeuchi, *Bioorg. Med. Chem. Lett.* **2015**, *25*, 5551-5554.
37. F. Hong, Y. Chen, B. Lu, J. Cheng, *Adv. Synth. Catal.* **2016**, *358*, 353-357.
38. M. K. Mehra, M. P. Tantak, I. Kumar, D. Kumar, *Synlett* **2016**, *27*, 604-610.
39. M. Ye, G.-L. Gao, A. J. F. Edmunds, P. A. Worthington, J. A. Morris, J.-Q. Yu, *J. Am. Chem. Soc.* **2011**, *133*, 19090-19093.
40. Y. Hayashi, *Chem. Sci.* **2016**, *7*, 866-880.

41. C. Vaxelaire, P. Winter, M. Christmann, *Angew. Chem. Int. Ed.* **2011**, *50*, 3605-3607.
42. R. Robinson, *J. Chem. Soc., Trans.* **1917**, *111*, 762-768.
43. R. Willstätter, *Ber. Dtsch. Chem. Ges.* **1901**, *34*, 129-144.
44. C. Grondal, M. Jeanty, D. Enders, *Nat. Chem.* **2010**, *2*, 167-178.
45. T. Mukaiyama, H. Ishikawa, H. Koshino, Y. Hayashi, *Chem. Eur. J.* **2013**, *19*, 17789-17800.
46. Y. Hayashi, S. Ogasawara, *Org. Lett.* **2016**, *18*, 3426-3429.
47. X. Ma, N. Gu, Y. Liu, P. Liu, J. Xie, B. Dai, Z. Liu, *Appl. Organomet. Chem.* **2015**, *29*, 50-56.
48. K. Matsumura, S. Yoshizaki, M. M. Maitani, Y. Wada, Y. Ogomi, S. Hayase, T. Kaiho, S. Fuse, H. Tanaka, T. Takahashi, *Chem. Eur. J.* **2015**, *21*, 9742-9747.
49. L. Ren, W. Chu, D. Guan, Y. Hou, M. Wang, X. Yuan, Z. Sun, *Appl. Organomet. Chem.* **2014**, *28*, 673-677.
50. A. El Akkaoui, S. Berteina-Raboin, A. Mouaddib, G. Guillaumet, *Eur. J. Org. Chem.* **2010**, *2010*, 862-871.
51. J. Koubachi, S. El Kazzouli, S. Berteina-Raboin, A. Mouaddib, G. Guillaumet, *J. Org. Chem.* **2007**, *72*, 7650-7655.
52. L. M. Geary, P. G. Hultin, *Org. Lett.* **2009**, *11*, 5478-5481.
53. W.-Y. Wang, X. Feng, B.-L. Hu, C.-L. Deng, X.-G. Zhang, *J. Org. Chem.* **2013**, *78*, 6025-6030.
54. D. I. Chai, M. Lautens, *J. Org. Chem.* **2009**, *74*, 3054-3061.
55. N. Nicolaus, P. T. Franke, M. Lautens, *Org. Lett.* **2011**, *13*, 4236-4239.
56. P. Dobrounig, M. Trobe, R. Breinbauer, *Monatsh. Chem.* **2017**, *148*, 3-35.
57. D. F. McMillen, D. M. Golden, *Annu. Rev. Phys. Chem.* **1982**, *33*, 493-532.
58. M. Lautens, Y.-Q. Fang, *Org. Lett.* **2003**, *5*, 3679-3682.
59. Y.-Q. Fang, M. Lautens, *J. Org. Chem.* **2008**, *73*, 538-549.
60. T. Saget, D. Perez, N. Cramer, *Org. Lett.* **2013**, *15*, 1354-1357.
61. S. G. Newman, M. Lautens, *J. Am. Chem. Soc.* **2010**, *132*, 11416-11417.
62. A. H. Roy, J. F. Hartwig, *J. Am. Chem. Soc.* **2001**, *123*, 1232-1233.

63. A. H. Roy, J. F. Hartwig, *J. Am. Chem. Soc.* **2003**, *125*, 13944-13945.
64. A. H. Roy, J. F. Hartwig, *Organometallics* **2004**, *23*, 1533-1541.
65. S. G. Newman, M. Lautens, *J. Am. Chem. Soc.* **2011**, *133*, 1778-1780.
66. Y. Lan, P. Liu, S. G. Newman, M. Lautens, K. Houk, *Chem. Sci.* **2012**, *3*, 1987-1995.
67. S. G. Newman, J. K. Howell, N. Nicolaus, M. Lautens, *J. Am. Chem. Soc.* **2011**, *133*, 14916-14919.
68. D. A. Petrone, M. Lischka, M. Lautens, *Angew. Chem. Int. Ed.* **2013**, *52*, 10635-10638.
69. X. Jia, D. A. Petrone, M. Lautens, *Angew. Chem. Int. Ed.* **2012**, *51*, 9870-9872.
70. D. A. Petrone, H. A. Malik, A. Clemenceau, M. Lautens, *Org. Lett.* **2012**, *14*, 4806-4809.
71. N. I. Shank, H. H. Pham, A. S. Waggoner, B. A. Armitage, *J. Am. Chem. Soc.* **2012**, *135*, 242-251.
72. L. Shi, T.-T. Wu, Z. Wang, J.-Y. Xue, Y.-G. Xu, *Eur. J. Med. Chem.* **2014**, *84*, 698-707.
73. A. J. Pickard, F. Liu, T. F. Bartenstein, L. G. Haines, K. E. Levine, G. L. Kucera, U. Bierbach, *Chem. Eur. J.* **2014**, *20*, 16174-16187.
74. C. H. Burgos, T. E. Barder, X. Huang, S. L. Buchwald, *Angew. Chem.* **2006**, *118*, 4427-4432.
75. H. Kaida, T. Goya, Y. Nishii, K. Hirano, T. Satoh, M. Miura, *Org. Lett.* **2017**, *19*, 1236-1239.
76. F. Ji, X. Li, W. Wu, H. Jiang, *J. Org. Chem.* **2014**, *79*, 11246-11253.
77. L. R. Whittell, K. T. Batty, R. P. Wong, E. M. Bolitho, S. A. Fox, T. M. Davis, P. E. Murray, *Bioorg. Med. Chem.* **2011**, *19*, 7519-7525.
78. N. Wang, M. Świtalska, M.-Y. Wu, K. Imai, T. A. Ngoc, C.-Q. Pang, L. Wang, J. Wietrzyk, T. Inokuchi, *Eur. J. Med. Chem.* **2014**, *78*, 314-323.
79. B. J. Margolis, K. A. Long, D. L. Laird, J. C. Ruble, S. R. Pulley, *J. Org. Chem.* **2007**, *72*, 2232-2235.
80. T. Okamoto, H. Hayatsu, Y. Baba, *Chem. Pharm. Bull.* **1960**, *8*, 892-899.
81. T. Zheng, H. Liao, J. Gao, L. Zhong, H. Gao, Q. Wu, *Polymer Chemistry* **2018**, *9*, 3088-3097.
82. T. Torigoe, T. Ohmura, M. Suginome, *Angew. Chem. Int. Ed.* **2017**, *56*, 14272-14276.

83. S. Würtz, C. Lohre, R. Fröhlich, K. Bergander, F. Glorius, *J. Am. Chem. Soc.* **2009**, *131*, 8344-8345.
84. M. Tajbakhsh, R. Hosseinzadeh, H. Alinezhad, S. Ghahari, A. Heydari, S. Khaksar, *Synthesis* **2011**, *2011*, 490-496.
85. R. A. da Silva, I. H. Estevam, L. W. Bieber, *Tetrahedron Lett.* **2007**, *48*, 7680-7682.
86. M. A. Topchiy, A. F. Asachenko, M. S. Nechaev, *Eur. J. Org. Chem.* **2014**, *2014*, 3319-3322.
87. J. P. Heiskanen, A. E. Tolkki, H. J. Lemmetyinen, O. E. O. Hormi, *J. Mater. Chem.* **2011**, *21*, 14766-14775.
88. A. V. Aksenov, D. A. Aksenov, N. A. Orazova, N. A. Aksenov, G. D. Griaznov, A. De Carvalho, R. Kiss, V. Mathieu, A. Kornienko, M. Rubin, *J. Org. Chem.* **2017**, *82*, 3011-3018.
89. R. M. Shanahan, A. Hickey, L. M. Bateman, M. E. Light, G. P. McGlacken, *J. Org. Chem.* **2020**, *85*, 2585-2596.
90. A. A. Altaf, A. Shahzad, Z. Gul, N. Rasool, A. Badshah, B. Lal, E. Khan, *J. Drug Des. Med. Chem.* **2015**, *1*, 1-11.
91. K. M. Engle, J.-Q. Yu, *J. Org. Chem.* **2013**, *78*, 8927-8955.
92. F. Shibahara, T. Murai, *Asian J. Org. Chem.* **2013**, *2*, 624-636.
93. D. E. Butler, P. Bass, I. C. Nordin, F. P. Hauck, Y. J. L'Italien, *J. Med. Chem.* **1971**, *14*, 575-579.
94. A. Klapars, S. L. Buchwald, *J. Am. Chem. Soc.* **2002**, *124*, 14844-14845.
95. A. J. Lin, T. L. Loo, *J. Med. Chem.* **1978**, *21*, 268-272.
96. A. E. Conroy, H. S. Mosher, F. C. Whitmore, *J. Am. Chem. Soc.* **1949**, *71*, 3236-3237.

General Conclusions

In Chapter 1, analogues of HHQ were synthesised with substitutions on the aryl ring, methylation at the nitrogen and oxygen atoms, a C-3 substituted quinazolinone analogue, and a HHQ analogue with a terminal alkene on the heptyl chain at C-2. An improved route to access 6-NO₂ HHQ via regioselective nitration of HHQ was developed, and the secondary and tertiary methylated analogues of Hartmann's antagonist were prepared. Through a collaboration with the BIOMERIT Research Centre at UCC, many of the HHQ analogues were shown to display antismearing activity towards the soil bacterium *B. atrophaeus*, and antibiofilm activity towards pathogenic species of fungi (*A. fumigatus*) and yeast (*C. albicans*). A study involving the C-3 substituted 6-NO₂ HHQ analogues elaborated on the role played by the C-3 position of AHQs in suppression of PqsR activation.

Chapter 2 described a new route towards the total synthesis of the nAChR agonist PHT which was developed during a placement project undertaken at Syngenta Crop Protection in Stein, Switzerland. After devising and pursuing two different retrosynthetic plans, the first six steps were optimised to produce good to excellent yields of the intermediate compounds. The key [3+2] cycloaddition step, which was required to access the bridged bicyclic framework of PHT, worked efficiently. Unfortunately, decarboxylation of the PHT substrate could not be achieved despite several attempts using various different approaches. A proof-of-concept debenzoylation indicated that if the challenges of the decarboxylation step could be overcome, the target compound PHT would indeed be accessible using this novel synthetic route.

The application of direct arylation methodology towards the synthesis of fused benzofuroquinoline products was demonstrated in Chapter 3. No added phosphine was required and the reactions were carried out in air. Using dibrominated substrates, a new one-pot tandem reaction was discovered, whereby a Suzuki-Miyaura coupling and direct arylation reaction occur on the same substrate, without requiring additional reagents or catalyst. Again, this tandem reaction occurs in the absence of added ligand and in air. Finally, reversible oxidative conditions allowed for the isolation of the C-7 brominated product of the direct arylation reaction.

Appendix I

Publications from Chapter 1



Cite this: DOI: 10.1039/c5ob00315f

A structure activity-relationship study of the bacterial signal molecule HHQ reveals swarming motility inhibition in *Bacillus atrophaeus*†

F. Jerry Reen,^a Rachel Shanahan,^b Rafael Cano,^b Fergal O'Gara^{*a,c} and Gerard P. McGlacken^{*b}

The sharp rise in antimicrobial resistance has been matched by a decline in the identification and clinical introduction of new classes of drugs to target microbial infections. Thus new approaches are being sought to counter the pending threat of a post-antibiotic era. In that context, the use of non-growth limiting small molecules, that target virulence behaviour in pathogens, has emerged as a solution with real clinical potential. We have previously shown that two signal molecules (HHQ and PQS) from the nosocomial pathogen *Pseudomonas aeruginosa* have modulatory activity towards other microorganisms. This current study involves the synthesis and evaluation of analogues of HHQ towards swarming and biofilm virulence behaviour in *Bacillus atrophaeus*, a soil bacterium and co-inhibitor with *P. aeruginosa*. Compounds with altered C6–C8 positions on the anthranilate-derived ring of HHQ, display a surprising degree of biological specificity, with certain candidates displaying complete motility inhibition. In contrast, anti-biofilm activity of the parent molecule was completely lost upon alteration at any position indicating a remarkable degree of specificity and delineation of phenotype.

Received 13th February 2015,

Accepted 9th April 2015

DOI: 10.1039/c5ob00315f

www.rsc.org/obc

Introduction

Quinolones are fused heterocyclic compounds that form the active structure of a wide range of potent broad-spectrum antimicrobial agents.¹ In fact, fluoroquinolones are the most successful non-natural product class of antibiotics.² Another important class of quinolones are the 2-alkyl-4-quinolones (AHQs) which are used as quorum sensing (QS) signaling molecules by pathogenic Gram-negative bacteria, including *Pseudomonas aeruginosa*,^{3,4} and certain *Burkholderia*,⁵ and *Alteromonas*⁶ strains. AHQ signaling pathways in these species have been shown to control production of multiple virulence determinants.^{7–9} This includes biofilm formation^{10,11} which is a structured community of bacterial cells enclosed in a self-produced polymeric matrix adhering to an inert or living surface.^{12,13} This mode of growth is particularly resistant to phagocytosis by white blood cells and to antibodies and antibiotics compared to planktonic cells.¹³ In multi-drug resistant

bacteria, biofilms play a key role in allowing the pathogen to overcome host defences and contribute to its virulence. The primary autoinducers of the *P. aeruginosa* AHQ signalling pathway are 2-heptyl-4-quinolone (referred to as the *Pseudomonas* quinolone signal, or PQS) and its biological precursor 2-heptyl-4-quinolone (HHQ) (Fig. 1)¹¹ and PQS has been shown to mediate biofilm formation in *P. aeruginosa*.⁷

Bacillus atrophaeus (also named *B. globigii* and previously *B. subtilis*) is a Gram positive bacterium which co-inhabits the soil environment with *P. aeruginosa*.¹⁴ It is indistinguishable from the typed *B. subtilis* strain except for the production of pigment, a feature that marks the organism as particularly useful in the phenotypic analysis described here. *Bacillus subtilis* species are an excellent and well-utilised model system for Gram positive bacteria, and a cross-species influence with *P. aeruginosa* has been shown.^{15–17} In light of the co-existence of both *B. atrophaeus* and *P. aeruginosa* in the soil, it is perhaps unsurprising that communication mechanisms

^aBIOMERIT Research Centre, Department of Microbiology, University College Cork, Ireland. E-mail: f.ogara@ucc.ie; Fax: +353 21 4903101

^bDepartment of Chemistry and Analytical & Biological Chemistry Research Facility (ABCRF), University College Cork, Ireland. E-mail: g.mcglacken@ucc.ie; Fax: +353 21 4274097

^cSchool of Biomedical Sciences, Curtin University, Perth, WA 6845, Australia

†Electronic supplementary information (ESI) available. See DOI: 10.1039/c5ob00315f

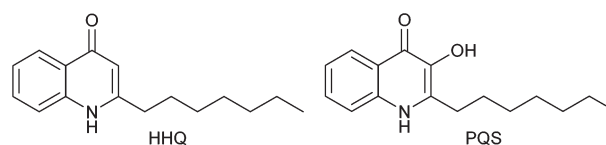
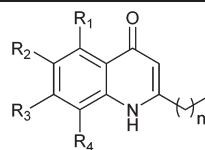


Fig. 1 *P. aeruginosa* signalling molecules HHQ and PQS.

Table 1 2-Alkyl-4-quinolones studied



Compound	<i>n</i>	R ₁	R ₂	R ₃	R ₄	Yield ^a [%]
1	6	H	Me	H	H	31
2	6	H	<i>n</i> -Hex	H	H	35
3	6	H	H	-CH-CH-CH-CH-	H	46
4	6	H	H	H	OMe	12
5	6	H	H	OMe	H	33
6	6	H	OMe	H	H	34
7	6	H	Cl	H	H	21
8	6	H	H	H	Cl	19
9	8	H	H	H	H	23
10	8	H	OMe	H	H	28
11	8	H	F	H	H	16
12	8	H	H	-CH-CH-CH-CH-	H	51
13	8	H	<i>n</i> -Hex	H	H	16

^a % yields are isolated yields over two steps.

between both organisms would exist and this type of community dynamic and microbiome has received considerable attention.¹⁸ However, the extent of these networks and molecular mechanisms remain to be ascertained. From a microbial control point of view, suppression of key virulence phenotypes in bacteria, independent of growth inhibition, should be less susceptible to the build-up of resistance than with traditional antibiotic treatment as metabolic processes and bacterial growth are not directly targeted.

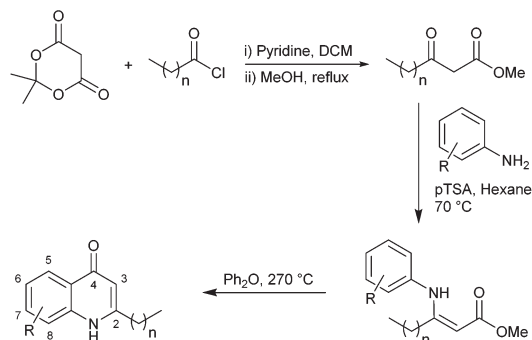
The SAR analysis presented in this study represents the preliminary steps in delineating the action of AHQs towards Gram positive bacteria, potentially providing a platform for future therapeutic developments.

Results and discussion

In light of the important roles played by PQS and HHQ in virulence, both molecules have been the subject of a number of structure–activity relationship (SAR) analyses in recent years.^{9,15,16,19} A study carried out by Hodgkinson's group showed evidence that the PQS regulator protein (PqsR), iron-chelating ability (specifically PqsR-independent production of pyoverdine) and membrane vesicle formation are altered upon changes to the PQS framework.¹⁹ For example, shortening or lengthening the C2 alkyl chain decreased activation of PqsR and substitution of the anthranilate ring compromised either the specific signalling, or membrane vesicle promotion. This indicates that there are multiple signalling mechanisms by which HHQ and PQS may possibly act. Antagonism of biofilm formation or any cross-species effects were not reported. A structure–activity investigation carried out by Reen *et al.*

focused on substitution of the C-3 position.¹⁶ HHQ was shown to inhibit biofilm formation in species that inhabit the same environment as *P. aeruginosa* whereas PQS and 3-halo-analogues did not. Very recently Steinbach and Hartmann also reported 'blocking' the C-3 position thus preventing hydroxylation to a PQS analogue.²⁰ Following on from their initial investigations, a simple quinolone was elegantly designed to target PqsR, and subsequently displayed antivirulence activity *in vivo*.

In the current work, we generated a diverse range of novel HHQ analogues by using derivatized anthranilates and, in some cases, by extension of the alkyl chain at C-2 from seven to nine carbons (Table 1). HHQ analogues were prepared using a procedure similar to that described by Somanathan *et al.*,²¹ and us,²² involving a Conrad–Limpach type cyclisation. Thus β-keto-esters were prepared by acylation of Meldrum's acid (2,2-dimethyl-1,3-dioxane-4,6-dione) with octanoyl chloride or decanoyl chloride, followed by methanolysis (Scheme 1). Condensation with a variety of anilines in the presence of acid using a Dean–Stark apparatus and subsequent cyclisation of the enamine at reflux in diphenyl ether gave the corresponding 2-heptyl- (1–8) or 2-nonyl-4-quinolone (9–13). During the course of this work, an alternative method for accessing the enamine intermediate was also used.²³ On occasion, this method provided a more efficient route. As mentioned earlier, *B. atrophaeus* was selected due to its co-existence with *P. aeruginosa* in the soil. Additionally, the organism is widely used as a surrogate for *B. anthracis* investigations in biodefense research,²⁴ as well as being used as a sterilisation control strain in industry.²⁵ *B. atrophaeus* also exhibits strong swarming and biofilm phenotypes that are characteristic of the multicellular behaviour underpinning virulence in many



Scheme 1 Synthesis of anthranilate-substituted 2-alkyl-4-quinolone.

pathogens.²⁶ Firstly, growth of *B. atrophaeus* was investigated in the presence of HHQ, PQS and the suite of analogues. Prepared in honeycomb 100-well plates, in TSB supplemented with 10 μ M of compound or equivalent volume of methanol as control, all readings were taken on a BioScreen Analyser.

Growth of *B. atrophaeus* was not significantly altered in the presence of any of the modified analogues (SM Fig. 1) and thus any virulence effects were likely to be growth independent. Swarming motility is a key multicellular behaviour in bacteria, considered a virulence phenotype in many organ-

isms²⁷ and underpinned by both intra and intercellular signalling. In the case of *B. atrophaeus*, swarming cells are joined in chain formations and the phenotype is promoted by the secretion of surfactant ahead of the swarm front.^{28,29} Previously, we showed that addition of PQS to swarm plates completely abolished swarming motility in *B. atrophaeus*, while addition of HHQ led to little reduction in this key virulence phenotype.¹⁵ However in the study reported herein, addition of HHQ analogues (1–13) to swarming media led to a significant alteration in activity compared to the parent compound HHQ. Remarkably, some analogues exhibited PQS like inhibition, while others had the effect of promoting swarming activity in the model organism (Fig. 2). Of the compounds tested, compounds 1, 3, 4, 6, 8, 12 and 14 led to a phenotype statistically similar to that observed with the carrier control MeOH. Quinolones 2, 5, 9, 11 and 13 gave a moderate decrease in swarming, whereas quinolones 7 and 10 completely abrogated swarming activity in *B. atrophaeus* as shown in Fig. 2. Overall substitution at the 6-position afforded the most response. In compounds with a C-2 heptyl chain, an electron withdrawing group (7) gave a dramatic decrease in swarming. Interestingly, this is consistent with Hartmann's observation, where a nitro group at the 6-position gave antagonistic behaviour in *P. aeruginosa*.²⁰ When we prepared an analogue possessing an electron releasing group (6) no decrease in swarming was observed.

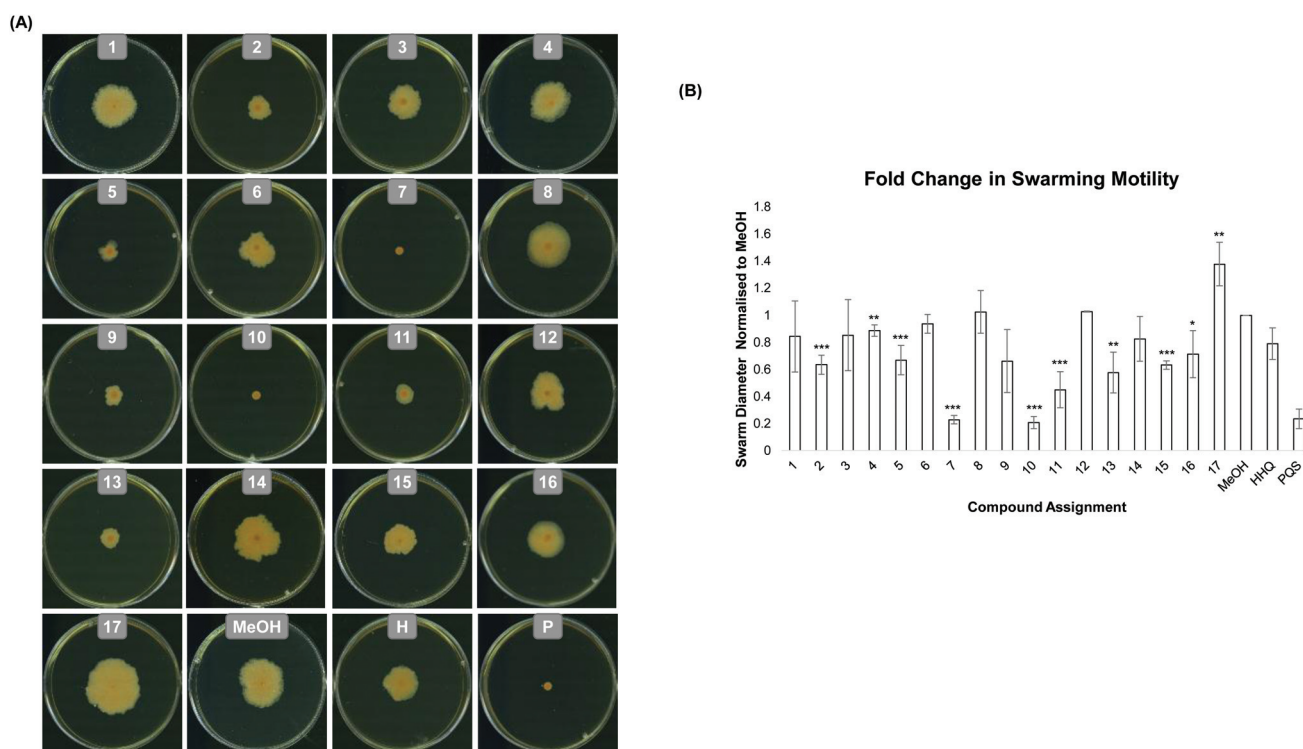
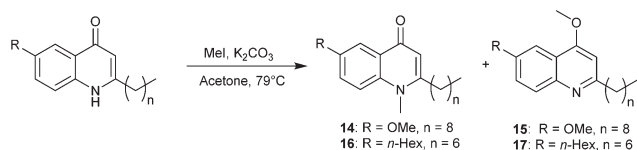


Fig. 2 Swarming motility of *B. atrophaeus* is modulated by HHQ, PQS and their analogues on 0.3% agar (w/v) TSA plates. Measurements reflect the total diameter of the swarm mass, and incorporates the point of inoculation which was performed by sterile toothpick. (A) is a visual representation of swarming motility in the presence of each analogue while (B) is a graphical representation of the combined data. All experimental datapoints represent the mean of at least 5 independent biological replicates. Error is presented as standard error of the mean and statistical analysis was performed using Student's *t*-test and Bootstratio analysis (* $p < 0.05$, ** $p < 0.005$, *** $p < 0.001$).



Scheme 2 Synthesis of *N*- and *O*-methylated compounds.

Remarkably, extension of the C-2 alkyl chain in the non-inhibitory analogue, afforded a molecule (**10**) capable of returning anti-motility behaviour.³⁰

4-Quinolones such as HHQ exist as two interconverting tautomeric forms (a 4-quinolone and a 4-hydroxyquinoline) and equilibrium tends towards the quinolone form under physiological conditions.³¹ We were intrigued to delineate these two structural isomers and elucidate if either structural form maintained activity if 'frozen out' by methylation at oxygen or nitrogen.

Preparation of the *N*- and *O*-methylated compounds was carried out by reaction of quinolone substrate **10** with methyl iodide in acetone and K₂CO₃. The resulting isomeric mixture was purified by column chromatography to afford the desired products **14** (quinolone) and **15** (quinoline) in 14 and 42% respectively (Scheme 2). When tested on *B. atrophaeus*, both compounds had lost anti-swarming activity (Fig. 2) relative to the parent quinolone (**10**) but the quinoline form **15** did show a slight enhancement of anti-swarming activity relative to quinolone **14**. We also chose to carry out a similar investigation using quinolone **2**, which displayed enhanced suppression of swarming motility relative to MeOH (and HHQ itself). In this case the *N*-Me derivative **16** (isolated in 10%) again showed little or no variation. However, addition of the *O*-Me variant **17**

(isolated in 37%) led to significant enhancement of swarming motility, in direct contrast to the parent molecule.

Having established the influence of the analogues on swarming motility, it was expected that a similar profile would emerge from an investigation of their impact on biofilm formation. Swarming motility is associated with biofilm formation in many pathogens, sometimes in what is an inverse relationship. Therefore, each analogue was tested for its impact on pellicle formation and attachment in *B. atrophaeus*. Surprisingly, all analogues had lost their anti-pellicle and anti-biofilm formation activity with respect to the parent molecule HHQ. Modification of any part of the quinolone framework led to loss of activity, even for those where suppression of swarming motility was enhanced (Fig. 3).

Conclusions

In this study we prepared a number of analogues of known *P. aeruginosa* signalling molecule HHQ, present in complex multi-bacterial and multi-kingdom environments, and tested them for anti-swarming and anti-biofilm activity towards *B. atrophaeus*. Several of the novel analogues show potent suppression of swarming motility, which suggests some degree of freedom regarding the structural interaction between the quinolone core molecule and the receiving organism. However, the lack of anti-biofilm activity exhibited by all the analogues would suggest that the anti-biofilm activity exhibited by HHQ is highly sensitive to structural modification and may reflect a highly specific protein–ligand interaction.

Previously, HHQ itself has shown very minor anti-swarming activity in a range of organisms in contrast to PQS, which completely abolished swarming activity.¹⁵ Strikingly, modification of the quinolone backbone structure described here, resulted in quinolones possessing potent suppression of swarming, similar to that with PQS. While there is no evidence of a pqsH type-activity encoded in a genome outside of *P. aeruginosa*, and thus no known mechanism for the hydroxylation of our HHQ analogues to PQS analogues,¹⁵ other biosynthetic steps could be at play and our investigations in this area will be published in due course.

Acknowledgements

The authors would like to thank David Woods for technical assistance. This research was supported in part by grants awarded to GMG by Science Foundation of Ireland (SFI) (SFI/12/TIDA/B2405, SFI/12/IP/1315, SFI/09/RFP/CHS2353 and SSPC2 12/RC/2275) and the Irish Research Council and to FOG (SFI: SSPC2 12/RC/2275; 13-TIDA-B2625; 07/ IN.1/B948; 12/TIDA/B2411; 12/TIDA/B2405; 09/RFP/BMT 2350); the Department of Agriculture, Fisheries and Food (DAFF11/F/009 MabS; FIRM/RSF/CoFoRD; FIRM 08/RDC/629); the Environmental Protection Agency (EPA 2008-PhD/S-2); the Irish Research Council for Science, Engineering and Technology

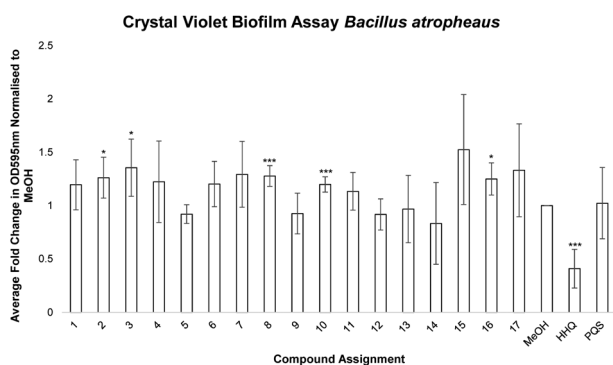
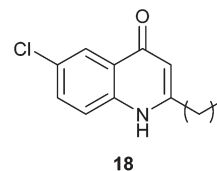


Fig. 3 Biofilm formation by *B. atrophaeus* in the presence of 10 μ M of compound, compared with an equivalent volume of methanol as control. A visualisation of the pellicle formed in the presence of each compound is presented above the graph. Each datapoint, which is presented as fold change in Abs_{595nm} relative to methanol control, is the average of at least 4 independent biological replicates. Error is presented as standard error of the mean and statistical analysis was performed using Student's *t*-test and Bootstratio analysis (* $p < 0.05$, ** $p < 0.005$, *** $p < 0.001$).

(GOIPG/2014/647; PD/2011/2414; RS/2010/2413); the European Commission (H20/20 EU-634486; FP7-PEOPLE-2013-ITN, 607786; OCEAN2012, 287589; FP7-KBBE-2012-6, CP-TP 311975; FP7-KBBE-2012-6, CP-TP-312184; Marie Curie 256596); the Marine Institute (Beaufort award C2CRA 2007/ 082); Teagasc (Walsh Fellowship 2013), the Health Research Board (HRA/2009/146) and the Irish Thoracic Society via the 2014 MRCG/HRB scheme (MRCG/2014/6).

Notes and references

- 1 D. C. Hooper and E. Rubinstein, *Quinolone Antimicrobial Agents*, ASM Press, Washington D.C., 2003.
- 2 D. O'Hagan, *J. Fluorine Chem.*, 2010, **131**, 1071.
- 3 S. Swift, J. A. Downie, N. A. Whitehead, A. M. Barnard, G. P. Salmond and P. Williams, *Adv. Microb. Physiol.*, 2001, **45**, 199.
- 4 C. Fuqua, M. R. Parsek and E. P. Greenberg, *Ann. Rev. Genet.*, 2001, **35**, 439.
- 5 S. P. Diggle, P. Cornelis, P. Williams and M. Camara, *Int. J. Med. Microbiol.*, 2006, **296**, 83.
- 6 R. A. Long, A. Qureshi, D. J. Faulkner and F. Azam, *Appl. Environ. Microbiol.*, 2003, **69**, 568.
- 7 S. P. Diggle, K. Winzer, S. R. Chhabra, K. E. Worrall, M. Camara and P. Williams, *Mol. Microbiol.*, 2003, **50**, 29.
- 8 E. C. Pesci, J. B. J. Milbank, J. P. Pearson, S. McKnight, A. S. Kende, E. P. Greenberg and B. H. Iglewski, *Proc. Natl. Acad. Sci. U. S. A.*, 1999, **96**, 11229.
- 9 L. Mashburn-Warren, J. Howe, K. Brandenburg and M. Whiteley, *J. Bacteriol.*, 2009, **191**, 3411.
- 10 J. F. Dubern and S. P. Diggle, *Mol. Biosyst.*, 2008, **4**, 882.
- 11 S. P. Diggle, S. Matthijs, V. J. Wright, M. P. Fletcher, S. R. Chhabra, I. L. Lamont, X. Kong, R. C. Hider, P. Cornelis, M. Camara and P. Williams, *Chem. Biol.*, 2007, **14**, 87.
- 12 J. W. Costerton, *Int. J. Antimicrob. Agents*, 1999, **11**, 217.
- 13 J. W. Costerton, P. S. Stewart and E. P. Greenberg, *Science*, 1999, **284**, 1318.
- 14 S. A. Burke, J. D. Wright, M. K. Robinson, B. V. Bronk and R. L. Warren, *Appl. Environ. Microbiol.*, 2004, **70**, 2786.
- 15 F. J. Reen, M. J. Mooij, L. J. Holcombe, C. M. McSweeney, G. P. McGlacken, J. P. Morrissey and F. O'Gara, *FEMS Microbiol. Ecol.*, 2011, **77**, 413.
- 16 F. J. Reen, S. L. Clarke, C. Legendre, C. M. McSweeney, K. S. Eccles, S. E. Lawrence, F. O'Gara and G. P. McGlacken, *Org. Biomol. Chem.*, 2012, **10**, 8903.
- 17 Y. Tashiro, S. Ichikawa, T. Nakajima-Kambe, H. Uchiyama and N. Nomura, *Microbes Environ.*, 2010, **25**, 120.
- 18 R. East, *Nature*, 2013, S18–S19, DOI: 10.1038/501S18a.
- 19 J. T. Hodgkinson, S. D. Bowden, W. R. Galloway, D. R. Spring and M. Welch, *J. Bacteriol.*, 2010, **192**, 3833.
- 20 C. Lu, C. K. Maurer, B. Kirsch, A. Steinbach and R. W. Hartmann, *Angew. Chem., Int. Ed.*, 2014, **53**, 1109.
- 21 R. Somanathan and K. M. Smith, *J. Heterocycl. Chem.*, 1981, **18**, 1077.
- 22 G. P. McGlacken, C. M. McSweeney, T. O'Brien, S. E. Lawrence, C. J. Elcoate, F. J. Reen and F. O'Gara, *Tetrahedron Lett.*, 2010, **51**, 5919.
- 23 A. V. Narsaiah, A. R. Reddy, B. V. S. Reddy and J. S. Yadav, *Open Catal. J.*, 2011, **4**, 43.
- 24 S. R. Kane, S. E. Létant, G. A. Murphy, T. M. Alfaro, P. W. Krauter, R. Mahnke, T. C. Legler and E. Raber, *J. Microbiol. Methods*, 2009, **76**, 278.
- 25 S. E. Létant, G. A. Murphy, T. M. Alfaro, J. R. Avila, S. R. Kane, E. Raber, T. M. Bunt and S. R. Shah, *Appl. Environ. Microbiol.*, 2011, **77**, 6570.
- 26 S. T. Rutherford and B. T. Bassler, *Cold Spring Harbor Perspect. Med.*, 2012, **2**(11), 1, DOI: 10.1101/cshperspect.a012427. pii: a012427.
- 27 D. E. Kearns, *Nat. Rev. Microbiol.*, 2010, **8**, 634.
- 28 K. Hamze, S. Autret, K. Hinc, S. Laalami, D. Julkowska, R. Briandet, M. Renault, C. Absalon, I. B. Holland, H. Putzer and S. J. S  ror, *Microbiol.*, 2011, **157**, 2456.
- 29 S. Heeb, M. P. Fletcher, S. R. Chhabra, S. P. Diggle, P. Williams and M. C  mara, *FEMS Microbiol. Rev.*, 2011, **35**, 247.
- 30 One Referee suggested the synthesis and biological testing of compound **18** to delineate the requirement for alteration at the C6 position and the length of the alkyl chain. No anti-swarming activity was observed, further demonstrating the exquisite specificity of the quinolone structure. No anti-biofilm activity was observed.
- 31 P. K. Singh, A. L. Schaefer, M. R. Parsek, T. O. Moninger, M. Welch and E. P. Greenberg, *Nature*, 2000, **407**, 762.



Exploiting Interkingdom Interactions for Development of Small-Molecule Inhibitors of *Candida albicans* Biofilm Formation

F. Jerry Reen,^a John P. Phelan,^a Lorna Gallagher,^a David F. Woods,^a Rachel M. Shanahan,^b Rafael Cano,^b Eoin Ó Muimhneacháin,^b Gerard P. McGlacken,^b Fergal O'Gara^{a,c}

Biomerit Research Centre, School of Microbiology, University College Cork—National University of Ireland, Cork, Ireland^a; School of Chemistry and Analytical and Biological Chemistry Research Facility (ABCRF), University College Cork—National University of Ireland, Cork, Ireland^b; School of Biomedical Sciences, Curtin Health Innovation Research Institute, Curtin University, Perth, Australia^c

A rapid decline in the development of new antimicrobial therapeutics has coincided with the emergence of new and more aggressive multidrug-resistant pathogens. Pathogens are protected from antibiotic activity by their ability to enter an aggregative biofilm state. Therefore, disrupting this process in pathogens is a key strategy for the development of next-generation antimicrobials. Here, we present a suite of compounds, based on the *Pseudomonas aeruginosa* 2-heptyl-4(1H)-quinolone (HHQ) core quinolone interkingdom signal structure, that exhibit noncytotoxic antibiofilm activity toward the fungal pathogen *Candida albicans*. In addition to providing new insights into what is a clinically important bacterium-fungus interaction, the capacity to modularize the functionality of the quinolone signals is an important advance in harnessing the therapeutic potential of signaling molecules in general. This provides a platform for the development of potent next-generation small-molecule therapeutics targeting clinically relevant fungal pathogens.

With the ever-increasing emergence of antibiotic-resistant pathogens and the lack of new antibiotics coming to market, we are entering a “postantibiotic era” (1–3). This realization has underpinned a global initiative to identify new and innovative approaches to infection management. As such, targeting virulence as a potential strategy for developing new antimicrobial drugs has been the focus of several research initiatives (4–11). In principle, suppressing virulence behavior and locking pathogens in a vegetative non-biofilm-forming lifestyle renders them less infective and more susceptible to conventional antibiotics (4, 12). While some success has been achieved against bacterial pathogens (6, 10, 13–19), less focus has been placed on fungal infections, which nevertheless continue to cause serious complications and mortality in patients (8, 20–22). Indeed, despite the medical and economic damage caused by fungal biofilms, there remains an urgent and largely unmet need for the identification of compounds able to specifically and selectively target and inhibit this mode of growth in clinically relevant fungal pathogens (23).

The predominant nosocomial fungal pathogens, which include *Candida* spp., *Aspergillus* spp., and *Fusarium* spp., are difficult to diagnose and cause high morbidity and mortality, even following antifungal therapy (21). *Candida albicans* causes a variety of complications ranging from mucosal disease to deep-seated mycoses, particularly in immunocompromised individuals (21, 24). Along with other fungal and yeast pathogens, *C. albicans* is known to form structured communities called biofilms on medical devices either pre- or postimplantation, leading to recurring infections and in some cases death (25, 26). Once established in the biofilm phase, *C. albicans* presents a significant clinical problem, with current treatment options severely limited by the intrinsic tolerance of fungal biofilms for antimycotics (20, 27, 28). Recent combination therapies incorporating antibacterial and antifungal agents have shown some success (29). However, as with all antibiotic-based strategies, reports of resistance continue to emerge (27), and biofilms themselves are considered a breeding ground for the emergence of antibiotic-resistant strains, effec-

tively hastening the onset of the perfect storm where the rapid decline in new antibiotic production has been met by an equally rapid increase in multidrug-resistant organisms (1). Thus, there is a need to consider new anti-infective strategies that do not target essential processes in the target organism. While blocking biofilms in these organisms remains a major clinical challenge (26, 30), exploiting our increased understanding of microbial signaling networks to control virulence and biofilm behavior is one innovative approach with significant potential.

Many sites of infection are colonized by communities of mixed fungal and bacterial organisms, and several layers of communication significantly impact the dynamics and flux of these populations (31, 32). For example, *C. albicans* is known to coexist with *Pseudomonas aeruginosa* in the cystic fibrosis (CF) lung, and interkingdom communication between the two organisms has previously been reported (16, 33). The *Pseudomonas* quinolone signal (PQS), 2-heptyl-3-hydroxy-4-quinolone, and its biological precursor, 2-heptyl-4-quinolone (HHQ), are important virulence factors produced by *P. aeruginosa*. Structurally, PQS and HHQ differ by the presence of a hydrogen at C-3 in HHQ and a hydroxyl group in PQS, giving rise to the increased interest in modulating

Received 22 January 2016 Returned for modification 21 April 2016

Accepted 1 July 2016

Accepted manuscript posted online 25 July 2016

Citation Reen FJ, Phelan JP, Gallagher L, Woods DF, Shanahan RM, Cano R, Ó Muimhneacháin E, McGlacken GP, O'Gara F. 2016. Exploiting interkingdom interactions for development of small-molecule inhibitors of *Candida albicans* biofilm formation. *Antimicrob Agents Chemother* 60:5894–5905. doi:10.1128/AAC.00190-16.

Address correspondence to Fergal O'Gara, f.ogara@ucc.ie.

F.J.R. and J.P.P. contributed equally to this work.

Supplemental material for this article may be found at <http://dx.doi.org/10.1128/AAC.00190-16>.

Copyright © 2016, American Society for Microbiology. All Rights Reserved.

this position to assign biological function to the structures of the molecules (34–37). Previously, we have shown that HHQ, but not PQS, suppresses biofilm formation by *C. albicans* (10). In response, *C. albicans* produces farnesol, which has been shown to modulate PQS production in *P. aeruginosa* (33). As both PQS and HHQ promote virulence and pathogenicity of *P. aeruginosa* (38, 39), their utility as an anti-*Candida* treatment falls short of being a viable antifungal treatment. However, the amenability of these small molecules to chemical modification provides an opportunity to develop compounds with specificity of function.

The transcriptional data and microscopic imaging described in this study have implicated components of the cell wall as key factors in the response of *C. albicans* to *P. aeruginosa* alkylhydroxyquinolone (AHQ) signaling. Furthermore, the biological activity of each class of analogue in bacterial, fungal, and host systems provides new insight into the possible interkingdom role of AHQs, particularly in a clinical setting such as the CF lung, where all three systems coexist. From a translational perspective, lead HHQ analogues with four key features were identified: (i) they have potent antibiofilm activity toward *C. albicans*, (ii) they have selective noncytotoxicity toward mammalian cell lines, (iii) they are nonagonistic and (iv) they are potentially antagonistic to the virulent pathogen *P. aeruginosa*. Several analogues retained the significant potency of the parent HHQ molecule against *C. albicans* biofilm formation while simultaneously becoming inactive in *P. aeruginosa* quorum sensing. This suggests that these molecules have the potential to be further optimized for use as anti-infectives for *Candida* without the concomitant limitation of *P. aeruginosa* virulence augmentation.

MATERIALS AND METHODS

***C. albicans* stock maintenance and culturing conditions.** *C. albicans* strain SC5314 was subcultured from 15% (vol/vol) glycerol stocks at -80°C onto yeast-peptone-dextrose (YPD) medium (1% [wt/vol] yeast extract, 2% [wt/vol] peptone, and 2% [wt/vol] dextrose) and incubated at 30°C overnight.

***P. aeruginosa* stock maintenance and culturing conditions.** *P. aeruginosa* strains, PAO1 and a *pqsA* mutant, containing the chromosomally inserted *pqsA-lacZ* promoter fusion on plasmid pUC18-mini-Tn7, were maintained on Luria-Bertani (LB) agar plates supplemented with carbenicillin (200 $\mu\text{g}/\text{ml}$) and 5-bromo-4-chloro-3-indolyl- β -D-galactopyranoside (X-Gal) (40 $\mu\text{g}/\text{ml}$) and incubated at 37°C overnight. Single colonies were inoculated into LB broth (20 ml) supplemented with carbenicillin (200 $\mu\text{g}/\text{ml}$) and incubated at 37°C with shaking at 180 rpm overnight. For subsequent experiments, the optical density at 600 nm (OD_{600}) was recorded, and a starting OD_{600} of 0.02 was inoculated into fresh LB broth supplemented with carbenicillin (200 $\mu\text{g}/\text{ml}$) and incubated at 37°C with shaking at 180 rpm.

Structural modification of HHQ. The synthesis of HHQ, PQS (40, 41), and other HHQ-based analogues (36, 37) was carried out via previously described methods. Novel compounds and compounds that required modified synthesis are described below and in the supplemental material.

TLC analysis. Silica thin-layer chromatographic (TLC) plates, activated by soaking in 5% (wt/vol) K_2HPO_4 for 30 min, were placed in an oven at 100°C for 1 h (42). Analogues (5 μl ; 10 mM) were spotted approximately 1 cm from the bottom. The spots were dried, and the plates were placed in a mobile phase comprising dichloromethane-methanol (95:5). The plate was viewed under UV light when the mobile phase had run 5 cm below the top of the plate.

Biofilm formation, quantification, and visualization. *C. albicans* biofilm formation was carried out in 96-well plates, as previously described (43). Seeding densities for all subsequent experiments ($n = 3$)

were an OD_{600} of 0.05. Biofilm formation was measured as previously described, using a semiquantitative tetrazolium salt, 2,3-bis-(2-methoxy-4-nitro-5-sulphophenyl)-2H tetrazolium-5-carboxanilide inner salt (XTT) reduction assay (44). Experiments were repeated at least three times, with at least eight technical replicates. Visualization of biofilm formation was performed on glass coverslips in 6-well plates using confocal scanning laser microscopy (CSLM). All images were captured using the Zeiss HBO-100 microscope illuminating system, processed using the Zen AIM application imaging program, and converted to JPGs using Axiovision 40 version 4.6.3.0. A minimum of three independent biological repetitions were carried out.

Viable-colony biofilm assay. *C. albicans* biofilms, supplemented with analogues and parent compounds, were grown in 6-well plates and incubated overnight at 37°C . Briefly, the OD_{600} s of *C. albicans* yeast nitrogen base (YNB) cultures were measured, and the cultures were diluted to an OD_{600} of 0.05 in YNB-NP (see below), supplemented with analogues, plated onto 6-well plates, and incubated for 1 h at 37°C . The medium was removed, and the wells were washed twice with sterile phosphate-buffered saline (PBS) and supplemented with fresh YNB-NP with analogues. The plates were incubated overnight at 37°C , after which the medium was removed and the wells were washed with sterile PBS. For serial dilutions, biofilms were harvested by scraping adherent cells into 1 ml PBS, vortexed, and serially diluted in sterile PBS. The serial dilutions (100 μl) were plated onto YPD agar and incubated overnight at 37°C . Colonies were counted and recorded the next day.

***C. albicans* growth curves.** Overnight *C. albicans* cultures grown in YNB were diluted to an OD_{600} of 0.05 in YNB supplemented with analogues. Cultures (200 μl) were added to each well of a 100-well plate and grown for 24-h period on a Bioscreen C spectrophotometer (Growth Curves USA).

RNA isolation and qRT-PCR transcriptional analysis. Overnight *C. albicans* cultures were diluted to an OD_{600} of 0.05 in either YNB or YNB-NP (Difco). The YNB cultures were supplemented with methanol, whereas YNB-NP cultures were supplemented with either 100 μM HHQ or the methanol volume equivalent. The cultures were grown at 37°C with agitation (180 rpm) for 6 h, after which they were centrifuged at 4,000 rpm, the supernatants were discarded, and the pellets were frozen at -20°C until they were processed. RNA was isolated using the MasterPure Yeast RNA purification kit (Cambio Ltd., Cambridge, United Kingdom) according to the manufacturer's specifications and quantified using an ND-1000 spectrophotometer (NanoDrop Technologies, USA). Genomic DNA was enzymatically removed using Turbo DNA-free DNase (Ambion), and samples were confirmed DNA free by PCR. RNA was converted to cDNA using random primers and avian myeloblastosis virus (AMV) reverse transcriptase (Promega) according to the manufacturer's instructions. Quantitative real-time (qRT)-PCR was carried out using the Universal Probe Library (UPL) system (Roche) according to the manufacturer's specifications, and samples were normalized to *C. albicans* actin transcript expression (*ACT1*). A full list of primers and UPL probes used in this study is provided in Table S1 in the supplemental material.

Phenazine extraction. *P. aeruginosa* strains were cultured as described above for 24 h, with the addition of analogues (100 μM), and pyocyanin was extracted as described previously (45). The cultures were centrifuged at 4,000 rpm for 10 min, and the cell-free supernatant (5 ml) was removed. Chloroform (3 ml) was added and mixed by vortexing. After centrifugation at 4,000 rpm for 5 min, the lower aqueous phase was transferred to 0.2 M HCl (2 ml). Samples were mixed by vortexing and centrifuged at 4,000 rpm for 5 min to separate the phases. An aliquot of the top phase (1 ml) was removed and spectrophotometrically analyzed at OD_{570} . Phenazine production was calculated using the following formula: $\text{OD}_{570} \times 2 \times 17.072$, with the units expressed in micrograms per milliliter.

Promoter fusion-based expression analysis. Promoter fusion analyses were performed in a 96-well format, with β -galactosidase activity measured as described previously (46). Briefly, overnight cultures of wild-type PAO1 *pqsA-lacZ* (pLP0996) and mutant strain PAO1 *pqsA* mutant *pqsA*-

lacZ were diluted to an OD₆₀₀ of 0.02 in LB broth. Analogues at 100 μ M final concentration were added, mixed, aliquoted into 96-well plates, and incubated overnight at 37°C with shaking. The next day, OD₆₀₀ values were recorded in a plate reader. Aliquots of cells (0.02 ml) were permeabilized (100 mM dibasic sodium phosphate [Na₂HPO₄], 20 mM KCl, 2 mM MgSO₄, 0.8 mg/ml CTAB [hexadecyltrimethylammonium bromide], 0.4 mg/ml sodium deoxycholate, 5.4 μ l/ml β -mercaptoethanol) and added to substrate solution (60 mM Na₂HPO₄, 40 mM NaH₂PO₄, 1 mg/ml *o*-nitrophenyl- β -D-galactoside [ONPG], 2.7 μ l/ml β -mercaptoethanol). The kinetics of color development was monitored, and the reactions were stopped using 1 M NaCO₃. OD₄₂₀ values were recorded as described above. Miller units were calculated using the following equation; $1,000 \times [(OD_{420}/OD_{600}) \times 0.02 \text{ ml} \times \text{reaction time (min)}]$.

Cytotoxicity assay. Lactate dehydrogenase (LDH) release from a panel of mammalian cells was assayed as a measure of cytotoxicity using an LDH colorimetric kit (Roche) according to the manufacturer's instructions (36). Briefly, IB3-1 lung epithelial cells, A549 human lung adenocarcinoma epithelial cells, DU-145 human prostate cancer cells, and HeLa cervical cancer cells were seeded onto 96-well plates and treated with methanol (control) and analogues. Following 16 h of incubation at 37°C and 5% CO₂, the supernatants were removed and added to a catalyst reaction mixture in a fresh plate and further incubated at 37°C and 5% CO₂ for 30 min to allow color development. After this period, the plate was analyzed on an enzyme-linked immunosorbent assay (ELISA) plate reader at OD₄₉₀. Cytotoxicity was expressed as a percentage of that of cells treated with 0.1% (vol/vol) Triton (100% cytotoxicity).

Statistical analysis. All graphs were compiled using GraphPad Prism (version 5.01) unless otherwise stated. All data were analyzed using built-in GraphPad Prism (version 5.01) functions as specified. The level of significance was set at a *P* value of 0.05, and *post hoc* comparisons between groups were performed using the Bonferroni multiple-comparison test.

RESULTS

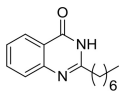
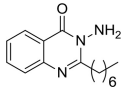
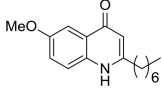
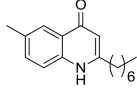
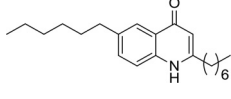
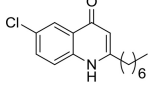
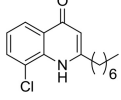
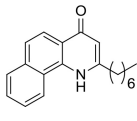
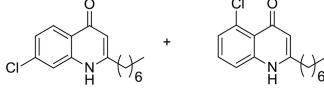
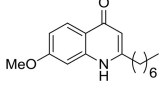
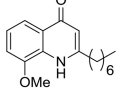
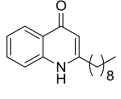
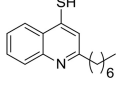
Key modifications of the quinolone framework retain antibiofilm activity toward *C. albicans*. The HHQ molecule has previously been shown to suppress biofilm formation in *C. albicans* at concentrations from 10 to 100 μ M (2.47 to 24.7 μ g/ml) independent of any effects on the growth of planktonic cells (10). Previous structure-function analysis of the activity of the quinolone framework had implicated the C-3 position as a key component of interspecies antibiofilm activity (36). We undertook further modification of the HHQ parent molecule with the aim of developing viable antibiofilm compounds to target *C. albicans*. These compounds were incorporated into a larger collection of alkylquinolone analogues, systematically modified at different positions on the molecule, and classified on the basis of their substitutions relative to the parent framework HHQ (Table 1).

The suite of analogues was first tested to establish their potency as antibiofilm compounds against *C. albicans* using an optimized XTT assay, a commonly used quantitative method to assess *Candida* biofilm mass and growth (47). As previously described (10), HHQ significantly suppressed biofilm formation compared to untreated and methanol-treated cells, whereas PQS appeared to induce biofilm formation (Fig. 1). When all the analogues were similarly screened by XTT assay, several had antibiofilm activities similar to that of HHQ (compounds 1 and 2 [class I; modified at C-3]; 3, 4, 6, 7, and 9 [class II; modified anthranilate ring]; and 12 [class III; modified alkyl chain]) (Fig. 2a). These analogues were diverse members of classes I, II, and III, suggesting that several components of the HHQ framework contribute to the antibiofilm activity of the parent compound. A number of substitutions led to intermediate antibiofilm activity, including 5, 8, 10, and 11 (class II; modified anthranilate ring) and 15 (class V; modified anthra-

nilate ring and alkyl chain length), while some analogues had completely lost the ability to suppress *C. albicans* biofilm formation, e.g., 13 (class IV; modified C-4) and the class V compounds 14, 16, and 17 (Fig. 2a). While modification of the C-3 position to produce PQS led to loss of antibiofilm activity (Fig. 1), incorporation of an -N-NH₂ moiety (compound 2) at the 3 position or substitution of C-3 with NH (1) did not affect the ability to suppress *C. albicans* biofilm formation (Fig. 2a). Addition of chlorine (Cl) at the C-6 and C-8 positions of the anthranilate ring (compounds 6 and 7) also did not lead to loss of antibiofilm activity. In contrast, the introduction of considerable steric bulk with the addition of an *n*-hexyl alkyl chain at C-6 of the anthranilate ring (compound 5) or elaboration of the aromatic group, as with the naphthyl compound (compound 8), resulted in compounds with significantly less potent antibiofilm activity than HHQ. These data suggest an exquisite level of specificity for the interaction between HHQ and the *C. albicans* biofilm intracellular machinery. Modification of the C-2 alkyl chain from *n*-heptyl (HHQ) to *n*-nonyl C₉ (compound 12) did not affect antibiofilm activity, while parallel modification of the anthranilate ring resulted in a complete loss, as with the class V compound 16 or 17. After modifying the C-4 position (C = O to C = S) (compound 13), the quinolone thiol exhibited an increase in XTT activity (*P* < 0.05) relative to controls (Fig. 2a), comparable to the increase observed in the presence of PQS (Fig. 1). Previously, we have shown that HHQ elicits a dose-dependent reduction in *C. albicans* biofilm formation (10). In order to determine if this also applied to the analogues that retain antibiofilm activity, dose-response analysis of selected compounds, 1, 2, 4, 6, and 12 representing classes I, II, and IV, was undertaken. This revealed compound-specific responses, with 10 μ M compounds 2, 4, and 12 being sufficient to elicit a statistically significant reduction in biofilm formation (Fig. 2b). All five compounds reduced biofilm formation when applied at 50 μ M and 100 μ M. To further confirm the antibiofilm activity of the lead compounds, viable-colony counts were performed on selected analogues using the maximum 100 μ M compound dose. This confirmed the outputs from the XTT assays; all the analogues, along with HHQ, significantly reduced viable biofilm cells in comparison to the control (see Fig. S1a in the supplemental material). Importantly, the antibiofilm activity was found to be independent of planktonic growth, which was unaffected in the presence of selected compounds (see Fig. S1b in the supplemental material).

Microscopic staining reveals structural changes in *C. albicans* biofilms. The formation of biofilms in bacteria, yeasts, and fungi is a highly ordered process involving multicellular behavior and has been defined in several stages (22). Confocal microscopy combined with intracellular staining was used to assess the structural integrity and cellular morphology of *C. albicans* incubated on coverslips. Biofilms were individually stained with each of the dyes, and multiple fields of view were visualized to accurately represent the effects of the analogues. The biofilms observed for methanol-treated and untreated controls displayed all the characteristics of a typical *C. albicans* biofilm and were classified as wild type (Fig. 1). Calcofluor, concanavalin A, and FUN-1 staining revealed uniform distribution of chitin/cellulose and cell wall mannosyl/glucosyl residues indicative of viable wild-type morphology (Fig. 1). The analogues identified by XTT assay as causing impaired biofilm formation (1, 2, 3, 4, 6, 7, 9, 12, and 15) exhibited markedly disrupted structures when grown on coverslips and were classified as atypical morphologies (Fig. 3). Cells treated with

TABLE 1 Compound data

Compound	Structure	Yield (%) ^a	MW	R _f ^b	Class ^c
1		76	244.3	0.319	I
2 ^d		3	259.3	0.907	I
3		34	273.4	0.252	II
4		31	257.4	0.286	II
5		35	327.5	0.504	II
6		21	277.8	0.403	II
7		19	277.8	0.630	II
8		46	293.4	0.294	II
9 ^d		6	277.8	0.361	II
10		33	273.4	0.261	II
11		12	273.4	0.504	II
12		23	271.4	0.395	III
13 ^d		48	259.4	1	IV

(Continued on following page)

TABLE 1 (Continued)

Compound	Structure	Yield (%) ^a	MW	R _f ^b	Class ^c
14		16	355.6	0.538	V
15		28	301.4	0.286	V
16		51	321.5	0.462	V
17		16	289.4	0.504	V

^a Yields were isolated over all steps.^b TLC on silica plates with dichloromethane-MeOH (95:5) mobile phase.^c Class I, modified C-3; class II, modified anthranilate ring; class III, modified alkyl chain; class IV, modified C-4; class V, modified anthranilate ring and alkyl chain.^d New compounds synthesized in this study.

class I analogues were found to be largely compromised in their biofilm-forming capabilities and were classified as morphologically atypical. Biofilms produced with both 1 and 2 were significantly distorted, displaying a spindle-like phenotype. Hyphae were short and predominantly displayed yeast cell types rather than hyphal structures. Other structure-disrupting analogues were from classes II, III, and V, suggesting that specific modifications on the anthranilate ring and alkyl chain variation do not significantly affect the antibiofilm activity compared to the parent compound (Fig. 3).

Some analogues, including those that exhibited intermediate activity in the XTT assay, did not alter the biofilm structure, with 5, 11, 13, 14, and 16 all placed into the wild-type morphology group. Biofilms formed in the presence of compound 13 showed

hyperproduction of short hyphae, creating a dense mycelial network (see Fig. S2 in the supplemental material). The remaining analogues from class II, 8 and 10 (see Fig. S1a in the supplemental material), caused significant biofilm disruption, with fragmented hyphae, stunted vegetative growth, and quite large cell debris fields. Cells incubated with the class V molecule 17 induced a severely compromised phenotype (see Fig. S2 in the supplemental material) where debris fields comprising yeast cells and blastospores characterized the structural phenotype.

Enhanced gene transcript expression of *HWP1*, *ECE1*, *ALS3*, *IHD1*, and the uncharacterized open reading frame (ORF) *orf19.2457* provides a molecular mechanism for alkyl quinolone activity toward *C. albicans*. In addition to providing new insights into the interkingdom relationship between these important

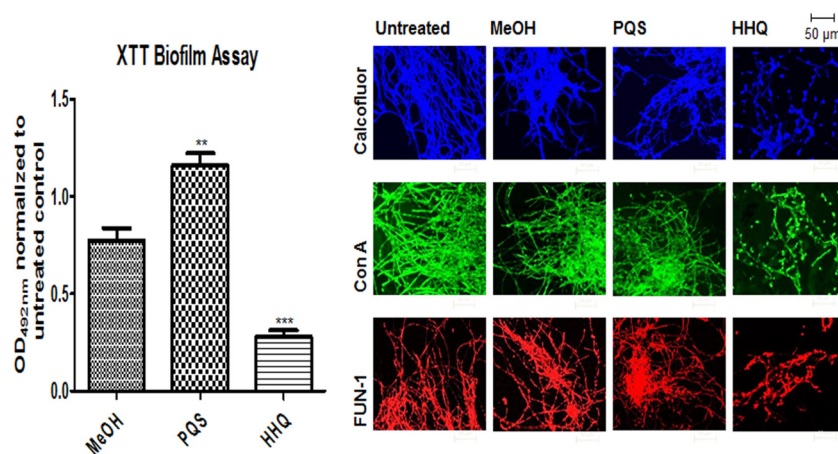


FIG 1 *C. albicans* biofilms are altered in the presence of HHQ. Filamentous *C. albicans* biofilms grown in the presence of PQS and HHQ (100 μ M) were assessed structurally by confocal microscopy and metabolically using the XTT biofilm assay. The data (means and standard errors of the mean [SEM]) are representative of three independent biological experiments and are presented relative to the untreated control. A two-tailed paired Student *t* test was performed by comparison of *C. albicans* in the presence of HHQ and PQS with *C. albicans* treated with methanol or ethanol (**, $P \leq 0.01$; ***, $P \leq 0.001$). ConA, concanavalin A.

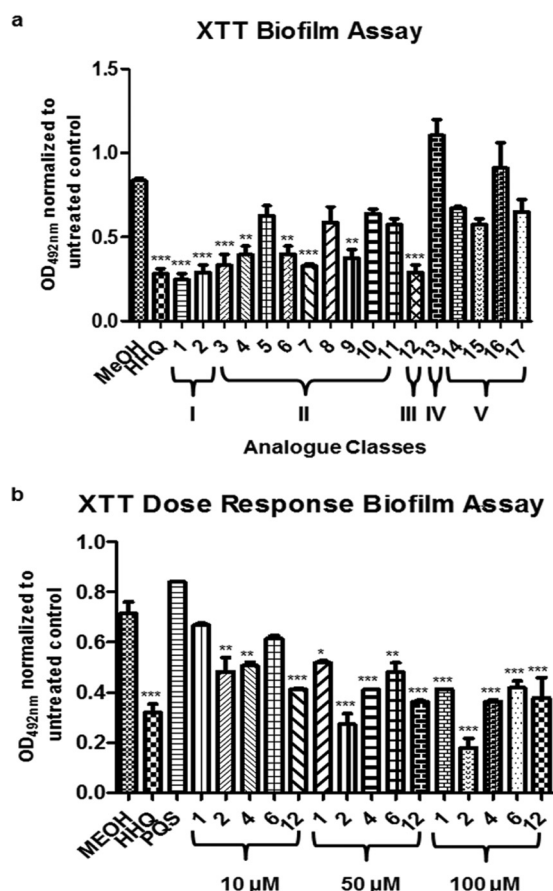


FIG 2 Decoration of HHQ exhibits variable biofilm activity against *C. albicans*. (a) A panel of HHQ-derivatized analogues were incubated with filamentous *C. albicans* and screened for biofilm formation using the metabolic XTT biofilm assay. The data are presented as OD₄₉₂ spectrophotometric output normalized to the untreated control and are representative of at least three independent biological replicates, with error bars representing SEM. (b) Dose-dependent XTT analysis of selected antibiofilm compounds applied at 10, 50, and 100 μM. The data are the averages from at least two independent biological replicates, each constituting eight technical replicates. Statistical analysis of both data sets was performed by one-way analysis of variance (ANOVA) with Bonferroni corrective testing, and the results are presented relative to the MeOH control values; *, $P \leq 0.05$; **, $P \leq 0.01$; ***, $P \leq 0.001$.

pathogens, strong emphasis has recently been placed on ligand-receptor interactions and the need to provide molecular mechanisms for the action of any potential therapeutic compound (48). We previously implicated *TUP1* in the HHQ-mediated suppression of biofilm formation in *C. albicans*, suggesting a role for the cell wall in this interaction (10, 16). More recently, several reports have shown changes in expression of cell wall-associated genes linked to biofilm formation in the organism (16, 20, 28, 49–51). They included a cohort of eight genes that are proposed to constitute the core filamentous response network, namely, *ALS3*, *ECE1*, *HGT2*, *HWP1*, *IHD1*, *RBT1*, *DCK1*, and the *orf19.2457* gene with unknown function (51). Therefore, transcript expression of a cohort of genes implicated in cell wall biogenesis, hyphal development, biofilm formation, and other related functions that were previously shown to be upregulated during the morphological transition from yeast to filamentous growth was investigated (see Table S1 in the supplemental material) (16, 51). The housekeep-

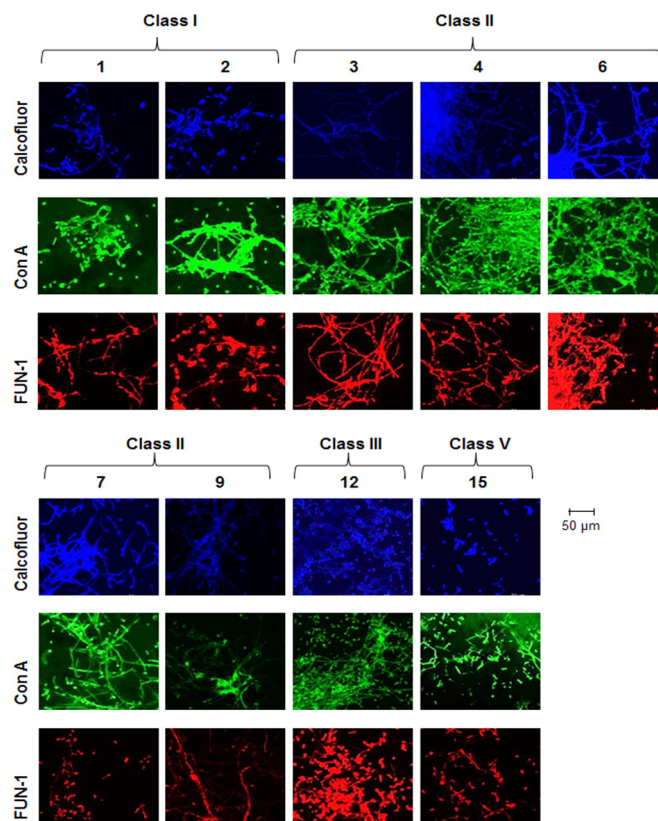


FIG 3 Microscopic analysis reveals altered biofilm structures. Analogues that lead to reduced *C. albicans* biofilm formation in the XTT assay (1, 2, 3, 4, 6, 7, 9, 12, and 15) exhibit compromised biofilm structures. Filamentous *C. albicans* biofilm in the presence of analogues (100 μM) was stained for chitin and cellulose (calcofluor; blue); lectins that bind to sugars, glycolipids, and glycoproteins (concanavalin A; green); and live/dead cells (FUN-1; red).

ing gene *ACT1* was chosen for normalization based on previous biofilm studies (52). We observed that several transcripts were hyperexpressed in an HHQ-dependent manner, specifically, *HWP1*, *ECE1*, *ALS3*, *IDH1*, and the as yet uncharacterized *orf19.2457* (Fig. 4). The remaining transcripts (*CPH1*, *EFB1*, *ESS1*, *RBT1*, *TUP1*, *BCR1*, *DCK1*, and *HGT2*) yielded expression patterns similar to those of control cells (see Fig. S3 in the supplemental material). It was perhaps somewhat surprising that, while treatment of *C. albicans* with *P. aeruginosa* supernatants has previously been shown to downregulate expression of the *RBT1*, *RBT5*, and *RBT8* genes (16), expression of *RBT1* was unaltered in the presence of HHQ (see Fig. S3 in the supplemental material). Taken together, these data suggest that HHQ induces a specific subset of cell wall proteins in *C. albicans*. Further work is needed to identify the upstream components of this response, although *in silico* screening of *C. albicans* genome sequences has ruled out the presence of an obvious PQS receptor (unpublished data).

Lead compounds display reduced cytotoxic activity toward specific mammalian cell lines. Evaluating the cytotoxicity of synthetic compounds is crucial in the context of developing targeted and highly optimized molecular therapeutics that are benign to human cellular physiology and ideal for use in a clinical environment. In previous work, we showed that analogue 1 was signifi-

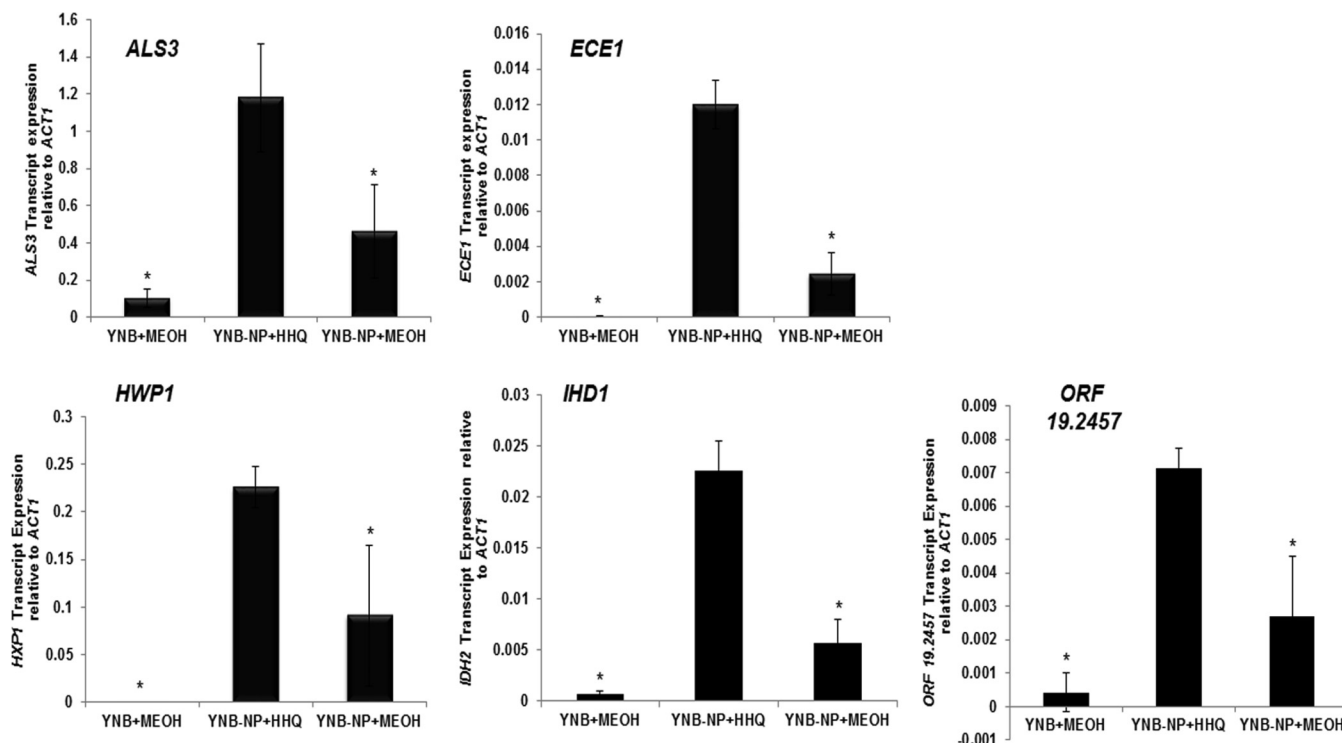


FIG 4 Hyphal pathway genes are hyperexpressed in response to HHQ. Transcript expression analysis (real-time RT-PCR) of a panel of biofilm genes was assessed in *C. albicans* grown in YNB-NP (filament-inducing medium) in 100 μ M HHQ for 6 h at 37°C. All the data were normalized to a housekeeping gene (*ACT1*). The error bars represent standard deviations (SD) of three independent biological replicates. A two-tailed paired Student *t* test was performed by comparison of HHQ-treated cells with methanol control in YNB-NP inducing medium (*, $P \leq 0.05$).

cantly less cytotoxic than HHQ, with an 80% reduction in LDH release relative to the parent compound (36). Therefore, the suite of analogues was tested for *in vitro* cytotoxicity toward IB3-1 airway epithelial cells. Class I analogues exhibited reduced cytotoxicity to IB3-1 cells, with compound 2 displaying approximately 34% toxicity (Fig. 5a). Several class II analogues (4, 6, and 9) exhibited reduced cytotoxicity relative to IB3-1 cells treated with HHQ, with 7 not reaching statistical significance. The class III analogue 12 was comparable to HHQ. Of the analogues that did not retain antibiofilm activity, 5, 8, 10, and 11 exhibited variable cytotoxicity to IB3-1 cells, whereas 13 exhibited considerably reduced cytotoxicity to IB3-1 cells (see Fig. S4 in the supplemental material). Finally, compound 16 exhibited very low levels of cytotoxicity, while 17 was reduced relative to HHQ-treated cells. Compound 15 was the most toxic, killing approximately 91% of all cells (Fig. 5a).

In order to achieve a more comprehensive understanding of the selective toxicity of the lead compounds, several additional cell lines were tested (Fig. 5b). LDH release assays were performed in A549, DU145, and HeLa cell lines in the presence of 100 μ M of the lead compounds and revealed distinct cytotoxicity profiles, with 1 and 9 consistently proving the least cytotoxic of the compounds tested. Compounds 4 and 6 exhibited reduced cytotoxicity in DU145 cells (although not statistically significant) but were comparable to HHQ in both the A549 and HeLa cell lines, while compound 2 exhibited increased cytotoxicity relative to HHQ in DU145 cells (Table 2). These data suggest that cell-specific cytotoxicity analysis will need to be performed prior to the introduction of these compounds in an applied setting.

HHQ analogues display a spectrum of agonist activity toward *P. aeruginosa* virulence. Taken together, compounds 1, 4, 6, and 9 pass both the first and second criteria described above, i.e., they retain antibiofilm activity toward *C. albicans* while exhibiting reduced selective cytotoxicity toward specific host cell lines. However, both HHQ and PQS are coinducers of the virulence-associated LysR-type transcriptional regulator PqsR (41). The structural moieties that underpin the interaction between HHQ/PQS and PqsR remain to be fully characterized, although recent studies have reported diverse classes of PqsR antagonists (53–55) and implicated the hydrophobic pocket situated within the PqsR protein (56). Therefore, in order to assess whether the lead compounds could elicit a virulence response from *P. aeruginosa*, phenazine production and *pqsA* promoter activity (57) were monitored in a *pqsA* mutant where the capacity to produce native HHQ and PQS had been lost.

Both HHQ and PQS restored phenazine production in the *pqsA* mutant strain (Fig. 6a). In contrast, the majority of analogues did not restore phenazine production in the strain, with the notable exception of compound 9. Several analogues from different classes did partially restore phenazine production in the mutant background, including compounds 10, 12, and 17 (Fig. 6; see Fig. S5 in the supplemental material). None of the analogues interfered with phenazine production in the wild-type PAO1 strain, suggesting that they are ineffective as PQS antagonists (see Fig. S5 in the supplemental material).

Similarly, while some degree of PqsR agonist activity was observed in the presence of compounds 6, 9, 10, 12, 13, and 17, only HHQ and PQS significantly induced promoter activity. All the

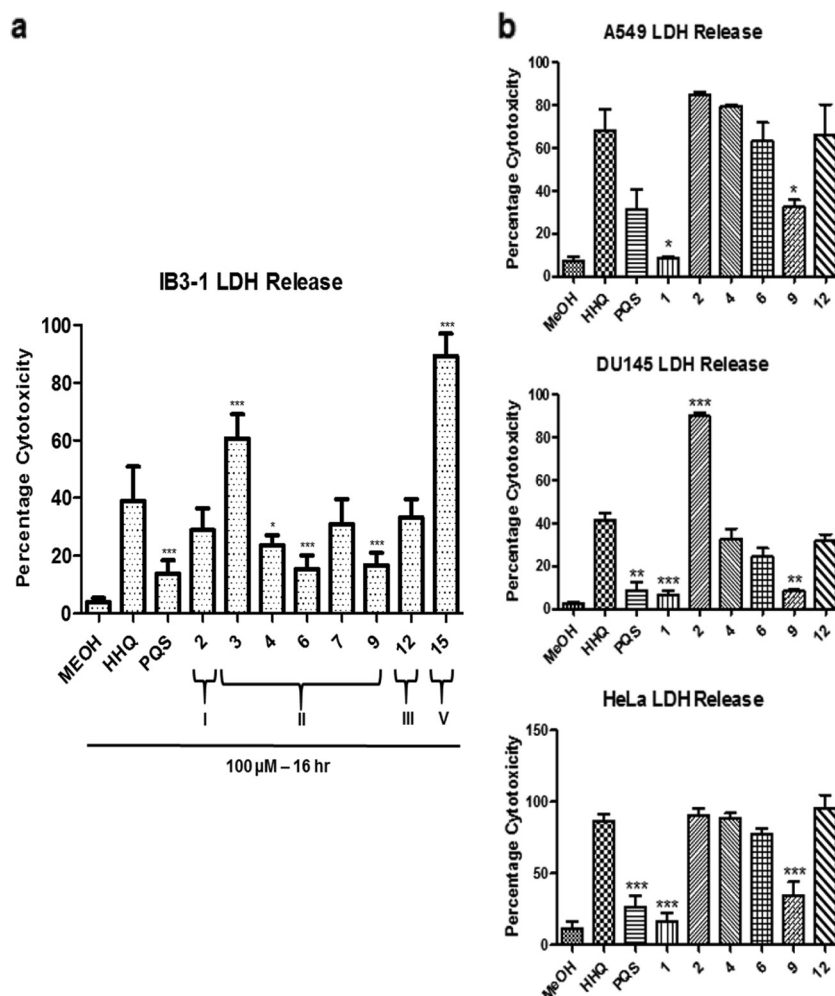


FIG 5 Cytotoxicity toward specific mammalian cell lines is reduced in lead compounds. (a) Cytotoxicity, measured as a percentage of total LDH released from IB3-1 cells treated with 0.1% Triton X-100 (100% cytotoxicity), was significantly reduced in the presence of several lead compounds. The data (means and SEM) are representative of three independent biological experiments. (b) Selected lead compounds were tested against A549, DU145, and HeLa cell lines. The data represent four independent biological replicates, and all the data points are normalized to Triton X-100 as described for panel a. One-way ANOVA was performed, with Bonferroni corrective testing on all data sets, and comparison to an MeOH control is presented; *, $P \leq 0.05$; **, $P \leq 0.01$; ***, $P \leq 0.001$.

other analogues did not influence promoter activity in this system (Fig. 6B; see Fig. S5 in the supplemental material). Somewhat surprisingly, antagonistic activity toward *pqsA* promoter activity was not observed, with almost all the analogues failing to significantly suppress *pqsA* promoter activity in the wild-type strain (see Fig. S5 in the supplemental material). The relative ineffectiveness of these

analogues as PQS antagonists may in part be due to hydroxylation of HHQ analogues (H at C-3) to PQS analogues (OH at C-3), thus establishing the nonantagonistic behavior explained by a recent report by Lu and colleagues, where the action of PqsH rendered anti-PQS compounds ineffective through bioconversion (55).

DISCUSSION

Current antimicrobial therapies tend to be non-pathogen specific, and there is evidence to suggest that the availability of relatively nontoxic broad-spectrum therapies has contributed to the emergence of resistance among both targeted and nontargeted microbes (58, 59). Consequently, there is an urgent need to create innovative new options for the targeted prevention of microbial infection while avoiding the inevitable emergence of resistance that is the hallmark of broad-spectrum antibiotic therapies (59, 60). Increasingly, industry, academia, and regulatory bodies have become interested in single-pathogen therapies to treat highly resistant or totally resistant bacterial pathogens, rightly viewed as an area of high unmet need (61–63). Exploiting interkingdom com-

TABLE 2 Selective toxicity indices of lead compounds

Compound	Selective toxicity index (% toxicity)			
	IB3-1	A549	DU145	HeLa
HHQ	26–50	51–75	26–50	76–100
PQS	0–25	26–50	0–25	0–25
1	0–25	0–25	0–25	0–25
2	26–50	76–100	76–100	76–100
4	0–25	76–100	26–50	76–100
6	26–50	51–75	0–25	76–100
9	0–25	26–50	0–25	26–50
12	26–50	51–75	26–50	76–100

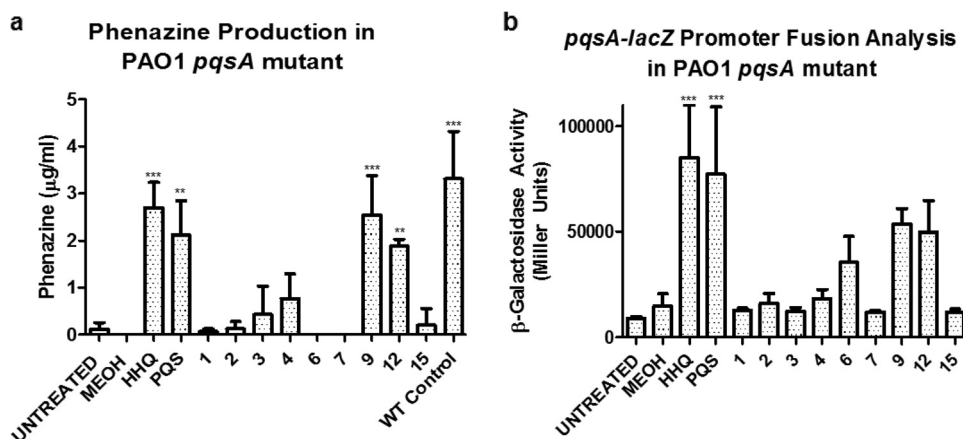


FIG 6 Influence of HHQ analogues on PQS-dependent virulence phenotypes in *P. aeruginosa*. Phenazine production (a) and *pqsA-lacZ* promoter activity (b) were quantified in a PAO1 *pqsA* mutant in the presence of HHQ, PQS, and lead compounds. The data are presented as means and SEM and are representative of at least three independent biological replicates. One-way ANOVA was performed, with Bonferroni corrective testing, and statistical significance relative to the MeOH control is presented; **, $P \leq 0.01$; ***, $P \leq 0.001$.

munication networks, and the mode of action of the chemical messages or signals employed therein, offers us a powerful platform from which to meet this need.

Previously, we showed that the HHQ interkingdom signal molecule from *P. aeruginosa* could suppress biofilm formation in *C. albicans* at concentrations ranging from 10 to 100 μ M (2.47 to 24.7 μ g/ml) (10). This suppression occurred independently of any growth limitation in planktonic cells, and morphogenesis on spider medium was also found to be unaffected (10). The design and subsequent analysis of a suite of analogues based on the core HHQ quinolone framework has led to the identification of several lead compounds that retain antibiofilm activity toward *C. albicans* but exhibit significantly reduced cytotoxicity toward IB3-1 epithelial cells compared with the parent HHQ molecule. The selective cytotoxicities of the lead compounds, together with the dose-dependent antibiofilm effects, will be key considerations in determining the cell line-specific therapeutic index of lead analogues as part of the ongoing development of these compounds. Furthermore, unlike HHQ, these lead compounds are now inactive toward the *P. aeruginosa* PqsR quorum-sensing system, a critical requirement for their potential future development as antibiofilm therapeutics. In addition, the ability to generate hydrochloride salts of the compounds (reference 36 and data not shown) suggests that the solubility of future therapeutics based on these scaffolds will not be a bottleneck. Several strategies have been proposed for the implementation of antibiofilm compounds as clinical therapeutics to target *C. albicans* biofilm infections (64). As the HHQ analogues possess antibiofilm, but not anti-*Candida*, activity, they would disrupt the formation of biofilms but not likely remove the planktonic cells that remain at the site of infection. Therefore, combination with conventional antifungal compounds would be required for effective clearance. Alternatively, where the potency of the antibiofilm activity can be synthetically enhanced through further derivatization, clearance by the immune system might also be realistic.

The molecular mechanisms through which AHQs and the lead compounds identified in this study disrupt the formation of biofilms by *C. albicans* remain to be fully elucidated. Previ-

ously, we have shown that HHQ does not affect adhesion, but rather directly impacts the subsequent developmental stages in a TUP1-dependent manner (10). In this study, we have shown that the expression of several cell wall-associated genes is increased in response to HHQ during the switch to hyphal growth. These genes have previously been implicated in the formation of *C. albicans* biofilms and have been shown to exhibit increased levels of expression during the hyphal transition (50, 51, 65). Therefore, antibiofilm compounds might be expected to suppress this induction rather than enhance it. However, five of the target genes tested exhibited an increase in expression relative to control cells under inducing conditions. This may be a reflection of the previous observation that HHQ interferes with the later stages of biofilm development (10). Alternatively, this hyperexpression phenotype may affect the capacity of the cell to engineer a community-based biofilm. Future studies will focus on elucidating the pathways through which *C. albicans* perceives and responds to challenge with HHQ with the aim of identifying potential therapeutic targets.

Further work using defined *in vivo* models of biofilms and infection will be required to further the development and evaluation of these small molecules as antibiofilm compounds. Models are now available for the investigation of infections involving medical devices, such as vascular catheters, dentures, urinary catheters, and subcutaneous implants, as well as mucosal biofilm infections (66). The ongoing development of cell-based or animal models to study *in vivo* infections (66–69), whether as single-pathogen or coculture systems (70), has provided a well-equipped tool kit for the preclinical assessment of these AHQ-based compounds.

Conclusions. In this study, we have functionalized the important microbial signaling molecules HHQ and PQS in order to exploit their interkingdom roles in controlling biofilm formation in *C. albicans*. In addition to deciphering further insights into the molecular mechanism through which these chemical messages elicit a biofilm-suppressive response from *C. albicans*, the bioactivity of several lead compounds has provided a viable platform for the development of next-generation therapeutics. Crucially, some of these compounds are nontoxic to mammalian cells and

have been rendered incapable of activating *P. aeruginosa* virulence systems, thus highlighting their potential utility as an effective therapy combatting human infection.

ACKNOWLEDGMENTS

F.J.R., G.P.M., and F.O. conceived and designed the investigation. F.J.R., J.P.P., L.G., and D.F.W. performed the biological experimentation, while R.C., R.M.S., and E.O.M. conducted the chemical synthesis. F.J.R., J.P.P., and F.O. wrote the manuscript, and we all read and edited the final draft.

FUNDING INFORMATION

This work, including the efforts of Gerard P. McGlacken, was funded by Science Foundation Ireland (SFI) (SFI/12/RC/2275). This work, including the efforts of Fergal O'Gara, was funded by Science Foundation Ireland (SFI) (SSPC-2 12/RC/2275, 13/TIDA/B2625, 12/TIDA/B2411, 12/TIDA/B2405, and 14/TIDA/2438). This work, including the efforts of Fergal O'Gara, was funded by European Commission (EC) (FP7-PEOPLE-2013-ITN 607786, FP7-KBBE-2012-6 CP-TP-312184, FP7-KBBE-2012-6 311975, OCEAN 2011-2 287589, Marie Curie 256596, and EU-634486). This work, including the efforts of Fergal O'Gara, was funded by Health Research Board (HRB) (Irish Thoracic Society MRCG-2014-6). This work, including the efforts of Fergal O'Gara, was funded by Teagasc (Walsh Fellowship 2013). This work, including the efforts of Fergal O'Gara, was funded by Department of Agriculture, Food and the Marine (FIRM/RSE/CoFoRD, FIRM 08/RDC/629, FIRM 1/F009/MabS, and FIRM 13/F/516). This work, including the efforts of Fergal O'Gara, was funded by Irish Research Council for Science, Engineering and Technology (IRCSET) (PD/2011/2414 and GOIPG/2014/647). This work, including the efforts of Fergal O'Gara, was funded by Marine Institute (Foras Na Mara) (Beaufort award C2CRA 2007/082).

G.P.M. thanks the Irish Research Council (R.M.S. and R.C.) and the UCC Strategic Research Fund (E.O.M.). The funders had no role in study design, data collection and interpretation, or the decision to submit the work for publication.

REFERENCES

- Cooper MA, Shlaes D. 2011. Fix the antibiotics pipeline. *Nature* 472:32. <http://dx.doi.org/10.1038/472032a>.
- European Centre for Disease Prevention and Control and European Medicines Agency. 2009. The bacterial challenge: time to react. European Centre for Disease Prevention and Control and European Medicines Agency, Stockholm, Sweden.
- Spellberg B, Powers JH, Brass EP, Miller LG, Edwards JE, Jr. 2004. Trends in antimicrobial drug development: implications for the future. *Clin Infect Dis* 38:1279–1286. <http://dx.doi.org/10.1086/420937>.
- Bjarnsholt T, Ciofu O, Molin S, Givskov M, Hoiby N. 2013. Applying insights from biofilm biology to drug development; can a new approach be developed? *Nat Rev Drug Discov* 12:791–808. <http://dx.doi.org/10.1038/nrd4000>.
- Davies D. 2003. Understanding biofilm resistance to antibacterial agents. *Nat Rev Drug Discov* 2:114–122. <http://dx.doi.org/10.1038/nrd1008>.
- Dong YH, Wang LH, Xu JL, Zhang HB, Zhang XF, Zhang LH. 2001. Quenching quorum-sensing-dependent bacterial infection by an N-acyl homoserine lactonase. *Nature* 411:813–817. <http://dx.doi.org/10.1038/35081101>.
- Fux CA, Costerton JW, Stewart PS, Stoodley P. 2005. Survival strategies of infectious biofilms. *Trends Microbiol* 13:34–40. <http://dx.doi.org/10.1016/j.tim.2004.11.010>.
- Hoiby N, Ciofu O, Johansen HK, Song ZJ, Moser C, Jensen PO, Molin S, Givskov M, Tolker-Nielsen T, Bjarnsholt T. 2011. The clinical impact of bacterial biofilms. *Int J Oral Sci* 3:55–65. <http://dx.doi.org/10.4248/IJOS11026>.
- Rasmussen TB, Givskov M. 2006. Quorum sensing inhibitors: a bargain of effects. *Microbiology* 152:895–904. <http://dx.doi.org/10.1099/mic.0.28601-0>.
- Reen FJ, Mooij MJ, Holcombe LJ, McSweeney CM, McGlacken GP, Morrissey JP, O'Gara F. 2011. The *Pseudomonas* quinolone signal (PQS), and its precursor HHQ, modulate interspecies and interkingdom behaviour. *FEMS Microbiol Ecol* 77:413–428. <http://dx.doi.org/10.1111/j.1574-6941.2011.01121.x>.
- Rutherford ST, Bassler BL. 2012. Bacterial quorum sensing: its role in virulence and possibilities for its control. *Cold Spring Harb Perspect Med* 2:a012427. <http://dx.doi.org/10.1101/cshperspect.a012427>.
- Ternent L, Dyson RJ, Krachler AM, Jabbari S. 2015. Bacterial fitness shapes the population dynamics of antibiotic-resistant and -susceptible bacteria in a model of combined antibiotic and anti-virulence treatment. *J Theor Biol* 372:1–11. <http://dx.doi.org/10.1016/j.jtbi.2015.02.011>.
- Cox CE, McClelland M, Teplitski M. 2013. Consequences of disrupting *Salmonella* AI-2 signaling on interactions within soft rots. *Phytopathology* 103:352–361. <http://dx.doi.org/10.1094/PHYTO-09-12-0237-FI>.
- Dong YH, Gusti AR, Zhang Q, Xu JL, Zhang LH. 2002. Identification of quorum-quenching N-acyl homoserine lactonases from *Bacillus* species. *Appl Environ Microbiol* 68:1754–1759. <http://dx.doi.org/10.1128/AEM.68.4.1754-1759.2002>.
- Hentzer M, Riedel K, Rasmussen TB, Heydorn A, Andersen JB, Parsek MR, Rice SA, Eberl L, Molin S, Hoiby N, Kjelleberg S, Givskov M. 2002. Inhibition of quorum sensing in *Pseudomonas aeruginosa* biofilm bacteria by a halogenated furanone compound. *Microbiology* 148:87–102. <http://dx.doi.org/10.1099/00221287-148-1-87>.
- Holcombe LJ, McAlester G, Munro CA, Enjalbert B, Brown AJ, Gow NA, Ding C, Butler G, O'Gara F, Morrissey JP. 2010. *Pseudomonas aeruginosa* secreted factors impair biofilm development in *Candida albicans*. *Microbiology* 156:1476–1486. <http://dx.doi.org/10.1099/mic.0.037549-0>.
- Janssens JC, Steenackers H, Robijns S, Gellens E, Levin J, Zhao H, Hermans K, De Coster D, Verhoeven TL, Marchal K, Vanderleyden J, De Vos DE, De Keersmaecker SC. 2008. Brominated furanones inhibit biofilm formation by *Salmonella enterica* serovar Typhimurium. *Appl Environ Microbiol* 74:6639–6648. <http://dx.doi.org/10.1128/AEM.01262-08>.
- O'Loughlin CT, Miller LC, Siryaporn A, Drescher K, Semmelhack MF, Bassler BL. 2013. A quorum-sensing inhibitor blocks *Pseudomonas aeruginosa* virulence and biofilm formation. *Proc Natl Acad Sci U S A* 110:17981–17986. <http://dx.doi.org/10.1073/pnas.1316981110>.
- Zambelloni R, Marquez R, Roe AJ. 2015. Development of antivirulence compounds: a biochemical review. *Chem Biol Drug Des* 85:43–55. <http://dx.doi.org/10.1111/cbdd.12430>.
- Desai JV, Mitchell AP, Andes DR. 2014. Fungal biofilms, drug resistance, and recurrent infection. *Cold Spring Harb Perspect Med* 4:a019729. <http://dx.doi.org/10.1101/cshperspect.a019729>.
- Perlroth J, Choi B, Spellberg B. 2007. Nosocomial fungal infections: epidemiology, diagnosis, and treatment. *Med Mycol* 45:321–346. <http://dx.doi.org/10.1080/13693780701218689>.
- Ramage G, Rajendran R, Sherry L, Williams C. 2012. Fungal biofilm resistance. *Int J Microbiol* 2012:528521. <http://dx.doi.org/10.1155/2012/528521>.
- Feldman M, Shenderovich J, Al-Quntar AA, Friedman M, Steinberg D. 2015. Sustained release of a novel anti-quorum-sensing agent against oral fungal biofilms. *Antimicrob Agents Chemother* 59:2265–2272. <http://dx.doi.org/10.1128/AAC.04212-14>.
- Moudgal V, Sobel J. 2010. Antifungals to treat *Candida albicans*. *Expert Opin Pharmacother* 11:2037–2048. <http://dx.doi.org/10.1517/14656566.2010.493875>.
- Chandra J, Mukherjee P, Ghannoum A. 2012. *Candida* biofilms associated with CVC and medical devices. *Mycoses* 55:46–57. <http://dx.doi.org/10.1111/j.1439-0507.2011.02149.x>.
- Lynch AS, Robertson GT. 2008. Bacterial and fungal biofilm infections. *Annu Rev Med* 59:415–428. <http://dx.doi.org/10.1146/annurev.med.59.110106.132000>.
- Bink A, Pellens K, Cammue BPA, Thevissen K. 2011. Anti-biofilm strategies: how to eradicate *Candida* biofilms. *Open Mycol J* 5:29–38. <http://dx.doi.org/10.2174/1874437001105010029>.
- Finkel JS, Xu W, Huang D, Hill EM, Desai JV, Woolford CA, Nett JE, Taff H, Norice CT, Andes DR, Lanni F, Mitchell AP. 2012. Portrait of *Candida albicans* adherence regulators. *PLoS Pathog* 8:e1002525. <http://dx.doi.org/10.1371/journal.ppat.1002525>.
- Miceli MH, Bernardo SM, Lee SA. 2009. *In vitro* analyses of the combination of high-dose doxycycline and antifungal agents against *Candida*

- albicans* biofilms. Int J Antimicrob Agents 34:326–332. <http://dx.doi.org/10.1016/j.ijantimicag.2009.04.011>.
30. Bose S, Ghosh AK. 2011. Biofilms: a challenge to medical science. J Clin Diagn Res 5:127–130.
 31. Peleg AY, Hogan DA, Mylonakis E. 2010. Medically important bacterial-fungal interactions. Nat Rev Microbiol 8:340–349. <http://dx.doi.org/10.1038/nrmicro2313>.
 32. Wargo MJ, Hogan DA. 2006. Fungal-bacterial interactions: a mixed bag of mingling microbes. Curr Opin Microbiol 9:359–364. <http://dx.doi.org/10.1016/j.mib.2006.06.001>.
 33. Cugini C, Morales DK, Hogan DA. 2010. *Candida albicans*-produced farnesol stimulates *Pseudomonas* quinolone signal production in LasR-defective *Pseudomonas aeruginosa* strains. Microbiology 156:3096–3107. <http://dx.doi.org/10.1099/mic.0.037911-0>.
 34. Hodgkinson JT, Galloway WR, Saraf S, Baxendale IR, Ley SV, Ladlow M, Welch M, Spring DR. 2011. Microwave and flow syntheses of *Pseudomonas* quinolone signal (PQS) and analogues. Org Biomol Chem 9:57–61. <http://dx.doi.org/10.1039/C0OB00652A>.
 35. Mashburn-Warren L, Howe J, Brandenburg K, Whiteley M. 2009. Structural requirements of the *Pseudomonas* quinolone signal for membrane vesicle stimulation. J Bacteriol 191:3411–3414. <http://dx.doi.org/10.1128/JB.00052-09>.
 36. Reen FJ, Clarke SL, Legendre C, McSweeney CM, Eccles KS, Lawrence SE, O'Gara F, McGlacken GP. 2012. Structure-function analysis of the C-3 position in analogues of microbial behavioural modulators HHQ and PQS. Org Biomol Chem 10:8903–8910. <http://dx.doi.org/10.1039/c2ob26823j>.
 37. Reen FJ, Shanahan R, Cano R, O'Gara F, McGlacken GP. 2015. A structure activity-relationship study of the bacterial signal molecule HHQ reveals swarming motility inhibition in *Bacillus atrophaeus*. Org Biomol Chem 13:5537–5541. <http://dx.doi.org/10.1039/C5OB00315F>.
 38. Deziel E, Lepine F, Milot S, He J, Mindrinos MN, Tompkins RG, Rahme LG. 2004. Analysis of *Pseudomonas aeruginosa* 4-hydroxy-2-alkylquinolines (HAQs) reveals a role for 4-hydroxy-2-heptylquinoline in cell-to-cell communication. Proc Natl Acad Sci U S A 101:1339–1344. <http://dx.doi.org/10.1073/pnas.0307694100>.
 39. Diggle SP, Matthijs S, Wright VJ, Fletcher MP, Chhabra SR, Lamont IL, Kong X, Hider RC, Cornelis P, Camara M, Williams P. 2007. The *Pseudomonas aeruginosa* 4-quinolone signal molecules HHQ and PQS play multifunctional roles in quorum sensing and iron entrapment. Chem Biol 14:87–96. <http://dx.doi.org/10.1016/j.chembiol.2006.11.014>.
 40. McGlacken GP, McSweeney CM, O'Brien T, Lawrence SE, Elcoate CJ, Reen FJ, O'Gara F. 2010. Synthesis of 3-halo-analogues of HHQ, subsequent cross-coupling and first crystal structure of *Pseudomonas* quinolone signal (PQS). Tetrahedron Lett 51:5919–5921. <http://dx.doi.org/10.1016/j.tetlet.2010.09.013>.
 41. Pesci EC, Milbank JB, Pearson JP, McKnight S, Kende AS, Greenberg EP, Iglewski BH. 1999. Quinolone signaling in the cell-to-cell communication system of *Pseudomonas aeruginosa*. Proc Natl Acad Sci U S A 96:11229–11234. <http://dx.doi.org/10.1073/pnas.96.20.11229>.
 42. Fletcher MP, Diggle SP, Camara M, Williams P. 2007. Biosensor-based assays for PQS, HHQ and related 2-alkyl-4-quinolone quorum sensing signal molecules. Nat Protoc 2:1254–1262. <http://dx.doi.org/10.1038/nprot.2007.158>.
 43. Ramage G, Vande Walle K, Wickes BL, Lopez-Ribot JL. 2001. Standardized method for in vitro antifungal susceptibility testing of *Candida albicans* biofilms. Antimicrob Agents Chemother 45:2475–2479. <http://dx.doi.org/10.1128/AAC.45.9.2475-2479.2001>.
 44. Hawser S. 1996. Comparisons of the susceptibilities of planktonic and adherent *Candida albicans* to antifungal agents: a modified XTT tetrazolium assay using synchronised C-albicans cells. J Med Vet Mycol 34:149–152. <http://dx.doi.org/10.1080/02681219680000231>.
 45. Essar DW, Eberly L, Hadero A, Crawford IP. 1990. Identification and characterization of genes for a second anthranilate synthase in *Pseudomonas aeruginosa*: interchangeability of the two anthranilate synthases and evolutionary implications. J Bacteriol 172:884–900.
 46. Miller JH. 1972. Experiments in molecular genetics. Cold Spring Harbor Laboratory Press, Cold Spring Harbor, NY.
 47. Nett JE, Cain MT, Crawford K, Andes DR. 2011. Optimizing a *Candida* biofilm microtiter plate model for measurement of antifungal susceptibility by tetrazolium salt assay. J Clin Microbiol 49:1426–1433. <http://dx.doi.org/10.1128/JCM.02273-10>.
 48. Baell J, Walters MA. 2014. Chemistry: chemical con artists foil drug discovery. Nature 513:481–483. <http://dx.doi.org/10.1038/513481a>.
 49. Bandara HM, Cheung BP, Watt RM, Jin LJ, Samaranyake LP. 2013. Secretory products of *Escherichia coli* biofilm modulate *Candida* biofilm formation and hyphal development. J Invest Clin Dent 4:186–199. <http://dx.doi.org/10.1111/jicd.12048>.
 50. Finkel JS, Mitchell AP. 2011. Genetic control of *Candida albicans* biofilm development. Nat Rev Microbiol 9:109–118. <http://dx.doi.org/10.1038/nrmicro2475>.
 51. Martin R, Albrecht-Eckardt D, Brunke S, Hube B, Hunniger K, Kurzai O. 2013. A core filamentation response network in *Candida albicans* is restricted to eight genes. PLoS One 8:e58613. <http://dx.doi.org/10.1371/journal.pone.0058613>.
 52. Nailis H, Coenye T, Van Nieuwerburgh F, Deforce D, Nelis HJ. 2006. Development and evaluation of different normalization strategies for gene expression studies in *Candida albicans* biofilms by real-time PCR. BMC Mol Biol 7:25. <http://dx.doi.org/10.1186/1471-2199-7-25>.
 53. Klein T, Henn C, de Jong JC, Zimmer C, Kirsch B, Maurer CK, Pistorius D, Muller R, Steinbach A, Hartmann RW. 2012. Identification of small-molecule antagonists of the *Pseudomonas aeruginosa* transcriptional regulator PqsR: biophysically guided hit discovery and optimization. ACS Chem Biol 7:1496–1501. <http://dx.doi.org/10.1021/cb300208g>.
 54. Lu C, Kirsch B, Zimmer C, de Jong JC, Henn C, Maurer CK, Musken M, Haussler S, Steinbach A, Hartmann RW. 2012. Discovery of antagonists of PqsR, a key player in 2-alkyl-4-quinolone-dependent quorum sensing in *Pseudomonas aeruginosa*. Chem Biol 19:381–390. <http://dx.doi.org/10.1016/j.chembiol.2012.01.015>.
 55. Lu C, Maurer CK, Kirsch B, Steinbach A, Hartmann RW. 2014. Overcoming the unexpected functional inversion of a PqsR antagonist in *Pseudomonas aeruginosa*: an in vivo potent antivirulence agent targeting pqs quorum sensing. Angew Chem Int Ed Engl 53:1109–1112. <http://dx.doi.org/10.1002/anie.201307547>.
 56. Ilangoan A, Fletcher M, Rampioni G, Pustelny C, Rumbaugh K, Heeb S, Camara M, Truman A, Chhabra SR, Emsley J, Williams P. 2013. Structural basis for native agonist and synthetic inhibitor recognition by the *Pseudomonas aeruginosa* quorum sensing regulator PqsR (MvR). PLoS Pathog 9:e1003508. <http://dx.doi.org/10.1371/journal.ppat.1003508>.
 57. McGrath S, Wade DS, Pesci EC. 2004. Dueling quorum sensing systems in *Pseudomonas aeruginosa* control the production of the *Pseudomonas* quinolone signal (PQS). FEMS Microbiol Lett 230:27–34. [http://dx.doi.org/10.1016/S0378-1097\(03\)00849-8](http://dx.doi.org/10.1016/S0378-1097(03)00849-8).
 58. Casadevall A. 1996. Crisis in infectious diseases: time for a new paradigm? Clin Infect Dis 23:790–794. <http://dx.doi.org/10.1093/clinids/23.4.790>.
 59. Casadevall A. 2009. The case for pathogen-specific therapy. Expert Opin Pharmacother 10:1699–1703. <http://dx.doi.org/10.1517/14656560903066837>.
 60. Spellberg B, Rex JH. 2013. The value of single-pathogen antibacterial agents. Nat Rev Drug Discov 12:963. <http://dx.doi.org/10.1038/nrd3957-cl>.
 61. European Medicines Agency. 2012. Addendum to the note for guidance on evaluation of medicinal products indicated for treatment of bacterial infections (CPMP/EWP/558/95 REV 2) to address indication-specific clinical data. European Medicines Agency, London, United Kingdom.
 62. Alemayehu D, Quinn J, Cook J, Kunkel M, Knirsch CA. 2012. A paradigm shift in drug development for treatment of rare multidrug-resistant gram-negative pathogens. Clin Infect Dis 55:562–567. <http://dx.doi.org/10.1093/cid/cis503>.
 63. Infectious Diseases Society of America. 2012. White paper: recommendations on the conduct of superiority and organism-specific clinical trials of antibacterial agents for the treatment of infections caused by drug-resistant bacterial pathogens. Clin Infect Dis 55:1031–1046. <http://dx.doi.org/10.1093/cid/cis688>.
 64. Nett JE. 2014. Future directions for anti-biofilm therapeutics targeting *Candida*. Expert Rev Anti Infect Ther 12:375–382. <http://dx.doi.org/10.1586/14787210.2014.885838>.
 65. Desai JV, Mitchell AP. 2015. *Candida albicans* biofilm development and its genetic control. Microbiol Spectr 3. <http://dx.doi.org/10.1128/microbiolspec.MB-0005-2014>.
 66. Nett JE, Andes DR. 2015. Fungal biofilms: in vivo models for discovery of anti-biofilm drugs. Microbiol Spectr 3. <http://dx.doi.org/10.1128/microbiolspec.MB-0008-2014>.
 67. Chauhan A, Bernardin A, Mussard W, Kriegl I, Esteve M, Ghigo

- JM, Beloin C, Semetey V. 2014. Preventing biofilm formation and associated occlusion by biomimetic glycocalyxlike polymer in central venous catheters. *J Infect Dis* 210:1347–1356. <http://dx.doi.org/10.1093/infdis/jiu249>.
68. Chauhan A, Ghigo JM, Beloin C. 2016. Study of in vivo catheter biofilm infections using pediatric central venous catheter implanted in rat. *Nat Protoc* 11:525–541. <http://dx.doi.org/10.1038/nprot.2016.033>.
69. Kucharikova S, Neirinck B, Sharma N, Vleugels J, Lagrou K, Van Dijck P. 2015. *In vivo Candida glabrata* biofilm development on foreign bodies in a rat subcutaneous model. *J Antimicrob Chemother* 70:846–856. <http://dx.doi.org/10.1093/jac/dku447>.
70. Sobue T, Diaz P, Xu H, Bertolini M, Dongari-Bagtzoglou A. 2016. Experimental models of *C. albicans*-streptococcal coinfection. *Methods Mol Biol* 1356:137–152. http://dx.doi.org/10.1007/978-1-4939-3052-4_10.



Harnessing Bacterial Signals for Suppression of Biofilm Formation in the Nosocomial Fungal Pathogen *Aspergillus fumigatus*

F. Jerry Reen¹, John P. Phelan¹, David F. Woods¹, Rachel Shanahan², Rafael Cano², Sarah Clarke², Gerard P. McGlacken² and Fergal O'Gara^{1,3*}

¹ BIOMERIT Research Centre, School of Microbiology, University College Cork – National University of Ireland, Cork, Ireland, ² Department of Chemistry and Analytical and Biological Chemistry Research Facility, University College Cork – National University of Ireland, Cork, Ireland, ³ School of Biomedical Sciences, Curtin Health Innovation Research Institute, Curtin University, Perth, WA, Australia

OPEN ACCESS

Edited by:

Christine Beemelmanns,
Hans Knöll Institute (LG), Germany

Reviewed by:

Henrietta Venter,
University of South Australia, Australia
Giordano Rampioni,
Roma Tre University, Italy

*Correspondence:

Fergal O'Gara
f.ogara@ucc.ie

Specialty section:

This article was submitted to
Antimicrobials, Resistance
and Chemotherapy,
a section of the journal
Frontiers in Microbiology

Received: 13 October 2016

Accepted: 08 December 2016

Published: 22 December 2016

Citation:

Reen FJ, Phelan JP, Woods DF,
Shanahan R, Cano R, Clarke S,
McGlacken GP and O'Gara F (2016)
Harnessing Bacterial Signals
for Suppression of Biofilm Formation
in the Nosocomial Fungal Pathogen
Aspergillus fumigatus.
Front. Microbiol. 7:2074.
doi: 10.3389/fmicb.2016.02074

Faced with the continued emergence of antibiotic resistance to all known classes of antibiotics, a paradigm shift in approaches toward antifungal therapeutics is required. Well characterized in a broad spectrum of bacterial and fungal pathogens, biofilms are a key factor in limiting the effectiveness of conventional antibiotics. Therefore, therapeutics such as small molecules that prevent or disrupt biofilm formation would render pathogens susceptible to clearance by existing drugs. This is the first report describing the effect of the *Pseudomonas aeruginosa* alkylhydroxyquinolone interkingdom signal molecules 2-heptyl-3-hydroxy-4-quinolone and 2-heptyl-4-quinolone on biofilm formation in the important fungal pathogen *Aspergillus fumigatus*. Decoration of the anthranilate ring on the quinolone framework resulted in significant changes in the capacity of these chemical messages to suppress biofilm formation. Addition of methoxy or methyl groups at the C5–C7 positions led to retention of anti-biofilm activity, in some cases dependent on the alkyl chain length at position C2. In contrast, halogenation at either the C3 or C6 positions led to loss of activity, with one notable exception. Microscopic staining provided key insights into the structural impact of the parent and modified molecules, identifying lead compounds for further development.

Keywords: biofilm, *Aspergillus fumigatus*, *Pseudomonas aeruginosa*, interkingdom interactions, alkylhydroxyquinolone (AHQ), PQS, HHQ

INTRODUCTION

Aspergillus fumigatus is an opportunistic pathogenic fungus associated with hospital-acquired infections. *A. fumigatus* infections contribute to morbidity and mortality in people with respiratory diseases such as cystic fibrosis (CF) and chronic obstructive pulmonary disease (COPD), as well as infecting open skin wounds in burn patients and medical implants (Peleg et al., 2010; Speirs et al., 2012). Indeed, there is a growing awareness of the importance of fungal pathogens in the lung and other sites of infection through global microbiome analyses (Kolwijck and van de Veerdonk, 2014; Kim et al., 2015). However, as with their bacterial counterparts, function and effect in relation to their contribution to the pathophysiology of disease can be harder to define. *Aspergillus* infection takes two principal forms; invasive pulmonary aspergillosis (IPA) and chronic

necrotising pulmonary aspergillosis, with the latter being characterized by the transformation of conidia to hyphae (germination), which can subsequently invade the tissue (Kaur and Singh, 2014; Kolwijck and van de Veerdonk, 2014). Hyphal stage cells typically adopt a structured biofilm, either as monospecies or multispecies, at which point the biofilm-embedded cells become highly resistant to antimicrobial drug therapy (Seidler et al., 2008; Manavathu et al., 2014). Several reasons have been proposed to explain this increased tolerance, such as biofilm specific upregulation of efflux proteins, the presence of extracellular matrices, and persister cells that are inherently drug resistant/tolerant due to their low metabolic rate (Manavathu et al., 2014).

These inherently resistant biofilm characteristics of *A. fumigatus* have led to conventional antifungal therapies rapidly becoming redundant in the treatment of not only nosocomial infections (e.g., hematologic disease) but also on indwelling medical devices (IMDs) and implants (Ramage and Williams, 2013). While both *Candida* and *Aspergillus* species are causative agents in approximately 8% of all implant infections, their potency and resistance to antifungals is increasing steadily with survival rates for some implant patient groups as low as 50% (Lynch and Robertson, 2008; Ramage and Williams, 2013). More recently, *Aspergillus* contamination of nebuliser devices used by CF patients has been reported (Peckham et al., 2016). The upward trend in Aspergillosis and other major fungal infections poses a significant clinical, financial and health threat and requires concerted and sustained efforts to identify and characterize novel anti-fungal agents to tackle these preventable diseases.

It is now becoming clear that the co-existence and mutual interaction of bacteria and fungi at the site of infection contributes to the pathogenesis of disease. In the case of CF, *A. fumigatus* has been isolated in up to 60% of patients with *Pseudomonas aeruginosa* infection, suggesting a close relationship between established colonization by *P. aeruginosa* and superinfection by *A. fumigatus* (Paugam et al., 2010; Briard et al., 2015). Interkingdom interactions between *A. fumigatus* and bacterial competitors has been described previously, with significant attention focused on the interaction with *P. aeruginosa* (McAlester et al., 2008; Mowat et al., 2010; Briard et al., 2015; Ferreira et al., 2015; Zheng et al., 2015). Perhaps somewhat surprisingly, given their co-occurrence, many of these studies describe an antagonistic influence of *P. aeruginosa* secreted factors on *A. fumigatus* biofilm formation. Mowat et al. (2010) ascribed the competitive inhibition of filamentous *A. fumigatus* growth by *P. aeruginosa* to the effects of small diffusible and heat-stable molecules. Interestingly, anti-biofilm activity in the supernatants of *P. aeruginosa* *lasR* and *lasI* quorum sensing mutants was reduced but not lost entirely, suggesting the factors responsible are not entirely under Acyl Homoserine Lactone (AHL) control. Several studies have described the impact of redox active metabolites produced by *P. aeruginosa* on biofilm formation and hyphal development in *A. fumigatus* (Briard et al., 2015; Zheng et al., 2015), effects that are likely to be strain and condition specific (Ferreira et al., 2015). More recently, Briard et al. (2016) demonstrated stimulation of *A. fumigatus* growth

by volatile compounds produced by *P. aeruginosa*. Moreover, strain specificity was also highlighted in a recent study by Shirazi et al. (2016) where biofilm filtrates of *P. aeruginosa* strains isolated from CF patients were shown to inhibit pre-formed *A. fumigatus* biofilms through apoptosis. Therefore, it is clear that the factors that govern the dynamics of the *P. aeruginosa* – *A. fumigatus* interaction *in vivo* remain to be fully understood. From a clinical perspective, a strategy that targets biofilm inhibition should be less susceptible than conventional antibiotic treatment to the emergence of resistance in pathogens, particularly as metabolic processes and bacterial growth are not directly targeted.

In this study, we investigated the anti-biofilm activity of *P. aeruginosa* alkylhydroxyquinolone (AHQ) autoinducers against *A. fumigatus*. Growth was unaffected, while biofilm biomass and structure was significantly altered in the presence of both 2-heptyl-4-quinolone (HHQ) and 2-heptyl-3-hydroxy-4-quinolone (PQS). Having established the activity of the parent molecules, a suite of analogs was tested for anti-biofilm activity and lead compounds were identified that retained activity against *A. fumigatus*. The synthesis of new compounds incorporating decorations on the anthranilate ring identified further lead compounds with activity comparable to the parent HHQ molecule, providing important insights into the structure function relationship underpinning the suppression of fungal biofilms. Importantly, anti-biofilm activity was retained against clinical isolates from a pediatric cohort, providing a framework for further functionalization and future clinical implementation.

MATERIALS AND METHODS

Fungal and Bacterial Culture Conditions

Aspergillus fumigatus Af293 was routinely grown on Sabouraud dextrose agar (SDA) in 100 ml cell culture flasks at 37°C for 3–4 days. Sputum samples from a pediatric CF cohort (Cork University Hospital) were cultured on SDA plates and incubated for 4–7 days at 37°C. Conidia were collected by scraping in PBS with 0.025% (v/v) Tween 20, and the Internal Transcribed Spacer (ITS) region was amplified by PCR using ITS4 (5'-TCCTCCGCTTATTGATATGC-3') and ITS5 (5'-GGAAGTAAAAGTCGTAACAAGG-3') for taxonomic identification. PCR reaction conditions were as follows: 30 cycles of alternating denaturation (94°C for 45 s), annealing (58°C for 45 s), and extension (72°C for 2 min). Yeast cultures of *Candida albicans* were routinely grown on yeast peptone dextrose (YPD) agar and were cultured at 30°C overnight. Bacterial cultures of *P. aeruginosa* containing the pLP0996 *pqsA-lacZ* promoter fusion were maintained on Luria Bertani (LB) plates supplemented with carbenicillin (200 µg/ml), and routinely grown at 37°C.

Spore Capture and Biofilm Assay

Conidia were harvested by flooding the surface of the agar plates with 5 ml PBS (Oxoid) containing 0.025% (v/v) Tween 20 and gently moving the liquid over the surface of the fungal lawn. The conidial suspension was transferred into a 25 ml

sterile container and conidia were counted using a Neubauer haemocytometer and light microscope. Conidia were adjusted to the required concentration in RPMI 1640 (Sigma) buffered to pH 7.0 with 0.165 M MOPS immediately prior to biofilm formation analysis.

To assess biofilm formation, counted *A. fumigatus* spores (1×10^5) in MOPS buffered RPMI 1640 were inoculated into 24- and 96-well plates and grown overnight in the presence of 100 μ M HHQ, PQS and the compound collection. After 24 h, the media was removed and the biofilm washed twice with distilled water after which 0.1 % crystal violet (CV) was added to each well and allowed to stand for 1 h at room temperature. The CV was removed and all wells washed in a water bath by inversion. Ethanol was added to each well to solubilize biofilms after which samples were read on a spectrophotometer at OD_{595nm}.

Analysis of preformed biofilms (24 h) was carried out by allowing biofilms to establish in buffered RPMI, or compound/carrier treated RPMI as described above. Disks were removed and washed gently in PBS to remove unattached cells. Disks from the buffered RPMI wells were transferred into 1 ml of buffered RPMI with 100 μ M HHQ, 1, or methanol control. In tandem, disks from pre-treated wells were also transferred and treated again with their respective compound or methanol control. All plates were incubated for 24 h at 37°C and biofilm quantified as before.

Staining and Microscopy

Aspergillus fumigatus spores (1×10^5) were inoculated onto plastic coverslips in 24 well plates and grown in the presence of analogs overnight at 37°C in RPMI buffered with MOPS pH 7.0. After 24 h, plastic coverslips were washed once in PBS and stained. Calcofluor (1 mg/ml) and 10% (w/v) potassium hydroxide were added drop-wise to coverslips, washed in PBS, mounted, and viewed. Concanavalin A (Con A) and FUN-1 were added at 50 μ g/ml in 1 ml PBS and incubated at 37°C for 30 min. All imaging was carried out on a Zeiss LSM5 confocal microscope. Confocal images were recorded under a bright field lens using $\times 20$ objective magnification. Filter cubes facilitating fluorescent imaging were used to record images for Calcofluor at Abs_{405nm}, Con A at Abs_{488nm} and FUN-1 at Abs_{543nm}. All images were captured using the Zeiss HBO-100 microscope illuminating system, processed using the Zen AIM application imaging program and converted to JPG using Axiovision 40 Ver. 4.6.3.0.

Growth Assays

Aspergillus fumigatus Af293 was grown in RPMI buffered media or YPD to assess sensitivity to HHQ, PQS, and lead analogs. Spore suspensions were collected from SDA plates in PBS Tween 20 (0.025%), counted using a haemocytometer, and inoculated into fresh YPD to a cell count of 1×10^5 spores/ml. Spore suspensions, either treated with lead compounds, carrier solvent, or untreated, were then added in quadruplicate to 96-well plates and incubated with gentle agitation for 24 h. The OD_{405nm} was determined spectrophotometrically.

Promoter Fusion Analysis

Alkylhydroxyquinolone signaling was monitored using the *pqsA-lacZ* promoter fusion pLP0996 in both the wild-type PAO1 strain and its isogenic *pqsA*[−] mutant (McGrath et al., 2004). Cells from overnight cultures were transferred to fresh LB media (carbenicillin 200 μ g/ml) to a starting OD_{600 nm} 0.02 in the presence of compounds 20–24 (100 μ M) or equivalent volumes of DMSO. Samples were taken at late log phase growth and β -galactosidase activity was measured as before (Reen et al., 2016).

Cytotoxicity Assays

Lactate dehydrogenase (LDH) release from HeLa (cervical epithelial adenocarcinoma) cells was assayed as a measure of cytotoxicity using an LDH colorimetric kit (Roche) according to manufacturers' instructions. HeLa cells were seeded into 96 well plates and treated with methanol (control) and analogs. Following a 16 h incubation at 37°C and 5% CO₂, supernatants were removed and added to catalyst reaction mixture in a fresh plate and further incubated at 37°C and 5% CO₂ for 30 min to allow for color development. After this period, the plate was analyzed by measuring the absorbance on a microplate spectrophotometer at OD_{490nm}.

XTT Biofilm Assays

The *C. albicans* biofilm response to analogs was assessed using the XTT [2,3-Bis-(2-Methoxy-4-Nitro-5-Sulphophenyl)-2H-Tetrazolium-5-Carboxanilide] assay in 96 well plates at 37°C. After overnight growth in the presence of methanol (control) and analogs, *C. albicans* biofilms were treated with 100 μ l freshly prepared XTT (Sigma) and menadione (Sigma). After a 2 h incubation at 37°C, biofilm formation was determined by measuring the absorbance at OD_{492nm} on a microplate spectrophotometer.

Statistical Analysis

Data presentation and statistical analysis was performed using the GraphPad Prism v5.03 software package or the Bootstratio algorithm (Cleries et al., 2012).

Compound Synthesis

The synthesis of HHQ, PQS (Pesci et al., 1999; McGlacken et al., 2010) and other HHQ-based analogs (Reen et al., 2012, 2015, 2016) was carried out via previously described methods. Novel compounds and compounds which required modified syntheses are described *vide infra* and in the Supplementary Data Sheet.

Ethics Statement

Sputum samples were collected from pediatric patients attending the CF clinic at Cork University Hospital, Ireland. This study was carried out in accordance with the recommendations of the Clinical Research Ethics Committee of the Cork Teaching Hospitals (CREC), with written informed consent from all subjects. All subjects gave written informed consent in accordance with the Declaration of Helsinki. The protocol was approved by the CREC and all samples were handled in accordance with the approved guidelines.

RESULTS

P. aeruginosa Signal Molecules Interfere with Biofilm Formation in *A. fumigatus*

The *P. aeruginosa* signaling molecules HHQ and PQS have previously been shown to possess interkingdom activity, influencing the phenotypic and transcriptional behavior of both microbes and higher order organisms (Reen et al., 2011; Tashiro et al., 2013; Trejo-Hernandez et al., 2014), including mammalian cells (Kim et al., 2010). While the *P. aeruginosa* secretome has previously been shown to suppress biofilm formation in *A. fumigatus* (Mowat et al., 2010), the extent of the active components remained to be defined. Our previous finding that HHQ suppressed biofilm formation in the pathogenic yeast, *C. albicans* (Reen et al., 2011), led us to investigate the anti-biofilm activity of these signals against *A. fumigatus*. Addition of either HHQ or PQS to the model strain *A. fumigatus* Af293 led to a significant reduction in attachment to the wells of polystyrene plates (Figure 1A). As expected, loss of the alkyl chain led to a significant reduction in the potency of this anti-biofilm activity, consistent with the functional requirement for this feature in AHQ signaling.

In order to visualize the biofilm structures, attached cells were treated with specific intracellular stains to assess impact on key cellular components. These included cellulose and chitin with Calcofluor; live cellular vacuolar stain FUN-1 which functions as a live/dead stain; and lectin (carbohydrate) structures with Concanavalin A. Confocal microscopic analysis confirmed the effect of HHQ and PQS on formation of biofilm mass and revealed a significant reduction and disruption of hyphal development (Figure 1B). Cells treated with either HHQ or PQS appeared locked in a spore form, with minimal evidence for formation of hyphal structures, and the absence of the interwoven network characteristic of *A. fumigatus*.

Structurally Modified AHQ Analogs Retain Anti-biofilm Activity

Having established that both HHQ and PQS interfered with biofilm formation, a suite of 4-quinolone analogs, bearing diverse structural features (Supplementary Figure S1), were tested for anti-biofilm activity toward *A. fumigatus*. Analogs included modifications at the C3 and C4 positions, on the anthranilate ring, and of the alkyl chain length, while substitutions were predominantly with halogen, *n*-hexyl, methyl or methoxy groups. The results of this analysis revealed that an exquisite degree of structural conservation is required for AHQ inter-kingdom activity (Figure 2A). Of these, compound 5 (*n*-hexyl at C6) and compound 12 (methoxy at C7) gave the greatest reduction in biofilm formation. Compound 14, in which the alkyl chain length was extended relative to the parent molecule HHQ, retained its anti-biofilm activity, while addition of halogen groups at C3 led to loss of anti-biofilm activity. Addition of a methoxy (3) or methyl (4) group to the C6 position of HHQ with a seven carbon alkyl chain led to loss of anti-biofilm activity (Figure 2B), while activity was retained in methoxy (11) and halogen (17) modified equivalents upon extension of the alkyl chain to nine carbons.

Isolation of quinolones with substituents at C5 is difficult, as the corresponding regioisomer (at C7) is also formed in the Conrad-Limpach cyclisation step. Thus we chose to focus on symmetrical aniline precursors, which allowed for further elaboration at the 6-position. Compounds were synthesized with Br (20), CO₂C₂H₅ (21), an electron withdrawing F (22), and an electron donating bulky C-C₃H₉ (23) at the C6 position (Figure 3). Use of the 3,5-dimethyl aniline precursor gave a C5-C7 substituted CH₃ (24). All analogs were assessed for antagonism of biofilm formation in *A. fumigatus* Af293. While two of the substituted analogs, 20 and 23, had lost their anti-biofilm activity, compounds 21, 22, and 24 retained activity against the fungus, suppressing biofilm formation to the same degree as lead compounds (Figure 4). It is clear that the structural organization of the anthranilate ring components is of critical importance to the anti-biofilm activity. The retention of anti-biofilm formation by analogs functionalized at the C6 and C8 positions was particularly interesting given that halogenation of these positions had previously been shown to enhance antagonism of PQS signaling in *P. aeruginosa* (Ilango et al., 2013).

Microscopic analysis of biofilms formed on plastic coverslips in the presence of selected compounds confirmed the disruption of hyphal structures in Af293 (Figure 5). Staining with Calcofluor revealed the absence of intact hyphal networks in samples treated with compounds 1, 12, 21, and 24 while inactive compounds 3 and 15 did not affect this phenotype. This anti-biofilm activity was shown to be independent of any impact on growth of Af293, with the exception of compound 2 which reduced the final OD_{600 nm} reached by 0.1 unit (Supplementary Figure S2).

Having determined that the alkylhydroxyquinolone derivative compounds could suppress biofilm formation in *A. fumigatus*, the next stage was to assess whether or not they could affect pre-formed *A. fumigatus* biofilms. The addition of HHQ or 1 to preformed biofilms on plastic disks led to a reduction relative to the methanol control, although only 1 reached statistical significance (Figure 6). Pre-treatment from the outset with either HHQ or 1 led to a marked reduction in biofilm formation on disks when compared with the control sample, further evidence that both attachment and the development of hyphal biofilms may be key targets for the lead compounds.

C6-Modified Analogs Exhibit Non-cytotoxic *A. fumigatus* Specific Activity

Any assessment of the utility of these compounds as anti-biofilm agents must consider the origin of the parent molecules HHQ and PQS as co-inducers of AHQ mediated virulence in *P. aeruginosa*. Both HHQ and PQS control multiple virulence phenotypes through activation of the PqsR transcriptional regulator (Xiao et al., 2006). Previously, we have shown that several of the lead analogs described here e.g., 1 and 2 are non-agonists of the AHQ signaling system in *P. aeruginosa*, are selectively non-cytotoxic, and are also effective biofilm blockers in *C. albicans* (Supplementary Table S1) (Reen et al., 2016). Therefore, this

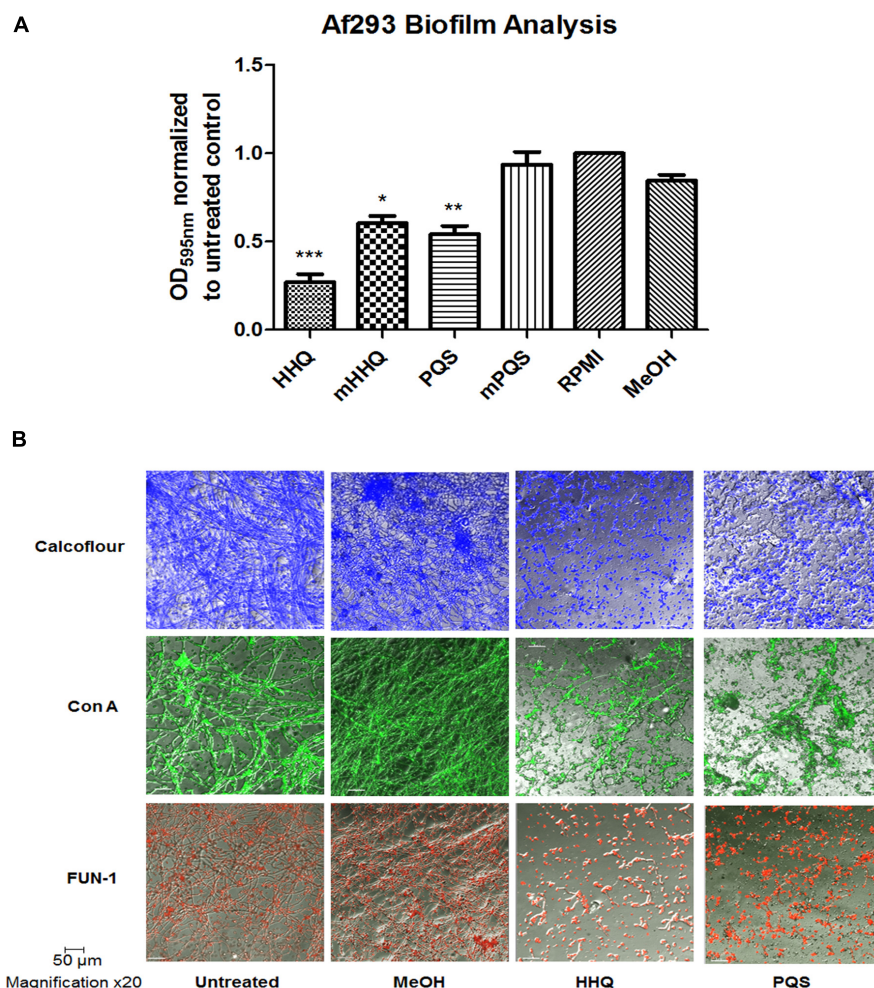


FIGURE 1 | Suppression of *A. fumigatus* biofilm formation in response to HHQ and PQS. (A) Biofilm assays using crystal violet (CV) staining. mPQS and mHHQ refer to the parent compounds with the C7 alkyl chain removed. RPMI constitutes the untreated sample whereby no compound or carrier has been added. Data is presented as mean fold change (\pm SEM) of Abs_{595nm} relative to untreated cells. Data is representative of five independent biological replicates. Statistical significance using methanol treated cells as reference is represented by one way ANOVA with *post hoc* Bonferroni correction (* $p < 0.05$, ** $p < 0.005$; *** $p < 0.001$). **(B)** Confocal microscopic analysis ($\times 20$) of biofilm formation on plastic coverslips. Staining was performed using Calcofluor-1 (cellulose and chitin), Concanavalin A (live cellular vacuoles), and FUN-1 (lectins/carbohydrates).

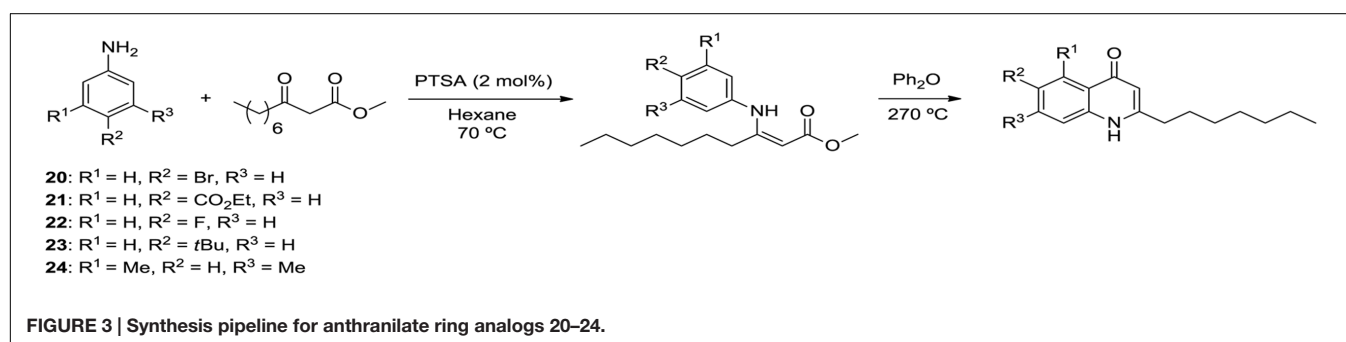
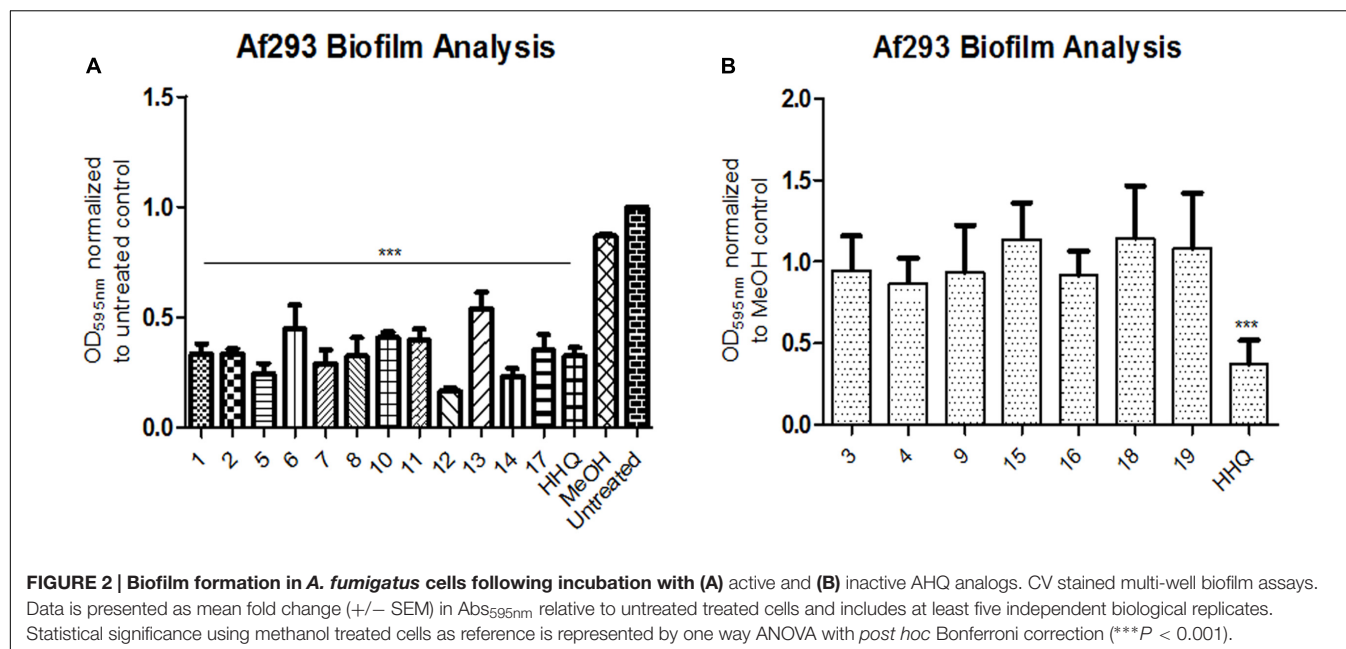
analysis was extended to the newly synthesized compounds 20–24 to provide a comprehensive profile of all the compounds described in this study. Addition of compounds 21, 23, and 24 did not lead to increased *pqsA* promoter activity in a PAO1 *pqsA*[−] mutant strain indicating that they are non-agonists of the PqsR virulence system (Figure 7A). In contrast, compounds 20 and 22 significantly increased expression relative to the control, suggesting that further modification would be required to silence this activity. In spite of being ineffective PqsR ligands, none of the five analogs were capable of interfering with AHQ signaling in the wild-type PAO1 strain, as seen with the comparable activity of the *pqsA* promoter in both treated and untreated cells (Figure 7B).

In order to determine whether or not the anti-biofilm activity extends to other fungal pathogens, *C. albicans* was tested for biofilm formation in the presence and absence of compounds 20–24 (Figure 7C). None of the compounds were found to be

active against *C. albicans* biofilm formation, in contrast to some of the other lead compounds identified in this study, such as 1 and 2 (Reen et al., 2016). Further extending the profile and characterization of these compounds, cytotoxicity was measured in a host cell line (Figure 7D). Only compound 24 elicited any measurable degree of cytotoxicity, and this was to a lesser extent than the parent molecule HHQ. The other four analogs were comparable to the methanol control.

AHQ Analogs Block Biofilm in Clinical *A. fumigatus* Isolates

There is a growing realization that the genomes of clinical isolates can vary markedly from typed environmental strains, with niche-specific selective pressures manifesting in considerable heterogeneity, even within species. This led us to investigate



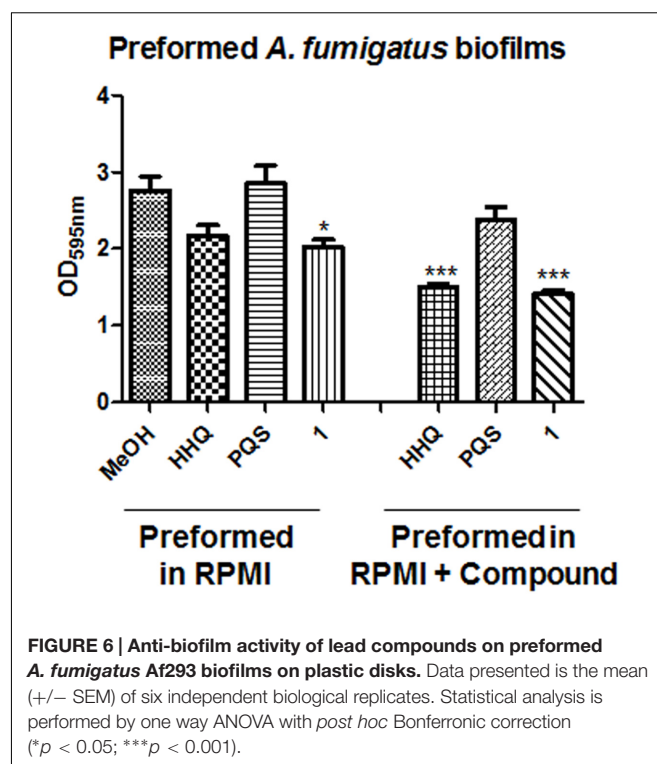
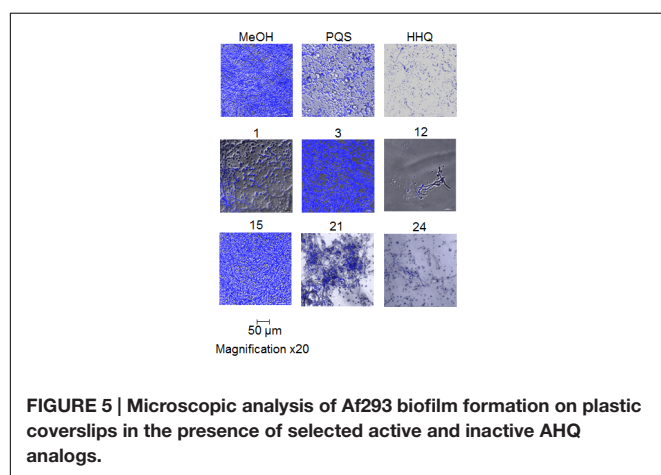
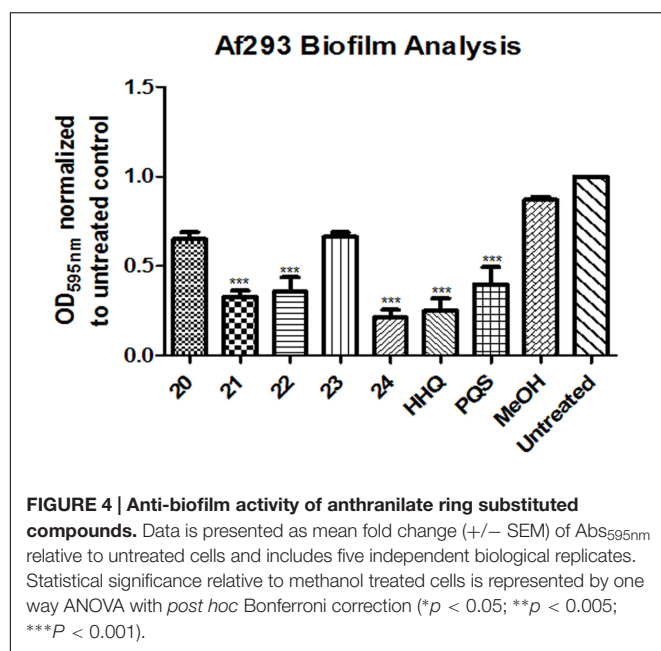
the effectiveness of the lead compounds against clinical isolates from a pediatric CF cohort, each of which exhibited significant wrinkling of the mycelial mat compared to the smoothness of Af293 (Figure 8). Both HHQ and PQS were capable of suppressing biofilm formation in each of the clinical isolates. It was notable, however, that the suppression of biofilm formation was not to same extent as that seen against the lab strain Af293, suggesting some degree of tolerance or adaptation in the clinical isolates (Figure 8). Lead compounds were also found to be effective against biofilm formation in clinical strains, underpinning their suitability for further therapeutic development (Figure 9).

The structural impact of lead compounds on biofilm formation in both Af293 and the clinical isolates was assessed using confocal microscopy of calcofluor stained cells. As expected, anti-biofilm compounds disrupted the formation of hyphal structures, while inactive compounds (e.g., 23) did not markedly affect this phenotype. In general, active compounds (e.g., 2 and 24) appeared to lock the fungal cells in the spore state, with little or no evidence for hyphal development (Figure 10). Although present in some of the clinical isolates (e.g., CFBRC2 and CFBRC3, 24), hyphal structures were weak and sparse,

indicating that a key mode of action of these compounds is the prevention of the hyphal switch.

DISCUSSION

Exposure of immunocompromised individuals to *A. fumigatus* can result in significant morbidity and even mortality in severe cases. The incidence is on the rise owing largely to the increased prevalence of respiratory conditions such as asthma, increased frequency of lung transplantation, and the ongoing use of immunosuppressive therapies. In many of these cases, *A. fumigatus* adopts a biofilm lifestyle, enhancing its persistence and contributing directly to morbidity and mortality associated with these infections. *A. fumigatus* has recently been associated with medical device infections (Ramage et al., 2012; Ramage and Williams, 2013; Nett and Andes, 2015). Cases of serious biomaterial-related infections of joint replacements, catheters, heart valves, cardiac pace makers, and breast augmentation implants have been reported. Often, high risk invasive surgical procedures are used to treat these *A. fumigatus* infections, as the formation of biofilm structures and the associated increased



HHQ and PQS were capable of interfering with the formation of *A. fumigatus* biofilms, leading to reduced biomass and the absence of intact hyphal structures in treated cells. Derivatization of the quinolone framework at the C6 and C8 positions revealed the anthranilate ring to be particularly important in the anti-biofilm activity. Several of these compounds have no agonistic activity toward *P. aeruginosa* virulence, unlike the parent molecules HHQ and PQS, thus presenting a viable framework for therapeutic development against medical device fungal pathogens [Figure 7 and (Reen et al., 2016)]. Furthermore, they are selectively non-cytotoxic to host cell lines, further supporting their development as viable molecular therapeutics. The next stage in the development of these lead compounds will be the characterization of the molecular mechanism(s) through which they elicit their anti-biofilm activity. One approach will be to investigate the possibility of fungal sensory and signal transduction systems that may be involved in perception of alkylhydroxyquinolones and transduction of that response to exist in a non-hyphal growth state. Alternatively, alkyl-quinolones, and PQS in particular, have also been reported previously to possess both pro- and anti-oxidant activity, while interaction with lipopolysaccharide, cellular membranes, and membrane vesicles has also been reported in several bacterial species (Haussler and Becker, 2008; Mashburn-Warren et al., 2009).

The modulation of *A. fumigatus* biofilm by HHQ and PQS adds another layer of complexity to the interkingdom interactions that are characteristic of mixed *P. aeruginosa* fungal communities. Phenazines, a redox active toxin controlled by PQS and secreted by *P. aeruginosa* reportedly undergo chemical

rate of antifungal resistance renders conventional treatment ineffectual (Desai et al., 2014; Nett and Andes, 2015). Antifungal tolerance in fungal infections has been attributed to the secretion of an extracellular polymeric matrix and increased activity of efflux pumps (Mowat et al., 2008; Rajendran et al., 2013). Therefore, therapies that combat biofilms directly are likely to enhance the survival and life expectancy of infected individuals.

In this study we have shown that two signal molecules secreted by the nosocomial pathogen *P. aeruginosa* can suppress biofilm formation in *A. fumigatus*. This may be a consequence of the proximity in which these organisms co-exist in clinical and environmental niches, including the lungs of immunocompromised patients and the plant ecosystem. Interactions between co-existing organisms have been widely reported, with signaling molecules showing activity ranging from inter-species to inter-kingdom (Reen et al., 2011; Chen et al., 2014; Michelsen et al., 2014; Kendall and Sperandio, 2016). Both

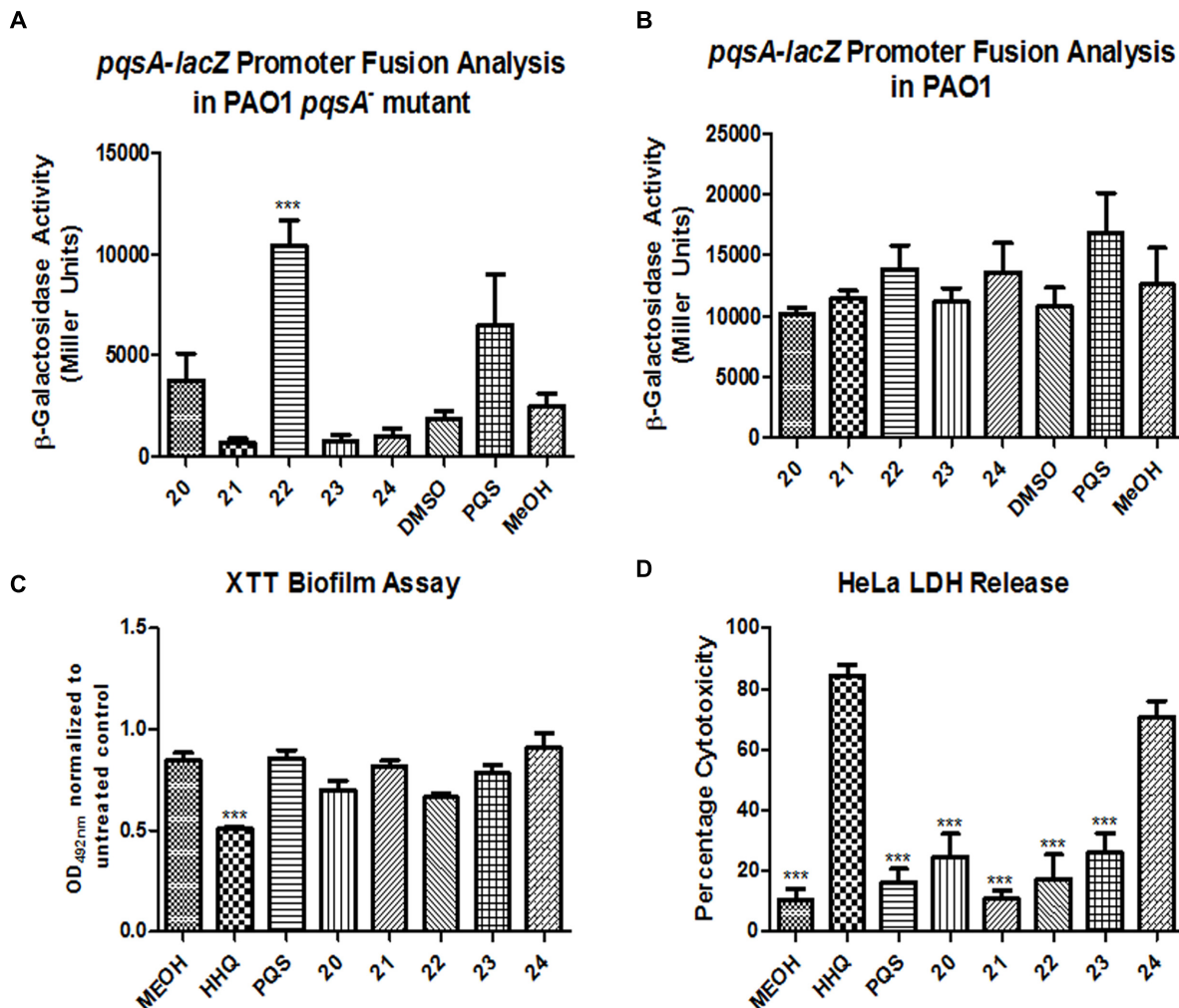


FIGURE 7 | Profiling the spectrum of activity of compounds 20–24. Promoter fusion analysis of the *pqsA-lacZ* pLP0996 plasmid in (A) a PAO1 *pqsA*⁻ mutant, and (B) PAO1 wild-type strain, (C) XTT biofilm analysis of *C. albicans* and (D) LDH release cytotoxicity assays using HeLa cell lines. Data in all experiments is the mean (+/- SEM) of at least three independent biological replicates. Statistical analysis was performed by one-way ANOVA with *post hoc* Bonferroni correction (***) $p \leq 0.001$.

transformation by *A. fumigatus* and *C. albicans* (Moree et al., 2012; Chen et al., 2014). The AHL class of quorum sensing signal has also been shown to play a role in modulating biofilm formation in these fungal pathogens (McAlester et al., 2008; Mowat et al., 2010), while HHQ and PQS have previously been shown to modulate biofilm formation in *C. albicans* (Reen et al., 2011, 2016). Apart from signal mediated interactions, there is recent evidence to suggest that interspecies and interkingdom interactions can foster mutability in co-existing organisms (Michelsen et al., 2014; Trejo-Hernandez et al., 2014). It must also be considered that microbial signals are just one factor in the process of fungal biofilm formation in the host. Other factors such as the availability of nutrients, host related factors such as the immune system and the surface upon which the biofilm will form, mechanical factors such as flow rate within the niche, and the presence of dispersion agents can have a significant influence on fungal biofilm formation. Notwithstanding this,

deciphering the chemical messages used by microbes themselves to control the behavior of pathogenic species, without disrupting the growth of the microbiome as a whole, remains a key goal in the age of molecular based therapeutics (Figure 11). As a greater understanding of the connection between microbiome dysbiosis and disease status continues to emerge, the critical need for therapeutics that retain the functionality of the core microbiome becomes ever more relevant.

CONCLUSION

Microbial communities are founded on intricate and long-evolved communication systems that determine the flux and dynamics of particular species in response to local and environmental cues. Therefore, deciphering these chemical messages has the potential to deliver on the new and innovative

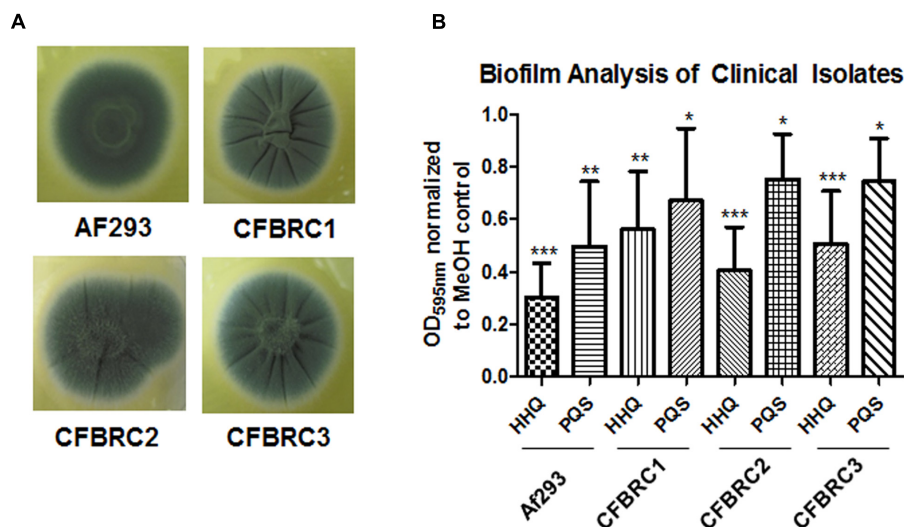


FIGURE 8 | AHQs suppress biofilm formation in clinical isolates. (A) Morphological analysis of clinical *A. fumigatus* isolates. **(B)** Biofilm formation in *A. fumigatus* treated cells following incubation with AHQ signals HHQ and PQS. Data is presented as mean fold change (\pm SEM) in OD_{595nm} relative to methanol treated cells and includes five independent biological replicates. Statistical significance is represented by Bootstratio analysis (* $p < 0.05$; ** $p < 0.005$; *** $p < 0.001$).

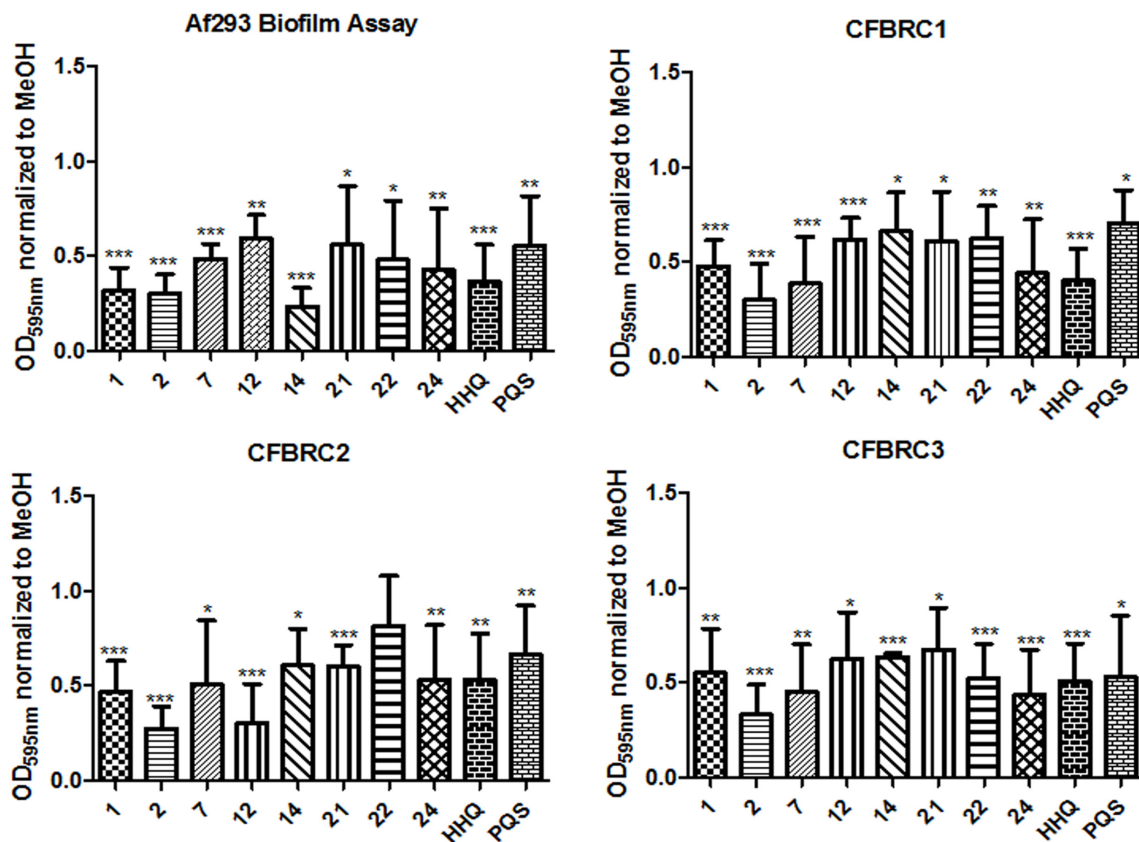


FIGURE 9 | Biofilm formation in *A. fumigatus* clinical isolates following incubation with AHQ analogs. Data is presented as mean fold change (\pm SEM) in OD_{595nm} relative to methanol treated cells and includes at least three independent biological replicates. Statistical significance is represented by Bootstratio analysis (* $p < 0.05$; ** $p < 0.005$; *** $p < 0.001$).

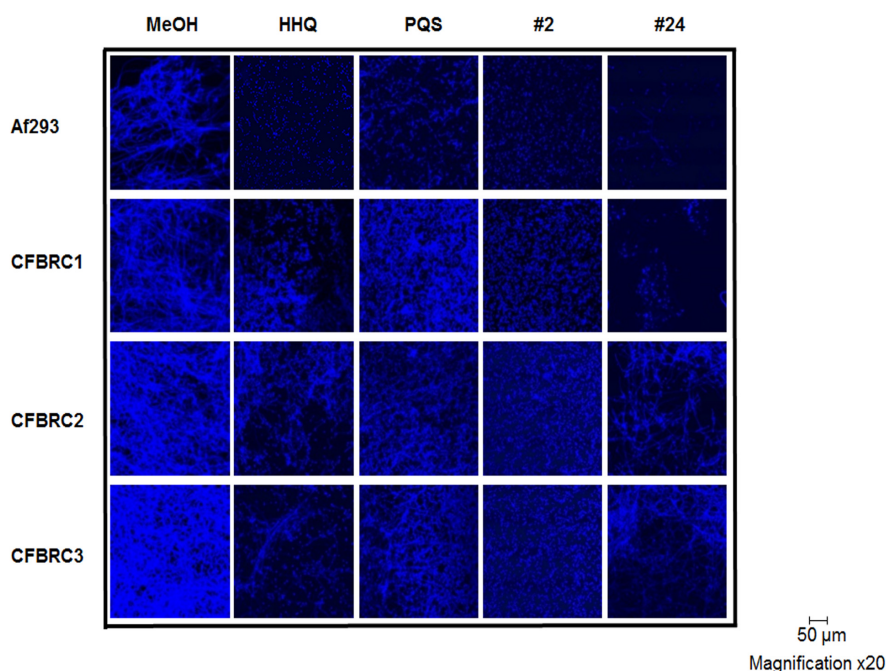
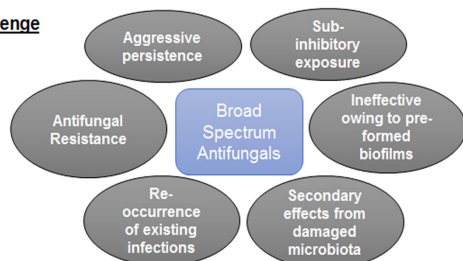
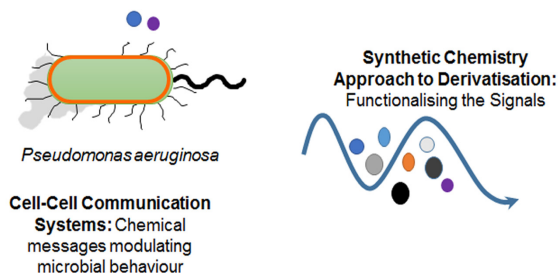


FIGURE 10 | CLSM analysis of biofilm formation in Af293 and clinical isolates in the presence of lead compounds 2 and 24. All data presented is representative of three independent biological replicates.

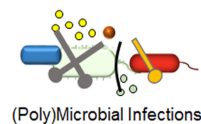
The Challenge



A Solution

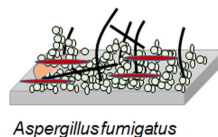


Current Broad Spectrum Antifungals

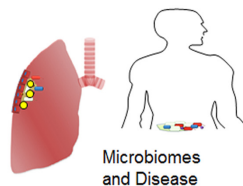


Non-specific Antifungal Eradication of Infection: Broad spectrum microbial death, potential for microbiome dysbiosis

Therapeutic Alternatives to Broad Spectrum Antibiotics



Non-Antibiotic Eradication of Infection: Biofilm blocking anti-infective molecules



Protecting the Good Microbiota: Targeted pathogen specific therapies

FIGURE 11 | The lead compounds identified in this study address a key clinical need for alternatives to broad spectrum antifungals. Challenge: While still the lead option for the management of microbial infections, broad spectrum growth limiting antifungals are increasingly being challenged by limiting factors including antifungal resistance, the aggressive persistence of known pathogens in a biofilm lifestyle, and the collateral damage caused to the host microbiome leading to dysbiosis, Solution: Exploiting new knowledge of cell-cell communication systems and utilizing synthetic chemistry approaches to generate suites of derivatized compounds, has made possible the development of anti-biofilm small molecules that are selectively non-toxic in mammalian cell lines. These have the potential to lock yeast and fungal pathogens such as *A. fumigatus* in the non-hyphal state, potentially rendering them more susceptible to immune challenge, and enhancing the effectiveness of conventional antifungal compounds.

alternatives being sought to conventional growth limiting antibiotics. This is an attractive route to therapy due to the chemical tractability of these signals, opening up avenues for functionalization to improve activity and drug-ability of lead compounds. The work described here is highly significant and potentially relevant to several sectors within the clinical and medical device arena where the occurrence of *in vivo* and nosocomial *Aspergillus* infections is destructive from both a human and financial perspective.

AUTHOR CONTRIBUTIONS

Conceptualization: FR, GM, and FO. Investigation: FR, JP, DW, RS, RC, and SC. Writing – Original Draft: FR. Writing – Review and Editing: FR, JP, DW, GM, and FG. Funding Acquisition: FR, GM, and FG.

FUNDING

This research was supported in part by grants awarded by the European Commission (FP7-PEOPLE-2013-ITN, 607786; FP7-KBBE-2012-6, CP-TP-312184; FP7-KBBE-2012-6, 311975; OCEAN 2011-2, 287589; Marie Curie

256596; EU-634486), Science Foundation Ireland (SSPC-2, 12/RC/2275; 13/TIDA/B2625; 12/TIDA/B2411; 12/TIDA/B2405; 14/TIDA/2438), the Department of Agriculture and Food (FIRM/RSF/CoFoRD; FIRM 08/RDC/629; FIRM 1/F009/MabS; FIRM 13/F/516), the Irish Research Council for Science, Engineering and Technology (PD/2011/2414; GOIPG/2014/647), the Health Research Board/Irish Thoracic Society (MRCG-2014-6), the Marine Institute (Beaufort award C2CRA 2007/082) and Teagasc (Walsh Fellowship 2013). GM thanks SFI, grant number SFI/12/RC/2275, and the Irish Research Council (RS and RC).

ACKNOWLEDGMENT

The authors thank Stephanie Flynn for excellent technical assistance.

SUPPLEMENTARY MATERIAL

The Supplementary Material for this article can be found online at: <http://journal.frontiersin.org/article/10.3389/fmicb.2016.02074/full#supplementary-material>

REFERENCES

- Briard, B., Bomme, P., Lechner, B. E., Mislin, G. L., Lair, V., Prevost, M. C., et al. (2015). *Pseudomonas aeruginosa* manipulates redox and iron homeostasis of its microbiota partner *Aspergillus fumigatus* via phenazines. *Sci. Rep.* 5:8220. doi: 10.1038/srep08220
- Briard, B., Heddergott, C., and Latge, J. P. (2016). Volatile compounds emitted by *Pseudomonas aeruginosa* stimulate growth of the fungal pathogen *Aspergillus fumigatus*. *MBio* 7, e00219–16. doi: 10.1128/mBio.00219-16
- Chen, A. I., Dolben, E. F., Okegbe, C., Harty, C. E., Golub, Y., Thao, S., et al. (2014). *Candida albicans* ethanol stimulates *Pseudomonas aeruginosa* WspR-controlled biofilm formation as part of a cyclic relationship involving phenazines. *PLoS Pathog.* 10:e1004480. doi: 10.1371/journal.ppat.1004480
- Cleries, R., Galvez, J., Espino, M., Ribes, J., Nunes, V., and de Heredia, M. L. (2012). Bootstratio: a web-based statistical analysis of fold-change in qPCR and RT-qPCR data using resampling methods. *Comput. Biol. Med.* 42, 438–445. doi: 10.1016/j.combiomed.2011.12.012
- Desai, J. V., Mitchell, A. P., and Andes, D. R. (2014). Fungal biofilms, drug resistance, and recurrent infection. *Cold Spring Harb. Perspect. Med.* 4:a019729. doi: 10.1101/cshperspect.a019729
- Ferreira, J. A., Penner, J. C., Moss, R. B., Haagsen, J. A., Clemons, K. V., Spormann, A. M., et al. (2015). Inhibition of *Aspergillus fumigatus* and its biofilm by *Pseudomonas aeruginosa* is dependent on the source, phenotype and growth conditions of the bacterium. *PLoS ONE* 10:e0134692. doi: 10.1371/journal.pone.0134692
- Hausser, S., and Becker, T. (2008). The *Pseudomonas* quinolone signal (PQS) balances life and death in *Pseudomonas aeruginosa* populations. *PLoS Pathog.* 4:e1000166. doi: 10.1371/journal.ppat.1000166
- Ilangoan, A., Fletcher, M., Rampioni, G., Pustelny, C., Rumbaugh, K., Heeb, S., et al. (2013). Structural basis for native agonist and synthetic inhibitor recognition by the *Pseudomonas aeruginosa* quorum sensing regulator PqsR (MvfR). *PLoS Pathog.* 9:e1003508. doi: 10.1371/journal.ppat.1003508
- Kaur, S., and Singh, S. (2014). Biofilm formation by *Aspergillus fumigatus*. *Med. Mycol.* 52, 2–9. doi: 10.3109/13693786.2013.819592
- Kendall, M. M., and Sperandio, V. (2016). What a dinner party! mechanisms and functions of interkingdom signaling in host-pathogen associations. *MBio* 7, e1748–e15. doi: 10.1128/mBio.01748-15
- Kim, K., Kim, Y. U., Koh, B. H., Hwang, S. S., Kim, S. H., Lepine, F., et al. (2010). HHQ and PQS, two *Pseudomonas aeruginosa* quorum-sensing molecules, down-regulate the innate immune responses through the nuclear factor-kappaB pathway. *Immunology* 129, 578–588. doi: 10.1111/j.1365-2567.2009.03160.x
- Kim, S. H., Clark, S. T., Surendra, A., Copeland, J. K., Wang, P. W., Ammar, R., et al. (2015). Global analysis of the fungal microbiome in cystic fibrosis patients reveals loss of function of the transcriptional repressor Nrg1 as a mechanism of pathogen adaptation. *PLoS Pathog.* 11:e1005308. doi: 10.1371/journal.ppat.1005308
- Kolwijck, E., and van de Veerdonk, F. L. (2014). The potential impact of the pulmonary microbiome on immunopathogenesis of *Aspergillus*-related lung disease. *Eur. J. Immunol.* 44, 3156–3165. doi: 10.1002/eji.201344404
- Lynch, A. S., and Robertson, G. T. (2008). Bacterial and fungal biofilm infections. *Annu. Rev. Med.* 59, 415–428. doi: 10.1146/annurev.med.59.110106.132000
- Manavathu, E. K., Vager, D. L., and Vazquez, J. A. (2014). Development and antimicrobial susceptibility studies of in vitro monomicrobial and polymicrobial biofilm models with *Aspergillus fumigatus* and *Pseudomonas aeruginosa*. *BMC Microbiol.* 14:53. doi: 10.1186/1471-2180-14-53
- Mashburn-Warren, L., Howe, J., Brandenburg, K., and Whiteley, M. (2009). Structural requirements of the *Pseudomonas* quinolone signal for membrane vesicle stimulation. *J. Bacteriol.* 191, 3411–3414. doi: 10.1128/JB.00052-09
- McAlester, G., O'Gara, F., and Morrissey, J. P. (2008). Signal-mediated interactions between *Pseudomonas aeruginosa* and *Candida albicans*. *J. Med. Microbiol.* 57, 563–569. doi: 10.1099/jmm.0.47705-0
- McGlacken, G. P., McSweeney, C. M., O'Brien, T., Lawrence, S. E., Elcoate, C. J., Reen, F. J., et al. (2010). Synthesis of 3-halo-analogues of HHQ, subsequent cross-coupling and first crystal structure of *Pseudomonas* quinolone signal (PQS). *Tetrahedron Lett.* 51, 5919–5921. doi: 10.1016/j.tetlet.2010.09.013
- McGrath, S., Wade, D. S., and Pesci, E. C. (2004). Dueling quorum sensing systems in *Pseudomonas aeruginosa* control the production of the *Pseudomonas* quinolone signal (PQS). *FEMS Microbiol. Lett.* 230, 27–34. doi: 10.1016/S0378-1097(03)00849-8
- Michelsen, C. F., Christensen, A. M., Bojer, M. S., Hoiby, N., Ingmer, H., and Jelsbak, L. (2014). *Staphylococcus aureus* alters growth activity, autolysis, and antibiotic tolerance in a human host-adapted *Pseudomonas aeruginosa* lineage. *J. Bacteriol.* 196, 3903–3911. doi: 10.1128/JB.02006-14

- Moree, W. J., Phelan, V. V., Wu, C. H., Bandeira, N., Cornett, D. S., Duggan, B. M., et al. (2012). Interkingdom metabolic transformations captured by microbial imaging mass spectrometry. *Proc. Natl. Acad. Sci. U.S.A.* 109, 13811–13816. doi: 10.1073/pnas.1206855109
- Mowat, E., Lang, S., Williams, C., McCulloch, E., Jones, B., and Ramage, G. (2008). Phase-dependent antifungal activity against *Aspergillus fumigatus* developing multicellular filamentous biofilms. *J. Antimicrob. Chemother.* 62, 1281–1284. doi: 10.1093/jac/dkn402
- Mowat, E., Rajendran, R., Williams, C., McCulloch, E., Jones, B., Lang, S., et al. (2010). *Pseudomonas aeruginosa* and their small diffusible extracellular molecules inhibit *Aspergillus fumigatus* biofilm formation. *FEMS Microbiol. Lett.* 313, 96–102. doi: 10.1111/j.1574-6968.2010.02130.x
- Nett, J. E., and Andes, D. R. (2015). Fungal biofilms: in vivo models for discovery of anti-biofilm drugs. *Microbiol. Spectr.* 3:E30.
- Paugam, A., Baixench, M. T., Demazes-Dufeu, N., Burgel, P. R., Sauter, E., Kanaan, R., et al. (2010). Characteristics and consequences of airway colonization by filamentous fungi in 201 adult patients with cystic fibrosis in France. *Med. Mycol.* 48(Suppl. 1), S32–S36. doi: 10.3109/13693786.2010.503665
- Peckham, D., Williams, K., Wynne, S., Denton, M., Pollard, K., and Barton, R. (2016). Fungal contamination of nebuliser devices used by people with cystic fibrosis. *J. Cyst. Fibros.* 15, 74–77. doi: 10.1016/j.jcf.2015.06.004
- Peleg, A. Y., Hogan, D. A., and Mylonakis, E. (2010). Medically important bacterial-fungal interactions. *Nat. Rev. Microbiol.* 8, 340–349. doi: 10.1038/nrmicro2313
- Pesci, E. C., Milbank, J. B., Pearson, J. P., McKnight, S., Kende, A. S., Greenberg, E. P., et al. (1999). Quinolone signaling in the cell-to-cell communication system of *Pseudomonas aeruginosa*. *Proc. Natl. Acad. Sci. U.S.A.* 96, 11229–11234. doi: 10.1073/pnas.96.20.11229
- Rajendran, R., Williams, C., Lappin, D. F., Millington, O., Martins, M., and Ramage, G. (2013). Extracellular DNA release acts as an antifungal resistance mechanism in mature *Aspergillus fumigatus* biofilms. *Eukaryot. Cell* 12, 420–429. doi: 10.1128/EC.00287-12
- Ramage, G., Rajendran, R., Sherry, L., and Williams, C. (2012). Fungal biofilm resistance. *Int. J. Microbiol.* 2012:528521. doi: 10.1155/2012/528521
- Ramage, G., and Williams, C. (2013). The clinical importance of fungal biofilms. *Adv. Appl. Microbiol.* 84, 27–83. doi: 10.1016/B978-0-12-407673-0.00002-3
- Reen, F. J., Clarke, S. L., Legendre, C., McSweeney, C. M., Eccles, K. S., Lawrence, S. E., et al. (2012). Structure-function analysis of the C-3 position in analogues of microbial behavioural modulators HHQ and PQS. *Org. Biomol. Chem.* 10, 8903–8910. doi: 10.1039/c2ob26823j
- Reen, F. J., Mooij, M. J., Holcombe, L. J., McSweeney, C. M., McGlacken, G. P., Morrissey, J. P., et al. (2011). The *Pseudomonas* quinolone signal (PQS), and its precursor HHQ, modulate interspecies and interkingdom behaviour. *FEMS Microbiol. Ecol.* 77, 413–428. doi: 10.1111/j.1574-6941.2011.01121.x
- Reen, F. J., Phelan, J. P., Gallagher, L., Woods, D. F., Shanahan, R. M., Cano, R., et al. (2016). Exploiting interkingdom interactions for the development of small molecule inhibitors of *Candida albicans* biofilm formation. *Antimicrob. Agents Chemother.* doi: 10.1128/AAC.00190-16 Epub ahead of print.
- Reen, F. J., Shanahan, R., Cano, R., O’Gara, F., and McGlacken, G. P. (2015). A structure activity-relationship study of the bacterial signal molecule HHQ reveals swarming motility inhibition in *Bacillus atrophaeus*. *Org. Biomol. Chem.* 13, 5537–5541. doi: 10.1039/c5ob00315f
- Seidler, M. J., Salvenmoser, S., and Muller, F. M. (2008). *Aspergillus fumigatus* forms biofilms with reduced antifungal drug susceptibility on bronchial epithelial cells. *Antimicrob. Agents Chemother.* 52, 4130–4136. doi: 10.1128/AAC.00234-08
- Shirazi, F., Ferreira, J. A., Stevens, D. A., Clemons, K. V., and Kontoyiannis, D. P. (2016). Biofilm filtrates of *Pseudomonas aeruginosa* strains isolated from cystic fibrosis patients inhibit preformed *Aspergillus fumigatus* biofilms via apoptosis. *PLoS ONE* 11:e0150155. doi: 10.1371/journal.pone.0150155
- Speirs, J. J., van der Ent, C. K., and Beekman, J. M. (2012). Effects of *Aspergillus fumigatus* colonization on lung function in cystic fibrosis. *Curr. Opin. Pulm. Med.* 18, 632–638. doi: 10.1097/MCP.0b013e328358d50b
- Tashiro, Y., Yawata, Y., Toyofuku, M., Uchiyama, H., and Nomura, N. (2013). Interspecies interaction between *Pseudomonas aeruginosa* and other microorganisms. *Microbes Environ.* 28, 13–24. doi: 10.1264/jsme2.ME12167
- Trejo-Hernandez, A., Andrade-Dominguez, A., Hernandez, M., and Encarnacion, S. (2014). Interspecies competition triggers virulence and mutability in *Candida albicans*-*Pseudomonas aeruginosa* mixed biofilms. *ISME J.* 8, 1974–1988. doi: 10.1038/ismej.2014.53
- Xiao, G., Deziel, E., He, J., Lepine, F., Lesic, B., Castonguay, M. H., et al. (2006). MvfR, a key *Pseudomonas aeruginosa* pathogenicity LTTR-class regulatory protein, has dual ligands. *Mol. Microbiol.* 62, 1689–1699. doi: 10.1111/j.1365-2958.2006.05462.x
- Zheng, H., Kim, J., Liew, M., Yan, J. K., Herrera, O., Bok, J. W., et al. (2015). Redox metabolites signal polymicrobial biofilm development via the NapA oxidative stress cascade in *Aspergillus*. *Curr. Biol.* 25, 29–37. doi: 10.1016/j.cub.2014.11.018

Conflict of Interest Statement: The authors declare that the research was conducted in the absence of any commercial or financial relationships that could be construed as a potential conflict of interest.

Copyright © 2016 Reen, Phelan, Woods, Shanahan, Cano, Clarke, McGlacken and O’Gara. This is an open-access article distributed under the terms of the Creative Commons Attribution License (CC BY). The use, distribution or reproduction in other forums is permitted, provided the original author(s) or licensor are credited and that the original publication in this journal is cited, in accordance with accepted academic practice. No use, distribution or reproduction is permitted which does not comply with these terms.



Cite this: *Org. Biomol. Chem.*, 2017, **15**, 306

Received 1st September 2016,
Accepted 24th November 2016

DOI: 10.1039/c6ob01930g

www.rsc.org/obc

The requirements at the C-3 position of alkylquinolones for signalling in *Pseudomonas aeruginosa*[†]

Rachel Shanahan,^{‡a} F. Jerry Reen,^{‡b} Rafael Cano,^a Fergal O'Gara^{*b,c} and Gerard P. McGlacken^{*a}

The 'perfect storm' of increasing bacterial antibiotic resistance and a decline in the discovery of new antibiotics, has made it necessary to search for new and innovative strategies to treat bacterial infections. Interruption of bacterial cell-to-cell communication signalling (Quorum Sensing), thus neutralizing virulence in pathogenic bacteria, is a growing area. 2-Alkyl-4-quinolones, HHQ and PQS, play a key role in the quorum sensing circuitry of *P. aeruginosa*. We report a new set of isosteres of 2-heptyl-6-nitroquinolin-4-one, with alterations at C-3, and evaluate the key structural requirements for agonistic and antagonistic activity in *Pseudomonas aeruginosa*.

Introduction

The dramatic increase in drug-resistant bacterial strains, along with a decrease in antibiotic research investment by pharmaceutical companies, is a serious cause of concern.^{1,2} It is now clear that new strategies³ must be developed to target bacterial infection. Non-biocidal approaches, which do not place an evolutionary stress on bacteria, could also avoid the acquisition of bacterial resistance.⁴

One of these strategies is based on the inhibition of the bacterial cell-to-cell communication system, known as Quorum-sensing (QS).^{5,6} QS uses extracellular signal molecules to coordinate cellular behaviour, motility, virulence and the formation of protective biofilms.⁷ Recently, efforts have been focused on the design of new molecules that could interfere with QS systems.^{8–10} Much work has focused on the important nosocomial pathogen *Pseudomonas aeruginosa*, in which multi-drug resistance continues to emerge.^{11,12}

P. aeruginosa^{13,14} is a highly adaptable Gram-negative bacterium, capable of colonizing a wide variety of environments including burn wounds and the lungs, primarily in immunocompromised or hospitalized patients. It is also the primary cause of morbidity and mortality in patients with cystic fibrosis (CF)¹⁵ and is one of six multi-drug resistant bacteria highlighted by the Centers for Disease Control and Prevention (CDC) as 'the most urgent and serious' threat to healthcare patients.¹⁶ Once *P. aeruginosa* has established itself in the lungs of immunocompromised patients, it adopts a chronic persistent lifestyle that is almost impossible to eradicate.

2-Alkyl-4-quinolones (AHQs) are used as QS signalling molecules by *P. aeruginosa* to control production of multiple virulence determinants,^{17–19} including biofilm formation.²⁰ The primary autoinducers of the *P. aeruginosa* AHQ signalling pathway are 2-heptyl-3-hydroxy-4-quinolone (*Pseudomonas* quinolone signal, or PQS) and its biological precursor 2-heptyl-4-quinolone (HHQ) (Fig. 1).^{21,22} HHQ is converted by the monooxygenase PqsH to PQS in *P. aeruginosa*. The action of PQS and HHQ on *P. aeruginosa* is complex.^{23,24} It is known to be dependent on the *pqsABCDE* biosynthetic operon which is positively regulated by the transcriptional regulator PqsR.^{25,26} PQS and HHQ activate PqsR, and thus enhance the expression of this operon and the subsequent virulence factors. Therefore PqsR is a key target in the search for a *P. aeruginosa* QS inhibitor.

Modifying the structural properties of HHQ and PQS in an effort to interfere with normal binding at PqsR, has recently been reported.^{27–30} Alterations to the alkyl chain¹¹ and the aromatic backbone³⁰ have given an insight into the structure-activity relationships of these molecules. What is clearly

^aDepartment of Chemistry and Analytical & Biological Chemistry Research Facility (ABCRF), University College Cork, Ireland. E-mail: g.mcglacken@ucc.ie;

Fax: +353 21 4274097

^bBIOMERIT Research Centre, Department of Microbiology, University College Cork, Ireland. E-mail: f.ogara@ucc.ie; Fax: +353 21 4903101

^cSchool of Biomedical Sciences, CHIRI, Curtin University, Perth WA 6845, Australia

[†]Electronic supplementary information (ESI) available. See DOI: 10.1039/c6ob01930g

[‡]Both authors contributed equally.

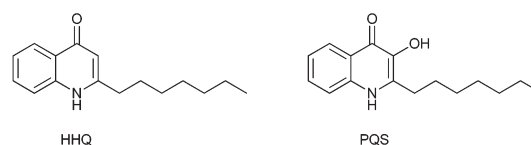


Fig. 1 Structure of the *P. aeruginosa* signalling molecules.

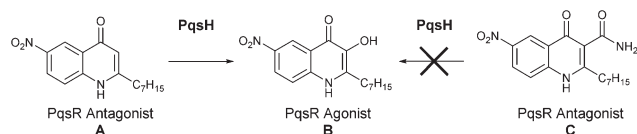


Fig. 2 Structure of the *P. aeruginosa* signalling molecules containing the nitro group at C-6 position.

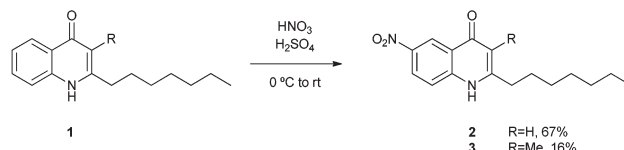
evident, is the exquisite structural specificity required for activity. A particularly interesting case has been recently reported by the Hartmann group.^{31,32} This study reported a potent PqsR antagonist could be accessed by placing a nitro group at the C-6 position of HHQ (Fig. 2, Compound A). However, when tested *in vivo* on *P. aeruginosa* (and *Escherichia coli*), the new compound displayed agonistic behaviour, reminiscent of PQS. Clever experiments and interpretation allowed for the discovery that the supposed antagonist was being hydroxylated by PqsH in *P. aeruginosa* into the corresponding PQS-like analogue (Fig. 2, Compound B), which was a strong PqsR agonist. In order to suppress this functional inversion, the Authors ‘blocked’ the C-3 position, leading to the development of a highly active antagonist (Fig. 2, Compound C).

Results and discussion

Prior to the Hartmann reports, we had previously shown the implications of altering the C-3 position of HHQ on phenazine production in *P. aeruginosa* and also on biofilm formation in *Bacillus subtilis*.²⁸ Since then, two important observations by Hartmann³¹ necessitate further investigation of the role played by the 3-position of alkylquinolones. Firstly, the insertion of the NO₂ group at C-6 in HHQ, greatly improves the antagonistic effects in *P. aeruginosa*. Thus moving forward, this group should remain a key factor in designing antagonists. Secondly, insertion of a C-3 blocking group prevents hydroxylation by *P. aeruginosa*, and thus the *in situ* formation of agonists. Thus, evaluation of the blocking group is crucial. For example, do the installed C-3 groups merely block the hydroxylation site? Or do they bestow additionally biological properties? In this report, we address these issues.

We suspected that addition of the amide group in compound C (Fig. 2) offered additional properties to the molecule, such as H-donor/acceptor capabilities as well as a new site for hydrophilic interaction. We were confident that the C-3 group did not purely act to prevent hydroxylation. Thus we set about preparing a number of analogues of HHQ,³³ all possessing the key 6-NO₂ group but with different groups at C-3. In this way we hoped to shed some light on the requirement at C-3 for antagonistic properties. Moreover, recent work on the structure of the PqsR active site,³⁴ would allow for a better interpretation of our results.

We started by developing a new route to 6-nitro-HHQ. Hartmann found that the final step *en route* to this molecule was low yielding (1%)²⁷ which probably reflects the lower



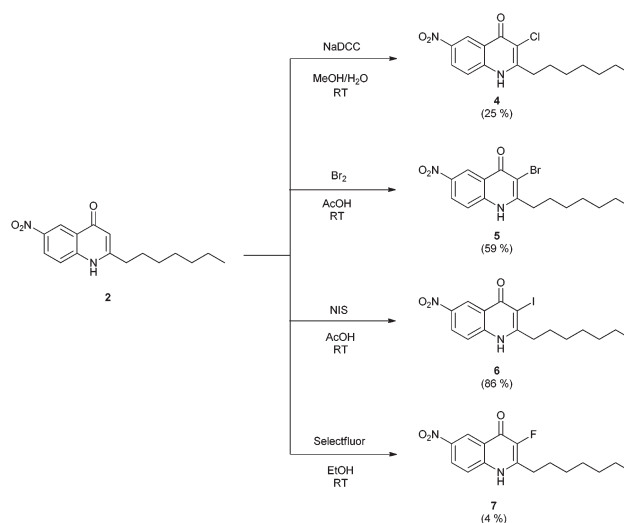
Scheme 1 Synthesis of 2-heptyl-6-nitroquinolin-4(1H)-one.

nucleophilicity of the nitro aniline in the Conrad-Limpach cyclisation steps. Instead we transformed HHQ itself into the nitro analogue in one step *via* electrophilic aromatic substitution in 67% yield (Scheme 1). Next, we installed a number of C-3 blocking groups. We began with a small non-polar methyl group, followed by nitration at C-6 (Scheme 1).

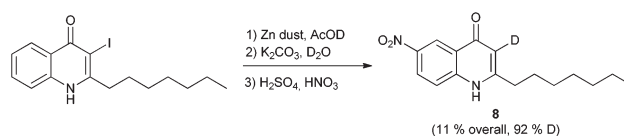
Using nitroquinolone 2, we then introduced Br, Cl and I-groups to give 4, 5 and 6 using Br₂, NaDCC (sodium dichloroisocyanurate) and NIS (*N*-iodosuccinimide) respectively (Scheme 2). Introduction of a fluorine group required extensive optimisation. However fluoroquinolone 7 could be isolated, pure, in 4% yield.

Lastly, an interesting deuterium-containing³⁵ compound 8 was prepared by a deuteriodehalogenation protocol (Scheme 3).

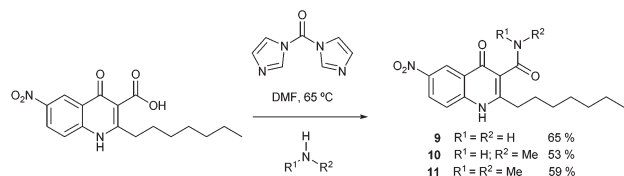
Next we sought to alter the H-donor/acceptor properties of the amide group at C-3 by preparing the corresponding secondary and tertiary amide. This was achieved by following Hartmann's synthesis of the carboxylic acid precursor followed by an amide coupling reaction using 1,1-carbonyldiimidazole (Scheme 4).



Scheme 2 Synthesis of 3-halo-2-heptyl-6-nitroquinolin-4(1H)-ones.



Scheme 3 Synthesis of 3-deutero-2-heptyl-6-nitroquinolin-4(1H)-one.



Scheme 4 Synthesis of 3-amido-2-heptyl-6-nitroquinolin-4(1H)-ones.

Biological results

As previously stated, the QS system (and HHQ/PQS production) is known to be dependent on the *pqsABCDE* biosynthetic operon, which is positively regulated by the transcriptional regulator PqsR.^{36,37} As PqsR controls the expression of *pqsA*, the monitoring of *pqsA* promoter activity can be used to determine PqsR agonism and antagonism.

Two genotypes of *P. aeruginosa* were chosen to be tested with the prepared molecules. Firstly a wild-type *P. aeruginosa* (PAO1) which would appropriately reflect the natural biochemistry of *P. aeruginosa* and secondly, an isogenic *pqsA* mutant (PAO1[−]) in which the ability to produce endogenous HHQ and PQS has been abolished. HHQ and PQS are co-inducers of PqsR signalling,³⁶ thus it is crucial to test our compounds on this genotype, to appropriately assess the actions of analogues, without interference from the naturally occurring activator, PQS. Thus all compounds (2–12) were tested using promoter fusion analysis of the PqsR-regulated *pqsA–E* operon in *P. aeruginosa* wild-type PAO1 and its isogenic *pqsA* mutant (Fig. 3).

Firstly, the deactivating effect of the 6-NO₂ group (on the anthranilate ring) towards PqsR was confirmed, as almost all of the compounds showed some decrease in PqsR activity (Fig. 3a and b). Compounds 4 and 9 exhibited a statistically significant antagonistic activity in the mutant strain, with compound 9 eliciting the greatest reduction. Compound 8 also elicited a reduction in *pqsA* activation, although this did not reach statistical significance. When tested in the wild-type

strain where *pqsA* activation occurs through endogenous PQS, compounds 2, 3, 8, and 9 were statistically active, with 9 being the most potent antagonist. Based on structural data related to the binding pocket of PqsR reported by Williams *et al.*³⁴ it is possible that the 6-NO₂ group interacts with an isoleucine residue (Ile-149) within the pocket, decreasing activation of the receptor. However, as might be expected, the level of deactivation was influenced by other parts of the molecule.

Compounds with a Cl, Br or I group at C-3 (4–6) showed activity similar to the unsubstituted analogue 2. Compound 8 (with deuterium at C-3 position) behaved similarly to the hydrogen analogue.

A very interesting case is the 3-F analogue (Compound 7). We predicted that this analogue would possess three key structural elements for antagonistic activity. 1: A nitro group at C6, as determined by Hartmann, 2: A robust blocking group at C3 to prevent hydroxylation and 3: A direct isosteric replacement at C3 (F for H) to minimise supplementary interactions. But in fact, 7 showed very little loss in activity relative to PQS. We suspected at this stage that the alteration at C3 had, in fact, negated the antagonist effects of the 6-nitro group. To probe this idea, we then decided to prepare a 3-F analogue, this time without the nitro-group. This should give a compound with enhanced agonistic effects. 3-Fluoro-2-heptylquinolin-4(1H)-one (Fig. 4, compound 12) was thus prepared (see ESI†). Gratifyingly, when tested, quinolone 12 displayed remarkable activation of the receptor, even stronger than PQS.

This suggests that there is a strong interaction between the fluorine atom and the PqsR binding pocket. It is well known that F can act as an isostere of the OH group,^{38,39} as it has a similar size (van der Waals radii: 1.47 Å for F; 1.53 Å for OH).⁴⁰ But the suspected key agonistic role of the –OH group in PQS (as a H-donor/acceptor) is now less certain.

Compounds 10 and 11, tested on the mutant strain, showed minimal inhibition and were less potent than compound 9. Inhibitory effects decreased with increasing substitution of the amide indicating that the amide group is not acting solely as a blocking group, suggesting that the H-bond donor capability of the nitrogen is important. The extensive study on AHQ-receptor interactions by Williams *et al.*³⁴ has also highlighted the requirement for an –NH₂ group at the C-3 position for competitive antagonism. They suggest that strengthened electrostatic interactions between the 3-NH₂ group and carbonyl groups in the Leu207 backbone within the pocket results in stronger binding than native ligands. Finally, analogues 9–11 were also tested with the wild type PAO1 strain. With this strain, the differences between the amides were more obvious and neither the secondary nor the tertiary amide showed comparable activity to the primary amide.

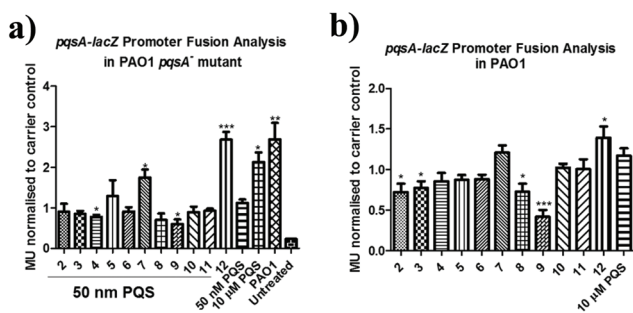


Fig. 3 Promoter fusion analysis (*pqsA-lacZ* pLP0996) of AHQ analogue treated PAO1 *pqsA*[−] and PAO1 strains. Where indicated, mutant cells were supplemented with 50 nM PQS upon inoculation. Data are normalized to the carrier control. All datapoints are the mean of at least three biological replicates. Statistical analysis was performed by Bootstratio (**p* ≤ 0.5, ***p* ≤ 0.005, ****p* ≤ 0.001). MeOH and DMSO were used as solvents depending on solubility. Where compounds were soluble in both, negligible activity differences were observed.

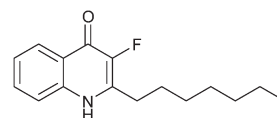


Fig. 4 Structure of compound 12, a very strong activator.

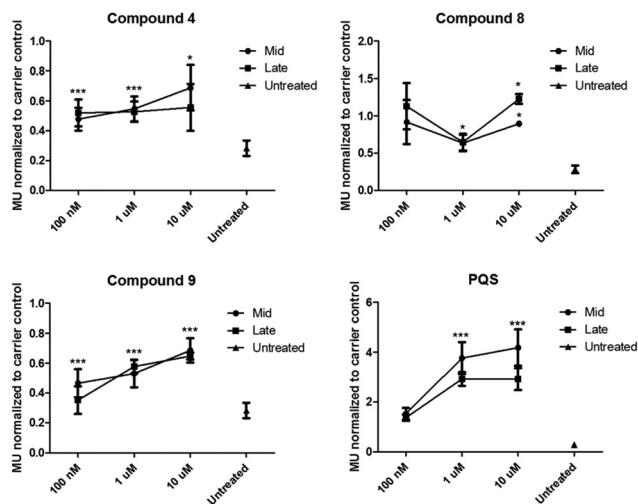


Fig. 5 Concentration and time-dependent *pqsA-lacZ* promoter fusion analysis in the PAO1 *pqsA*[−] mutant strain supplemented with 50 nM PQS and individual compounds. Data are presented as MU normalized to the carrier control (MeOH or DMSO as appropriate) treated with 50 nM PQS. ML refers to mid-log phase samples (OD_{600 nm} 0.4–0.6), while ES refers to early stationary phase samples (OD_{600 nm} 1.0–1.4). The untreated sample was not supplemented with 50 nM PQS. All data are the mean and SEM of at least 3 independent biological replicates. Statistical analysis was performed using Bootstratio (**p* < 0.05, ****p* < 0.001).

Heretofore, all analysis was performed using a single concentration (10 μM) of compound. Therefore, we undertook a concentration dependent investigation of lead compounds, selecting **4**, **8** and **9**. Concentrations of 100 nM, 1 μM and 10 μM were tested against the PAO1 *pqsA*[−] mutant strain supplemented with 50 nM PQS. Samples were taken during mid-logarithmic (ML) and early stationary (ES) phase growth for comparison. As expected, the control test involving addition of PQS, led to enhanced promoter activity at all concentrations, with the most significant increases occurring upon addition of 1 μM and 10 μM PQS (Fig. 5). In contrast, addition of all three analogues led to a concentration-dependent reduction in *pqsA* promoter activity. Compounds **4** and **9** displayed antagonistic activity at both time points and at all three concentrations tested. Compound **8** activity was less potent at 100 nM in mid-log phase samples and at early stationary phase growth, possibly owing to PqsH-mediated conversion to the parent molecule PQS.

Finally and importantly, growth curve analysis ruled out any growth limiting effects from these compounds (ESI, Fig. S1†).

Conclusions

The preparation of a variety of 6-nitro-quinolones, isosteric at C-3 are reported. We have shown that the group at C-3 has further roles beyond acting as a blocking group to prevent hydroxylation by PqsH. It appears that a primary amide is needed to achieve optimised antagonistic activity. This is con-

sistent with an interaction with the PqsR pocket, *via* establishing H bonds with the Leu207 carbonyl group, as postulated in previous studies. Finally, enhanced agonistic activity towards the PqsR receptor was observed with a novel 3-F quinolone. Importantly, the structural elements which lead to strong agonistic activity, can also be helpful in the pursuit of antagonists.^{41,42} Overall, it appears that while antagonistic behaviour seems to be strongly dependent on the ability of the molecule to engage in hydrogen-bonding interactions at the C-3 position, agonistic behaviour does not, and may be ruled by more polar dipole interactions.

Acknowledgements

This research was supported in part by grants awarded to GMG by Science Foundation of Ireland (SFI) (SFI/12/TIDA/B2405, SFI/12/IP/1315, SFI/09/RFP/CHS2353 and SSPC2 12/RC/2275) and the Irish Research Council and to FOG (SFI: SSPC2 12/RC/2275; 13-TIDA-B2625; 07/IN.1/B948; 12/TIDA/B2411; 12/TIDA/B2405; 09/RFP/BMT 2350); the Department of Agriculture, Fisheries and Food (DAFF11/F/009MabS; FIRM/RSF/CoFoRD; FIRM 08/RDC/629); the Environmental Protection Agency (EPA 2008-PhD/S-2); the Irish Research Council for Science, Engineering and Technology (GOIPG/2014/647; PD/2011/2414; RS/2010/2413); the European Commission (H20/20 EU-634486; FP7-PEOPLE-2013-ITN, 607786; OCEAN2012, 287589; FP7-KBBE-2012-6, CP-TP 311975; CP-TP-312184; Marie Curie 256596); the Marine Institute (Beaufort award C2CRA 2007/082); Teagasc (Walsh Fellowship 2013), the Health Research Board (HRA/2009/146) and the Irish Thoracic Society *via* the 2014 MRCG/HRB scheme (MRCG/2014/6).

Notes and references

- 1 C. A. Arias and B. E. Murray, *N. Engl. J. Med.*, 2009, **360**, 439–443.
- 2 C. Walsh, *Nature*, 2000, **406**, 775–781.
- 3 S. Wagner, R. Sommer, S. Hinsberger, C. Lu, R. W. Hartmann, M. Empting and A. Titz, *J. Med. Chem.*, 2016, **59**, 5929–5969.
- 4 M. Hentzer and M. Givskov, *J. Clin. Invest.*, 2003, **112**, 1300–1307.
- 5 S. Swift, J. A. Downie, N. A. Whitehead, A. M. L. Barnard, G. P. C. Salmond and P. Williams, *Adv. Microb. Physiol.*, 2001, **45**, 199–270.
- 6 T. R. de Kievit and B. H. Iglewski, *Infect. Immun.*, 2000, **68**, 4839–4849.
- 7 S. Atkinson and P. Williams, *J. R. Soc., Interface*, 2009, **6**, 959–978.
- 8 G. Rampioni, L. Leoni and P. Williams, *Bioorg. Chem.*, 2014, **55**, 60–68.
- 9 R. P. Singh, *Med. Chem. Commun.*, 2015, **6**, 259–272.

- 10 S. Scutera, M. Zucca and D. Savoia, *Expert Opin. Drug Discovery*, 2014, **9**, 353–366.
- 11 J. Hodgkinson, S. D. Bowden, W. R. J. D. Galloway, D. R. Spring and M. Welch, *J. Bacteriol.*, 2010, **192**, 3833–3837.
- 12 K. M. Smith, Y. Bu and H. Suga, *Chem. Biol.*, 2003, **10**, 81–89.
- 13 M. Campo, M. Bendinelle and H. Friedman, *Infectious Agents and Pathogenesis, Chapter: Pseudomonas aeruginosa as an Opportunistic Pathogen*, Springer, 1993.
- 14 E. S. Snitkin and J. A. Segre, *Nat. Genet.*, 2015, **47**, 2–3.
- 15 P. K. Singh, A. L. Schaefer, M. R. Parsek, T. O. Moninger, M. J. Welsh and E. P. Greenberg, *Nature*, 2000, **407**, 762–764.
- 16 <http://www.cdc.gov/media/releases/2016/p0303-superbugs.html>, accessed on 22-8-2016.
- 17 S. P. Diggle, K. Winzer, S. R. Chhabra, K. E. Worrall, M. Camara and P. Williams, *Mol. Microbiol.*, 2003, **50**, 29–43.
- 18 E. C. Pesci, J. B. J. Milbank, J. P. Pearson, S. McKnight, A. S. Kende, E. P. Greenberg and B. H. Iglewski, *Proc. Natl. Acad. Sci. U. S. A.*, 1999, **96**, 11229–11234.
- 19 L. Mashburn-Warren, J. Howe, K. Brandenburg and M. Whiteley, *J. Bacteriol.*, 2009, **191**, 3411–3414.
- 20 J. F. Dubern and S. P. Diggle, *Mol. Biosyst.*, 2008, **4**, 882–888.
- 21 S. P. Diggle, S. Matthijs, V. J. Wright, M. P. Fletcher, S. R. Chhabra, I. L. Lamont, X. Kong, R. C. Hider, P. Cornelis, M. Camara and P. Williams, *Chem. Biol.*, 2007, **14**, 87–96.
- 22 F. J. Reen, M. J. Mooij, L. J. Holcombe, C. M. McSweeney, G. P. McGlacken, J. P. Morrissey and F. O’Gara, *FEMS Microbiol. Ecol.*, 2011, **77**, 413–428.
- 23 S. L. Drees, C. Li, F. Prasetya, M. Saleem, I. Dreveny, P. Williams, U. Hennecke, J. Emsley and S. Fetzner, *J. Biol. Chem.*, 2016, **291**, 6610–6624.
- 24 P. N. Jimenez, G. Koch, J. A. Thompson, K. B. Xavier, R. H. Cool and W. J. Quax, *Microbiol. Mol. Biol. Rev.*, 2012, **76**, 46–55.
- 25 H. Cao, G. Krishnan, B. Goumnerov, J. Tsongalis, R. Tompkins and L. G. Rahme, *Proc. Natl. Acad. Sci. U. S. A.*, 2001, **98**, 14613–14618.
- 26 L. A. Gallagher, S. L. McKnight, M. S. Kuznetsova, E. C. Pecsí and C. Manoil, *J. Bacteriol.*, 2002, **184**, 6472–6480.
- 27 C. Lu, B. Kirsch, C. Zimmer, J. C. de Jong, C. Henn, C. K. Maurer, M. Müsken, S. Haüssler, A. Steinbach and R. W. Hartmann, *Chem. Biol.*, 2012, **19**, 381–390.
- 28 F. J. Reen, S. L. Clarke, C. Legendre, C. M. McSweeney, K. S. Eccles, S. L. Lawrence, F. O’Gara and G. P. McGlacken, *Org. Biomol. Chem.*, 2012, **10**, 8903–8910.
- 29 J. T. Hodgkinson, W. R. J. D. Galloway, M. Welch and D. R. Spring, *Nat. Protoc.*, 2012, **7**, 1184–1192.
- 30 F. J. Reen, R. Shanahan, R. Cano, F. O’Gara and G. P. McGlacken, *Org. Biomol. Chem.*, 2015, **13**, 5537–5541.
- 31 C. Lu, C. K. Maurer, B. Kirsch, A. Steinbach and R. W. Hartmann, *Angew. Chem., Int. Ed.*, 2014, **53**, 1109–1112.
- 32 C. Lu, B. Kirsch, C. K. Maurer, J. C. de Jong, A. Braunshausen, A. Steinbach and R. W. Hartmann, *Eur. J. Med. Chem.*, 2014, **79**, 173–183.
- 33 G. P. McGlacken, C. M. McSweeney, T. O’Brien, S. E. Lawrence, C. J. Elcoate, F. J. Reen and F. O’Gara, *Tetrahedron Lett.*, 2010, **51**, 5919–5921.
- 34 A. Ilangovan, M. Fletcher, G. Rampioni, C. Pustelny, K. Rumbaugh, S. Heeb, M. Cámara, A. Truman, S. R. Chhabra, J. Emsley and P. Williams, *PLoS Pathog.*, 2013, **9**, e1003508.
- 35 Deuterated compounds as potential targets, have been touted. See: G. H. Timmins, *Expert Opin. Ther. Pat.*, 2014, **24**, 1067–1075. The presumption is that deuterated compounds would exhibit improved pharmacokinetic and toxicological properties due an altered metabolism rate as a result of a stronger C–D bond.
- 36 G. Xiao, E. Déziel, J. He, F. Lepine, B. Lesic, M.-H. Castonguay, S. Milot, A. P. Tampakaki, S. E. Stachel and L. G. Rahme, *Mol. Microbiol.*, 2006, **62**, 1689–1699.
- 37 E. Déziel, S. Golapan, A. P. Tampakaki, F. Lépine, K. E. Padfield, M. Saucier, G. Xiao and L. G. Rahme, *Mol. Microbiol.*, 2005, **55**, 998–1014.
- 38 J. A. K. Howard, V. J. Hoy, D. O’Hagan and G. T. Smith, *Tetrahedron*, 1996, **52**, 12613–12622.
- 39 N. Brown, *Bioisosteres in Medicinal Chemistry*, Wiley-VCH Verlag, Weinheim, Germany, 2012.
- 40 G. Bott, L. D. Field and S. Sternhell, *J. Am. Chem. Soc.*, 1980, **102**, 5618–5626.
- 41 K. M. Smith, Y. Bu and H. Suga, *Chem. Biol.*, 2003, **10**, 563–571.
- 42 G. D. Geske, J. C. O’Neill, D. M. Miller, M. E. Mattmann and H. E. Blackwell, *J. Am. Chem. Soc.*, 2007, **129**, 13613–13625.

Appendix II

Publications from Chapter 3

SPECIAL
ISSUE

Direct Arylation

Synthesis of Benzofuroquinolines via Phosphine-Free Direct Arylation of 4-Phenoxyquinolines in Air

Rachel M. Shanahan,^[a] Aobha Hickey,^[a] F. Jerry Reen,^[b] Fergal O'Gara,^[c,d] and Gerard P. McGlacken^{*[a]}

Abstract: A palladium-catalysed, phosphine-free, direct arylation of 4-phenoxyquinolines, in air is described. Using an intramolecular approach, the ring-closed products are formed in

yields of up to 95 %. This approach allows access to a range of benzofuroquinolines. An array of functional groups on both the quinoline and phenoxy rings are tolerated.

Introduction

The quinoline nucleus occurs in many natural and synthetic pharmacologically active compounds,^[1] and is ranked 22nd in the top 100 most frequently used ring systems present in FDA approved drugs.^[2] Thus, the quinoline motif is considered a privileged biological scaffold, utilised by synthetic chemists to build molecular complexity, and ultimately improve biological activity. As a versatile heterocycle, it displays reactivity similar to that of other aromatic (pyridine/benzene) analogues, and thus can undergo a wide range of synthetic transformations.^[3,4]

One of the most important transformations in organic synthesis remains the linking of two (hetero)aryl groups via a new carbon–carbon bond.^[5] Traditionally, the most reliable class of C–C bond forming reactions involves the palladium-catalysed coupling of an aryl or vinyl halide with an organometallic reagent.^[6–9] Examples include the Suzuki–Miyaura coupling,^[10] Stille coupling,^[11] and Negishi coupling.^[12] An alternative is the use of direct arylation protocols, which are less reliant on the installation of a reactive functionality prior to cross-coupling.^[13–15]

Direct arylation of simple arenes has been increasingly utilised in organic synthesis to access complex polycyclic ring systems.^[16–20] By comparison, similar reactions involving heterocycles tend to require specialised catalyst/ligand systems and are therefore less prevalent in the literature.^[21] One of the earliest relevant examples of an intramolecular direct arylation of a

heteroarene was reported in 1984 by Ames and Opalko.^[22] As a recent example, Ha et al. reported a palladium-catalysed synthesis of benzofuroquinolines in moderate to excellent yields.^[23]

Herein we report a palladium-catalysed direct arylation of 4-phenoxyquinolines as a route to benzofuro[3,2-c]quinolines (Figure 1). Access to these products will aid exploration of their untapped biological potential, given that similar quinoline-based compounds exhibit anticancer,^[24] antimalarial^[25] and antibacterial^[26] effects.

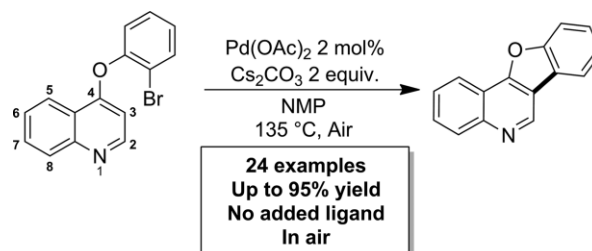


Figure 1. Intramolecular direct arylation of 4-phenoxyquinolines.

Previous syntheses of some of these substrates via direct arylation have relied upon positioning the activated carbon-halide on the C-3 position of the quinoline coupling partner^[27,28] which limits the accessibility and versatility of products

Yu et al., *J. Am. Chem. Soc.*, 2011, 133, 19090:

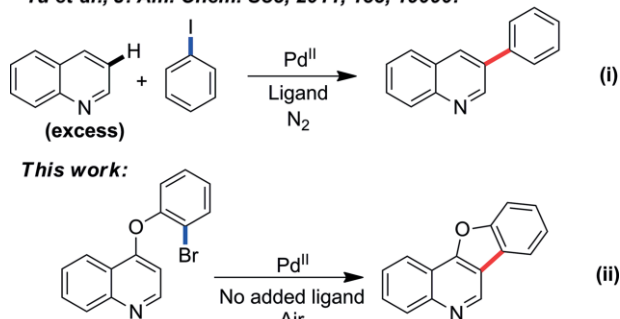


Figure 2. Palladium-catalysed direct arylation at the C-3 position of quinolines.

[a] Analytical and Biological Research Facility (ABCRF) & School of Chemistry, University College Cork, Cork, Ireland
E-mail: g.mcglacken@ucc.ie
<http://research.ucc.ie/profiles/D004/gmcglacken>

[b] School of Microbiology, University College Cork, Cork, Ireland

[c] BIOMERIT Research Centre, School of Microbiology, University College Cork, Cork, Ireland

[d] School of Biomedical Sciences, Curtin Health Innovation Research Institute, Curtin University, Perth, WA 6102, Australia

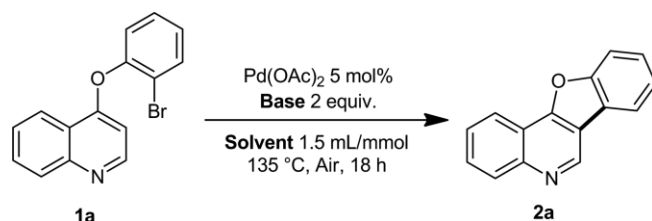
Supporting information and ORCID(s) from the author(s) for this article are available on the WWW under <https://doi.org/10.1002/ejoc.201800923>.

formed. The first example of non-directed direct arylation/C–H activation of the C-3 position of pyridines and quinolines was reported by Yu and co-workers (Figure 2(i)), using phenanthroline ligands under inert reaction conditions.^[29] This method also relies upon the use of a large excess of the quinoline or pyridine substrate, which is only applicable to an intermolecular system. Herein we describe a system that requires no added ligand for arylation of the C-3 position of the quinoline ring, via intramolecular direct arylation, in air [Figure 2 (ii)].

Results and Discussion

Initially, 4-(2-bromophenoxy)quinoline **1a** was chosen as a model substrate, which was readily accessible from reaction of 4-chloroquinoline and 2-bromophenol. Our initial coupling conditions allowed formation of the fused product **2a** in 57 % isolated yield in air (Table 1 entry 1). Next, a variety of reaction parameters were assessed (Table 1). A solvent screen indicated that high-boiling point amide solvents were necessary for good conversion (entries 1–3). Other organic solvents gave little or no conversion to product (entries 4–8). Changing the base from Na₂CO₃ to K₂CO₃ or Cs₂CO₃ allowed the reaction to reach 100 % conversion (entry 9 and 10), while use of a stronger butoxide base resulted in partial decomposition of the starting material (entry 11). A further reduction in catalyst loading to 2 mol-% was also achieved (entry 12), at which point the desired product **2a** could be obtained in 95 % isolated yield under the optimised conditions.

Table 1. Optimisation of reaction conditions.

				
Entry	Base	Solvent	Yield by NMR [%] ^[a]	Isolated Yield [%]
1	Na ₂ CO ₃	DMA	–	57
2	Na ₂ CO ₃	DMF	67	–
3	Na ₂ CO ₃	NMP	70	72
4	Na ₂ CO ₃	DMSO	0	–
5 ^[b]	Na ₂ CO ₃	1,4-dioxane	0	–
6 ^[b]	Na ₂ CO ₃	EtOH	0	–
7 ^[b]	Na ₂ CO ₃	1,2-DCE	0	–
8 ^[b]	Na ₂ CO ₃	MeCN	0	–
9	K ₂ CO ₃	NMP	72	–
10	Cs ₂ CO ₃	NMP	83	–
11	NaOtBu	NMP	39 ^[c]	–
12 ^[d]	Cs ₂ CO ₃	NMP	99	95
13 ^[e]	Cs ₂ CO ₃	NMP	33	–

[a] Yields determined by ¹H NMR analysis of the crude reaction mixture using 1,3,5-trimethoxybenzene as internal standard. [b] Reaction carried out at the reflux temperature of solvent. [c] Decomposition of starting material observed. [d] 2 mol-% Pd(OAc)₂ used. [e] 1 mol-% Pd(OAc)₂ used.

With optimised conditions in hand, the substrate scope of the reaction was evaluated (Figure 3). Overall, it was observed that the reaction could tolerate a variety of functional groups

on both the phenoxy and quinoline coupling partners. Substrates bearing weakly electron-withdrawing substituents (**2b–f**) on the phenoxy ring were well tolerated. Additionally, the chlorides in **2e** and **2f** were retained as a synthetic handle for further cross-coupling. The more strongly electron-withdrawing substituents on **2g** and **2h** led to cyclisation in excellent yields of 88 % and 90 %, respectively. Moderate yields were observed in the case of the nitro (**2i**) and ester (**2j**) analogues.

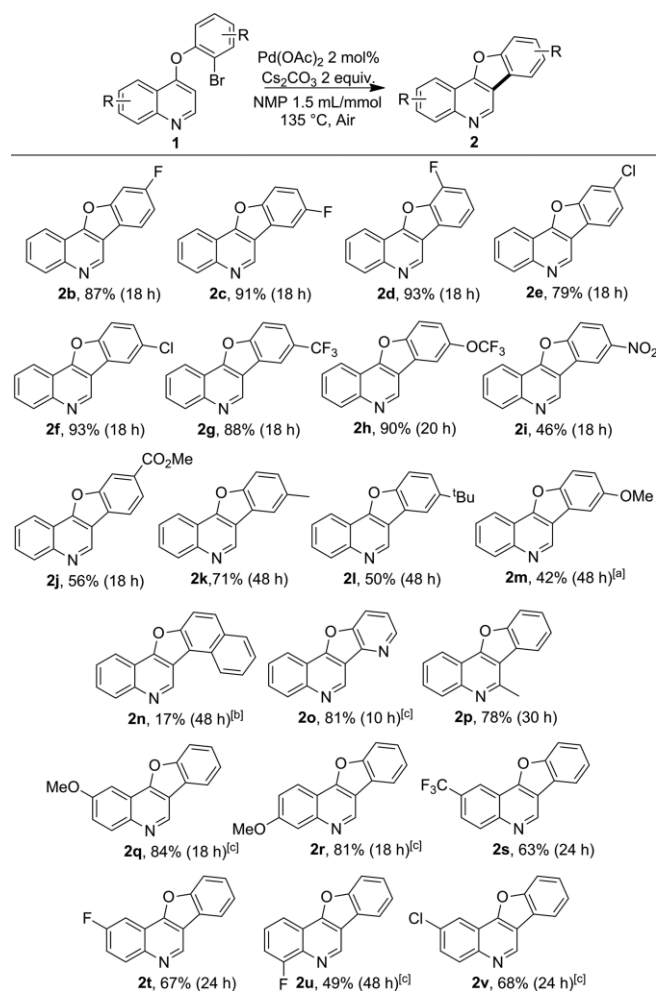


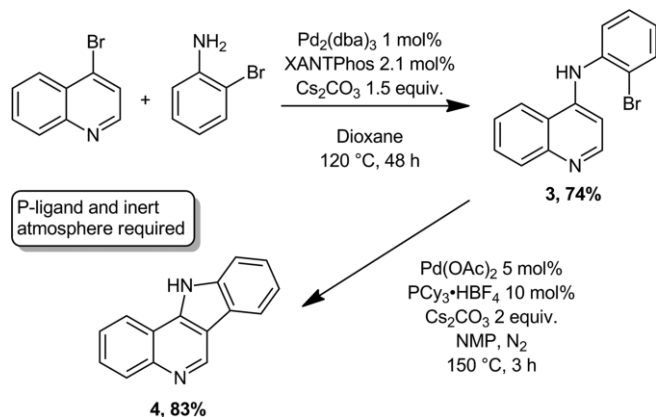
Figure 3. Substrate scope. All yields are isolated yields. [a] The yield of this product could be improved to 60 % when using the following conditions: 5 mol-% Pd(OAc)₂, 10 mol-% PCy₃·HBF₄, 2 equiv. Cs₂CO₃ under N₂ at 135 °C for 18 h. [b] The yield of this product could be improved to 66 % when using the same conditions described in [a]. [c] 5 mol-% Pd(OAc)₂ used.

Longer reaction times were required in the case of electron-rich phenoxy substrates (**2k–m**). In the case of the naphthyl analogue **2n**, the desired product could only be obtained in 17 % isolated yield, with the majority of the remaining material attributed to unreacted starting material. This may be due to the steric bulk of the naphthyl group hindering access to the coupling site. Pleasingly, compound **2o** bearing a pyridine moiety instead of an aryl was obtained in an excellent yield of 81 %.

The scope of the reaction with respect to the quinoline was also examined. A methyl group at the C-2 position was well tolerated (**2p**). On the aryl backbone, both electron donating –OMe substituents (**2q** and **2r**) and electron withdrawing –CF₃,

-F and -Cl substituents (**2s–v**) also led to very good yields of product. The reaction conditions were also applicable to a 4-phenoxy pyridine substrate.^[30] A few quinoline analogues (*p*-pyridinyl, aldehydic, and those with an *S*-linker) failed to cyclise under these conditions.^[31]

Compounds containing fused indolquinoline rings are known to possess antimalarial,^[32] antiproliferative and anticancer activity.^[33] Thus, we hoped to access similar compounds by including this functionality in our substrate scope. A Hartwig–Buchwald coupling gave the precursor **3** in 74 % isolated yield (Scheme 1). However, when this compound was subjected to the previously optimised direct arylation conditions given above, no product was observed. Even when using the protected (*N*-Boc) substrate, coupling could not be achieved under these conditions.^[34] We reasoned at this point that inhibitive *N*-ligation to palladium could be avoided by the addition of competitive phosphine ligands.^[35] Indeed, when a new catalytic system of 5 mol-% Pd(OAc)₂ and 10 mol-% PCy₃·HBF₄ was employed, the fused product could be obtained in 83 % isolated yield after 3 h. An inert atmosphere was required (Scheme 1).^[36]



Scheme 1. Synthesis and direct arylation of 4-anilinoquinoline substrate.

The mechanism probably proceeds via an initial oxidative addition followed by a rate-determining C–H activation via a concerted metalation deprotonation (CMD).^[29,37–40] A CMD mechanism is often characterised by the acidity of the key C–H bond. To probe this, a number of competition experiments were carried out using a basic quinoline substrate **1a** and those substituted with an electron-withdrawing (**1s**) and an electron-donating (**1q**) group (Figure 4 and SI). In all cases the experiment revealed that the electron-poor substrate outpaced the electron-rich substrate.

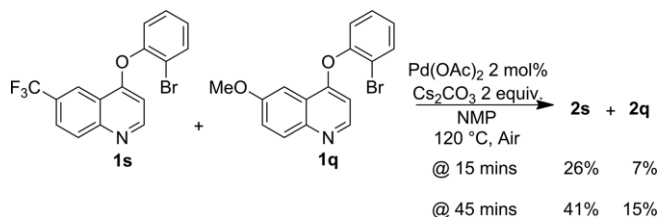


Figure 4. Competition experiment between **1s** and **1q**.

We then wished to apply the methodology to a more challenging quinoline of potential biological importance. Many spe-

cies of bacteria use a sophisticated communication system termed “quorum sensing” (QS).^[41] This coordinated behaviour allows for the construction of protective biofilms and the production of virulence factors, ultimately for the benefit of the entire colony. In contrast to antibiotic treatment, disrupting QS, termed “quorum quenching”, is non-biocidal and thus as a strategy, is less likely to promote bacterial resistance by reducing the level of mutant dominance.^[42] *Pseudomonas aeruginosa* uses quinolones such as 4-hydroxy-2-heptylquinoline (HHQ) and its 3-OH analogue *Pseudomonas* quinolone signal (PQS) to modulate quorum sensing (Figure 5). Thus analogues of these molecules could be used as competitive binders, disrupting numerous downstream processes.

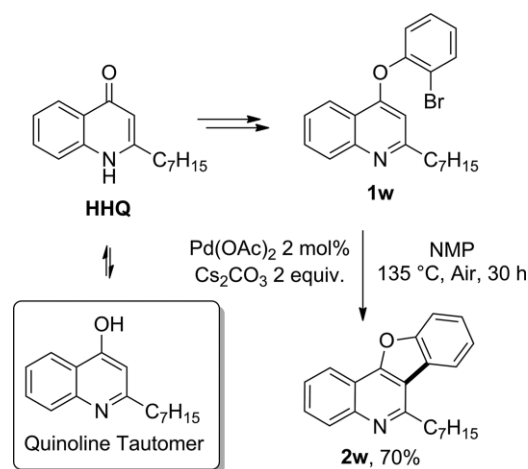


Figure 5. HHQ-like substrate blocked at C-3.

Following on from our continuing investigation of quinolone and quinoline analogues of HHQ and PQS,^[43–49] using molecules which are “blocked” at the C-3 position, we chose to apply our intramolecular arylation methodology to a HHQ/PQS analogue (Figure 5). Substitution of C-3 is often crucial as it prevents hydroxylation of HHQ at this position by PqsH. Analogues with a hydroxyl group at C-3 can lead to unwanted agnostic behaviour.^[50,51]

Thus HHQ was converted into the phenoxy precursor, which cyclised well, considering the steric encumbrance of the heptyl chain (the heptyl chain is critical for most biological activity). The impact of compound **2w** on quinolone signalling (more specifically PqsR signalling) was then investigated. HHQ (and PQS) are known to act as co-inducer signals of the PqsR LysR-type transcriptional regulator, leading to transcriptional activation of the *pqsA* promoter. Thus, the *pqsA* promoter itself acts as a proxy for activation of PqsR signalling. A *pqsA* fusion plasmid reporter (pLP0996) contains the *pqsA* promoter sequence upstream of the *lacZ* encoding gene and thus was ultimately used as indicator.^[52] Wild-type *P. aeruginosa* produces endogenous HHQ, and thus any interference with activation of the plasmid encoded *pqsA*-promoter would likely infer antagonism of natural co-inducer binding. However, no such interference was observed and levels of *pqsA* transcriptional activation were comparable in carrier and cells treated with cyclised quinoline **2w** (Figure 6). Activation of the pLP0996 encoded *pqsA* promoter in a *pqsA* mutant lacking endogenous HHQ and PQS can only

occur upon addition of exogenous signal. In this case, while HHQ activated promoter activity, addition of quinoline **2w** had no effect beyond baseline. Thus quinoline **2w** displayed neither agonist nor antagonist behaviour with respect to PqsR signalling. This was further evident from the lack of inhibition of pyocyanin production in a wild-type strain and the lack of pyocyanin restoration in the *pqsA* mutant.

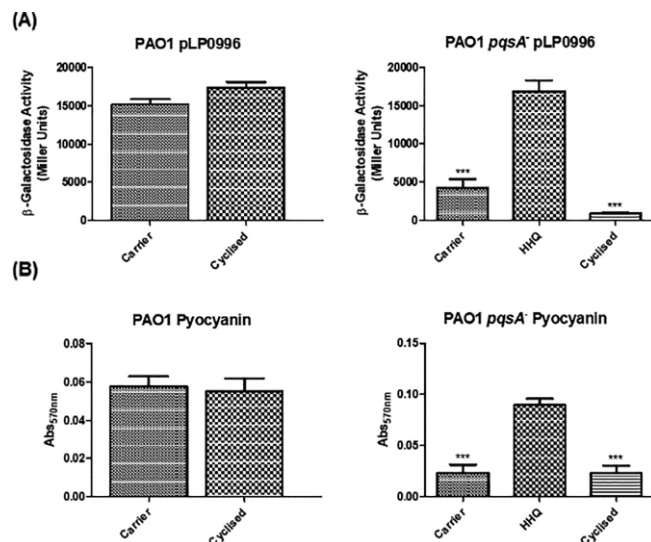


Figure 6. (A) Transcriptional activation of the *pqsA* promoter was unaffected in wild-type (PAO1 pMP0996) and mutant (PAO1 *pqsA*⁻ pLP0996) cells upon addition of **2w**. This suggests that the compound is neither an antagonist nor an agonist of PqsR signalling under conditions tested. (B) Pyocyanin production followed a similar pattern, i.e. unaffected in the presence of **2w** in either the wild-type or mutant cells. All data presented is the mean (\pm SEM) of three independent biological replicates. Statistical analysis was performed by Students t-test and one way ANOVA with Bonferroni post-hoc testing (*** $p < 0.001$).

The production of HHQ-like compounds which do not and cannot be hydroxylated *in vivo* at C-3^[51] and thus do not exhibit any strong agonistic or antagonist behaviour, make for an excellent molecular framework for further modification and structure-activity studies. Further details of the biological activity will be published in due course.

Conclusions

In summary, the application of direct arylation methodology towards the synthesis of fused benzofuroquinoline products has been demonstrated. Placement of the halide on the phenoxy component of the coupling precursor allows for easy access to cyclised products. No added phosphine is required and the reactions can be carried out in air. Modification of the methodology allows for the inclusion of 4-anilinoquinoline substrates, without the requirement for *N*-protection. Finally, electron-poor quinolines appear to work best as evidenced by competition experiments. Application to a sterically hindered (C-2 = *n*-heptyl) HHQ mimic proceeds well.

Experimental Section

General Methods: Solvents and reagents were used as obtained from commercial sources and without purification. Melting points

were measured in a Thomas Hoover Capillary Melting Point apparatus. Infrared spectra were measured on a Perkin-Elmer FT-IR spectrometer. Nuclear Magnetic Resonance (NMR) samples were run in deuterated chloroform (CDCl_3) or deuterated dimethylsulfoxide ($[\text{D}_6]\text{DMSO}$) as specified. ^1H NMR (600 MHz), ^1H NMR (500 MHz), ^1H NMR (400 MHz), and ^1H NMR (300 MHz) spectra were recorded on Bruker Avance 600, Bruker Avance 500, Bruker Avance 400 and Bruker Avance 300 NMR spectrometers, respectively, in proton coupled mode using tetramethylsilane (TMS) as the internal standard. ^{13}C NMR (150 MHz), ^{13}C NMR (125 MHz), ^{13}C NMR (100 MHz), and ^{13}C NMR (75 MHz) spectra were recorded on Bruker Avance 600, Bruker Avance 500, Bruker Avance 400 and Bruker Avance 300 NMR spectrometers, respectively, in proton decoupled mode at 20 °C using tetramethylsilane (TMS) as the internal standard. ^{19}F NMR (282 MHz) spectra were recorded on a Bruker Avance 300 NMR spectrometer in proton decoupled mode at 20 °C. All spectra were run at University College Cork. Chemical shifts (δ) are expressed as parts per million (ppm), positive shift being downfield from TMS; coupling constants (*J*) are expressed in Hertz [Hz]. Splitting patterns in ^1H NMR spectra are designated as: s (singlet), bs (broad singlet), d (doublet), dd (doublet of doublets), ddd (doublet of doublets of doublets), t (triplet), td (triplet of doublets), q (quartet), quin (quintet) and m (multiplet). High resolution precise mass spectra (HRMS) were recorded on a Waters LCT Premier ToF LC-MS instrument in electrospray ionisation (ESI) mode using 50 % acetonitrile/water containing 0.1 % formic acid as eluent; samples were made up in acetonitrile at a concentration of ca. 1 mg/mL. Column chromatography was carried out using 60 Å (35–70 μm) silica. TLC was carried out on pre-coated silica gel plates (Merck 60 PF254). The developed plates were visualized under UV light.

Palladium-catalysed intramolecular direct arylation reactions were carried out in sealed reaction tubes which were placed in a solid multi-reaction heating plate.

General Procedures for Synthesis of 4-(2-Bromophenoxy)quinoline Substrates 1a–1w

Method (a): Compounds 1a–1c, 1f, 1i, 1k, 1l, 1o–1w: A mixture of the 4-chloroquinoline substrate (1 equiv.), the substituted 2-bromophenol (5 equiv.) and sodium hydroxide (crushed pellets) (1.5 equiv.) was stirred at 120 °C until reaction was completed (2–6 h) as evident by thin layer chromatography (hexane/ethyl acetate, 8:2). The cooled reaction mixture was diluted with 10 % aq. NaOH (5 mL) and stirred at room temperature for 1 h. The aqueous phase was extracted with DCM (3 \times 20 mL). The combined organic layers were washed with 6 M NaOH (3 \times 10 mL), water (10 mL) and brine (10 mL), dried with MgSO_4 , filtered and concentrated in vacuo. The crude mixture was purified by column chromatography over silica gel using hexane/ethyl acetate (8:2) as eluent.

Method (b): Compounds 1d, 1e, 1g, 1h, 1j, 1m, 1n: A mixture of 4-chloroquinoline (1 equiv.), the substituted 2-bromophenol (1.5 equiv.) and 4-dimethylaminopyridine (3 equiv.) in toluene (1.5 mL/mmol) was stirred at 130 °C until the reaction was completed as evident by thin layer chromatography (hexane/ethyl acetate, 8:2). The cooled reaction mixture was diluted with 10 % aq. NaOH (5 mL) and stirred at room temperature for 1 h. The aqueous phase was extracted with DCM (3 \times 20 mL). The combined organic layers were washed with 3 M NaOH (3 \times 10 mL), 1 M HCl (2 \times 10 mL), water (10 mL) and brine (10 mL), dried with MgSO_4 , filtered and concentrated in vacuo. The crude mixture was purified by column chromatography over silica gel using hexane/ethyl acetate (8:2) as eluent.

4-(2-Bromophenoxy)quinoline (1a): Method (a) – white solid (2.89 g, 78 %); m.p. 62–64 °C. IR (film): $\tilde{\nu}_{\text{max}}$ = 3434, 1596, 1305,

1223, 659 cm⁻¹. ¹H NMR (300 MHz, CDCl₃): δ = 6.41 (d, *J* = 5.1 Hz, 1 H), 7.18–7.27 (m, 2 H), 7.43 (ddd, *J* = 8.1, 7.3, 1.6 Hz, 1 H), 7.61 (ddd, *J* = 8.2, 6.9, 1.1 Hz, 1 H), 7.70–7.82 (m, 2 H), 8.12 (d, *J* = 8.2 Hz, 1 H), 8.42 (dd, *J* = 8.3, 0.9 Hz, 1 H), 8.68 (d, *J* = 5.1 Hz, 1 H) ppm. ¹³C NMR (75 MHz, CDCl₃): δ = 103.7, 116.4, 121.1, 121.9, 123.2, 126.3, 127.3, 129.1, 129.2, 130.2, 134.3, 149.8, 151.0, 151.2, 160.7 ppm. HRMS (ESI-TOF) *m/z*: [M + H]⁺ calcd. for C₁₅H₁₁BrNO: 300.0024, found 300.0016.

4-(2-Bromo-5-fluorophenoxy)quinoline (1b): Method (a) – pale yellow solid (0.891 g, 91 %); m.p. 77–78 °C. IR (film): ν_{max} = 3066, 1476, 1305, 1252, 1159, 601 cm⁻¹. ¹H NMR (300 MHz, CDCl₃): δ = 6.49 (d, *J* = 5.1 Hz, 1 H), 6.94–7.01 (m, 1 H), 6.99 (d, *J* = 8.1 Hz, 1 H), 7.57–7.74 (m, 2 H), 7.80 (ddd, *J* = 8.4, 6.9, 1.4 Hz, 1 H), 8.13 (d, *J* = 8.5 Hz, 1 H), 8.37 (dd, *J* = 8.4, 1.0 Hz, 1 H), 8.73 (d, *J* = 5.1 Hz, 1 H) ppm. ¹³C NMR (75 MHz, CDCl₃): δ = 104.1, 110.7, 110.9 [d, ²*J*(C,F) = 25 Hz], 114.5 [d, ²*J*(C,F) = 22 Hz], 120.9, 121.7, 126.5, 129.2, 130.4, 134.7 [d, ³*J*(C,F) = 9 Hz], 149.9, 151.0, 152.0 [d, ³*J*(C,F) = 11 Hz], 160.1, 162.4 [d, ¹*J*(C,F) = 250 Hz] ppm. ¹⁹F NMR (282 MHz, CDCl₃): δ = -111 ppm. HRMS (ESI-TOF) *m/z*: [M + H]⁺ calcd. for C₁₅H₁₀BrFNO: 317.9930, found 317.9936.

4-(2-Bromo-4-fluorophenoxy)quinoline (1c): Method (a) – pale yellow solid (0.188 g, 38 %); m.p. 100–103 °C. IR (film): ν_{max} = 3065, 1480, 1305, 1248, 1183, 765 cm⁻¹. ¹H NMR (300 MHz, CDCl₃): δ = 6.39 (d, *J* = 5.1 Hz, 1 H), 7.10–7.29 (m, 2 H), 7.48 (dd, *J* = 7.7, 2.8 Hz, 1 H), 7.62 (ddd, *J* = 8.2, 5.5, 1.2 Hz, 1 H), 7.79 (ddd, *J* = 8.5, 6.9, 1.5 Hz, 1 H), 8.12 (d, *J* = 8.5 Hz, 1 H), 8.40 (dd, *J* = 8.3, 0.9 Hz, 1 H), 8.69 (d, *J* = 5.1 Hz, 1 H) ppm. ¹³C NMR (75 MHz, CDCl₃): δ = 103.4, 116.1 [d, ²*J*(C,F) = 23 Hz], 116.9 [d, ³*J*(C,F) = 10 Hz], 120.9, 121.3 [d, ²*J*(C,F) = 26 Hz], 121.8, 124.3 [d, ³*J*(C,F) = 9 Hz], 126.4, 129.2, 130.3, 147.4, 149.8, 151.0, 159.9 [d, ¹*J*(C,F) = 250 Hz], 160.7 ppm. ¹⁹F NMR (282 MHz, CDCl₃): δ = -114 ppm. HRMS (ESI-TOF) *m/z*: [M + H]⁺ calcd. for C₁₅H₁₀BrFNO: 317.9930, found 317.9935.

4-(2-Bromo-6-fluorophenoxy)quinoline (1d): Method (b) – pale yellow solid (0.318 g, 72 %); m.p. 118–119 °C. IR (film): ν_{max} = 3064, 1502, 1471, 1305, 1271, 1042, 665 cm⁻¹. ¹H NMR (300 MHz, CDCl₃): δ = 6.39 (d, *J* = 5.1 Hz, 1 H), 7.15–7.30 (m, 2 H), 7.47–7.54 (m, 1 H), 7.63 (ddd, *J* = 8.1, 7.0, 1.1 Hz, 1 H), 7.79 (ddd, *J* = 8.4, 6.9, 1.5 Hz, 1 H), 8.13 (d, *J* = 8.5 Hz, 1 H), 8.46 (dd, *J* = 8.3, 1.1 Hz, 1 H), 8.69 (d, *J* = 5.0 Hz, 1 H) ppm. ¹³C NMR (75 MHz, CDCl₃): δ = 102.5, 116.5 [d, ²*J*(C,F) = 19 Hz], 118.3, 120.6, 121.9, 126.4, 127.7 [d, ³*J*(C,F) = 8 Hz], 129.10, 129.16, 130.2, 139.3 [d, ²*J*(C,F) = 14 Hz], 149.8, 150.9, 155.6 [d, ¹*J*(C,F) = 255 Hz], 159.8 ppm. ¹⁹F NMR (282 MHz, CDCl₃): δ = -124 ppm. HRMS (ESI-TOF) *m/z*: [M + H]⁺ calcd. for C₁₅H₁₀BrFNO: 317.9930, found 317.9921.

4-(2-Bromo-5-chlorophenoxy)quinoline (1e): Method (b) – white solid (0.290 g, 89 %); m.p. 79–81 °C. IR (film): ν_{max} = 3370, 1562, 1464, 1305, 1252, 765, 665 cm⁻¹. ¹H NMR (300 MHz, CDCl₃): δ = 6.48 (d, *J* = 5.1 Hz, 1 H), 7.16–7.29 (m, 2 H), 7.57–7.69 (m, 2 H), 7.79 (ddd, *J* = 8.5, 6.9, 1.5 Hz, 1 H), 8.13 (d, *J* = 8.6 Hz, 1 H), 8.36 (dd, *J* = 8.4, 0.9 Hz, 1 H), 8.72 (d, *J* = 5.1 Hz, 1 H) ppm. ¹³C NMR (75 MHz, CDCl₃): δ = 104.1, 114.4, 120.9, 121.7, 123.3, 126.5, 127.4, 129.2, 130.4, 134.5, 134.8, 149.9, 151.0, 151.9, 160.1 ppm. HRMS (ESI-TOF) *m/z*: [M + H]⁺ calcd. for C₁₅H₁₀BrClNO: 333.9634, found 333.9622.

4-(2-Bromo-4-chlorophenoxy)quinoline (1f): Method (a) – off-white solid (1.97 g, 96 %); m.p. 112–115 °C. IR (film): ν_{max} = 3403, 1596, 1465, 1392, 1257, 824, 765 cm⁻¹. ¹H NMR (300 MHz, CDCl₃): δ = 6.42 (d, *J* = 5.1 Hz, 1 H), 7.17 (d, *J* = 8.6 Hz, 1 H), 7.40 (dd, *J* = 8.7, 2.5 Hz, 1 H), 7.61 (ddd, *J* = 8.2, 6.9, 1.2 Hz, 1 H), 7.70–7.84 (m, 2 H), 8.12 (d, *J* = 8.5 Hz, 1 H), 8.38 (dd, *J* = 8.4, 0.9 Hz, 1 H), 8.70 (d, *J* = 5.1 Hz, 1 H) ppm. ¹³C NMR (75 MHz, CDCl₃): δ = 103.7, 117.0, 120.9, 121.7, 123.8, 126.4, 129.2, 129.3, 130.3, 132.0, 133.9, 149.9,

150.0, 151.0, 160.4 ppm. HRMS (ESI-TOF) *m/z*: [M + H]⁺ calcd. for C₁₅H₁₀BrClNO: 333.9634, found 333.9629.

4-[2-Bromo-4-(trifluoromethyl)phenoxy]quinoline (1g): Method (b) – sticky colourless oil (0.0731 g, 20 %). IR (film): ν_{max} = 1623, 1569, 1320, 1263, 1231, 1130, 588 cm⁻¹. ¹H NMR (300 MHz, CDCl₃): δ = 6.50 (d, *J* = 5.1 Hz, 1 H), 7.28 (d, *J* = 8.5 Hz, 1 H), 7.54–7.70 (m, 2 H), 7.79 (ddd, *J* = 8.4, 6.9, 1.4 Hz, 1 H), 8.00 (d, *J* = 1.7 Hz, 1 H), 8.14 (d, *J* = 8.5 Hz, 1 H), 8.34 (dd, *J* = 8.4, 0.9 Hz, 1 H), 8.73 (d, *J* = 4.9 Hz, 1 H) ppm. ¹³C NMR (75 MHz, CDCl₃): δ = 104.7, 116.5, 121.0, 121.7, 122.6, 122.9 [q, ¹*J*(C,F) = 272 Hz], 126.4 [q, ³*J*(C,F) = 4 Hz], 126.7, 129.2 [q, ²*J*(C,F) = 34 Hz], 129.3, 130.5, 131.7 [q, ³*J*(C,F) = 4 Hz], 150.0, 150.9, 154.4, 159.8 ppm. ¹⁹F NMR (282 MHz, CDCl₃): δ = -62 ppm. HRMS (ESI-TOF) *m/z*: [M + H]⁺ calcd. for C₁₆H₁₀BrF₃NO: 367.9898, found 367.9886.

4-[2-Bromo-4-(trifluoromethoxy)phenoxy]quinoline (1h): Method (b) – pale yellow solid (0.3015 g, 78 %); m.p. 50–52 °C. IR (film): ν_{max} = 1640, 1597, 1306, 1253, 1218, 1187, 567 cm⁻¹. ¹H NMR (300 MHz, CDCl₃): δ = 6.44 (d, *J* = 5.1 Hz, 1 H), 7.22–7.35 (m, 2 H), 7.55–7.69 (m, 2 H), 7.79 (ddd, *J* = 8.5, 6.9, 1.5 Hz, 1 H), 8.13 (d, *J* = 8.4 Hz, 1 H), 8.38 (dd, *J* = 8.4, 0.9 Hz, 1 H), 8.71 (d, *J* = 5.1 Hz, 1 H) ppm. ¹³C NMR (75 MHz, CDCl₃): δ = 103.8, 116.9, 120.4 [q, ¹*J*(C,F) = 259 Hz], 120.9, 121.7, 121.8, 123.7, 126.5, 127.0, 129.2, 130.4, 146.6, 149.9, 150.0, 151.0, 160.3 ppm. ¹⁹F NMR (282 MHz, CDCl₃): δ = -58 ppm. HRMS (ESI-TOF) *m/z*: [M + H]⁺ calcd. for C₁₆H₁₀BrF₃NO₂: 383.9847, found 383.9843.

4-(2-Bromo-4-nitrophenoxy)quinoline (1i): Method (a) – pale yellow solid (0.192 g, 80 %); m.p. 151–152 °C. IR (film): ν_{max} = 3376, 1523, 1346, 1305, 1257, 665 cm⁻¹. ¹H NMR (300 MHz, CDCl₃): δ = 6.65 (d, *J* = 5.0 Hz, 1 H), 7.23 (d, *J* = 8.9 Hz, 1 H), 7.64 (ddd, *J* = 8.1, 7.1, 0.7 Hz, 1 H), 7.83 (ddd, *J* = 8.4, 7.0, 1.3 Hz, 1 H), 8.17 (d, *J* = 8.5 Hz, 1 H), 8.25 (d, *J* = 8.8 Hz, 1 H), 8.27 (dd, *J* = 8.9, 2.7 Hz, 1 H), 8.65 (d, *J* = 2.6 Hz, 1 H), 8.80 (d, *J* = 5.0 Hz, 1 H) ppm. ¹³C NMR (75 MHz, CDCl₃): δ = 106.0, 115.9, 121.1, 121.2, 121.5, 124.6, 127.1, 129.5, 129.9, 130.7, 144.9, 150.2, 151.0, 157.2, 159.1 ppm. HRMS (ESI-TOF) *m/z*: [M + H]⁺ calcd. for C₁₅H₁₀BrN₂O₃: 344.9875, found 344.9865.

Methyl 4-Bromo-3-(quinolin-4-yloxy)benzoate (1j): Method (b) – off white solid (0.258 g, 62 %); m.p. 87–89 °C. IR (film): ν_{max} = 3586, 2950, 1724, 1565, 1502, 1392, 1294, 1241, 765 cm⁻¹. ¹H NMR (300 MHz, CDCl₃): δ = 3.92 (s, 3 H), 6.43 (d, *J* = 5.1 Hz, 1 H), 7.63 (ddd, *J* = 8.2, 6.9, 1.1 Hz, 1 H), 7.76–7.90 (m, 4 H), 8.13 (d, *J* = 8.5 Hz, 1 H), 8.40 (dd, *J* = 8.3, 0.9 Hz, 1 H), 8.70 (d, *J* = 5.1 Hz, 1 H) ppm. ¹³C NMR (75 MHz, CDCl₃): δ = 52.6, 103.9, 121.0, 121.7, 122.0, 123.9, 126.5, 128.0, 129.2, 130.4, 131.6, 134.5, 149.9, 151.0, 152.4, 160.3, 165.4 ppm. HRMS (ESI-TOF) *m/z*: [M + H]⁺ calcd. for C₁₇H₁₃BrNO₃: 358.0079, found 358.0089.

4-(2-Bromo-4-methylphenoxy)quinoline (1k): Method (a) – orange solid (0.242 g, 84 %); m.p. 122–125 °C. IR (film): ν_{max} = 3064, 1568, 1485, 1392, 1255, 765 cm⁻¹. ¹H NMR (300 MHz, CDCl₃): δ = 2.41 (s, 3 H), 6.40 (d, *J* = 5.2 Hz, 1 H), 7.13 (d, *J* = 8.2 Hz, 1 H), 7.22 (dd, *J* = 8.2, 1.5 Hz, 1 H), 7.54 (d, *J* = 1.4 Hz, 1 H), 7.61 (ddd, *J* = 8.1, 6.9, 1.1 Hz, 1 H), 7.78 (ddd, *J* = 8.4, 6.9, 1.4 Hz, 1 H), 8.11 (d, *J* = 8.5 Hz, 1 H), 8.43 (dd, *J* = 8.3, 1.0 Hz, 1 H), 8.67 (d, *J* = 5.1 Hz, 1 H) ppm. ¹³C NMR (75 MHz, CDCl₃): δ = 20.7, 103.5, 115.9, 121.1, 121.9, 122.9, 126.2, 129.1, 129.8, 130.1, 134.5, 137.5, 148.8, 149.8, 151.0, 161.0 ppm. HRMS (ESI-TOF) *m/z*: [M + H]⁺ calcd. for C₁₆H₁₃Br NO: 314.0181, found 314.0169.

4-[2-Bromo-4-(tert-butyl)phenoxy]quinoline (1l): Method (a) – pale yellow solid (0.073 g, 56 %); m.p. 68–70 °C. IR (film): ν_{max} = 2963, 1568, 1488, 1391, 1306, 1263, 766 cm⁻¹. ¹H NMR (300 MHz, CDCl₃): δ = 1.36 (s, 9 H), 6.43 (d, *J* = 5.1 Hz, 1 H), 7.16 (d, *J* = 8.5 Hz,

1 H), 7.41 (dd, $J = 8.5, 2.2$ Hz, 1 H), 7.60 (t, $J = 7.6$ Hz, 1 H), 7.65–7.83 (m, 2 H), 8.11 (d, $J = 8.5$ Hz, 1 H), 8.42 (d, $J = 8.3$ Hz, 1 H), 8.67 (d, $J = 5.0$ Hz, 1 H) ppm. ^{13}C NMR (75 MHz, CDCl_3): $\delta = 31.3, 34.7, 103.6, 115.8, 121.1, 121.9, 122.6, 126.2, 126.3, 129.0, 130.2, 131.2, 148.5, 149.7, 150.9, 151.1, 160.9$ ppm. HRMS (ESI-TOF) m/z : $[\text{M} + \text{H}]^+$ calcd. for $\text{C}_{19}\text{H}_{19}\text{BrNO}$: 356.0650, found 356.0642.

4-(2-Bromo-4-methoxyphenoxy)quinoline (1m): Method (b) – beige solid (0.304 g, 56 %); m.p. 184–185 °C. IR (film): $\tilde{\nu}_{\text{max}} = 3062, 2835, 1595, 1487, 1392, 1212, 765$ cm^{-1} . ^1H NMR (300 MHz, CDCl_3): $\delta = 3.86$ (s, 3 H), 6.38 (d, $J = 5.2$ Hz, 1 H), 6.96 (dd, $J = 8.9, 2.9$ Hz, 1 H), 7.17 (d, $J = 8.9$ Hz, 1 H), 7.24 (d, $J = 2.9$ Hz, 1 H), 7.60 (ddd, $J = 8.1, 6.9, 1.1$ Hz, 1 H), 7.77 (ddd, $J = 8.5, 6.9, 1.5$ Hz, 1 H), 8.11 (d, $J = 8.5$ Hz, 1 H), 8.43 (dd, $J = 8.3, 0.9$ Hz, 1 H), 8.67 (d, $J = 5.0$ Hz, 1 H) ppm. ^{13}C NMR (75 MHz, CDCl_3): $\delta = 55.9, 103.3, 114.9, 116.7, 118.9, 121.0, 121.9, 123.7, 126.2, 129.0, 130.1, 144.5, 149.7, 151.0, 157.9, 161.3$ ppm. HRMS (ESI-TOF) m/z : $[\text{M} + \text{H}]^+$ calcd. for $\text{C}_{16}\text{H}_{13}\text{BrNO}_2$: 330.0130, found 330.0125.

4-[(1-Bromonaphthalen-2-yl)oxy]quinoline (1n): Method (a) – off-white solid (0.318 g, 61 %); m.p. 197–200 °C. IR (film): $\tilde{\nu}_{\text{max}} = 3062, 1594, 1568, 1499, 1392, 1253, 764$ cm^{-1} . ^1H NMR (300 MHz, CDCl_3): $\delta = 6.42$ (d, $J = 5.1$ Hz, 1 H), 7.36 (d, $J = 8.8$ Hz, 1 H), 7.55–7.72 (m, 3 H), 7.80 (ddd, $J = 8.5, 6.9, 1.5$ Hz, 1 H), 7.92 (d, $J = 8.1$ Hz, 1 H), 7.93 (d, $J = 8.8$ Hz, 1 H), 8.14 (d, $J = 8.5$ Hz, 1 H), 8.33 (d, $J = 8.5$ Hz, 1 H), 8.51 (dd, $J = 8.3, 1.0$ Hz, 1 H), 8.56 (d, $J = 5.1$ Hz, 1 H) ppm. ^{13}C NMR (75 MHz, CDCl_3): $\delta = 103.9, 115.2, 121.1, 121.3, 122.0, 126.3, 126.6, 127.1, 128.2, 128.4, 129.1, 129.8, 130.3, 132.4, 133.2, 149.0, 149.8, 151.1, 160.8$ ppm. HRMS (ESI-TOF) m/z : $[\text{M} + \text{H}]^+$ calcd. for $\text{C}_{19}\text{H}_{13}\text{BrNO}$: 350.0181, found 350.0178.

4-[(2-Bromopyridin-3-yl)oxy]quinoline (1o): Method (a) – pale pink solid (0.2378 g, 79 %); m.p. 170–173 °C. IR (film): $\tilde{\nu}_{\text{max}} = 1639, 1503, 1305, 1268, 666$ cm^{-1} . ^1H NMR (300 MHz, CDCl_3): $\delta = 6.45$ (d, $J = 5.1$ Hz, 1 H), 7.38 (dd, $J = 8.0, 4.6$ Hz, 1 H), 7.47–7.70 (m, 2 H), 7.79 (ddd, $J = 8.4, 7.0, 1.4$ Hz, 1 H), 8.13 (d, $J = 8.5$ Hz, 1 H), 8.28–8.47 (m, 2 H), 8.72 (d, $J = 5.1$ Hz, 1 H) ppm. ^{13}C NMR (75 MHz, CDCl_3): $\delta = 104.1, 121.0, 121.7, 124.0, 126.7, 129.2, 130.5, 130.5, 136.6, 147.0, 148.7, 149.9, 150.8, 159.9$ ppm. HRMS (ESI-TOF) m/z : $[\text{M} + \text{H}]^+$ calcd. for $\text{C}_{14}\text{H}_{10}\text{BrN}_2\text{O}$: 300.9976, found 300.9986.

4-(2-Bromophenoxy)-2-methylquinoline (1p): Method (a) – pale pink solid (0.331 g, 93 %); m.p. 98–101 °C. IR (film): $\tilde{\nu}_{\text{max}} = 2923, 1599, 1470, 1342, 1235, 754$ cm^{-1} . ^1H NMR (300 MHz, CDCl_3): $\delta = 2.60$ (s, 3 H), 6.29 (s, 1 H), 7.15–7.29 (m, 2 H), 7.42 (ddd, $J = 8.6, 7.3, 1.6$ Hz, 1 H), 7.54 (ddd, $J = 8.2, 6.9, 1.2$ Hz, 1 H), 7.68–7.79 (m, 2 H), 8.02 (d, $J = 8.4$ Hz, 1 H), 8.35 (dd, $J = 8.4, 1.0$ Hz, 1 H) ppm. ^{13}C NMR (75 MHz, CDCl_3): $\delta = 25.8, 104.2, 116.3, 119.5, 121.7, 123.2, 125.4, 127.1, 128.3, 129.1, 130.2, 134.3, 149.4, 151.3, 159.9, 160.8$ ppm. HRMS (ESI-TOF) m/z : $[\text{M} + \text{H}]^+$ calcd. for $\text{C}_{16}\text{H}_{13}\text{BrNO}$: 314.0181, found 314.0179.

4-(2-Bromophenoxy)-6-methoxyquinoline (1q): Method (a) – yellow sticky oil (0.599 g, 70 %). IR (film): $\tilde{\nu}_{\text{max}} = 3392, 1596, 1467, 1365, 1262, 1223, 778$ cm^{-1} . ^1H NMR (300 MHz, CDCl_3): $\delta = 3.98$ (s, 3 H), 6.40 (d, $J = 5.1$ Hz, 1 H), 7.16–7.29 (m, 2 H), 7.37–7.47 (m, 2 H), 7.64 (d, $J = 2.8$ Hz, 1 H), 7.73 (dd, $J = 8.0, 1.5$ Hz, 1 H), 8.01 (d, $J = 9.2$ Hz, 1 H), 8.54 (d, $J = 5.1$ Hz, 1 H) ppm. ^{13}C NMR (75 MHz, CDCl_3): $\delta = 55.7, 99.4, 104.2, 116.4, 121.8, 122.9, 123.2, 127.2, 129.2, 130.7, 134.3, 145.9, 148.4, 151.3, 157.8, 159.7$ ppm. HRMS (ESI-TOF) m/z : $[\text{M} + \text{H}]^+$ calcd. for $\text{C}_{16}\text{H}_{13}\text{BrNO}_2$: 330.0130, found 330.0130.

4-(2-Bromophenoxy)-7-methoxyquinoline (1r): Method (a) – pale yellow solid (0.380 g, 74 %); m.p. 99–100 °C. IR (film): $\tilde{\nu}_{\text{max}} = 3388, 1622, 1428, 1315, 1227, 665$ cm^{-1} . ^1H NMR (300 MHz, CDCl_3): $\delta = 3.98$ (s, 3 H), 6.30 (d, $J = 5.2$ Hz, 1 H), 7.15–7.29 (m, 3 H), 7.36–7.47 (m, 2 H), 7.72 (dd, $J = 7.9, 1.5$ Hz, 1 H), 8.29 (d, $J = 9.2$ Hz, 1 H), 8.59

(d, $J = 5.2$ Hz, 1 H) ppm. ^{13}C NMR (75 MHz, CDCl_3): $\delta = 55.5, 102.4, 107.3, 115.8, 116.3, 119.2, 123.1, 123.2, 127.1, 129.1, 134.2, 151.2, 151.5, 151.8, 160.7, 161.3$ ppm. HRMS (ESI-TOF) m/z : $[\text{M} + \text{H}]^+$ calcd. for $\text{C}_{16}\text{H}_{12}\text{BrNO}_2$: 330.0130, found 330.0128.

4-(2-Bromophenoxy)-6-(trifluoromethyl)quinoline (1s): Method (a) – off-white solid (0.254 g, 80 %); m.p. 67–69 °C. IR (film): $\tilde{\nu}_{\text{max}} = 3069, 1570, 1467, 1316, 1224, 1126, 739$ cm^{-1} . ^1H NMR (300 MHz, CDCl_3): $\delta = 6.47$ (d, $J = 5.2$ Hz, 1 H), 7.21–7.32 (m, 2 H), 7.46 (ddd, $J = 8.1, 7.3, 1.6$ Hz, 1 H), 7.75 (dd, $J = 7.9, 1.3$ Hz, 1 H), 7.95 (dd, $J = 8.9, 2.1$ Hz, 1 H), 8.22 (d, $J = 8.9$ Hz, 1 H), 8.76 (s, 1 H), 8.77 (d, $J = 5.2$ Hz, 1 H) ppm. ^{13}C NMR (125 MHz, CDCl_3): $\delta = 104.4, 116.4, 120.2, 120.3$ [q, $^3J(\text{C},\text{F}) = 5$ Hz], 123.4, 124.1 [q, $^1J(\text{C},\text{F}) = 272$ Hz], 126.0 [q, $^3J(\text{C},\text{F}) = 3$ Hz], 127.8, 128.2 [q, $^2J(\text{C},\text{F}) = 33$ Hz], 129.4, 130.3, 134.5, 150.6, 150.7, 153.2, 161.3 ppm. ^{19}F NMR (282 MHz, CDCl_3): $\delta = -62$ ppm. HRMS (ESI-TOF) m/z : $[\text{M} + \text{H}]^+$ calcd. for $\text{C}_{16}\text{H}_{10}\text{BrF}_3\text{NO}$: 367.9898, found 367.9894.

4-(2-Bromophenoxy)-6-fluoroquinoline (1t): Method (a) – pale yellow solid (0.344 g, 65 %); m.p. 75–79 °C. IR (film): $\tilde{\nu}_{\text{max}} = 3422, 1630, 1262, 1222, 1177, 657$ cm^{-1} . ^1H NMR (300 MHz, CDCl_3): $\delta = 6.43$ (d, $J = 5.1$ Hz, 1 H), 7.19–7.24 (m, 1 H), 7.25 (d, $J = 8.7$ Hz, 1 H), 7.44 (t, $J = 7.4$ Hz, 1 H), 7.54 (td, $J = 8.7, 2.8$ Hz, 1 H), 7.73 (d, $J = 9.9$ Hz, 1 H), 8.02 (dd, $J = 9.3, 2.8$ Hz, 1 H), 8.12 (dd, $J = 9.2, 5.2$ Hz, 1 H), 8.64 (d, $J = 5.1$ Hz, 1 H) ppm. ^{13}C NMR (75 MHz, CDCl_3): $\delta = 104.0, 105.7$ [d, $^2J(\text{C},\text{F}) = 24$ Hz], 116.3, 120.4 [d, $^2J(\text{C},\text{F}) = 26$ Hz], 121.7 [d, $^3J(\text{C},\text{F}) = 10$ Hz], 123.3, 127.5, 129.3, 131.7 [d, $^3J(\text{C},\text{F}) = 10$ Hz], 134.4, 146.9, 150.3 [d, $^6J(\text{C},\text{F}) = 3$ Hz], 150.8, 160.3 [d, $^4J(\text{C},\text{F}) = 5$ Hz], 160.4 [d, $^1J(\text{C},\text{F}) = 248$ Hz] ppm. ^{19}F NMR (282 MHz, CDCl_3): $\delta = -113$ ppm. HRMS (ESI-TOF) m/z : $[\text{M} + \text{H}]^+$ calcd. for $\text{C}_{15}\text{H}_{10}\text{BrFNO}$: 317.9930, found 317.9917.

4-(2-Bromophenoxy)-8-fluoroquinoline (1u): Method (a) – pale yellow crystalline solid (0.2519 g, 53 %); m.p. 87–90 °C. IR (film): $\tilde{\nu}_{\text{max}} = 1631, 1597, 1264, 1224, 949, 612$ cm^{-1} . ^1H NMR (300 MHz, CDCl_3): $\delta = 6.45$ (d, $J = 5.1$ Hz, 1 H), 7.12–7.29 (m, 2 H), 7.34–7.58 (m, 3 H), 7.70 (dd, $J = 8.0, 1.4$ Hz, 1 H), 8.19 (d, $J = 8.0$ Hz, 1 H), 8.71 (d, $J = 5.1$ Hz, 1 H) ppm. ^{13}C NMR (75 MHz, CDCl_3): $\delta = 104.4, 114.3$ [d, $^4J(\text{C},\text{F}) = 19$ Hz], 116.2, 117.7 [d, $^4J(\text{C},\text{F}) = 5$ Hz], 122.7 [d, $^3J(\text{C},\text{F}) = 3$ Hz], 123.2, 126.0 [d, $^3J(\text{C},\text{F}) = 8$ Hz], 127.55, 129.3, 134.3, 140.0 [d, $^2J(\text{C},\text{F}) = 13$ Hz], 150.7, 151.2, 157.9 [d, $^1J(\text{C},\text{F}) = 256$ Hz], 160.6 [d, $^4J(\text{C},\text{F}) = 4$ Hz] ppm. ^{19}F NMR (282 MHz, CDCl_3): $\delta = -125$ ppm. HRMS (ESI-TOF) m/z : $[\text{M} + \text{H}]^+$ calcd. for $\text{C}_{15}\text{H}_{10}\text{BrFNO}$: 317.9930, found 317.9918.

4-(2-Bromophenoxy)-6-chloroquinoline (1v): Method (a) – off-white solid (0.4525 g, 90 %); m.p. 89–90 °C. IR (film): $\tilde{\nu}_{\text{max}} = 1642, 1563, 1262, 1222, 666, 643$ cm^{-1} . ^1H NMR (300 MHz, CDCl_3): $\delta = 6.41$ (d, $J = 5.2$ Hz, 1 H), 7.17–7.30 (m, 2 H), 7.44 (ddd, $J = 8.2, 7.3, 1.6$ Hz, 1 H), 7.65–7.69 (m, 2 H), 8.04 (d, $J = 9.0$ Hz, 1 H), 8.40 (d, $J = 2.3$ Hz, 1 H), 8.66 (d, $J = 5.2$ Hz, 1 H) ppm. ^{13}C NMR (75 MHz, CDCl_3): $\delta = 104.2, 116.3, 121.0, 121.6, 123.2, 127.5, 129.3, 130.8, 131.1, 132.2, 134.3, 148.1, 150.7, 151.2, 160.0$ ppm. HRMS (ESI-TOF) m/z : $[\text{M} + \text{H}]^+$ calcd. for $\text{C}_{15}\text{H}_{10}\text{BrClNO}$: 333.9634, found 333.9628.

4-(2-Bromophenoxy)-2-heptylquinoline (1w): Method (a) – off-white solid (0.205 g, 90 %); m.p. 75–77 °C. IR (film): $\tilde{\nu}_{\text{max}} = 2926, 2855, 1600, 1470, 1359, 1234, 763$ cm^{-1} . ^1H NMR (300 MHz, CDCl_3): $\delta = 0.85$ (t, $J = 6.7$ Hz, 3 H), 1.14–1.42 (m, 8 H), 1.68 (m, 2 H), 2.80 (t, $J = 8.1$ Hz, 2 H), 6.30 (s, 1 H), 7.17–7.25 (m, 2 H), 7.42 (ddd, $J = 8.5, 7.2, 1.5$ Hz, 1 H), 7.53 (ddd, $J = 8.1, 7.0, 1.1$ Hz, 1 H), 7.63–7.81 (m, 2 H), 8.05 (d, $J = 8.4$ Hz, 1 H), 8.34 (dd, $J = 8.3, 0.9$ Hz, 1 H) ppm. ^{13}C NMR (75 MHz, CDCl_3): $\delta = 14.1, 22.6, 29.2, 29.4, 30.0, 31.8, 39.7, 103.8, 116.3, 119.7, 121.7, 123.1, 125.4, 127.1, 128.5, 129.2, 130.1, 134.3, 149.5, 151.4, 160.7, 164.2$ ppm. HRMS (ESI-TOF) m/z : $[\text{M} + \text{H}]^+$ calcd. for $\text{C}_{22}\text{H}_{25}\text{BrNO}$: 398.1120, found 398.1135.

General Procedure for Palladium-Catalysed Intramolecular Direct Arylation Reactions for the Preparation of Compounds 2a–2w: A mixture of the 4-(2-bromophenoxy)quinoline substrate **1** (1 equiv.), Pd(OAc)₂ (2–5 mol-%), and anhydrous caesium carbonate (2 equiv.) in anhydrous *N*-methylpyrrolidone (1.5 mL/mmol) was stirred at 135 °C in a sealed reaction tube until the reaction was completed as evident by ¹H NMR analysis. The cooled reaction mixture was diluted with DCM, filtered through a short plug of Celite and concentrated in vacuo. The crude mixture was purified by column chromatography over silica gel using DCM/EtOAc (99:1–95:5) as eluent.

Benzofuro[3,2-*c*]quinoline (2a):^[27] White solid (0.068 g, 95 %); m.p. 132–135 °C (lit.^[27] 135–138 °C). IR (film): $\tilde{\nu}_{\max}$ = 3369, 1566, 1510, 1399, 1190 cm⁻¹. ¹H NMR (300 MHz, CDCl₃): δ = 7.44–7.58 (m, 2 H), 7.65–7.83 (m, 3 H), 8.12 (dd, *J* = 7.2, 0.9 Hz, 1 H), 8.28 (d, *J* = 8.4 Hz, 1 H), 8.44 (dd, *J* = 8.1, 1.0 Hz, 1 H), 9.51 (s, 1 H) ppm. ¹³C NMR (75 MHz, CDCl₃): δ = 112.1, 116.3, 117.2, 120.6, 120.8, 122.7, 124.1, 127.0, 127.2, 129.3, 129.9, 144.4, 147.4, 156.0, 157.5 ppm. HRMS (ESI-TOF) *m/z*: [M + H]⁺ calcd. for C₁₅H₁₀NO: 220.0762, found 220.0755.

9-Fluorobenzofuro[3,2-*c*]quinoline (2b):^[53] White solid (0.064 g, 88 %); m.p. 149–150 °C (lit.^[53] 148–150 °C). IR (film): $\tilde{\nu}_{\max}$ = 3052, 1564, 1512, 1396, 1254, 1134 cm⁻¹. ¹H NMR (300 MHz, CDCl₃): δ = 7.22 (ddd, *J* = 8.9, 6.9, 2.2 Hz, 1 H), 7.45 (dd, *J* = 8.6, 2.2 Hz, 1 H), 7.63–7.85 (m, 2 H), 8.00 (dd, *J* = 8.6, 5.3 Hz, 1 H), 8.25 (d, *J* = 8.3 Hz, 1 H), 8.36 (dd, *J* = 8.1, 1.1 Hz, 1 H), 9.43 (s, 1 H) ppm. ¹³C NMR (75 MHz, CDCl₃): δ = 100.3 [d, ²*J*(C,F) = 27 Hz], 112.3 [d, ²*J*(C,F) = 24 Hz], 115.8, 117.0, 118.9 [d, ⁴*J*(C,F) = 4 Hz], 120.6, 121.2 [d, ³*J*(C,F) = 10 Hz], 127.2, 129.4, 129.8, 143.9, 147.1, 156.1 [d, ³*J*(C,F) = 14 Hz], 158.1 [d, ⁵*J*(C,F) = 3 Hz], 162.2 [d, ¹*J*(C,F) = 247 Hz] ppm. ¹⁹F NMR (282 MHz, CDCl₃): δ = –112 ppm. HRMS (ESI-TOF) *m/z*: [M + H]⁺ calcd. for C₁₅H₉FNO: 238.0668, found 238.0668.

8-Fluorobenzofuro[3,2-*c*]quinoline (2c):^[27] White solid (0.087 g, 91 %); m.p. 163–164 °C (lit.^[27] 162–163 °C). IR (film): $\tilde{\nu}_{\max}$ = 3368, 1565, 1479, 1319, 1247, 1146 cm⁻¹. ¹H NMR (300 MHz, CDCl₃): δ = 7.21–7.33 (m, 1 H), 7.65–7.87 (m, 4 H), 8.28 (d, *J* = 8.4 Hz, 1 H), 8.41 (dd, *J* = 8.1, 1.0 Hz, 1 H), 9.45 (s, 1 H) ppm. ¹³C NMR (75 MHz, CDCl₃): δ = 106.7 [d, ²*J*(C,F) = 26 Hz], 112.9 [d, ³*J*(C,F) = 9 Hz], 114.7 [d, ²*J*(C,F) = 26 Hz], 116.1 [d, ⁴*J*(C,F) = 4 Hz], 117.0, 120.8, 123.6 [d, ³*J*(C,F) = 11 Hz], 127.2, 129.6, 129.9, 144.2, 147.5, 151.9, 158.6, 159.7 [d, ¹*J*(C,F) = 241 Hz] ppm. ¹⁹F NMR (282 MHz, CDCl₃): δ = –118 ppm. HRMS (ESI-TOF) *m/z*: [M + H]⁺ calcd. for C₁₅H₉FNO: 238.0668, found 238.0659.

10-Fluorobenzofuro[3,2-*c*]quinoline (2d):^[27] White solid (0.104 g, 93 %); m.p. 156–157 °C (lit.^[27] 157–158 °C). IR (film): $\tilde{\nu}_{\max}$ = 3368, 1564, 1496, 1347, 1200, 1189 cm⁻¹. ¹H NMR (300 MHz, CDCl₃): δ = 7.27–7.35 (m, 1 H), 7.42 (td, *J* = 8.0, 4.4 Hz, 1 H), 7.73 (ddd, *J* = 8.1, 7.0, 1.2 Hz, 1 H), 7.79–7.92 (m, 2 H), 8.29 (d, *J* = 8.2 Hz, 1 H), 8.49 (dd, *J* = 8.1, 0.9 Hz, 1 H), 9.50 (s, 1 H) ppm. ¹³C NMR (75 MHz, CDCl₃): δ = 113.7 [d, ²*J*(C,F) = 16 Hz], 116.0, 116.1 [d, ⁴*J*(C,F) = 4 Hz], 117.0, 120.8, 124.8 [d, ³*J*(C,F) = 6 Hz], 126.2 [d, ³*J*(C,F) = 3 Hz], 127.3, 129.7, 129.8, 142.7 [d, ²*J*(C,F) = 11 Hz], 144.3, 147.7, 148.3 [d, ¹*J*(C,F) = 251 Hz], 157.8 ppm. ¹⁹F NMR (282 MHz, CDCl₃): δ = –135 ppm. HRMS (ESI-TOF) *m/z*: [M + H]⁺ calcd. for C₁₅H₉FNO: 238.0668, found 238.0662.

9-Chlorobenzofuro[3,2-*c*]quinoline (2e): White solid (0.086 g, 79 %); m.p. 198–199 °C. IR (film): $\tilde{\nu}_{\max}$ = 3047, 1562, 1508, 1338, 1049, 755 cm⁻¹. ¹H NMR (300 MHz, CDCl₃): δ = 7.47 (dd, *J* = 8.3, 1.8 Hz, 1 H), 7.66–7.87 (m, 3 H), 8.00 (d, *J* = 8.3 Hz, 1 H), 8.27 (d, *J* = 8.4 Hz, 1 H), 8.40 (d, *J* = 8.0 Hz, 1 H), 9.46 (s, 1 H) ppm. ¹³C NMR (75 MHz, CDCl₃): δ = 112.8, 115.7, 117.0, 120.7, 121.1, 121.4, 124.8,

127.2, 129.6, 129.9, 132.9, 144.1, 147.5, 156.0, 157.8 ppm. HRMS (ESI-TOF) *m/z*: [M + H]⁺ calcd. for C₁₅H₉ClNO: 254.0373, found 254.0363.

8-Chlorobenzofuro[3,2-*c*]quinoline (2f):^[27] White solid (0.071 g, 93 %); m.p. 187–189 °C (lit.^[27] 189–190 °C). IR (film): $\tilde{\nu}_{\max}$ = 2917, 1564, 1511, 1395, 1194, 871 cm⁻¹. ¹H NMR (300 MHz, CDCl₃): δ = 7.51 (dd, *J* = 8.8, 2.2 Hz, 1 H), 7.69 (dd, *J* = 8.8, 0.4 Hz, 1 H), 7.72 (ddd, *J* = 8.1, 7.0, 1.2 Hz, 1 H), 7.82 (ddd, *J* = 8.5, 7.0, 1.5 Hz, 1 H), 8.08 (dd, *J* = 2.2, 0.4 Hz, 1 H), 8.28 (d, *J* = 8.2 Hz, 1 H), 8.41 (dd, *J* = 8.2, 0.9 Hz, 1 H), 9.46 (s, 1 H) ppm. ¹³C NMR (100 MHz, CDCl₃): δ = 113.1, 115.5, 117.0, 120.5, 120.8, 124.1, 127.28, 127.34, 129.75, 129.78, 130.0, 144.2, 147.6, 154.2, 158.2 ppm. HRMS (ESI-TOF) *m/z*: [M + H]⁺ calcd. for C₁₅H₉ClNO: 254.0373, found 254.0370.

8-(Trifluoromethyl)benzofuro[3,2-*c*]quinoline (2g): White crystalline solid (0.0533 g, 88 %); m.p. 170–173 °C. IR (film): $\tilde{\nu}_{\max}$ = 1627, 1567, 1333, 1310, 1151, 1110 cm⁻¹. ¹H NMR (400 MHz, CDCl₃): δ = 7.65–7.91 (m, 4 H), 8.29 (d, *J* = 8.5 Hz, 1 H), 8.35–8.48 (m, 2 H), 9.52 (s, 1 H) ppm. ¹³C NMR (75 MHz, CDCl₃): δ = 112.5, 115.4, 116.8, 118.3 [q, ³*J*(C,F) = 4 Hz], 120.7, 123.0, 124.3 [q, ³*J*(C,F) = 4 Hz], 124.3 [q, ¹*J*(C,F) = 272 Hz], 126.8 [q, ²*J*(C,F) = 33 Hz], 127.4, 129.9, 130.0, 144.1, 147.8, 157.2, 158.4 ppm. ¹⁹F NMR (282 MHz, CDCl₃): δ = –61 ppm. HRMS (ESI-TOF) *m/z*: [M + H]⁺ calcd. for C₁₆H₉F₃NO: 288.0636, found 288.0629.

8-(Trifluoromethoxy)benzofuro[3,2-*c*]quinoline (2h): White crystalline solid (0.1367 g, 90 %); m.p. 124–126 °C. IR (film): $\tilde{\nu}_{\max}$ = 1641, 1512, 1280, 1247, 1206, 1141, 1156 cm⁻¹. ¹H NMR (300 MHz, CDCl₃): δ = 7.41 (ddd, *J* = 8.9, 2.4, 0.8 Hz, 1 H), 7.64–7.88 (m, 3 H), 7.95 (d, *J* = 1.1 Hz, 1 H), 8.28 (d, *J* = 8.4 Hz, 1 H), 8.41 (dd, *J* = 8.1, 1.0 Hz, 1 H), 9.47 (s, 1 H) ppm. ¹³C NMR (75 MHz, CDCl₃): δ = 113.0, 113.6, 115.9, 117.0, 120.6 [q, ¹*J*(C,F) = 257 Hz], 120.7, 120.8, 123.8, 127.4, 129.9, 130.0, 144.2, 145.8, 147.8, 153.9, 158.7 ppm. ¹⁹F NMR (282 MHz, CDCl₃): δ = –58 ppm. HRMS (ESI-TOF) *m/z*: [M + H]⁺ calcd. for C₁₆H₉F₃NO₂: 304.0585, found 304.0574.

8-Nitrobenzofuro[3,2-*c*]quinoline (2i): Orange solid (0.028 g, 46 %); m.p. > 250 °C. IR (film): $\tilde{\nu}_{\max}$ = 3030, 1528, 1397, 1344, 1200 cm⁻¹. ¹H NMR (300 MHz, CDCl₃): δ = 7.77 (ddd, *J* = 8.1, 7.2, 1.0 Hz, 1 H), 7.84–7.91 (m, 2 H), 8.32 (d, *J* = 8.5 Hz, 1 H), 8.41–8.52 (m, 2 H), 9.02 (d, *J* = 2.3 Hz, 1 H), 9.56 (s, 1 H) ppm. ¹³C NMR (100 MHz, CDCl₃): δ = 112.6, 115.4, 116.8, 117.1, 120.8, 123.0, 123.6, 127.8, 130.1, 130.5, 144.1, 144.9, 148.1, 158.6, 159.3 ppm. HRMS (ESI-TOF) *m/z*: [M + H]⁺ calcd. for C₁₅H₉N₂O₃: 265.0613, found 265.0611.

Methyl Benzofuro[3,2-*c*]quinoline-9-carboxylate (2j): Beige solid (0.043 g, 56 %); m.p. 192–193 °C. IR (film): $\tilde{\nu}_{\max}$ = 3402, 1717, 1565, 1434, 1397, 1281, 1234 cm⁻¹. ¹H NMR (300 MHz, CDCl₃): δ = 4.00 (s, 3 H), 7.70 (m, 1 H), 7.81 (ddd, *J* = 8.5, 7.0, 1.5 Hz, 1 H), 8.09 (d, *J* = 7.8 Hz, 1 H), 8.16 (dd, *J* = 8.2, 1.3 Hz, 1 H), 8.26 (d, *J* = 8.4 Hz, 1 H), 8.36–8.43 (m, 2 H), 9.46 (s, 1 H) ppm. ¹³C NMR (75 MHz, CDCl₃): δ = 52.5, 113.6, 115.5, 116.9, 120.2, 121.0, 125.5, 126.8, 127.3, 129.0, 129.9, 130.0, 144.5, 147.8, 155.4, 159.0, 166.6 ppm. HRMS (ESI-TOF) *m/z*: [M + H]⁺ calcd. for C₁₇H₁₂NO₃: 278.0817, found 278.0811.

8-Methylbenzofuro[3,2-*c*]quinoline (2k):^[27] White solid (0.062 g, 71 %); m.p. 145–148 °C (lit.^[27] 149–150 °C). IR (film): $\tilde{\nu}_{\max}$ = 2917, 1564, 1510, 1321, 1192 cm⁻¹. ¹H NMR (300 MHz, CDCl₃): δ = 2.57 (s, 3 H), 7.35 (ddd, *J* = 8.5, 1.8, 0.5 Hz, 1 H), 7.61–7.73 (m, 2 H), 7.78 (ddd, *J* = 8.5, 6.9, 1.6 Hz, 1 H), 7.89–7.92 (m, 1 H), 8.26 (d, *J* = 8.5 Hz, 1 H), 8.41 (dd, *J* = 8.1, 0.9 Hz, 1 H), 9.47 (s, 1 H) ppm. ¹³C NMR (75 MHz, CDCl₃): δ = 21.4, 111.5, 116.2, 117.2, 120.5, 120.8, 122.6, 126.8, 128.3, 129.1, 129.8, 133.7, 144.3, 147.3, 154.3, 157.6 ppm. HRMS (ESI-TOF) *m/z*: [M + H]⁺ calcd. for C₁₆H₁₂NO: 234.0919, found 234.0921.

8-(*tert*-Butyl)benzofuro[3,2-*c*]quinoline (2l):^[27] Pale yellow solid (0.025 g, 50 %); m.p. 97–100 °C (lit.^[27] 99–100 °C). IR (film): $\tilde{\nu}_{\max}$ =

2962, 1567, 1488, 1392, 1201 cm^{-1} . ^1H NMR (600 MHz, CDCl_3): δ = 1.47 (s, 9 H), 7.61 (dd, J = 8.7, 2.0 Hz, 1 H), 7.67–7.72 (m, 2 H), 7.79 (ddd, J = 8.4, 6.9, 1.5 Hz, 1 H), 8.10 (d, J = 1.7 Hz, 1 H), 8.27 (d, J = 8.4 Hz, 1 H), 8.42 (dd, J = 8.2, 1.0 Hz, 1 H), 9.52 (s, 1 H) ppm. ^{13}C NMR (150 MHz, CDCl_3): δ = 31.9, 35.0, 111.4, 116.7, 116.9, 117.3, 120.8, 122.3, 125.1, 126.9, 129.2, 129.8, 144.4, 147.3, 147.4, 154.2, 157.8 ppm. HRMS (ESI-TOF) m/z : $[\text{M} + \text{H}]^+$ calcd. for $\text{C}_{19}\text{H}_{18}\text{NO}$: 276.1388, found 276.1377.

8-Methoxybenzofuro[3,2-*c*]quinoline (2m):^[28] Off-white solid (0.032 g, 42 %); m.p. 165–167 °C (lit.^[28] 160–162 °C). IR (film): $\tilde{\nu}_{\text{max}}$ = 3350, 1570, 1486, 1330, 1186, 1164 cm^{-1} . ^1H NMR (300 MHz, CDCl_3): δ = 3.96 (s, 3 H), 7.13 (dd, J = 9.0, 2.6 Hz, 1 H), 7.54 (d, J = 2.6 Hz, 1 H), 7.59–7.85 (m, 3 H), 8.26 (d, J = 8.4 Hz, 1 H), 8.40 (dd, J = 8.1, 1.0 Hz, 1 H), 9.46 (s, 1 H) ppm. ^{13}C NMR (75 MHz, CDCl_3): δ = 56.1, 103.3, 112.6, 115.5, 116.6, 117.3, 120.8, 123.3, 127.0, 129.3, 129.8, 144.4, 147.3, 150.7, 156.9, 158.1 ppm. HRMS (ESI-TOF) m/z : $[\text{M} + \text{H}]^+$ calcd. for $\text{C}_{16}\text{H}_{12}\text{NO}_2$: 250.0868, found 250.0858.

Naphtho[1',2':4,5]furo[3,2-*c*]quinoline (2n): Off-white solid (0.014 g, 17 %); m.p. 203–205 °C. IR (film): $\tilde{\nu}_{\text{max}}$ = 2919, 1562, 1507, 1310, 1223 cm^{-1} . ^1H NMR (600 MHz, CDCl_3): δ = 7.64 (ddd, J = 8.0, 6.9, 1.1 Hz, 1 H), 7.75 (ddd, J = 8.0, 6.9, 1.1 Hz, 1 H), 7.79–7.85 (m, 2 H), 7.94 (d, J = 8.9 Hz, 1 H), 8.02 (d, J = 8.9 Hz, 1 H), 8.09 (d, J = 8.2 Hz, 1 H), 8.33 (d, J = 8.4 Hz, 1 H), 8.51 (dd, J = 8.4, 1.1 Hz, 1 H), 8.69 (d, J = 8.2 Hz, 1 H), 9.97 (s, 1 H) ppm. ^{13}C NMR (150 MHz, CDCl_3): δ = 112.7, 117.0, 117.3, 117.7, 120.7, 124.2, 125.3, 127.2, 127.7, 128.5, 128.8, 129.2, 129.4, 129.8, 131.0, 145.1, 146.4, 154.1, 157.0 ppm. HRMS (ESI-TOF) m/z : $[\text{M} + \text{H}]^+$ calcd. for $\text{C}_{19}\text{H}_{12}\text{NO}$: 270.0919, found 270.0916.

Pyrido[2',3':4,5]furo[3,2-*c*]quinoline (2o): Pale yellow solid (0.0896 g, 81 %); m.p. 174–175 °C. IR (film): $\tilde{\nu}_{\text{max}}$ = 1637, 1570, 1306, 1264 cm^{-1} . ^1H NMR (300 MHz, CDCl_3): δ = 7.42 (dd, J = 8.4, 4.8 Hz, 1 H), 7.60–7.86 (m, 2 H), 7.96 (dd, J = 8.4, 1.3 Hz, 1 H), 8.17–8.43 (m, 2 H), 8.71 (dd, J = 4.8, 1.2 Hz, 1 H), 9.66 (s, 1 H) ppm. ^{13}C NMR (75 MHz, CDCl_3): δ = 115.3, 116.9, 119.0, 120.6, 121.3, 127.3, 130.0, 130.2, 142.8, 144.4, 146.6, 148.2, 149.2, 159.1 ppm. HRMS (ESI-TOF) m/z : $[\text{M} + \text{H}]^+$ calcd. for $\text{C}_{14}\text{H}_9\text{N}_2\text{O}$: 221.0715, found 221.0710.

6-Methylbenzofuro[3,2-*c*]quinoline (2p):^[27] Pale yellow solid (0.029 g, 78 %); m.p. 132–134 °C (lit.^[27] 132–133 °C). IR (film): $\tilde{\nu}_{\text{max}}$ = 3380, 1563, 1509, 1364, 1084 cm^{-1} . ^1H NMR (300 MHz, CDCl_3): δ = 3.16 (s, 3 H), 7.41–7.69 (m, 3 H), 7.72–7.79 (m, 2 H), 8.10 (dd, J = 7.6, 2.1 Hz, 1 H), 8.18 (d, J = 8.4 Hz, 1 H), 8.38 (dd, J = 8.1, 2.1 Hz, 1 H) ppm. ^{13}C NMR (75 MHz, CDCl_3): δ = 24.3, 112.1, 115.5, 116.2, 120.7, 121.8, 123.5, 124.0, 126.1, 126.7, 128.9, 129.4, 146.9, 154.8, 155.9, 157.5 ppm. HRMS (ESI-TOF) m/z : $[\text{M} + \text{H}]^+$ calcd. for $\text{C}_{16}\text{H}_{12}\text{NO}$: 234.0919, found 234.0915.

2-Methoxybenzofuro[3,2-*c*]quinoline (2q):^[27] Off-white solid (0.095 g, 84 %); m.p. 150–152 °C (lit.^[27] 150–153 °C). IR (film): $\tilde{\nu}_{\text{max}}$ = 2954, 1350, 1514, 1468, 1228, 1191, 1031 cm^{-1} . ^1H NMR (300 MHz, CDCl_3): δ = 3.96 (s, 3 H), 7.28–7.53 (m, 4 H), 7.64 (d, J = 8.1 Hz, 1 H), 7.97 (dd, J = 7.4, 0.8 Hz, 1 H), 8.08 (d, J = 9.2 Hz, 1 H), 9.23 (s, 1 H) ppm. ^{13}C NMR (75 MHz, CDCl_3): δ = 55.6, 98.5, 111.9, 116.4, 117.7, 120.6, 121.7, 122.8, 123.9, 127.1, 131.3, 141.5, 143.3, 155.8, 156.7, 158.2 ppm. HRMS (ESI-TOF) m/z : $[\text{M} + \text{H}]^+$ calcd. for $\text{C}_{16}\text{H}_{12}\text{NO}_2$: 250.0868, found 250.0858.

3-Methoxybenzofuro[3,2-*c*]quinoline (2r): Off-white solid (0.091 g, 81 %); m.p. 146–147 °C. IR (film): $\tilde{\nu}_{\text{max}}$ = 3022, 1639, 1452, 1345, 1324, 1242, 1168 cm^{-1} . ^1H NMR (300 MHz, CDCl_3): δ = 3.97 (s, 3 H), 7.31 (dd, J = 9.0, 2.3 Hz, 1 H), 7.36–7.54 (m, 2 H), 7.58 (d, J = 2.3 Hz, 1 H), 7.68 (d, J = 8.0 Hz, 1 H), 7.99 (d, J = 7.1 Hz, 1 H), 8.25 (d, J = 9.0 Hz, 1 H), 9.37 (s, 1 H) ppm. ^{13}C NMR (75 MHz, CDCl_3): δ = 55.5, 108.4, 111.7, 112.0, 115.0, 119.7, 120.3, 121.9, 122.8, 123.9,

126.7, 144.6, 149.3, 155.8, 157.8, 160.7 ppm. HRMS (ESI-TOF) m/z : $[\text{M} + \text{H}]^+$ calcd. for $\text{C}_{16}\text{H}_{12}\text{NO}_2$: 250.0868, found 250.0865.

2-(Trifluoromethyl)benzofuro[3,2-*c*]quinoline (2s): Yellow solid (0.049 g, 63 %); m.p. 141–143 °C. IR (film): $\tilde{\nu}_{\text{max}}$ = 2917, 1567, 1443, 1348, 1167, 1111 cm^{-1} . ^1H NMR (300 MHz, CDCl_3): δ = 7.43–7.67 (m, 2 H), 7.80 (d, J = 8.2 Hz, 1 H), 7.96 (dd, J = 9.0, 2.0 Hz, 1 H), 8.13 (d, J = 8.4 Hz, 1 H), 8.38 (d, J = 8.9 Hz, 1 H), 8.75 (s, 1 H), 9.60 (s, 1 H) ppm. ^{13}C NMR (100 MHz, CDCl_3): δ = 112.3, 116.3, 117.3, 119.1 [q, $^3J(\text{C},\text{F})$ = 5 Hz], 120.8, 122.1, 124.3 [q, $^1J(\text{C},\text{F})$ = 270 Hz], 124.5, 124.9 [q, $^3J(\text{C},\text{F})$ = 3 Hz], 127.9, 128.8 [q, $^2J(\text{C},\text{F})$ = 33 Hz], 131.0, 146.4, 148.0, 156.1, 157.5 ppm. ^{19}F NMR (282 MHz, CDCl_3): δ = –62 ppm. HRMS (ESI-TOF) m/z : $[\text{M} + \text{H}]^+$ calcd. for $\text{C}_{16}\text{H}_9\text{F}_3\text{NO}$: 288.0636, found 288.0634.

2-Fluorobenzofuro[3,2-*c*]quinoline (2t):^[53] White solid (0.025 g, 67 %); m.p. 146–148 °C (lit.^[53] 148–149 °C). IR (film): $\tilde{\nu}_{\text{max}}$ = 3399, 1515, 1462, 1364, 1195, 1175 cm^{-1} . ^1H NMR (300 MHz, CDCl_3): δ = 7.45–7.61 (m, 3 H), 7.76 (d, J = 8.1 Hz, 1 H), 8.00 (dd, J = 8.6, 2.8 Hz, 1 H), 8.10 (dd, J = 7.6, 0.8 Hz, 1 H), 8.26 (dd, J = 9.3, 5.2 Hz, 1 H), 9.45 (s, 1 H) ppm. ^{13}C NMR (75 MHz, CDCl_3): δ = 104.7 [d, $^2J(\text{C},\text{F})$ = 24 Hz], 112.2, 116.8, 117.8 [d, $^3J(\text{C},\text{F})$ = 11 Hz], 119.3 [d, $^2J(\text{C},\text{F})$ = 26 Hz], 120.8, 122.5, 124.2, 127.6, 132.5 [d, $^3J(\text{C},\text{F})$ = 9 Hz], 143.6 [d, $^6J(\text{C},\text{F})$ = 3 Hz], 144.4, 156.1, 157.1 [d, $^4J(\text{C},\text{F})$ = 5 Hz], 160.8 [d, $^1J(\text{C},\text{F})$ = 249 Hz] ppm. ^{19}F NMR (282 MHz, CDCl_3): δ = –111 ppm. HRMS (ESI-TOF) m/z : $[\text{M} + \text{H}]^+$ calcd. for $\text{C}_{15}\text{H}_9\text{FNO}$: 238.0668, found 238.0659.

4-Fluorobenzofuro[3,2-*c*]quinoline (2u): White crystalline solid (0.0405 g, 49 %); m.p. 153–155 °C. IR (film): $\tilde{\nu}_{\text{max}}$ = 1640, 1596, 1300, 1249, 949 cm^{-1} . ^1H NMR (300 MHz, CDCl_3): δ = 7.40–7.68 (m, 4 H), 7.75 (d, J = 8.1 Hz, 1 H), 7.99–8.27 (m, 2 H), 9.53 (s, 1 H) ppm. ^{13}C NMR (100 MHz, CDCl_3): δ = 112.2, 113.7 [d, $^2J(\text{C},\text{F})$ = 19 Hz], 116.6 [d, $^2J(\text{C},\text{F})$ = 19 Hz], 117.3, 118.9 [d, $^3J(\text{C},\text{F})$ = 3 Hz], 120.9, 122.4, 124.3, 127.1 [d, $^3J(\text{C},\text{F})$ = 8 Hz], 127.7, 137.3 [d, $^2J(\text{C},\text{F})$ = 12 Hz], 144.6, 156.0, 157.0 [d, $^4J(\text{C},\text{F})$ = 5 Hz], 158.6 [d, $^1J(\text{C},\text{F})$ = 257 Hz] ppm. ^{19}F NMR (282 MHz, CDCl_3): δ = –122 ppm. HRMS (ESI-TOF) m/z : $[\text{M} + \text{H}]^+$ calcd. for $\text{C}_{15}\text{H}_9\text{FNO}$: 238.0668, found 238.0661.

2-Chlorobenzofuro[3,2-*c*]quinoline (2v):^[53] White crystalline solid (0.0865 g, 68 %); m.p. 141–142 °C (lit.^[53] 139–141 °C). ^1H NMR (300 MHz, CDCl_3): δ = 7.38–7.58 (m, 2 H), 7.59–7.76 (m, 2 H), 8.02 (dd, J = 7.6, 0.6 Hz, 1 H), 8.12 (d, J = 9.0 Hz, 1 H), 8.27 (d, J = 2.3 Hz, 1 H), 9.38 (s, 1 H) ppm. ^{13}C NMR (75 MHz, CDCl_3): δ = 112.2, 116.9, 117.7, 119.8, 120.7, 122.3, 124.2, 127.6, 130.0, 131.4, 132.9, 144.4, 145.5, 156.0, 156.3 ppm. HRMS (ESI-TOF) m/z : $[\text{M} + \text{H}]^+$ calcd. for $\text{C}_{15}\text{H}_9\text{ClNO}$: 254.0373, found 254.0368.

6-Heptylbenzofuro[3,2-*c*]quinoline (2w): White solid (0.056 g, 70 %); m.p. 90–92 °C. IR (film): $\tilde{\nu}_{\text{max}}$ = 2917, 1559, 1445, 1363, 1202 cm^{-1} . ^1H NMR (300 MHz, CDCl_3): δ = 0.88 (t, J = 6.7 Hz, 3 H), 1.22–1.64 (m, 8 H), 1.95 (dt, J = 15.7, 7.7 Hz, 2 H), 3.40 (t, J = 8.0 Hz, 2 H), 7.40–7.67 (m, 3 H), 7.69–7.79 (m, 2 H), 8.00 (d, J = 7.3 Hz, 1 H), 8.19 (d, J = 8.4 Hz, 1 H), 8.35 (d, J = 8.1 Hz, 1 H) ppm. ^{13}C NMR (75 MHz, CDCl_3): δ = 14.1, 22.7, 28.6, 29.2, 29.9, 31.8, 38.0, 112.1, 114.8, 116.2, 120.7, 121.8, 123.1, 124.0, 126.0, 126.6, 129.1, 129.3, 146.9, 155.9, 157.7, 159.0 ppm. HRMS (ESI-TOF) m/z : $[\text{M} + \text{H}]^+$ calcd. for $\text{C}_{22}\text{H}_{24}\text{NO}$: 318.1858, found 318.1845.

Synthesis of *N*-(2-Bromophenyl)quinolin-4-amine (3): To a degassed solution of $\text{Pd}_2(\text{dba})_3$ (2 mol-%) and XantPhos (4 mol-%) in anhydrous 1,4-dioxane (4 mL/mmol) were added caesium carbonate (1.4 equiv.), 4-bromoquinoline (1 equiv.) and 2-bromoaniline (1.1 equiv.) under a nitrogen atmosphere. The reaction mixture was stirred at 120 °C under nitrogen for 24 h. The cooled reaction mixture was diluted with DCM, filtered through Celite and concentrated in vacuo. The crude mixture was purified by column chromatogra-

phy over silica gel using DCM/EtOAc (3:1) as eluent to yield the product as a yellow solid (0.322 g, 74 %); m.p. 238–241 °C. IR (film): $\tilde{\nu}_{\max}$ = 3360, 3061, 1572, 1526, 1335, 747 cm^{-1} . ^1H NMR (300 MHz, CDCl_3): δ = 6.88 (br. s, 1 H), 7.02 (td, J = 8.0, 1.5 Hz, 1 H), 7.08 (d, J = 5.2 Hz, 1 H), 7.31–7.38 (m, 1 H), 7.51–7.61 (m, 2 H), 7.65–7.78 (m, 2 H), 8.01 (d, J = 8.3 Hz, 1 H), 8.09 (d, J = 8.0 Hz, 1 H), 8.66 (d, J = 5.2 Hz, 1 H) ppm. ^{13}C NMR (75 MHz, CDCl_3): δ = 103.4, 116.9, 120.0, 120.3, 122.2, 125.0, 125.8, 128.4, 129.6, 130.1, 133.5, 138.3, 146.2, 149.2, 150.8 ppm. HRMS (ESI-TOF) m/z : $[\text{M} + \text{H}]^+$ calcd. for $\text{C}_{15}\text{H}_{12}\text{BrN}_2$: 299.0184, found 299.0187.

Synthesis of 11H-Indolo[3,2-c]quinoline (4):^[54] *N*-(2-bromophenyl)quinolin-4-amine **3** (1 equiv.), $\text{Pd}(\text{OAc})_2$ (5 mol-%), $\text{PCy}_3 \cdot \text{HBF}_4$ (10 mol-%) and caesium carbonate (2 equiv.) were added to degassed *N*-methylpyrrolidone (1.5 mL/mmol) under Schlenk conditions under a nitrogen atmosphere. The reaction mixture was stirred at 150 °C (sand bath) for 3 h. The cooled reaction mixture was diluted with DCM and filtered through Celite. The mixture was washed with water (3 \times 10 mL) and brine (15 mL), dried with MgSO_4 , filtered and concentrated in vacuo. The crude mixture was purified by column chromatography over silica gel using DCM/EtOAc (7:3) as eluent to yield the product as an off-white solid (0.030 g, 83 %); m.p. > 250 °C (lit.^[54] 340–341 °C). IR (film): $\tilde{\nu}_{\max}$ = 3355, 2916, 2849, 1567, 1512, 1459, 1236 cm^{-1} . ^1H NMR (300 MHz, D_6DMSO): δ = 7.35 (t, J = 7.5 Hz, 1 H), 7.51 (t, J = 7.6 Hz, 1 H), 7.63–7.81 (m, 3 H), 8.15 (dd, J = 8.2, 1.3 Hz, 1 H), 8.33 (d, J = 7.8 Hz, 1 H), 8.53 (dd, J = 8.0, 1.4 Hz, 1 H), 9.60 (s, 1 H), 12.72 (s, 1 H) ppm. ^{13}C NMR (75 MHz, D_6DMSO): δ = 112.3, 114.8, 117.6, 120.6, 121.1, 122.4, 122.6, 126.0, 126.1, 128.5, 130.0, 139.3, 140.2, 145.3, 145.9 ppm. HRMS (ESI-TOF) m/z : $[\text{M} + \text{H}]^+$ calcd. for $\text{C}_{15}\text{H}_{11}\text{N}_2$: 219.0922, found 219.0911.

Supporting Information (see footnote on the first page of this article): Additional competition experiments, as well as ^1H , ^{13}C and ^{19}F NMR spectra of all new compounds, key intermediates and final products.

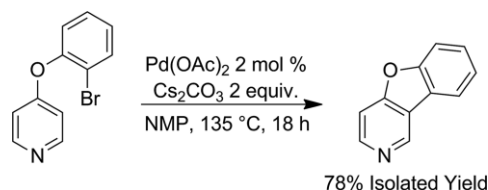
Acknowledgments

Our research is supported by Science Foundation Ireland (grant number SFI/12/IP/1315) and the Synthesis and Solid State Pharmaceutical Centre (SSPC) (SFI/12/RC/2275). The Authors thank the European Cooperation in Science and Technology COST initiative for funding CA15106, C-H Activation in Organic Synthesis (CHAOS). FJR, GMG, and FOG acknowledge support from Enterprise Ireland (CF-2017-0757-P).

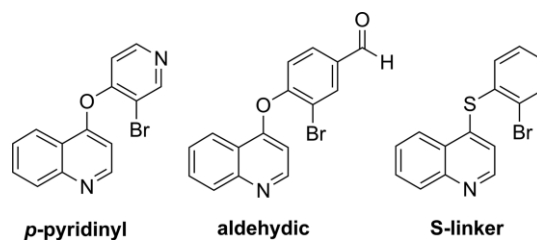
Keywords: Quinoline · Direct arylation · CH activation · Ring closure

- [1] J. P. Michael, *Nat. Prod. Rep.* **2008**, 25, 166–187.
- [2] R. D. Taylor, M. MacCoss, A. D. G. Lawson, *J. Med. Chem.* **2014**, 57, 5845–5859.
- [3] G. Jones *The Chemistry of Heterocyclic Compounds - Quinolines*, Vol. 104, Wiley, **2009**.
- [4] M. J. Mphahlele, L. G. Lesenyehlo, *J. Heterocycl. Chem.* **2013**, 50, 1–16.
- [5] Y. Nishihara *Applied cross-coupling reactions*, Vol. 80, Springer Science & Business Media, **2012**.
- [6] J. Stille, *Angew. Chem. Int. Ed.* **1986**, 25, 508–524; *Angew. Chem.* **1986**, 98, 504–519.
- [7] S. L. Buchwald, K. Fugami, T. Hiyama, M. Kosugi, M. Miura, N. Miyaura, A. Muci, M. Nomura, E. Shirakawa, K. Tamao *Cross-coupling reactions: a practical guide*, Vol. 219, Springer, **2003**.
- [8] T.-Y. Luh, M.-k. Leung, K.-T. Wong, *Chem. Rev.* **2000**, 100, 3187–3204.

- [9] J. Hassan, M. Sévignon, C. Gozzi, E. Schulz, M. Lemaire, *Chem. Rev.* **2002**, 102, 1359–1470.
- [10] N. Miyaura, A. Suzuki, *Chem. Rev.* **1995**, 95, 2457–2483.
- [11] D. Milstein, J. Stille, *J. Am. Chem. Soc.* **1978**, 100, 3636–3638.
- [12] E.-I. Negishi, *Acc. Chem. Res.* **1982**, 15, 340–348.
- [13] D. Alberico, M. E. Scott, M. Lautens, *Chem. Rev.* **2007**, 107, 174–238.
- [14] G. P. McGlacken, L. M. Bateman, *Chem. Soc. Rev.* **2009**, 38, 2447–2464.
- [15] L. Ackermann, R. Vicente, A. R. Kapdi, *Angew. Chem. Int. Ed.* **2009**, 48, 9792–9826; *Angew. Chem.* **2009**, 121, 9976.
- [16] L.-C. Campeau, M. Parisien, M. Leblanc, K. Fagnou, *J. Am. Chem. Soc.* **2004**, 126, 9186–9187.
- [17] K. Mackey, L. M. Pardo, A. M. Prendergast, M.-T. Nolan, L. M. Bateman, G. P. McGlacken, *Org. Lett.* **2016**, 18, 2540–2543.
- [18] M.-T. Nolan, L. M. Pardo, A. M. Prendergast, G. P. McGlacken, *J. Org. Chem.* **2015**, 80, 10904–10913.
- [19] M.-T. Nolan, J. T. W. Bray, K. Eccles, M. S. Cheung, Z. Lin, S. E. Lawrence, A. C. Whitwood, I. J. S. Fairlamb, G. P. McGlacken, *Tetrahedron* **2014**, 70, 7120–7127.
- [20] Y. Yang, J. Lan, J. You, *Chem. Rev.* **2017**, 117, 8787–8863.
- [21] R. Rossi, F. Bellina, M. Lessi, C. Manzini, *Adv. Synth. Catal.* **2014**, 356, 17–117.
- [22] D. Ames, A. Opalko, *Tetrahedron* **1984**, 40, 1919–1925.
- [23] W. S. Yoon, S. J. Lee, S. K. Kang, D.-C. Ha, J. Du Ha, *Tetrahedron Lett.* **2009**, 50, 4492–4494.
- [24] Y.-L. Chen, C.-H. Chung, I. L. Chen, P.-H. Chen, H.-Y. Jeng, *Bioorg. Med. Chem.* **2002**, 10, 2705–2712.
- [25] Z. Xiao, N. C. Waters, C. L. Woodard, Z. Li, P.-K. Li, *Bioorg. Med. Chem. Lett.* **2001**, 11, 2875–2878.
- [26] M. Zhao, T. Kamada, A. Takeuchi, H. Nishioka, T. Kuroda, Y. Takeuchi, *Bioorg. Med. Chem. Lett.* **2015**, 25, 5551–5554.
- [27] F. Hong, Y. Chen, B. Lu, J. Cheng, *Adv. Synth. Catal.* **2016**, 358, 353–357.
- [28] M. K. Mehra, M. P. Tantak, I. Kumar, D. Kumar, *Synlett* **2016**, 27, 604–610.
- [29] M. Ye, G.-L. Gao, A. J. F. Edmunds, P. A. Worthington, J. A. Morris, J.-Q. Yu, *J. Am. Chem. Soc.* **2011**, 133, 19090–19093.
- [30] The authors wish to thank the reviewers for the suggestion to try the following reaction:



- [31] Substrates that failed to undergo clean coupling under the optimised conditions:



- [32] L. R. Whittell, K. T. Batty, R. P. Wong, E. M. Bolitho, S. A. Fox, T. M. Davis, P. E. Murray, *Bioorg. Med. Chem.* **2011**, 19, 7519–7525.
- [33] N. Wang, M. Świtalska, M.-Y. Wu, K. Imai, T. A. Ngoc, C.-Q. Pang, L. Wang, J. Wietrzyk, T. Inokuchi, *Eur. J. Med. Chem.* **2014**, 78, 314–323.
- [34] When the Boc-protected substrate was subjected to the optimized conditions, deprotected starting material (**3**) was recovered exclusively.
- [35] J. P. Heiskanen, A. E. Tolkki, H. J. Lemmetyinen, O. E. O. Hormi, *J. Mater. Chem.* **2011**, 21, 14766–14775.
- [36] Under aerobic conditions the reaction proceeded sluggishly. Decomposition of starting material was evident by analysis of the ^1H NMR spectra of the reaction mixture.
- [37] A. M. Prendergast, G. P. McGlacken, *Eur. J. Org. Chem.* **2018**, 2018.
- [38] M. Lafrance, K. Fagnou, *J. Am. Chem. Soc.* **2006**, 128, 16496–16497.

- [39] D. García-Cuadrado, A. A. Braga, F. Maseras, A. M. Echavarren, *J. Am. Chem. Soc.* **2006**, *128*, 1066–1067.
- [40] D. García-Cuadrado, P. de Mendoza, A. A. Braga, F. Maseras, A. M. Echavarren, *J. Am. Chem. Soc.* **2007**, *129*, 6880–6886.
- [41] M. Whiteley, S. P. Diggle, E. P. Greenberg, *Nature* **2017**, *551*, 313.
- [42] F. J. Reen, G. P. McGlacken, F. O'Gara, *FEMS Microbiol. Lett.* **2018**, *365*, fny076.
- [43] G. P. McGlacken, C. M. McSweeney, T. O'Brien, S. E. Lawrence, C. J. Elcoate, F. J. Reen, F. O'Gara, *Tetrahedron Lett.* **2010**, *51*, 5919–5921.
- [44] F. J. Reen, S. L. Clarke, C. Legendre, C. M. McSweeney, K. S. Eccles, S. E. Lawrence, F. O'Gara, G. P. McGlacken, *Org. Biomol. Chem.* **2012**, *10*, 8903–8910.
- [45] F. J. Reen, M. J. Mooij, L. J. Holcombe, C. M. McSweeney, G. P. McGlacken, J. P. Morrissey, F. O'Gara, *FEMS Microbiol. Ecol.* **2011**, *77*, 413–428.
- [46] F. J. Reen, J. P. Phelan, L. Gallagher, D. F. Woods, R. M. Shanahan, R. Cano, E. Ó. Muimhneacháin, G. P. McGlacken, F. O'Gara, *Antimicrob. Agents Chemother.* **2016**, *60*, 5894–5905.
- [47] F. J. Reen, J. P. Phelan, D. F. Woods, R. Shanahan, R. Cano, S. Clarke, G. P. McGlacken, F. O'Gara, *Front. Microbiol.* **2016**, *7*, 2074.
- [48] F. J. Reen, R. Shanahan, R. Cano, F. O'Gara, G. P. McGlacken, *Org. Biomol. Chem.* **2015**, *13*, 5537–5541.
- [49] R. Shanahan, F. J. Reen, R. Cano, F. O'Gara, G. P. McGlacken, *Org. Biomol. Chem.* **2017**, *15*, 306–310.
- [50] C. Lu, B. Kirsch, C. Zimmer, J. C. de Jong, C. Henn, C. K. Maurer, M. Müsken, S. Häussler, A. Steinbach, R. W. Hartmann, *Chem. Biol.* **2012**, *19*, 381–390.
- [51] C. Lu, C. K. Maurer, B. Kirsch, A. Steinbach, R. W. Hartmann, *Angew. Chem. Int. Ed.* **2014**, *53*, 1109–1112; *Angew. Chem.* **2014**, *126*, 1127.
- [52] S. McGrath, D. S. Wade, E. C. Pesci, *FEMS Microbiol. Lett.* **2004**, *230*, 27–34.
- [53] F. Ji, X. Li, W. Wu, H. Jiang, *J. Org. Chem.* **2014**, *79*, 11246–11253.
- [54] A. V. Aksenov, D. A. Aksenov, N. A. Orazova, N. A. Aksenov, G. D. Griaznov, A. De Carvalho, R. Kiss, V. Mathieu, A. Kornienko, M. Rubin, *J. Org. Chem.* **2017**, *82*, 3011–3018.

Received: June 13, 2018

One-Pot Cross-Coupling/C–H Functionalization Reactions: Quinoline as a Substrate and Ligand through N–Pd Interaction

Rachel M. Shanahan,¹ Aobha Hickey,¹ Lorraine M. Bateman, Mark E. Light, and Gerard P. McGlacken*Cite This: *J. Org. Chem.* 2020, 85, 2585–2596

Read Online

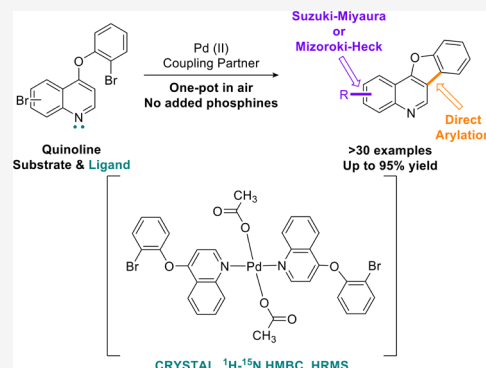
ACCESS |

Metrics & More

Article Recommendations

Supporting Information

ABSTRACT: Herein, we report a one-pot process that marries mechanistically distinct, traditional cross-coupling reactions with C–H functionalization using the same precatalyst. The reactions proceed in yields of up to 95%, in air, and require no extraneous ligand. The reactions are thought to be facilitated by harnessing the substrate quinoline as an N-ligand, and evidence of the palladium–quinoline interaction is provided by ¹H-¹⁵N HMBC NMR spectroscopy and X-ray crystallographic structures. Application of the methodology is demonstrated by the quick formation of fluorescent, π -extended frameworks.



INTRODUCTION

The formation of multiple carbon–carbon bonds in a telescoped, one-pot procedure is an efficient and environmentally friendly approach to the construction of new chemical entities.¹ However, carrying out two or more chemical reactions in a single vessel places significant demands on the methodologies involved, specifically in terms of reagent, catalyst, and substrate compatibility.² Additionally, avoiding secondary manipulation during a reaction is highly preferable if the procedures are to be applied industrially.

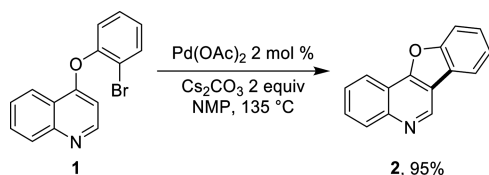
Pyridine, quinoline, and furan moieties are prominent in synthetic and naturally occurring pharmacologically active compounds.³ In drugs, they represent the 2nd, 22nd, and 25th most common ring systems, respectively.⁴ We recently reported a palladium-catalyzed intramolecular direct arylation (DA) protocol that gives a variety of benzofuro[3,2-*c*]quinolines **2** from 4-(2-bromophenoxy)quinolines **1** in excellent yields (Scheme 1).⁵

Chemoselectivity and regioselectivity proved to be very predictable in these mono-halogenated systems. Conversely, cross-coupling reactions involving substrates bearing more than one halogen are far less predictable.^{2,6} The selective

functionalization of substrates with two different halogens usually relies upon the marked difference in the rates of oxidative addition (OA) at the C–X bonds. Using halogens of the same type is considerably more difficult as significant rate differences in the oxidation step (I vs Br or Br vs Cl) are not easily harnessed.⁷ A limited number of one-pot reactions combining C–H functionalization with a Suzuki–Miyaura reaction have been reported.⁸ However, we are aware of very few protocols that do not require perturbation of the reaction setup by the addition of secondary reactants, reagents, or catalysts subsequent to reaction initiation.⁹ In all cases, added phosphine ligand is required. The use of phosphine ligands adds significantly to the cost of any catalytic process; in fact, they are often the most expensive component of a catalytic system.¹⁰

This report describes a selection of one-pot tandem Suzuki–Miyaura/direct arylation (SM/DA) and Mizoroki–Heck/direct arylation (MH/DA) reactions with di- and tribromoquinolines. Once the reaction is initiated, no further manipulation is required, and no subsequent addition of solvents, reagents, reactants, or catalysts is needed. Overall, the reaction proceeds using 2 mol % Pd(OAc)₂, in air, and without recourse to extraneous ligands. Through further development to a one-pot Mizoroki–Heck/direct arylation protocol, π -extended quinolines, with structural features of interest to

Scheme 1. Intramolecular Direct Arylation of **1**



Received: December 10, 2019

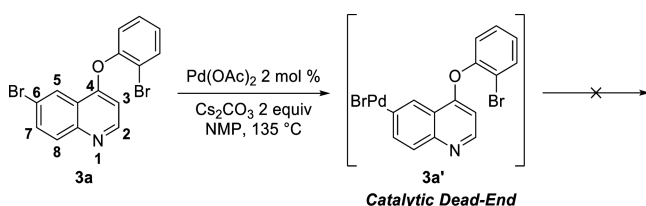
Published: January 23, 2020

medicinal¹¹ and materials¹² chemists, were prepared. These entities are challenging to synthesize by traditional, stepwise cross-coupling techniques.¹³ We provide structural characterization of initially formed palladium–quinoline (Pd–Q) complexes using crystallography, mass spectrometry, and heteronuclear multiple bond correlation (HMBC) NMR spectroscopy.

RESULTS AND DISCUSSION

Our initial aim was to test the chemoselectivity of **3a** and perhaps exploit entropic factors to carry out the intramolecular DA reaction while leaving the bromide on the quinoline backbone untouched. Using the reaction conditions that had so efficiently furnished **2** from **1**, no DA was observed (Scheme 2). We doubted that the bromine on the quinoline ring would

Scheme 2. Failed Intramolecular DA of Dibromoquinoline 3a



affect the electronics of the C-3 position to such an extent that C–H functionalization would be prevented. Thus, we rationalized that OA at the quinoline–Br was favored over the phenoxy–Br. In the absence of a suitable coupling partner, the OA product **3a'** was a catalytic dead end, with the palladium trapped at a nonproductive site.

In an effort to liberate the palladium, phenylboronic acid was introduced into the reaction mixture. Indeed, after optimization, the Suzuki–Miyaura reaction occurred, along with the direct arylation, giving 2-phenyl-benzofuro[3,2-*c*]quinoline **4a** in 83% isolated yield (Table 1).

A broad range of substituted phenylboronic acids underwent one-pot tandem SM/DA coupling, allowing access to novel benzofuroquinolines in good to excellent yields. Both electron-releasing (**4b** and **4c**) and electron-withdrawing (**4d–4k**) groups were well tolerated. The chloride on **4f** and **4l** was retained as a synthetic handle. Considering the prevalence of the pyridine moiety in biologically active compounds,¹⁴ we also applied the SM/DA reaction conditions to this substrate and were pleased to furnish the benzofuropyridine **4m** in good yield. The Suzuki–Miyaura coupling was also conducive to positioning the bromine at C-7 (**4n–4r**) (Figure 1a).

We were then keen to expand the scope of our one-pot process to include Mizoroki–Heck transformations. Using either *tert*-butyl acrylate or styrene derivatives, the one-pot tandem MH/DA products were obtained in very good yields (**5a–5h**) (Figure 1b). Both transformations also worked efficiently when the second bromine was placed on the phenoxy ring (**6a–6c**) (Figure 1c). Given the apparent versatility of our methodology, a three-component tandem process was devised using tribrominated substrates and two equivalents of either coupling partner (**7a–7c**) (Figure 1d). The structures of **4a**, **4n**, and **5b** were confirmed by X-ray diffraction analysis of single crystals (Figure 2 and see Supporting Information S3–S6).

Table 1. Solvent and Base Screen for Tandem SM/DA Reaction of 3a

entry	base	solvent	conv. (%)	yield ^a (%)
1	Cs ₂ CO ₃	NMP	100	73 (75)
2 ^b	Cs ₂ CO ₃	1,4-dioxane	90	68
3 ^c	Cs ₂ CO ₃	toluene	25	
4 ^c	Cs ₂ CO ₃	xylene	16	
5 ^c	Cs ₂ CO ₃	cyclohexanone	85	61
6 ^c	Cs ₂ CO ₃	<i>i</i> -PrOAc	25	
7 ^c	Cs ₂ CO ₃	<i>n</i> -BuOAc	20	
8	Na ₂ CO ₃	NMP	100	80
9	K ₂ CO ₃	NMP	100	86 (83)
10	KOH	NMP	30	20
11	NaOH	NMP	65	44
12	NaOt-Bu	NMP	0 ^d	

^aYields determined by ¹H NMR analysis of the crude reaction mixture using 1,3,5-trimethoxybenzene as an internal standard; values in parentheses represent isolated yields. ^bReaction carried out at 125 °C. ^cReaction carried out at 110 °C. ^dComplete decomposition of **3a** was observed.

Incorporating heteroatomic substrates in cross-coupling reactions usually necessitates the employment of an added ligand and inert atmosphere,¹⁵ and in the reported C–H functionalization of pyridines and quinolines,¹⁶ ancillary ligands are also required. Considering that pyridines,¹⁷ and indeed quinolines,¹⁸ possess the propensity to act as ligands for palladium, we suspected that our methodology might be underpinned by Pd–Q coordination. In order to determine any Pd–Q interaction, we undertook ¹H–¹⁵N HMBC NMR spectroscopy. Inherent in this powerful technique are gradient-enhanced pulse sequences, which allow for suppression of *t*₁ noise facilitating the observation of the relatively weak long-range ¹H–¹⁵N correlations.¹⁹ Overall, the low natural abundance and low gyromagnetic ratio are overcome. Using this technique, structures **8a** and **8b** were elucidated. Initially, 0.5 equiv of Pd(OAc)₂ was added to **1** and **3b** in CDCl₃ (Scheme 3), and the ¹H, ¹³C, and ¹H–¹⁵N HMBC NMR spectra were recorded (see Supporting Information S14).

Complete consumption of both substrates was observed, accompanied by upfield shifts in the ¹H signals of the C-2, C-3, and C-8 protons and a dramatic upfield shift in the ¹⁵N nucleus resonance (for example, from 291.7 ppm **1** to 196.7 ppm **8a**) in the respective ¹H–¹⁵N HMBC spectra (Figure 3 and Supporting Information S14–S25). The significant shielding of the nitrogen atom and the considerable accompanying shift in both the C-2 and C-8 protons are indicative of direct Pd–N coordination.²⁰ Upon addition of Pd(OAc)₂ to **3h**, ¹H and ¹³C NMR shifts analogous to those in **8a** and **8b** were observed. Similar downfield shifts were also discerned in the ¹H NMR spectra of **8a** in dioxane-*d*₈ and ACN-*d*₃ (Supporting Information S16 and S20). Crystal structures for complexes **8a** and **8c** were obtained (Figure 4), and the compositions of **8a–8c** were also verified by HRMS data (Supporting Information S8–S13).

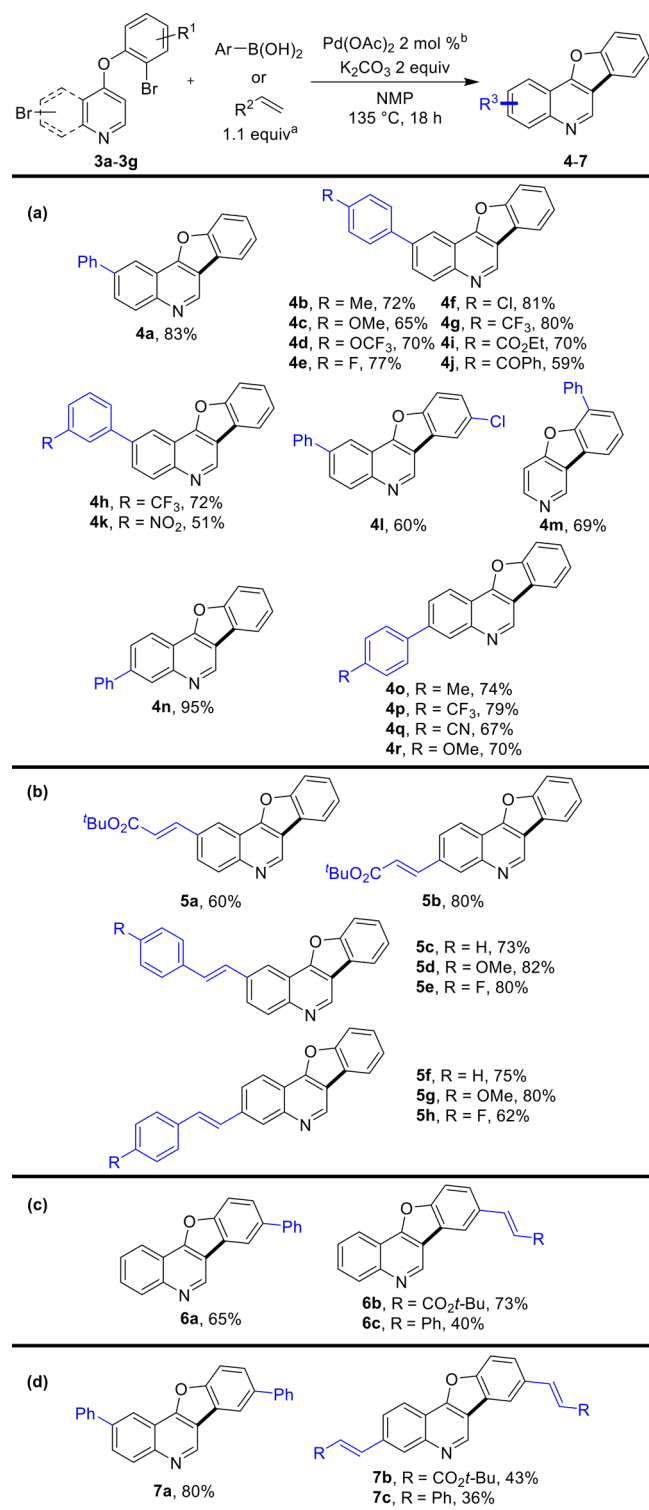


Figure 1. One-pot tandem SM/DA and MH/DA substrate scope. All yields are isolated. ^a2.2 equiv. of coupling partner employed in the synthesis of 7a–7c. ^b5 mol % Pd(OAc)₂ used for all styrene-based derivatives.

We consider the Suzuki–Miyaura reaction to be the initial transformation in the sequence (Supporting Information Schemes S1 and S2), progressing via the typical Pd(II)/Pd(0) mechanistic cycle. For the DA step, we postulate two plausible mechanisms: first, OA at C–Br followed by C–H activation via, for example, concerted metalation–deprotona-

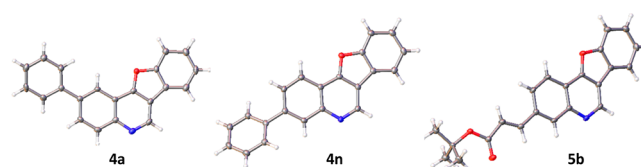


Figure 2. Crystal structures of 4a, 4n, and 5b drawn at the 50% probability level. Second molecule in the asymmetric unit of 4a omitted for clarity (see Supporting Information S4 for further information).

Scheme 3. Precatalyst Formation and Structure

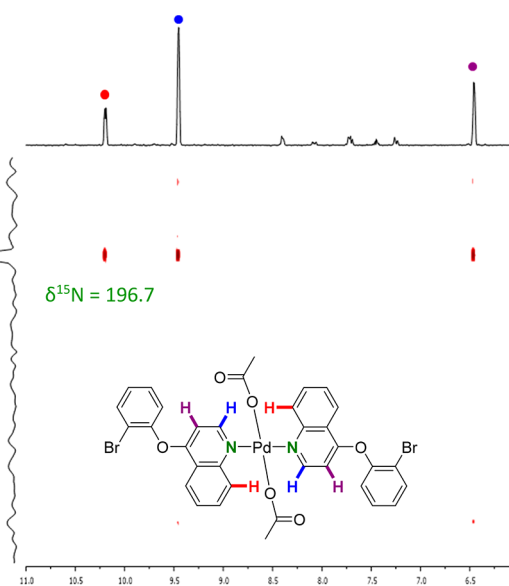
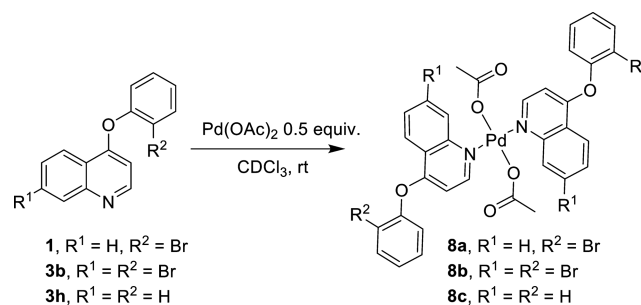


Figure 3. ¹H-¹⁵N HMBC NMR spectrum of 8a in CDCl₃ at 300 K as recorded at 600 MHz (¹H) and 60 MHz (¹⁵N). All chemical shifts δ reported in ppm.

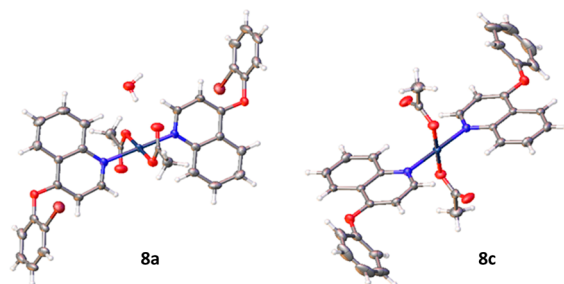
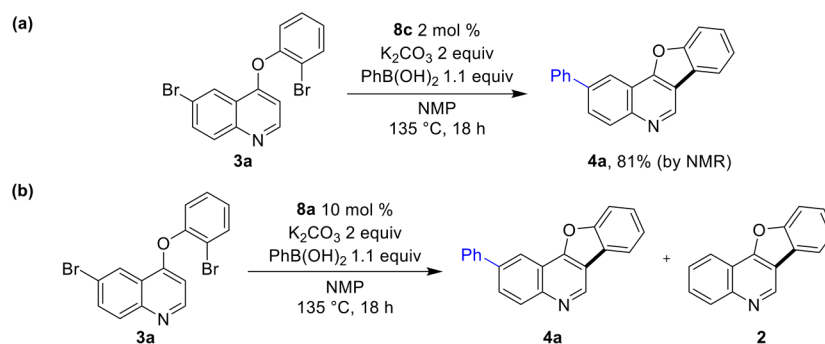


Figure 4. Crystal structures of 8a and 8c drawn at the 50% probability level. Disordered solvent (methanol) treated using solvent masking techniques for structure 8c (see Supporting Information S4–S7 for further information).

Scheme 4. Preformed 8c/8a as Competent Precatalysts for the SM/DA Reaction



tion (CMD),²¹ and second, a Pd(II)/Pd(IV) route is also plausible, as proposed by Yu and Morokuma.^{16a,22}

Albeit undefined at this stage, we envisage these complexes playing an important role as precatalysts, with the quinoline aiding precatalyst-to-catalyst transformation, although it is difficult to rule out an additional role of the quinoline in preventing catalyst decomposition.²³ Importantly, 8c was deemed a competent precatalyst for the SM/DA reaction (Scheme 4a). A further experiment using mono-bromo-Pd complex 8a as the sole catalytic-source for the SM/DA reaction yielded both 2 and 4a, proving that the Pd–Q interaction is fluxional and ruling out a spectator-only role for the quinoline ligands (analogous to phosphine ligands for example) in the initially formed complexes 8a and 8b (Scheme 4b).²⁴

Many small, conjugated organic molecules have the ability to emit fluorescent light and can be exploited for a variety of applications, such as in selective probes for ion detection^{12,25} and optoelectronic devices²⁶ and as dyes or tags in bioimaging.²⁷ We were intrigued to investigate if our π -extended MH/DA products displayed any useful photophysical characteristics. Thus, UV–Visible absorption data for the styrene-functionalized compounds 2, 5c–5h, 6c, and 7c was obtained, and their fluorescent properties were investigated. The standard benzofuro[3,2-c]quinoline framework 2 is given for comparison (Table 2).

All compounds exhibit their maximum absorption band (λ_{max}) in the UV or near-UV region and yield large molar absorption coefficients (ϵ) in the range of $10^4 \text{ dm}^3 \text{ mol}^{-1} \text{ cm}^{-1}$. The addition of further auxochromes to the substituted frameworks resulted in notable shifts in λ_{max} . For example,

Table 2. UV–Vis Data, Fluorescence Emission (em.) Data, and Molar Absorption Coefficients (ϵ) for Compounds 2, 5c–5h, 6c, and 7c (See Supporting Information S125–S133 for More Information)

compd	abs. λ_{max} (nm)	em. λ_{em} (nm)	ϵ^a ($\text{dm}^3 \text{ mol}^{-1} \text{ cm}^{-1}$)
2	257	353	63,300
5c	301	389	45,188
5d	259	416	38,338
5e	300	388	42,000
5f	337	387	38,500
5g	260	421	31,700
5h	336	386	43,638
6c	258	382	36,538
7c	342	346	51,438

^a ϵ calculated at $8 \times 10^{-6} \text{ mol dm}^{-3}$.

the introduction of an electron releasing methoxy group (5d and 5g) induced a hypsochromic shift relative to the parent styrene compounds 5c and 5f. In contrast, the more electronically poor quinoline frameworks (5e and 5h) were blueshifted by a single nanometer. A significant bathochromic shift and increased intensity are displayed in the emission spectra for all compounds with respect to 2. The addition of electron-poor/rich groups to our molecular framework gives rise to tunable differences in emission intensity and wavelength.

In summary, we report the occurrence of two mechanistically distinct reactions in one pot using the same precatalyst and without a requisite for an added ligand. The reactions work well in air, furnishing substituted benzofuroquinolines, which represent an interesting molecular framework for biological investigations. Direct evidence that the substrate quinoline forms a precatalytic species with palladium is provided, and excellent characterization data is furnished. The π -extended products also display interesting and potentially useful fluorescence properties.

EXPERIMENTAL SECTION

Materials and Methods. Solvents and reagents were used as obtained from commercial sources and without purification.

Melting points were measured in a Thomas Hoover Capillary Melting Point apparatus.

Infrared spectra were measured on a Perkin-Elmer FT-IR spectrometer as thin films in dichloromethane (DCM).

Column chromatography was carried out using 60 Å (35–70 μm) silica. Thin-layer chromatography (TLC) was carried out on precoated silica gel plates (Merck 60 PF254). The developed plates were visualized under UV light.

High-resolution precise mass spectra (HRMS) were recorded on a Waters LCT Premier ToF LC-MS instrument in University College Cork. Samples were run in electrospray ionization (ESI) mode using 50% acetonitrile/water containing 0.1% formic acid as an eluent; samples were made up at a concentration of ca. 1 mg mL^{-1} . HRMS of metal-containing complexes were recorded on a Bruker compact TOF-MS in the University of York. Samples were run in electrospray ionization (ESI) mode using 50% MeOH/water as eluent; samples were made up at a concentration of ca. 1 mg mL^{-1} . Acquisitions were internally calibrated using sodium formate clusters.

Nuclear magnetic resonance (NMR) samples were run in deuterated chloroform (CDCl_3), deuterated dimethyl sulfoxide ($(\text{CD}_3)_2\text{SO}$), deuterated dioxane ($\text{C}_4\text{D}_8\text{O}_2$), or deuterated acetonitrile ($\text{C}_2\text{D}_3\text{N}$) as specified. ^1H NMR (600 MHz) and ^1H NMR (300 MHz) spectra were recorded on Bruker Avance III 600 and Bruker Avance III 300 NMR spectrometers, respectively, in proton-coupled mode using tetramethylsilane (TMS) as the internal standard. ^{13}C NMR (150 MHz), ^{13}C NMR (100 MHz), and ^{13}C NMR (75 MHz) spectra were recorded on Bruker Avance III 600, Bruker Avance 400, and Bruker Avance III 300 NMR spectrometers, respectively, in

proton-decoupled mode at 300 K using TMS as the internal standard. ^{19}F NMR (282 MHz) spectra were recorded on a Bruker Avance III 300 NMR spectrometer in proton-decoupled mode at 300 K. ^1H - ^{15}N HMBC spectra were recorded on a Bruker Avance III 600 NMR spectrometer [600 MHz (^1H) and 60 MHz (^{15}N)] equipped with Bruker BBFO cryoprobe. All spectra recorded at 300 K and referenced externally to nitromethane at 380.2 ppm, and the value of which was uncorrected. ^1H - ^{15}N HMBC spectra were acquired using the Bruker HMBC pulse program (2D ^1H - ^{15}N correlation via heteronuclear zero and double quantum coherence optimized on long-range couplings) with four scans and a spectral width of 600–650 ppm. All spectra were run at University College Cork. Chemical shifts (δ) are expressed as parts per million (ppm), positive shift being downfield from TMS; coupling constants (J) are expressed in hertz (Hz). Splitting patterns in ^1H NMR spectra are designated as follows: s (singlet), bs (broad singlet), d (doublet), dd (doublet of doublets), ddd (doublet of doublets of doublets), t (triplet), td (triplet of doublets), q (quartet), quin (quintet), and m (multiplet).

Single-crystal X-ray analysis was performed on a Rigaku AFC12 FRE-HF diffractometer equipped with an Oxford Cryosystems low-temperature device. The crystals were kept at a steady $T = 100(2)$ K during data collection. The structures were solved with the ShelXT²⁸ structure solution program using the Intrinsic Phasing solution method and by using Olex2²⁹ as the graphical interface. The models were refined with version 2016/6 of ShelXL²⁸ using least-squares minimization. Cell parameters were retrieved and refined using the CrysAlisPro (Rigaku, V1.171.40.37a, 2019). All nonhydrogen atoms were refined anisotropically. Hydrogen atom positions were calculated geometrically and refined using the riding model. Further information is available in the Supporting Information.

UV–Visible absorption was performed on a Thermo Scientific Evolution 60S UV–Visible spectrophotometer. All solutions were made up in DCM, and measurements were performed in high-precision quartz cells of 10 mm in path length. A baseline in DCM was recorded by an internal reference detector. Molar absorption values were calculated using Beer's law at a concentration of 8×10^{-6} mol dm^{-3} . Fluorescence intensities were measured on a PerkinElmer Fluorescence Spectrometer LS 55. All solutions were made up in DCM, and measurements were performed in high-precision quartz cells of 10×10 mm in path length. Spectra were recorded in the range of 200–700 nm, and compounds were excited at 257 nm.

General Procedure for the Synthesis of 4-Phenoxyquinoline Substrates. A mixture of the 4-chloroquinoline substrate (1 equiv), the phenol (5 equiv), and NaOH (crushed pellets) (1.5 equiv) was stirred at 120 °C in an aluminum heating mantle until the reaction was complete (2–6 h) as evidenced by TLC (Hex/EtOAc 8:2). The cooled reaction mixture was diluted with 10% aqueous NaOH (5 mL) and stirred at room temperature for 1 h. The aqueous phase was extracted with DCM (3×20 mL). The combined organic layers were washed with 6 M NaOH (3×10 mL), water (10 mL), and brine (10 mL), dried over MgSO_4 , filtered, and concentrated in vacuo. The crude mixture was purified by column chromatography over silica gel using Hex/EtOAc (8:2) as an eluent unless otherwise specified.

6-Bromo-4-(2-bromophenoxy)quinoline (3a). 6-Bromo-4-chloroquinoline (0.970 g, 4.0 mmol), 2-bromophenol (2.32 mL, 20 mmol), and NaOH (0.240 g, 6.0 mmol) were reacted according to the general procedure for the synthesis of 4-phenoxyquinolines above to give the title product as a pale yellow solid; yield: 1.406 g (93%); m.p. 97–98 °C; IR (NaCl): ν 3399, 1590, 1491, 1350, 1221, 665 cm^{-1} ; ^1H NMR (300 MHz, CDCl_3) δ : 6.41 (d, $J = 5.2$ Hz, 1H), 7.19–7.28 (m, 2H), 7.39–7.47 (m, 1H), 7.73 (dd, $J = 8.3, 1.5$ Hz, 1H), 7.84 (dd, $J = 9.0, 2.2$ Hz, 1H), 7.98 (d, $J = 9.0$ Hz, 1H), 8.58 (d, $J = 2.2$ Hz, 1H), 8.67 (d, $J = 5.2$ Hz, 1H) ppm; $^{13}\text{C}\{^1\text{H}\}$ NMR (75 MHz, CDCl_3) δ : 104.2, 116.4, 120.3, 122.2, 123.3, 124.3, 127.6, 129.3, 130.9, 133.7, 134.4, 148.4, 150.8, 151.4, 159.8 ppm; HRMS (ESI-TOF) m/z : $[\text{M} + \text{H}]^+$ calcd for $\text{C}_{15}\text{H}_{10}\text{Br}_2\text{NO}$ 377.9129; found: 377.9132.

7-Bromo-4-(2-bromophenoxy)quinoline (3b). 7-Bromo-4-chloroquinoline (0.970 g, 4.0 mmol), 2-bromophenol (2.32 mL, 20.0 mmol), and NaOH (0.240 g, 6.0 mmol) were reacted according to the

general procedure for the synthesis of 4-phenoxyquinolines above to give the title product as a pale yellow solid; yield: 1.397 g (92%); m.p. 73–74 °C; IR (NaCl): ν 3064, 1561, 1468, 1301, 1220, 657 cm^{-1} ; ^1H NMR (300 MHz, CDCl_3) δ : 6.41 (d, $J = 5.2$ Hz, 1H), 7.19–7.30 (m, 2H), 7.39–7.48 (m, 1H), 7.66–7.76 (m, 2H), 8.25–8.33 (m, 2H), 8.66 (d, $J = 5.2$ Hz, 1H) ppm; $^{13}\text{C}\{^1\text{H}\}$ NMR (75 MHz, CDCl_3) δ : 103.9, 116.3, 119.7, 123.3, 123.5, 124.6, 127.6, 129.3, 129.8, 131.4, 134.4, 150.5, 150.8, 152.1, 160.8 ppm; HRMS (ESI-TOF) m/z : $[\text{M} + \text{H}]^+$ calcd for $\text{C}_{15}\text{H}_{10}\text{Br}_2\text{NO}$ 377.9129; found: 377.9119.

6-Bromo-4-(2-bromo-4-chlorophenoxy)quinoline (3c). 6-Bromo-4-chloroquinoline (0.500 g, 2.06 mmol), 2-bromo-4-chlorophenol (2.140 g, 10.31 mmol), and NaOH (0.126 g, 3.14 mmol) were reacted according to the general procedure for the synthesis of 4-phenoxyquinolines above to give the title product as a pale pink solid; yield: 531 mg (77%); m.p. 157–159 °C; IR (NaCl): ν 3392, 1590, 1467, 1349, 1256, 729, 667 cm^{-1} ; ^1H NMR (300 MHz, CDCl_3) δ : 6.41 (d, $J = 5.1$ Hz, 1H), 7.18 (d, $J = 8.6$ Hz, 1H), 7.42 (dd, $J = 8.6, 2.5$ Hz, 1H), 7.74 (d, $J = 2.4$ Hz, 1H), 7.84 (dd, $J = 9.0, 2.2$ Hz, 1H), 7.98 (d, $J = 9.0$ Hz, 1H), 8.55 (d, $J = 2.2$ Hz, 1H), 8.68 (d, $J = 5.1$ Hz, 1H) ppm; $^{13}\text{C}\{^1\text{H}\}$ NMR (75 MHz, CDCl_3) δ : 104.1, 117.0, 120.5, 122.0, 124.0, 124.2, 129.4, 131.0, 132.4, 133.9, 134.0, 148.4, 149.6, 151.3, 159.5 ppm; HRMS (ESI-TOF) m/z : $[\text{M} + \text{H}]^+$ calcd for $\text{C}_{15}\text{H}_9\text{Br}_2\text{ClNO}$ 411.8739; found: 411.8730.

4-(2,6-Dibromophenoxy)pyridine (3d). A neat mixture of 4-chloropyridine (0.250 g, 1.66 mmol) and 2,6-dibromophenol (0.630 g, 2.50 mmol) was stirred at 120 °C in an aluminum heating mantle until the reaction was complete (16 h) as evidenced by TLC (Hex/EtOAc 8:2). The cooled reaction mixture was diluted with 10% aqueous NaOH (5 mL) and stirred at room temperature for 1 h. The aqueous phase was extracted with DCM (3×20 mL). The combined organic layers were washed with 6 M NaOH (3×10 mL), water (10 mL), and brine (10 mL), dried over MgSO_4 , filtered, and concentrated in vacuo. The crude mixture was purified by recrystallization from cyclohexane to give the title product as an off-white solid; yield: 365 mg (66%); m.p. 91–93 °C; IR (NaCl): ν 3393, 1590, 1434, 1261, 1200, 665 cm^{-1} ; ^1H NMR (300 MHz, CDCl_3) δ : 6.75 (d, $J = 5.0$ Hz, 2H), 7.07 (t, $J = 8.1$ Hz, 1H), 7.63 (dd, $J = 8.1, 1.9$ Hz, 2H), 8.49 (d, $J = 5.2$ Hz, 2H) ppm; $^{13}\text{C}\{^1\text{H}\}$ NMR (75 MHz, CDCl_3) δ : 110.8, 118.3, 128.3, 133.1, 147.7, 151.5, 162.5 ppm; HRMS (ESI-TOF) m/z : $[\text{M} + \text{H}]^+$ calcd for $\text{C}_{11}\text{H}_8\text{Br}_2\text{NO}$ 327.8973; found: 327.8961.

4-(2,4-Dibromophenoxy)quinoline (3e). 4-Chloroquinoline (0.260 g, 1.60 mmol), 2,4-dibromophenol (2.00 g, 7.90 mmol), and NaOH (0.095 g, 2.40 mmol) were reacted according to the general procedure for the synthesis of 4-phenoxyquinolines above to give the title product as a pale yellow solid; yield: 517 mg (85%); m.p. 125–126 °C; IR (NaCl): ν 3394, 1596, 1464, 1305, 1224, 667 cm^{-1} ; ^1H NMR (300 MHz, CDCl_3) δ : 6.43 (d, $J = 5.1$ Hz, 1H), 7.13 (d, $J = 8.6$ Hz, 1H), 7.50–7.68 (m, 2H), 7.79 (ddd, $J = 8.5, 6.9, 1.4$ Hz, 1H), 7.88 (d, $J = 2.3$ Hz, 1H), 8.12 (d, $J = 8.4$ Hz, 1H), 8.38 (dd, $J = 8.4, 0.9$ Hz, 1H), 8.70 (d, $J = 5.1$ Hz, 1H) ppm; $^{13}\text{C}\{^1\text{H}\}$ NMR (75 MHz, CDCl_3) δ : 103.8, 117.4, 119.3, 120.9, 121.8, 124.3, 126.5, 129.2, 130.4, 132.3, 136.6, 149.8, 150.5, 151.0, 160.3 ppm; HRMS (ESI-TOF) m/z : $[\text{M} + \text{H}]^+$ calcd for $\text{C}_{15}\text{H}_{10}\text{Br}_2\text{NO}$ 377.9129; found: 377.9114.

6-Bromo-4-(2,4-dibromophenoxy)quinoline (3f). 6-Bromo-4-chloroquinoline (0.240 g, 0.99 mmol), 2,4-dibromophenol (1.247 g, 4.95 mmol), and NaOH (0.059 g, 1.5 mmol) were reacted according to the general procedure for the synthesis of 4-phenoxyquinolines above to give the title product as a pale yellow solid; yield: 268 mg (59%); m.p. 162–163 °C; IR (NaCl): ν 3370, 1590, 1449, 1349, 1255, 665 cm^{-1} ; ^1H NMR (300 MHz, CDCl_3) δ : 6.42 (d, $J = 5.1$ Hz, 1H), 7.12 (d, $J = 8.6$ Hz, 1H), 7.56 (dd, $J = 8.6, 2.3$ Hz, 1H), 7.80–7.91 (m, 2H), 7.98 (d, $J = 9.0$ Hz, 1H), 8.54 (d, $J = 2.2$ Hz, 1H), 8.68 (d, $J = 5.1$ Hz, 1H) ppm; $^{13}\text{C}\{^1\text{H}\}$ NMR (75 MHz, CDCl_3) δ : 104.2, 117.4, 119.7, 120.5, 122.0, 124.2, 124.4, 131.0, 132.4, 133.9, 136.7, 148.4, 150.1, 151.3, 159.4 ppm; HRMS (ESI-TOF) m/z : $[\text{M} + \text{H}]^+$ calcd for $\text{C}_{15}\text{H}_9\text{Br}_3\text{NO}$ 455.8234; found: 455.8233.

7-Bromo-4-(2,4-dibromophenoxy)quinoline (3g). 7-Bromo-4-chloroquinoline (0.243 g, 1.0 mmol), 2,4-dibromophenol (1.26 g,

5.0 mmol), and NaOH (0.06 g, 1.5 mmol) were reacted according to the general procedure for the synthesis of 4-phenoxyquinolines above to give the title product as a white solid; yield: 398 mg (87%); m.p. 140–142 °C; IR (NaCl) ν 3583, 1615, 1559, 1302, 1096, 666 cm^{-1} ; ^1H NMR (300 MHz, CDCl_3) δ : 6.42 (d, J = 5.2 Hz, 1H), 7.13 (d, J = 8.6 Hz, 1H), 7.56 (dd, J = 8.6, 2.3 Hz, 1H), 7.70 (dd, J = 8.9, 1.9 Hz, 1H), 7.88 (d, J = 2.3 Hz, 1H), 8.18–8.36 (m, 2H), 8.68 (d, J = 5.2 Hz, 1H) ppm; $^{13}\text{C}\{^1\text{H}\}$ NMR (75 MHz, CDCl_3) δ : 103.9, 117.4, 119.6, 119.7, 123.3, 124.4, 124.7, 130.0, 131.5, 132.4, 136.7, 150.2, 150.5, 152.1, 160.5 ppm; HRMS (ESI-TOF) m/z : $[\text{M} + \text{H}]^+$ calcd for $\text{C}_{15}\text{H}_9\text{Br}_3\text{NO}$ 455.8229; found: 455.8233.

4-Phenoxyquinoline (3h).³⁰ 4-Chloroquinoline (0.164 g, 1.0 mmol), phenol (0.471 g, 5.0 mmol), and NaOH (0.06 g, 1.5 mmol) were reacted according to the general procedure for the synthesis of 4-phenoxyquinolines above to give the title product as a yellow oil; yield: 192 mg (87%); ^1H NMR (300 MHz, CDCl_3) δ : 6.54 (d, J = 5.2 Hz, 1H), 7.13–7.22 (m, 2H), 7.23–7.33 (m, 1H), 7.39–7.50 (m, 2H), 7.56 (ddd, J = 8.2, 6.9, 1.1 Hz, 1H), 7.74 (ddd, J = 8.5, 6.9, 1.5 Hz, 1H), 8.10 (d, J = 8.3 Hz, 1H), 8.36 (dd, J = 8.4, 1.1 Hz, 1H), 8.66 (d, J = 5.1 Hz, 1H) ppm; $^{13}\text{C}\{^1\text{H}\}$ NMR (75 MHz, CDCl_3) δ : 104.4, 121.1, 121.5, 121.8, 125.6, 126.1, 129.1, 130.1, 130.3, 149.8, 151.1, 154.4, 161.9 ppm; HRMS (ESI-TOF) m/z : $[\text{M} + \text{H}]^+$ calcd for $\text{C}_{15}\text{H}_{12}\text{NO}$ 222.0913; found: 222.0913.

6-Bromo-4-phenoxyquinoline (3i). 6-Bromo-4-chloroquinoline (0.500 g, 2.1 mmol), phenol (0.970 g, 10.31 mmol), and NaOH (0.126 g, 3.14 mmol) were reacted according to the general procedure for the synthesis of 4-phenoxyquinolines above to give the title product as a pale yellow solid; yield: 517 mg (83%); m.p. 84–86 °C; IR (NaCl) ν 3401, 1561, 1487, 1351, 1213, 667 cm^{-1} ; ^1H NMR (300 MHz, CDCl_3) δ : 6.54 (d, J = 5.2 Hz, 1H), 7.13–7.22 (m, 2H), 7.25–7.36 (m, 1H), 7.41–7.53 (m, 2H), 7.80 (dd, J = 9.0, 2.2 Hz, 1H), 7.95 (d, J = 9.0 Hz, 1H), 8.53 (d, J = 2.2 Hz, 1H), 8.65 (d, J = 5.2 Hz, 1H) ppm; $^{13}\text{C}\{^1\text{H}\}$ NMR (75 MHz, CDCl_3) δ : 104.7, 120.2, 121.1, 122.6, 124.3, 125.9, 130.4, 130.9, 133.6, 148.3, 151.5, 154.0, 161.0 ppm; HRMS (ESI-TOF) m/z : $[\text{M} + \text{H}]^+$ calcd for $\text{C}_{15}\text{H}_{11}\text{BrNO}$ 300.0024; found: 300.0013.

General Procedure for Palladium-Catalyzed One-Pot Suzuki–Miyaura and Intramolecular Direct Arylation Reactions. A mixture of the 4-(2-bromophenoxy)quinoline substrate (1 equiv), $\text{PhB}(\text{OH})_2$ (1.1 equiv), $\text{Pd}(\text{OAc})_2$ (2 mol %), and anhydrous K_2CO_3 (2 equiv) in anhydrous NMP (1.5 mL mmol^{-1}) was stirred at 135 °C in a sealed reaction tube in an aluminum multireaction heating mantle until the reaction was complete as evidenced by ^1H NMR analysis. The cooled reaction mixture was diluted with DCM, filtered through a short plug of Celite, and concentrated in vacuo. The crude mixture was purified by column chromatography over silica gel using DCM/EtOAc (99:1–95:5) as an eluent unless otherwise specified.

2-Phenylbenzofuro[3,2-*c*]quinoline (4a). A mixture of substrate 3a (0.100 g, 0.26 mmol), phenylboronic acid (0.035 g, 0.29 mmol), $\text{Pd}(\text{OAc})_2$ (1.2 mg, 2 mol %), and anhydrous K_2CO_3 (0.073 g, 0.53 mmol) in anhydrous NMP (0.4 mL, 1.5 mL mmol^{-1}) was reacted according to the general one-pot SM/DA procedure above to give the title product as a pale yellow solid; X-ray quality crystals were obtained via vapor diffusion from a saturated solution of toluene in hexane, the CCDC number is 1967876; yield: 63 mg (83%); m.p. 169–171 °C; IR (NaCl) ν 3450, 1559, 1460, 1359, 1193 cm^{-1} ; ^1H NMR (300 MHz, CDCl_3) δ : 7.39–7.61 (m, 5H), 7.74–7.87 (m, 3H), 8.02–8.15 (m, 2H), 8.33 (d, J = 8.8 Hz, 1H), 8.62 (d, J = 1.7 Hz, 1H), 9.49 (s, 1H) ppm; $^{13}\text{C}\{^1\text{H}\}$ NMR (75 MHz, CDCl_3) δ : 112.1, 116.6, 117.3, 118.4, 120.6, 122.7, 124.1, 127.3, 127.5, 127.9, 128.8, 129.0, 130.2, 139.7, 140.1, 144.2, 146.7, 156.0, 157.6 ppm; HRMS (ESI-TOF) m/z : $[\text{M} + \text{H}]^+$ calcd for $\text{C}_{21}\text{H}_{14}\text{NO}$ 296.1075; found: 296.1062.

2-(*p*-Tolyl)benzofuro[3,2-*c*]quinoline (4b). A mixture of substrate 3a (0.150 g, 0.396 mmol), *o*-tolylboronic acid (0.059 g, 0.435 mmol), $\text{Pd}(\text{OAc})_2$ (1.8 mg, 2 mol %), and anhydrous K_2CO_3 (0.109 g, 0.79 mmol) in anhydrous NMP (0.6 mL, 1.5 mL mmol^{-1}) was reacted according to the general one-pot SM/DA procedure above to give the title product as a white solid; yield: 89 mg (72%); m.p. 183–185 °C; IR (NaCl) ν 3583, 3401, 1505, 1460, 1358, 1190 cm^{-1} ; ^1H NMR

(300 MHz, CDCl_3) δ : 2.45 (s, 3H), 7.35 (d, J = 7.9 Hz, 2H), 7.44–7.62 (m, 2H), 7.69–7.82 (m, 3H), 8.02–8.16 (m, 2H), 8.33 (d, J = 8.8 Hz, 1H), 8.61 (d, J = 1.9 Hz, 1H), 9.49 (s, 1H) ppm; $^{13}\text{C}\{^1\text{H}\}$ NMR (75 MHz, CDCl_3) δ : 21.2, 112.1, 116.5, 117.4, 118.0, 120.7, 122.7, 124.1, 127.27, 127.34, 128.8, 129.8, 130.2, 137.2, 137.9, 139.6, 144.0, 146.6, 156.0, 157.6 ppm; HRMS (ESI-TOF) m/z : $[\text{M} + \text{H}]^+$ calcd for $\text{C}_{22}\text{H}_{16}\text{NO}$ 310.1232; found: 310.1222.

2-(4-Methoxyphenyl)benzofuro[3,2-*c*]quinoline (4c). A mixture of substrate 3a (0.150 g, 0.396 mmol), 4-methoxyphenylboronic acid (0.066 g, 0.435 mmol), $\text{Pd}(\text{OAc})_2$ (4.5 mg, 5 mol %), and anhydrous K_2CO_3 (0.109 g, 0.79 mmol) in anhydrous NMP (0.6 mL, 1.5 mL mmol^{-1}) was reacted according to the general one-pot SM/DA procedure above to give the title product as a white solid; yield: 84 mg (65%); m.p. 189–191 °C; IR (NaCl) ν 3320, 1505, 1460, 1359, 1246, 1190 cm^{-1} ; ^1H NMR (300 MHz, CDCl_3) δ : 3.90 (s, 3H), 7.01–7.12 (m, 2H), 7.43–7.60 (m, 2H), 7.71–7.81 (m, 3H), 8.01 (dd, J = 8.8, 2.1 Hz, 1H), 8.10 (dd, J = 7.6, 0.9 Hz, 1H), 8.30 (d, J = 8.8 Hz, 1H), 8.55 (d, J = 1.9 Hz, 1H), 9.46 (s, 1H) ppm; $^{13}\text{C}\{^1\text{H}\}$ NMR (75 MHz, CDCl_3) δ : 55.4, 112.1, 114.5, 116.5, 117.4, 117.5, 120.6, 122.7, 124.1, 127.2, 128.56, 128.61, 130.2, 132.6, 139.3, 143.9, 146.4, 156.0, 157.5, 159.7 ppm; HRMS (ESI-TOF) m/z : $[\text{M} + \text{H}]^+$ calcd for $\text{C}_{22}\text{H}_{16}\text{NO}_2$ 326.1181; found: 326.1185.

2-(4-(Trifluoromethoxy)phenyl)benzofuro[3,2-*c*]quinoline (4d). A mixture of substrate 3a (0.150 g, 0.396 mmol), 4-(trifluoromethoxy)phenylboronic acid (0.090 g, 0.435 mmol), $\text{Pd}(\text{OAc})_2$ (1.8 mg, 2 mol %), and anhydrous K_2CO_3 (0.109 g, 0.79 mmol) in anhydrous NMP (0.6 mL, 1.5 mL mmol^{-1}) was reacted according to the general one-pot SM/DA procedure above to give the title product as a yellow solid; yield: 105 mg (70%); m.p. 148–150 °C; IR (NaCl) ν 3583, 1504, 1459, 1283, 1210, 1191, 1165 cm^{-1} ; ^1H NMR (300 MHz, CDCl_3) δ : 7.37 (dd, J = 8.8, 0.9 Hz, 2H), 7.43–7.62 (m, 2H), 7.72–7.86 (m, 3H), 7.97 (dd, J = 8.8, 2.1 Hz, 1H), 8.09 (dd, J = 7.6, 0.8 Hz, 1H), 8.31 (d, J = 8.8 Hz, 1H), 8.54 (d, J = 2.0 Hz, 1H), 9.47 (s, 1H) ppm; $^{13}\text{C}\{^1\text{H}\}$ NMR (75 MHz, CDCl_3) δ : 112.1, 116.8, 117.4, 118.6, 120.5 (q, $^1J_{\text{C(F)}} = 257$ Hz), 120.7, 121.4, 122.6, 124.2, 127.4, 128.5, 128.9, 130.5, 138.3, 138.9, 144.5, 146.7, 149.2 (q, $^3J_{\text{C(F)}} = 2$ Hz), 156.0, 157.5 ppm; $^{19}\text{F}\{^1\text{H}\}$ NMR (282 MHz, CDCl_3) δ : –58 ppm; HRMS (ESI-TOF) m/z : $[\text{M} + \text{H}]^+$ calcd for $\text{C}_{22}\text{H}_{13}\text{F}_3\text{NO}_2$ 380.0898; found: 380.0889.

2-(4-Fluorophenyl)benzofuro[3,2-*c*]quinoline (4e). A mixture of substrate 3a (0.150 g, 0.396 mmol), 4-fluorophenylboronic acid (0.061 g, 0.435 mmol), $\text{Pd}(\text{OAc})_2$ (1.8 mg, 2 mol %), and anhydrous K_2CO_3 (0.109 g, 0.79 mmol) in anhydrous NMP (0.6 mL, 1.5 mL mmol^{-1}) was reacted according to the general one-pot SM/DA procedure above to give the title product as a pale yellow solid; yield: 95 mg (77%); m.p. 185–186 °C; IR (NaCl) ν 3391, 1561, 1460, 1334, 1192, 1123 cm^{-1} ; ^1H NMR (300 MHz, CDCl_3) δ : 7.16–7.29 (m, 2H), 7.46–7.62 (m, 2H), 7.72–7.83 (m, 3H), 8.00 (dd, J = 8.8, 2.1 Hz, 1H), 8.13 (dd, J = 7.2, 1.3 Hz, 1H), 8.33 (d, J = 8.8 Hz, 1H), 8.57 (d, J = 2.0 Hz, 1H), 9.50 (s, 1H) ppm; $^{13}\text{C}\{^1\text{H}\}$ NMR (75 MHz, CDCl_3) δ : 112.1, 115.9 (d, $^2J_{\text{C(F)}} = 22$ Hz), 116.7, 117.4, 118.2, 120.7, 122.7, 124.1, 127.3, 128.6, 129.1 (d, $^3J_{\text{C(F)}} = 8$ Hz), 130.4, 136.2, 138.7, 144.3, 146.6, 156.0, 157.5, 162.9 (d, $^1J_{\text{C(F)}} = 247$ Hz) ppm; $^{19}\text{F}\{^1\text{H}\}$ NMR (282 MHz, CDCl_3) δ : –115 ppm; HRMS (ESI-TOF) m/z : $[\text{M} + \text{H}]^+$ calcd for $\text{C}_{21}\text{H}_{13}\text{FNO}$ 314.0981; found: 314.0971.

2-(4-Chlorophenyl)benzofuro[3,2-*c*]quinoline (4f). A mixture of substrate 3a (0.150 g, 0.396 mmol), 4-chlorophenylboronic acid (0.068 g, 0.435 mmol), $\text{Pd}(\text{OAc})_2$ (1.8 mg, 2 mol %), and anhydrous K_2CO_3 (0.109 g, 0.79 mmol) in anhydrous NMP (0.6 mL, 1.5 mL mmol^{-1}) was reacted according to the general one-pot SM/DA procedure above to give the title product as a pale yellow solid; yield: 106 mg (81%); m.p. 191–192 °C; IR (NaCl) ν 3389, 1556, 1458, 1356, 1191, 821 cm^{-1} ; ^1H NMR (300 MHz, CDCl_3) δ : 7.38–7.57 (m, 4H), 7.61–7.75 (m, 3H), 7.89 (dd, J = 8.8, 2.1 Hz, 1H), 8.02 (dd, J = 7.6, 0.8 Hz, 1H), 8.24 (d, J = 8.8 Hz, 1H), 8.43 (d, J = 2.0 Hz, 1H), 9.39 (s, 1H) ppm; $^{13}\text{C}\{^1\text{H}\}$ NMR (75 MHz, CDCl_3) δ : 112.1, 116.7, 117.3, 118.2, 120.7, 122.6, 124.1, 127.3, 128.3, 128.6, 129.1, 130.4, 134.1, 138.3, 138.5, 144.4, 146.7, 155.9, 157.4 ppm; HRMS

(ESI-TOF) m/z : $[M + H]^+$ calcd for $C_{21}H_{13}ClNO$ 330.0680; found: 330.0676.

2-(4-(Trifluoromethyl)phenyl)benzofuro[3,2-*c*]quinoline (4g). A mixture of substrate **3a** (0.150 g, 0.396 mmol), (4-(trifluoromethyl)phenyl)boronic acid (0.083 g, 0.435 mmol), $Pd(OAc)_2$ (1.8 mg, 2 mol %), and anhydrous K_2CO_3 (0.109 g, 0.79 mmol) in anhydrous NMP (0.6 mL, 1.5 mL $mmol^{-1}$) was reacted according to the general one-pot SM/DA procedure above to give the title product as a pale yellow solid; yield: 114 mg (80%); m.p. 194–195 °C; IR (NaCl): ν 3384, 1614, 1460, 1331, 1189, 1116 cm^{-1} ; 1H NMR (300 MHz, $CDCl_3$) δ : 7.46–7.63 (m, 2H), 7.74–7.85 (m, 3H), 7.93 (d, J = 8.2 Hz, 2H), 8.04 (dd, J = 8.8, 2.1 Hz, 1H), 8.13 (d, J = 7.4 Hz, 1H), 8.37 (d, J = 8.8 Hz, 1H), 8.65 (d, J = 1.9 Hz, 1H), 9.53 (s, 1H) ppm; $^{13}C\{^1H\}$ NMR (75 MHz, $CDCl_3$) δ : 112.1, 116.8, 117.3, 119.0, 120.7, 122.6, 124.22, 124.23 (q, $^1J_{C,F}$ = 270 Hz), 125.9 (q, $^3J_{C,F}$ = 4 Hz), 127.5, 127.7, 128.4, 130.0 (q, $^2J_{C,F}$ = 33 Hz), 130.6, 138.1, 143.6, 144.8, 146.9, 156.0, 157.5 ppm; $^{19}F\{^1H\}$ NMR (282 MHz, $CDCl_3$) δ : –62 ppm; HRMS (ESI-TOF) m/z : $[M + H]^+$ calcd for $C_{22}H_{13}F_3NO$ 364.0949; found: 364.0938.

2-(3-(Trifluoromethyl)phenyl)benzofuro[3,2-*c*]quinoline (4h). A mixture of substrate **3a** (0.150 g, 0.396 mmol), (3-(trifluoromethyl)phenyl)boronic acid (0.083 g, 0.435 mmol), $Pd(OAc)_2$ (1.8 mg, 2 mol %), and anhydrous K_2CO_3 (0.109 g, 0.79 mmol) in anhydrous NMP (0.6 mL, 1.5 mL $mmol^{-1}$) was reacted according to the general one-pot SM/DA procedure above to give the title product as a pale yellow solid; yield: 104 mg (72%); m.p. 171–173 °C; IR (NaCl): ν 3391, 1561, 1446, 1334, 1166, 1123 cm^{-1} ; 1H NMR (300 MHz, $CDCl_3$) δ : 7.45–7.73 (m, 4H), 7.79 (d, J = 7.9 Hz, 1H), 7.95–8.09 (m, 3H), 8.13 (dd, J = 7.6, 0.8 Hz, 1H), 8.37 (d, J = 8.8 Hz, 1H), 8.63 (d, J = 2.0 Hz, 1H), 9.52 (s, 1H) ppm; $^{13}C\{^1H\}$ NMR (75 MHz, $CDCl_3$) δ : 112.1, 116.8, 117.3, 118.7, 120.7, 122.6, 124.19, 124.20 (q, $^1J_{C,F}$ = 273 Hz), 124.3 (q, $^3J_{C,F}$ = 4 Hz), 124.6 (q, $^3J_{C,F}$ = 4 Hz), 127.5, 128.4, 129.5, 130.6, 130.7, 131.5 (q, $^2J_{C,F}$ = 32 Hz), 138.1, 140.9, 144.7, 146.8, 156.0, 157.5 ppm; $^{19}F\{^1H\}$ NMR (282 MHz, $CDCl_3$) δ : –62 ppm; HRMS (ESI-TOF) m/z : $[M + H]^+$ calcd for $C_{22}H_{13}F_3NO$ 364.0944; found: 364.0947.

Ethyl 4-(Benzofuro[3,2-*c*]quinolin-2-yl)benzoate (4i). A mixture of substrate **3a** (0.150 g, 0.396 mmol), 4-ethoxycarbonylphenylboronic acid (0.084 g, 0.435 mmol), $Pd(OAc)_2$ (1.8 mg, 2 mol %), and anhydrous K_2CO_3 (0.109 g, 0.79 mmol) in anhydrous NMP (0.6 mL, 1.5 mL $mmol^{-1}$) was reacted according to the general one-pot SM/DA procedure above to give the title product as a beige solid; yield: 105 mg (70%); m.p. 160–161 °C; IR (NaCl): ν 2922, 1715, 1607, 1460, 1357, 1278, 1190 cm^{-1} ; 1H NMR (300 MHz, $CDCl_3$) δ : 1.45 (t, J = 7.1 Hz, 3H), 4.44 (q, J = 7.1 Hz, 2H), 7.43–7.63 (m, 2H), 7.79 (d, J = 7.9 Hz, 1H), 7.84–7.95 (m, 2H), 8.02–8.28 (m, 4H), 8.36 (d, J = 8.8 Hz, 1H), 8.67 (d, J = 1.7 Hz, 1H), 9.52 (s, 1H) ppm; $^{13}C\{^1H\}$ NMR (75 MHz, $CDCl_3$) δ : 14.4, 61.1, 112.1, 116.7, 117.2, 118.8, 120.7, 122.5, 124.1, 127.3, 127.4, 128.8, 129.8, 130.2, 130.5, 138.3, 144.2, 144.6, 146.9, 155.9, 157.4, 166.4 ppm; HRMS (ESI-TOF) m/z : $[M + H]^+$ calcd for $C_{24}H_{18}NO_3$ 368.1281; found: 368.1282.

4-(Benzofuro[3,2-*c*]quinolin-2-yl)phenyl)methanone (4j). A mixture of substrate **3a** (0.150 g, 0.396 mmol), (4-benzoylphenyl)boronic acid (0.098 g, 0.435 mmol), $Pd(OAc)_2$ (1.8 mg, 2 mol %), and anhydrous K_2CO_3 (0.109 g, 0.79 mmol) in anhydrous NMP (0.6 mL, 1.5 mL $mmol^{-1}$) was reacted according to the general one-pot SM/DA procedure above to give the title product as a pale yellow solid; yield: 94 mg (59%); m.p. 184–187 °C; IR (NaCl): ν 3401, 1652, 1602, 1460, 1357, 1190 cm^{-1} ; 1H NMR (300 MHz, $CDCl_3$) δ : 7.46–7.70 (m, 5H), 7.79 (d, J = 8.3 Hz, 1H), 7.84–8.04 (m, 6H), 8.05–8.20 (m, 2H), 8.38 (d, J = 8.8 Hz, 1H), 8.71 (d, J = 1.9 Hz, 1H), 9.53 (s, 1H) ppm; $^{13}C\{^1H\}$ NMR (75 MHz, $CDCl_3$) δ : 112.1, 116.8, 117.4, 119.0, 120.7, 122.6, 124.2, 127.3, 127.5, 128.4, 128.5, 130.0, 130.6, 130.9, 132.5, 136.8, 137.6, 138.4, 144.0, 144.7, 146.9, 156.0, 157.5, 196.2 ppm; HRMS (ESI-TOF) m/z : $[M + H]^+$ calcd for $C_{28}H_{18}NO_2$ 400.1332; found: 400.1331.

2-(3-Nitrophenyl)benzofuro[3,2-*c*]quinoline (4k). A mixture of substrate **3a** (0.150 g, 0.396 mmol), 3-nitrophenylboronic acid (0.072 g, 0.435 mmol), $Pd(OAc)_2$ (1.8 mg, 2 mol %), and anhydrous K_2CO_3 (0.109 g, 0.79 mmol) in anhydrous NMP (0.6 mL, 1.5 mL $mmol^{-1}$)

was reacted according to the general one-pot SM/DA procedure above to give the title product as a yellow solid; yield: 69 mg (51%); m.p. 227–228 °C; IR (NaCl): ν 3392, 1529, 1460, 1348, 1321, 1191 cm^{-1} ; 1H NMR (300 MHz, $CDCl_3$) δ : 7.47–7.64 (m, 2H), 7.72 (t, J = 8.0 Hz, 1H), 7.80 (d, J = 8.0 Hz, 1H), 8.06 (dd, J = 8.8, 2.2 Hz, 1H), 8.10–8.19 (m, 2H), 8.30 (ddd, J = 8.2, 2.2, 1.0 Hz, 1H), 8.40 (d, J = 8.8 Hz, 1H), 8.65–8.73 (m, 2H), 9.55 (s, 1H) ppm; $^{13}C\{^1H\}$ NMR (75 MHz, $CDCl_3$) δ : 112.2, 117.0, 117.4, 119.1, 120.8, 122.3, 122.5, 122.6, 124.3, 127.6, 128.2, 130.0, 131.0, 133.3, 137.1, 141.9, 145.1, 147.0, 148.9, 156.1, 157.5 ppm; HRMS (ESI-TOF) m/z : $[M + H]^+$ calcd for $C_{21}H_{13}N_2O_3$ 341.0921; found: 341.0919.

8-Chloro-2-phenylbenzofuro[3,2-*c*]quinoline (4l). A mixture of substrate **3c** (0.200 g, 0.60 mmol), phenylboronic acid (0.080 g, 0.658 mmol), $Pd(OAc)_2$ (2.7 mg, 2 mol %), and anhydrous K_2CO_3 (0.165 g, 1.20 mmol) in anhydrous NMP (0.9 mL, 1.5 mL $mmol^{-1}$) was reacted according to the general one-pot SM/DA procedure above to give the title product as a pale yellow solid; yield: 118 mg (60%); m.p. 213–214 °C; IR (NaCl): ν 3583, 1461, 1359, 1192, 665 cm^{-1} ; 1H NMR (300 MHz, $CDCl_3$) δ : 7.38–7.60 (m, 4H), 7.66 (d, J = 8.8 Hz, 1H), 7.75–7.87 (m, 2H), 7.99–8.12 (m, 2H), 8.31 (d, J = 8.8 Hz, 1H), 8.55 (d, J = 1.8 Hz, 1H), 9.41 (s, 1H) ppm; $^{13}C\{^1H\}$ NMR (75 MHz, $CDCl_3$) δ : 113.1, 115.8, 117.2, 118.4, 120.5, 124.2, 127.4, 127.5, 128.1, 129.1, 129.3, 129.9, 130.4, 140.0, 140.1, 144.0, 147.0, 154.3, 158.4 ppm; HRMS (ESI-TOF) m/z : $[M + H]^+$ calcd for $C_{21}H_{13}ClNO$ 330.0681; found: 330.0684.

6-Phenylbenzofuro[3,2-*c*]pyridine (4m). A mixture of substrate **3d** (0.150 g, 0.456 mmol), phenylboronic acid (0.061 g, 0.50 mmol), $Pd(OAc)_2$ (2.0 mg, 2 mol %), and anhydrous K_2CO_3 (0.126 g, 0.912 mmol) in anhydrous NMP (0.7 mL, 1.5 mL $mmol^{-1}$) was reacted according to the general one-pot SM/DA procedure above and purified via column chromatography using 100% Et_2O as an eluent to give the title product as a pale yellow solid; yield: 77 mg (69%); m.p. 66–68 °C; IR (NaCl): ν 3402, 3032, 1577, 1450, 1332, 1168 cm^{-1} ; 1H NMR (300 MHz, $CDCl_3$) δ : 7.35–7.63 (m, 5H), 7.67 (dd, J = 7.6, 1.3 Hz, 1H), 7.83–7.92 (m, 2H), 8.01 (dd, J = 7.7, 1.3 Hz, 1H), 8.67 (d, J = 5.7 Hz, 1H), 9.30 (s, 1H) ppm; $^{13}C\{^1H\}$ NMR (75 MHz, $CDCl_3$) δ : 107.6, 120.1, 121.6, 122.4, 124.4, 126.4, 128.07, 128.13, 128.77, 128.80, 135.8, 143.7, 147.5, 153.1, 160.9 ppm; HRMS (ESI-TOF) m/z : $[M + H]^+$ calcd for $C_{17}H_{12}NO$ 246.0913; found: 246.0914. Note: Here, a second Suzuki–Miyaura reaction occurred in competition with the direct arylation. These products were separable by careful column chromatography.

3-Phenylbenzofuro[3,2-*c*]quinoline (4n). A mixture of substrate **3b** (0.200 g, 0.528 mmol), phenylboronic acid (0.071 g, 0.58 mmol), $Pd(OAc)_2$ (2.4 mg, 2 mol %), and anhydrous K_2CO_3 (0.146 g, 1.06 mmol) in anhydrous NMP (0.8 mL, 1.5 mL $mmol^{-1}$) was reacted according to the general one-pot SM/DA procedure above to give the title product as a pale yellow solid; X-ray quality crystals were obtained via vapor diffusion from a saturated solution of toluene in hexane, the CCDC number is 1967484; yield: 146 mg (95%); m.p. 172–173 °C; IR (NaCl): ν 3275, 1559, 1452, 1379, 1188 cm^{-1} ; 1H NMR (300 MHz, $CDCl_3$) δ : 7.37–7.64 (m, 5H), 7.72–7.88 (m, 3H), 7.98 (dd, J = 8.5, 1.7 Hz, 1H), 8.12 (dd, J = 7.5, 1.0 Hz, 1H), 8.42–8.59 (m, 2H), 9.54 (s, 1H) ppm; $^{13}C\{^1H\}$ NMR (75 MHz, $CDCl_3$) δ : 112.2, 116.1, 116.4, 120.6, 121.3, 122.8, 124.1, 126.6, 127.3, 127.5, 127.6, 128.0, 129.1, 140.2, 142.2, 144.9, 147.8, 156.1, 157.5 ppm; HRMS (ESI-TOF) m/z : $[M + H]^+$ calcd for $C_{21}H_{14}NO$ 296.1070; found: 296.1072.

3-(*p*-Tolyl)benzofuro[3,2-*c*]quinoline (4o). A mixture of substrate **3b** (0.150 g, 0.396 mmol), *o*-tolylboronic acid (0.059 g, 0.435 mmol), $Pd(OAc)_2$ (1.8 mg, 2 mol %), and anhydrous K_2CO_3 (0.109 g, 0.79 mmol) in anhydrous NMP (0.6 mL, 1.5 mL $mmol^{-1}$) was reacted according to the general one-pot SM/DA procedure above to give the title product as a white solid; yield: 90 mg (74%); m.p. 200–202 °C; IR (NaCl): ν 3150, 1554, 1450, 1379, 1190 cm^{-1} ; 1H NMR (300 MHz, $CDCl_3$) δ : 2.45 (s, 3H), 7.34 (d, J = 7.9 Hz, 2H), 7.44–7.60 (m, 2H), 7.66–7.81 (m, 3H), 7.97 (dd, J = 8.5, 1.5 Hz, 1H), 8.11 (dd, J = 7.6, 0.9 Hz, 1H), 8.42–8.52 (m, 2H), 9.51 (s, 1H) ppm; $^{13}C\{^1H\}$ NMR (75 MHz, $CDCl_3$) δ : 21.2, 112.1, 115.9, 116.2, 120.5, 121.1, 122.7, 124.0, 126.4, 127.1, 127.2, 127.3, 129.8, 137.3, 137.9, 142.0,

144.7, 147.9, 156.0, 157.4 ppm; HRMS (ESI-TOF) m/z : $[M + H]^+$ calcd for $C_{22}H_{16}NO$ 310.1232; found: 310.1244.

3-(4-(Trifluoromethyl)phenyl)benzofuro[3,2-*c*]quinoline (4p). A mixture of substrate **3b** (0.150 g, 0.396 mmol), (4-(trifluoromethyl)phenyl)boronic acid (0.083 g, 0.435 mmol), $Pd(OAc)_2$ (1.8 mg, 2 mol %), and anhydrous K_2CO_3 (0.109 g, 0.79 mmol) in anhydrous NMP (0.6 mL, 1.5 mL $mmol^{-1}$) was reacted according to the general one-pot SM/DA procedure above to give the title product as a yellow solid; yield: 114 mg (79%); m.p. 205–208 °C; IR (NaCl): ν 3251, 1559, 1450, 1329, 1188, 1110 cm^{-1} ; 1H NMR (300 MHz, $CDCl_3$) δ : 7.46–7.63 (m, 2H), 7.76–7.82 (m, 3H), 7.86–8.02 (m, 3H), 8.13 (dd, J = 7.6, 0.9 Hz, 1H), 8.49–8.57 (m, 2H), 9.55 (s, 1H) ppm; $^{13}C\{^1H\}$ NMR (75 MHz, $CDCl_3$) δ : 112.2, 116.7, 120.7, 121.6, 122.6, 124.21, 124.22 (q , $^1J_{C,F}$ = 270 Hz), 126.0 (q , $^3J_{C,F}$ = 4 Hz), 126.2, 127.5, 127.7, 128.2, 129.9 (q , $^2J_{C,F}$ = 32 Hz), 140.4, 143.7, 145.1, 147.6, 156.1, 157.3 ppm; $^{19}F\{^1H\}$ NMR (282 MHz, $CDCl_3$) δ : –62 ppm; HRMS (ESI-TOF) m/z : $[M + H]^+$ calcd for $C_{22}H_{13}F_3NO$ 364.0949; found: 364.0951. Note: ^{13}C NMR shift at 116.7 ppm represents two individual carbon signals as confirmed by 2D NMR experiments.

4-(Benzofuro[3,2-*c*]quinolin-3-yl)benzonitrile (4q). A mixture of substrate **3b** (0.150 g, 0.396 mmol), 4-cyanophenylboronic acid (0.065 g, 0.435 mmol), $Pd(OAc)_2$ (4.4 mg, 5 mol %), and anhydrous K_2CO_3 (0.109 g, 0.79 mmol) in anhydrous NMP (0.6 mL, 1.5 mL $mmol^{-1}$) was reacted according to the general one-pot SM/DA procedure above to give the title product as a white solid; yield: 85 mg (67%); m.p. >250 °C; IR (NaCl): ν 3348, 2223, 1553, 1447, 1344, 1184 cm^{-1} ; 1H NMR (300 MHz, $CDCl_3$) δ : 7.45–7.64 (m, 2H), 7.73–7.80 (m, 6H), 8.13 (dd, J = 7.6, 0.8 Hz, 1H), 8.45–8.60 (m, 2H), 9.55 (s, 1H) ppm; $^{13}C\{^1H\}$ NMR (75 MHz, $CDCl_3$) δ : 111.7, 112.3, 116.9, 117.0, 118.8, 120.8, 121.9, 122.6, 124.3, 126.0, 127.6, 128.1, 128.4, 132.9, 139.9, 144.7, 145.3, 147.5, 156.2, 157.2 ppm; HRMS (ESI-TOF) m/z : $[M + H]^+$ calcd for $C_{22}H_{13}N_2O$: 321.1028; found: 321.1033.

3-(4-Methoxyphenyl)benzofuro[3,2-*c*]quinoline (4r). A mixture of substrate **3b** (0.150 g, 0.396 mmol), 4-methoxyphenylboronic acid (0.066 g, 0.435 mmol), $Pd(OAc)_2$ (1.8 mg, 2 mol %), and anhydrous K_2CO_3 (0.109 g, 0.79 mmol) in anhydrous NMP (0.6 mL, 1.5 mL $mmol^{-1}$) was reacted according to the general one-pot SM/DA procedure above to give the title product as a white solid; yield: 88 mg (70%); m.p. 157–158 °C; IR (NaCl): ν 3369, 2998, 1607, 1450, 1303, 1245, 1188 cm^{-1} ; 1H NMR (300 MHz, $CDCl_3$) δ : 3.88 (s, 3H), 6.99–7.10 (m, 2H), 7.41–7.57 (m, 2H), 7.68–7.77 (m, 3H), 7.91 (dd, J = 8.6, 1.7 Hz, 1H), 8.07 (dd, J = 7.5, 1.5 Hz, 1H), 8.37–8.45 (m, 2H), 9.47 (s, 1H) ppm; $^{13}C\{^1H\}$ NMR (75 MHz, $CDCl_3$) δ : 55.4, 112.1, 114.5, 115.7, 116.1, 120.5, 121.2, 122.8, 124.1, 126.3, 126.8, 127.1, 128.5, 132.7, 141.7, 144.8, 148.0, 156.0, 157.5, 159.8 ppm; HRMS (ESI-TOF) m/z : $[M + H]^+$ calcd for $C_{22}H_{16}NO_2$ 326.1176; found: 326.1173.

General Procedure for Palladium-Catalyzed One-Pot Mizoroki–Heck and Intramolecular Direct Arylation Reactions. A mixture of the 4-(2-bromophenoxy)quinoline substrate (1 equiv), Heck coupling partner (1.1 equiv), $Pd(OAc)_2$ (2 mol % for *tert*-butyl acrylate or 5 mol % for styrene derivatives), and anhydrous K_2CO_3 (2 equiv) in anhydrous NMP (1.5 mL $mmol^{-1}$) was stirred at 135 °C in a sealed reaction tube in an aluminum multireaction heating mantle until the reaction was completed as evidenced by 1H NMR analysis (18–24 h). The cooled reaction mixture was diluted with DCM, filtered through a short plug of Celite, and concentrated in vacuo. The crude mixture was purified by column chromatography over silica gel using DCM/EtOAc (99:1–95:5) as an eluent.

***tert*-Butyl (E)-3-(Benzofuro[3,2-*c*]quinolin-2-yl)acrylate (5a).** A mixture of substrate **3a** (0.050 g, 0.132 mmol), *tert*-butyl acrylate (21 μ L, 0.145 mmol), $Pd(OAc)_2$ (0.6 mg, 2 mol %), and anhydrous K_2CO_3 (0.036 g, 0.264 mmol) in anhydrous NMP (0.2 mL, 1.5 mL $mmol^{-1}$) was reacted according to the general one-pot MH/DA procedure above to give the title product as a white solid; yield: 27 mg (60%); m.p. 169–170 °C; IR (NaCl): ν 3393, 2976, 1701, 1560, 1460, 1366, 1238, 1151 cm^{-1} ; 1H NMR (300 MHz, $CDCl_3$) δ : 1.58 (s, 9H), 6.60 (d, J = 16.0 Hz, 1H), 7.44–7.65 (m, 2H), 7.73–7.89

(m, 2H), 7.94 (dd, J = 8.9, 2.0 Hz, 1H), 8.11 (dd, J = 7.6, 0.8 Hz, 1H), 8.24 (d, J = 8.8 Hz, 1H), 8.51 (d, J = 1.9 Hz, 1H), 9.49 (s, 1H) ppm; $^{13}C\{^1H\}$ NMR (100 MHz, $CDCl_3$) δ : 28.2, 80.9, 112.3, 117.0, 117.3, 120.8, 121.6, 122.0, 122.5, 124.3, 127.4, 127.6, 130.5, 133.4, 142.5, 145.1, 147.9, 156.1, 157.5, 166.1 ppm; HRMS (ESI-TOF) m/z : $[M + H]^+$ calcd for $C_{22}H_{20}NO_3$: 346.1438; found: 346.1434.

***tert*-Butyl (E)-3-(Benzofuro[3,2-*c*]quinolin-3-yl)acrylate (5b).** A mixture of substrate **3b** (0.050 g, 0.132 mmol), *tert*-butyl acrylate (21 μ L, 0.145 mmol), $Pd(OAc)_2$ (0.6 mg, 2 mol %), and anhydrous K_2CO_3 (0.036 g, 0.264 mmol) in anhydrous NMP (0.2 mL, 1.5 mL $mmol^{-1}$) was reacted according to the general one-pot MH/DA procedure above to give the title product as a pale yellow solid; X-ray quality crystals were obtained via vapor diffusion from a saturated solution of toluene in hexane, the CCDC number is 1967537; yield: 36 mg (80%); m.p. 160–162 °C; IR (NaCl): ν 3393, 2976, 1703, 1560, 1452, 1366, 1285, 1149 cm^{-1} ; 1H NMR (300 MHz, $CDCl_3$) δ : 1.58 (s, 9H), 6.59 (d, J = 16.0 Hz, 1H), 7.44–7.63 (m, 2H), 7.71–7.92 (m, 3H), 8.11 (dd, J = 7.6, 0.8 Hz, 1H), 8.30–8.46 (m, 2H), 9.51 (s, 1H) ppm; $^{13}C\{^1H\}$ NMR (75 MHz, $CDCl_3$) δ : 28.2, 80.8, 112.2, 117.1, 117.7, 120.8, 121.4, 122.0, 122.5, 124.3, 125.1, 127.6, 130.7, 135.6, 142.8, 145.2, 147.4, 156.2, 157.1, 166.0 ppm; HRMS (ESI-TOF) m/z : $[M + H]^+$ calcd for $C_{22}H_{20}NO_3$: 346.1438; found: 346.1432.

(E)-2-Styrylbenzofuro[3,2-*c*]quinoline (5c). A mixture of substrate **3a** (0.114 g, 0.30 mmol), styrene (38 μ L, 0.33 mmol), $Pd(OAc)_2$ (3.4 mg, 5 mol %), and anhydrous K_2CO_3 (0.083 g, 0.60 mmol) in anhydrous NMP (0.5 mL, 1.5 mL $mmol^{-1}$) was reacted according to the general one-pot MH/DA procedure above to give the title product as a white solid; yield: 70 mg (73%); m.p. 201–202 °C; IR (NaCl): ν 3379, 1662, 1561, 1377, 1188 cm^{-1} ; 1H NMR (300 MHz, $CDCl_3$) δ : 7.22–7.66 (m, 9H), 7.76 (d, J = 8.1 Hz, 1H), 7.98 (dd, J = 8.9, 2.0 Hz, 1H), 8.07 (dd, J = 7.6, 0.8 Hz, 1H), 8.22 (d, J = 8.9 Hz, 1H), 8.39 (d, J = 1.8 Hz, 1H), 9.41 (s, 1H) ppm; $^{13}C\{^1H\}$ NMR (75 MHz, $CDCl_3$) δ : 112.1, 116.7, 117.4, 118.6, 120.7, 122.7, 124.1, 126.8, 127.2, 127.3, 127.8, 128.1, 128.8, 130.1, 130.6, 136.1, 137.0, 143.9, 147.0, 156.0, 157.4 ppm; HRMS (ESI-TOF) m/z : $[M + H]^+$ calcd for $C_{23}H_{16}NO$ 322.1226; found: 322.1223.

(E)-2-(4-Methoxystyryl)benzofuro[3,2-*c*]quinoline (5d). A mixture of substrate **3a** (0.114 g, 0.30 mmol), 4-methoxystyrene (44 μ L, 0.33 mmol), $Pd(OAc)_2$ (3.4 mg, 5 mol %), and anhydrous K_2CO_3 (0.083 g, 0.60 mmol) in anhydrous NMP (0.5 mL, 1.5 mL $mmol^{-1}$) was reacted according to the general one-pot MH/DA procedure above to give the title product as a white solid; yield: 86 mg (82%); m.p. 190–192 °C; IR (NaCl): ν 3388, 1656, 1602, 1562, 1346, 1250, 1110 cm^{-1} ; 1H NMR (300 MHz, $CDCl_3$) δ : 3.86 (s, 3H), 6.84–7.04 (m, 2H), 7.12–7.38 (m, 2H), 7.40–7.65 (m, 4H), 7.76 (d, J = 8.1 Hz, 1H), 7.97 (dd, J = 8.9, 1.8 Hz, 1H), 8.09 (d, J = 7.4 Hz, 1H), 8.21 (d, J = 8.9 Hz, 1H), 8.38 (d, J = 1.7 Hz, 1H), 9.41 (s, 1H) ppm; $^{13}C\{^1H\}$ NMR (75 MHz, $CDCl_3$) δ : 55.4, 112.1, 114.3, 116.7, 117.5, 118.1, 120.7, 122.8, 124.1, 125.7, 127.2, 127.3, 128.0, 129.8, 130.1, 130.2, 136.5, 143.7, 146.9, 156.0, 157.4, 159.7 ppm; HRMS (ESI-TOF) m/z : $[M + H]^+$ calcd for $C_{24}H_{18}NO_2$ 352.1332; found: 352.1328.

(E)-2-(4-Fluorostyryl)benzofuro[3,2-*c*]quinoline (5e). A mixture of substrate **3a** (0.114 g, 0.30 mmol), 4-fluorostyrene (39 μ L, 0.33 mmol), $Pd(OAc)_2$ (3.4 mg, 5 mol %), and anhydrous K_2CO_3 (0.083 g, 0.60 mmol) in anhydrous NMP (0.5 mL, 1.5 mL $mmol^{-1}$) was reacted according to the general one-pot MH/DA procedure above to give the title product as a yellow solid; yield: 82 mg (80%); m.p. 189–191 °C; IR (NaCl): ν 3404, 1676, 1598, 1559, 1346, 1234, 1096 cm^{-1} ; 1H NMR (300 MHz, $CDCl_3$) δ : 7.00–7.15 (m, 2H), 7.17–7.34 (m, 2H), 7.41–7.63 (m, 4H), 7.75 (d, J = 8.1 Hz, 1H), 7.95 (dd, J = 8.9, 2.0 Hz, 1H), 8.07 (d, J = 7.5 Hz, 1H), 8.21 (d, J = 8.9 Hz, 1H), 8.37 (d, J = 1.8 Hz, 1H), 9.41 (s, 1H) ppm; $^{13}C\{^1H\}$ NMR (75 MHz, $CDCl_3$) δ : 112.1, 115.8 (d, $^2J_{C,F}$ = 22 Hz), 116.7, 117.4, 118.6, 120.7, 122.7, 124.1, 127.1, 127.3, 127.6 (d, $^6J_{C,F}$ = 2 Hz), 128.3 (d, $^3J_{C,F}$ = 8 Hz), 129.4, 130.2, 133.2 (d, $^4J_{C,F}$ = 3 Hz), 135.9, 144.0, 147.0, 156.0, 157.4, 162.6 (d, $^1J_{C,F}$ = 248 Hz) ppm; $^{19}F\{^1H\}$ NMR (282 MHz, $CDCl_3$) δ : –113 ppm; HRMS (ESI-TOF) m/z : $[M + H]^+$ calcd for $C_{23}H_{15}FNO$ 340.1132; found: 340.1135.

(*E*)-3-Styrylbenzofuro[3,2-*c*]quinoline (**5f**). A mixture of substrate **3b** (0.114 g, 0.30 mmol), styrene (38 μ L, 0.33 mmol), Pd(OAc)₂ (3.4 mg, 5 mol %), and anhydrous K₂CO₃ (0.083 g, 0.60 mmol) in anhydrous NMP (0.5 mL, 1.5 mL mmol⁻¹) was reacted according to the general one-pot MH/DA procedure above to give the title product as a yellow solid; yield: 72 mg (75%); m.p. 179–182 °C; IR (NaCl) ν 3583, 1656, 1632, 1561, 1348, 1190 cm⁻¹; ¹H NMR (300 MHz, CDCl₃) δ : 7.20–7.65 (m, 9H), 7.74 (d, *J* = 7.9 Hz, 1H), 7.91 (dd, *J* = 8.6, 1.5 Hz, 1H), 8.07 (dd, *J* = 7.5, 0.9 Hz, 1H), 8.27 (d, *J* = 1.3 Hz, 1H), 8.36 (d, *J* = 8.6 Hz, 1H), 9.46 (s, 1H) ppm; ¹³C{¹H} NMR (75 MHz, CDCl₃) δ : 112.1, 116.3, 120.6, 121.1, 122.7, 124.1, 124.9, 126.8, 127.2, 128.0, 128.1, 128.8, 130.7, 137.0, 138.5, 144.8, 147.9, 156.1, 157.4 ppm; HRMS (ESI-TOF) *m/z*: [M + H]⁺ calcd for C₂₃H₁₆NO 322.1226; found: 322.1227. Note: ¹³C NMR shifts at 116.3 and 128.1 ppm represent two individual carbon signals as confirmed by 2D NMR experiments.

(*E*)-3-(4-Methoxystyryl)benzofuro[3,2-*c*]quinoline (**5g**). A mixture of substrate **3b** (0.114 g, 0.30 mmol), 4-methoxystyrene (44 μ L, 0.33 mmol), Pd(OAc)₂ (3.4 mg, 5 mol %), and anhydrous K₂CO₃ (0.083 g, 0.60 mmol) in anhydrous NMP (0.5 mL, 1.5 mL mmol⁻¹) was reacted according to the general one-pot MH/DA procedure above to give the title product as a yellow solid; yield: 84 mg (80%); m.p. 168–170 °C; IR (NaCl) ν 3379, 1687, 1603, 1560, 1347, 1176, 1033 cm⁻¹; ¹H NMR (300 MHz, CDCl₃) δ : 3.86 (s, 3H), 6.89–7.00 (m, 2H), 7.13–7.39 (m, 2H), 7.42–7.65 (m, 4H), 7.75 (d, *J* = 7.8 Hz, 1H), 7.92 (dd, *J* = 8.6, 1.5 Hz, 1H), 8.09 (dd, *J* = 7.2, 1.3 Hz, 1H), 8.27 (d, *J* = 1.2 Hz, 1H), 8.38 (d, *J* = 8.6 Hz, 1H), 9.47 (s, 1H) ppm; ¹³C{¹H} NMR (75 MHz, CDCl₃) δ : 55.4, 112.1, 114.3, 116.0, 116.2, 120.5, 121.0, 122.8, 124.1, 124.8, 126.0, 127.1, 127.5, 128.1, 129.8, 130.3, 138.9, 144.7, 148.0, 156.0, 157.4, 159.7 ppm; HRMS (ESI-TOF) *m/z*: [M + H]⁺ calcd for C₂₄H₁₈NO₂ 352.1332; found: 352.1333.

(*E*)-3-(4-Fluorostyryl)benzofuro[3,2-*c*]quinoline (**5h**). A mixture of substrate **3b** (0.114 g, 0.30 mmol), 4-fluorostyrene (39 μ L, 0.33 mmol), Pd(OAc)₂ (3.4 mg, 5 mol %), and anhydrous K₂CO₃ (0.083 g, 0.60 mmol) in anhydrous NMP (0.5 mL, 1.5 mL mmol⁻¹) was reacted according to the general one-pot MH/DA procedure above to give the title product as a yellow solid; yield: 63 mg (62%); m.p. 209–211 °C; IR (NaCl) ν 3049, 1682, 1637, 1508, 1347, 1228, 1012 cm⁻¹; ¹H NMR (300 MHz, CDCl₃) δ : 7.02–7.16 (m, 2H), 7.20–7.38 (m, 2H), 7.42–7.64 (m, 4H), 7.76 (dd, *J* = 7.6, 0.7 Hz, 1H), 7.91 (dd, *J* = 8.6, 1.6 Hz, 1H), 8.04–8.15 (m, 1H), 8.28 (d, *J* = 1.4 Hz, 1H), 8.39 (d, *J* = 8.6 Hz, 1H), 9.48 (s, 1H) ppm; ¹³C{¹H} NMR (75 MHz, CDCl₃) δ : 112.1, 115.8 (d, ²*J*_(C,F) = 22 Hz), 116.31, 116.34, 120.6, 121.1, 122.7, 124.1, 124.8, 127.3, 127.86, 127.89, 128.3 (d, ³*J*_(C,F) = 8 Hz), 129.4, 133.2 (d, ⁴*J*_(C,F) = 3 Hz), 138.3, 144.8, 147.9, 156.0, 157.4, 162.6 (d, ¹*J*_(C,F) = 248 Hz) ppm; ¹⁹F{¹H} NMR (282 MHz, CDCl₃) δ : -113 ppm; HRMS (ESI-TOF) *m/z*: [M + H]⁺ calcd for C₂₃H₁₅FNO 340.1132; found: 340.1135.

General Procedure for the Synthesis of Phenoxy-Substituted SM/DA and MH/DA Products. The same procedures and purification methods outlined for the SM/DA and MH/DA reactions were employed here using 4-(2,4-dibromphenoxy)quinoline **3e** (1 equiv) as the substrate.

8-Phenylbenzofuro[3,2-*c*]quinoline (**6a**). A mixture of substrate **3e** (0.200 g, 0.528 mmol), phenylboronic acid (0.071 g, 0.58 mmol), Pd(OAc)₂ (2.4 mg, 2 mol %), and anhydrous K₂CO₃ (0.146 g, 1.06 mmol) in anhydrous NMP (0.8 mL, 1.5 mL mmol⁻¹) was reacted according to the general one-pot SM/DA procedure above to give the title product as a yellow solid; yield: 103 mg (65%); m.p. 153–155 °C; IR (NaCl) ν 2922, 1567, 1460, 1325, 1202 cm⁻¹; ¹H NMR (300 MHz, CDCl₃) δ : 7.36–7.45 (m, 1H), 7.46–7.56 (m, 2H), 7.67–7.86 (m, 6H), 8.24–8.35 (m, 2H), 8.45 (dd, *J* = 8.1, 1.6 Hz, 1H), 9.55 (s, 1H) ppm; ¹³C{¹H} NMR (75 MHz, CDCl₃) δ : 112.2, 116.4, 117.2, 119.1, 120.8, 123.3, 126.7, 127.1, 127.4, 127.5, 128.9, 129.4, 129.9, 137.9, 140.9, 144.4, 147.5, 155.5, 158.0 ppm; HRMS (ESI-TOF) *m/z*: [M + H]⁺ calcd for C₂₁H₁₄NO 296.1070; found: 296.1072.

tert-Butyl (*E*)-3-(Benzofuro[3,2-*c*]quinolin-8-yl)acrylate (**6b**). A mixture of substrate **3e** (0.076 g, 0.20 mmol), *tert*-butyl acrylate (32 μ L, 0.22 mmol), Pd(OAc)₂ (0.9 mg, 2 mol %), and anhydrous K₂CO₃ (0.055 g, 0.40 mmol) in anhydrous NMP (0.3 mL, 1.5 mL mmol⁻¹)

was reacted according to the general one-pot MH/DA procedure above to give the title product as a white solid; yield: 50 mg (73%); m.p. 157–158 °C; IR (NaCl) ν 3434, 1703, 1638, 1594, 1566, 1367, 1203, 1151 cm⁻¹; ¹H NMR (300 MHz, CDCl₃) δ : 1.58 (s, 9H), 6.47 (d, *J* = 15.9 Hz, 1H), 7.50–7.89 (m, 5H), 8.09–8.30 (m, 2H), 8.36 (dd, *J* = 8.1, 1.1 Hz, 1H), 9.45 (s, 1H) ppm; ¹³C{¹H} NMR (75 MHz, CDCl₃) δ : 28.3, 80.7, 112.5, 115.9, 117.1, 120.2, 120.4, 120.8, 123.5, 127.22, 127.24, 129.6, 130.0, 131.2, 143.0, 144.3, 147.7, 156.7, 158.2, 166.2 ppm; HRMS (ESI-TOF) *m/z*: [M + H]⁺ C₂₂H₂₀NO₃: 346.1438; found: 346.1430.

(*E*)-8-Styrylbenzofuro[3,2-*c*]quinoline (**6c**). A mixture of substrate **3e** (0.076 g, 0.20 mmol), styrene (25 μ L, 0.22 mmol), Pd(OAc)₂ (2.5 mg, 5 mol %), and anhydrous K₂CO₃ (0.055 g, 0.40 mmol) in anhydrous NMP (0.3 mL, 1.5 mL mmol⁻¹) was reacted according to the general one-pot MH/DA procedure above to give the title product as a yellow solid; yield: 25 mg (40%); m.p. 200–203 °C; IR (NaCl) ν 3583, 1650, 1598, 1567, 1324, 1195 cm⁻¹; ¹H NMR (300 MHz, CDCl₃) δ : 7.11–7.47 (m, 5H), 7.55–7.61 (m, 2H), 7.63–7.87 (m, 4H), 8.11–8.32 (m, 2H), 8.39 (dd, *J* = 8.1, 1.3 Hz, 1H), 9.50 (s, 1H) ppm; ¹³C{¹H} NMR (75 MHz, CDCl₃) δ : 112.2, 116.2, 117.2, 118.2, 120.8, 123.3, 126.0, 126.5, 127.1, 127.8, 128.1, 128.8, 128.9, 129.4, 129.9, 133.9, 137.2, 144.4, 147.5, 155.6, 158.0 ppm; HRMS (ESI-TOF) *m/z*: [M + H]⁺ calcd for C₂₃H₁₆NO 322.1226; found: 322.1223.

General Procedure for the Synthesis of Three-Component SM/DA and MH/DA Products. The same procedures and purification methods outlined for the SM/DA and MH/DA reactions were employed here using bromo-4-(2,4-dibromphenoxy)quinoline (1 equiv) as the substrate and double the equivalent of coupling partner (2.2 equiv).

2,8-Diphenylbenzofuro[3,2-*c*]quinoline (**7a**). A mixture of substrate **3f** (0.200 g, 0.437 mmol), phenylboronic acid (0.117 g, 0.96 mmol), Pd(OAc)₂ (2.0 mg, 2 mol %), and anhydrous K₂CO₃ (0.121 g, 0.873 mmol) in anhydrous NMP (0.7 mL, 1.5 mL mmol⁻¹) was reacted according to the general one-pot SM/DA procedure above to give the title product as a pale yellow solid; yield: 129 mg (80%); m.p. 206–207 °C; IR (NaCl) ν 3054, 2920, 1682, 1560, 1460, 1358, 1200 cm⁻¹; ¹H NMR (300 MHz, CDCl₃) δ : 7.37–7.60 (m, 6H), 7.68–7.88 (m, 6H), 8.07 (dd, *J* = 8.8, 2.1 Hz, 1H), 8.28–8.40 (m, 2H), 8.64 (d, *J* = 1.7 Hz, 1H), 9.54 (s, 1H) ppm; ¹³C{¹H} NMR (75 MHz, CDCl₃) δ : 112.2, 116.6, 117.4, 118.4, 119.1, 123.3, 126.8, 127.4, 127.50, 127.54, 128.0, 128.9, 129.0, 130.3, 137.9, 139.8, 140.1, 140.9, 144.2, 146.8, 155.5, 158.1 ppm; HRMS (ESI-TOF) *m/z*: [M + H]⁺ calcd for C₂₇H₁₈NO 372.1388; found: 372.1384. Note: ¹³C NMR shift at 128.9 ppm represents two individual carbon signals as confirmed by 2D NMR experiments.

*Di-tert-butyl 3,3'-(Benzofuro[3,2-*c*]quinoline-3,8-diyl)(2*E*,2'*E*)-diacrylate (**7b**)*. A mixture of substrate **3g** (0.050 g, 0.11 mmol), *tert*-butyl acrylate (35 μ L, 0.242 mmol), Pd(OAc)₂ (0.5 mg, 2 mol %), and anhydrous K₂CO₃ (0.030 g, 0.22 mmol) in anhydrous NMP (0.3 mL, 1.5 mL mmol⁻¹) was reacted according to the general one-pot MH/DA procedure above to give the title product as a white solid; yield: 23 mg (43%); m.p. 217–219 °C; IR (NaCl) ν 3402, 1703, 1638, 1559, 1512, 1368, 1201, 1148 cm⁻¹; ¹H NMR (300 MHz, CDCl₃) δ : 1.50–1.61 (m, 18H), 6.40–6.67 (m, 2H), 7.66–7.94 (m, 5H), 8.23 (d, *J* = 0.8 Hz, 1H), 8.29–8.44 (m, 2H), 9.49 (s, 1H) ppm; ¹³C{¹H} NMR (75 MHz, CDCl₃) δ : 28.22, 28.24, 80.7, 80.9, 112.6, 116.6, 117.6, 120.3, 120.5, 121.4, 122.3, 123.3, 125.3, 127.5, 130.7, 131.4, 136.0, 142.7, 142.8, 145.0, 147.7, 156.9, 157.8, 166.0, 166.1 ppm; HRMS (ESI-TOF) *m/z*: [M + H]⁺ calcd for C₂₉H₃₀NO₅: 472.2118; found: 472.2117.

3,8-Di(*E*)-styrylbenzofuro[3,2-*c*]quinoline (**7c**). A mixture of substrate **3g** (0.115 g, 0.25 mmol), styrene (63 μ L, 0.55 mmol), Pd(OAc)₂ (2.8 mg, 5 mol %), and anhydrous K₂CO₃ (0.069 g, 0.50 mmol) in anhydrous NMP (0.4 mL, 1.5 mL mmol⁻¹) was reacted according to the general one-pot MH/DA procedure above to give the title product as a white solid; yield: 76 mg (36%); m.p. >250 °C; IR (NaCl) ν 3387, 1691, 1594, 1560, 1326, 1044 cm⁻¹; ¹H NMR (600 MHz, (CD₃)₂SO) δ : 7.20–7.54 (m, 9H), 7.59 (app. s, 2H), 7.63–7.75 (m, 4H), 7.87 (dd, *J* = 8.6, 1.6 Hz, 1H), 7.94 (d, *J* = 8.5

H₂, 1H), 8.17 (dd, *J* = 8.7, 1.4 Hz, 1H), 8.35 (d, *J* = 1.3 Hz, 1H), 8.41 (d, *J* = 8.5 Hz, 1H), 8.61 (d, *J* = 1.5 Hz, 1H), 9.69 (s, 1H) ppm; ¹³C{¹H} NMR (150 MHz, (CD₃)₂SO) δ : 112.8, 115.9, 116.4, 119.1, 121.4, 123.2, 127.0, 127.2, 127.3, 128.29, 128.33, 128.6, 129.0, 129.3, 131.2, 134.3, 137.3, 137.5, 139.0, 146.0, 148.1, 155.5, 157.4 ppm; HRMS (ESI-TOF) *m/z*: [M + H]⁺ calcd for C₃₁H₂₃NO 424.1696; found: 424.1690. Note: This compound was highly insoluble, spectra were acquired on <3 mg of this compound after heating in (CD₃)₂SO, and it was difficult to directly assign. As with other compounds, some ¹³C shifts from this spectrum represent more than one signal as confirmed by 2D NMR experiments.

Isolation of Suzuki–Miyaura Only Products. To further probe the hypothesis that the Suzuki–Miyaura reaction was occurring at the C-6 position before direct arylation at the C-3 position, substrate **3i** was synthesized. This substrate could only undergo the Suzuki–Miyaura reaction and proceeded as anticipated (Supporting Information Scheme S1).

4-Phenoxy-6-phenylquinoline (4s). A mixture of substrate **3i** (0.200 g, 0.666 mmol, 1 equiv), phenylboronic acid (0.081 g, 0.666 mmol, 1 equiv), Pd(OAc)₂ (3.0 mg, 2 mol %), and anhydrous K₂CO₃ (0.184 g, 1.333 mmol, 2 equiv) in anhydrous NMP (1.0 mL, 1.5 mL mmol^{−1}) was stirred at 135 °C in a sealed reaction tube in an aluminum multireaction heating mantle until the reaction was completed as evidenced by ¹H NMR analysis (4 h). The cooled reaction mixture was diluted with DCM, filtered through a short plug of Celite, and concentrated in vacuo. The crude mixture was purified by column chromatography over silica gel using Hex/EtOAc (7:3–6:4) as an eluent to give the title product as a pale yellow solid; yield: 168 mg (84%); m.p. 78–80 °C; IR (NaCl): ν 3058, 1562, 1487, 1460, 1360, 1203 cm^{−1}; ¹H NMR (300 MHz, CDCl₃) δ : 6.58 (d, *J* = 5.1 Hz, 1H), 7.16–7.57 (m, 8H), 7.72–7.74 (m, 2H), 8.03 (dd, *J* = 8.8, 2.1 Hz, 1H), 8.17 (d, *J* = 8.8 Hz, 1H), 8.58 (d, *J* = 2.0 Hz, 1H), 8.67 (d, *J* = 4.9 Hz, 1H) ppm; ¹³C{¹H} NMR (75 MHz, CDCl₃) δ : 104.6, 119.6, 121.2, 121.7, 125.7, 127.5, 127.7, 129.0, 129.6, 129.8, 130.3, 139.0, 140.5, 149.1, 151.1, 154.4, 162.1 ppm; HRMS (ESI-TOF) *m/z*: [M + H]⁺ calcd for C₂₁H₁₆NO 298.1226; found: 298.1228.

The tandem reaction was carried out on **3a** at a lower temperature to see if the Suzuki–Miyaura only product could be isolated and prove that it was happening prior to the direct arylation reaction. At this temperature, the major product was the uncyclized Suzuki–Miyaura product **4t**, although some of the tandem product **4a** and starting material **3a** were also isolated (Supporting Information Scheme S2).

4-(2-Bromophenoxy)-6-phenylquinoline (4t). A mixture of substrate **3a** (0.150 g, 0.396 mmol), phenylboronic acid (0.048 g, 0.396 mmol), Pd(OAc)₂ (1.8 mg, 2 mol %), and anhydrous K₂CO₃ (0.109 g, 0.79 mmol) in anhydrous NMP (0.6 mL, 1.5 mL mmol^{−1}) was stirred at 100 °C in a sealed reaction tube in an aluminum multireaction heating mantle for 24 h. The cooled reaction mixture was diluted with DCM, filtered through a short plug of Celite, and concentrated in vacuo. The crude mixture was purified by column chromatography over silica gel using Hex/EtOAc (8:2–7:3) as an eluent to give the title product as a pale yellow solid; yield: 73 mg (49%); m.p. 85–87 °C; IR (NaCl): ν 3059, 1564, 1460, 1361, 1222, 667 cm^{−1}; ¹H NMR (300 MHz, CDCl₃) δ : 6.43 (d, *J* = 5.2 Hz, 1H), 7.16–7.32 (m, 2H), 7.34–7.57 (m, 4H), 7.70–7.84 (m, 3H), 8.05 (dd, *J* = 8.8, 2.1 Hz, 1H), 8.20 (d, *J* = 8.7 Hz, 1H), 8.62 (d, *J* = 2.0 Hz, 1H), 8.69 (d, *J* = 5.3 Hz, 1H) ppm; ¹³C{¹H} NMR (75 MHz, CDCl₃) δ : 103.9, 116.4, 119.6, 121.3, 123.3, 127.6, 127.9, 129.0, 129.3, 130.2, 134.4, 139.4, 140.3, 148.2, 150.5, 151.0, 161.5 ppm; HRMS (ESI-TOF) *m/z*: [M + H]⁺ calcd for C₂₁H₁₅BrNO 376.0332; found: 376.0331. Note: ¹³C NMR shifts at 127.6 and 129.0 ppm each represent two individual carbon signals as confirmed by 2D NMR experiments.

The Synthesis of Palladium–Quinoline Complexes. **4-(2-Bromophenoxy)quinoline Palladium Diacetate Dimer (8a).** To an NMR tube were added **1** (61.5 mg, 0.204 mmol, 1.0 equiv), Pd(OAc)₂ (22.9 mg, 0.102 mmol, 0.5 equiv), and CDCl₃ (0.6 mL); X-ray quality crystals were obtained via vapor diffusion from a

saturated solution of toluene/methanol in hexane, the CCDC number is 1970630; decomposition >150 °C; IR (NaCl) ν 3436, 1615, 1589, 1573, 1303, 1217, 1075, 695 cm^{−1}; ¹H NMR (300 MHz, CDCl₃) δ : 1.53 (s, 6H), 6.47 (d, *J* = 6.2 Hz, 2H), 7.11–7.34 (m, 4H), 7.37–7.54 (m, 2H), 7.59–7.84 (m, 4H), 8.08 (ddd, *J* = 8.6, 7.0, 1.4 Hz, 2H), 8.41 (dd, *J* = 8.1, 0.9 Hz, 2H), 9.46 (d, *J* = 6.2 Hz, 2H), 10.20 (d, *J* = 8.6 Hz, 2H) ppm; ¹³C{¹H} NMR (150 MHz, CDCl₃) δ : 22.6, 103.9, 116.2, 121.3, 122.0, 123.4, 127.4, 128.1, 129.0, 129.4, 132.1, 134.5, 147.9, 150.2, 156.1, 162.6, 178.3 ppm; HRMS (ESI-TOF) *m/z*: [M – OAc]⁺ calcd for C₃₂H₂₃Br₂N₂O₄Pd 762.9054; found: 762.9081.

7-Bromo-4-(2-bromophenoxy)quinoline Palladium Diacetate Dimer (8b). To an NMR tube were added **3b** (60.8 mg, 0.160 mmol, 1.0 equiv), Pd(OAc)₂ (18.0 mg, 0.080 mmol, 0.5 equiv), and CDCl₃ (0.6 mL). Decomposition >190 °C; IR (NaCl) ν 3419, 1623, 1590, 1511, 1306, 1219, 1063, 733, 693 cm^{−1}; ¹H NMR (600 MHz, CDCl₃) δ : 1.59 (s, 6H), 6.46 (d, *J* = 6.2 Hz, 2H), 7.16–7.37 (m, 4H), 7.41–7.57 (m, 2H), 7.66–7.93 (m, 4H), 8.29 (d, *J* = 8.8 Hz, 2H), 9.43 (d, *J* = 6.2 Hz, 2H), 10.36 (d, *J* = 1.7 Hz, 2H) ppm; ¹³C{¹H} NMR (150 MHz, CDCl₃) δ : 22.7, 104.2, 116.1, 120.1, 123.3, 123.5, 127.0, 128.4, 129.6, 131.2, 134.6, 148.4, 149.9, 157.4, 162.8, 178.4 ppm; HRMS (ESI-TOF) *m/z*: [M – OAc]⁺ calcd for C₃₂H₂₁Br₄N₂O₄Pd 918.7264; found: 918.7284. Note: ¹³C NMR shift at 131.2 ppm represents two individual carbon signals as confirmed by 2D NMR experiments.

4-Phenoxyquinoline Palladium Diacetate Dimer (8c). To 25 mL of RBF were added **3h** (55.0 mg, 0.249 mmol, 1.0 equiv), Pd(OAc)₂ (27.9 mg, 0.124 mmol, 0.5 equiv), and CDCl₃ (2 mL); X-ray quality crystals were obtained via vapor diffusion from a saturated solution of toluene/methanol in hexane, the CCDC number is 1970507; decomposition >150 °C; IR (NaCl) ν 3413, 1621, 1595, 1305, 1512, 1203, 1063 cm^{−1}; ¹H NMR (300 MHz, CDCl₃) δ : 1.53 (s, 6H), 6.50 (d, *J* = 6.2 Hz, 2H), 7.03–7.21 (m, 4H), 7.23–7.51 (m, 6H), 7.61 (ddd, *J* = 8.2, 7.0, 1.0 Hz, 2H), 7.99 (ddd, *J* = 8.6, 7.0, 1.4 Hz, 2H), 8.28 (dd, *J* = 8.4, 1.0 Hz, 2H), 9.34 (d, *J* = 6.2 Hz, 2H), 10.08 (d, *J* = 8.6 Hz, 2H) ppm; ¹³C{¹H} NMR (75 MHz, CDCl₃) δ : 22.7, 104.3, 121.4, 121.8, 122.0, 126.7, 127.3, 129.1, 130.7, 132.0, 148.0, 153.4, 156.1, 163.9, 178.3 ppm; HRMS (ESI-TOF) *m/z*: [M – OAc]⁺ calcd for C₃₂H₂₅N₂O₄Pd 607.0844; found: 607.0849.

Experiments To Prove Viability of Palladium–Quinoline Complexes. **1.** A 0.062 M stock solution of **8c** in CDCl₃ was prepared, and 0.1 mL (4.1 mg, 2 mol %) was transferred to a reaction tube and concentrated in vacuo to give a yellow residue. To the tube containing this residue were added substrate **3a** (0.118 g, 0.310 mmol, 1 equiv), phenylboronic acid (0.042 g, 0.341 mmol, 1.1 equiv), anhydrous K₂CO₃ (0.086 g, 0.62 mmol), and NMP (0.5 mL, 1.5 mL mmol^{−1}). The resulting mixture was stirred at 135 °C in the sealed reaction tube in an aluminum multireaction heating mantle until the reaction was complete as evidenced by ¹H NMR analysis (20 h). The cooled reaction mixture was diluted with DCM, filtered through a short plug of Celite, and concentrated in vacuo. A yield of 81% **4a** was determined by ¹H NMR analysis of the crude reaction mixture using 1,3,5-trimethoxybenzene as an internal standard (Scheme 4a).

2. A 0.062 M stock solution of **8c** in CDCl₃ was prepared, and 0.1 mL (4.1 mg, 2 mol %) was transferred to a reaction tube and concentrated in vacuo to give a yellow residue. To the tube containing this residue were added substrate **1** (0.093 g, 0.310 mmol, 1 equiv), anhydrous K₂CO₃ (0.086 g, 0.62 mmol), and NMP (0.5 mL, 1.5 mL mmol^{−1}). The resulting mixture was stirred at 135 °C in the sealed reaction tube in an aluminum multireaction heating mantle until the reaction was complete as evidenced by ¹H NMR analysis (20 h). The cooled reaction mixture was diluted with DCM, filtered through a short plug of Celite, and concentrated in vacuo. A 99% yield of **2** was determined by ¹H NMR analysis of the crude reaction mixture using 1,3,5-trimethoxybenzene as an internal standard (Supporting Information Scheme S3).

3. A 0.10 M stock solution of **8a** in CHCl₃ was prepared, and 0.2 mL (16.5 mg, 10 mol %) was transferred to a reaction tube and concentrated in vacuo to give a yellow residue. To the tube containing this residue were added substrate **3a** (0.076 g, 0.20 mmol, 1 equiv), phenylboronic acid (0.027 g, 0.22 mmol, 1.1 equiv), anhydrous

K₂CO₃ (0.055 g, 0.40 mmol), and NMP (0.3 mL, 1.5 mL mmol⁻¹). The resulting mixture was stirred at 135 °C in the sealed reaction tube in an aluminum multi-reaction heating mantle until the reaction was complete as evidenced by ¹H NMR analysis (18 h). The cooled reaction mixture was diluted with DCM, filtered through a short plug of Celite, and concentrated in vacuo. Upon analysis of the crude reaction mixture, no starting material remained, and the peaks for both products **4a** and **2** were present. The signals for **4a** and **2** were too close to obtain accurate NMR yields and were nonseparable by column chromatography (Scheme 4b).

■ ASSOCIATED CONTENT

Supporting Information

The Supporting Information is available free of charge at <https://pubs.acs.org/doi/10.1021/acs.joc.9b03321>.

Copies of the ¹H, ¹³C, and ¹H-¹⁵N HMBC NMR spectra, additional experiments, X-ray crystallography data, HRMS data for metal-containing complexes, fluorescence emission, and UV–Vis absorption data (PDF)

X-ray crystallography data for **4a**, **4n**, **5b**, **8a**, and **8c** (CIF)

■ AUTHOR INFORMATION

Corresponding Author

Gerard P. McGlacken – School of Chemistry, Analytical and Biological Chemistry Research Facility (ABCRF) and Synthesis and Solid State Pharmaceutical Centre (SSPC), University College Cork, Cork T12 YN60, Ireland; orcid.org/0000-0002-7821-0804; Email: g.mcglacken@ucc.ie

Authors

Rachel M. Shanahan – School of Chemistry, Analytical and Biological Chemistry Research Facility (ABCRF), University College Cork, Cork T12 YN60, Ireland

Aobha Hickey – School of Chemistry, Analytical and Biological Chemistry Research Facility (ABCRF), University College Cork, Cork T12 YN60, Ireland

Lorraine M. Bateman – School of Chemistry, Analytical and Biological Chemistry Research Facility (ABCRF), Synthesis and Solid State Pharmaceutical Centre (SSPC), and School of Pharmacy, University College Cork, Cork T12 YN60, Ireland

Mark E. Light – Department of Chemistry, University of Southampton, Southampton SO17 1BJ, United Kingdom

Complete contact information is available at:

<https://pubs.acs.org/doi/10.1021/acs.joc.9b03321>

Author Contributions

[†]R.M.S. and A.H. contributed equally.

Notes

The authors declare no competing financial interest.

■ ACKNOWLEDGMENTS

The authors would like to thank Dr. Trevor Carey, Prof John Sodeau, Dr. Peter Byrne, and Dr. Leticia Pardo for useful discussion. The authors acknowledge the Irish Research Council (IRC) and Science Foundation Ireland (SFI) (grant number SFI/12/IP/1315) and the Synthesis and Solid State Pharmaceutical Centre (SSPC) (SFI/12/RC/2275 and SFI/12/RC/2275_P2). The authors thank the European Cooperation in Science and Technology COST initiative for funding CA15106, C-H Activation in Organic Synthesis (CHAOS). This publication has emanated from research conducted with

the financial support of SFI through a research infrastructure award for process flow spectroscopy (Prospect) under the grant number 15/RI/3221.

■ REFERENCES

- (1) (a) Hayashi, Y. Pot economy and one-pot synthesis. *Chem. Sci.* **2016**, *7*, 866–880. (b) Vaxelaire, C.; Winter, P.; Christmann, M. One-Pot Reactions Accelerate the Synthesis of Active Pharmaceutical Ingredients. *Angew. Chem., Int. Ed.* **2011**, *50*, 3605–3607.
- (2) Dobrounig, P.; Trobe, M.; Breinbauer, R. Sequential and iterative Pd-catalyzed cross-coupling reactions in organic synthesis. *Monatsh. Chem.* **2017**, *148*, 3–35.
- (3) Majumdar, K. C.; Chattopadhyay, S. K. *Heterocycles in Natural Product Synthesis*; John Wiley & Sons: Weinheim, Germany, 2011.
- (4) Taylor, R. D.; MacCoss, M.; Lawson, A. D. G. Rings in Drugs. *J. Med. Chem.* **2014**, *57*, 5845–5859.
- (5) Shanahan, R. M.; Hickey, A.; Reen, F. J.; O’Gara, F.; McGlacken, G. P. Synthesis of Benzofuroquinolines via Phosphine-Free Direct Arylation of 4-Phenoxyquinolines in Air. *Eur. J. Org. Chem.* **2018**, *2018*, 6140–6149.
- (6) Newman, S. G.; Lautens, M. The role of reversible oxidative addition in selective palladium (0)-catalyzed intramolecular cross-couplings of polyhalogenated substrates: synthesis of brominated indoles. *J. Am. Chem. Soc.* **2010**, *132*, 11416–11417.
- (7) Wang, J.-R.; Manabe, K. Transition-Metal-Catalyzed Site-Selective Cross-Coupling of Di- and Polyhalogenated Compounds. *Synthesis* **2009**, *2009*, 1405–1427.
- (8) (a) Ma, X.; Gu, N.; Liu, Y.; Liu, P.; Xie, J.; Dai, B.; Liu, Z. One-pot synthesis of polyfluoroterphenyls via palladium-catalyzed Suzuki-Miyaura coupling of chlorobromobenzene and C-H bond functionalization of perfluoroarenes. *Appl. Organomet. Chem.* **2015**, *29*, 50–56. (b) Matsumura, K.; Yoshizaki, S.; Maitani, M. M.; Wada, Y.; Ogomi, Y.; Hayase, S.; Kaiho, T.; Fuse, S.; Tanaka, H.; Takahashi, T. Rapid Synthesis of Thiophene-Based, Organic Dyes for Dye-Sensitized Solar Cells (DSSCs) by a One-Pot, Four-Component Coupling Approach. *Chem. – Eur. J.* **2015**, *21*, 9742–9747. (c) Ren, L.; Chu, W.; Guan, D.; Hou, Y.; Wang, M.; Yuan, X.; Sun, Z. Chemoselective one-pot synthesis of terphenyl derivatives by sequential directed C-H functionalization-Suzuki coupling. *Appl. Organomet. Chem.* **2014**, *28*, 673–677. (d) El Akkaoui, A.; Berteina-Raboin, S.; Mouaddib, A.; Guillaumet, G. Direct Arylation of Imidazo[1,2-b]pyridazines: Microwave-Assisted One-Pot Suzuki Coupling/Pd-Catalysed Arylation. *Eur. J. Org. Chem.* **2010**, *2010*, 862–871. (e) Koubachi, J.; El Kazzouli, S.; Berteina-Raboin, S.; Mouaddib, A.; Guillaumet, G. Synthesis of polysubstituted imidazo[1,2-a]pyridines via microwave-assisted one-pot cyclization/Suzuki coupling/palladium-catalyzed heteroarylation. *J. Org. Chem.* **2007**, *72*, 7650–7655.
- (9) (a) Geary, L. M.; Hultin, P. G. Modular Construction of 2-Substituted Benzo[b]furans from 1,2-Dichlorovinyl Ethers. *Org. Lett.* **2009**, *11*, 5478–5481. (b) Wang, W.-Y.; Feng, X.; Hu, B.-L.; Deng, C.-L.; Zhang, X.-G. Synthesis of 6-(Trifluoromethyl) Phenanthridines via Palladium-Catalyzed Tandem Suzuki/C-H Arylation Reactions. *J. Org. Chem.* **2013**, *78*, 6025–6030. (c) Chai, D. I.; Lautens, M. Tandem Pd-Catalyzed Double C-C Bond Formation: Effect of Water. *J. Org. Chem.* **2009**, *74*, 3054–3061. (d) Nicolaus, N.; Franke, P. T.; Lautens, M. Modular Synthesis of Naphthothiophenes by Pd-Catalyzed Tandem Direct Arylation/Suzuki Coupling. *Org. Lett.* **2011**, *13*, 4236–4239. (e) Leclerc, J.-P.; André, M.; Fagnou, K. Heck, Direct Arylation, and Hydrogenation: Two or Three Sequential Reactions from a Single Catalyst. *J. Org. Chem.* **2006**, *71*, 1711–1714.
- (10) Friedman, D.; Masiangoli, T.; Olson, S. *The Role of the Chemical Sciences in Finding Alternatives to Critical Resources: A Workshop Summary*; National Academies Press: Washington, DC, 2012.
- (11) (a) Zhao, M.; Kamada, T.; Takeuchi, A.; Nishioka, H.; Kuroda, T.; Takeuchi, Y. Structure–activity relationship of indoloquinoline analogs anti-MRSA. *Bioorg. Med. Chem. Lett.* **2015**, *25*, 5551–5554. (b) Chen, Y.-L.; Chung, C.-H.; Chen, I. L.; Chen, P.-H.; Jeng, H.-Y.

Synthesis and cytotoxic activity evaluation of indolo-, pyrrolo-, and benzofuro-quinolin-2(1H)-ones and 6-anilinoindoloquinoline derivatives. *Bioorg. Med. Chem.* **2002**, *10*, 2705–2712.

(12) Chang, Y.; Fu, J.; Yao, K.; Li, B.; Xu, K.; Pang, X. Novel fluorescent probes for sequential detection of Cu²⁺ and citrate anion and application in living cell imaging. *Dyes Pigm.* **2019**, *161*, 331–340.

(13) Although conventional EAS would not be useful here, it is worth noting that C–H borylation could be considered a viable route, as demonstrated in the following reports: (a) Mkhaliid, I. A. I.; Coventry, D. N.; Albesa-Jove, D.; Batsanov, A. S.; Howard, J. A. K.; Perutz, R. N.; Marder, T. B. Ir-Catalyzed Borylation of C–H Bonds in N-Containing Heterocycles: Regioselectivity in the Synthesis of Heteroaryl Boronate Esters. *Angew. Chem., Int. Ed.* **2006**, *45*, 489–491. (b) Tajuddin, H.; Harrisson, P.; Bitterlich, B.; Collings, J. C.; Sim, N.; Batsanov, A. S.; Cheung, M. S.; Kawamorita, S.; Maxwell, A. C.; Shukla, L.; Morris, J.; Lin, Z.; Marder, T. B.; Steel, P. G. Iridium-catalyzed C–H borylation of quinolines and unsymmetrical 1,2-disubstituted benzenes: insights into steric and electronic effects on selectivity. *Chem. Sci.* **2012**, *3*, 3505–3515.

(14) Altaf, A. A.; Shahzad, A.; Gul, Z.; Rasool, N.; Badshah, A.; Lal, B.; Khan, E. A review on the medicinal importance of pyridine derivatives. *J. Drug Des. Med. Chem.* **2015**, *1*, 1–11.

(15) Yang, Y.; Lan, J.; You, J. Oxidative C–H/C–H Coupling Reactions between Two (Hetero)arenes. *Chem. Rev.* **2017**, *117*, 8787–8863.

(16) (a) Ye, M.; Gao, G.-L.; Edmunds, A. J. F.; Worthington, P. A.; Morris, J. A.; Yu, J.-Q. Ligand-Promoted C3-Selective Arylation of Pyridines with Pd Catalysts: Gram-Scale Synthesis of (±)-Preclamol. *J. Am. Chem. Soc.* **2011**, *133*, 19090–19093. (b) Iwai, T.; Sawamura, M. Transition-Metal-Catalyzed Site-Selective C–H Functionalization of Quinolines beyond C2 Selectivity. *ACS Catal.* **2015**, *5*, 5031–5040. (c) Hilton, M. C.; Dolewski, R. D.; McNally, A. Selective Functionalization of Pyridines via Heterocyclic Phosphonium Salts. *J. Am. Chem. Soc.* **2016**, *138*, 13806–13809. (d) Konishi, S.; Kawamorita, S.; Iwai, T.; Steel, P. G.; Marder, T. B.; Sawamura, M. Site-Selective C–H Borylation of Quinolines at the C8 Position Catalyzed by a Silica-Supported Phosphane-Iridium System. *Chem. – Asian J.* **2014**, *9*, 434–438.

(17) Park, H.; Chekshin, N.; Shen, P.-X.; Yu, J.-Q. Ligand-Enabled, Palladium-Catalyzed β -C(sp³)-H Arylation of Weinreb Amides. *ACS Catal.* **2018**, *8*, 9292–9297.

(18) (a) Wasa, M.; Chan, K. S. L.; Zhang, X.-G.; He, J.; Miura, M.; Yu, J.-Q. Ligand-Enabled Methylene C(sp³)-H Bond Activation with a Pd(II) Catalyst. *J. Am. Chem. Soc.* **2012**, *134*, 18570–18572. (b) He, Y.; Wu, Z.; Ma, C.; Zhou, X.; Liu, X.; Wang, X.; Huang, G. Palladium-Catalyzed Selective C–H Activation: A Simple Method to Synthesize C-3 Site Arylated Quinoline Derivatives. *Adv. Synth. Catal.* **2016**, *358*, 375–379.

(19) Martin, G. E.; Hadden, C. E. Long-Range 1H–15N Heteronuclear Shift Correlation at Natural Abundance. *J. Nat. Prod.* **2000**, *63*, 543–585.

(20) (a) Rosar, V.; Dedeic, D.; Nobile, T.; Fini, F.; Balducci, G.; Alessio, E.; Carfagna, C.; Milani, B. Palladium complexes with simple iminopyridines as catalysts for polyketone synthesis. *Dalton Trans.* **2016**, *45*, 14609–14619. (b) Pereira, M. T.; Antelo, J. M.; Adrio, L. A.; Martínez, J.; Ortigueira, J. M.; López-Torres, M.; Vila, J. M. Novel Bidentate [N,S] Palladacycle Metalloligands. 1H–15N HMBC as a Decisive NMR Technique for the Structural Characterization of Palladium-Rhodium and Palladium-Palladium Bimetallic Complexes. *Organometallics* **2014**, *33*, 3265–3274. (c) Villarreal, W.; Colina-Vegas, L.; Rodrigues de Oliveira, C.; Tenorio, J. C.; Ellena, J.; Gozzo, F. C.; Cominetti, M. R.; Ferreira, A. G.; Ferreira, M. A. B.; Navarro, M.; Batista, A. A. Chiral Platinum(II) Complexes Featuring Phosphine and Chloroquine Ligands as Cytotoxic and Monofunctional DNA-Binding Agents. *Inorg. Chem.* **2015**, *54*, 11709–11720.

(21) (a) García-Cuadrado, D.; Braga, A. A. C.; Maseras, F.; Echavarren, A. M. Proton Abstraction Mechanism for the Palladium-Catalyzed Intramolecular Arylation. *J. Am. Chem. Soc.* **2006**, *128*, 1066–1067. (b) Gorelsky, S. I.; Lapointe, D.; Fagnou, K. Analysis of

the Concerted Metalation-Deprotonation Mechanism in Palladium-Catalyzed Direct Arylation Across a Broad Range of Aromatic Substrates. *J. Am. Chem. Soc.* **2008**, *130*, 10848–10849. (c) Boutadla, Y.; Davies, D. L.; Macgregor, S. A.; Poblador-Bahamonde, A. I. Mechanisms of C–H bond activation: rich synergy between computation and experiment. *Dalton Trans.* **2009**, *2009*, 5820–5831.

(22) Jiang, J.; Yu, J.-Q.; Morokuma, K. Mechanism and Stereoselectivity of Directed C(sp³)-H Activation and Arylation Catalyzed by Pd(II) with Pyridine Ligand and Trifluoroacetate: A Computational Study. *ACS Catal.* **2015**, *5*, 3648–3661.

(23) Cabrera, P. J.; Lee, M.; Sanford, M. S. Second-Generation Palladium Catalyst System for Transannular C–H Functionalization of Azabicycloalkanes. *J. Am. Chem. Soc.* **2018**, *140*, 5599–5606.

(24) While it is difficult to rule out a role for NMP-stabilized Pd nanoparticles, it is noted that these reactions work in dioxane. Also, the addition of quinoline ligands to the DA reaction of non-coordinating substrates increases turnover significantly; these reactions will be published in due course.

(25) Zhao, X. J.; Huang, C. Z.; Huang, C. Z. Small organic molecules as fluorescent probes for nucleotides and their derivatives. *TrAC, Trends Anal. Chem.* **2010**, *29*, 354–367.

(26) Hou, L.; Zhang, X.; Cotella, G. F.; Carnicella, G.; Herder, M.; Schmidt, B. M.; Pätz, M.; Hecht, S.; Cacialli, F.; Samori, P. Optically switchable organic light-emitting transistors. *Nat. Nanotechnol.* **2019**, *14*, 347–353.

(27) Terai, T.; Nagano, T. Small-molecule fluorophores and fluorescent probes for bioimaging. *Pflugers Arch - Eur. J. Physiol.* **2013**, *465*, 347–359.

(28) Sheldrick, G. M. Crystal Structure Refinement with SHELXL. *Acta Crystallogr. Sect. C, Struct. Chem.* **2015**, *71*, 3–8.

(29) Dolomanov, O. V.; Bourhis, L. J.; Gildea, R. J.; Howard, J. A. K.; Puschmann, H. OLEX2: A Complete Structure Solution, Refinement and Analysis Program. *J. Appl. Crystallogr.* **2009**, *42*, 339–341.

(30) Mehra, M. K.; Tantak, M. P.; Arun, V.; Kumar, I.; Kumar, D. Metal-free regioselective formation of C–N and C–O bonds with the utilization of diaryliodonium salts in water: facile synthesis of N-arylquinolones and aryloxyquinolones. *Org. Biomol. Chem.* **2017**, *15*, 4956–4961.